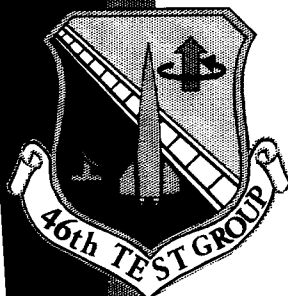




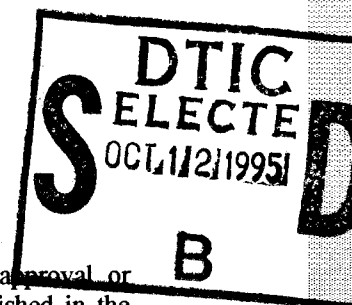
AFDTC-TR-95-24
VOLUME I



SEVENTEENTH BIENNIAL GUIDANCE TEST SYMPOSIUM

PREPARED BY
746TH TEST SQUADRON
(CENTRAL INERTIAL GUIDANCE TEST FACILITY)
1644 VANDERGRIFT ROAD
HOLLOMAN AFB, NEW MEXICO 88330-7850

2, 3, & 4 MAY 1995



Publication of this report does not constitute approval or disapproval of the ideas or findings. It is published in the interest of exchanging scientific and technical information.

DISTRIBUTION STATEMENT: Approved for public release; distribution is unlimited.

The Public Affairs Office has reviewed this report, and it is releasable to the National Technical Information Service where it will be available to the general public, including foreign nationals.

DTIC QUALITY INSPECTED 8

19951011 011

REPORT DOCUMENTATION PAGE			Form Approved OMB No. 0704-0188	
Public reporting burden for this collection of information is estimated to average 1 hour per response, including the time for reviewing instructions, searching existing data sources, gathering and maintaining the data needed, and completing and reviewing the collection of information. Send comments regarding this burden estimate or any other aspect of this collection of information, including suggestions for reducing this burden, to Washington Headquarters Services, Directorate for Information Operations and Reports, 1215 Jefferson Davis Highway, Suite 1204, Arlington, VA 22202-4302, and to the Office of Management and Budget, Paperwork Reduction Project (0704-0188), Washington, DC 20503.				
1. AGENCY USE ONLY (Leave blank)	2. REPORT DATE MAY 1995	3. REPORT TYPE AND DATES COVERED SYMPOSIUM PAPERS 2-4 MAY 1995		
4. TITLE AND SUBTITLE SEVENTEENTH BIENNIAL GUIDANCE TEST SYMPOSIUM (VOLUME I)		5. FUNDING NUMBERS JON: 9993NGTS PE: 65708F		
6. AUTHOR(S) The authors' names are indicated on the individual papers.				
7. PERFORMING ORGANIZATION NAME(S) AND ADDRESS(ES) 746 TS/CC (AFMC) 1644 Vandergrift Road Holloman AFB NM 88330-7850		8. PERFORMING ORGANIZATION REPORT NUMBER AFDTC-TR-95-24 Volume I		
9. SPONSORING/MONITORING AGENCY NAME(S) AND ADDRESS(ES) 746 TS/CC (AFMC) 1644 Vandergrift Road Holloman AFB NM 88330-7850		10. SPONSORING/MONITORING AGENCY REPORT NUMBER AFDTC-TR-95-24 Volume I		
11. SUPPLEMENTARY NOTES				
12a. DISTRIBUTION/AVAILABILITY STATEMENT Approved for public release; distribution is unlimited.		12b. DISTRIBUTION CODE		
13. ABSTRACT (Maximum 200 words) These proceedings contain papers which were presented at the Seventeenth Biennial Guidance Test Symposium. This symposium, hosted by the 746th Test Squadron, Central Inertial Guidance Test Facility, Holloman Air Force Base, New Mexico, on 2-4 May, was directed toward the exchange of information, stimulation of new ideas, and discussion of current techniques associated with the development and evaluation of inertial guidance and navigation systems and global positioning systems. The papers presented included such topics as new test and calibration techniques for guidance systems, advances in flight referenced systems, global positioning systems integrations, and software developments. Volume I contains papers which are unclassified and have no distribution restriction.				
14. SUBJECT TERMS		15. NUMBER OF PAGES 395		16. PRICE CODE
17. SECURITY CLASSIFICATION OF REPORT UNCLASSIFIED	18. SECURITY CLASSIFICATION OF THIS PAGE UNCLASSIFIED	19. SECURITY CLASSIFICATION OF ABSTRACT UNCLASSIFIED	20. LIMITATION OF ABSTRACT UNCLASSIFIED	

THIS PAGE LEFT BLANK INTENTIONALLY

FOREWORD

The Seventeenth Biennial Guidance Test Symposium was held at the Ruidoso Civic and Events Center, Ruidoso, New Mexico, on 2-3 May. A classified session was held at Holloman Air Force Base, New Mexico, on 4 May 1995. This symposium was hosted by the Central Inertial Guidance Test Facility (746th Test Squadron), of the 46th Test Group.

The purpose of the symposium was to provide a forum for approximately 250 people from industry, universities, foreign governments, Department of Defense, and other government agencies to exchange technical information. Papers covered a wide spectrum of topics related to the test and evaluation of systems and components for missile guidance and aircraft navigation applications with emphasis on advances and new information.


Forty-five excellent papers were presented at this symposium; time constraints limited the number presented to only a portion of those papers submitted.

The Paper Selection Committee included Mr. Norman Ingold, Mr. William Ritter, Dr. Mike Hooser, Mr. Francisco Ramirez, Capt Britt Snodgrass, Mr. Derryl Stutz, Capt Dan Uribe, Mr. Coy Hunt, Ms. Barbara Cosentino, Mr. Dennis Ruff, Mr. Robert Lawrence, and Mr. Philip Simpson from the 746th Test Squadron, Holloman Air Force Base, New Mexico.

In addition to those people mentioned above and the contributing authors, a large number of people contributed to the success of this symposium. I wish to express my appreciation to each of them for their efforts. Special thanks go to our Symposium Manager, Mr. Robert Kelher, our Technical Managers, Mr. Reese Sturdevant and Mr. Derryl Stutz, and to the Symposium Coordinator, Ms. Mary Landers.

Publication of this report does not constitute approval or disapproval of the ideas or findings stated within. It is published in the interest of exchanging scientific and technical information.

Accession For	
NTIS GRA&I	<input checked="checked" type="checkbox"/>
DTIC TAB	<input type="checkbox"/>
Unannounced	<input type="checkbox"/>
Justification	
By _____	
Distribution/	
Availability Codes	
Dist	Avail and/or Special
A-1	


DENNIS R. FURMAN, Lt Col, USAF
Commander, 746th Test Squadron

THIS PAGE LEFT BLANK INTENTIONALLY

TABLE OF CONTENTS
SEVENTEENTH BIENNIAL GUIDANCE TEST SYMPOSIUM
PROCEEDINGS
VOLUME I
UNCLASSIFIED

	PAGE
REPORT DOCUMENTATION PAGE.....	i
FOREWORD	iii
TABLE OF CONTENTS.....	v
SESSION I-A: OPENING SESSION.....	1
<i>Advanced Inertial Technology for Military and Commercial Use</i>	
John Elwell, Charles Start Draper Laboratory, Cambridge MA, and Robert Christiansen, Rockwell International, Anaheim CA	3
<i>Performance Testing of a Military GPS Attitude Determining System</i>	
Charles Rodgers, Adroit Systems, Inc., Alexandria VA	18
SESSION II-A: ADVANCED SYSTEMS I.....	29
<i>Results of Carrier Phase Measurement Incorporation Into CHAPS</i>	
Captains Anthony Nash, John Raquet, Britt Snodgrass and Dr. Mike Hooser, 746th Test Squadron, Holloman AFB NM	31
<i>Future Guidance, Navigation & Control Issues.....</i>	
Tom Reed, The Reed Company, Charlton MA	42
SESSION III-A: FIBER OPTIC GYROS.....	62
<i>Cluster Sampling Technique for Gyro Noise Analysis</i>	
M. M. Tehrani, Litton G&C Systems, Woodland Hills CA	64
<i>Fiber Optic Gyro Development for Navy Shipboard Inertial.....</i>	
Reference Systems Applications Joseph DeFato, NCCOSC, Warminster PA	78

<i>Fiber Optic Gyro for Land Navigation</i>	88
Sid Bennett, Andrew Corporation, Orland Park IL	
SESSION II-B: INTEGRATED GPS	98
<i>MAPS Hybrid Engineering Test & Evaluation Results.....</i>	100
Brian Fly, Honeywell Military Avionics, St. Petersburg FL	
<i>Qualification Test Methodology and Results of the Enhanced.....</i>	113
<i>Performance Miniaturized Airborne GPS Receiver</i>	
Redge Bartholomew, Rockwell International, Cedar Rapids IA	
<i>A New Approach to Simulation and Test of Integrated GPS/INS.....</i>	126
Systems	
Axel Lehmann, LITEF, Republic of Germany	
SESSION III-B: GPS TOPICS I.....	132
<i>Integrity Monitoring in the DOD Standard Miniaturized Airborne.....</i>	134
<i>GPS Receiver</i>	
Redge Bartholomew, Rockwell International, Cedar Rapids IA	
<i>Enhancement to C/A-Only Mode Operation of the DOD.....</i>	150
<i>Standard MAGR</i>	
Roger Kirpes, Brent Disselkoen, and Barry Breffle, Rockwell International, Cedar Rapids IA	
<i>Evaluating the Effects of Different Satellite Selection Strategies</i>	166
<i>for Nap of the Earth (NOE) and Ground-Based Global Positioning System (GPS) Users</i>	
Ms. Van Tran, U. S. Army CECOM, Ft. Monmouth NJ and James Adametz, Intermetrics, Inc., Eatontown NJ	
SESSION IV-A: INERTIAL INSTRUMENTS	202
<i>Thermal Analysis of the HRG to Determine Its GAP</i>	204
<i>Sensitivity/Compensation</i>	
Lalit Kumar, Delco Systems Operations, Goleta CA	
<i>G2000 Miniature Gyroscope.....</i>	218
Robert Burlingame, Litton G&C Systems, Salt Lake City UT	

SESSION VI-A: T&E METHODOLOGY II	228
--	-----

ONLY PRESENTATIONS WERE GIVEN DURING THIS SESSION

SESSION VII-A: ADVANCED SYSTEMS II.....	232
---	-----

<i>Fly-By-Light Advanced Systems Hardware (FLASH) Program</i>	<i>234</i>
---	------------

Advanced Research Projects Agency (ARPA) Technology

Reinvestment Project (TRP)

Carlos A. Bedoya, McDonnell Douglas Aerospace, St. Louis MO

<i>The Precision Navigation Systems (PNS)</i>	<i>247</i>
---	------------

Paul Olson, U. S. Army CECOM, Ft. Monmouth NJ and Mark Berry,

Intermetrics, Inc., Wall Township NJ

SESSION IV-B: DIFFERENTIAL GPS	270
--------------------------------------	-----

<i>Wide Area Differential GPS Navigation System Analysis.....</i>	<i>272</i>
---	------------

and Testing

Dirk DeDoes, Intermetrics, Inc., Huntington Beach CA

<i>Results of Differential GPS Support for a Coast to Coas.....</i>	<i>294</i>
---	------------

Flight Test

Dan Crouch and Capt Daniel Uribe, 746th Test Squadron,

Holloman AFB NM

SESSION V-B: GPS SIMULATORS	307
-----------------------------------	-----

<i>Real Time GPS Simulator Integrated with the High</i>	<i>309</i>
---	------------

Fidelity Manned Flight Simulator

Frederick A. Ventrone, Jr., Patuxent River MD, Gary Green,

Pacer Systems, Lexington Park MD, and Christ Bartone, Athens OH

<i>Receiver Time Delay Calibration Using a GPS Signal Simulator.....</i>	<i>316</i>
--	------------

James Brad, U. S. Naval Research Lab, Washington DC

SESSION VI-B: INTEGRATED GPS II.....	331
--------------------------------------	-----

<i>GPS Inertial Navigation Assembly (GINA) Design.....</i>	<i>333</i>
--	------------

and Performance

Dick Hogg and Stan Zugay, NCCOSC, Warminster PA

SESSION VII-B: GPS TOPICS II..... 343

Statistical Significance for Global Positioning System..... 345
(GPS) Test and Evaluation
Dr. Robert Rogers, Rogers Engineering & Associates, Gainesville FL

Investigation into the Reliability of the DOD Miniaturized 356
Airborne GPS Receiver
G. (Phil) Barnes, Rockwell International, Cedar Rapids IA

ATTENDANCE LIST 377

THIS PAGE LEFT BLANK INTENTIONALLY

SESSION I-A
OPENING SESSION

CHAIRMAN

FREDRIC R. NADEAU

*746TH TEST SQUADRON
CIGTF*

THIS PAGE LEFT BLANK INTENTIONALLY

**"Advanced Inertial Technology
for Military and Commercial Use"**

R. G. Christiansen, Rockwell

J. Elwell, The Charles Stark Draper Laboratory

THIS PAGE LEFT BLANK INTENTIONALLY

Abstract

Micromachined silicon inertial sensors are expected to have substantial cost, size, and applications advantages over many competing gyro technologies. Using batch processing techniques that are typical in today's semiconductor industry, thousands of identical sensors, less than a few square millimeters in area, can be fabricated simultaneously. Because of the inherent size, cost, and ruggedness advantages over existing inertial sensors, expanded GN&C applications will be the result.

The Charles Stark Draper Laboratories (Draper) and Rockwell have formed an alliance to address opportunities this new technology presents. The Draper-Rockwell Team is in the process of design to cost, transition to production, and marketing this new class of small, low-cost inertial sensors for commercial and military products. Work on the initial product, a yaw rate gyro for the automotive industry, is well under way. High volume production implemented for consumer markets, such as automotive systems and camcorders, will drive down unit costs. Following in the footsteps of semiconductors, new military inertial applications, previously limited by size or economic feasibility, are quickly becoming a reality.

Draper has been conducting research on micromechanical inertial sensors for more than eight years with gradual success and recent performance breakthroughs. Government contracts have followed for miniature IMUs and high-g capable instruments for competent munitions. Rockwell has the full range of vertical integration necessary to bring this technology to market, including extensive experience in GN&C, silicon manufacturing, high-volume production facilities for electronics/packaging, and a strong position in existing principle markets.

This paper describes the development of silicon micromachined inertial sensors, potential products and applications, and our alliance plan as an example of a successful defense conversion/dual use activity.

THIS PAGE LEFT BLANK INTENTIONALLY

Introduction

Inertial sensors, gyros and accelerometers, have a long and distinguished history in military systems applied to guidance, control, platform stabilization and navigation. Major drawbacks to most commercial applications of gyros and accelerometers have been due to cost. Work at the Draper Lab has led to a breakthrough in utilizing volume production techniques developed for integrated circuit manufacturing to fabricate miniature, rugged inertial sensors. In order to capitalize on the commercial potential of these breakthroughs, Draper entered into an alliance with Rockwell to transition the technology to production and commercial sales. The functioning of the alliance has Draper doing initial design and development while Rockwell transitions the Draper process to production and sales.

Rockwell's technical expertise in supporting the transition effort is derived from several of its operation divisions:

Autonetics Electronic Systems Division (AESD) - Extensive experience in operation and application of inertial sensors and systems

Electro-Optical Center (EOC) - Production capability for specialty silicon devices

Telecommunications (Operations and Digital Communication Division) - High-volume production capability for ASICs and packaging requirements

Science Center - Research and development support for technology development and transfer

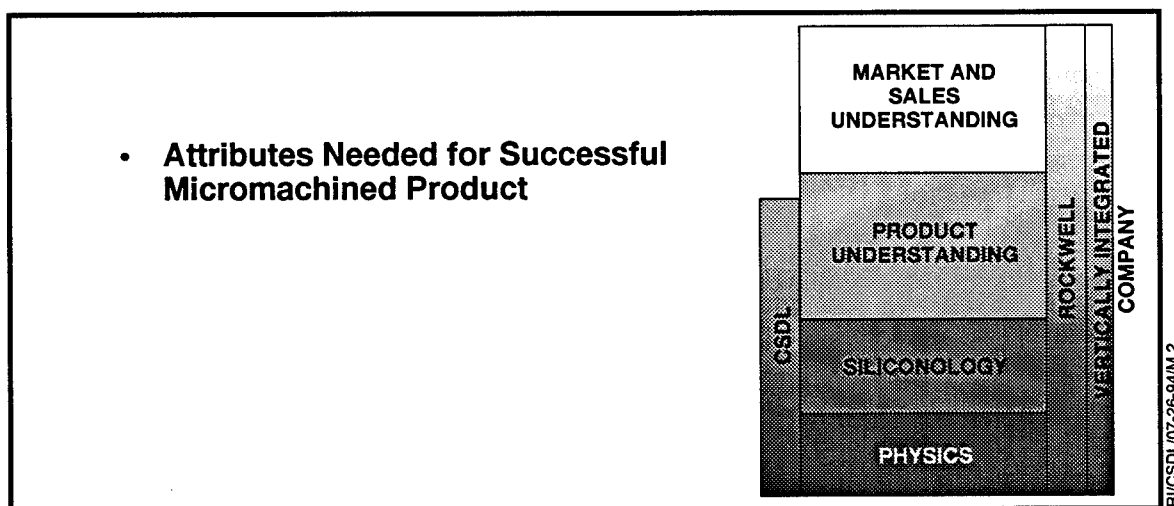


Figure 1. Alliance Strengths

In addition to technical support, Rockwell also provides the alliance with an existing market position in the principle areas that will be targeted, such as automotive applications, military guidance, and commercial electronics. Figure 1 depicts the attributes needed to successfully transition a micromachined product from laboratory to the market place.

The first product to be developed and transitioned is a low-cost, moderate performance rotational rate sensor known as the Draper/Rockwell Micromachined Gyro (DRMG). The further intent is to leverage the work on the DRMG into a long term relationship between Rockwell and Draper to develop and produce additional micromachined sensors and products. This product is an ideal match to the definition of defense conversion, or dual use, since it will support closely coupled commercial and military applications.

The Micromechanical Gyro Market

The initial focus of the research and development at CSDL was for military application. With the demise of the Soviet block and the end of the Cold War, a reassessment of how we use our technical skills to expand the areas where gyros and accelerometers could be applied was undertaken. Figure 2 shows the general segmentation of the market for 0.1°/sec - 10°/sec class of gyros. Some of the applications, like automotive (see Figure 3), have the potential for high volume sales in the near term. The military market has all of the usual application for gyros in the indicated performance class and one major, realizable, new market - competent munitions. The competent munitions market includes artillery and mortar shells. These applications are made possible because of the extreme ruggedness of micromachined gyros and accelerometers. Both gyros and accelerometers have survived and functioned properly following in excess of 60,000 g's shock. Another new application area for micromachined gyros is in the Line-of-Sight (LOS) stabilization of video cameras, cameras, binoculars, and other optical instruments. Although the LOS problem for these applications is very similar in technical content to that of seeker or array stabilization in military systems, serious consideration for commercial application could only emerge when the very low price, small size and ruggedness of micromachined gyros were considered. Finally, when price has been lowered to the level of a few dollars, application of these devices to toys, personal computers, robotics, factory application will occur.

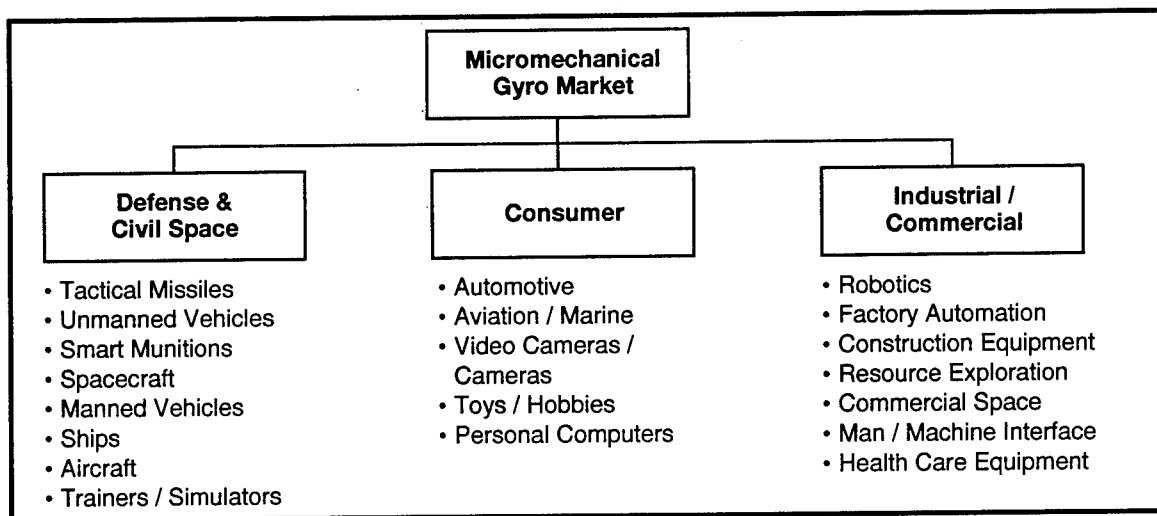


Figure 2. Micromechanical (Micromachined) Gyro Market and Segmentation

The emergence of a large commercial (10^7 or more) market for gyros has a corresponding positive benefit on the military. A comparison with the microprocessor market will serve as a good

analogy. Military systems are a major consumer of commercial microprocessors - to the benefit of the military systems. If, as in the past, the military had to develop, sustain, and maintain an industrial base by itself, the cost of the micro-processor would be prohibitive for all but the high-end weapons (strategic, high-end aircraft, ships, etc.). In this area one thing is clear - a strong and robust commercial business base, grounded in the U.S., is good for the military application in that low cost quality products are available for existing and future military systems.

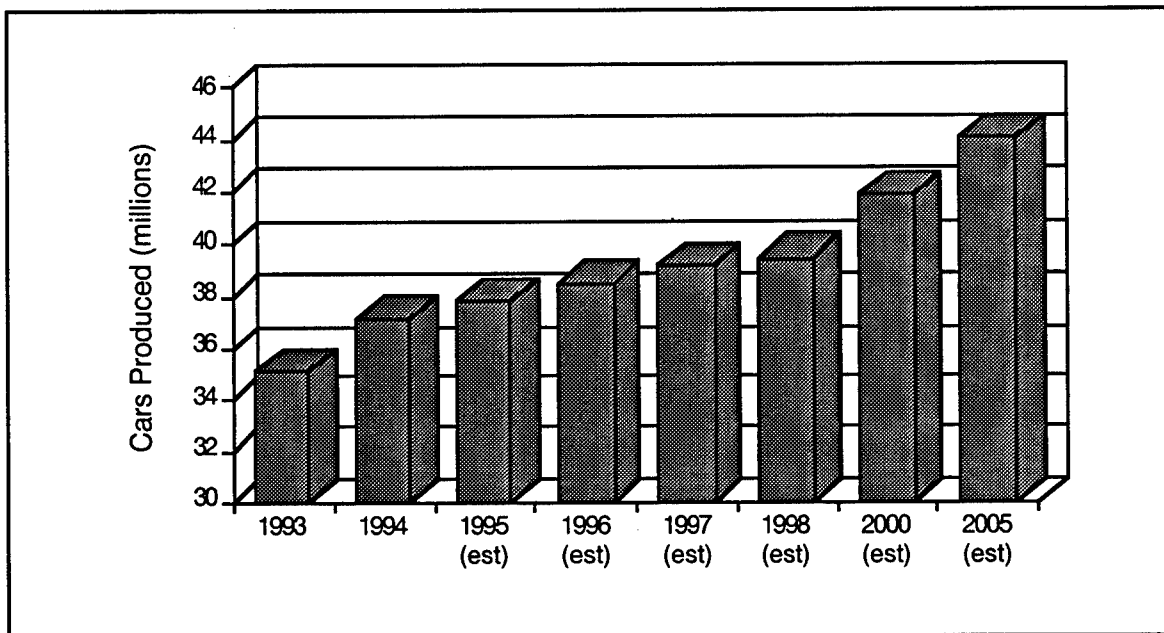


Figure 3. World Automobile Production

DRMG Description

The micromachined rate sensors are single crystal silicon "resonating structure" gyros that are extremely rugged, inherently balanced, physically small, and inexpensive to fabricate. To achieve the cost goals for commercial applications, gyros must shrink to nearly microscope size. However, as the size of the inertial elements shrink, mechanical interfaces cause frictional forces that are large in comparison to inertial forces. As a result, the Draper micromechanical gyroscopes are designed to utilize vibrating inertial elements to avoid the use of mechanical interfaces such as sliding contacts or bearings. The lack of friction makes these microsensors extremely rugged as well.

The principle of operation uses a resonating structure device that, under excitation, will induce a velocity in the structure sensing masses (Figure 4). Electrostatic combs are utilized to drive the masses with opposite oscillatory phases. Small changes in the motion of the vibrating masses occur when the device is rotated about the sense axis, which is parallel to the plane in which the masses move and normal to their velocities. The Coriolis effect causes the masses to oscillate slightly out of their original plane of motion by an amount proportional to the rotation rate. Measurement of the mass deflection is accomplished by synchronously demodulating the sense signal, which is $\pi/2$ out of phase with the drive signal, as shown in Figure 4. Macroscopic tuning

fork gyroscopes, that take advantage of this effect, have been used for many years and are well understood.

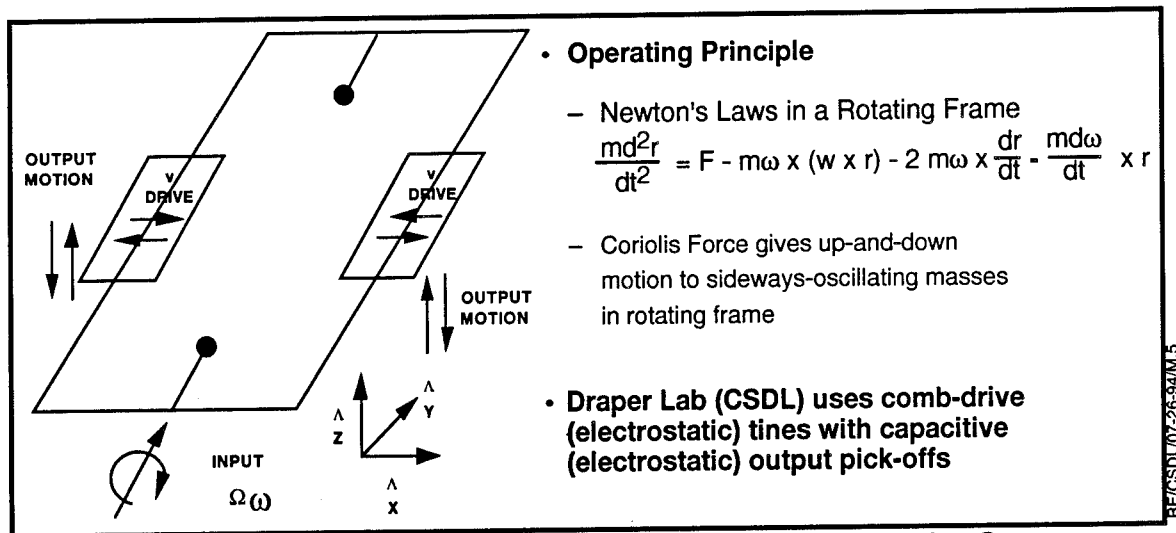


Figure 4. How They Work: Device Concept Evaluation - Rotation Sensor

The utilization of micromachining process technology provides a major advantage of size and cost over these macroscopic devices. The micromechanical gyro chips, with surface areas of a few square millimeters, capitalize on the inherent low cost associated with silicon wafer fabrication techniques while providing sensitivity and ruggedness suitable for automotive use. The structure is fabricated using a dissolved wafer process with dry etch and boron diffusion process steps utilized to define the final dimensions. This structure is then anodically bonded to a glass substrate that has been prepared with a metal deposition step that becomes an integral part of the rate sensor operation.

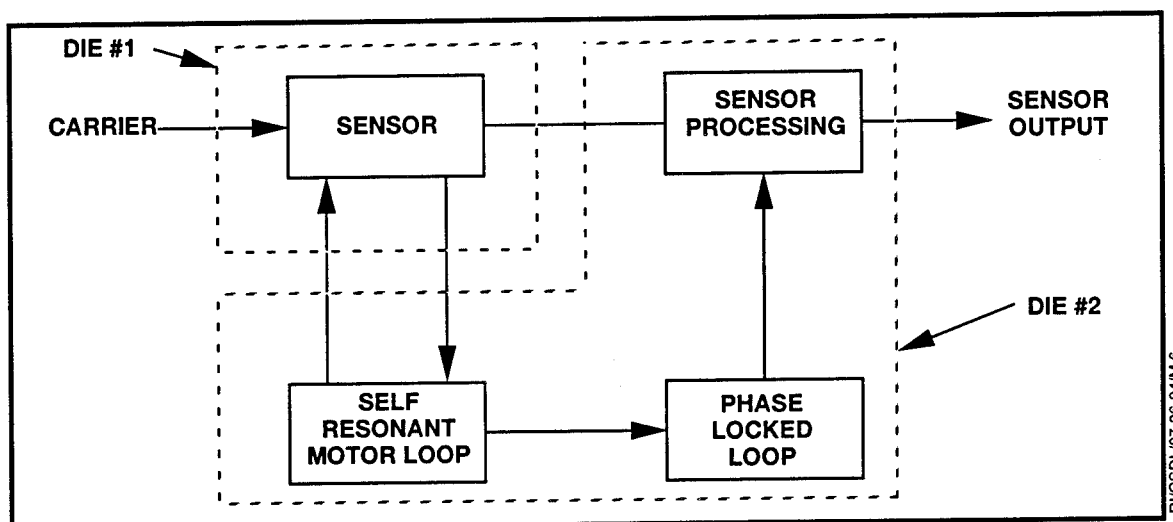


Figure 5. Micromachine Gyro Block Diagram

The physical characteristics of the micromachined sensor are delineated in Table 1. The market or application consequence of attribute is also noted.

Table 1. Sensor Characteristics

		Comment
• Material	• Single crystal silicon on glass	• Simple manufacturing process (4 masks), well understood material
• Volume	• $\sim 4 \text{ mm}^3$	• Very small, goes anywhere
• Mass of Die	• < 3.5 milligram	• Same
• Fork Natural Frequency	• 25 KHz	• Vibration Insensitive
• Mass of Fork	• < 1 microgram	• Shock insensitive (20,000 g+)
• Sensor pick-up	• Capacitance	• Thermally Insensitive

The performance potential of the micromachined gyro is shown in Figures 6 and 7. Figure 6 shows bias and scale factor data taken over 125°C ($-45 - + 85^\circ\text{C}$) with the gyro rated at $\pm 70^\circ/\text{sec}$ and at $0^\circ/\text{sec}$. The temperature measure is chamber temperature. Figure 6 shows that the gyro has more than adequate performance for the automotive application it was targeted for. Figure 7 shows the same data after compensation for the chamber temperature effect on output bias and scale factor. There is a dramatic improvement in the data, and it clearly shows the potential for performance in the $50 - 100^\circ/\text{hr}$ class over this temperature. This is a dramatic example of potential dual use - extended test of an automotive grade gyro elevating it to a military grade gyro.

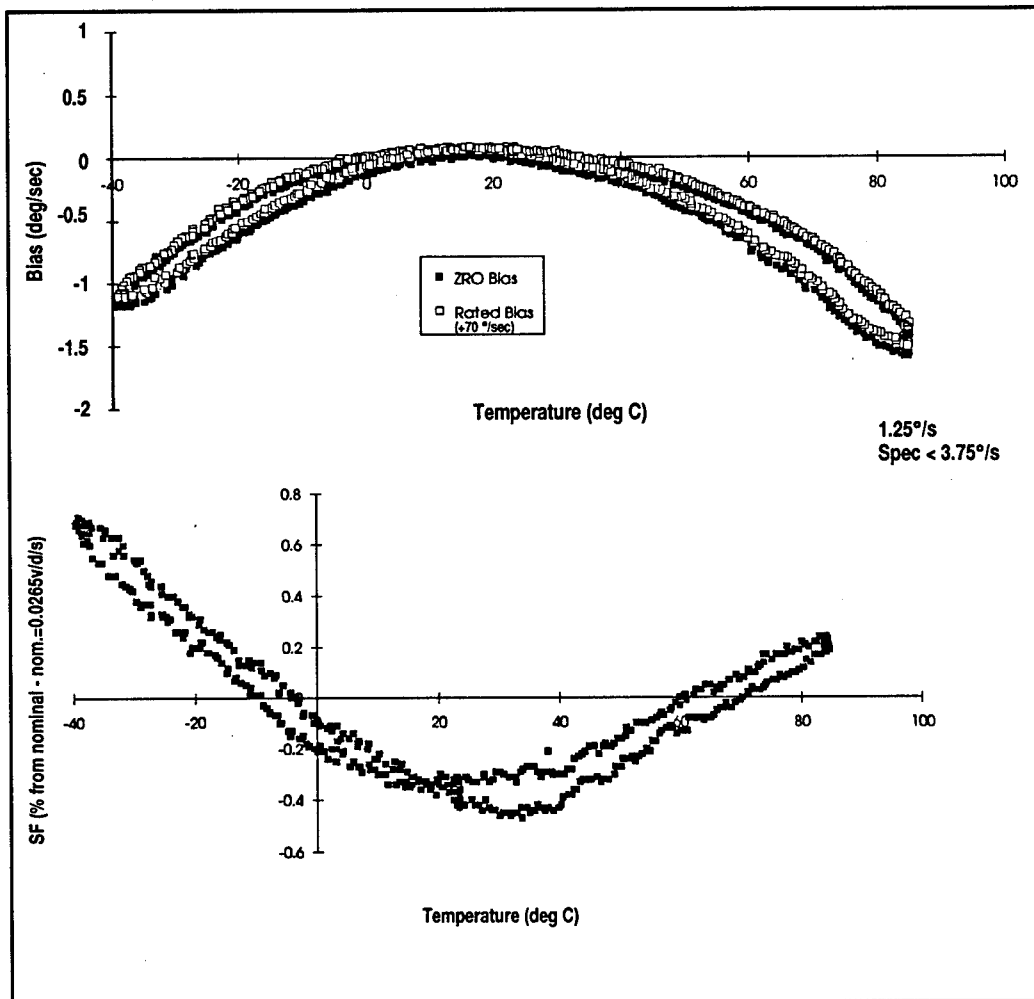


Figure 6.

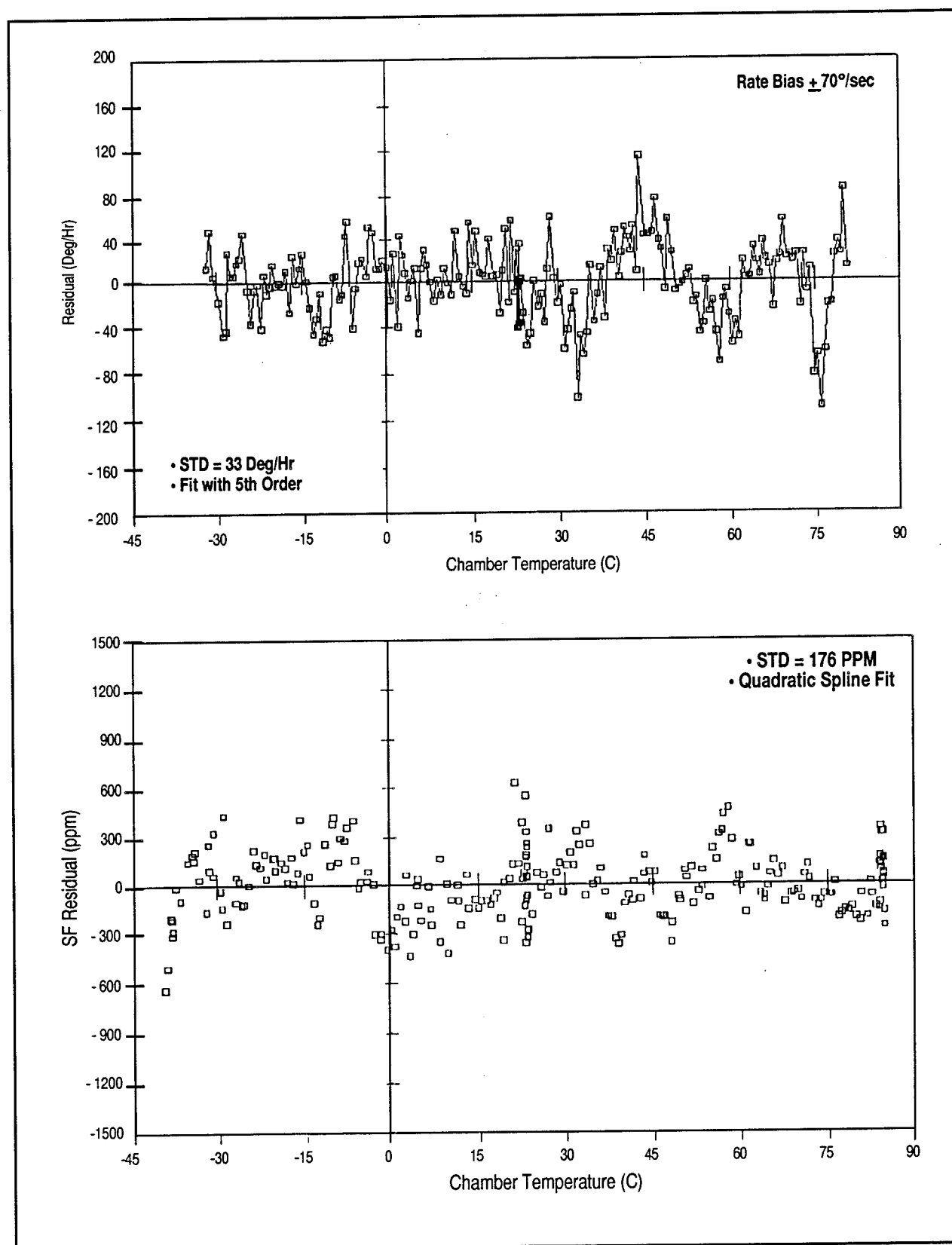


Figure 7.

Production Transition Activities

The objective of the production transition plan is to take the prototype developmental work done at Draper and scale up/modify the processes to allow high-volume production at Rockwell facilities.

Draper and Rockwell jointly developed a sensor process/design transition plan that utilizes a sequence of six formal lot builds. The goal is to start with a build process that closely duplicates the exact sequence of steps used in the Draper fabrication process, and at the end of the six lots have a fully qualified production capability utilizing Rockwell equipment with an process changes developed during the transition sequence. Each lot would be developed and assessed over a 2 to 3 month time frame. Specific goals were defined for each of the six lots:

- Lot 1 - Basic mask designs, process steps in primarily single wafer fabrication steps, manual wafer test capability
- Lot 2 - Initial process improvements and initial integration of some batch wafer fabrication steps
- Lot 3 - Improved mask designs, further process improvements, additional batch wafer fabrication steps
- Lot 4 - Final mask designs, automated wafer test capability, final batch wafer fabrication steps, process improvements as required
- Lot 5 - Preliminary assessment of production process, process step and documentation corrections
- Lot 6 - Formal validation of production process

Common to many technical developments, the ability to test and characterize performance in a cost-effective manner (i.e., minimization of time in test) is critical in producing a viable, affordable product. This is even more appropriate in the wafer level fabrication of micromechanical structures that do not lend themselves to traditional methods of wafer level electrical testing. The approach to test in the six lot transfer sequence, is to develop novel test techniques that not only adequately characterize performance, but also minimize test time. A series of steps have been implemented to assess basic device parameters (electrical, mechanical, and inertial) at a wafer probe level. (see Figure 8) Inertial performance characteristics are then verified by integrating the sensor into a complete instrument package and performing controlled rate and thermal evaluation testing. Data from actual instrument performance testing will then be fed back and correlated to both the process control sequence and to the wafer probe test level. This iterative loop will be used to correlate the appropriate device parameters with inertial level performance. The goal is to identify the minimal number of critical test procedures during the earliest phases of the overall fabrication sequence to avoid adding value to nonfunctional parts.

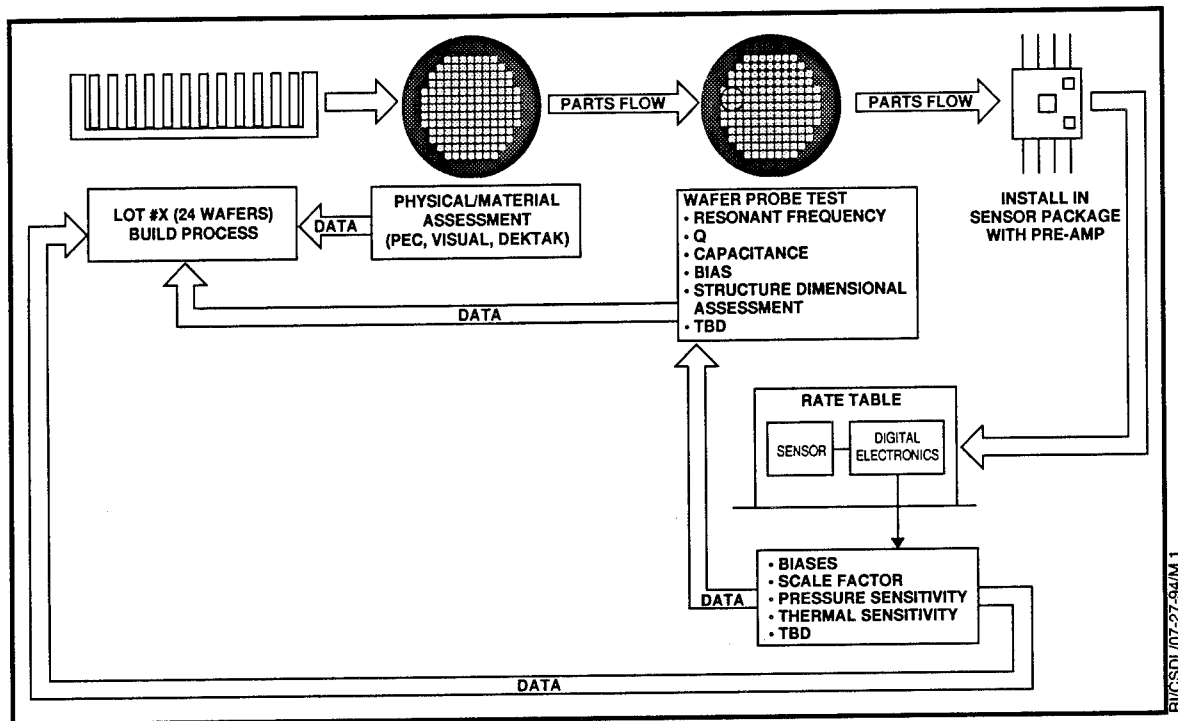


Figure 8. Sensor Test Sequence

Transfer of the electronics design is following a three-phase approach. The initial design architecture was defined following the assessment of critical instrument requirements, both performance and cost. The basic architecture is currently being evaluated for compliance to requirements by utilization of discrete components in an Engineering Developmental. Concurrently, efforts to convert the architecture into an ASIC design have begun utilizing the design capabilities of the CMOS fabrication facility at Rockwell. This mechanization is being implemented utilizing the full spectrum of design and process rules available from the foundry. Mechanization simulations and test results from the EDM testing are being used for design modification necessary to achieve both cost and performance goals.

Following fabrication of the first version ASIC, a series of extensive evaluations for both electrical performance and sensor compatibility will determine the need for further design adjustments. Any necessary modifications or improvements to the design will then be incorporated for a second pass ASIC build. Testing of the second ASIC will determine the readiness for pilot production fabrication.

Activities are under way to define the final prototype packaging approach that will be used for the production rate sensing instrument. The current plans are to integrate the sensor die and the ASIC die within a plastic leadless chip carrier (PLCC) type of package with module level integration available for specific customer requirements. Figure 9 shows one of the packaging concepts under evaluation.

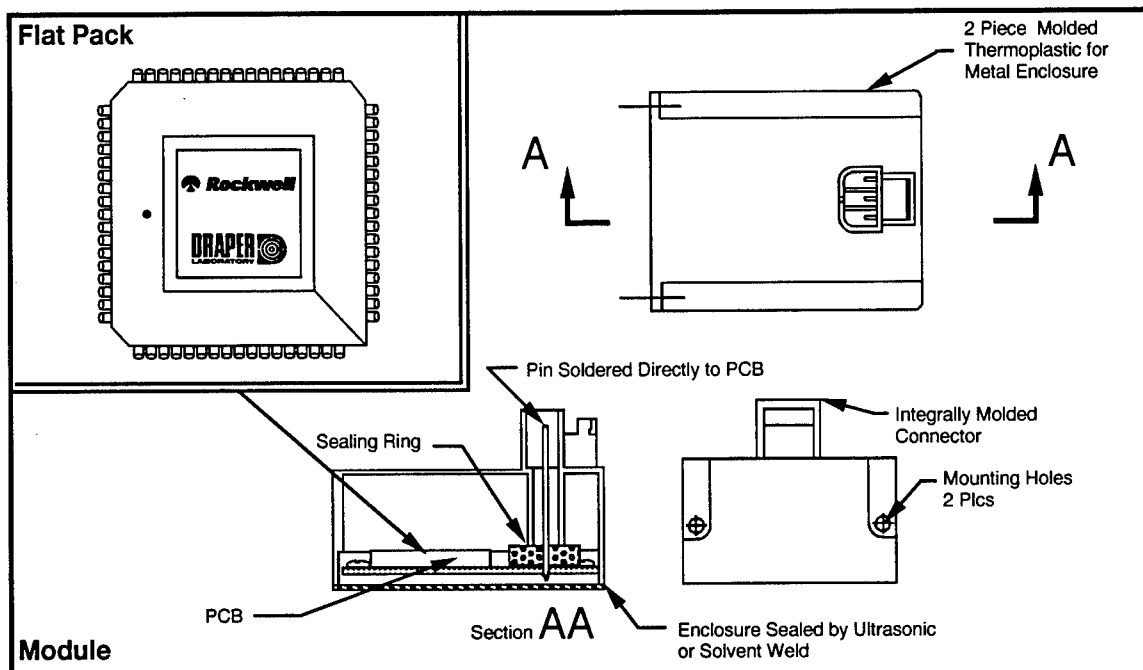


Figure 9. Proposed Packaging Concepts

Manufacture of the rate sensor will be performed by various facilities within Rockwell (see Figure 10). The sensor will be produced by Rockwell's Electro-Optical Center in Anaheim, CA. This facility is a medium volume, specialty silicon production site capable of fabricating 750 wafers per month, with a potential of reaching production of five million sensor die per year.

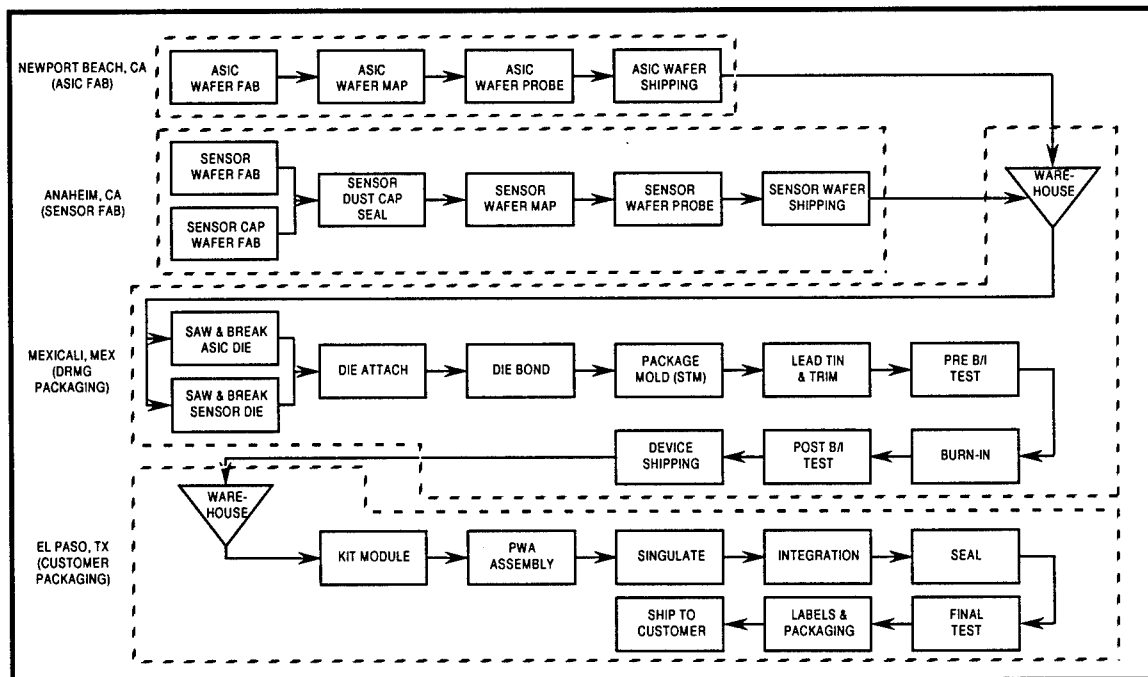


Figure 10. DRMG Manufacturing Process

The ASIC will be manufactured in Newport Beach by Telecommunications Operations Production Facility. This facility is a world-class, high-volume silicon production complex, which currently

produces approximately 80 percent of all fax/modem chips sold in the world. The operation runs 24 hours a day, 7 days per week, with a current capacity of 650 5" wafers per day. An extensive upgrade is currently in progress to install and qualify an 8" wafer line, which could effectively double the daily output of chips.

Integration of the sensor and ASIC will take place in the Telecommunications Operations Production facility in Mexicali, Mexico. This facility currently performs all die level packaging for Newport Beach product and is fully automated with a high quality output. Module level integration will be performed in El Paso, TX at the Telecommunications Operations Production Packaging facility. This location is a modern 90,000 sq. ft. plant that is currently producing 100,000 modules and systems per month, with a potential rate of 400,000 modules per month. This site currently fabricates and tests a product line of automotive electronic modules for the Rockwell Automotive Operations division.

Current production implementation schedules indicate that completion of all initial transition activities, including process transfer, documentation and any necessary fabrication equipment integration will be completed by the fall of 1995. This will meet current plans for the first pilot production run and full qualification of the device, including fabrication process control. Initial low rate production capability is being planned for the second quarter of 1996.

Conclusion

The emergence of micromachining technology, as applied to inertial sensors, has great potential in advancing the applicability of these devices to an array of new applications. This will include not only traditional and nontraditional military applications, but also allow penetration into commercial markets that, due to cost constraints, have not been able to integrate such components into deliverable products. The inclusion of gyros and accelerometers into these commercial applications, with their cost and volume needs will provide a great benefit to the military in that there will be an industrial base of products with direct military applicability which DoD does not have to maintain (like micro-processors). Rockwell and Draper have allied themselves to take advantage of both organization's strengths in order to nurture and grow this industrial base.

Transitioning the research and development efforts into a high-volume, repeatable manufacturing environment is providing a great challenge to the resources of both companies. A comprehensive transfer plan for design, fabrication and test has been defined and is currently under way to move this technology into the marketplace. Cooperative design and process transfer efforts for both the electronics and sensor components will help satisfy both performance and time-to-market pressures.

It is expected that these inexpensive instruments will meet the needs of many current and future performance requirements. In addition, with the production volume capabilities being developed by the Draper/Rockwell alliance, the availability and cost of the devices will most certainly lead to applications that have not yet been defined.

THIS PAGE LEFT BLANK INTENTIONALLY

PERFORMANCE TESTING OF A MILITARY GPS ATTITUDE DETERMINING SYSTEM

Charles Rodgers
Geoff Hazel
Darrell Greenlee

Adroit Systems, Inc.
209 Madison St.
Alexandria VA 22314

(703) 684-2900

APPROVED FOR PUBLIC RELEASE; DISTRIBUTION IS UNLIMITED.

ABSTRACT

Adroit Systems, Inc. has developed a military GPS attitude determining system (ADS) under contract to the U.S. Army Topographic Engineering Center (TEC). The system has three configurations to satisfy the accuracy requirements of three different Army applications. One version is designed to meet the requirements of the Multiple Launch Rocket System (MLRS) and other artillery for determining pointing attitude, position, and time to facilitate "shoot and scoot" tactics. Another version is designed to meet the requirements of the Trailblazer electronic warfare van. A man-pack version that has applications for Forward Observer/Forward Air Controller (FO/FAC) precise targeting is also being developed. All versions depend on the measurement of the GPS carrier phase at three antennas to determine platform attitude or pointing angle.

The first phase of the development effort involved testing and analysis of the factors that determine the performance of a GPS ADS. Phase II, just completed, consisted of final system design, system integration, and performance testing. Phase III will involve military wide demonstrations.

This paper discusses the system design, hardware integration, and performance testing. It presents the performance test designs, analysis, and results. These test results will be compared to the system requirements. Test

results for all three configurations will be reported. Any deviations from requirements or predictions will be addressed. Strategies for achieving the requirements in a production version will be discussed.

INTRODUCTION

The Army Topographic Engineering Center (TEC) has contracted with Adroit Systems, Inc. (ASI) to develop a real-time attitude determining system (ADS) that will meet the needs of the Multiple Launch Rocket System (MLRS), the Trailblazer Electronic Warfare (EW) vehicle, and a man-portable system. This GPS-based system will provide accurate attitude, time, and position in real-time. It will enable the Army to determine quickly and accurately the pointing angle or attitude of all types of artillery and vehicles.

Adroit's ADS uses carrier phase interferometry of GPS signals to measure the signal arrival time difference at two closely separated antennas that form a baseline. The carrier phase is measured at each antenna and the difference between the measurements is used to determine which antenna is closer to each satellite. The phase difference is used to calculate an angle between each GPS satellite and the antenna baseline. These angles, combined with the satellite and user positions, are used to calculate the baseline attitude^{1,2,3}.

A GPS-based system for vehicle attitude determination has many advantages. It's real-time solutions are not susceptible to magnetic deviations or gravity, temperature, and pressure variations. This greatly enhances heading accuracy, particularly at high latitudes. Current attitude systems utilize gyroscopes and inertial platforms, whose performance degrades with time. They must be calibrated initially and then updated periodically. Adroit's attitude determining system does not require initial calibration or surveying, and its error is bounded over time. In addition, all measurements are relative to the worldwide GPS coordinate frame. Referencing all measurements to the GPS will allow targeting and attack without digital data bases or maps.

Phase I of the contract consisted of testing and analysis of GPS ADS performance factors. The data collected during Phase I was used to analyze the performance of three prototype baseplane configurations. These baseplanes used an equilateral triangle of baselines with antenna separations of 0.17, 0.5, and 0.85 meters. The subsequent phase I analysis examined the effects of baseline length, antenna type, baseplane tilt, and baseplane environment on ADS performance. The goal of the phase I effort was to use the results of this analysis to optimize the ADS system design implemented in the phase II ADS prototype.

Phase II of the contract consisted of three main parts. First, results of the phase I analysis were incorporated into the phase II prototype designs. Next, the prototype ADS hardware and software were developed simultaneously. Lastly, the system was tested to optimize/tune the software configurable ADS parameters, and to verify that the ADS meets the Army's specified performance requirements.

The phase II prototype ADS (TEC ADS) was designed to be a modular system that allows components to be substituted with minimal engineering. A block diagram of the TEC ADS is shown in figure 1. It consists of only one main receiver processing unit (RPU) and three separate antenna assembly units (AAU). The RPU (boxed item in figure 1) consists of three Magnavox N-Channel PPS/SPS receivers driven by a common OCXO, a 80486DX2/66 single board computer (SBC) which holds all of the ADS processing and interface software, a DC/DC power converter, a 1553 bus interface card, and a few other interface cables and modules. Each AAU consists of three dual frequency microstrip patch GPS antennas (equilateral triangle arrangements), a corresponding dual bandpass, low noise amplifier (LNA) and 4 dB attenuator for each antenna, an inclinometer assembly to aid in pitch and roll solution searching, and several interface cables. The Trailblazer, Manpack, and MLRS baseplanes have antenna separations of 0.5, 0.85, and 2.0 meters respectively, and are designed to give the ADS performances indicated in table 1. Only one baseplane assembly can be used with the RPU at a time.

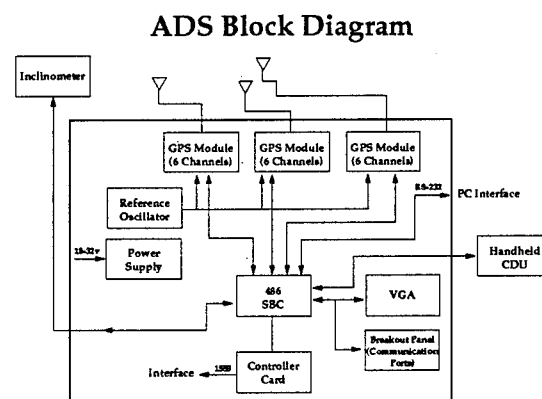


Figure 1

As with the TEC ADS hardware, the software design goals were to achieve a modular system. The main attitude determining algorithm is complemented with several integrity moni-

system. The main attitude determining algorithm is complemented with several integrity monitoring, and solution optimizing software modules.

This paper describes the phase II performance tests and their results.

TEST OBJECTIVES

The tests were designed to accomplish two objectives. One was to tune and optimize the attitude determining software, and the other was to verify the contracted azimuth performance specification. ASI has identified and characterized the major sources of GPS attitude determining error⁴. Major contributors of error include receiver phase measurement noise, multipath, and satellite geometry factors. The system under test incorporates new software mechanisms for mitigating the effects of these error sources. Integrity monitoring software is also included to detect and remove attitude solutions corrupted by residual error. The first objective of the testing was to collect sufficient data to thoroughly tune, test, and verify these algorithms.

The second objective of this testing was to analyze sufficient data to verify the achievement of the Army performance specifications. The azimuth performance specifications for the system under test are shown in Table 1. Performance of the Trailblazer and Manpack configurations were evaluated by comparison of the GPS ADS results against accurately surveyed azimuth truths. Since the MLRS configuration was too large to mount on a tripod and align with a surveyed truth, its performance was evaluated by a self-survey technique.

Table 1: ADS Performance Requirements

Configuration	Pointing Error at 4 seconds		Est. Baseline Length
	Azimuth	Elevation	
MLRS	1.0 mil (.056°)	3.5 mil (.197°)	2.0 meters
Man-Portable	2.5 mil (.141°)	8 mil (.450°)	1.0 meters
Trailblazer	5.5 mil (.310°)	17.0 mil (.956°)	0.5 meters

TEST DESIGN

The Trailblazer AAU consists of one large saucer like ground plane measuring approximately 1.0 meter in diameter. Its three antennas are separated by 0.5 meters in an equilateral triangular configuration. To provide a repeatable means of aligning the baseplane towards a target, a telescopic sight was attached underneath the tripod mounting support. The sight was aligned with the pointing vector associated with the Trailblazer AAU.

The Manpack AAU consists of three small round ground planes measuring about 40 centimeters in diameter, each containing one antenna, connected to a central support base by a rectangular metal arm. The arms support the individual ground planes/antennas in an equilateral triangle configuration with 0.85 meter separations. The telescopic sight is mounted on a support arm underneath one of the small groundplanes. The scope alignment errors are calibrated out during the data analysis.

To facilitate static testing, Army TEC set up calibrated azimuth targets from a location on ASI's lower and upper roofs. The lower roof test site is located within a few meters

of a high brick wall with two large metal doors. As they make good multipath reflectors, the site was chosen as a hostile or worst case environment.

The MAPS inertial system was used to survey in more than a dozen azimuth targets. The survey accuracy is about 0.029 degrees. The closest target was at a distance of 3/4 mile, but the average target distance was approximately 2 miles. In general, the longer the distance to the target, the less sensitive the result is to accurate test positioning. It also reduces alignment error due to target thickness with respect to the telescopic sight cross-hair thickness.

Azimuth accuracy for the Trailblazer and Manpack systems was tested on the lower roof test site at ASI. Each baseplane was placed on the test tripod located at the survey marker on the lower roof. Raw test data was collected with each baseplane aligned at five distinct surveyed azimuth targets. However, the targets were chosen to require baseplane rotation of greater than 270 degrees in azimuth throughout a baseplane test suite.

At each of the five targets, approximately 30 minutes of data was collected. The data consisted of receiver carrier phase data, receiver position data, time data, satellite data, and other information necessary to post process complete attitude solutions. An identical test suite (same targets for each baseplane) except for the time of day was repeated on the following day. The test start time was offset so that a different GPS constellation was present. A minimum of five hours of data (18,000 attitude calculations) for each baseplane configuration was collected. However, high wind during one day's test caused the manpack baseplane to oscillate. That day's test will be repeated but it is not in time for this paper.

The MLRS baseplane, similar to the Manpack, consists of three small round groundplanes of about 40 centimeters in diameter. Each having a microstrip patch antenna mounted on it. The groundplanes are supported by a triangular metal skeleton structure with 2 meter sides. The groundplanes are mounted at the apexes of the support triangle structure. Unlike the Trailblazer and Manpack baseplanes, the MLRS is too unwieldy to be mounted on a tripod. Therefore telescopic sight alignment to a known truth is not possible with this baseplane. Instead, long duration testing for self-surveying was used.

The MLRS baseplane was placed on equal height risers at the upper roof test site. The risers maintained the baseplane at nominally 0 degrees in pitch and roll throughout the test suites (not accounting for wind effects). In addition, the risers helped to reduce the multipath reflections originating from the metal lip surrounding the

upper roof. In addition, nearby air conditioning equipment could produce multipath.

The baseplane was fixed in a single position for a total of approximately 15 hours of data (54,000 attitude solutions). The data was collected in four 3.5 hour data blocks. As with the Trailblazer and Manpack test suites, the data collection was time offset to capture a variety of different GPS satellite constellations. The details of the data analysis is presented in the next section.

DATA ANALYSIS

The two aspects of the data analysis correspond to the two test objectives outlined above. First extensive analysis was performed to tune, test, and verify the new error reduction and integrity monitoring software. The algorithms were tuned to optimize azi-

muth performance as characterized by the azimuth CEP metric described below. Once the optimal software configuration was established, tests were performed to characterize the azimuth performance of the system under test.

Both aspects of the analysis were performed in post-mission processing of the collected raw receiver data. It is important to recognize, however, that the post-mission analysis used the identical software as the real-time system. The software runs more quickly from a disk file in post-mission analysis than it did in real-time where it is required to wait for data from the receivers at each epoch. The correspondence of the real-time and post-mission attitude results was verified experimentally. Hence, the post-mission analysis of the data serves as a valid measure of the performance of the real-time software.

Self-survey of the MLRS baseplane was achieved by computing the average azimuth solution over a twelve hour (one full satellite orbit) data set. This long-term average azimuth

served as the self-surveyed truth for the MLRS baseplane. A similar procedure was used to calibrate the scope alignment error of the Manpack baseplane. Long-term static averages were used to calibrate the constant azimuth bias caused by sight misalignment.

The metric used to characterize the azimuth performance of the system corresponds roughly to an azimuth circular error probability (CEP). Army specifications were in terms of CEP. Specifically, it represents the range about the known truth (or self-surveyed truth, in the case of the MLRS baseplane) within which one half of the solutions fell.

This CEP number was calculated for the static tests by first finding the mean and standard deviation of the azimuth solution. The standard deviation was scaled by $2/e$ to find the range about the mean within which one half of the solutions fell. Finally, this deviation was added to the difference between the truth and the solution mean (long term bias). This metric captures the performance effects of both long term bias and short term instabilities.

Due to multipath and other error sources, the phase measurements are infrequently so seriously distorted as to produce a spurious solution. ASI has developed software that recognizes and excludes spurious solutions. This integrity monitoring software is a real-time software module which computes a measure of confidence in each computed solution and removes low confidence solutions from the output stream. They are never seen by the user. As a result, these low confidence solutions were not incorporated in the characterization of azimuth performance. The percentage of solutions removed by the integrity monitoring software was about 1%.

TEST RESULTS

Figure 2 summarizes the results of the tests on the 0.5 meter baseline system. The number of solutions in each data set is above the bar. The labels at the bottom of each bar indicate the test date and the surveyed target it was aligned with (T1, T2, etc.)

Individual test results varied from a minimum of 0.227 degree to a maximum of 0.342 degrees CEP. The pooled CEP for all data sets was 0.265 degree. The environment is high in multipath because there is a high brick wall several meters behind the surveyed test point. This baseline's design goal was 0.310 degrees.

AZIMUTH ACCURACY PERFORMANCE - 0.5 METER BASELINES
 POOLED CEP = 0.2651 DEG. (4.7 MIL)
 20,229 TOTAL MEASUREMENTS; 98.0% GOOD SOLUTIONS

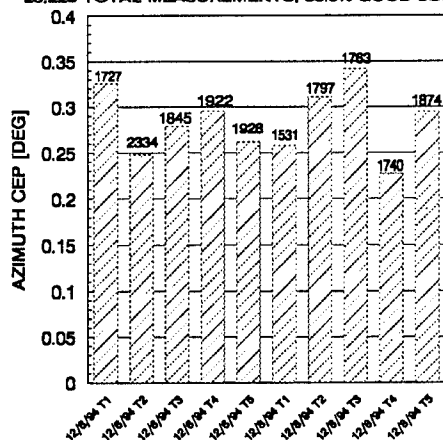


Figure 2

Figures 3 and 4 show the complete solution set for the two tests aligned with target two. The first data set, taken on December 6, 1994, has a CEP of 0.248 degree. The second set of data, taken on December 8, 1994, has a CEP of 0.311 degree. Different satellite geometries and their effect on multipath cause the difference in accuracy levels between sets. Multipath errors are the major cause of the periodic peaks and valleys of the solution. The multipath phase distortions on each satellite signal appear to combine much like phasors. Sometimes they reenforce each other resulting in a major peak, while at other times they almost cancel each other.

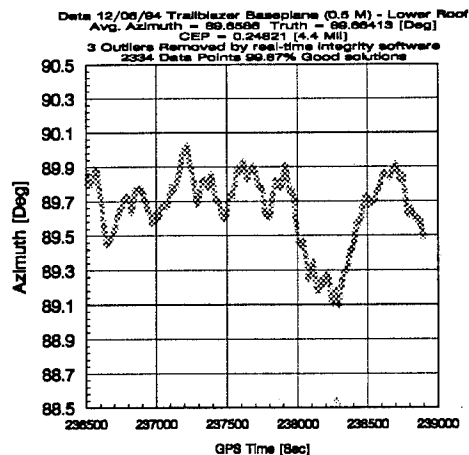


Figure 3

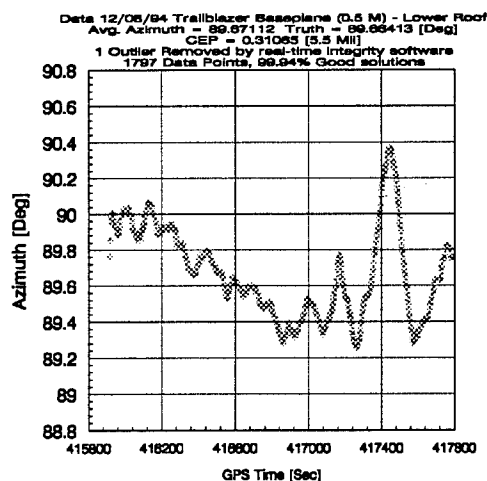


Figure 4

Figure 5 summarizes the results of the tests on the 0.85 meter baseline system. The CEP figure for each data set is at the top the bar. The number of solutions in each data set is in parenthesis above the bar. Labels at the bottom of each bar indicate the test date and the surveyed target it was aligned with (T1, T2, etc.)

The results are from half as many data sets as the 0.5 meter baseline tests. One day's data was unusable because of a high wind that caused the baseplane to oscillate about the

truth. The results of that data set were an order of magnitude greater than those in figure 5. This is inconsistent with other data collected on this baseline during system development, as well as with theory. Therefore, it is not being presented here. More data will be collected to replace the unusable sets when possible. We do not expect the results to change the pooled CEP significantly.

Individual test results on the 0.85 meter baseline system varied from a minimum of 0.0942 degree to a maximum of 0.1524 degrees CEP. The pooled CEP for all the data was 0.1268 degree. Again, the environment is high in multipath because of a high wall several meters behind the baseplane. The design goal for this baseline was 0.141 degrees.

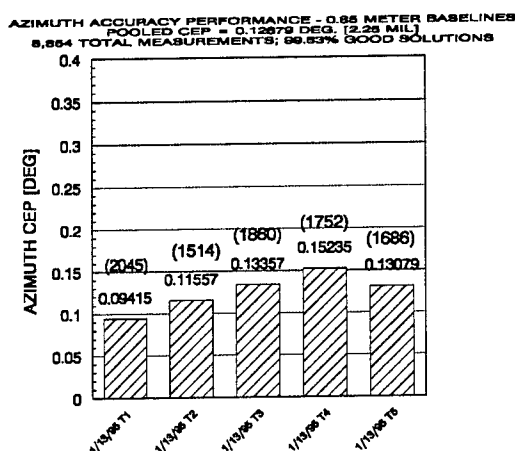


Figure 5

Figure 6 is a plot of the entire solution set for the 0.85 meter baseplane aligned with target two. The same type of multipath peaks and valleys as in 0.5 meter plots (Figs. 3 & 4) is evident here. Note, however, that the variation is contained in a smaller envelope. As the baseline lengths increase, the phase error present becomes a smaller portion of the phase difference being measured between two antennas. This reduces the azimuth solution error. Our real-time integrity algorithms removed the few solution outliers shown on

the plot from the solution statistics. These solutions would not be output to the system user. However, they remain in this plot for the development team's information.

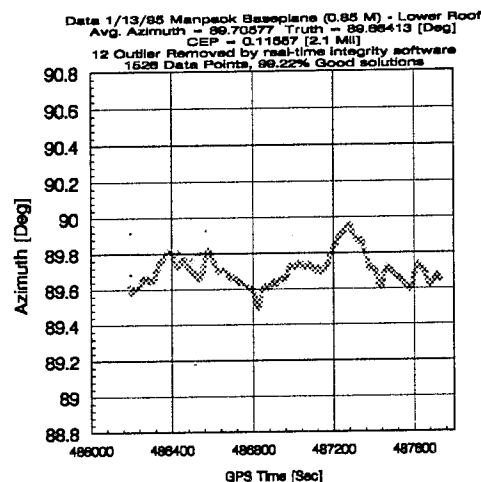


Figure 6

Figure 7 summarizes the results of the tests on the 2.0 meter baseline system. The CEP figure for each data set is at the top the bar. The number of solutions in each data set is in parenthesis above the bar. Data sets were designed to collect data once per second over a period of three and one half hours. We had to shorten one test due to equipment problems. All data were taken without moving the baseplane assembly. The long duration tests were used to self survey the truth used for the CEP calculation.

Individual test results on the 2.0 meter baseline system varied from a minimum of 0.0776 degree to a maximum of 0.0890 degree CEP. The pooled CEP for all the data sets was 0.0831 degree. The environment was relatively low in multipath because the data was taken on the highest roof structure. No wall was present. However, nearby air conditioning did provide the opportunity for multipath reflections. The design goal for this baseline was 0.058 degree.

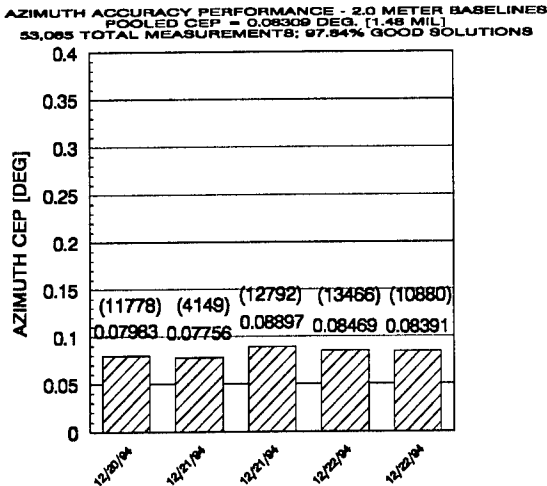


Figure 7

Figure 8 is a plot of about the first 4500 solutions for the 2.0 meter baseline on December 22, 1994. To display the entire data set, four such plots would be required. Note, the multipath variation is contained in a smaller envelope than the 0.85 meter baseline. Again, the real-time integrity algorithms removed the few solution outliers shown on the plot from the solution statistics.

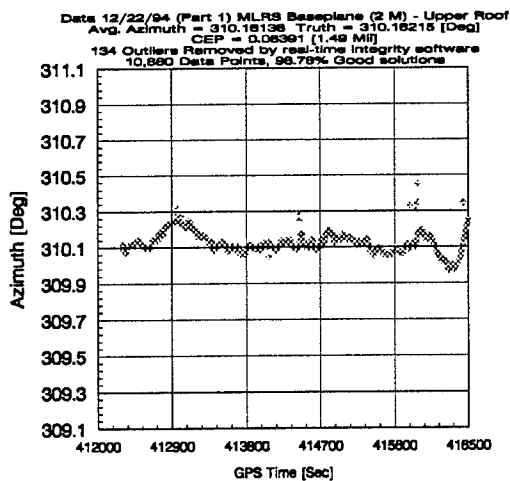


Figure 8

SUMMARY AND CONCLUSIONS

Adroit Systems, Inc. has developed a GPS attitude determining system for the U.S. Army. It is a dual frequency, P(Y) code system that can work with any of three baseplane designs to achieve a range of attitude accuracies. The baseplanes have different antenna separations that allow different levels of accuracy. ASI tested the unit's azimuth performance against Army surveyed targets.

Figure 9 shows how the measured azimuth performance varied with baseline length. The figure also compares the test results to the design objectives. The shorter baselines exceeded the design goals. The 0.5 meter baseline demonstrated 0.045 degree better performance than its goal. The 0.85 meter baseline performance was 0.014 degree better than its goal. However, the longest baseline system performance fell 0.027 degree short of its goal. A longer baseline will be tried to reach the desired level of performance.

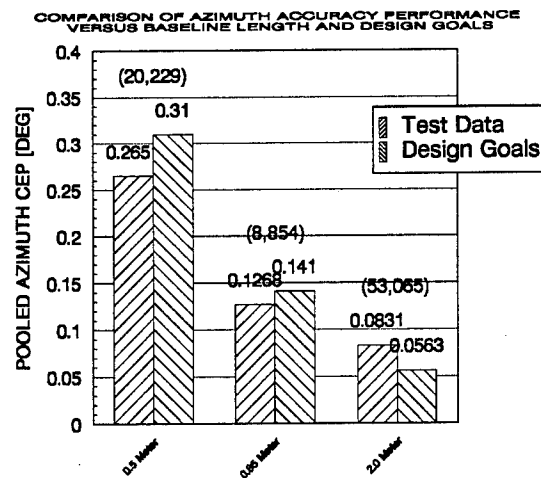


Figure 9

The major error source preventing the system from being more accurate is multipath.

Adroit tested algorithms to reduce multipath by rejecting satellite signals that exhibited multipath characteristics. This caused the software to use fewer satellites when calculating the solutions. This could cause geometric biases that can also affect azimuth accuracy. The most effective means of increasing system accuracy is to improve GPS receivers so that they can correct multipath errors. If multipath was eliminated, according to theory, accuracies for a 2.0 meter baseline could be as good as 0.04 degree⁴.

The results demonstrate that GPS attitude determination can fulfill the requirements of military applications for precise real-time attitude, position, time, and velocity. We can mitigate the problems of signal blockage and jamming by integrating a low cost IMU with the GPS system. Adroit is currently developing such a system for NASA.

ACKNOWLEDGMENTS

The authors thank Army Space Command and Army TEC for supporting this work. Special thanks go to our recently retired COTR Mr. Malone "Tony" Hawker and his supervisor Mr. Richard Marth at Army TEC for their assistance and supervision. Jim Washington at Army Space Command was instrumental in arranging funding the effort. Thanks also go to Jerry Johnson for introducing us to the military users.

Lastly, the authors thank Mark Sullivan, Raj Aggarwal, and Amy Gardner of ASI for their help on this successful project. Mark and Raj were major contributors to the attitude and test software development. Amy helped design and directed fabrication of the baseplanes and low noise amplifiers.

ENDNOTES

1. Jurgens, Richard., "Realtime GPS Azimuth Determining System", Proceedings of the National Technical Meeting of the Institute of Navigation, San Diego, January 23-25, 1990, pp. 105-110.
2. Jurgens, R., Rodgers, C., and Fan, L., "GPS Azimuth Determining System (ADS) Cycle Resolution, System Design, and Army Test Results", Proceedings of the National Technical Meeting of the Institute of Navigation, Jan. 22-24, 1991.
3. Rodgers, C., Jurgens, R., and Fan, L., "Advances in GPS Attitude Technology as Developed for The Strategic Defense Command", Proceedings of the Fourth International Technical Meeting of The Institute of Navigation, Albuquerque, September 11-13, 1991.
4. Rodgers, C., Gardner, A., and Stroup, D., "Testing and Analysis of Baseline Length as a Performance Factor in GPS Attitude Determining Systems (ADS)," Proceedings of the 1994 National Technical Meeting, San Diego, January 24 - 26, 1994.

BIOGRAPHY

Charles Rodgers

Mr. Rodgers is the GPS Engineering Manager at Adroit Systems. He has a BSEE and a MSEE from The Georgia Institute of Technology. At Adroit he has been involved with GPS ADS development for seven years. He has three patents pending for GPS ADS applications.

Mr. Rodgers has designed and built a GPS satellite signal simulator. He is presently leading ASI's project to develop a military ADS for the Army. His concept for applying precision GPS positioning to precision targeting and strike is scheduled to be tested by the Air Force in 1995. He has won a Best Paper Award from the Institute of Navigation

(ION) for a paper on GPS multipath. He is currently the Principal Investigator on a NASA project to develop a high dynamic GPS ADS for flight test.

Geoffrey G. Hazel

Mr. Hazel is a Member of the Technical Staff at ASI. He has a BSEE and a MSEE from the University of Maryland. Mr. Hazel is a member of the GPS Applications Group at Adroit. In this role, he is involved in the algorithm design, system integration, software development, and system test and analysis efforts supporting the development of Adroit's GPS Attitude Determining Systems (ADSs). He is currently leading the software development efforts on several ADS prototype production projects. In this capacity he is working to implement innovative solution search strategies and optimize the accuracy and speed of the search algorithms. In addition, he is working extensively with real-time multi-tasking kernels for embedded applications. Since the completion of his Master's degree in Electrophysics and Semiconductor lasers, Mr. Hazel has also completed the intensive one week course "NAVSTAR GPS for Engineers" (Navtech Seminars' Course 354).

Darrell F. Greenlee

Mr. Greenlee is a Member of the Technical Staff at ASI. He has a BSEE and graduated Magna Cum Laude from the University of Maryland. He is a member of the GPS Group at Adroit Systems, Inc. His major technical experience is in the design, analysis, and implementation of embedded systems. He has most recently developed and integrated the hardware for a GPS based attitude determining system for the U.S. Army. Project responsibilities included hardware component/module specification, module interface planning, printed circuit design, embedded control/interface software development, and hardware system testing. Since joining Adroit in February 1993, Mr. Greenlee has

also been an integral member of the design/development team for Adroit's commercial GPS based Attitude determining system. Mr. Greenlee college studies concentrated on the hardware and software operations of micro-processor based digital systems. In addition, he participated in several software controlled integration projects using a V40 based single board computer. Mr. Greenlee also gained testing and documentation skills working at Allied-Signal Aerospace during the summer of his senior year.

THIS PAGE LEFT BLANK INTENTIONALLY

SESSION II-A

ADVANCED SYSTEMS I

CHAIRMAN

ROBERT CHRISTIANSEN

*ROCKWELL INTERNATIONAL
ANAHEIM CA*

THIS PAGE LEFT BLANK INTENTIONALLY

Results of Carrier Phase Measurement Incorporation into SARS I

Capt Anthony R. Nash, Capt John F. Raquet, Capt F. Britt Snodgrass, Dr. Michael D. Hooser
746th Test Squadron, Holloman AFB, NM

Abstract

The CIGTIF High Accuracy Post-processing System (SARS I) is a flight reference system used by the 746 Test Squadron (746 TS) which provides high accuracy reference position and velocity information. The system incorporates differentially corrected code and carrier measurements from GPS, inertial navigation systems (INS) measurements, and ground based transponder measurements. This data is used by a post-processing extended Kalman filter to compute precise position and velocity. Of primary concern, is validating the system under flight conditions. These tests include high speed test track runs, flight testing, and van testing. The validation test results are given which show that the GPS carrier phase hardware and software do perform well under the high dynamic conditions of an aircraft flight. It has been demonstrated that the incorporation of GPS carrier phase measurements, as well as several enhancements to the extended Kalman filter, have improved the SARS I position accuracy to below one meter.

1. INTRODUCTION

The 46th Guidance Test Squadron (also known as the Central Inertial Guidance Test Facility or CIGTF) located at Holloman AFB, New Mexico has been the principal test agency for developmental testing of military aircraft navigation systems since 1966. Due to tremendous accuracy improvements brought about by the integration of Global Positioning System (GPS) receivers with inertial navigation systems (INS), CIGTF needed an improved flight test reference system. In Aug 1994, work was started on the CIGTF Sub-Meter Accuracy Reference System I (SARS I). SARS I is CIGTF's new reference system for testing GPS,

INS, and embedded GPS/INS navigation systems on cargo or large bomber aircraft.

SARS I is a replacement for the High Accuracy Reference System (CHAPS). SARS I has a similar design to its predecessor, CHAPS, but is smaller (one C-12 rack compared to two for CHAPS), is written entirely in Ada, and most importantly, incorporates differential carrier phase GPS measurements.

The SARS I development project started with five major design goals. In order of priority, they were: (1) improved accuracy (below one meter), (2) rapid development, (3) operation during GPS jamming, (4) flexibility for future development, and (5) simplicity of operation.

The overall position and velocity accuracies are achieved by using four different, complementary sensors: an INS, differentially corrected GPS, differentially corrected GPS carrier phase, and ground based transponders. The information from these four systems is combined in a post-mission Kalman filter. The software architecture of the filter was designed to easily accommodate more sophisticated sensor error models as they are developed and validated. This supports planned accuracy improvements throughout the life of the system.

SARS I was developed over an 8 month period using the CHAPS baseline, by a small, in-house team of engineers and technicians. Limited time and personnel resources required use of many "off-the-shelf" components whenever possible. The INS and GPS receiver are widely used on U.S. Air Force aircraft, while the transponder and interrogator equipment was taken from previous reference system development efforts. The carrier phase GPS receiver is a commercially available Ashtech Z-XII receiver.

The 46th GTS is a leader in field testing GPS equipment in an electromagnetic combat (jamming and/or spoofing) environment. During such tests, GPS alone cannot normally be used as a valid reference. The SARS I transponder/interrogator subsystem continues to provide range and delta-range measurements when the GPS L1 and L2 frequencies are jammed because it operates in the higher 2 GHz band.

For ease of operation, SARS I is designed to be self-initializing and requires minimal pre-flight input. No transponder location data is required at the start of the test mission because SARS I automatically interrogates all possible transponders and builds its own database of responsive transponders.

The overall system architecture and data flow for SARS I is presented in Section 2. The Kalman filter is described in Section 3, followed by the software architecture in Section 4. Section 5 presents the concept of operations for a typical test mission. Section 6 presents some

preliminary test results from the validation test program. Section 7 concludes the article with a discussion of planned future enhancements.

2. SYSTEM ARCHITECTURE

SARS I has two fundamental parts — the navigation sensor/data collection system and the post-flight data processing software.

The navigation sensor/data collection system includes a pallet which is flown aboard the testbed aircraft, a differential GPS ground station, and multiple ground based transponders. The SARS I pallet includes a strapdown INS, a two GPS receivers, two transponder interrogators, and a VME bus computer for control and data acquisition. These subsystems are illustrated in Figure 1.

The post-flight Kalman filter processes GPS pseudo-range and delta-range measurements, carrier phase generated position and velocity

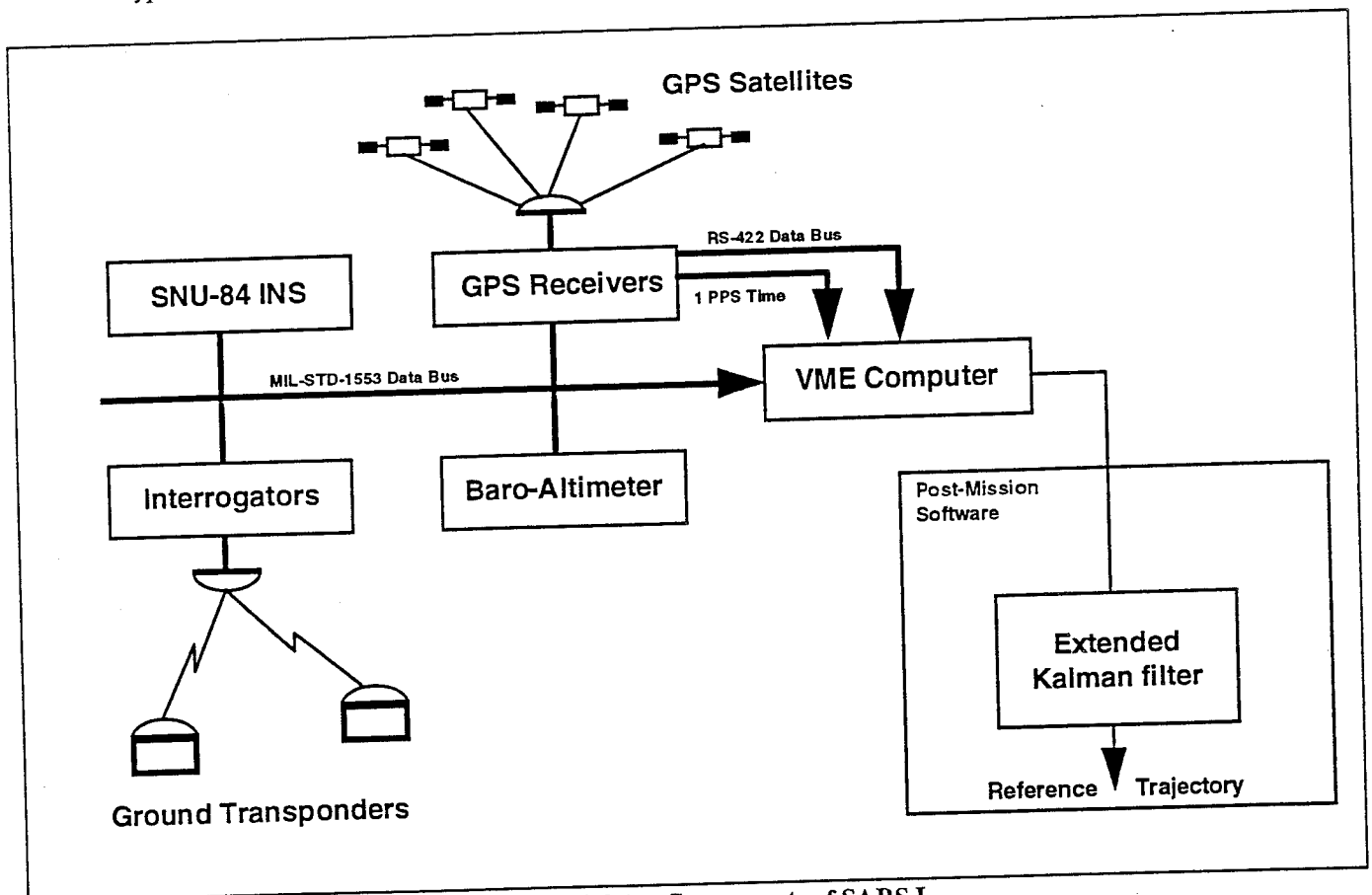


Figure 1: Major Components of SARS I

measurements, as well as interrogator/transponder range and delta-range measurements to estimate errors in the INS's indicated trajectory. The filter models the INS errors in an earth-centered earth-fixed (ECEF) Cartesian coordinate frame, which results in much simpler measurement processing. The post-flight filter is written entirely in Ada and hosted on an HP-9000 workstation. The software architecture is designed to easily accommodate new navigation sensors.

2.1. Navigation Sensor Pallet

GPS Receiver Subsystem — The GPS receiver is a standard Rockwell-Collins RCVR 3A. This is a five channel, dual frequency, keyable receiver. The only modification to the receiver is an added provision for a precise frequency input (10.23 MHz Rubidium clock). It is also possible to use a Rockwell-Collins Miniature Airborne GPS Receiver (MAGR) instead of the RCVR 3A.

The raw pseudo-range and delta-range measurements are collected through the RS-422 port on the GPS receiver. Before use by the filter, these measurements are corrected for Selective Availability (SA) effects, and differential corrections are applied based upon measurements from the CIGTF Satellite Reference Station (SRS). The station uses a modified GPS RCVR 3A with special software that permits externally commanded satellite selection and provides a time-shared "all-in-view" capability on this five channel receiver. The receiver is keyed to permit dual-frequency Y-code operation. Raw pseudo-range and delta-range information is recorded from the instrumentation port to the local hard disk. The SRS was developed separately from SARS I.

Differential GPS Carrier Phase Subsystem -- The differential GPS carrier phase subsystem consists of an Ashtech Z-XII receiver and PNAV post-processing software developed by Ashtech. The Ashtech is a dual frequency Z code receiver, and tracks the carrier phase on L1. It requires a minimum of 5 satellites to develop a solution, and can track as many as 10. PNAV is used in a post processing mode to resolve integer ambiguities, detect cycle slips, and to generate a position solution. The position solution is then incorporated into the

post mission Kalman filter as latitude, longitude and altitude.

Range and Range-Rate Subsystem (RRS) — The RRS consists of multiple ground-based transponders and one or more interrogators. It was originally manufactured by Cubic Corporation for use in the CIRIS system. The transponders are portable and are arranged to provide good geometry throughout the aircraft flight profile. Up to 255 different transponder IDs are available although a typical flight test uses only 10-50 different transponders.

The interrogator transmits and receives on one of three channels in the 2325 to 2412 MHz range. Since this frequency band is much higher than the GPS L1 and L2 frequencies, the interrogator can continue to collect measurements in the presence of GPS jamming.

The interrogator normally talks to two transponders each second. The range measurement is made by a continuous wave phase comparison technique in which the slant range between the transponder and interrogator antennas is proportional to the round trip phase delay. The range measurement is normally accurate to within 1-2 meters including atmospheric delays, survey errors, and calibration errors. The "range-rate" measurements are actually delta-ranges where the change in carrier phase is tracked over a short integration interval. The resulting line-of-sight range-rate is accurate to within 0.03 m/s.

Inertial Navigation Subsystem — Two different inertial navigation systems have been used in the SARS I prototype--a Litton LN-93 and a Honeywell H423. Both of these strapdown ring-laser-gyro systems comply with the USAF standard medium accuracy (0.8 nmi/hr) navigation unit specification, SNU 84-1.

Altitude aiding of the INS is performed using a combination of GPS altitude from the RCVR 3A and baro-altimeter altitude. When the RCVR 3A has a valid altitude solution, it is directly used as the aiding altitude input to the INS. Meanwhile, the bias between the GPS altitude and the baro-altimeter altitude is continuously calculated. When the RCVR3A's altitude solution becomes invalid due to jamming, antenna shading, or other disturbances, this bias

is used to correct the baro-altimeter altitude for aiding the INS until the RCVR 3A obtains a good altitude solution.

Real-Time Control and Data Acquisition Subsystem — The real-time control and data acquisition subsystem (RCDAS) is a flight qualified VME bus computer. It includes a Motorola 68030 processor card, a 330 Mb hard disk, and MIL-STD-1553B, RS-422, and SCSI interface cards. Software in the RCDAS performs all initialization functions and records navigation sensor data to the hard disk. All time-tags are referenced to GPS time using the one pulse per second (1PPS) signal from the GPS receiver.

2.2. Post-Flight Filter

The filter software is based on models of the error behavior of all navigation sensors. These error models are utilized in an extended Kalman filter algorithm to estimate accurate position, velocity, and attitude. The filter is described in detail in the next section.

3. FILTER ARCHITECTURE

At the highest level, the SARS I filter is a traditional aided INS navigation filter: the INS output serves as the indicated (nominal) trajectory and GPS/transponder measurements are processed to estimate position, velocity, and other errors. The estimated errors are then subtracted from the indicated trajectory to produce the reference position, velocity, and attitude.

The error models for the INS, GPS, and RRS subsystems are specified at run-time, and there are ten or more error states, depending upon the selection of error models. RRS error models are generally transponder dependent, so the total size of the error state is also a function of the number of transponders that were used on a given mission. A typical filter error state vector is listed in Table 1.

3.1. INS Error Model

The INS position, velocity, and attitude errors are modeled in World Geodetic System 1984 (WGS 84) earth-centered earth-fixed (ECEF) Cartesian coordinates. This is the same

coordinate frame in which the GPS and RRS measurements are defined. This use of a common coordinate frame minimizes the need for coordinate transformations in the measurement incorporation algorithms. The algorithms and matrix definitions for this ECEF

Table 1: Typical SARS I Error State Vector

Error State	Definition
1	INS X_{ECEF} position error
2	INS Y_{ECEF} position error
3	INS Z_{ECEF} position error
4	INS X_{ECEF} velocity error
5	INS Y_{ECEF} velocity error
6	INS Z_{ECEF} velocity error
7	INS X_{ECEF} attitude error
8	INS Y_{ECEF} attitude error
9	INS Z_{ECEF} attitude error
10	INS X_{sensor} gyro rate bias
11	INS Y_{sensor} gyro rate bias
12	INS Z_{sensor} gyro rate bias
13	INS X_{sensor} accelerometer bias
14	INS Y_{sensor} accelerometer bias
15	INS Z_{sensor} accelerometer bias
16	Aiding altitude error
17	GPS clock bias
18	GPS clock drift
19	GPS Chan 1 LOS range error
20	GPS Chan 2 LOS range error
21	GPS Chan 3 LOS range error
22	GPS Chan 4 LOS range error
23	Trans 1 Chan 1 LOS range error
24	Trans 1 Chan 2 LOS range error
25	Trans 2 Chan 1 LOS range error
26	Trans 2 Chan 2 LOS range error
M	M
59	Trans 19 Chan 1 LOS range error
60	Trans 19 Chan 2 LOS range error
61	Trans 20 Chan 1 LOS range error
62	Trans 20 Chan 2 LOS range error

filter model were derived from information in references [1], [2], and [3].

The INS accelerometer biases and gyro drifts are modeled in the sensor frame as first order Markov processes. These errors are mapped into the ECEF frame through attitude-derived transformation matrices embedded in the filter's fundamental dynamics matrix.

The final INS error state models the aiding altitude error as a first order Markov process. This state is required for accurate modeling of the INS vertical channel. No baro-altimeter readings are incorporated into the filter as measurements.

3.2. Differential GPS Error Model

Under normal conditions, four GPS pseudo-range/delta-range measurements are recorded each second. Originally, two error states were used to model the GPS errors—receiver clock bias and receiver clock drift. After initial testing of the filter, four states were added which model line-of-sight (LOS) bias-like errors in each of the pseudo-range measurements as first order Markov processes. Note that these LOS errors represent the residual error after correcting for relativity, satellite clock error, tropospheric and ionospheric delay errors, and applying the differential corrections.

Each of the LOS error states corresponds with measurements to a single satellite. When the GPS receiver switches to a new satellite, the corresponding LOS error state is reinitialized by setting the error state element to zero, resetting the covariance matrix diagonal element to an initial value, and zeroing out the off-diagonal (cross-correlation) terms of the covariance matrix. This final step is necessary because the cross-covariance information is rendered invalid by the state switch. Resetting the covariance matrix diagonal term to an initial (higher) value causes the filter to rely less heavily upon the new satellite pseudo-range measurement until its error characteristics are more accurately determined, which minimizes the typical spikes observed during satellite changeovers.

3.3. RRS Measurement Model

Under normal conditions two interrogators on the aircraft are used to take six measurements each second (three range and three deltarange). The RRS range measurement errors are modeled as first order Markov processes. Range errors for the RRS system are primarily a result of calibration errors, residual unmodeled atmospheric refraction errors, and transponder survey errors. The calibration and refraction errors are different for each channel on each transponder, so a total of two error states per

transponder are used. On a typical test flight, 30-40 transponders may be used which results in 60-80 RRS error states. When added to the 16 INS error states and 6 differential GPS error states, this results in a total state size of 82-102 error states, which can be processed in near real-time.

If a higher rate of processing is desired, the transponder measurements can be processed without error-state modeling, or a limited number of transponders can be included in the error state vector, and transponders can be swapped in and out using a method similar to the GPS satellite swapping procedure described in section 3.2. The SARS I filter also has the capability to model transponder survey errors for selected transponders using three additional states per transponder, but this technique has not yet been fully exercised.

4. SOFTWARE ARCHITECTURE

Because SARS I is intended to be the second step in a series of reference system development efforts, the Ada language software for the SARS I Kalman filter was designed with an emphasis on flexibility, portability, and maintainability.

The SARS I Kalman filter allows the overall model (state vector, dynamics model, measurement models) to be reconfigured at run time without code recompilation or relinking. The system includes a number of different INS models, transponder models, and differential GPS models. A run-time control file read at the start of filter execution specifies which error model to use for each subsystem. The filter's state vector, state transition matrix, and other quantities corresponding to the desired models are created at the start of filter execution before any data is processed. Each predefined subsystem model includes default values for initial conditions and filter tuning parameters. These defaults may be overridden by new values from the run-time control file. This reconfiguration feature is used to support research on new models by minimizing the need for recompilation.

The SARS I software is portable to most types of modern computers. The software was originally written on an HP 9000/375 workstation using the HP-UX Unix operating system and Verdex

Ada. It has since been ported to an HP 9000/735 workstation using a new Verdex Ada compiler. Only minor changes were required to handle differences between the compilers and operating systems.

5. CONCEPT OF OPERATIONS

This section describes how SARS I is used to support a typical flight test mission. Flight tests of an embedded GPS/INS (EGI) are usually conducted using a C-12 aircraft. The C-12 is the military designation for a Beechcraft Super King Air, a twin turbo-prop cargo aircraft capable of flying at altitudes of 9500 meters at cruise speeds ranging from 70 to 130 meters per second. The flights begin and end at Holloman AFB, in the middle of New Mexico's Tularosa Basin. Transponders are deployed throughout the Tularosa Basin and on surrounding mountain tops. Additional transponders are currently located throughout New Mexico. The primary SRS ground station is located at Holloman AFB.

When the INS alignment is initiated, the control computer commands the interrogator to begin interrogating transponders. Starting with a randomized list of all possible transponders, the computer builds an internal database, called the "active set," of up to 120 transponders that respond to interrogations and provide valid measurements. The active set list is randomized after each cycle to increase the probability of good transponder geometry. Occasional measurements are attempted using transponders that are not in the current active set, in case they have come within range of the aircraft. During flight, transponders are moved in and out of the active set, depending upon their ability to generate valid measurements.

A typical flight test for investigating GPS jamming response takes place entirely within the Tularosa Basin, in White Sands Missile Range airspace. GPS jammers are placed at various locations in the mountains surrounding the basin. After taking off from Holloman AFB, the C-12 flies a simulated ground attack mission against stationary targets within the jamming zone. The GPS receiver under test may be jammed for several minutes until the C-12 flies back out of the jamming zone. During a two

hour test, the C-12 will make between 6 and 10 passes through the jamming zone before landing back at the base. Most of the flight takes place within 100 km of the Satellite Reference Station.

After landing, the data is downloaded off the aircraft and transferred to the SARS I ground station where it is then used by the SARS I Kalman filter to generate the final reference data.

6. SARS I TEST RESULTS

6.1. SARS I Accuracy

An extensive test series has been conducted to validate the SARS I system, including van testing, low-velocity sled track testing, cargo aircraft testing, and high-velocity sled track testing. Because of the ongoing nature of the system, only the results from the high-velocity sled track testing during Jul-Aug 94, are presented.

Sled Tests —The Holloman High Speed Test Track has been precisely surveyed and instrumented with a series of bevel-edged interrupter blades positioned at nominal intervals of 4.33 feet along the track. An infrared beam in a sled-borne sensing head was interrupted each time the sensing head passed over an interrupter, generating a series of pulses as the sled moved along the track. From the timing of these pulses, downtrack position and velocity were derived to an accuracy better than 0.0008 m and 0.0004 m/sec respectively.

The sled run consisted of a two-stage rocket firing, which generated peak accelerations of 30 m/s² and peak velocities of 160 m/s. The sled traveled from south to north with a true heading of 355.8 degrees. After the test, the SARS I data was processed and compared with the sled reference data. The results are shown in Table 2. A set of plots showing the results from sled run #3 is shown in Figures 2a and 2b. Figure 2a is a plot of the position errors for sled run #3 with out incorporating carrier phase measurements into the filter. Figure 2b is a plot of the position errors for sled run #3 incorporating carrier phase measurements. The step jumps in the Up Position Error of Figure 2a result from the 4 ft resolution in the INS altitude output.

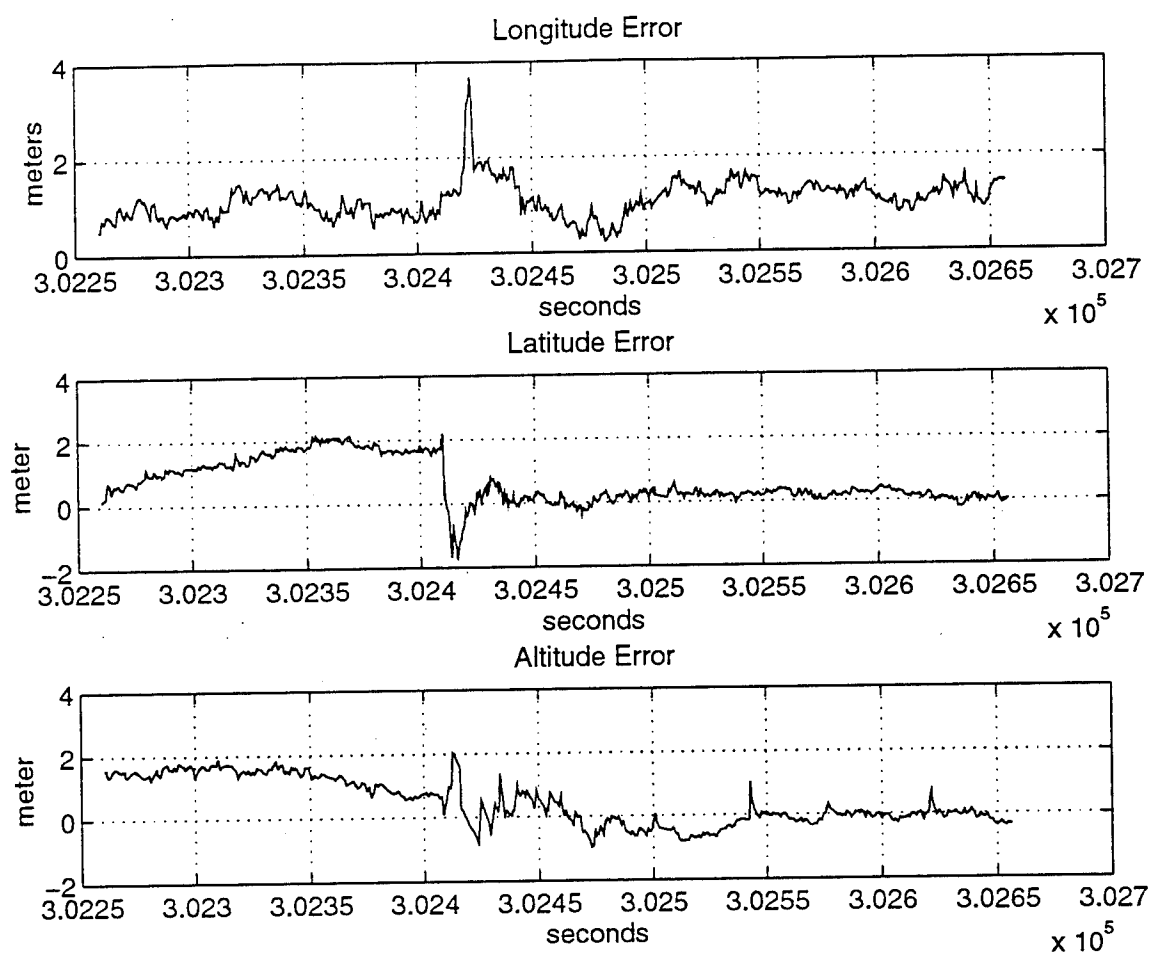


Figure 2A: Position Errors (w/o Carrier Phase) for Sled Run #3

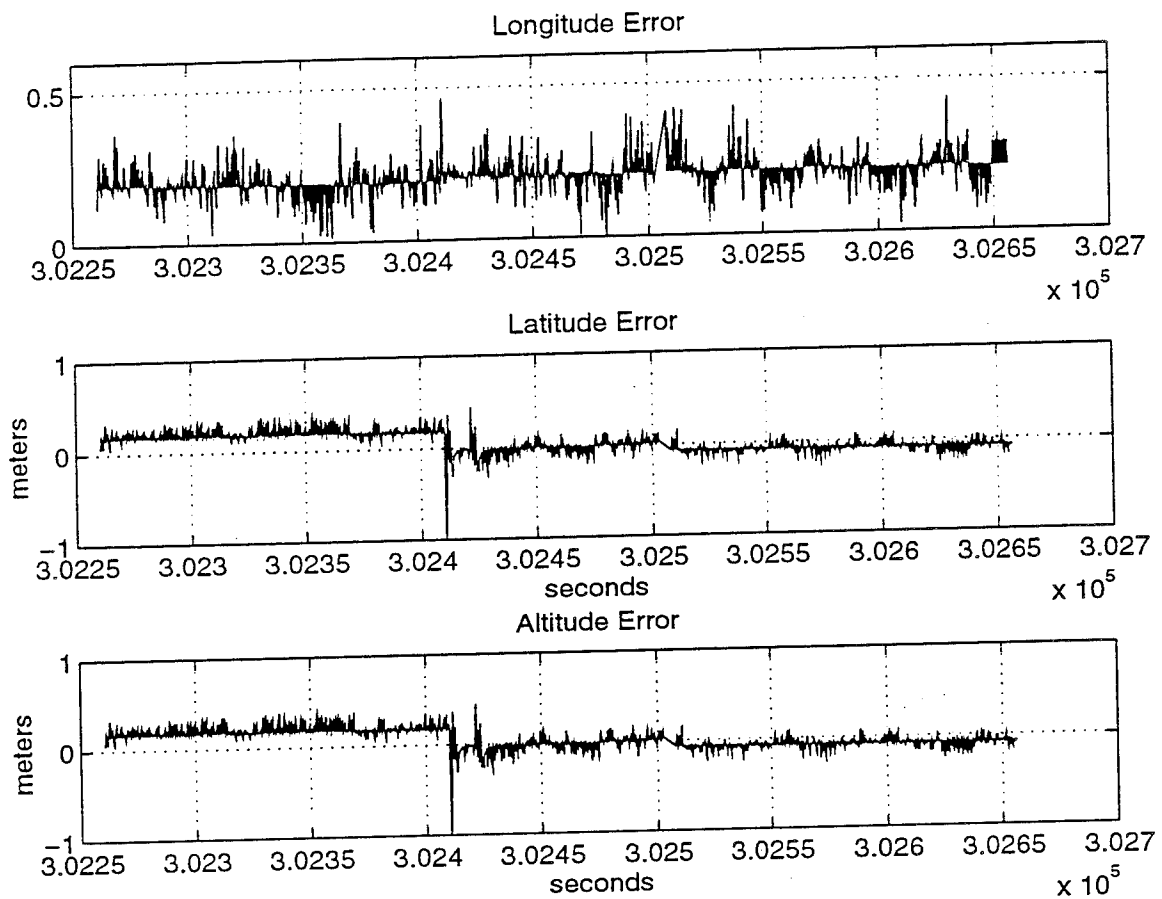


Figure 2B: Position Errors (with Carrier Phase) for Sled Run #3

Table 2: Difference Between SARS I (w/o CP) and Test Track Solution (SARS I - Track)

Error Type	Sled Run 1 25 Jul 94			Sled Run 2 3 Aug 94			Sled Run 3 10 Aug 94			All Runs Combined		
	Mean	Std Dev	Error RMS	Mean	Std Dev	Error RMS	Mean	Std Dev	Error RMS	Mean	Std Dev	Error RMS
East Pos Err (m)	0.68	0.44	0.80	0.87	0.71	1.12	1.09	0.34	1.13	0.88	0.50	1.02
North Pos Err (m)	-0.05	0.37	0.37	-0.05	0.37	0.37	0.64	0.74	0.97	0.18	0.49	0.57
Up Pos Err (m)	0.12	0.41	0.43	0.06	0.63	0.63	0.46	0.78	0.91	0.21	0.61	0.66
East Vel Err (m/s)	-0.029	0.061	0.068	0.000	0.073	0.073	-0.038	0.078	0.087	-0.024	0.070	0.074
North Vel Err (m/s)	0.013	0.057	0.059	-0.006	0.060	0.061	0.052	0.099	0.112	0.022	0.079	0.082
Up Vel Err (m/s)	-0.030	0.105	0.109	-0.046	0.110	0.120	-0.032	0.108	0.113	-0.035	0.108	0.113

Table 2 shows the difference between the track derived position and velocity and the SARS I

6.2 IMPROVEMENTS DUE TO CARRIER PHASE MEASUREMENTS

In order to show the improvements expected from incorporating carrier phase measurements into the filter, the carrier phase data gathered during CHAPS validation track tests last summer were incorporated into the post mission filter and compared to the SARS I data without carrier phase. However, some problems were encountered. During sled run #1, we lost carrier lock for 100 seconds. Loss occurred at ignition of the first rocket motor, and was not regained until the vehicle had stopped. Sled run #2 also lost carrier phase lock, but for only 15 seconds. This time loss occurred at ignition of the second rocket and was quickly regained while the sled was still in motion. Finally, the receiver maintained carrier phase lock for the entire sled run #3.

Despite the problems maintaining carrier phase lock for two of the runs, the results of incorporating carrier phase data greatly improved the results as can be seen in Table 3.

derived position and velocity, without incorporating carrier phase measurements.

Figures 2a and 2b, show that not only does carrier phase data greatly improve the accuracy of the system, but it improves the precision of the system as well. Tables 2 & 3 show that the standard deviation for each run is significantly smaller when carrier phase data is incorporated.

7. FUTURE DEVELOPMENT

Although SARS I is just emerging from initial development, planning for future changes and improvements is already underway. Concurrently, the 46th Guidance Test Squadron is testing its next generation Satellite Reference Station which uses a dual frequency, Y-code, all-in-view, carrier phase receiver. When the new SRS becomes operational, the RCVR 3A currently used by SARS I will be replaced by the new receiver.

SARS I filter development will continue into the future. A backwards smoother has been implemented, and testing is underway to determine how to use it most effectively. Sometimes it is not feasible to use the interrogator/transponder subsystem, and

Table 3: Difference Between SARS I and Test Track Solution (SARS I - Track)

Error Type	Sled Run 1 25 Jul 94			Sled Run 2 3 Aug 94			Sled Run 3 10 Aug 94			All Runs Combined		
	Mean	Std Dev	Error RMS	Mean	Std Dev	Error RMS	Mean	Std Dev	Error RMS	Mean	Std Dev	Error RMS
East Pos Err (m)	0.16	0.14	0.21	0.12	0.37	0.39	0.20	0.06	0.21	-0.59	0.19	0.63
North Pos Err (m)	-0.07	0.11	0.13	0.03	0.21	0.21	0.05	0.15	0.15	-0.25	0.16	0.30
Up Pos Err (m)	0.20	0.55	0.59	0.02	0.19	0.19	0.01	0.11	0.11	0.08	0.28	0.30
East Vel Err (m/s)	-0.002	0.025	0.025	-0.016	0.075	0.077	-0.054	0.029	0.030	-0.024	0.043	0.044
North Vel Err (m/s)	0.008	0.035	0.036	0.003	0.099	0.099	-0.012	0.050	0.051	0.000	0.061	0.062
Up Vel Err (m/s)	-0.005	0.051	0.051	-0.009	0.057	0.058	-0.024	0.066	0.070	-0.013	0.058	0.060

effective backwards smoothing becomes valuable during periods of jamming when no GPS measurements are available.

Another important long-term goal is the replacement of the transponder/interrogator subsystem with something less costly to operate and maintain. Several alternatives are being investigated. The final solution must provide measurements in the presence of both L1 and L2 GPS jammers.

In the interest of miniaturization, an embedded INS/carrier-phase GPS receiver may eventually replace the SNU-84 INS. This type of embedded GPS/INS is not currently available but one may be within a few years. In order to use an embedded system with the SARS I software, the embedded system must have a mode where the inertial navigation solution and raw GPS measurements are provided as separate outputs.

REFERENCES

1. "Computer Program Product Specification (C5) for the GPS Radio Receiver R-2332D&E/AR (RCVR 3A) of the User Equipment Segment, NAVSTAR Global Positioning System, CI No. 6228078", Specification Number CP-RCVR-3010, Part II of Two Parts, 9 January 1990, Collins Government Avionics Division, Rockwell International Corporation, Cedar Rapids, Iowa.
2. Carlson, Neal A., "Strapdown Inertial Navigation System Simulation Model," TM-90-002, February 1990, Integrity Systems, Inc. Winchester MA.
3. Wei, M. and K. P. Schwarz, "A Strapdown Inertial Algorithm Using an Earth-Fixed Cartesian Frame," NAVIGATION, Journal of the Institute of Navigation, Vol. 37 No. 2, Summer 1990.

THIS PAGE LEFT BLANK INTENTIONALLY

FUTURE GUIDANCE, NAVIGATION & CONTROL ISSUES

**by
Tom Reed
Consultant
Milli Sensor Systems & Actuators, Inc.
(MSSA, Inc.)**

**Presented at the
Seventeenth Biennial Guidance Test Symposium
Holloman Air Force Base, New Mexico**

THIS PAGE LEFT BLANK INTENTIONALLY

FUTURE GN&C ISSUES:

ABSTRACT

The world of GN&C is changing, components, programs and funding have been dramatically reduced while requirements and areas of opportunity have increased. The need for simplicity, reliability, adaptability and low cost is apparent and now appear possible with the development of smaller and less expensive inertial sensors. The era of multi-million dollar designs of inertial systems where the emphasis was on schedule and performance with little cost reduction incentives have essentially disappeared. Cost, of both development and procurement, has become the driving factor. In the area of electronic design, functional integration has replaced component selection, digital processing has replaced linear design and software idiosyncrasies have replaced "strange electronic phenomena". Strapdown designs dramatically reduce the need for moving parts but have minimized the ability for pre-flight calibration. GPS can supply the necessary updates but brings its own problems. Optimal filtering must be extended from today's slow pre-flight calibration calculations to real time operational upgrades using multi-sensor inputs. While these changes have brought about new system engineering challenges, there is a need to blend them into the prior knowledge of solid engineering practices that evolved from the scars of yesterday.

Strategic grade inertial instruments have traditionally been based on gyroscopic elements. Other basic methods have evolved, including laser type gyros, RLGs, ZLGs, FOGs and IFOGs; and crystal type accelerometers, VBAs and others. Lately, the development of micro-miniature instruments has been in the forefront, with both gyros and accelerometers in the millimeter range. With the possible exception of the RLG, none of these non-gyroscopic units can be considered strategic grade.

The advent of an operational GPS will allow future guidance to be better while using less precise inertial instruments. In fact, where GPS is available, all that is needed is essentially an autopilot function for control. In military use, however, there are applications where GPS access may be denied by enemy action. These applications will be addressed. The many orders of magnitude reduction from the strategic grade instruments to the micro-miniature units, in both size and performance, has left a large gap in the intermediate area. This is the area, where instrument size is in proper balance with the size of the support electronics and computational devices and performance for military applications. A projected set of these instruments will be used to illustrate a system of tomorrow. This strawman system will be used to present the issues of future GN&C systems.

This paper will attempt to outline a series of thought disciplines that are intended to reduce the iterative process of system design. It will show that state theory and linear design can be the enemy of good digital process design, that design for analytical simplicity can, at times, produce system complexity and sub-optimal operation. It will try to replace rote with common sense direction, producing some new perspectives for old problems and translating old ones for the new.

THIS PAGE LEFT BLANK INTENTIONALLY

FUTURE GUIDANCE, NAVIGATION & CONTROL ISSUES:

by
T. E. Reed
MSSA, Inc.

INTRODUCTION

I believe that any paper, except perhaps a mystery, should start off with an explanation of the title. But there should be some explanation or, in this case, a statement of limitation because the title is all encompassing. I will first define the word system — it is a functioning entity that consists of a set of sub-systems, each of which performs one of the various functions that make up the whole. It is the interaction of these sub-systems that comprise the main complexity of the system. My interest and training lie in the realm of ICBM inertial guidance systems, which I can state, with only a few disagreements, represents the most precise, multi-disciplined complexity crammed into the smallest space; multi-million dollar production systems that can be carried by one man. It will also cover, to a lesser degree, SLBMs and by inference, Cruise Missiles.

The world has changed dramatically in the last ten years, as electronics, sensors and funding have all shrunk. As system sizes and costs get smaller, the areas of opportunity have and will grow. The addition of an effective GPS system yielding accurate positional information compliments the shorter term accuracy of inertial sensors; allowing significant reduction in both size and cost by reducing the accuracy requirements of inertial instruments, including pre-flight calibration eliminating the complexity of gimbals. Previously, only ships, large missiles and aircraft were candidates for inertial guidance systems because of size, weight and cost. Now it is possible to design systems that can guide weapons as small as a howitzer shell with incredible absolute accuracy.

This paper will address the dramatic changes in new instrument designs, their uses and future considerations from a system standpoint. It will also attempt to translate the knowledge and scars of past GN&C designs into this new era of small parts and small funding. Its primary value is that it tries to define the basis behind good engineering and how design approaches should change to be more compatible with the rapid changes in technical capabilities and fiscal realities.

GN&C systems will be divided into two discrete categories based on weapons: nuclear and conventional; and each section divided into two more: nuclear into the ICBM and the SLBM; conventional into high explosive or kinetic.

NUCLEAR

The dissolution of the USSR has reduced, but not eliminated, the need for a nuclear strike force. As long as there are untrustworthy nations capable of delivering nuclear devices through the atmosphere to our country there will be a need for a nuclear deterrent force. The past triad of nuclear deterrent capability, ICBMs, SLBMs and long range bombers, performed its job well. The future of this triad is in question. The high manning necessary to maintain the submarines and bombers, as well as their possible dual role will most likely result in perpetuation of these capabilities. The ICBM, which requires little manning, relatively, will most likely be slowly reduced unless saved by more fiscally responsible heads. Its future is, however, probably secure for the next twenty to thirty years.

The present ICBM force is limited to Minuteman IIIs and Peacekeepers, with the Peacekeepers scheduled to be retired in the near future and the MM IIIs being emasculated

by the elimination of multiple warheads. These deterrents are augmented by the Navy's SLBMs fleet whose effectiveness will also be severely reduced by treaties and funding.

There is a basic criteria for both the ICBM and the SLBM, that they must be able to operate under all possible environments including hostile actions, and these actions could include neutralizing our GPS satellite system. This dictates that all GN&C for these missiles will be either pure inertial or stellar-inertial, as they are now.

The Navy appears to be satisfied with its present Trident Mk 6 system and, while continuing some development programs, has no immediate plans for upgrading. Long term maintenance can become a problem in a few years, requiring production lines to be reopened, but there is no indication that the Navy will start a new system for its nuclear SLBMs in the next decade.

The Air Force, on the other hand, is in the process of having a new system developed but, because of intermittent funding problems, it will probably be obsolete before it is accepted or needed. There are no plans, that I know of, to replace the present MM III or Peacekeeper systems.

Future Needs

For both services, the time will probably come when a new system is needed before the world gets safe enough to eliminate the need—if ever! If this happens, and if you can assume that the GPS is still vulnerable, instruments with the following performance¹ will be needed:

Missile	Gyro		Accelerometer	
	Bias Deg/hr	Scale Factor ppm	Bias μg's	Scale Factor ppm
Pure Inertial	0.00001	20	5	1
Stellar-Inertial	0.001	100	10	2

The pure inertial requires either the floated Single-Degree-of-Freedom gyro or the larger RLGs and either a PIGA type accelerometer or an improvement in the present VBAs. There is little chance that the world will ever see another pure inertial strategic missile system. The stellar-inertial will require either the present two-degree-of-freedom type gyro or a RLG while the accelerometer requirements follow those of the pure inertial.

CONVENTIONAL PRECISION STRIKE MISSILES

By increasing the accuracy of our present long range missiles, this country could have the ability to strike anywhere in the world with an essentially invulnerable, surgically precise weapon. Its ability to fly above the protected airspace of other countries, its ability to effect minimal collateral damage and its fast reaction time makes it an ideal supplement to present weapons. Use of these long range missiles will probably be limited to high value targets such as command posts, large munitions storage areas, launch sites, strategic bridges and manufacturing plants. They could be equipped with explosive warheads for soft targets, buildings, bridges, etc.; and kinetic penetrators for deeply located command posts. These penetrators may or may not contain explosives.

¹ The use of single scalar numbers to define the performance of an instrument is regrettable and actually inadequate—see Appendix A.

Requirements

It is assumed that GPS will be used to aid an inertial system in order to obtain the necessary accuracy. While strategic grade inertial instruments will not be required for this application, there will be a need for pure inertial operation within approximately twenty miles from the target. Even without jamming the reentry velocity will generate plasma that will make GPS ineffective during part of the trajectory. This requires inertial instruments with the following range of performance:

Weapon	Gyro		Accelerometer	
	Bias Deg/hr	Scale Factor ppm	Bias μ g's	Scale Factor ppm
Explosive	5	500	100	100
Kinetic Penetrator	1	300	50	50

The lesser requirements for the explosive weapon are due to its ability to strike at a higher speed, taking less time to traverse the twenty miles. The kinetic weapon, on the other hand, requires a slower speed to assure that it will not explode on impact². There would probably not be two guidance systems designed for the two types of warheads so the better quality instruments will be assumed.

INSTRUMENT REQUIREMENTS

The four types of systems show a spread in the requirements for both the gyros and the accelerometers. There appears to be no need for gyros in the 1 to 0.001 deg/hr range, nor for accelerometers in the 10 to 50 μ g bias range, and the 2 to 50 ppm scale factor range. This information should set the goals for future instrument designs.

It is the contention of this author that the evolution of the μ -miniature instruments will not reach the 1 deg/hr and the 50 ppm range within the foreseeable future. They are the instruments of the future with a promise of significant reductions in cost, weight and power, opening up the use of inertial instruments in applications heretofore unheard of. In the meantime there are small instruments in development, not micro but milli, instruments based on well proven gyroscopic principles of the past. These instruments could be the basis for the next evolution of conventional strike GN&C systems.

SPONSOR SPECIFICATIONS

The sponsors working with smaller budgets should sharpen their pencils in the area of system specifications. More time must be spent, and more items opened for negotiation if costs are to be held down.

In the past the dynamic and hostile environments have been specified in a worst-worst condition, in contrast to the use of statistical methods for other requirements. This has cost the military literally millions of dollars both in unnecessary development and procurement costs. There appears to be little difference between live-through and operate-through specifications.

² One rule of the thumb which may not be too accurate is that a penetrator must hit at a speed less than the speed of sound in the penetrator material.

Three dimensional vibration spec's: amplitude, frequency and endurance, have been simplified in order to present them on a two dimensional chart by eliminating the dimension of endurance. This allows a short time "spike" of vibration to become a sustained input. This has resulted in vibrational power specifications as much as four orders of magnitude higher than an actual flight.

The probability of hostile nuclear events should be made statistically realistic. The ability of a system to circumvent radiation induced shutdown depends on the induced downtime. The probability of precisely sequential events is statistically small and should be reflected in the specification.

The overall problem is the intractability of written specifications. Many items are overspec'ed without recognition of the overall effect on performance or design.

It goes without saying that micro-management is costly. Meetings need to be divided into two parts, the first should be the designer presentation with the sponsor and their aides, SETA, consultants, etc. constrained to listen with a minimum of questions—no directions. The sponsor should then hold a caucus and generate a list of clarifications, suggestions and other comments. A second meeting is then held where as many items are clarified as possible, and the remaining ones formally submitted as Requests for Actions (RFAs).

SYSTEM ENGINEERING

This paper contends that the majority of system problems can be separated into the following categories:

1. Temperature—All aspects of temperature, absolute value as well as its spatial and temporal gradients.
2. Grounds—The distribution and interconnects of system voltage references, both power and signal, and their short and long term effects on system operation.
3. Analytical—A catchall term relating to the non-physical, algorithms and software design of the system.

Temperature

Instruments are temperature sensitive, but the majority, due to their inherent symmetry, are more sensitive to thermal gradient changes than "soak" temperature. This requires that the thermal management design control both temperature and temperature gradients about the sensitive parts of the instruments. Now throw in the fact that thermal gradients are time dependent and the problem expands to four dimensions, three spatial, one temporal. To actively control or compensate in four dimensions becomes impossible or, at best, highly complex. The answer lies in the following:

1. The thermal interference comes, primarily, from outside, not inside.
2. Gradients are best constrained passively by lowering tangential resistance and increasing radial.
3. Constrain instrument power flow to specific paths and control the temperature of that path.
4. Eliminate all passive convective heat flow, eliminate all voids $> 0.030"$.

It is assumed that the instruments are designed to minimize internal power variations. This being true, the problem reduces to minimizing the effect of the outside environment. Ideally, this can be done by designing an instrument interface so that all power flows through a single point and then control the temperature of that point. While this ideal design is impossible, it can be approached by minimizing power flow "leakage" radially

and moving the control point away from the instrument, allowing passive smoothing of gradients.

An effective method of maintaining a constant thermal pattern across an instrument is to wrap it in consecutive layers of insulation and conductor, e. g. mylar and aluminum, which not only minimizes external temperature effects but also minimizes changing internal gradients. Remember, gradients only become a problem when they change.

If the instrument is tumbled to determine parameters, try reversing the trajectory. If the coefficients are different, then a g-dependent thermal gradient, i. e. convection, is the most likely culprit.

Electrical Grounds

Grounding techniques for large, spread out, high power systems appears to be non-essential for small, compact, low power systems. This is not necessarily true. Power may be reduced but so is voltage and the signal levels become more sensitive, so application of standard grounding techniques remains important.

Another oversight, especially as high frequency and digital signals become the standard, is the use of ground planes, where grounds are attached to supporting conductive structures. This is proper in many applications but care must be taken to assure that the current path is not dependent on mechanical, i.e. clamped, connections between dissimilar metals. This can lead to major problems in system reliability. The passing of electrical current across dissimilar metallic interfaces can, over time, change the conductance and inherent galvanic potential of the clamped joint. All current carrying dissimilar clamped connections should have welded or soldered parallel conductive connections.

The increased use of digital signals has reduced the problem of ground isolation across sub-system interfaces. Transformers and optical isolators allow near perfect ground noise isolation. If analog signals are required to interface with other subsystems, forward ground sensing techniques should be used. This technique senses the difference in the noise on the two ground systems and sums it into the outgoing signal.

Computations

The largest change from past practices in the development of any future system is the move from serial to parallel processing. The digitizing of functions has brought us greater precision, but not necessarily greater accuracy. It should bring simplicity, but could evolve into greater complexity. There are two areas of specific interest here, one is the digitizing of closed loop servo functions and the other is the use of optimum or quasi-optimum filters.

The design of an analog servo is straightforward, there are only resistors, capacitors, inductors and amplifiers. Leads, lags, inertias damping and spring constants are all linear and well suited for analytical definition. Bode plots, S-plane analysis and other tools of the trade allowed rapid convergence to an operating servo. Even the introduction of some non-linearities were allowed as Z-plane and state theory analysis provided more effective tools. Then came digitization and parallel computation. Immediately we began to construct parallel processing modules that represented leads and lags, of linear transfers and we started to bang up against throughput problems, quantization noise and granularity non-linearities.

First forget linear analysis, that was invented to handle the limitations of analog components. Second, get a good description of the data content. Was the true output an analog signal that was digitized? or was it a pure digital output? If it was digitized was it conservative³? Did it contain all the information of the analog signal or was the digitizing process an incomplete sampling with accumulative error?

The best digitizing method uses a Sigma-Delta Modulator. This method performs a continuous integration of the analog signal minus the resulting digitized output to assure that the entire low frequency contents of the input signal has been properly translated into a digital output. This assures that the integral of the digital signal does not diverge from the integral of the analog, which can happen in sample and hold type digitizers.

Now comes the servo design. Assume a positional servo wherein the input error signal is proportional to angular error and the output will supply torque. What is known? Positional error and its uncertainty, rate of change of positional error and its uncertainty! The dynamics of the servo driven member to a torque command is known. The rest is no different than an optimum filter, just compute the optimum torque command.

The problem of initial turn-on will probably require special attention, but again, the computer knows everything, with some uncertainty. At turn-on the analog and digital signals are saturated, containing only error polarity information. In a linear servo the torque would be full on, and the servo would have to be designed with enough lead time after getting out of saturation to properly reverse the torque prior to cross-over or the system goes unstable.

In the digital servo, the computer can be told how far out the positional stop are, and it can regulate the amount of torque, and therefore the velocity acquired when it comes out of saturation. Once in the linear region it can compute the torque profile required to achieve an optimum convergence.

Kalman Filtering

In the case of inertial systems, the Kalman type filters were used to extract system calibration parameters in the field prior to launch. Once launched there was no additional information that could allow parameter updates. In the case of the Navy systems which use a star tracker, there is addition information but the updating of system parameters is a closed form one-time calculation. In today's and tomorrow's systems where GPS signals can allow parameter updates through most of the flight, the filter must be updated in flight. On the ground the filter operation could be slow with solutions updated in minutes. In flight this needs needs to be speeded up to operate in seconds or less.

The required increase in filter speed by more than two orders of magnitude requires some major modifications. One offsetting advantage is that available processing is getting faster, but more is required. The only three methods for speeding up this process, other than getting a faster processor, is to either reduce the number of state variables, find ways to partition the filter or to use better sparse matrix techniques. The first, or reducing the number of filter states, is the most straightforward. During ground calibration, parameter stabilities over long periods were of interest and the number of filter states was increased. During flight the number of parameters that are expected to shift significantly is reduced allowing constants to be substituted for dynamic variables.

³ The term conservative, in this context, refers to conversion errors that are non-accumulative.

The next method of speeding up the filter is to partition variables into independent or near independent sets. As the complexity of large numbers of parameters are reduced, the ability to partition increases. Two matrices with half the size can be manipulated in considerably less time than the original large matrix. The use of better matrix manipulation techniques will undoubtedly be automatic so will not be expounded on here.

GPS has another advantage, it has a method of determining its own credibility, this is the Degree of Precision (DOP) calculations that are performed using the relative positions of the satellites. This allows the filter to dynamically modify its GPS weightings empirically and independently. There are two considerations or variables unique to flight that need to be optimized. One is the "initialization" of a new satellite and the other is the losing of GPS information due to natural or hostile action.

When a new satellite is observed, then its computed range must be compared with the accumulated positional data and then given a constant bias. This is in addition to the uncertainty associated with the DOP. Also the loss of any or all satellites, either through hostile action or occultation must be judged immediately and the filter must make the proper adjustments.

A major concern is data latency, information from the GPS must be accurately time tagged before merging with the inertial instrument information. Only dynamic testing will indicate latency problems.

TESTING

Testing can be a major cost item in the design and production of a system, sometimes even exceeding the cost of manufacturing. It is very important that the entire test program be given as much attention in early-on planning as any other design or production item. Reexamination of the test program during manufacturing should occur periodically to maintain an optimum and responsive production action.

Why, When and How

There are four basic reasons for performing a test. Adequacy, definition, reliability and circus act. Adequacy tests are used to determine if the unit will fulfill its intended role. Definition is the quantification of a unit's parameters. Reliability is to determine its expected lifetime and circus act testing is to impress your superiors or sponsors.

The inputs to these tests can be one or more of the following: time, temperature, acceleration (linear, sinusoidal, acoustical, random or shock), angular rate (and its derivatives), radiation (photons, neutrons, gamma rays, etc.), pressure (gas or liquid), fungus, corrosive materials and abrasion.

Testing will occur in the various phases of design and manufacturing, from the incoming inspections to the final system acceptance tests. There are two basic criteria for determining the viability of a specific test. First, define the possible results of the test and define the response to each — if they are all the same, don't do it. In other words, if a test does not influence the future then why do it? Second criteria, if the same test can be done at a higher level of integration and the negative results of that test multiplied by their probability costs less than doing the lower level test(s) then do away with the lower level tests. This is the area that needs periodic review, as information comes in as to the pass fail ratio and the cost of retrofitting becomes better known. For example, if a particular test on part "A" costs \$100 and past history shows that the failure rate is 1.0%, then this test is not cost effective unless a failure at the next level costs more than \$10,000. A few words of caution! The

type of failure that will be found at the lower level must be visible at the next test level! Also the manufacturing flow must be capable of handling the retrofit as a well cost defined action.

Every system test should have well defined results with proper pretest analysis to assure convergence. This is especially true with some of the more expensive engineering tests. One of the requirements of a GPS aided INS is the proper time merging of sensor information, this probably will require dynamic testing such as quantitative rocket sled testing.

MISCELLANEOUS CRITERIA

Besides the technical areas there is the design management criteria that require some comment. Communication with the sponsor must be a two way street. If the sponsor decrees a change that you believe is wrong, make sure they understand the possible ramifications.

Its never too late!

When a condition or design error is found that could possibly jeopardize system operation in the future, never say its too late to fix! If it is not a show stopper then don't stop the show — but don't ignore it either! Set up a parallel action with the intent of working on a fix. Be candid with your sponsors, let them know about the problem and what you are doing about it. If your fears don't materialize then good, but if they do you will be closer to a program saving fix.

There will be times during early system testing when an error is found that must be corrected. This does not mean that everything stop until the fix is made unless further testing is impossible. Continue testing to determine as many errors or weaknesses as possible as early as possible and then work them in parallel.

Adequacy not Perfection

Perfection is the enemy of good engineering. Perfection begets indecision and indecision is the Achilles heel of engineers and their managers. When a problem is encountered, define it in relation to its specific effect on the required system performance and then strive for an adequate solution.

Failure Reports

As systems are required to be more reliable and as they become more reliable, the need for more accurate failure reporting and effective failure actions become increasingly more important. Every failure should be looked upon as an positive opportunity to effectively increase reliability.

The first criteria is to impress on all personnel that honest and thorough failure reporting is an absolute necessity. One of the cleanest failure to act upon is one caused by operator error. It must be stressed that the reporting of an operator error will not result in reprimand. What it should result in, is a review of procedures to determine if changes could be made that would minimize this type of error from occurring again. This cannot be stressed enough, the working environment should not be laden with the fear of operator penalties for errors.

Once a fault is found it must be thoroughly understood. I was once reviewing fault reports at a large avionics firm that was in the initial stages of producing a highly sophisticated and expensive system. One report caught my eye, it stated that the system had automatically shutdown and after teardown (a three day effort) and troubleshooting (a two day effort) a broken wire was found. The corrective action section of the failure report, signed by a member of the QC team stated, "Replaced Wire".

What should have happened was a thorough investigation of why the wire broke. Was it a poor solder joint? an improperly stripped wire? a defective wire? a poor holddown? What? This failure should have triggered an investigation that should, in turn, resulted in some change in procedures, either manufacturing, testing or inspection. It should assure that it has minimized the chance of this type of failure of ever occurring again.

STRAWMAN DESIGN

The best way to tie all of the above together is to actually go through the preliminary steps of designing a system of the future. Most of the ideas are possible today and some must wait, but only a few years. The same for the mission need and the political atmosphere, but we shouldn't need to wait long.

Mission

This strawman system will guide a hypothetical weapon to any point on earth in less than two hours. Its primary warhead is a five hundred pound penetrator that contains fifty pounds of HE and a fuse that can be set to detonate at any prescribed depth. The system in design will guide the missile from boost through freefall and reentry until impact.

Operational Constraints

The missile system must be capable of a fifteen minute reaction time, this includes target and trajectory information upload and GPS acquisition. The guidance will consist of a GPS aided inertial system with differential or relative GPS upgrade capability. The guidance must be capable of achieving a 20 foot CEP with an impact speed of not more than 5,000 feet per second.

The only hostile countermeasures expected will be GPS jamming which should effectively make GPS unusable below 90,000 feet. Reentry velocity is at 17,500 ft/sec with sufficient deceleration to achieve 10,500 ft/sec at 90,000 feet followed by a deceleration at approximately 3 g's to the optimal penetrator impact velocity of 6,500 ft/sec with a vertical, ± 3 degree, impact.

This trajectory will be essentially invulnerable to anti-missile weapons up to and including the US Patriot system. No form of anti-anti-missile device will be needed for the foreseeable future.

The above constraints can be translated into the following requirements and specifications:

1. One or more atmospheric "skips" must be made to decrease velocity and properly calibrate the INS parameters.
2. The 20 foot CEP represents a 90 arc second half-cone angle from 90,000 feet.
3. The pure inertial flight will last for approximate 8 seconds.

Error Budget

From the above constraints the following error budget was generated: (in feet)

Parameter	Error	Down Range	Cross Range
At time of GPS loss			
Velocity Vector Misalignment	20 arc seconds	9	9
Position Error	10 feet	10	10
Non-Thrust Gyro Rate Errors ⁴	1 deg/hour	8	8
Non-Thrust Accel. Bias Error	500 μ g's	4	4
Target Uncertainty		10	10
Control Error		4	4
Other Errors		<5	<5
RSS		19.5	19.5
CEP			20.0

The above numbers are realistic, assuming that the GPS has accuracies in the < 0.1 feet/second range with corresponding incremental position accuracy. The absolute position accuracy assumes the use of differential or relative GPS updates prior to signal loss.

Instrument Selection

Every pound of guidance weight subtracts from the weight of the weapon and reduces its lethality. This "non-lethal" weight includes not only the guidance system but also the actuators, the ablative shield and the batteries. The reduction of the actuators and ablative shields were assumed to be near optimum, or at least outside the design of the guidance unit. The battery weight is a function of the amp-hour requirement so that the guidance system should not only weigh less but use less power. The use of μ -miniature inertial instruments would fulfill both the weight and power requirements but their ability to meet the above performance requirements are many years away. The next available off-the-shelf instruments were orders of magnitude heavier in both weight and power consumption.

MSSA, Inc is developing an intermediate set of inertial instruments. These instruments are not expected to reach strategic accuracies, but the conservative estimates of performance will easily meet the requirements of this system. While their weight is larger than the μ -miniature units, their total contribution to system weight is insignificant when all other guidance elements are considered.

The strawman instruments to be used in this strawman system, both the gyro and the accelerometer are packaged in a one inch square and less than one-half inch thick. This packaging is compatible with electronic packaging being developed by the Air Force Phillips Laboratory under the direction of Capt Lyke.

Combining these instruments with these electronics can produce a one inch square stack, say four inches long, that contains one each accelerometer and gyro plus all the direct support electronics. The entire guidance system consists of three of these units with a fourth similarly size unit that contains the processors. The configuration of these "sticks", being long and narrow has other advantages to be covered later.

⁴ The sensitivity of this term is a function of its ability to be calibrated and its direct effect on reentry guidance.

GPS Selection

The GPS will be a miniaturized system capable of receiving up to six satellites. It will be packaged in a unit external but in close proximity to the INS. It will receive velocity information from the INS processor in order to allow use of narrow capture loops.

Thermal Management

By wrapping these "sticks" in alternate layers of conductors and insulators, e.g. aluminum and mylar, the vast majority of the internal power flow can be forced to exit through the ends. These ends can be designed to pinch down the thermal path so that a single temperature controller at each end can make the entire package thermally stable with practically no sensitivity to the outside environment. Its small thermal capacitance will allow it to reach thermal equilibrium well within the required reaction time of the missile. The size and number of wires required to run these "sticks" becomes the limiting factor in controlling wattage flows, any electrical conductor is also an excellent thermal conductor. This wire problem can be minimized, almost eliminated by reducing the number of wires to two—for DC power and use optical couplers with small optical fibers, a better thermal insulator, for all frequency references into the unit and all signals leaving.

Computations

One of the major costs in the design of a guidance system is the software development. In this system this cost is to be held at a minimum by the use of federated processors. Parkinson's law is compounded many times in the field of software development. The interfaces between separate programmers becomes extremely critical. Federated processors can define these interfaces in both software areas but also physically. The primary problem of federation is synchronizing their interfaces. This problem is to be circumvented by macro-synchronism with all processors connected on a single bus.

Assume a total computational cycle as 0.25 seconds or 4 Hz and equal or less than eight processors. Now take each processor and break its functions into 2^n , where $n = 1, 2, \dots, 5$, approximately equal parts. Now the controlling function will be an eight bit timing word occurring at a 1024 Hz rate. Expressed octally it would send words from 000 to 3778 on the bus not only for the usual communication window but also to begin each program segment.

Each software segment is running at the internal processor speed but it must finish its entire sequence within the allotted time, then wait for its next operational key. Communication between processors will be done by the time segment that computes that data. The data will be placed on the bus immediately after that processor and segment is called. The processor and segment that requires this data will be designed to be on the previous code word and will wait that $1/1024$ second to pull off the data.

This allows a system designer to define the data products, the generator and receiver, and then set the sequence of software segments and processors. At this point the individual segments can be defined and parceled out to programmers thereby essentially controlling all communication from a single person's action, minimizing the Parkinson's law syndrome. Also throughput computations will be done on segments which again breaks down the large central computer type problem into as many as 256 smaller almost independent problems.

The following is a list of the basic functions and the operations per second:

Function	Operations/Second
A. Gyro and Accelerometer Corrections	512
B. Coning Corrections	512
C. INS Quaternion	16
D. GPS Solution	4
E. DGPS or RGPS Correction	4
F. Coordinate Transformation	4
G. GPS/INS Filter	4

Figure 1 shows an example using processor I which processes INS output.

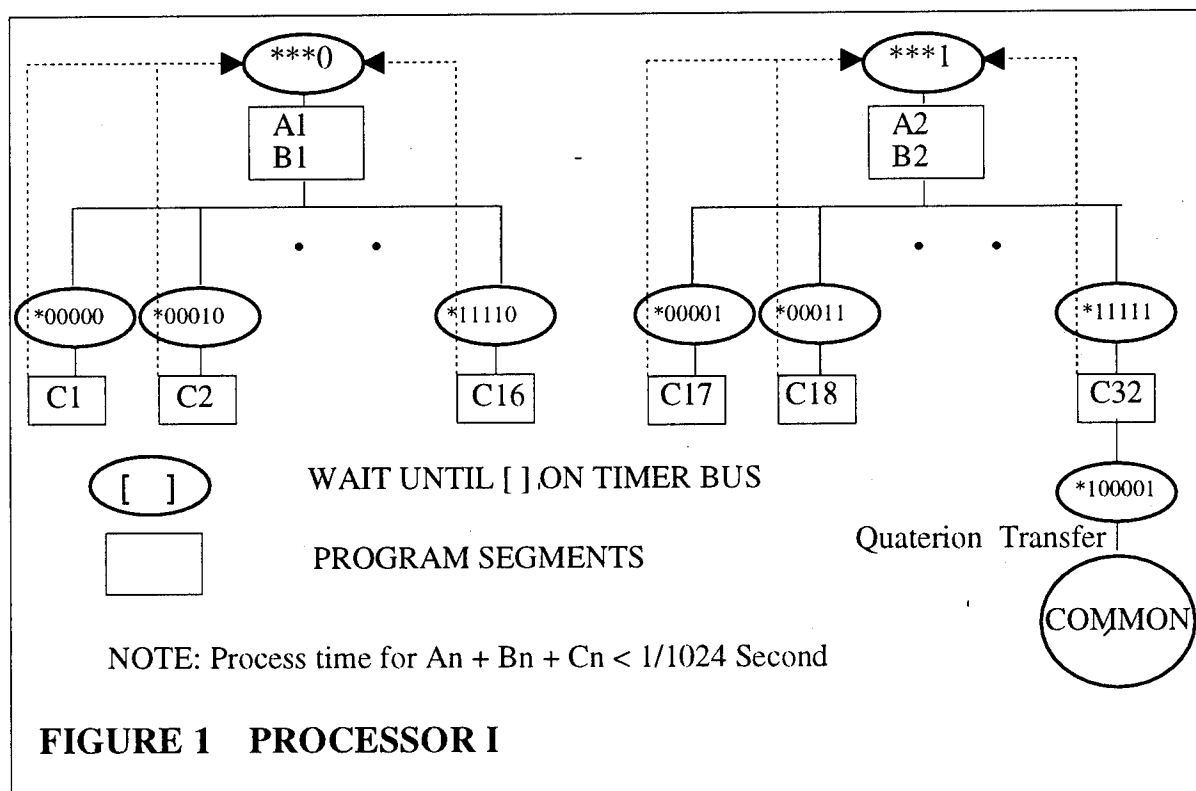


FIGURE 1 PROCESSOR I

Package Integrity & Mounting

The relative alignment of the inertial instruments over time is extremely important as their calibration would have been done prior to missile integration, and relied on for the rest of its field life. The basic "stick" design can be made extremely stiff, with heavy frames on the outside and light electronic boards in the center.

The INS will be packaged as a unit, leaving the GPS unit with its coax cables external without mechanical isolation. The INS package will be mounted using isolators yielding a natural frequency of approximately 50 Hz requiring a throw space of approximately three inches, assuming a package weight of five pounds. It is important that this isolation design be as isoelastic as possible to minimize the translation of linear vibration into coherent rotations which can introduce coning errors.

SUMMARY

There will be a need for future long range missile guidance, both for nuclear and precision strike weapons. The cost of pure inertial systems will undoubtedly eliminate them as future candidates. The "softness" of GPS will eliminate its uses as the primary sensor for nuclear missiles. Precision strike missiles will require continuous guidance and will undoubtedly use GPS with terminal upgrades using differential or relative GPS methods.

As the development of GPS/INS systems proliferate standard ASIC designs, antenna technology and less expensive inertial instruments will dramatically reduce the size and costs of effective guidance systems. The development of an intermediate set of inertial instruments using gyroscopic principles will fill the gap between the accurate but present expensive instruments and the future inexpensive but inaccurate μ -miniature units.

THIS PAGE LEFT BLANK INTENTIONALLY

APPENDIX A

INERTIAL INSTRUMENT UNCERTAINTY

Inertial instrument performance is often characterized by a single scalar number, e.g. a 10 degree per hour gyro or a 10 micro-g accelerometer. This is totally inadequate for system design. Inertial instrument uncertainties and their effect on system operation are much too complicated for a single value. Well then! What is needed?

If the instrument is to be used in a GPS aided system then the uncertainty of interest is the short term noise, essentially for the time of flight as the instrument is dynamically calibrated prior to pure inertial use. If the instrument is to be used in a pure inertial or stellar inertial then its parameters will probably be calibrated using a Kalman filter. If this is true the instrument should be defined in the linear terms compatible with the filter. These terms are white noise, random walk⁵ and ramps. Even this is artificial as instruments seldom exhibit random walk or ramps, the more common phenomena is 1/f noise and exponentials both of which are incompatible with Kalman computations. This then requires a force fit of the linear terms to the instrument reality.

In order to give a better understanding of instrument behavior, the following is a look at possible causes of imperfect, non-ideal instrument behavior:

	DESIGN RESPONSIBILITY	
	SYSTEM	INSTRUMENT
NOISE		
Excitation Jitter	Electronics	
"Shot" Noise	Preamp	Low Sensitivity
Mechanical Vibration	Isolators, Resonances	Resonances
Quantization	Readout	Bandwidth
Inadequate Filter	Filter Design	
RANDOM WALK		
Incomplete Readout (Lost Data)	Readout Method	
RAMP		
Wearout		Moving Contact
EXPONENTIALS & 1/F NOISE		
Thermal Environment	Thermal Control	Symmetry, $\partial(\text{Power})$
Material Relaxation or Fatigue		Material
Corrosion		Material, Seal
Outgassing		Preparation
Electronic Parameters	Electronic Design	

⁵ In a gyro this is angle random walk and rate random walk, in an accelerometer it is velocity random walk and acceleration random walk.

THIS PAGE LEFT BLANK INTENTIONALLY

SESSION III-A
FIBER OPTIC GYROS

CHAIRMAN

DR. RICHARD GREENSPAN

*C. S. DRAPER LABORATORY
CAMBRIDGE MA*

THIS PAGE LEFT BLANK INTENTIONALLY

Cluster Sampling Technique for Gyro Noise Analysis

M. M. Tehrani

Litton Guidance and Control Systems, Woodland Hills, CA 91367

Abstract

In 1979, the author adapted the Allan Variance technique to the analysis of the ring laser gyro (RLG) data. Allan Variance is a time domain analysis method originally developed to study the frequency stability of oscillators. In his treatment of RLG noise analysis, the author defined the Cluster Variance as twice the Allan Variance and related that to the noise power spectral density (PSD) of the gyro. The reason for this definition was the fact that the RLG output is the result of the interference of the two counter-propagating beams. And, considering each beam as an oscillator, the RLG output variance is the sum of the variances of the two beams.

In this talk, we will briefly review the fundamentals of the cluster sampling technique (CST) and discuss the Cluster Variances of a number of prominent noise terms and their physical origins in RLG. We will also present the Cluster Variance of the RLG quantization noise that was not treated in the 1979 work.

THIS PAGE LEFT BLANK INTENTIONALLY

Cluster Sampling Technique for RLG Noise Analysis

M. M. Tehrani

Litton Guidance and Control Systems, Woodland Hills, CA 91367

I. Introduction

Cluster Sampling Technique (CST) uses the Allan Variance methodology of data analysis. The latter is a time domain analysis technique originally developed to study the frequency stability of oscillators^[1]. It can be used to determine the characters of the underlying random processes which give rise to the data noise. As such, it helps identify the source of a given noise term present in the data; whether it is inherently in the instrument or, in the absence of any plausible mechanism within the instrument, its origin should be sought in the test set up. In 1979 the author adapted the Allan Variance technique to identify various noise terms in ring laser gyro (RLG) data. Equations were developed to relate the effect of each noise term on the RLG data. Since the RLG output is the difference (beat frequency) between the frequencies of the two counter-propagating laser beams its variance is the sum of the variances of the two beams. Considering each laser beam as an oscillator, the RLG output variance, which we call Cluster Variance, will be twice the Allan Variance.

The cluster variance technique may be used as a stand alone method of data analysis or in conjunction with any of the frequency domain methods of analysis. It should also be mentioned that the technique can be applied to the noise study of other gyros as well as accelerometers. Its value, however, depends on the degree of understanding the physics of the instrument.

Following is an overview of the Cluster Variance and its adaptation to the noise properties of RLG. With the exception of the quantization noise, detailed derivations of all the equations are given in Reference 2 and will not be repeated here. Instead, emphasis will be on discussions of origins of various noise terms in RLG and the method by which a particular noise manifests itself in the cluster variance.

II. Methodology

Consider N sampled data of an oscillator with a sample time of t_0 . Let us form data clusters of lengths $t_0, 2t_0, \dots, Kt_0$ ($K < N/2$) and obtain averages of the sum of the data points contained in each cluster over the length of that cluster. A new set of random variables can now be generated by taking the difference of averages of each two adjoining clusters. Allan variance is defined as one half the statistical variance of the new random variable. As discussed earlier, laser gyro output is the (heterodyne) combination of the two counter-propagating laser beams. As such, the gyro noise variance is twice that of each laser beam treated as an independent oscillator. Thus, the laser gyro output variance, called cluster variance^[2] is twice the Allan variance. Since the following exposition is a summary of the derivations given in Reference 2 we employ the same definitions.

The cluster variances obtained by performing the prescribed operations are related to the power spectral density (PSD) of the noise terms in the original data set. An underlying assumption in the formulation is that the random processes affecting the gyro output are all stationary in time^[3]. The relationship between cluster variance and the noise PSD is given by :

$$\sigma^2(f) = 8 \int_0^\infty df \frac{\sin^4(\pi f T)}{(\pi f T)^2} S_\Omega(f) \quad (1)$$

where $S_\Omega(f)$ is the rate noise PSD, and T is the cluster time ($T = Kt_0$). Equation (1) is the key result that will be used throughout to characterize the rate noise PSD from the cluster variance calculations. Its physical interpretation is that the cluster variance is proportional to the total noise power of the gyro rate output when passed through a filter with the transfer function of $\sin^4(x)/(x)^2$. This particular transfer function is the result of the method used to create and operate on the clusters.

It is seen from Equation (1) and the above interpretation that the filter bandpass depends on the cluster time T . This suggests that different types of random processes can be examined by adjusting the filter bandpass, namely by varying T . Thus a plot of cluster variance versus cluster time provides a means of identifying and quantifying various noise terms that exist in the data.

The following paragraphs show the application of Equation (1) to a number of noise terms that are either known to exist in RLG or are suspected to influence the data.

1. Angular Random Walk

There are two main sources for this error which will be discussed separately:

- Randomized dither--In mechanically dithered RLGs the dither amplitude is randomized in each dither cycle. This is to avoid the build up of angular errors during the zero rate crossings of the sinusoidal dither^[4]. Accomplishing this, however, is at the expense of creating a random walk in the gyro phase angle. Laser gyros which do not employ dither as a means of lock-in avoidance (such as the multioscillator gyro) do not possess this type of random walk.
- Spontaneous emission of photons-- A smaller component of the RLG angular random walk is caused by the spontaneously emitted photons which are always present in the laser action. Its magnitude is smaller than the dither-induced random walk by a factor of 2 to 10. Unlike the dither-induced random walk, however, this portion is unavoidable. For this reason the angular random walk due to spontaneously emitted photons is called the "Quantum Limit" of the gyro random walk^[5].

Other "high frequency" noise terms can also contribute to the gyro random walk although most of these sources can be eliminated by design. These noise terms are all characterized by a white noise spectrum on the gyro rate output. Thus the associated PSD is represented by:

$$S_{\Omega}(f) = q^2 \quad (2)$$

where q is the noise amplitude. If we use Equation (2) in (1) and carry out the integration we obtain:

$$\sigma^2(T) = \frac{2q^2}{T} \quad (3)$$

As shown in Fig. 1, Equation (3) indicates that a log-log plot of $\sigma(T)$ versus T has a slope of $-1/2$. Furthermore, the numerical value of q can be obtained directly by reading the slope line at $T=2$ hours.

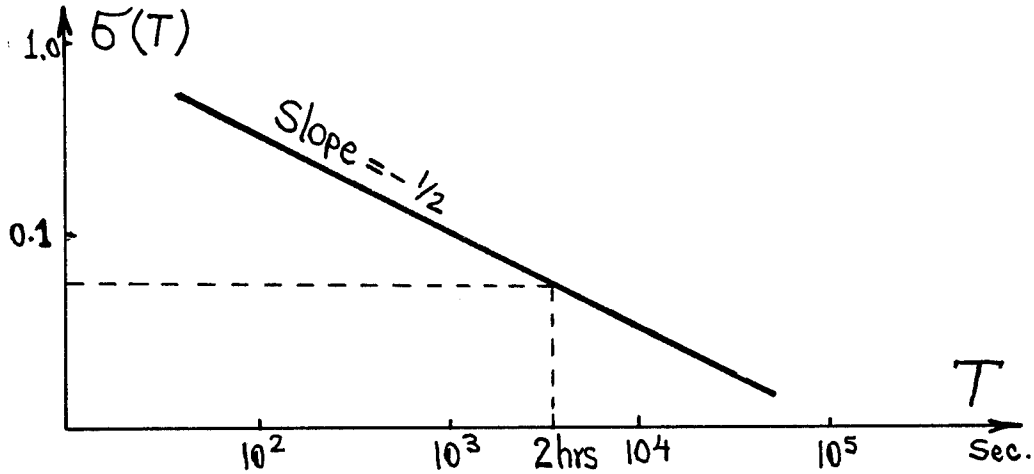


Fig. 1. Log-log plot of $\sigma(T)$ vs. T for the angular random walk

II. Exponentially Correlated (Markov) Noise

The correlated noise is a generalization of the white noise by having a finite (non zero) correlation time. Its PSD is a Lorentzian whose bandwidth is determined by the noise correlation time. Amongst the contributors to this noise term is the randomized mechanical dither. This is due to the resonant nature of the dither mechanism which does not allow all frequencies being imparted to the gyro body with equal amplitude. Thus, in reality the randomized dither introduces a correlated noise to the gyro whose correlation time can be shown to be related to the mechanical Q of the dither spring^[6]. The rate PSD of this type of noise is :

$$S_{\Omega}(f) = \frac{(q_c T_c)^2}{1 + (2\pi f T_c)^2} \quad (4)$$

where q_c is the noise amplitude and T_c is the correlation time. Substitution of (4) in Equation (1) and performing the integration yield:

$$\sigma^2(T) = \frac{2(q_c T_c)^2}{T} \left\{ 1 - \frac{T_c}{2T} [3 - 4 \exp(-\frac{T}{T_c}) + \exp(-2\frac{T}{T_c})] \right\} \quad (5)$$

Fig. 2 shows a log-log plot of Equation (5). It is instructive to examine various limits of this equation. For cluster times much longer than the correlation time, we find:

$$\sigma^2(T) \rightarrow \frac{2(q_c T_c)^2}{T} \quad \text{for } T \gg T_c \quad (6)$$

which, as expected, is the expression for the angular random walk with the identification $q = q_c T_c$. In the opposite limit, Equation (5) reduces to:

$$\sigma^2(T) \rightarrow \frac{2q_c^2}{3} T \quad \text{for } T \ll T_c \quad (7)$$

This is known as the rate random walk. In some gyros it shows up in the region of long cluster times and is caused by a correlated noise of yet longer correlation time. In most cases it is an error which is introduced at the system level.

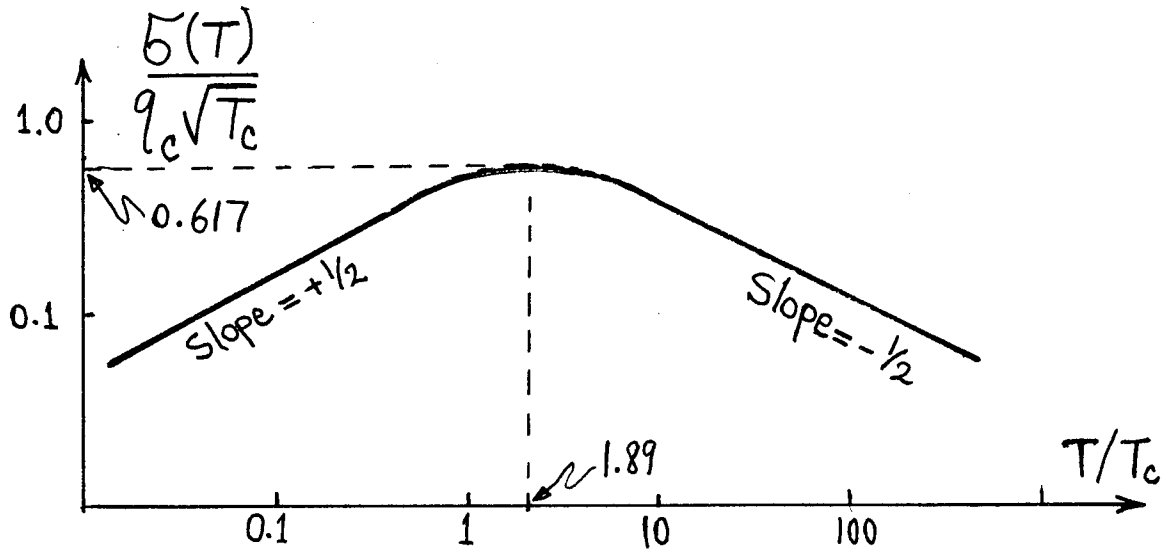


Fig. 2. Log-log plot of $\sigma(T)$ vs. T for exponentially correlated noise.

3. Quantization Noise

This noise is strictly due to the digital nature of the RLG output. The readout electronics registers a count only when the gyro phase changes by 2π . The rate PSD, $S_{\Omega}(f)$, for such a process can be derived from the corresponding angle PSD, $S_{\Phi}(f)$, given in Reference 7 and the equation $S_{\Omega}(2\pi f) = (2\pi f)^2 S_{\Phi}(2\pi f)$ relating the two. We obtain:

$$S_{\Omega}(f) = \frac{4Q^2}{T} \sin^2(\pi f T) \quad (8)$$

whose use in Equation (1) yields:

$$\sigma^2(T) = \frac{6Q^2}{T^2} \quad (9)$$

where Q is the quantization noise amplitude. Equation (9) indicates that the quantization noise is represented by a slope of -1 in a log-log plot of $\sigma(T)$ versus T , as shown in Fig. 3. The magnitude of this noise can be read off the slope line at $T = \sqrt{6}$ hour.

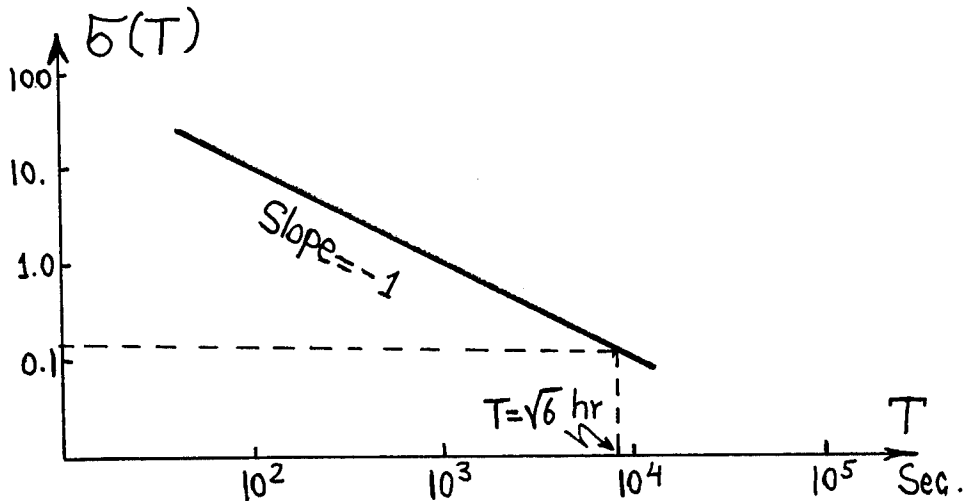


Fig. 3. Log-log plot of $\sigma(T)$ vs. T for quantization noise.

4. Flicker Noise

The origin of this noise is in the RLG discharge assembly, the electronics, or other components susceptible to random "flickering". Because of its low frequency nature it shows up as the bias fluctuations in the data. For this reason it may be called the limit of bias stability. The rate PSD associated with this noise is:

$$S_{\Omega}(f) = \begin{cases} \left(\frac{B^2}{2\pi} \right) \frac{1}{f} & \text{for } f \leq f_0 \\ 0 & \text{for } f > f_0 \end{cases} \quad (10)$$

where B is the noise amplitude and f_0 is the cut off frequency. Application of (10) to Equation (1) results in:

$$\sigma^2(T) = \frac{4B^2}{\pi} \left\{ \ln 2 - \frac{\sin^3(\pi f_0 T)}{2(\pi f_0 T)^2} [\sin(\pi f_0 T) + 4\pi f_0 T \cos(\pi f_0 T)] + Ci(2\pi f_0 T) - Ci(4\pi f_0 T) \right\} \quad (11)$$

Where $Ci(x)$ is the cosine-integral function^[8]. Figure 4 represents a log-log plot of Equation (11) which shows that the cluster variance for flicker noise reaches a plateau for cluster times of much longer than the inverse cut off frequency. Thus, the flat region of the cluster plot can be examined to estimate the limit of bias stability as well as the cut off frequency of the underlying flicker noise.

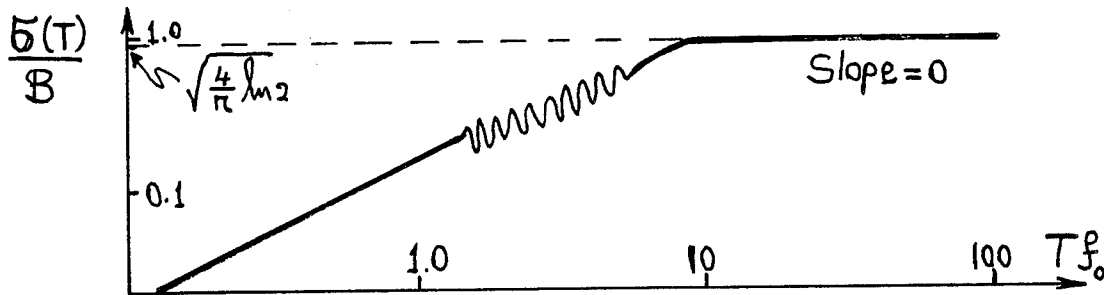


Fig. 4. Log-log plot of $\sigma(T)$ vs. T . for the flicker noise.

5. Sinusoidal Error

The PSD of this noise is characterized by a number of distinct frequencies. Amongst its origin in the high frequency range is the plasma oscillations in the laser discharge. A low frequency contributor to this noise could be the slow motion of the test platforms subjected to periodic environmental changes. A representation of the PSD of this noise containing a single frequency is given as:

$$S_{\Omega}(f) = \frac{1}{2}\Omega_0^2\delta(f-f_0) \quad (12)$$

where Ω_0 is the amplitude, f_0 is the frequency, and $\delta(x)$ is the Dirac delta function. Multiple frequency sinusoidal errors can be similarly represented by a sum of terms such as (12) at their respective frequencies. Applying Equation (1) to (12), we obtain:

$$\sigma^2(T) = 2\Omega_0^2 \left(\frac{\sin^2(\pi f_0 T)}{\pi f_0 T} \right)^2 \quad (13)$$

Figure 5 shows a log-log plot of Equation (13). Identification and estimation of this noise in RLG data require the observation of several peaks. As is seen, however, the amplitudes of consecutive peaks fall off rapidly. This can cause masking of the second or higher order peaks by other noise terms which makes the observation of this noise difficult.

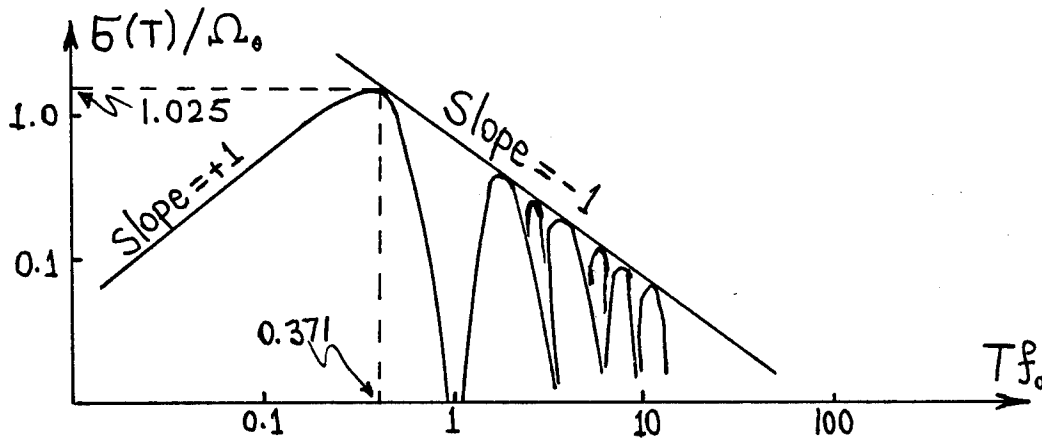


Fig. 5. Log-log plot of $\sigma^2(T)$ vs. T for sinusoidal error

6. Rate Ramp

This is more of a deterministic error rather than a random noise. Its presence in the data may indicate a very slow degradation of the RLG intensity persisting over a long period of time and in the same direction (decreasing or increasing). It could also be due to a very small acceleration of the platform in the same direction and persisting over a long period of time. Whatever the source, it appears as a genuine input to the RLG given by:

$$\Omega = Rt \quad (14)$$

where R is the ramp rate. By forming and operating on the clusters on data containing an input given by (14), we obtain:

$$\sigma^2(T) = R^2 T^2 \quad (15)$$

which shows that a slope of $+1$ in the log-log plot of $\sigma(T)$ versus T , as depicted in Figure 6, is indicative of rate ramp in the data. The magnitude of R can be obtained from the slope line at $T = 1$ hour.

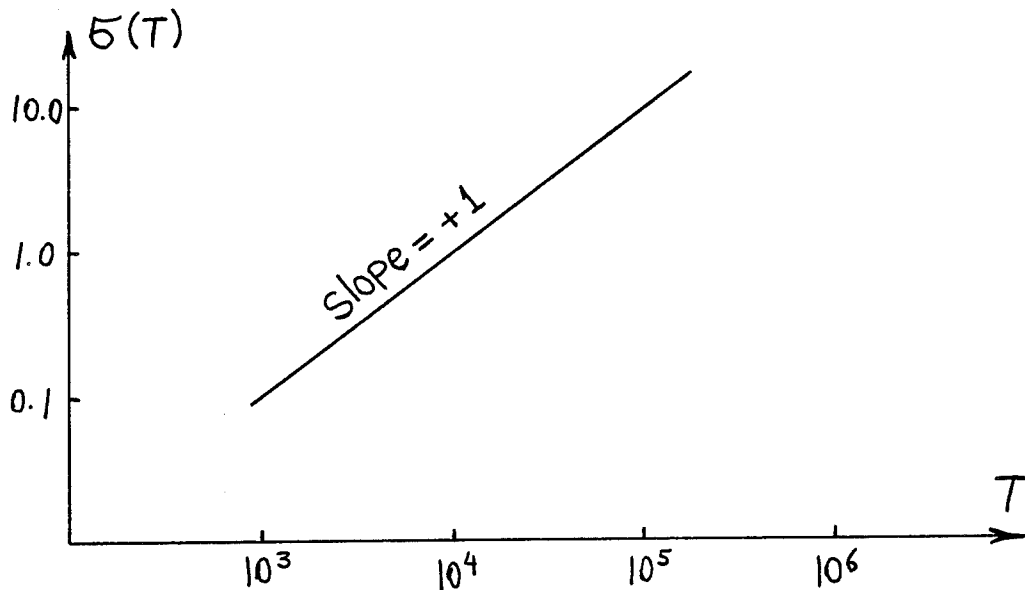


Fig. 6. Log-log plot of $\sigma(T)$ vs. T for rate ramp

III. Combined Effects of All Random Processes

In general, any number of the random processes discussed above (plus others) can be present in the data. Thus, a typical cluster variance plot looks like the one shown in Figure 7. Experience shows that, in most cases, different noise terms appear in different regions of the cluster time. This allows easy identification of various random processes that exist in the data. If it can be assumed that the existing random processes are all statistically independent then it can be shown that the cluster variance at any given cluster time is the sum of cluster variances due to the individual random processes at the same cluster time. In other words,

$$\sigma_{tot}^2(T) = \sigma_{ARW}^2(T) + \sigma_{Quant.}^2(T) + \sigma_{flick}^2(T) + \dots \quad (16)$$

Thus, estimating the amplitude of a given random noise in any region of cluster time requires a knowledge of the amplitudes of the other random noises in the same region.

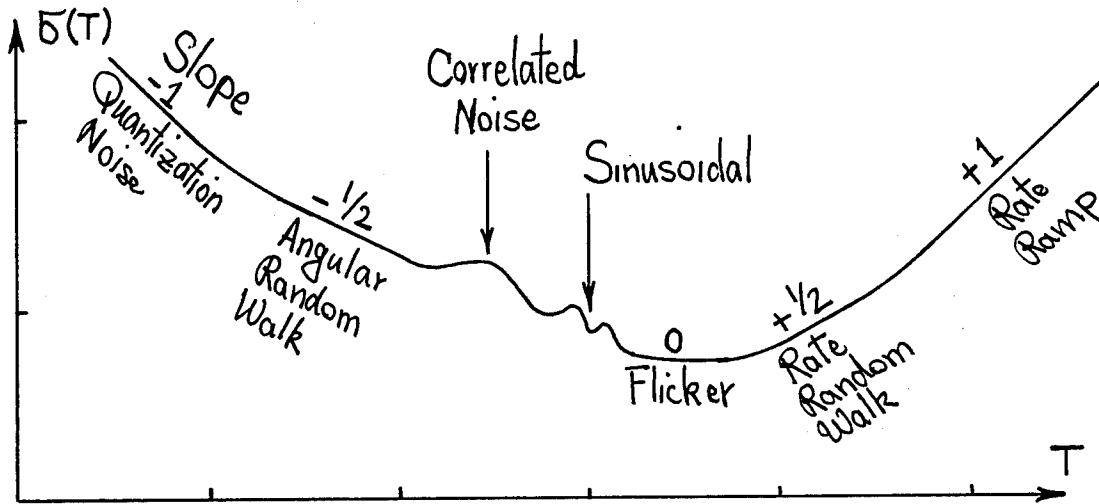


Fig. 7. Log-log plot of $\sigma(T)$ vs. T containing all six noise terms discussed.

IV. Estimation Accuracy and Test Design

A finite number of clusters can be generated from any finite set of data. Cluster variance of any noise term is estimated using the *total* number of clusters of a given length that can be created. On the other hand, estimation accuracy of the cluster variance for a given cluster time depends on the

number of *independent* clusters within the data set. It can be shown^[2] that the percentage error, δ , in estimating $\sigma(T)$ when using clusters containing K data points from a data set of N points is given by:

$$\delta = \frac{1}{\sqrt{2\left(\frac{N}{K}-1\right)}} \quad (17)$$

Equation (17) shows that the estimation errors in the regions of short (long) cluster times are small (large) as the number of independent clusters in these regions is large (small). In fact, this equation can be used to design a test to observe a particular noise of certain characteristics to within a given accuracy. For example, let us say we wish to verify the existence of a random process with a characteristic time of 24 hours in the data to within an error of 25 percent. We first set $\delta = 0.25$ in Equation (17) and obtain:

$$K_{\max} = \frac{N}{9} \quad (18)$$

Since the suspected characteristic time is 24 hours we create clusters of the same length. Thus the total test length needed for such a test is $24 \times 9 = 216$ hours.

References:

- [1]. Allan, D.W., Proc. IEEE, Vol. 54, p. 221 (1966)
- [2]. Tehrani, M.M., Proc. SPIE, Vol. 412, p. 207 (1983)
- [3]. Since the Allan variance technique deals with the second order (two-time) correlation function, the only requirement is that the random processes be "stationary in the wide sense". See Reference 7 below.
- [4]. Killpatrick, J.E., Proc. SPIE, Vol. 487, p. 85 (1984)
- [5]. Simpson, J.H., Proc. NAECON, Vol. 1, p. 80 (1980); See also: Dorshner, T.A., *et al*, IEEE J. Quant. El. QE-16, p. 1376 (1980)
- [6]. Tehrani, M. M., Proc. Sixteenth Biennial Guidance Test Symposium, pp. 585-597 (1993)
- [7]. Papoulis, A., Probability, Random Variables, and Stochastic Processes, Third Edition, McGraw-Hill, Inc. (1991)
- [8]. See, for example, Gradshteyn, I.S. and Ryzhik, I.M., Table of Integrals, Series, and Products, Academic Press (1980)

THIS PAGE LEFT BLANK INTENTIONALLY

Fiber Optic Gyro Development for Navy Shipboard Inertial Reference System Applications

Joseph De Fato
Naval Command Control and Ocean Surveillance Center
RDT&E Division Detachment
Warminster, Pennsylvania

and

Ralph A. Patterson
Litton Guidance & Control Systems Division
Woodland Hills, California

APPROVED FOR PUBLIC RELEASE; DISTRIBUTION IS UNLIMITED.

ABSTRACT

In support of the Navigation and Aircraft Command, Control Communication and Technology Program sponsored by the Office of Naval Research and the Fiber Optic Basic Technology Program sponsored by the Naval Sea Systems Command, the NCCOSC RDT&E Division Detachment is assessing the viability of using fiber optic gyro technology for Navy shipboard inertial reference system applications. The capabilities and facilities available at NCCOSC's Inertial Navigation Facility (INFAC) are being used to investigate, test, and evaluate industry fiber optic gyro designs. This will result in assessment of gyro performance, identification of sensor technology deficiencies, and promotion of industry development tasks for fiber optic gyro enhancements.

To date, NCCOSC has completed an in-house laboratory evaluation of two industry first generation interferometric fiber optic gyro (IFOG) designs and is currently directing the development of a second generation IFOG that will be suitable for shipboard gyrocompass system applications. This new development incorporates sensor component and architecture advances made by industry to resolve the deficiencies found to be present in first-generation IFOGs. NCCOSC has conducted a competitive procurement and awarded a contract to Litton Guidance and Control Systems for the development of an IFOG design intended for use in high accuracy stabilized shipboard gyrocompass equipment. Two engineering model gyros have been fabricated and delivered to NCCOSC.

This paper describes the Litton gyrocompass IFOG design and the gyro acceptance testing of the two demonstration IFOGs conducted at the Litton Woodland

Hills facility. Acceptance test results are presented and are shown to be consistent with contract requirements. A discussion of the ongoing laboratory evaluation by NCCOSC of the Litton hardware deliverables is also provided.

INTRODUCTION

The spinning mass electromechanical gyro technology now used in Navy shipboard gyrocompass equipments is antiquated and increasingly costly to support in the fleet. The need to improve reliability and to reduce the high costs of procuring and maintaining shipboard gyrocompass systems are recognized drivers for the development of a new generation of shipboard gyrocompasses based on the utilization of interferometric fiber optic gyro (IFOG) technology. The factors governing the ship mission are long endurance, reliability, low speeds, and slow maneuvers. The successful use of IFOG technology in marine inertial reference systems requires not only the attainment of adequate performance levels with respect to gyro bias stability, scale factor and white noise but also the achievement of long term (days) gyro bias drift and calibration stability in the temperature controlled environment of an unaided system mechanization. These issues are not considered in current IFOG technology based developments such as the ARPA sponsored GPS Guidance Package Program (GGP) and the Air Force Precision Fiber Optic Gyro (PFOG) Program.

Exploratory IFOG development for shipboard gyrocompass system applications has been conducted by the Naval Command, Control and Ocean Surveillance

Center (NCCOSC) RDT&E Division Detachment Warminster, PA as a subtask of the Navigation System Technology (RC32N10) Project Plan sponsored by the Office of Naval Research (ONR). This program has demonstrated the inherent capability of IFOG technology to meet the most stringent performance requirements of the Navy's Gyrocompass Systems (AN/WSN-2 and 2A), utilized aboard submarines. This was accomplished by NCCOSC test and evaluation of industry first generation brassboard IFOG models. However, the NCCOSC evaluation also showed the need for gyro architecture and component improvements to remedy IFOG temperature sensitivity and IFOG light source reliability deficiencies.

With funding support provided by ONR and the Naval Sea System Command, NCCOSC is currently directing the development of a second generation IFOG design that will be suitable for shipboard gyrocompass system applications. This new development will incorporate gyro technology advances made by industry to resolve the deficiencies found to be present in first generation IFOG designs. In addition to IFOG sensor architecture enhancements, these advances include improved gyro rotation sensing coil fabrication techniques to minimize performance degrading thermal effects, new light source technology for increasing gyro lifetime and reliability, and integrated optic development enabling the manufacture of reduced cost photonics components with improved optical characteristics.

NCCOSC conducted a competitive procurement and awarded a contract, effective September 1993, to the Litton Guidance and Control Systems Division, Woodland Hills, California for the design, fabrication, and contractor acceptance testing of two second generation Gyrocompass IFOG demonstration units (Demo No. 1 and Demo No. 2). The Litton gyro build and acceptance test effort has been completed and the two units were delivered to NCCOSC Warminster Inertial Navigation Facility (INFAC) in December 1994. NCCOSC laboratory test and evaluation of the Litton Gyrocompass IFOG hardware, now in progress, is planned for completion in FY 1995.

GYROCOMPASS IFOG DESIGN DESCRIPTION

The emergence and accelerating maturation of IFOG technology offers an approach to achieve high reliability and low life-cycle cost in high accuracy shipboard gyrocompasses for new applications. The IFOG, unlike

spinning wheel gyros and conventional two-mode ring laser gyros, does not require any moving parts. Since the IFOG consists of solid-state optical and electro-optical components that are available from multiple sources, the acquisition costs of IFOGs are extremely competitive and limited life/reliability parts are virtually eliminated.

Application of IFOG technology to shipboard gyrocompass systems imposes certain stringent gyro performance requirements that must be met so that the overall system meets its mission requirements. From the standpoint of reliability and life-cycle-cost, a pure strapdown system mechanization without environmental control for the sensors offers the most advantageous approach. This approach, however, does not provide any gyro calibration capability and exposes the inertial sensors to the full range of operating environments. Consequently, the gyrocompass IFOG is required to maintain its bias drift values within the gyro error budget limits over the life of the system and under all shipboard environments. Test results presented below indicate that with software compensation IFOGs are approaching this capability.

Significant progress has been made in IFOG technology at Litton since the delivery of the first generation IFOG brassboard models to NCCOSC nearly five years ago. This progress resolves the deficiencies observed on those earlier models, and results in generally improved performance characteristics. The resolution of those deficiencies is discussed below.

Minimizing Thermal Effects. One of the main weaknesses of fiber optic gyroscopes in the past was the strong sensitivity of their bias to temperature transients. As early as 1980, D. M. Shupe published a paper warning that the sensor coil in the IFOG could exhibit strong thermally-induced non-reciprocities and, thus, large bias errors if subjected to rapidly changing temperature. These thermal perturbations modify the phase of the two light waves propagating through the coil via the temperature dependence of the refractive index and the length of the fiber. The Shupe bias error arises because a thermal perturbation acting on any given segment of coil affects the two counterpropagating waves at different times due to the finite speed of light. If the sensor coil is wound placing segments of coil that are equidistant from the coil midpoint in very close proximity, then the perturbations acting on the two counterpropagating waves at a given time are almost identical and their effects tend to cancel. This is the principle on which the modern IFOG coil winding techniques used at Litton are based.

A good indicator of the overall sensitivity of the IFOG bias to temperature transients is the Shupe coefficient, that is, the slope of the bias versus temperature rate of change curve. Figure 1. shows the results of development progress during the past four years concerning bias sensitivity to thermal transients. This progress chart shows a significant reduction of the Shupe coefficient by a factor of 200 over four years. This important result is due to the improvements Litton has made in winding techniques, spool material and coil design.

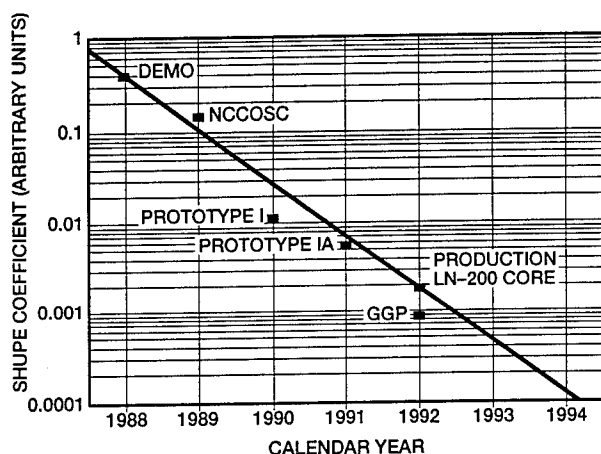


Figure 1. Litton's IFOG Bias Progress — Shupe Error Reduction of >200x in less than four years

Increased Lifetime and Reliability. The key to the increased lifetime and reliability of the Litton IFOG is the improved broadband solid state light source. The previous design utilized a commercial superluminescent diode (SLD) source and therefore exhibited unacceptably short life. The improved light source is projected to have a lifetime of more than 500,000 hours in typical gyrocompass environments. Predictions of MTBF for complete Litton IFOG triads in the shipboard gyrocompass environment, Naval Sheltered (NS), are shown in Table 1. This prediction indicates that the IFOG MTBF for a single axis including electronics will be more than 150,000 hours.

Integrated Optics Advances for Lower Optical Losses and Reduced Costs. The multi-function integrated optics chip (MIOC) developed is based on the LiNbO₃ waveguide technique and features low insertion loss and excellent polarization operation. The typical loss for a device made in production is <6.0 dB which is an improvement of more than 5 dB over the older technology.

TRIAD ASSEMBLY/PART	FAILURE RATE (PER MILLION HRS)
SOURCE	1.6478
COUPLER	.0082
PHOTODETECTOR	1.1275
COIL	.5644
MIOC	.1784
SPLICES	.0264
INTERCONNECT ASSEMBLY	.0181
SOURCE CARD	7.1313
PREAMPLIFIER CARD	4.3983
PROCESSOR CARD	3.7837
TOTAL FAILURE RATE	18.8841
TRIAD MTBF	52,955 hrs
SINGLE AXIS MTBF	158,865 hrs

TABLE 1. Predicted Litton IFOG Triad reliability in a Naval sheltered environment.

One of the technology hurdles which hindered use of integrated optic chips in IFOGs was the fiber pigtail requirement. In general, this was a labor intensive, high cost process. To overcome this problem, Litton has designed and built a fully automated MIOC pigtailing and packaging station. It has been put into operation at the Litton manufacturing facility located in Salt Lake City, Utah. This station needs only a small amount of operator touch time to complete the pigtailing and packaging process because of its fully automated design.

Optical Architecture. The Gyrocompass IFOG utilizes a very simple optical architecture, as shown in Figure 2, consisting of five optical components. Fiber pigtails from each component are spliced together to form the optical circuit (the optical equivalent of soldering electronics parts). Because the interconnecting fibers between components can be several meters long, IFOG designers enjoy an unprecedented level of flexibility in packaging design which has led to reduction in system size and weight, better performance and lower manufacturing cost.

Litton Gyrocompass IFOG development has taken full advantage of the burgeoning optical telecommunication industries development of low-cost, low-failure rate components and processes required by the new information highway. Litton is also developing low cost IFOG manufacturing processes through factory automation. Specific processes being automated are coil winding, pigtailing and packaging, assembly and test. By

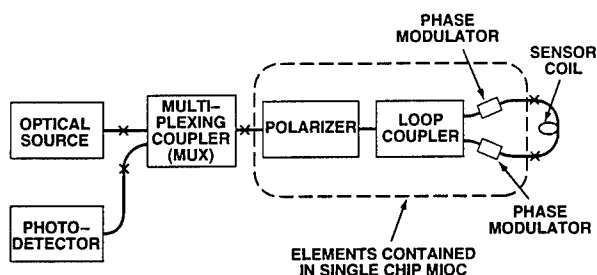


Figure 2. Gyrocompass IFOG Block Optical Architecture. X indicates a fiber-optic splice.

establishing and maintaining this synergy with telecommunications industries, and by implementing the newest automation technologies, IFOG based navigation systems will continue to improve in affordability and reliability.

The physics upon which the fiber optic gyro operates is the Sagnac effect [1]. In short, the relative phase between two counterpropagating waves of light within a closed path is proportional to the path's rotation rate. The Gyrocompass IFOG is an instrument which utilizes this phenomenon in an optical fiber interferometer.

Referring to Figure 2, broadband, stable-wavelength light propagates from the solid state optical source via a first fiber segment to the multiplexing (MUX) coupler. Half of this light propagates from the MUX coupler to the multifunction integrated optics chip (MIOC) via a second fiber segment. The remaining half is radiated into free space. Low loss optical waveguides formed in the lithium niobate MIOC material transmit the light to the polarizer segment where it is linearly polarized with an extinction ratio of >60 dB. The waveguide transmits the polarized light on to the loop coupler where the light is divided equally into two waveguides. The polarized and divided light propagates down the two waveguides to the phase modulator segments and on to the optical fiber leads of the sensor coil constructed of polarization maintaining (pm) fiber [2]. In the Litton Gyrocompass IFOG, the coil is less than 7.0 cm in diameter and consists of 1 Km of fiber wound in a quadrupole fashion for optimum bias performance [3, 4]. The high power source, low loss optical components and low-noise optical receiver provide for best random walk performance. The two wavefronts propagate in opposite directions around the sensor coil where they undergo equal and opposite phase shifts due to any rotation of the sensor about the coil axis due to the Sagnac effect. The wavefronts, now carrying the rotation information, propagate

back into the MIOC via the sensor coil leads and through the phase modulators to the loop coupler where the two wavefronts interfere coherently, thereby converting the Sagnac induced rotation information into a more easily measured intensity variation. The combined wave propagates via the MIOC waveguide through the polarizing segment where spurious optical signals are suppressed and into the fiber segment which carries the light on to the MUX coupler. Half the light is coupled via a third fiber segment to the low-noise receiver module consisting of a PINFET detector and a transimpedance amplifier. The other half is coupled along the first fiber segment to the source where it is absorbed and re-radiated.

Modulation/Demodulation Electronics. The closed-loop electronics scheme employed ensures the greatest sensitivity, output linearity, and minimizes bias errors due to changes in optical gains and losses. As shown in Figure 3 the analog signal from the photodetector is amplified and converted to digital format. The processor operates on this signal such that when converted to an analog signal and applied to the phase modulators, this signal results in an optical phase shift equal and opposite to the Sagnac (rotation induced) phase shift. The optics, therefore, operate at a null and the phase modulator voltage required to produce the null becomes the measurement of rotation.

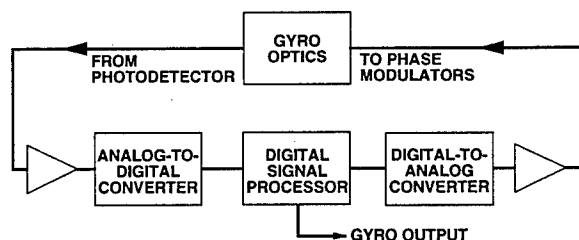


Figure 3. Closed Loop Modulation/Demodulation Electronics Block Diagram. Loop closure drives Gyrocompass IFOG output to null.

Gyrocompass IFOG Demonstration Unit Packaging. Each demonstration unit consists of two modules connected by an umbilical containing both optical and electrical cable as shown in Figure 4. The coil subassembly module consists of optical components, temperature sensors, supporting structures and a magnetic shield. The electronics module is comprised of a chassis, power supplies, modulation/demodulation electronics, electro-optical components, temperature sensors and an

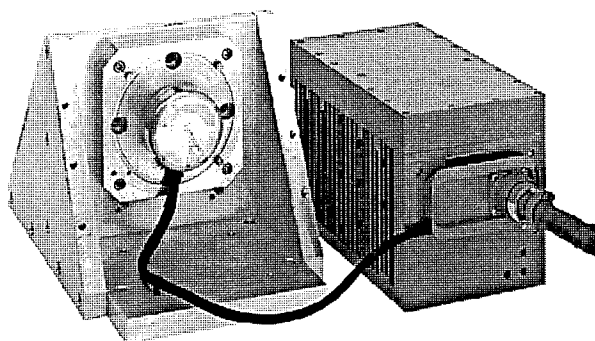


Figure 4. Gyrocompass IFOG Demonstration Unit

input/output connector for test interface to the instrument. The umbilical is not a feature of the baseline Gyrocompass IFOG design and is provided only to facilitate test configuration change-overs and to minimize fixturing complexity.

Gyrocompass IFOG Acceptance Test Procedure. As an essential element in its gyroscope development program, Litton has established and maintained test facilities and analysis techniques which are necessary to assess the status of current designs. The demonstration units were tested on a Contraves rate table mounted to a seismic isolation pier. A computer controlled oven enclosed the rotating rate-table platform and all test data were acquired at intervals from one to sixty seconds under computer control.

Data analysis techniques were applied to allow separation of error sources and to assess residual errors which are present after compensating the Gyrocompass IFOG output. Quantization reduction (triangular) filtering was employed to minimize the gyro noise due to the angle pulse output. An Allan Variance analysis technique implemented in the program "AUTOFIT" was used to allow separation of the angle random walk (ARW) effects, quantization effects, correlated noise, rate random walk effects and bias trending [5].

Calibration. In preparation for the formal testing Litton performed on the deliverable gyros, a set of tests were performed to establish the modeling coefficients of the instrument. These coefficients could then be applied, within a predetermined model, to the data, thereby providing a means for assessing the performance of each of the instruments. The operating range of the gyros during calibration was -5 to $+60^{\circ}\text{C}$ to cover the anticipated operating range with some margin.

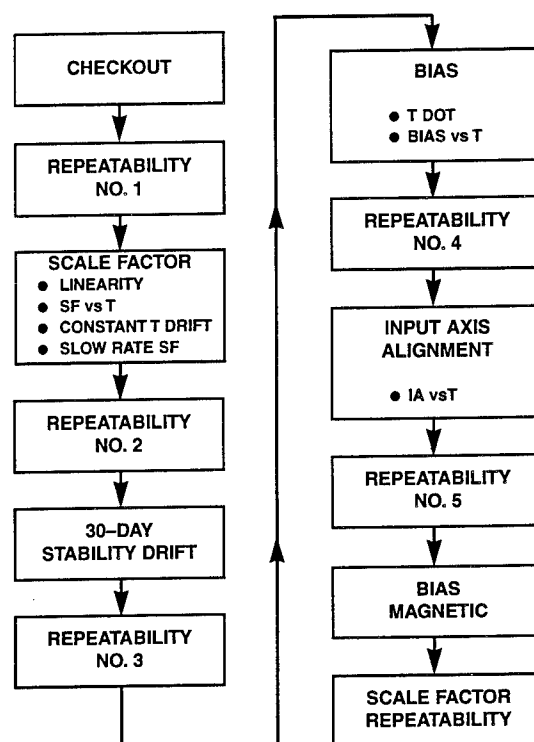


Figure 5. Demonstration Unit Test Sequence

Acceptance Test Procedure (ATP). The purpose of the ATP portion of the program was to measure the performance of the deliverable gyros, to validate the error budget established for the high accuracy IFOG and support the design approach proposed for the next generation high accuracy gyrocompass. The philosophy of the testing was to evaluate the environmental performance and the long-term (> 30 days) drift characteristics of the two demonstration units in a series of environmental tests separated by a sequence of measurements to assess bias and input axis alignment repeatability that was repeated five times throughout ATP. Scale factor repeatability was measured in a separate sequence of tests two weeks in duration. The actual order of testing is shown in Figure 5.

LITTON ACCEPTANCE TEST RESULTS

The Litton acceptance testing of the two Gyrocompass IFOG demonstration units has been completed and the analysis of the data is underway in preparation for a formal Acceptance Test Report. Preliminary results of bias, scale factor and input axis alignment testing are summarized in Table 2. In the table, ATP results are shown in comparison to the goals which were established based

PERFORMANCE PARAMETER	UNITS (1σ)	GOAL	ATP RESULTS	
			DEMO NO. 1	DEMO NO. 2
I. BIAS				
a. Angular Random Walk	deg/rt-hr	0.004	0.0038	0.0033
b. Repeatability	deg/hr	0.007	0.008	0.033
c. Correlated Noise (6-hr time constant)	deg/hr	0.007	0.007	None
d. Rate Random Walk	deg/hr/rt-hr	0.0003	0.00018	0.00029
e. Trend	deg/hr/hr	0.00003	0.000013	0.00003
f. Temp. Model Residual	deg/hr	0.007	0.012	0.007
II. SCALE FACTOR				
a. Linearity	ppm	10	1.1	2.1
b. Asymmetry	ppm	1	0.28	0.62
c. Repeatability	ppm	20	4.5	9.8
d. Temp. Model Residual	ppm	20	15.6	8.6
III. INPUT AXIS ALIGNMENT				
a. Repeatability	arcsecs	2	0.07	0.29
b. Temp. Model Residual	arcsecs	2	0.06	0.29

Table 2. Litton Gyrocompass IFOG Acceptance Tests Results Summary

on system simulations under "worst-case" conditions with no turn-table which would allow in-run bias calibrations.

Bias

The three bias uncertainty tests conducted were bias repeatability, 30-day bias stability, and bias modelability. The bias repeatability was determined through a series of constant temperature drift runs, during which the gyro rotated at earth's rate (Los Angeles latitude, with the input axis vertical). Figure 6 is a plot of the bias measured at periodic intervals throughout ATP for both instruments. The one sigma repeatability of the bias was determined to be 0.008 deg/hr for Demo Unit No. 1 and 0.033 deg/hr for Demo Unit No. 2.

A 30-day bias drift of each instrument was performed to observe the long-term behavior of the gyro bias, and to assess whether or not a turntable should be included as part of the proposed IFOG-based next generation gyrocompass. The gyros were both allowed to drift with their input axis facing true North, using a polar mount, to minimize any drift due to input axis alignment errors. The temperature of the instruments was held constant, and the bias was observed continuously for 33.8 days. Demo No. 2 performance is shown in Figure 7. In addition to the one sigma bias uncertainty of 0.0068 and

0.0081 deg/hr for Demo Unit No. 1 and 2, respectively, the results of autofit analyses presented in Table 2 show that the contributions of the bias drift due to rate random walk and trend for the two instruments meet the goals for the gyrocompass IFOG system.

The bias modelability measurement allows visibility into the correlated noise of the gyro and its constituent parameters. A typical bias drift versus temperature is

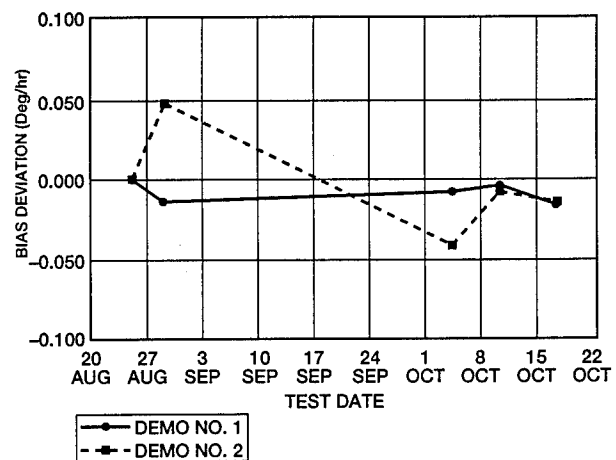
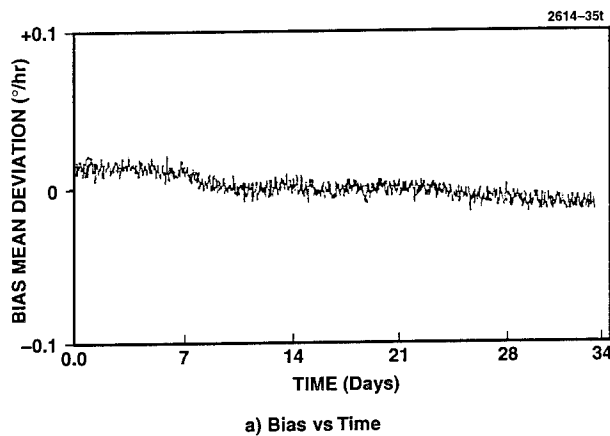


Figure 6. Gyrocompass IFOG Performance — Bias Repeatability



No.	Coefficient	Estimate	Std Err	Err/Est Ratio
1	Trend	.00002	(± 0.00000)	Deg/hr/hr 25.14%
2	Rt Rndm Walk	.00029	(± 0.00004)	Deg/hr/rt-hr 14.96%
2	Angle Rw	.00341	(± 0.00023)	Deg/rt-hr 6.85%

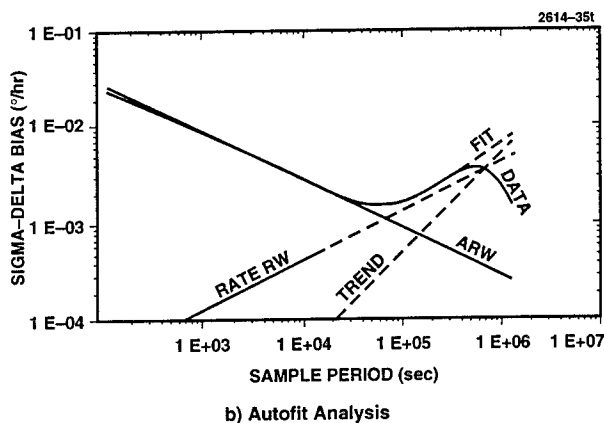


Figure 7. Bias Drift Results over 33-day constant temperature drift run on Demo No. 2.

shown for Demo Unit No. 2 in Figure 8 during which the ambient temperature was varied between 4 and 50 deg C. The figure shows the gyro output after the calibration model and previously measured coefficients were applied, resulting in bias residuals of 0.007°/hr (one sigma).

Scale Factor

The linearity, asymmetry, repeatability and modelability of the delivered gyros' scale factor were evaluated as part of ATP. The linearity and asymmetry of each gyro was determined from a series of three consecutive linearity tests. The scale factor linearity of Demo Unit No. 1 was measured to be 1.09 ppm over a range of

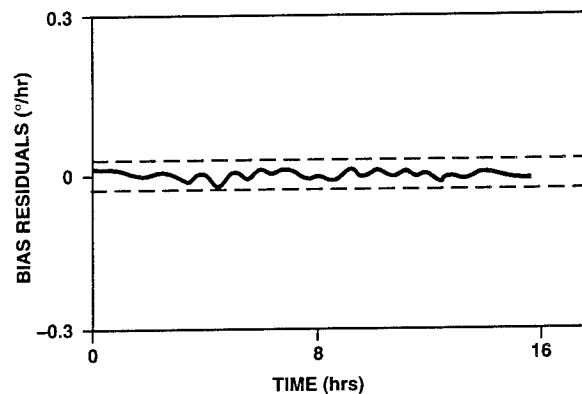


Figure 8. Bias Modelability Test Results for Demo No. 2. One-Sigma value for the bias residuals was measured to be 0.007°/hr after applying a 30-minute filter to reduce angular random walk effects.

± 100 deg/second as shown in Figure 9. The corresponding asymmetry was determined to be 0.28 ppm. The scale factor linearity of Demo Unit No. 2 was measured to be 2.06 ppm, with an asymmetry of 0.62 ppm.

The scale factor repeatability of the gyros was measured by allowing the gyros to rotate at 30 deg/sec in a Maytag fashion (5 revolutions clockwise, then 5 counterclockwise) at constant temperature for 1 hour, during which the scale factor of each instrument was monitored. This test was repeated 30 times throughout a two week period. A plot of the scale factor repeatability of each instrument versus time is presented in Figure 10. The one sigma repeatability for the two gyros were 4.5 and 9.8 ppm, respectively, for Demo Units No. 1 and No. 2.

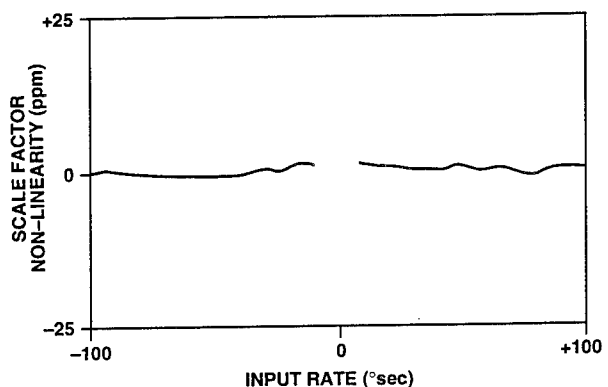


Figure 9. Gyrocompass IFOG Scale Factor non-linearity and asymmetry test results. Non-linearity = 1.09 ppm and asymmetry = 0.28 ppm.

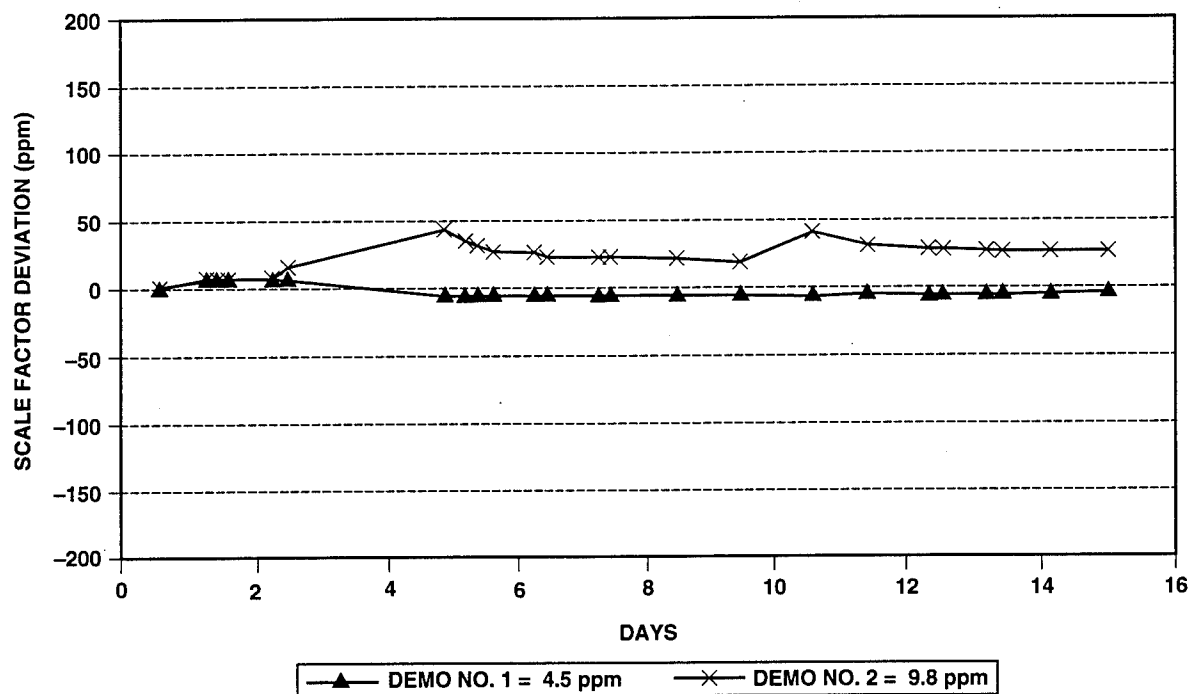


Figure 10. Gyrocompass IFOG Performance — Scale factor repeatability test results

Scale factor modelability measurements were performed by measuring the gyros' scale factor during a temperature profile. Model residuals over 4 to 50 deg C range were measured to be 15.6 and 8.6 ppm for Demo No. 1 and Demo No. 2, respectively.

IA Alignment

As part of the ATP, the input axis alignment repeatability and modelability were measured for each gyro. The input axis alignment repeatability measurements were performed at constant temperature, at intervals throughout the ATP. The results of the input axis alignment repeatability measurements were 0.68 arcsec (one sigma) for Demo Unit No. 1, and 1.2 arcsec (one sigma) for Demo Unit No. 2 as shown in Figure 11.

The input axis alignment modelability was measured while the gyros were subjected to thermal cycling from 4 to 50 deg C. The residual input axis misalignment, after applying the model developed during calibration was 0.29 arcsec for Demo Unit No. 1 and 0.065 arcsec for Demo Unit No. 2.

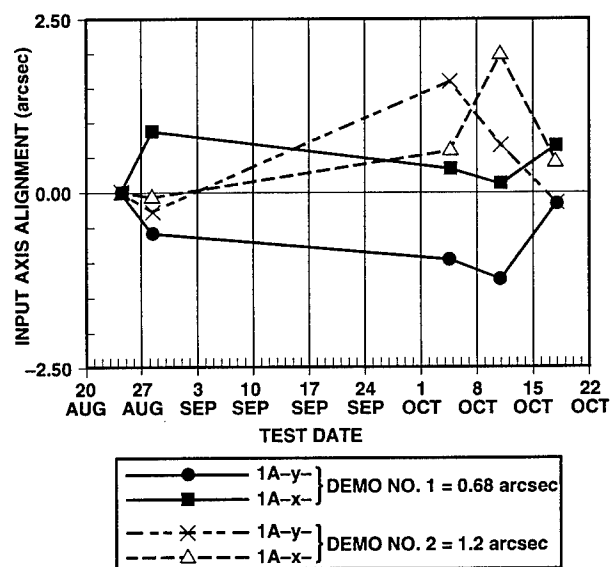


Figure 11. Gyrocompass IFOG Performance — Input Axis Alignment Repeatability

NCCOSC GYROCOMPASS IFOG TEST AND EVALUATION PROGRAM

The NCCOSC laboratory test program is planned to verify the suitability of the Litton IFOG design for the gyrocompass application and to provide the gyro data baseline needed to support the future implementation of fiber optic technology in Navy marine inertial navigation systems. Testing of the Litton Gyrocompass IFOG Demonstration units at NCCOSC's Warminster Inertial Navigational Facility (INFAC) will be conducted in accordance with a Laboratory Gyro Test Plan prepared by NCCOSC [6]. Subsequent to the completion of the laboratory gyro test program, a Final Report will be issued by NCCOSC providing an assessment of the Litton gyro design with recommendations of readiness for transition to a shipboard gyrocompass system development.

Contract gyro hardware was received from Litton on 13 December 1994. NCCOSC has successfully integrated the Demonstration Units with the IFOG test station at INFAC and initiated in-house gyro testing. Data obtained from a 97 hour test run of Demo No. 1 at laboratory ambient exhibited an angle random walk coefficient of 0.004 deg/rt-hr (1σ) which is comparable with the white noise performance level obtained by Litton during Demo No. 1 gyro acceptance testing. NCCOSC in-house scale factor performance testing of Demo No. 1 and Demo No. 2 is in progress.

BIBLIOGRAPHY

- [1] S. Ezekiel and H. J. Arditty, Eds., Fiber Optic Rotation Sensors, Springer Series in Optical Sciences, 32, Springer-Verlag, NY (1982).
- [2] W. K. Burns et al., "Fiber-optic gyroscope with polarization-holding fiber," Opt. Lett., 8, 540 (1983).
- [3] D. M. Shupe, "Thermally induced nonreciprocity in the fiber-optic interferometer," Appl. Opt., 19, 654 (1980).
- [4] N. J. Frigo, "Compensation of linear sources of nonreciprocity in Sagnac interferometers," Proc. SPIE, 412, 268 (1983).
- [5] D. Sargent and B. O. Wyman, "Extraction of stability statistics from integrated rate data," AIAA Guidance and Control Conference, Danvers, MA (1980).
- [6] W. Sapp, J. De Fato, "NCCOSC Test Plan for the Laboratory Assessment of the Litton Second Generation Interferometric Fiber Optic Gyro", Naval Command Control and Ocean Surveillance Center, RDT&E Division Detachment, Warminster, Pennsylvania, 16 May 1994.

THIS PAGE LEFT BLANK INTENTIONALLY

Fiber Optic Gyro for Land Navigation

by

S. M. Bennett, R. B. Dyott, D. Allen, J. Brunner and S. Emge

Andrew Corporation

10500 W. 153rd St.

Orland Park, IL 60462

ABSTRACT

Requirements for a gyroscope intended for use in land navigation in a coupled dead-reckoning/GPS are governed more by cost than by performance. As a result, explicit performance measures are poorly defined. The development of a low-cost fiber optic gyro for this application is described. Using open-loop signal processing, a short coil length, and simple packaging concepts, it represents an evolutionary approach to meeting market demands.

Based on elliptical-core polarization maintaining fiber, fused fiber couplers and an on-fiber polarizer, the components are assembled by fusion splicing. The optical circuit exhibits stability of less than 6 deg/hr RMS, although the overall gyro bias performance exhibits a temperature-dependent offset due to the analog signal processing technique. The optical circuit loss is low, permitting use of a low-power optical source.

INTRODUCTION

We have previously reported the development of a low-cost fiber optic gyro based on all-fiber construction¹. It had the form of a right circular cylinder and contained both the optical and electronic circuits within the same housing. The initial electronics approach was a pseudo-closed-loop circuit², realized with analog electronics. External interfaces were intended to permit operation from unconditioned vehicle power, and either analog or digital data outputs are provided. Our initial experience with this approach, which was intended to cover a wide range of applications with input angular rates from less than 100 to greater than 1000 degrees per second with high linearity and low drift has been satisfactory, but we continue to review the concept to look for further cost reductions. Our cost model allocates approximately 30 percent of the product cost to the electronics, and the current approach is about double that. One of our goals is a very-low-cost fiber-optic gyro that can be built in large quantities, and we have undertaken the development of a

new mechanical configuration and electronics approach as the next step along the way. This is a report on our progress.

The right circular cylinder form factor of the existing gyro is inconvenient for mounting in electronics assemblies or in an inconspicuous way in the trunk of a vehicle, and we have changed the form factor to rectangular with minimum height. Along with a simplification of the electronics approach this permits all of the electronics to be accommodated on a single circuit board. We have retained the vehicle power interface and both analog and digital data output options.

We describe the design philosophy and present some initial results. In addition, we present some test data taken in the automotive environment.

DISCUSSION

Navigation systems for land vehicles are relatively new, with most work dating from the early 1980s, although the concepts, and several actual systems date a decade earlier³. Initially the systems utilized dead reckoning navigation, with a gyro or magnetometer and odometer and, in some instances, rudimentary map matching. More recently, the widespread use of the standard positioning service (SPS) of the Global Positioning System (GPS), including differential GPS (DGPS), has made the location of a vehicle simple and accurate in most instances. There still exists a class of problems where GPS alone cannot be relied upon: urban environments where buildings block the satellite signal and heavily wooded areas where attenuation of the radio waves has a similar result. Dead reckoning functions as a gap filler for those systems where no outage is permissible, but the GPS data can be used to periodically correct the dead reckoning sensors, reducing the demands on each.

As yet, there is no standard specification for performance of a gyroscope in this application, and only some of the parameters, such as maximum angular rate, can be derived from vehicle dynamics considerations. Our perception of the performance requirements are given in Table 1. As the overall system evolves, the specification will become more comprehensive.

Characteristic	Requirement
Rotation Rate, deg/sec	± 100
Scale Factor Linearity: constant temp full temp	< 0.5 percent, rms < 1 percent, rms
Scale Factor vs Temperature	< 1 percent
Angle Random Walk, deg/hr/rt-Hz	20
Instantaneous Bandwidth, Hz	100
Bias Drift, deg/sec	0.025 (fixed temp) 0.050 (temp range) 0.025 (repeatability)
Temperature range, deg C Operating Storage	-40 to +75 -50 to +85
Power Supply Voltage, VDC	+12
Output Data Analog Digital	TBD 16 bits, serial, RS-232
Power Consumption Analog Digital	< 2 watts < 3 watts
Cost (qty 1 x 10⁶), \$	100

Table 1. Fiber Optic Gyro Performance Requirements

We believe that the angle random walk specification needs to be as low as possible, consistent with cost, as this influences the speed with which the bias offset can be estimated when the vehicle is stopped. Our experience with the digital output is that the 12 bit data in our previous design did not result in the least significant bit being consistently

toggled by the gyro angle random walk, and the estimate of bias offset contained an error which could be significant in some applications. For our new design, we have chosen to err on the side of excess, using a 16 bit ADC.

The all-fiber interferometric fiber-optic gyro shown in Figure 1. uses fiber for the coil, couplers and polarizer. Bias modulation is mechanically applied by a piezoelectric transducer (PZT). The PZT has a very limited bandwidth, and closed-loop operation is not possible, but the cost of the components is low, and an integrated optics chip (IOC) is avoided.

The usual minimum configuration is employed, with a 3dB directional coupler attached to the polarization-maintaining fiber coil, connecting the coupler to an on-fiber polarizer. The source-detector coupler is polarization maintaining as well, and a conventional laser diode operated below threshold yields a sufficiently broad band source to ensure a short coherence length in the fiber. Aided by the properties of **ECORE®** fiber which has low sensitivity to temperature and physical stress, this reduces the effect of polarization cross-coupling points on bias drift. Our objective is to reduce the overall insertion loss of the gyro optical circuit in order to employ the lowest power source possible. In addition to reducing overall power consumption, it gives us a wider choice of sources.

The optical circuit is integrated with the electronics in a rectangular form factor enclosure which measures (4.25 in x 3.25 in x 1.5 in) and is shown in Figure 2. Both the analog and digital output versions appear identical and differ only in the output interface circuitry. The unit operates from +12 VDC unconditioned power such as would be found in an automobile. The data presented here are for a typical analog output instrument.

From a cost viewpoint, we believe that the very lowest cost fiber optic gyro will have to use a synchronous detector operating at the fundamental frequency of modulation. As is well known, the optical scale factor and modulation depth must be tightly controlled in order to minimize scale factor variation with temperature. In addition, the output response exhibits a sinusoidal variation with rate. Control of the optical scale factor is achieved by a circuit that maintains a constant optical power at the detector, while the sinusoidal variation is minimized by employing a coil with a small Sagnac scale factor compared with the maximum specified rotation rate (Figure 3).

Achieving the specified angle random walk depends on the source power, and meeting the overall optical loss budget. Table 2 summarizes the loss values associated with typical components used in the manufacture of our gyro. Since our report last year, we have made progress in reducing both the insertion loss of some of the components and the number of splices. Table 3 compares the insertion losses used in our design budget in June 1994 and April 1995. Except for the coil, whose length has been reduced from 150 to 50 meters, the loss reductions have been a result of reduced variability in the component manufacture.

Component	Maximum Insertion Loss (one-way), dB	
	July 1994	April 1995
Directional coupler	0.5	0.5
Polarizer	1.5	1.0
Source Polarization Loss	1.5	1.5
Coil	1.2	0.4
Splice	0.5	0.4

Table 2. Optical Component Losses

Table 3 applies these component loss characteristics to the "minimum" configuration gyro, which we assemble with a total of 3 splices. We have eliminated the splices previously used to attach the source and detector to the directional coupler. This reduces the number of splice transits to 6. We are developing a combination directional coupler and polarizer, which will eliminate a further splice, resulting in only 4 splice transits per optical circuit.

Path	Loss, dB	
	July 1994	July 1995
Splice transits (8,4)	4	1.6
Polarizer transits (2)	3	2.0
Source polarization (in polarizer)	1.5	1.5
Directional coupler transits (4)	2	2
Coil	1.2	0.40
Coupler splitting loss (source-detector)	6	6
Total Optical Path	18	13.5

Table 3. Optical Circuit Loss Budget

Andrew Corporation has developed an elliptical-core polarization-maintaining fiber, which is the basis of the fiber components of this gyro. The fiber is produced in two cladding cross sections: circular and D-shaped. The D-shaped fiber is useful for fabricating components, such as directional couplers and polarizers. The overall diameter of the fiber matrix is 80 microns, which has become standard in the production of fiber optic gyros as the best compromise between reducing the bending stresses associated with coiling and the practical aspects of fiber splicing. The fiber is protected from damage by a dual-acrylate coating, whose primary layer has a glass transition temperature below the minimum gyro operating temperature.

The individual optical components have previously been described, but are summarized here. The directional coupler made with D fiber which has been etched, threaded in a tube which has been collapsed around it, and subsequently thermally diffused. The characteristics are stable with temperature, as there are no dissimilar expansion coefficients in the coupling area. We also have developed an on-fiber polarizer, made with D-fiber, which is an approximately 7 cm long region of the fiber where etching has exposed evanescent fields which interact with a deposited layer of indium. Various optical sources have been evaluated in our devel-

opment program, and several conventional laser diode sources have been found to yield acceptable coherence lengths in the context of the overall optical system.

It is important that there should be only one optical path through the Sagnac interferometer, comprising the polarizer, coupler and coil. There is the likelihood that any discontinuity to the guided light wave, such as that produced by a splice or by the fused region of the coupler, will couple optical power from one mode in the elliptical fiber to the orthogonal mode, which has a different propagation constant. In order that these coupling points be phase-incoherent, the distance between them must be greater than the decoherence length:

$$L_{DC} > \frac{L_S}{\Delta n_g} \quad (1)$$

where L_S is the coherence length of the source with wavelength λ and a line width $\Delta\lambda$.

$$L_S = \frac{\lambda^2}{\Delta\lambda} \quad (2)$$

and Δn_g is the difference in group refractive index between the two fundamental modes.

$$\Delta n_g = \Delta\bar{\beta} - \lambda \frac{d(\Delta\bar{\beta})}{d\lambda} \quad (3)$$

where $\Delta\bar{\beta}$ is the normalized birefringence. The fiber is designed to operate near the point of maximum birefringence⁴ where the second term in (3) is zero.

For elliptical-core fiber with an axial ratio of 0.5,

$$\frac{\Delta\bar{\beta}}{(\Delta n)^2} = 0.2$$

With a typical refractive index difference between the core and cladding of $\Delta n = 0.035$, the normalized birefringence is

$$\Delta\bar{\beta} = 2.45 \times 10^{-4} \quad (4)$$

For a source wavelength of 815 nm and a line width of 20 nm, the source coherence length is

$$L_S = 3.32 \times 10^{-5} \text{m} \quad (5)$$

and substituting in (1), we find that the decoherence length to be 0.135 meters. This is easily obtained with the all-fiber gyro construction method.

Temperature changes are manifest in both modelable and unmodelable variations in the bias offset. The wide temperature environment in which land vehicles operate, such as leaving a heated garage in winter, make the unmodelable portion of the bias offset an important parameter. Fig 4 illustrates the performance of a typical optical circuit, utilizing laboratory electronics. The data represents a single cycle temperature excursion in a thermal chamber at a rate of 1 deg C/minute, and exhibits a RMS value of 0.002 deg/sec (6 deg/hr). The measurements were made on a 75 meter coil of 66mm diameter, and are indicative of the results expected from the shorter coil that we have decided to use. The bias trend with temperature is believed to be the result of electronic pickup of the dither modulation, as it is not characteristic of the Shupe effect. It is small in the context of the product specification. The electronics offset variation with temperature is expected to be somewhat greater than this, but has not as yet been measured. The modelable temperature dependence of scale factor is shown in Figure 5, which includes the source wavelength temperature dependence.

An informal road test of the gyro was conducted to determine if there were any artifacts that were not uncovered by preliminary laboratory testing. A digital gyro was mounted to the floor of a light truck with Velcro and the data collected at 0.1 sec increments by a portable computer. The data shown is for a 15 minute segment of on-the-road driving in suburban Chicago. Figure 6 is the angle rate data. It is measured as the average rate per 0.1 seconds and expressed as an equivalent instantaneous rate. The vehicle angle change is the integral of this rate, and is shown in Figure 7, with the initial angle arbitrarily set to zero. Initially, the vehicle was parked in the company parking lot, and the maneuvering in the half minute brought the vehicle onto the public roads. Although we are located almost 35 miles from the center of Chicago, the road grid system extends well outward, especially to the southwest, and the first several turns result in navigating the right angle turns in the immediate vicinity. After 600 seconds the character of the roads changes and at about 660 seconds a short winding section is encountered. The remainder of the run has similar characteristics. The final 60 seconds of data is for the vehicle stopped, but with the motor running. One can see that the rate data is quieter than when in motion, and only the least significant bit is toggled.

The manufacture of components is now well established, and many of the processes are being automated as they mature. Assembly of the gyro, comprising fusion splicing of the optical components, recoating the fiber, packing into the housing, integration with the electronics assembly and final test is still evolving. Figure 8 is a view of our final assembly and test cell, which has a current one-shift capacity of 1500 gyros per year. Methods developed in this area will be used in the manufacturing scale-up process.

CONCLUSION

Low-cost fiber optic gyros appear to be practical to manufacture, providing that the specifications are modest, and a simple approach to design is taken. Continuing development of each of the component parts is required, but the assembly and test phases of manufacture are becoming more important as we near our goal.

REFERENCES

1. D. Allen, S. M. Bennett, J. Brunner, and R. B. Dyott, "A low cost fiber optic gyro for land navigation", SPIE vol. 2292, Fiber Optic and Laser Sensors XII (1994), 203-217.
2. A. B. Tveten, A. D. Kersey, E. C. McGarry and A. Dandridge, "Electronic Interferometric Sensor Simulator/Demodulator", Optical Fiber Sensors 1988 Technical Digest Series, Volume 2, Part 1, 277-290.
3. R. L. French and G. M. Lang, "Automatic Route Control System", IEEE Transactions on Vehicular Technology", Vol CT-22, May 1973, 36-41.
4. R. B. Dyott, J. R. Cozens and D. G. Morris, "Preservation of Polarization in Optical-Fibre Waveguides with Elliptical Cores", Elec. Lett., Vol, 15, No. 13, June 21, 1979, 380-382.

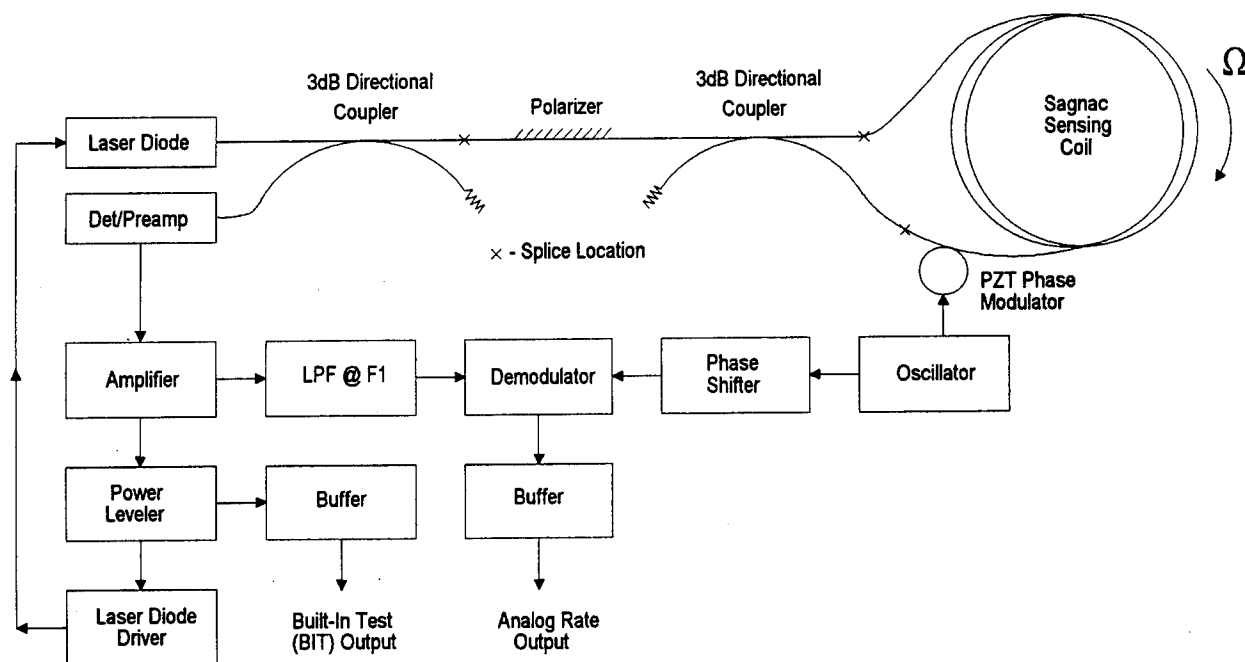
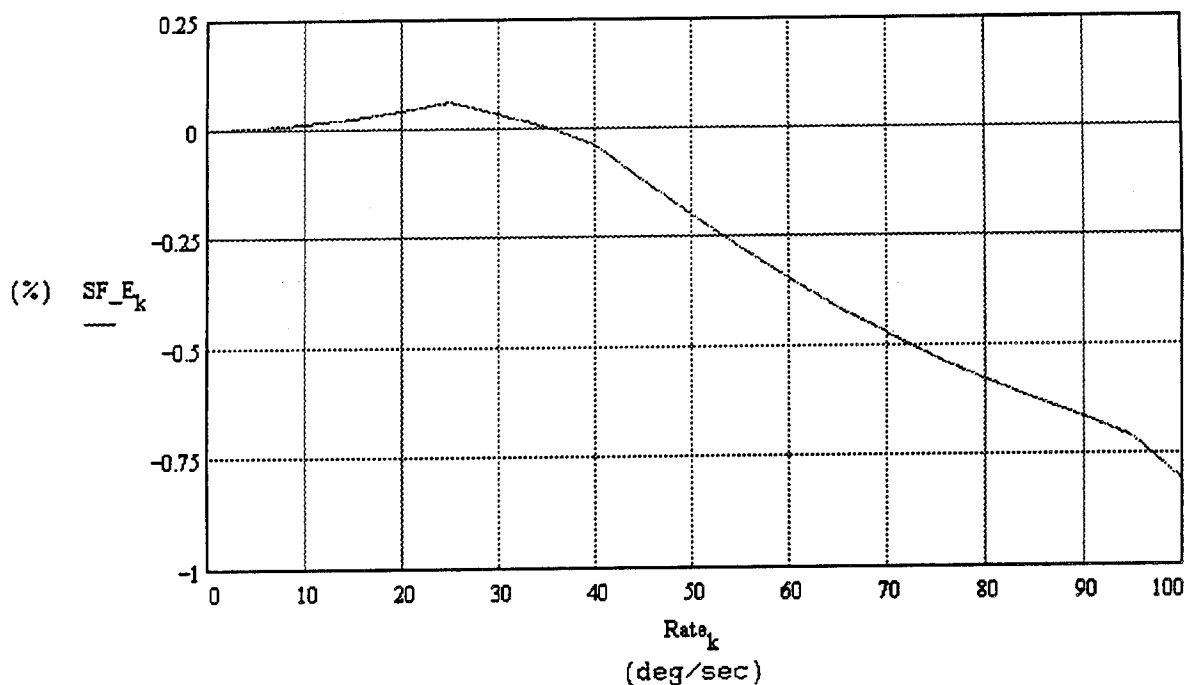


Figure 1. Optical and Electrical Block Diagram



Figure 2. Gyro Packaging



$SF_{E_{rms\ 50}} = 0.0758$ % RMS, SF Non-linearity, 0-50 °/sec.

$SF_{E_{rms\ 100}} = 0.3941$ % RMS, SF Non-linearity, 0-100 °/sec.

Figure 3. Predicted Scale Factor Linearity Response

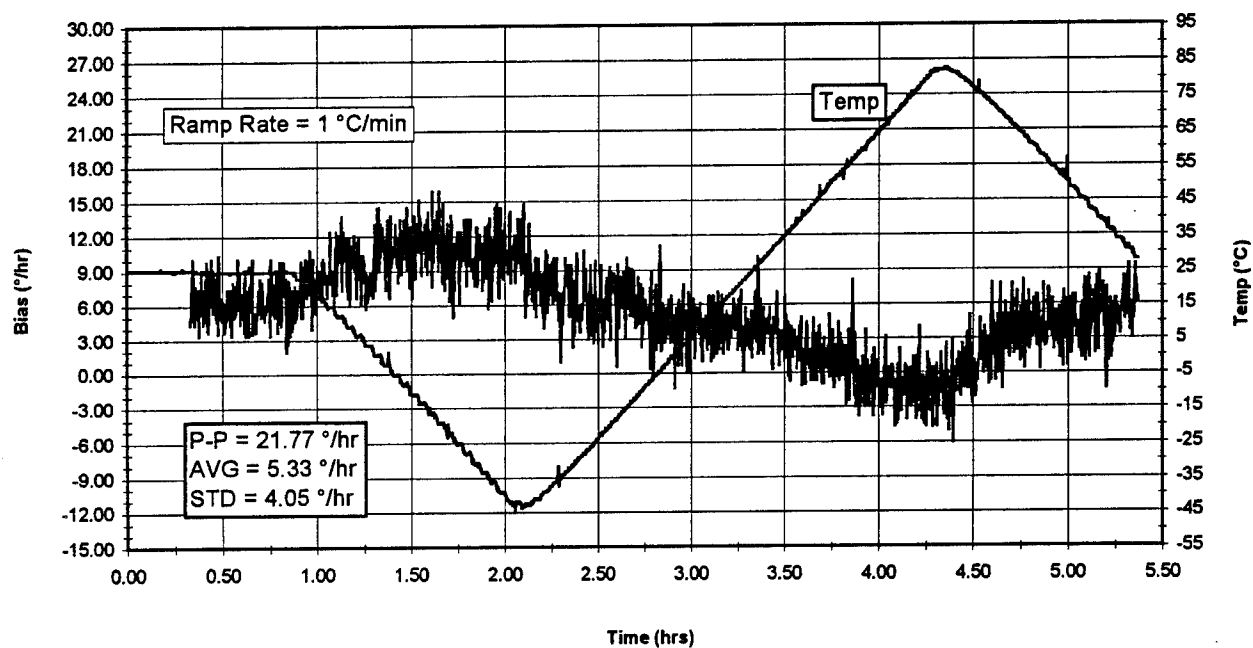


Figure 4. Bias vs Temperature Response for Optical Circuit

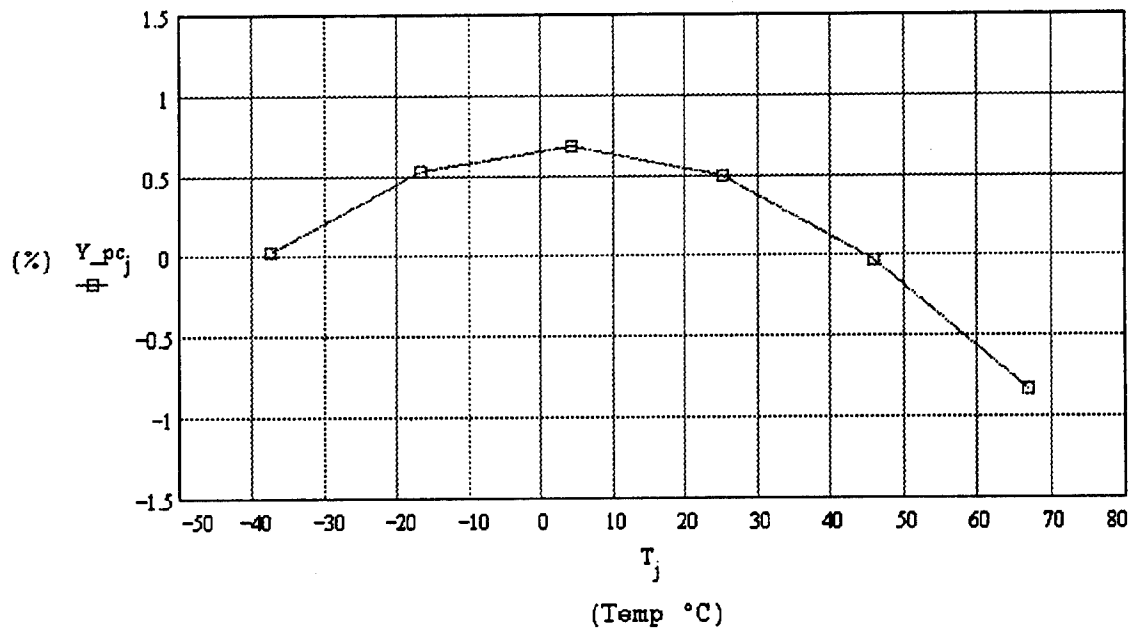


Figure 5. Predicted Scale Factor vs Temperature Response

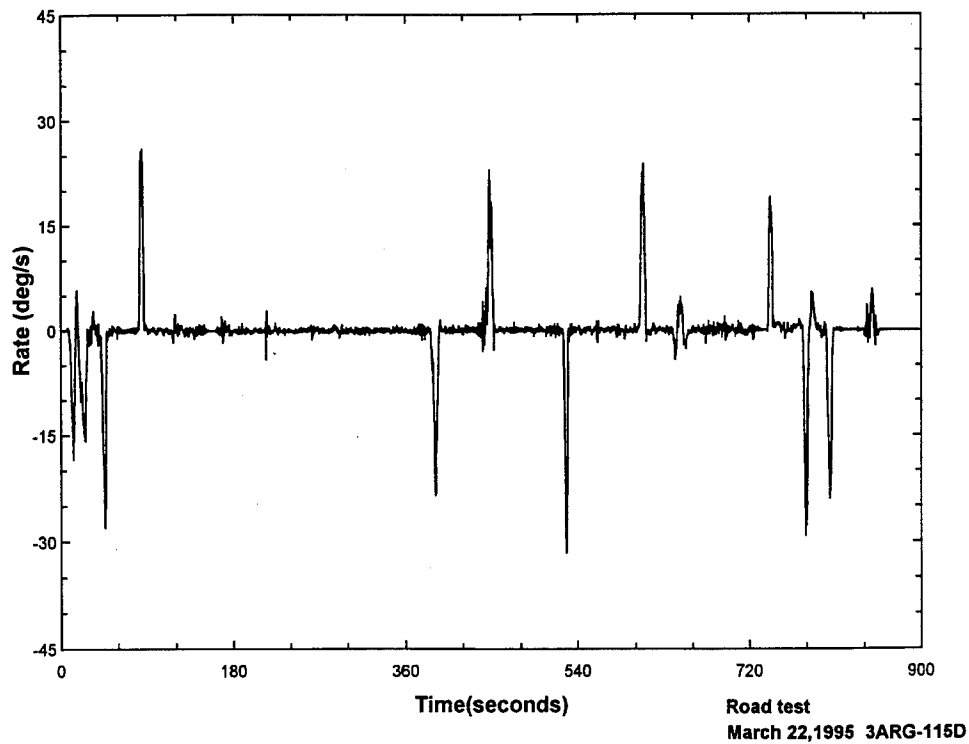


Figure 6. Rate Data from Road Test

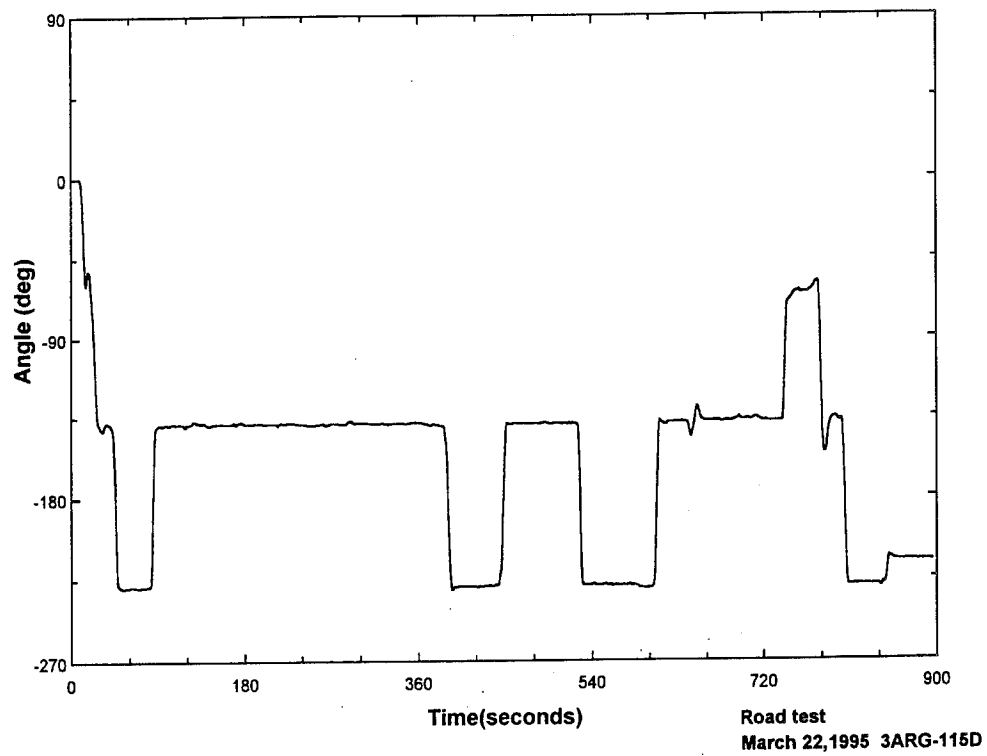


Figure 7. Angle Data from Road Test



Figure 8. Gyro Assembly and Test Cell

THIS PAGE LEFT BLANK INTENTIONALLY

SESSION II-B
INTEGRATED GPS I

CHAIRMAN

LT COL ROBERT RIGGINS

*AFIT/ENG
WRIGHT-PATTERSON AFB OH*

THIS PAGE LEFT BLANK INTENTIONALLY

MAPS HYBRID ENGINEERING AND DEVELOPMENT TEST RESULTS

Brian E. Fly
Honeywell Military Avionics
Guidance and Navigation Operation
11601 Roosevelt Blvd
St. Petersburg, FL 33716-2202
813-579-6733
FAX: 813-579-6832

Michael D. Slama
US Army Topographic
Engineering Center
ATTN: CETEC-TD-GS
7701 Telegraph Rd, Bldg 2592
Alexandria, VA 22310-3864
703-355-2821
FAX: 703-355-3176

Abstract

This paper presents the Engineering and Development Test (EDT) results of the Modular Azimuth Position System Hybrid (MAPS-H) program. The MAPS-H land navigation and orientation system consists of the Honeywell Dynamic Reference Unit-Hybrid (DRU-H), the Precision LightWeight GPS Receiver (PLGR), the Vehicle Motion Sensor (VMS), and a system unique Control Unit (CU). The MAPS-H program is being developed by the US Army PM Paladin/FAASV Program office which is upgrading the present MAPS DRU to integrate with the PLGR. The PLGR is the standard hand-held GPS receiver for the DoD, and the MAPS is the standard land navigation (positioning and orientation) system for the US Army. Current US Army systems using the MAPS are the M109A6 Paladin Self Propelled Howitzer, the AN/TPQ-36(V)7 and AN/TPQ-37 FireFinder Radar Systems. The MAPS-H has completed EDT testing at Aberdeen Proving Grounds (APG), Maryland and at Yuma Proving Grounds (YPG), Arizona. EDT was performed by the Combat Systems Testing Activity (CSTA) in order to validate the design and software enhancements prior to the start of the formal qualification testing. This paper provides the results of the following tests:

Operational/Performance test results in the HMMWV test vehicle

Operational/Performance test results in the Paladin

Operational/Performance test results in the FireFinder vehicle

Dynamic Alignment (capabilities and limitations)

Added capabilities of the MAPS-H versus the MAPS or PLGR (stand alone)

Kalman Filter improvement for compensation of gravity anomalies and deflections

In addition, this paper will address some of the unique test equipment developed for the effort and many of the challenges encountered, and solutions which were implemented.

Introduction and System History

The MAPS Hybrid is a self contained inertial positioning and pointing system that operates in conjunction with a Precision Lightweight GPS Receiver (PLGR), for use in survey, radar, weapon and target acquisition systems. Honeywell has been under contract with PM Paladin since September, 1992 to develop and integrate the PLGR with the DRU. The combined system provides initial position coordinates, position aiding and inertial error bounding during travel, and allows for Dynamic Alignments. The MAPS Hybrid system has completed Engineering Development Testing (EDT) and the results of this test phase are presented herein.

MAPS History

The Modular Azimuth Position System (MAPS) program was started in 1983 as part of the Howitzer Improvement Program (HIP). The MAPS consists of three components, the Dynamic Reference Unit (DRU), the Control and Display Unit (CDU) and the Vehicle Motion Sensor (VMS). The DRU is the position/orientation component, the CDU is the man/machine interface, and the VMS reads speedometer rotations (providing inertial damping to the DRU). Three contractors participated in MAPS initial development, Honeywell, Litton, and Singer. At the conclusion of the development effort, Honeywell was chosen for DRU production.

The HIP program was eventually replaced with the Paladin Program, and the first production DRU was delivered to the Paladin program in March of 1993. The production DRU is currently used on the M109A6 Paladin, the FireFinder TPQ-36, and has been selected for the FireFinder TPQ-37. International applications include the British Warrior Forward Observer Post Vehicle and the Swedish POS2 system for use with the Bkan 1 (Self propelled Howitzer), FH 77B Towed Howitzer, EPBV 90 and EPBV 3022 Target Acquisition Vehicles, the BV206 equipped with the Artillery Hunting Radar (ARTHUR), and the Tgb 11 Artillery Survey and Reconnaissance Vehicle. Other applications that are using the DRU include the Ground Based Radar (GBR) program, various mortar improvement programs, the Theater High Altitude Air Defense (THAAD) program (launch vehicles), the Advanced Field Artillery System (AFAS) program, and the Large Area Mobile Projected Smoke System (LAMPSS). Also, the DRU (repackaged with additional capabilities) is being considered as a Position and Azimuth Determination System (PADS) replacement. Civilian applications include use by the Naval Surface Weapons Center for a position/orientation reference, and NASA Wallops Island as a ship board navigator and attitude reference unit. Also, the Air Force uses the system on a robotic runway grader. Finally, the Bureau of Mines uses it for mine surveying and various mining companies are using the DRU for orientation of their mining machines in both high wall and tunneling applications.

MAPS Hybrid History

The next logical step for the MAPS program was to integrate a Global Position System (GPS) receiver into the MAPS DRU. It was the objective of the Department of Defense (DoD) and the Joint Program Office (JPO) to limit the proliferation of the GPS receivers and therefore directed PM Paladin to use the Precision Lightweight GPS Receiver (PLGR) as the GPS receiver for the integration effort. The combined system of modified DRU and PLGR is the MAPS Hybrid, and the DRU became the DRU Hybrid (DRUH). The MAPS Hybrid contract was awarded to Honeywell in September 1992. The program consists of 4 phases. Phase I was System Development and ran from September 92 to April 94. Phase II was Engineering Development Testing (EDT) and it ran from May 94 to February 95. Phase III will be Qualification Testing and it will run from May 95 to September 95. Phase IV will be Production Planning and it will run from Oct 95 to June 96.

MAPS Hybrid System Description

The MAPS Hybrid (reference Figure 1) consists of a DRU Hybrid, a PLGR, a VMS, a Control and Display Unit (CDU), system interconnection cables and a DC power source. In the Paladin, the CDU consists of the Automatic Fire and Control System (AFCS) which not only interfaces with the DRUH, but also provides ballistic calculations, automatic laying of the weapon, and backup power. For the TPQ-36, the PM FireFinder office is developing an improved CDU Hybrid that provides the operator with position, attitude and system information. However, since the MAPS Hybrid system is modular, the user is not required to utilize a PLGR and VMS, and therefore these items are not used in all applications. The various components of the MAPS Hybrid system are as follows:

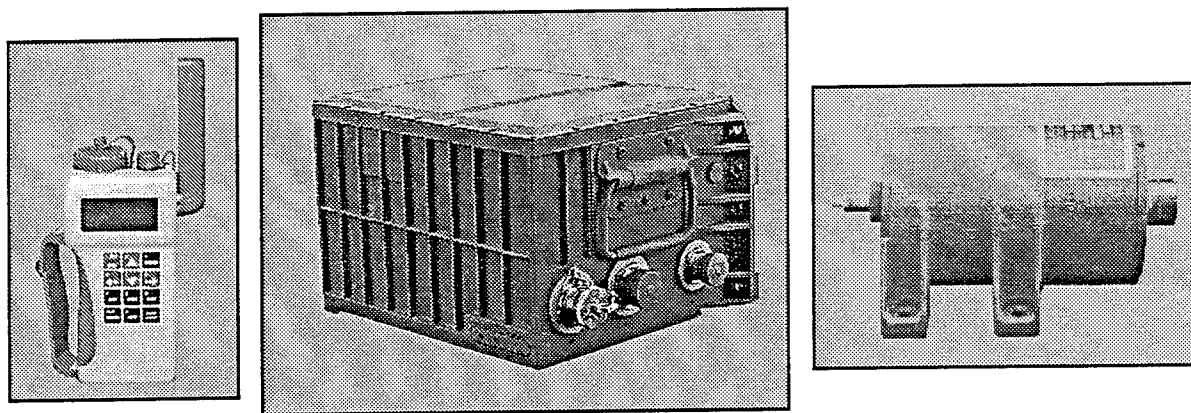


Figure 1. MAPS Hybrid Components

DRUH: The DRUH hardware differs from the DRU in that it communicates with the PLGR over a dedicated RS-422 data bus line. It also incorporates a standard MIL-STD-1553B data bus, and has an improved navigation processor board. Survey software can be electronically loaded over the data bus lines, and the DRUH is backwards compatible with standard MAPS software and application configurations. The improvements to software include expanded status message, new PLGR related BIT, RS422 and 1553 bus commands, expanded configuration data, geodetic data information, 1553 data bus structure, software download commands, dynamic alignment, absolute and relative GPS aiding, and datum conversions (including operator defined datums). The rest of the DRUH matches the standard production DRU hardware currently being delivered to a variety of customers. Therefore, it is not expected that the current DRU Mean Time Between Failures (MTBF) will decrease from the current 19,054 hours that has been calculated from the fielded Paladin unit data.

PLGR Mount and Antenna: The PLGR is the DoD standard hand held GPS receiver (AN/PSN-11). Honeywell has designed and developed the associated cables, the PLGR vehicle power supply, and the PLGR Remote Antenna which will be used in the Paladin Howitzer and the FireFinder vehicles. The MAPS-H program also had to develop its own PLGR mount for the Paladin Howitzer because of gunfire shock and vibration environments which are experienced in this vehicle. The PLGR Mount employs shock isolators that allow the standard (supplied) PLGR mount to be used in the howitzer. Additionally, the mount is used in the TPQ-36 because of security concerns. The remote antenna assembly was designed to match the SINCARS antenna bolt pattern and spring design and therefore can be easily installed on most Army vehicles. The PLGR remote antenna is designed to raise the antenna above any obstructions on the vehicle that might block, shade or interfere with GPS signals. This antenna assembly has been selected for use on the Field Artillery Ammunition Support Vehicle (FAASV). Other Army

systems, such as the FOX vehicle, have also tested the PLGR antenna design. Finally, the PLGR power is derived from the host vehicle through a modified PLGR power cable.

Vehicle Motion Sensor: The VMS is an odometer pick-off unit that measures speedometer rotations (forward and reverse odometer pulses which represent incremental distance traveled) and transmits this data over a RS-422 bus to the DRUH to bound inertial errors. The VMS is currently used on the Paladin, TPQ-36, and TPQ-37 and a variety of international vehicles.

Control and Display Unit: The CDU used in the Paladin is the AFCS which is the man/machine interface for all operations in the Paladin. An engineering version of AFCS software has been developed to operate with the MAPS-H system during the upcoming Qualification Testing which the Government will conduct. Although this software will not be used in the field, it will be the baseline for further upgrades of the Paladin AFCS. The CDU used in the TPQ-36 is being upgraded to interface with the MAPS-H system. The FireFinder CDU is a hand held unit which performs basic DRUH command and control. Operational capabilities include initial position entry, position display in UTM coordinates, azimuth output, MAPS-H system control (GPS Enabled/Disabled, VMS Enabled/Disabled), and system status, alerts, or BITs. The CDU Hybrid will undergo qualification as part of the MAPS-H Qualification testing effort.

MAPS-H EDT Overview

MAPS-H Engineering Development Testing (EDT) started on 2 May 94 at Aberdeen Proving Grounds, Maryland. The program plan was to deliver 3 drops of MAPSH software during EDT to allow software maturity to progress during testing. Because of the modular design, a variety of system configurations and alignment types had to be tested. These configurations break down as follows:

System Survey Configurations:

Free Inertial (FI): DRUH is aided by Zero Velocity Updates (ZUPTs) to bound inertial errors. No PLGR or VMS used.

Odometer Aided (OA) - DRUH is aided by VMS. No PLGR, and ZUPTs are used fortuitously.

Integrated (IN) - DRUH is aided by the PLGR, VMS and ZUPTs.

Alignment Types:

Static Alignment (STA) - A standard 15 minute (or less) stationary alignment between latitudes between 65° North and 65° South. The DRUH can gyrocompass at latitudes up to 84° North with degraded accuracy. Anytime that the host vehicle stops for more than 30 seconds, the DRUH will automatically revert to gyrocompass alignment and continue refining the azimuth accuracy. This capability eliminates degradation of the azimuth alignment accuracy as a function of time.

Stored Heading Alignment (SHA) - A 35 second alignment is available if the vehicle had not been moved since the DRUH was shutdown. For a stored heading alignment, the DRUH simply stores the azimuth of the DRUH at shutdown in an EEPROM location and then uses this data at the next turn on. If the DRUH determines that the stored azimuth agrees with the present azimuth within a preset limit, then the DRUH declares SHA valid and transitions to the Survey Mode. In addition, several other tests are performed to determine whether the vehicle has been moved between the shutdown and the subsequent application of power. If any of these tests fail, the DRUH will revert to a standard gyrocompass static alignment.

Dynamic Alignment (DYN) - An alignment performed while the vehicle is moving. The system must be configured in the Integrated mode. This mode is discussed in more detail in the Hybrid Features section of this paper.

The following table recaps the various alignment modes of the DRUH:

Alignment Mode	PLGR Status	VMS Status	Time to complete	Comments
Dynamic	required EPE < 16 meters	used if available	15 minutes nominal Will decrease to 5 minutes once DRUH estimated azimuth PE < 1 mil	Automatic entry into dynamic alignment mode
Static	N/A	N/A	15 minutes nominal between 65° N and 65° S latitudes	Automatically decreases time to complete based on present latitude
Stored Heading	N/A	N/A	35 seconds from initiation of command	Requires no vehicle motion since last power down

During EDT, it was not possible to perform all combinations of configurations with each software version, because of time and equipment requirements. Therefore not all software versions were run in each vehicle, but most probable mission scenarios were performed and validated during the EDT effort.

Because of the upgraded performance capabilities of the MAPS-H, some innovative test measuring equipment had to be developed. One such device is the CDU Simulator (CDUS). The CDUS is a ruggedized 486 based portable lightweight computer (LCU) which allows for operator interaction with the DRUH. Not only can position and configuration data be sent to the DRUH via the CDUS, the CDUS also can examine, store, and or modify any of the DRUH memory addresses. The CDUS incorporates a digital I/O board for setting programmable discretes in the DRUH (software loading, vehicle configuration flags, and Hybrid/MAPS mode) and can communicate over any of the DRUH RS-422 Busses and 1553 Busses. The CDUS can operate either on 120 volt AC or 24 volt DC power which makes it an ideal field test computer. Additionally, the CDUS is based on the same system as the U.S. Army Computer Test Set (CTS) so it can be used for field trouble shooting of the DRUH.

Another support system developed for the test program is a Differential GPS positioning system. This DIF-GPS system was developed by the US Army Topographic Engr Center (TEC) for the Corps of Engineers for real time, on the fly, corrected GPS positions. The Combat System Test Activity (CSTA) worked with TEC to develop a similar system that could be used at APG to position test equipment to within 0.5 meters CEP (Circular Error Probable). The DIF-GPS system can interface with the CDUS to allow simultaneous data collection of the DIF-GPS and the MAPS-H. This data can then be processed for comparison of the DRUH position output to that of the DIF-GPS. The DIF-GPS is only limited by the range of the data transmission devices (radios).

MAPS Hybrid EDT Results

The results of the EDT effort are shown in the following tables. The data is segregated into the host vehicle type (i.e., HMMWV, Paladin, or FireFinder) and is presented by the type of mission. As can be seen from the results, the MAPS-H performed at approximately 35% of the specification requirement.

Table 1. HMMWV Data

DRUH Configuration	S/W Drop	Number of Missions	Horizontal Error (CEP, m)	Altitude Error (PE, m)
STA/SHA -FI	1	5	5	4
	2	16	4	1
	3	2	1	1
Requirement			18	10
STA/SHA-OA	1	12	0.12% x Dist Trav	0.03% x Dist Trav
	2	53	0.12% x Dist Trav	0.03% x Dist Trav
	3	23	0.10% x Dist Trav	0.04% x Dist Trav
Requirement			0.25% x Dist Trav	0.067% x Dist Trav
STA/SHA-IN	1	27	8	6
	2	58	8	3
	3	6	7	4
Requirement			10	10
DYN-IN	1	N/A	N/A	N/A
	2	61	6	4
	3	18	5	5
Requirement			10	10



Figure 2. HMMWV Test Vehicle

Table 2. Paladin Data

DRUH Configuration	S/W Drop	Number of Missions	Horizontal Error (CEP, m)	Altitude Error (PE, m)
STA/SHA -FI	1	10	2	1
	2	-	-	-
	3	2	1	1
Requirement			18	10
STA/SHA-OA	1	12	.13% x Dist Trav	.05% x Dist Trav
	2	2	.16% x Dist Trav	.04% x Dist Trav
	3	-	-	-
Requirement			0.25% x Dist Trav	0.067% x Dist Trav
STA/SHA-IN	1	17	5	3
	2	-	-	-
	3	-	-	-
Requirement			10	10
DYN-IN	1	N/A	N/A	N/A
	2	6	5	3
	3	-	-	-
Requirement			10	10

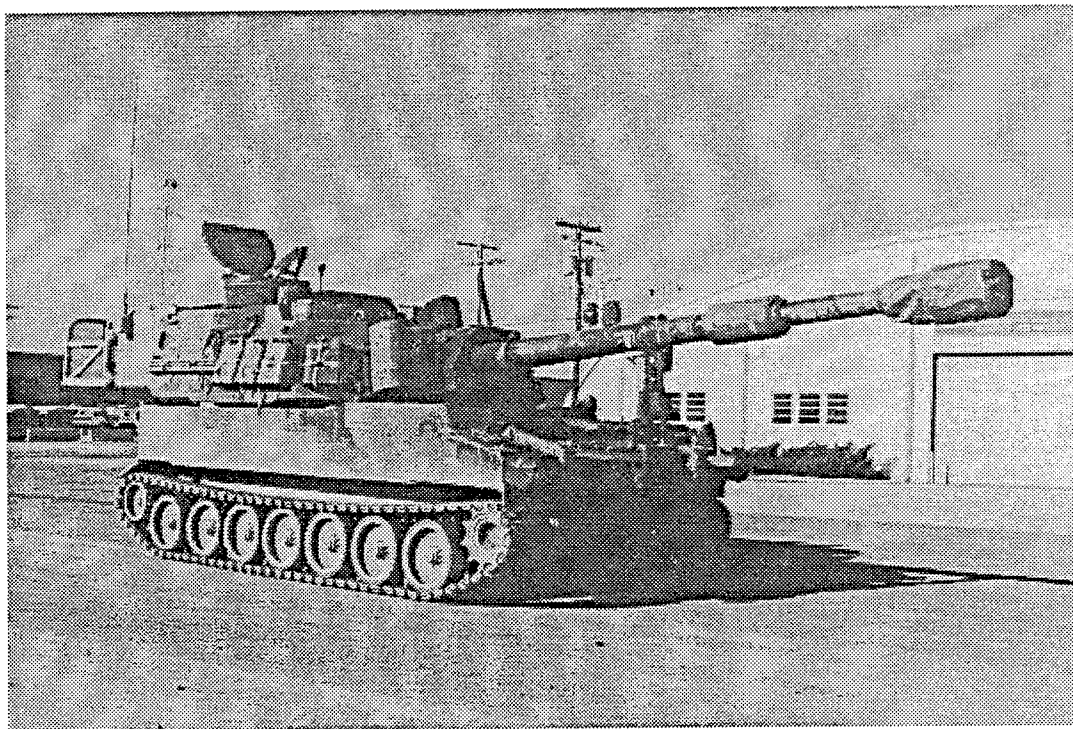


Figure 3. Paladin Howitzer

Table 3. FireFinder Data

DRUH Configuration	S/W Drop	Number of Missions	Horizontal Error (CEP, m)	Altitude Error (PE, m)
STA/SHA -FI	1	N/A	N/A	N/A
	2	5	2	1
	3	-	-	-
Requirement			18	10
STA/SHA-OA	1	N/A	N/A	N/A
	2	48	.08% x Dist Trav	.04% x Dist Trav
	3	-	-	-
Requirement			0.25% x Dist Trav	0.067% x Dist Trav
STA/SHA-IN	1	N/A	N/A	N/A
	2	23	7	3
	3	-	-	-
Requirement			10	10
DYN-IN	1	N/A	N/A	N/A
	2	8	3	4
	3	-	-	-
Requirement			10	10

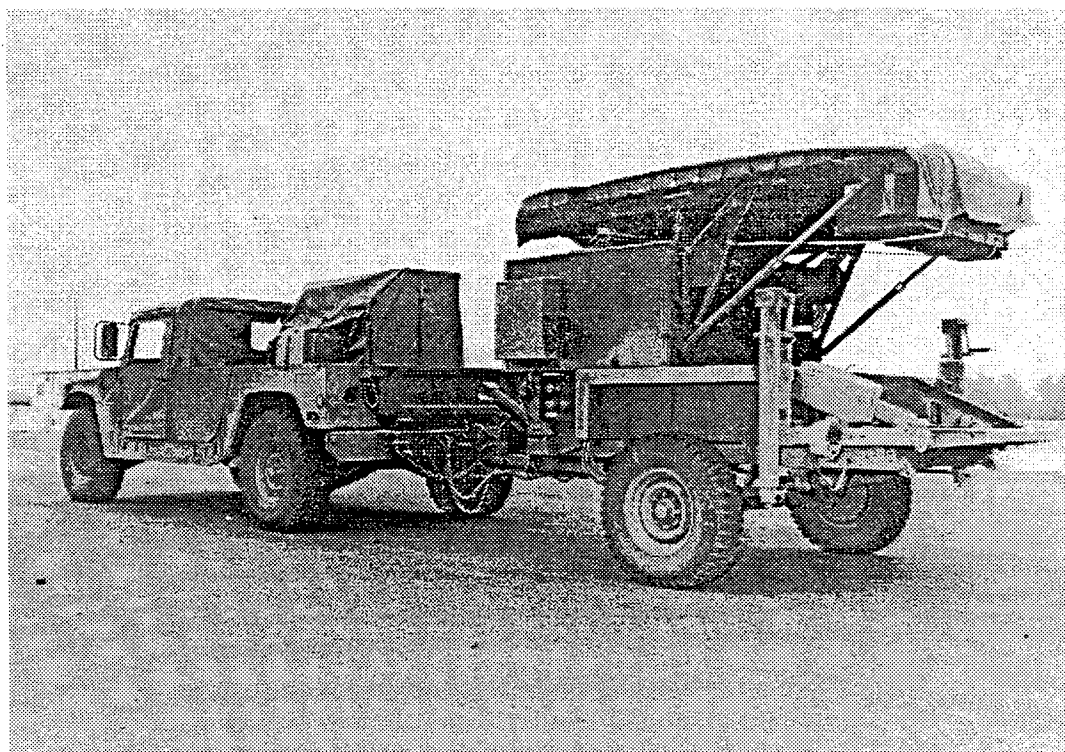


Figure 4. TPQ-37 FireFinder

MAPS Hybrid Unique Features

Dynamic Alignment

The MAPS-H has the capability to perform dynamic alignment (align on the move) if the PLGR is enabled and transmitting valid position data to the DRUH. The Dynamic Alignment is automatically initiated if the MAPS-H detects movement at power up or during any phase of the alignment process. This includes the gyro compassing and fine alignment periods. Additionally, Dynamic align can be initiated during vehicle motion (MAPS-H is powered on after vehicle motion has already started). The normal static alignment of the MAPS-H is 15 minutes (or less depending on the latitude). This same time period is used during dynamic alignment, with the Align Time to Go timer starting at 15 minutes and decrementing from this point once valid PLGR data is received by the DRUH. Valid PLGR data is defined as a PLGR Estimated Position Error (EPE) of less than 16 meters. In other words, once the PLGR internal Kalman Filter determines that it has a 'good' solution, then the DRUH will begin to use the velocity and position data from the PLGR to provide damping data to the DRUH Kalman Filter. In addition, the Vehicle Motion Sensor (VMS) data is used as a velocity input to the kalman filter if it is available (the DRUH alternately samples the GPS input and the VMS input). If valid PLGR data is not received during the dynamic alignment, the MAPS-H will continue to reset the align time to go counter until PLGR data is available or the operator stops the vehicle and performs a position update. Reasons for poor PLGR data vary, but the usual culprits are trees, buildings, terrain features, electromagnetic influences, or the PLGR itself. Testing has shown that trees and overhead foliage will cause GPS receivers to lose satellite lock. This is further compounded by the movement of the receiver along a road that has trees on either side since the PLGR is not able to lock on to a satellite or constellation. Usually, if the PLGR is not locked on to the constellation, it will enter a world wide search for any available satellite. This search may take many minutes to complete. Additionally, further interference can be caused by buildings which create multipathing inputs to the PLGR. This will sometimes result in high PLGR EPE (usually above what the DRUH will accept as input unless the operator commands the DRUH to use Poor PLGR Data). And finally, the PLGR itself can be the cause of an unsuccessful dynamic alignment. If the PLGR is powered on and allowed to acquire the present GPS constellation prior to the initiation of the mission, the EPE will usually be within the limit and the DRUH will transition to Dynamic Align. But, if it is powered on concurrently with the DRUH, there may be a wait of up to 18 minutes before the PLGR is sending valid data and the DRUH makes the jump to the Dynamic Alignment mode.

However, if the PLGR data is valid, dynamic alignment will usually requires about 7 to 10 minutes to complete. This is possible because the align time will decrease to 5 minutes (left in alignment) as soon as the DRUH determines that its azimuth output error is less than 1.0 mil Probable Error (0.05625 degrees). The time required for the DRUH to make this determination varies, but usually occurs within 2 to 5 minutes from the time that valid PLGR data is available and the align time has started to decrement. If, at any time, the DRUH detects that the host vehicle is not moving, it will revert to normal static alignment. If motion is detected prior to the completion of the static alignment, the DRUH will automatically enter the dynamic align mode if PLGR data is available and valid.

Added Capabilities

The introduction of the PLGR to the MAPS system has enhanced the capabilities of both systems in relation to their stand alone attributes. Since MAPS is a inertially based unit, errors in the position and velocity estimate tend to build up over time and distance traveled. In the past, the user had to update the position of the MAPS at various intervals. The frequency of these updates is determined by the users accuracy requirements, or the user could choose to operate in a mode known as ZUPT Mode which mandates periodic stops for a Zero Velocity Update (ZUPT). Nominally, after approximately 20 to 30 minutes of sustained travel, the MAPS-H position error should exceed the PLGR position solution. Therefore, for long periods of travel (as was the case in Operation Desert Storm), the PLGR is an ideal performance aid for the MAPS-H. Conversely, the MAPS-H makes the PLGR a more robust and reliable tool for users with the DRUH's ability to output precise attitude data (azimuth, pitch and roll) and provide navigation and position data during periods of PLGR data outages. If the PLGR data becomes unusable due to forest or brush cover, multipathing, jamming, spoofing environments, or unavailability of GPS constellation data, the DRUH will continue to operate inertially, until PLGR is again valid and can provide updated information.

Also, in response to the desires of the Artillery community, there two safety checks for the PLGR vs map sheet miss-matched datum situation. First, the DRUH automatically checks an entered position's datum, with a valid PLGR position datum. If the two datums don't agree, the DRUH will set a Status message that warns the operator the datums don't agree. A system's integrator can use this status to make the operator perform a coordinate check. Second, the DRUH can operate in the Relative Aiding Mode. In this mode, the DRUH computes the offsets between a PLGR position and an entered Survey Control Point (SCP) position that are on two different datums. After an operator inputs the coordinates from the SCP, the DRUH (if commanded) will compute the X, Y, and Z offsets (differences) between the PLGR supplied coordinates and the SCP coordinates. The DRUH will then continue to apply these offsets to bring the DRUH and the PLGR coordinates into coincidence. The DRUH can be configured to either update the offsets automatically each time a position update is performed, or give the operator the choice to command or not command a re-computation of the offsets with the position update. These two features act as safety checks for the miss-matched datum condition between the PLGR and a set of Survey Control Points, or positions relative to a map sheet.

Gravity Anomaly State

The DRUH utilizes a 22 state Kalman Filter which calibrates the odometer scale factor, and provides estimates and trims for the attitude alignment angles of the DRUH relative to the earth coordinate frame and the vehicle frame, the scale factor and bias parameters of the accelerometers, and the gyro bias parameters. The filter eliminates the need for periodic calibrations since the filter operation is transparent to the user while it is continuously modifying the trim estimates as conditions change. One of the unique features of the MAPS-H Kalman filter is the addition of a gravity anomaly state model for handling gravity anomalies (variances in the local gravity field and deflections of vertical). This state allows the DRUH to properly model changes in the gravity vector as the host vehicle traverses the gravity field. The DRUH employs a First Order Markov estimate which allows for the proper modeling of the gravity estimate versus real gravity magnitude. Results of testing over the gravity anomaly at Yuma Proving Grounds are shown in the following table:

Table 4. Gravity Anomaly Test Results

S/W Version	SCP	Error E	Error N	Error A
LNAV12	95 to TRH	-6	-8	-1
	TRH to 95	9	0	19
	95 to TRH	-11	-4	8
	TRH to 95	3	-1	17
	95 to TRH	-4	-4	7
	TRH to 95	7	-3	13
MNAV15A	TRH to 95	12	-3	-17
	95 to TRH	8	7	-8
	TRH to 95	12	3	-19
	95 to TRH	-2	5	-13
	TRH to 95	12	5	-11
	95 to TRH	10	29	0
	TRH to 95	1	-3	-19
	95 to TRH	6	9	-13
	TRH to 95	17	-1	-10
Hybrid	95 to TRH	-4	3	-1
	TRH to 95	3	-2	2
	95 to TRH	-3	5	-1
	TRH to 95	-2	0	1
	TRH to 95	0	-3	0
	95 to TRH	3	0	0
	TRH to 95	2	-9	1
	95 to TRH	2	2	0
	TRH to 95	-1	-9	5
	95 to TRH	1	-1	-4
	95 to TRH	6	-2	-1
	TRH to 95	-3	5	1

Notes:

LNAV12 = PreProduction DRU Software Version

MNAV15a = Production DRU Software Version

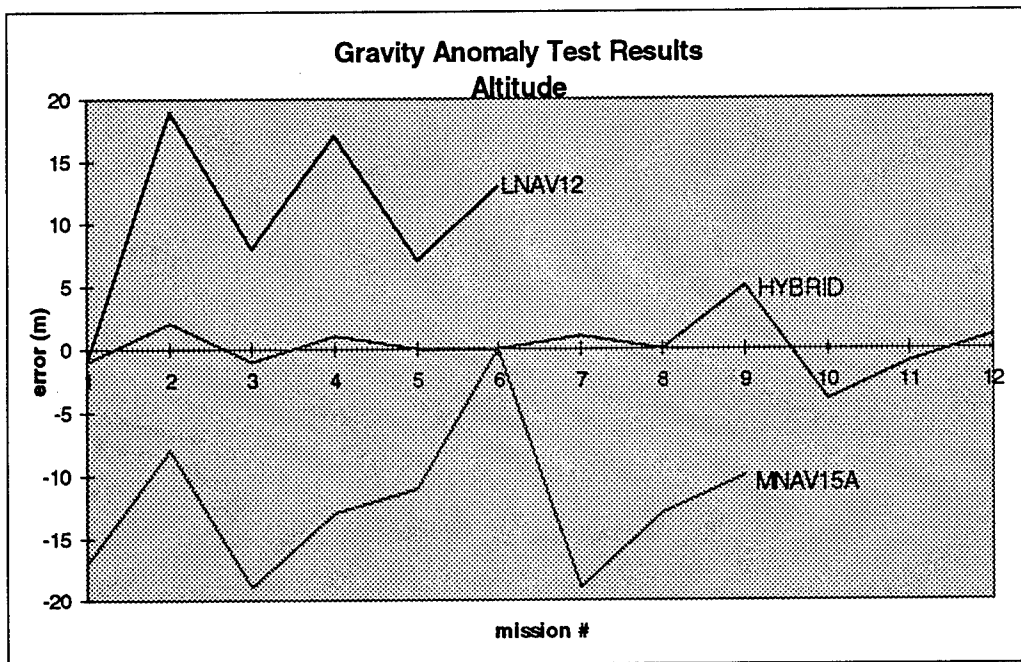
Hybrid = PreProduction DRUH Software Versions (Odo Mode only - No PLGR damping)

TRH = Truck Rolling Hills Course Survey Control Point

95 = Highway 95 Survey Control Point

Errors are shown in meters

As the data shows, performance is significantly improved with the introduction of the Hybrid Kalman filter which utilizes a separate state for the gravity anomalies and deflections encountered during missions. The anomaly is located under and in the vicinity of the TRH survey control point. Distance traveled for each mission was approximately 10 to 15 km (depending on the route chosen). The following charts depict the data (for altitude error only) from the earlier software versions to the latest testing performed in January of 1995.



Conclusion and Summary

As can be seen from the aforementioned results and capabilities, the MAPS-H is an extremely accurate and reliable land navigation device that is suited for any vehicle. The mating of this premier land navigator and the standard Army GPS receiver is a plus for both systems by allowing each to draw upon their strengths and negating each others weaknesses. The MAPS-H is currently undergoing contractor qualification testing and will start government qualification on May 1, 1995. Results of this testing will be made available by fall of this year. Copies of the MAPS Hybrid EDT Test Report can be obtained by contacting Mike Slama at the US Army Topographic Engineering Center (703) 355-2821.

THIS PAGE LEFT BLANK INTENTIONALLY

QUALIFICATION TEST METHODOLOGY AND RESULTS OF THE ENHANCED PERFORMANCE MINIATURIZED AIRBORNE GPS RECEIVER

R.G. BARTHOLOMEW, V.D. MOEN, R.C. WELLS
COLLINS AVIONICS & COMMUNICATIONS DIVISION, ROCKWELL INTERNATIONAL

The GPS Joint Program Office, in responding to their users' identification of additional requirements, has enhanced the capabilities and the performance of the DoD Standard Miniaturized Airborne GPS Receiver (MAGR). In doing so it also has responded to the need to have prototype equipment available early on in the integration cycle -- in parallel with its development: it has used an inverted test methodology compared to previous practice. In the modified receiver velocity accuracy has been brought to .008 m/s (RMS) and in a helicopter environment (when the antenna is mounted under the rotor next to the hub) velocity noise has been reduced, jamming resistance is now 70 dB J/S, and underdetermined (one or two satellite tracking) time accuracy now is better than 40 ns. In addition, control over satellite mask angle and antenna gain pattern has been added to compensate for a less than optimal antenna placement. So that verification of these changes could be accelerated, functionality was field verified with prototype receivers while development of performance levels continued: contractor qualification testing was held subsequent to integration testing so that field qualification testing (DT/OT) at the government's test facilities could proceed immediately upon receipt of the pre-production qualification units.

MAGR was developed to provide a smaller and lighter 3A receiver: its name originally was the 3A-M (Miniature). As such its requirements were determined in the late 70's: without significant change, the MAGR's requirements proceed in a direct line from the Phase IIB F-16 and B-52 receivers (defined by SS-US-200) to the 3A (defined by an interface change -- ECP COM-P-36A -- to the Phase IIB receivers) to the MAGR (CI-MAGR-300 -- which, for the most part, defines a smaller and lighter 3A with the same functional and performance capabilities). The anti-jamming performance, the position, velocity and time accuracies, the acquisition and reacquisition performance and the tracking reliability all are the same. In the intervening years since the original definition -- and in particular, in the years since the Gulf War -- the DoD has identified new functional and performance requirements. The Army has identified new requirements specific to the helicopter environment, and the Air Force has defined new anti-jamming and antenna compensation capabilities.

The paper will define the MAGR's architecture, describe in detail the added capabilities, and describe the changes made to the receiver to implement them. It will describe the functional and performance qualification testing that verified the changes, and also will describe the engineering development and simultaneous field testing that allowed for an accelerated government test and acceptance schedule. Finally, it will show data comparing the receiver's original performance with the enhanced performance.

THIS PAGE LEFT BLANK INTENTIONALLY

**QUALIFICATION TEST METHODOLOGY AND RESULTS
OF THE ENHANCED PERFORMANCE
MINIATURIZED AIRBORNE GPS RECEIVER**

Prepared By:
R. G. Bartholomew
V. D. Moen
R. C. Wells
S. L. Patton

March 10, 1995

Mail Station 153-160
Collins Avionics and Communications Division
Rockwell International
350 Collins Road, NE
Cedar Rapids, Iowa 52498
TEL: 319 395 1906 / 8633
FAX: 319 395 1642

Approved for Public Release; distribution is unlimited.

THIS PAGE LEFT BLANK INTENTIONALLY

QUALIFICATION TEST METHODOLOGY AND RESULTS OF THE ENHANCED PERFORMANCE MINIATURIZED AIRBORNE GPS RECEIVER

R.G. BARTHOLOMEW, V.D. MOEN, R.C. WELLS, S. L. PATTON
COLLINS AVIONICS & COMMUNICATIONS DIVISION, ROCKWELL INTERNATIONAL

INTRODUCTION

Engineering Change Proposal 005 adds functional and performance capability to the Miniaturized Airborne GPS Receiver (MAGR) designed and manufactured by the Collins Avionics & Communications Division of Rockwell International. Velocity accuracy has been improved, velocity noise in the helicopter environment (when the antenna is mounted under the rotor next to the hub) has been reduced, minimum signal acquisition and track has been improved, and underdetermined (less than 4 satellite tracking) time accuracy also has been improved. In addition, control over satellite mask angle and antenna gain pattern has been added to compensate for a less than optimal antenna placement.

The MAGR's original capabilities were derived back in the late 70's with the General Development Model (GDM): given the target aircraft and the perceived mission needs, they were considered necessary and sufficient. They were codified in SS-US-200, and in the early 80's came to be satisfied by the F-16/B-52 receiver. Without significant modification (beyond adding aircraft interface capabilities), these were the requirements to be satisfied by the production equipment -- the 3A receiver: the production receiver was defined as a modification of the Phase II prototype. The MAGR, as a follow-on activity, was a response to a need for smaller size, weight, and power, without significant improvements in functional or performance capabilities -- again, nothing beyond interfaces with the other aircraft systems. No improvements to position, velocity, or time accuracy were needed, none to jamming resistance, neither tracking reliability nor acquisition speed. Available enhancements were acknowledged; none were needed.

As a result of several factors -- the most obvious of which was the Gulf War, but also a maturing of experience with GPS receiver integrations, greater awareness of limitations, better understanding of potential -- shortly after the deployment of the MAGR Engineering Development Models (EDM), both the Army and the Air Force determined potential mission enhancements -- to the EH-60, the Apache, the F-117, and the B-2. In some instances, the new capability was a response to an observable mission deficiency: GPS could be further exploited to provide further mission capability. These came from operational experience as well as prototype testing. In other instances, it was a response to rapidly evolving integration plans: moving additional performance requirements into the GPS receiver was a tradeoff allowing inclusion of additional combat or transport capability elsewhere in the platform. In some instances the need for further size, weight, and power reductions lead the platform to move beyond the stand alone GPS function: the capability and its effectiveness in adding or enhancing mission capability was demonstrated on a MAGR (where proof of concept could be established without impact to an embedded module's host) but transported to a GPS module embedded in an inertial or a Doppler system for operational use.

Regardless of the end integration plan of the funding platform, demonstrated and verified capability was added to the baseline MAGR. So that platforms that had no need for the enhanced capability would be in no way affected by the change to the receiver, the hardware and software part numbers were split so that production orders could specify the baseline hardware and either the baseline software or the new software. Since ECP005 is a software change only, and since the MAGR is field reprogrammable, if the platform wants to integrate the new capability, the upgrade to the MAGR can be made without its removal from the aircraft. To protect existing integrations, ECP005 is completely backward compatible -- no integration changes are required if only baseline capabilities are used.

The purpose here is to describe the new capabilities, how they have been implemented -- both within the receiver as well as at the aircraft interface -- and in summary fashion to what extent its implementation represents a departure from the baseline architecture and design. The paper presents a brief description of the baseline software architecture as an aid in identifying what parts of the software have been changed, and to what degree they affect the basic GPS capability (the software that identifies which satellites should be acquired and tracked, that processes measurements, and determines position, velocity, and time). Then, each change is described. Finally, the qualification tests are described, along with lab results.

SOFTWARE ARCHITECTURE

MAGR's functional capabilities are divided into two groups separated by the boundaries of MAGR's two AAMP2 processors. One group collectively is responsible for the per se GPS function and is performed by the Navigation Processor: selecting satellites, acquiring and tracking them, determining pseudo-range and delta-range, and (therefrom) deriving a position, velocity, and time solution. The other group is responsible for the interfaces with the aircraft and its other subsystems and is performed by the I/O Processor: the Interface Manager and Interface Descriptor functions allow communication over the 1553 interfaces (both ICD-GPS-059 and ICD-GPS-104), the ARINC 429 interface (ICD-GPS-073), the PTTI interface (ICD-GPS-060), and the instrumentation interface (ICD-GPS-204A). The waypoint navigation function (RNAV) and the coordinate transformations are performed here as well. The receiver's navigation-related capabilities and its interface functions are consequently independent, each one performed in isolation, so that neither impacts the other.

MAGR software resides in EEPROM. As a consequence, new capability can be added and existing capability can be modified without removing the receiver from the aircraft. A program residing in protected memory can take in a new load module from either the 1553 interface (both the ICD-059 version and the ICD-104 version) or the RS-422 interface, and reprogram the EEPROM. Both the I/O processor and the NAV Processor can be reprogrammed in this way.

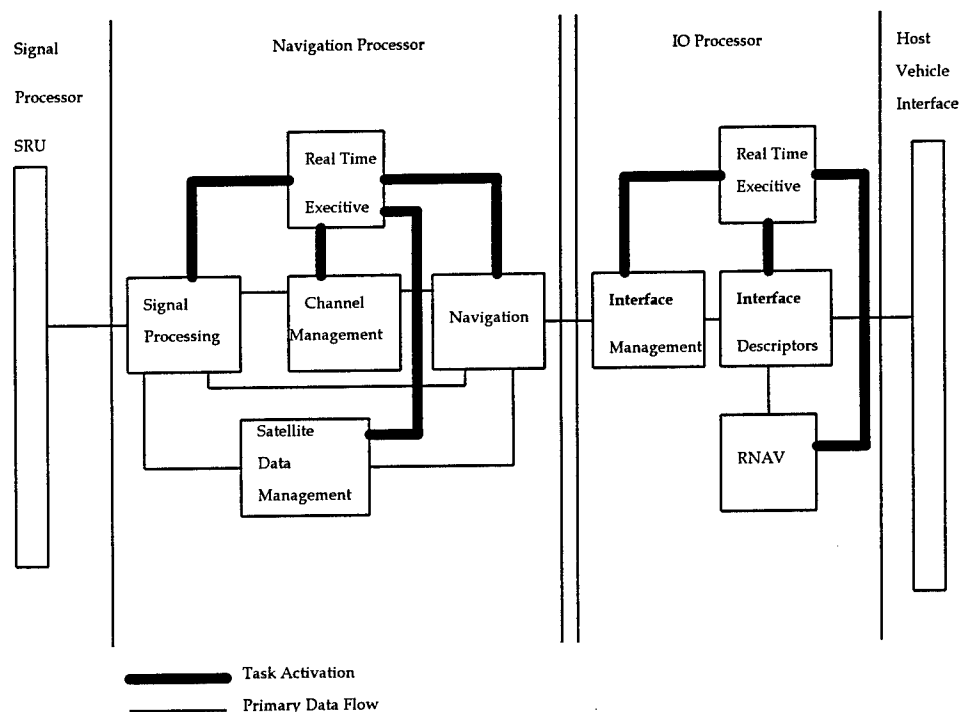


Figure 1. MAGR Software Architecture

The receiver's functions all are performed by tasks, each of which is initiated and iterated under the control of a multitasking executive. The executive initiates tasks on a priority basis (which priorities were assigned to tasks during the system definition phase of the development) so that time critical functions are neither delayed nor interrupted by background tasks. A system of interrupts and timers allows the executive to iterate tasks in either a time interval or interrupt driven manner. In this way the executive exerts real-time control over the execution of receiver functions.

CHANGE DESCRIPTION

Each of the three services, independently -- and to varying degrees -- motivated the prototyping of these capabilities. Primarily they evolved as unique requirements from unique integrations: each was developed as a unique prototype -- even within services, separately funded capabilities were developed and delivered in unique prototype receivers. Subsequent to proof of concept testing, separate software configuration items were merged into a single item and delivered for contractor qualification testing and government development and operational testing. They are presented here as they were funded: organized by the original funding service.

NAVY:

- Add another Sync Mode time tagging mechanism to the ICD-GPS-059 1553 interface (i.e., add the I-26 message)

ARMY:

- Rotary wing performance improvements
 - Create a filtered ECEF velocity vector for the RNAV computations.
 - Change the Kalman filter Sleep Mode to correct problems with large position error growth.
 - Add delta range validity processing to correct velocity spikes caused by loss of lock during delta range measurement interval.
 - Add 4-to-3 SV Augmentation to correct spikes in EHE/EVE caused by recomputation of Kalman filter covariance augmentation under conditions of less than 4 SVs.
 - Suppress velocity excursions after satellite switch during hover
- Add time only mode.
- Add 5 Hz. delta range processing capability.

AIR FORCE:

- Use antenna orientation, antenna gain pattern and aircraft attitude information as criteria for SV selection.
- Improve acquisition/reacquisition and State 5 tracking performance
- Add constellation freeze capability.
- Allow selective disabling of SVs.
- Create a velocity quality parameter equivalent to EHE/EVE

NAVY

ADD ANOTHER SYNC MODE TIME TAGGING MECHANISM TO THE ICD-GPS-059 1553 INTERFACE (I.E., ADD THE I-26 MESSAGE)

This data message is meant to operate on platforms that require the 1553 synchronize mode time tagging mechanism but are unable to generate the necessary Synchronization Mode Command With Data Word: the use of this data message has the identical effect. The addition of the I-26 Synchronization Time Word Input Message will apply only to 1553 architectures controlled by ICD-GPS-059 (Rev C, 21 September 1993 -- where it is described as the *****-GPS26 message): bus architectures controlled by ICD-GPS-104 will have no such capability. The implementation of this function will be limited to Protocol A. This limitation assumes one or another of the Synchronization Mode Commands is available on other bus architectures.

ARMY

ROTARY WING PERFORMANCE IMPROVEMENTS

Several additions and changes have been made to the MAGR to accommodate the helicopter unique mission. In particular, they apply where hovering below tree top level and flight close to the ground is the norm -- where more than likely the receiver is continuously underdetermined, perhaps undetermined (i.e., tracking no satellites at all); and where the antenna has been placed close to the mast and is subject to momentary obscuration by the spinning rotor.

When the MAGR is receiving no inertial aiding data, it uses its Kalman filter's 1 Hz acceleration estimate to propagate velocity at a 10 Hz rate (when receiving aiding, the MAGR uses the inertial acceleration to propagate the 1 Hz velocity at the input aiding rate). This propagated velocity was used by the RNAV computations -- some of which produce data at 10 Hz and 20 Hz rates. The output RNAV data although accurate with respect to RMS criteria were nonetheless noisy relative to the magnitude of the velocity vector -- inversely so: as the magnitude of the vector decreased, relative noise increased. Since they were being used to drive flight instruments, this noise made them unusable at low velocities (less than 30 m/s). To neutralize this phenomenon, the MAGR's RNAV now passes the unaided, 10 Hz velocity through a first order, low pass filter: with low magnitude velocities, the filtering is heavy; with increasing magnitude, the effect diminishes to zero. This affects ground track, ground speed, wind speed, wind direction, time-to-go, track angle error, and drift angle.

When underdetermined (when processing measurements from fewer than four satellites) the MAGR's Kalman filter output data when inertially aided is over time increasingly affected by the inertial input data. Beyond some threshold determined by time and measurements, the receiver's output data almost exclusively reflects the input data -- and to all appearances the Kalman filter is dormant, a condition in the MAGR called Filter Sleep Mode. The MAGR uses this same mode when it is Doppler aided by a source of inertial quality. In this case integration testing showed pathological conditions in which entry to sleep mode or subsequent exit caused significant errors in the MAGR's still-underdetermined output data. This same effect was seen in its recovery from the underdetermined condition.

The response to these problems had several aspects. When underdetermined, the MAGR now will use a count down rate for entry to Kalman Filter Sleep Mode so that the minimum time-to-sleep is 8 seconds (versus the previous 180 seconds). This change affects the receiver only when the *****-GPS 20 block is being used with the Sensor Configuration bits set for INS quality (AHRS = 0100). Also, during Filter Sleep Mode, the MAGR will drive the ECEF position vector toward the Baro corrected altitude when it is receiving Baro aiding. It will apply a position correction to drive the current position error state toward 0 (this has little effect when external position is being received at 1 Hz, but prevents the position from being driven off when Sleep Mode is entered and no external position is being supplied). Finally, it now will maintain nominal position when provided by the DRS aiding source, allowing GPS position to decay to the externally provided nominal when the GPS Kalman Filter is in Sleep Mode.

When the rotor is spinning, the blades can cause momentary signal loss -- not to the extent that the receiver must abandon the delta range measurement or declare loss of carrier lock, but enough so that the resulting velocity has more than the normal amount of noise. To overcome this, the MAGR now continuously checks for loss of lock over each of its 60 ms intervals; and when it identifies an inconsistent segment, marks the individual piece of the delta range measurement invalid.

Another data stability problem showed up when the helicopter was flying close to the ground, suffering nearly continuous obscuration -- alternately losing, then reacquiring satellites. Many GPS integrations use the receiver's output of estimated GPS errors to evaluate the quality of the GPS data -- in addition to or instead of the output figure of merit -- to know if the data can be used for the intended mission. This leaves the flight management system susceptible to anomalies in the error estimates. The Covariance Augmentation Matrix -- from which these output data are derived -- is normally computed once per second when the receiver is tracking four satellites. When there is a four satellite to three satellite transition and valid altitude aiding is available, the three satellites plus altitude

give the necessary observability in four directions to continue computing the Covariance Augmentation Matrix at a 1 Hz rate.

However, the use of altitude caused the covariance to increase, resulting in a "spike" in the Estimated Horizontal Error, sometimes in the Estimated Vertical Error. This spike was not indicative of the actual solution behavior since little position change would occur in the short term from a four satellite to three satellite plus baro measurement condition. To prevent the spike -- and to preclude the consequent rejection of data by the flight management system -- the Covariance Augmentation Matrix computation now is "frozen" when a three satellite plus baro condition exists. It remains in this state for 15 seconds or until a four satellites are once again available. At the end of the 15 second period the Covariance Augmentation Matrix is recomputed and another 15 second wait period is begun. Upon the return to a 4 SV navigation condition, the Covariance Augmentation Matrix is again computed at a 1 Hz rate. Note that a "spike" may still occur at the end of the 15 second period. The intent of this change is to mitigate the EHE/EVE spikes caused by transitory SV tracking conditions, not to address the effects of satellite measurements and aiding data on the Covariance Augmentation Matrix.

The receiver switching from tracking one satellite to another (e.g., to sustain the best GDOP) may be reflected in a minor drift in its position output with a corresponding but artificial non-zero velocity. This same phenomenon may occur subsequent to the download of new ephemeris data from one of the satellites currently in use. To compensate for this unacceptable velocity, expected measurement residuals now are used to adapt the position state process noise proportional to the size of the maximum expected residual. This allows position changes of this kind to occur without introducing the artificial velocity.

ADD TIME ONLY MODE

Given an accurate 3-D position from the pilot, the receiver will provide an accurate time output (equivalent in accuracy to the four satellite solution) when only one or two satellites are available. A Time Only Mode filter will process measurements from all receivable satellites. Since a known stationary position has been entered, the only variables that remain unknown are the user clock bias and clock drift. Therefore, only the 2 clock states of the Kalman Filter will be modeled. The non-time states of the Kalman Filter covariance matrix and non-time states of the process noise will be zeroed. Due to the uncertain accuracy of the entered position, the Figure of Merit will be set to 9 during time only mode operation.

ADD 5 HZ. DELTA RANGE PROCESSING CAPABILITY

This is being added to achieve greater velocity and therefore position accuracy when GPS is operating in a low dynamics, unaided mode (i.e., without inertial or inertial quality aiding). The fast-rate (up to 25 Hz) velocity output in the GPS 26-***** 1553 message (ICD-GPS-104) is based on the extrapolation of the 1 Hz GPS velocity data (i.e., based on 1 Hz GPS measurements) by inertial acceleration input (up to 25 Hz). In the unaided mode -- lacking any other fast rate, intermeasurement estimate of acceleration -- the MAGR uses its own 1 Hz acceleration estimate to propagate velocity (and therefore position) at a 10 Hz rate. Since that data first gets processed into velocity about 0.2 sec after its time of validity, the 10 Hz unaided velocity reflects extrapolation by 0.2 to 1.2 seconds.

When a change in velocity occurs between 1 Hz measurement samples, acceleration and jerk derived from delta range can become coarse -- the extrapolation error can be large. Such an incapacity in a precision approach or landing context -- where wind gusts may cause intermeasurement position changes made significant by the need to drive flight instruments in a fine scale mode -- neutralizes a capability available with inertial aiding. The solution to this problem is to sample delta range at a faster rate -- i.e., to determine a more timely estimate of acceleration and jerk, and therefore a more timely estimate of velocity and position.

The MAGR's one second delta range interval previously had been subdivided into five subintervals of 200 msec each, with a delta range measurement provided at the end of each subinterval. The MAGR now has been updated to use those 5 Hz measurements in real-time -- rather than summing them at a 1 Hz rate -- to better estimate acceleration and jerk. Once per second, the fast rate delta range solution is recalibrated to the Kalman Filter position and velocity solution.

AIR FORCE

ANTENNA ORIENTATION/ANTENNA GAIN PATTERN

The object here is to improve the satellite selection mechanism in cases where antenna placement and the antenna gain pattern degrade performance. Loading an antenna orientation allows the integrator to define the fore/aft and left/right orientation of the platform antenna. This will allow the MAGR receiver to redefine "local level" and decide which satellites actually are in view given the antenna placement -- to optimize the best GDOP determination. This makes use of attitude aiding data input from the 1553 bus. As long as Pitch and Heading are available, the MAGR will combine the attitude data with the antenna orientation to optimize the satellite selection function. If there is no aiding data, then the antenna orientation will default to the current implementation, where the antenna is assumed to be lined up with local level. Roll is not used due to its transitory nature and the subsequent transitory effect on satellite visibility. The antenna orientation data are stored in non-volatile RAM (battery backed).

The antenna gain pattern will be defined by two angles (with 1553 data entered in INIT mode only) relative to the antenna unit vertical, and can be interpreted as two points along the antenna gain pattern curve. These angles will define two cones of visibility, one for initial acquisition and a wider cone for normal track. The SV selection process will include redefining local level using antenna orientation and attitude aiding and computing the best GDOP within the cone defined by entered antenna angles. If too few satellites are visible in the first cone, the cone will be widened, as defined by the second set of entered angles, to include more satellites. The angle defining the narrow cone should be chosen based on minimum satellite signal power and antenna angle (gain) such that all satellites in the cone will be acquirable at the resultant signal power (e.g. -167 dBw, -170 dBw). The second angle will be chosen to take advantage of the fact that most satellites are above minimum required power levels. The gain pattern angles also are stored in non-volatile RAM.

ENHANCED ACQUISITION/REACQUISITION AND STATE 5 (CARRIER) TRACKING

This allows the MAGR to perform acquisitions at reduced signal power levels (-167 dBw C/A, -170 dBw P L1, -173 dBw P L2 IF; -168 dBw C/A, -171 dBw P L1, -174 dBw P L2 RF). It involves increasing the acquisition search and dwell times, allowing faster growth of search sizes, and increasing the maximum search limit. Narrowing the MAGR's tracking loop bandwidth, allows it to track in State 5 down to -170 dBw L1, L2 P IF and -171 dBw L1, L2 P RF. A reduction in the carrier loop filter bandwidth reduces carrier loop noise while still being able to handle frequency shifts due to dynamics.

CONSTELLATION FREEZE CAPABILITY

To further diminish position and velocity discontinuities resulting from best-GDOP motivated satellite switches, this function allows the 1553 interface (ICD-GPS-059) to inhibit all satellite switching. When this mode is enabled, the current four satellite constellation being tracked will be the "frozen" constellation. This constellation will continue to be used, even if one or more of the satellites cannot be tracked (e.g. satellites being masked, satellites setting, etc.), until it is deselected via the 1553 interface, or a NAV-INIT-NAV mode change occurs, or a short or a long term power outage occurs. Upon termination of this mode, normal satellite selection will resume.

ALLOW SELECTIVE DISABLING OF SVS

This function allows the removal of selected satellites from the visible satellites list. If a satellite being tracked is disabled, it will be dropped and an attempt will be made to switch in an alternate immediately. This is similar to what would happen if loss of lock occurred while the receiver was unaided. This function -- the list of satellites to be removed -- is selectable in Nav mode by the 1553 interface. Upon exiting this mode, all satellites in view will be returned to the candidate lists and normal satellite selection will resume. This function will be disabled upon a long term power outage but will be retained upon NAV-INIT-NAV mode transitions and short term power outages. It also can be selected in INIT mode to influence initial acquisitions and Cold Starts.

CREATE A VELOCITY QUALITY PARAMETER EQUIVALENT TO EHE/EVE

The implementation of this function makes the Estimated Horizontal Velocity Error and Estimated Vertical Velocity Error (EHVE and EVVE) available to the 1553 interface (both ICD-GPS-059 and ICD-GPS-104). They are equal to the square root of the corresponding horizontal and vertical velocity variances (but rescaled) previously available in the Kalman Filter Navigation Output blocks (ICD-GPS-204A).

TEST DESCRIPTIONS AND TEST RESULTS

The primary goal of the ECP005 development was to add useful capability -- both functional and performance -- without degrading existing capability. Determining that this goal had been met required using a measurement system whose accuracy had previously been established. The ECP005 lab testing was performed using the Simulation, Evaluation and Verification System (SEVS), validated and used by the DoD for the MAGR's baseline performance qualification testing. Similar simulated flight profiles (e.g., host vehicle dynamics, signal power, jamming, satellite masking) used during the MAGR baseline test program were used to measure the ECP005 performance capability (although in some instances, to verify new capabilities, new profiles had to be created). Because of the merging of independently developed capabilities, an additional challenge to the test methodology was in confirming that none of the newly developed capabilities that previously had been verified in isolation had been compromised by the process of merging them together.

TEST DESCRIPTIONS

Three basic profiles were used to test the ECP005 performance capability - similar to the ones used by the DoD to validate the baseline MAGR: (1) Medium Dynamics Racetrack, (2) Static, and (3) Acquisition. Using the SEVS, motion is simulated with varying dynamics (velocity, acceleration, and jerk), as are jamming, satellite masking and signal attenuation effects, ionospheric and tropospheric delays, clock errors, host vehicle sensor data (as well as sensor errors), antenna characteristics, varying signal strengths, and so on. The profiles are repeated, varying the simulated conditions, as often necessary to verify all aspects of performance.

1. Medium Dynamics Racetrack: The racetrack begins with a stationary period of five minutes to allow initialization of the test by the test operator. The profile then accelerates to 450 m/sec at an altitude of 3300 m. After a period of constant dynamics, the profile decelerates to 250 m/sec, climbs to 5000 meters, and executes a 4 g, 20 meter/sec/sec/sec jerk coordinated turn. After alternating periods of constant velocity and medium dynamics, the profile returns to its starting point and starts its second lap. Although the racetrack profile was designed with PVT performance analysis in mind, it also is applicable to both reacquisition and tracking performance. The reacquisitions are accomplished by removing signal power from one satellite for a 10 second period during either a constant or medium dynamic segment. The tracking performance tests with this profile determine the receiver's response to jamming and ability to maintain code and/or carrier lock.

2. Static: The static profile uses external factors that vary from benign to extreme. The profile is tested under State 3 jamming conditions for PVT performance. Quick acquisition response is tested in categories of TTFF-1. Tracking reliability and reacquisition after loss-of-lock are also investigated.

3. Acquisition: The acquisition profile was developed specifically for the purposes of testing initial acquisitions (TTFF-1) under dynamics. In researching the TTFF-1 requirements, it was determined that performance is nearly independent of reasonable initial position and time uncertainties. Therefore, all position and time uncertainties are manually entered as 3 sigma (worst case) values. However, TTFF-1 performance is very dependent on the velocity uncertainty during the trial. The velocity uncertainty will be a gaussian distribution as a function of time with a manually entered initial velocity error of up to 150 m/sec, based on a constant velocity racetrack.

TEST RESULTS

Performance Evaluation

Two levels of formal testing were performed: regression (to confirm no baseline capability was lost) and qualification (to verify new requirements were met). Regression testing includes maximum dynamics and line of sight profiles and confirms the receiver continues to meet its spec requirements. Qualification testing covered five categories, using test plans and procedures that were similar to those used for evaluating the baseline receiver's performance with additional tests created to verify capabilities specific to the ECP. Position, velocity, and time accuracy were measured over the course of many different trials involving varying levels of dynamics, signal powers, jamming levels, and sensor aiding types. Acquisition speed was measured - again, under varying initial conditions - for Time-To-First-Fix-1 (TTFF-1): search and acquisition using C/A code followed by a handover to P(Y) code. Reacquisition time (subsequent to signal masking or momentary power loss) and tracking reliability (during unmasked periods of minimum signal power, dynamics, and jamming) were also measured. Table 1 shows the results of the ECP005 performance testing. Note that TTFF is measured from the initiation of the navigation mode to the point at which the accuracy of the present position and current time outputs fall within the required ranges. Reacquisition performance is measured from the time at which the signal is no longer masked until the recovery of signal from that same satellite, under varying conditions of host vehicle dynamics, external sensor aiding, and jamming. Tracking performance is evaluated in two ways. The first is a measure of the receiver's ability to maintain signal lock under conditions of jamming and host vehicle dynamics. The second is a measure of pseudo-range and delta-range accuracy under these same conditions.

Table 1. ECP005 Performance Test Results

PVT PERFORMANCE									
	A/U	Jam ?	Profile	HORT POS (M)	VERT POS (M)	3D VEL (M/S)		TIME MARK (NSEC)	PTTI (NSEC)
						CONST	MAX		
CHALS	A	No	RACE *	0.71	1.17	.0098	.0136	21	14
CHALS	A	Yes	RACE *	1.26	1.68	.0096	.0131	16	17
TIME ONLY (1 SV)	U	No	STATIC	0.85	0.25	N/A	N/A	21	21
TIME ONLY (2 SV)	U	No	STATIC	0.85	0.25	N/A	N/A	29	29
TIME ONLY (3 SV)	U	No	STATIC	0.85	0.25	N/A	N/A	18	7
EXTENDED ST 5	U	No	RACE	2.66	1.69	.038	.462	20	23
EXTENDED ST 5	U	Yes	RACE	2.03	1.73	.053	.510	15	15
EXTENDED ST 5	A	No	RACE	1.92	1.07	.011	.024	22	7
EXTENDED ST 5	A	Yes	RACE	1.99	1.63	.014	.027	27	15
* Low dynamics									
TTFF-1									
	A/U	Jam ?	Profile	% SUCCESSFUL		AVG TTFF1			
100 KM INIT ERROR	U	Yes	ACQ	100%		76 S			
10 KM INIT ERROR	U	Yes	STATIC	100%		73 S			
REACQUISITION									
SIGNAL	A/U	Jam ?	Profile	% SUCCESSFUL		AVG RECOVERY			
P CODE (St 5)	A	Yes	RACE	100%		3.7 S			
P CODE (St 3)	A	Yes	RACE	100%		1.5 S			
TRACKING RELIABILITY									
SIGNAL	A/U	Jam ?	Profile	% SUCCESSFUL					
P CODE, L1/L2	U	No	RACE	100%					
P CODE, L1/L2	U	Yes	RACE	100%					
TRACKING ACCURACY (PER SV - WORST CASE)									
SIGNAL	A/U	Jam ?	Profile	PSEUDORANGE ERROR (M)		DELTARANGE ERROR (M)			
P CODE, L1	U	No	RACE	0.8380		0.0078			
P CODE, L2	U	No	RACE	1.045		0.0135			
P CODE, L1	U	Yes	RACE	1.100		0.0157			
P CODE, L2	U	Yes	RACE	0.9752		0.0163			

THIS PAGE LEFT BLANK INTENTIONALLY

A New Approach to Simulation and Test of Integrated GPS/INS Systems

Manfred Bäumker - Fachhochschule Bochum, FRG

Axel Lehmann - LITEF GmbH Freiburg, FRG

Approved for Public Release; distribution is unlimited.

BIOGRAPHY

Manfred Bäumker received his M.S. and Ph.D. degree in Geodesy at the University of Hannover, Germany in 1980 resp. 1984. From 1984 to 1992 he was system and chief engineer in the development department of LITEF, Germany, where he was responsible for the mechanisation of AHRS and Inertial Navigation Systems including GPS and DGPS integration. Since 1992 he is professor for physics and surveying at the Fachhochschule in Bochum, Germany.

Axel Lehmann received his M.S. degree in Communications Engineering from the Technical University of Berlin. He now has fifteen years of experience in the design, test and application of inertial systems. His expertise goes from low accuracy AHRS to very high precision marine laser navigation systems. He presently serves as the project manager of the FOG-AHRS / GPS development at LITEF.

ABSTRACT

This paper addresses a new approach to the simulation and test problem during the development of integrated GPS/Inertial systems.

Normally, one simulates a GPS/Inertial system with known or assumed error sources. A major problem is the stimulation of the errors by an appropriate dynamic environment, i.e. flight profiles. Based upon the initial approach refinements are derived from test results of the system compared to a reference system of higher performance. This procedure is then repeated several times until the system meets its requirements. This phase is very time consuming and expensive.

The new approach of system development uni-

fies system simulation and system test by collecting raw data of all sources, i.e. INS and GPS. This approach enables the use of test data later on as simulation input. Using this method any test can be repeated a thousand times with identical conditions offline. System optimization can be done more easily and cost effective, because expensive flight tests do not have to be repeated.

The approach can be tested and verified by introducing additional known errors and observing the system response ("Software-in-the-loop").

In 1993 an implementation was started with the definition of hardware and software building blocks and the definition of the interfaces and protocols. As far as possible commercial standards were used. Special definitions were introduced only if no standards were available. The first system tests were performed in early 1994.

The approach enables the user to compare GPS, DGPS, INS/GPS, INS/DGPS and OTF solutions. The DGPS and OTF solutions are used as the reference for the measurements.

The paper will show the benefits of this approach with an example of a GPS/AHRS integration optimized for helicopter use.

INTRODUCTION

From the beginning of the development of inertial systems high effort was put in the study of error models of these systems and especially the inertial sensors, i.e. accelerometers and gyros, to evaluate system performance. The development of inertial systems was and still is costly, so there is a major interest to establish a reasonable confidence level in a design before

a costly development is started. Regarding inertial navigation systems and especially strap-down systems the error behaviour depends considerably on the vehicle dynamics. So, for the evaluation of such systems realistic vehicle dynamics have to be additionally simulated.

All simulation approaches are limited with respect to the vehicle dynamics and the error models of the sensors. Therefore, a new approach is presented here to overcome limitations and shortcomings of the conventional error simulation programs. The paper starts with an overview over simulation tools developed and used at LITEF, which in the authors' opinion do not differ largely from those, used in other companies and institutions.

INS and SENSOR ERROR MODELS

The first programs to simulate (platform) INS error behaviour integrated the error equations assuming a constant and a random bias for the gyros and accelerometers [1..3]. Running these simulations several times with different statistically distributed parameters and taking the root-sum-square (Monte-Carlo-Method) produced reasonable results, if the behaviour of the sensors was modelled correctly. Gyros made and still make problems, because the measurement of gyro noise is not a trivial task, and models have to be set up very carefully. There exists extensive literature on this subject, which shows the importance of these models. A very good overview on that subject, citing many references, can be found in [9, 10].

With the invention of strapdown technology the case of modelling the behaviour of inertial systems became even more complicated. Because the sensors now are strapped to the body of the vehicle, all its movements influence the error behaviour of the sensors. While in platform systems the sensors are (more or less) decoupled of the vehicle's movement, in a strapdown system many errors become significant, i.e. acceleration dependent bias of the gyros, because the measurement axes of the instruments change continuously with respect to the navigation frame [8].

For strapdown systems error simulation pro-

grams had to be re-written completely and because vehicle dynamics and more complicated sensor error models had to be included, these programs consumed hours of CPU time for a single run [4]. In its time (1982) a state-of-the-art program at LITEF needed ten to twelve hours on an IBM-360 for a complete Monte-Carlo-Run of a two-hour vehicle scenario.

Today, there are no such restrictions on computing power, but the primary tools are still the same. The discussion about error models is still going on as can be seen in the contemporary literature [5..7]. But there was always a difference in performance between the simulated and the real system, and according to Murphy's Law the real system always was worse than the simulated one.

Kalman-filter technique added another problem to system simulation: The verification of filter performance in the target system. The problems of simulating sensor errors correctly were addressed before, but now also the implementation played an important role. Until today, many simulation programs are written in FORTRAN, the code in the target system is written in Assembler (10 years ago), in C (5 years ago) or Ada (today). The differences in code, resulting from the different languages, result often in different outputs of the same software design.

Consequently, the next tool to add to our simulation toolbox was a sensor simulation program, which could serve as a front end for the error simulation program (which propagated the errors) as well as for the "real" navigation program in the target system (which propagated the complete sensor data). This was used to verify the software performance on a very high level.

As mentioned before, simulation and reality differed, sometimes largely. In the authors' experience the most important shortcoming of the simulation technique is the inability to simulate the environment, i.e. the behaviour of the vehicle in motion, temperature dependent errors, the vibration and the interaction between the sensors. In this context an additional error source due to the platform and navigation algorithm, i. e. sculling and coning should be mentioned.

GPS ERROR MODELS

From the beginning of GPS the benefit of combining INS and GPS was obvious: GPS offered the long term accuracy, which INS lacked and INS offered the dynamic behaviour and jamming resistance, which GPS lacked.

In the early days of GPS the main interest was to simulate the satellite orbits to answer the question: At which time today can I observe three satellites for at least 30 minutes [11, 12]? For the case of simulating the aiding of an INS simple models could be applied by adding noise to the velocities and position, generated by a flight path generator.

For the simulation of centralized Kalman-filters models for the pseudo-range measurements were developed [13]. Even more sophisticated models for DGPS were recently published [14].

Again, these models were helpfull in estimating the overall performance, but could not simulate a lot of real world errors, i.e. multipath effects and real-time behaviour of GPS receivers in a moving vehicle.

With the completion of the GPS constellation GPS and DGPS became an important tool in testing INS, because a continuous reference became available [15].

THE NEW APPROACH

The more GPS became available, receivers became cheaper and smarter. Very soon GPS receivers became available, which allowed the user to take the "raw" GPS measurements, i.e. pseudo-ranges and delta-ranges, and to process this data the way he wanted. At the same time computers became more powerful and smaller. It became apparent, that it was much easier to observe GPS and use the real data than to simulate GPS.

The former approach of simulating inertial systems, then testing them, then analyse the errors and then start all over again was thought over. The ideal would be to have the test data available at the start to optimize the system already within the development.

The missing link for GPS / INS integration was the availability of "raw" INS data. This is normally not available from INS systems. The rate and acceleration output of an INS is usually limited in resolution, therefore an external integration with sufficient accuracy is not possible. LITEF, being a manufacturer of inertial equipments, had the possibility to change this for it's own purposes.

A new measurement system was designed, which could collect all primary data of the sensors in real time. These data then could be used in a host computer not just for simulation of the errors, but for driving the "real" software with the "real" data.

THE MEASUREMENT SYSTEM

For the first experiments an existing AHRS (Attitude and Heading Reference System), the LITEF LCR-88, was used. This system uses the ARINC-429 high-speed serial output bus, which has a sufficient data rate to handle the data needed in real time. The output was modified by adding special labels, which were used to output the raw data, i.e. the angular increments of the gyros and the velocity increments of the accelerometers, with full accuracy.

This data is compensated for all known systematic errors, i.e. scalefactor, misalignments and biases, and this data is the input to the analytical platform and the navigation equations.

The data to be stored has a rate of up to 10 MByte/hr. Data from the GPS receivers is much slower in rate and much less - about 1 MByte/hr. This data rate can be handled with modern computers and storage media. The important problem to be solved was to preserve the timing relationship between the inertial and the GPS measurements with an accuracy of some milliseconds.

The measurement system has been realised using a portable PC for industrial purposes with an Intel 486DX33 processor and EISA-Bus. The GPS data is received via a RS-232 or RS-422 port, depending on the type of receiver. The data from the IMU (inertial measurement unit, i.e. the AHRS) is received by an intelligent

ARINC interface, which selects the labels of interest and adds a 1 ms resolution time tag. To preserve the timing relationship between the data, the 1PPS signal of the GPS receiver is fed to the printer port of the PC. This generates an interrupt, which reads out the 1 ms timer of the ARINC interface, thus the timing between the data is preserved (Fig. 1).

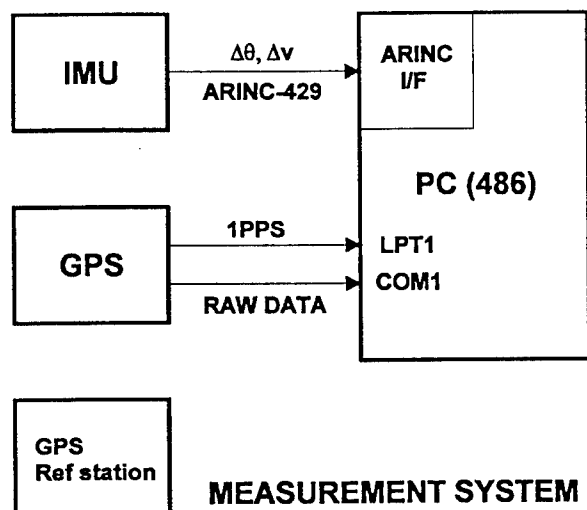


Fig. 1

While this description is quite short, the process to solve the problems with this system consumed quite some time. The software was written in C and runs under normal MSDOS, which is not known for its good real time behaviour.

APPLICATIONS

The system was used in a first trial in March 1993 for test flights in Münster. The system then was upgraded and used very successfully for flight tests at Manching Airbase in a helicopter in January 1994. This data is presently used to design and optimize a new AHRS/(D)GPS integrated system for aerial applications. Further tests have been carried out in a truck to evaluate the performance of such a system for land navigation purposes.

The benefit of the measurement system and this kind of data is manifold:

- GPS/DGPS offers an excellent reference, especially in those cases when an OTF solution is possible

- on a host computer the data can drive the real software and not an error simulation, only the real time behaviour is missing
- using Ada as programming language, as we do now, differences in code between the host and the target system can be minimized
- Kalman-filter technique enables the user to estimate the residual errors
- Kalman-filter can be tested by adding artificial (known) errors to the real-time data
- different Kalman-filters, i.e. centralized or cascaded or different states, can be compared and analysed using the same data base
- the recorded test can be repeated as often as needed with different mechanisations.

CONCLUSIONS

A new approach to the development and test of inertial systems and integrated INS/GPS was presented. The main difference to the conventional approach is the bottom up method of development. First, the test data is gathered as raw data from an IMU and GPS (and other sensors, if applicable) with well preserved timing relationship. Then, this data is used to drive the navigation software, which now can be optimized in a host computer, without repeating costly tests in a vehicle.

It should be pointed out that the idea behind this approach is not new at all, but today's availability of computing power and software tools made this approach feasible.

Presently, this system is used at LITEF to develop an integrated FOG-AHRS/GPS system. Based on this experience a software was written, which collects the raw data and also incorporates the navigation equations and a Kalman-filter.

REFERENCES

- [1] C. Broxmeyer, *Inertial Navigation Systems*, McGraw-Hill, New York 1964
- [2] M. Kayton and W. R. Fried (eds), *Avionics Navigation Systems*, Wiley, New York 1969
- [3] J. L. Farrell, *Integrated Aircraft Navigation*, Academic Press, New York 1969
- [4] V. Wetzig, Hao Zhuge, *Simulation of Strapdown-System Errors and Error Compensation Methods*, DFVLR-Mitteilung 84-22, Köln 1984
- [5] I. Y. Bar-Itzhack and D. Goshen-Meskin, *Unified Approach to Inertial Navigation System Error Modelling*, Journal of Guidance and Control, Vol. 15 No. 3
- [6] G. Arshal, *Error Equations of Inertial Navigation*, Journal of Guidance and Control, Vol. 10 No. 4
- [7] B. M. Scherzinger and D. B. Reid, *Modified Strapdown Inertial Navigator Error Models*, IEEE PLANS 1994
- [8] D. K. Joos and U. K. Krogmann, *Estimation of Strapdown Sensor Parameters for Inertial System Error Compensation*, AGARD Conference Proceedings No. 298, London 1980
- [9] F. Saggio III, *Strapdown Gyro Random Drift Models from Power Spectral Density Estimates*, 10th IMACS World Congress on System Simulation and Scientific Computing, 1982
- [10] G. W. Erickson, *An Overview of Dynamic and Stochastic Modelling of Gyros*, Proceedings of ION Technical Meeting, 1993
- [11] Kalafus et al., *NAVSTAR GPS Simulation and Analysis Program*, DOT-TSC-RSPA-83-11, Dec. 1983
- [12] G. Matchett, *Stochastic Simulation of GPS S/A Errors Technical Memorandum*, TASC DTRS-57-83-C-00077, June 1985
- [13] M.S. Braasch, *A Signal Model for GPS*, Navigation Vol. 37 No. 4
- [14] J. Rankin, *GPS and Differential GPS: An Error Model for Sensor Simulation*, IEEE PLANS 1994
- [15] A. K. Brown, A. Matthews, T. Varty, *Low Cost Testing of High Accuracy INS using GPS*, Proceedings ION Technical Meeting 1986

THIS PAGE LEFT BLANK INTENTIONALLY

SESSION III-B

GPS TOPICS I

CHAIRMAN

MICHAEL HADFIELD

*746TH TEST SQUADRON
HOLLOMAN AFB NM*

THIS PAGE LEFT BLANK INTENTIONALLY

INTEGRITY MONITORING IN THE DOD STANDARD MINIATURIZED AIRBORNE GPS
RECEIVER
R. W. HOECH, R. G. BARTHOLOMEW
COLLINS AVIONICS AND COMMUNICATION DIVISION, ROCKWELL INTERNATIONAL

This paper will present the integrity monitoring capability of the DoD Standard Miniaturized Airborne GPS Receiver (MAGR) and the additional, RAIM, capability of the Enhanced MAGR (EMAGR). It will describe the standard MAGR's least squares residual comparison, and the hardware and software architectures that sustain it but that also define its performance limits. It will describe the EMAGR's RAIM capability as an increment to the standard receiver, and will describe the hardware and software architectures that enable it and that allow it to overcome the shortcomings of the standard receiver. This will include a discussion not only of the detection schemes -- and in the case of the EMAGR, the isolation scheme -- but as well it will describe the several annunciation capabilities. It also will identify test methodologies that verify performance equivalent to that established by TSO-C129.

Early on for the DoD's receivers, the concept of integrity applied exclusively to the real-time verification of the receiver's hardware and software. The accuracy of its navigation data was doubtful if for example the GDOP exceeded some large value; or if some memory chip was failing. As time passed (and confidence increased), test and analysis engineers felt it appropriate to make at least some kind of rudimentary consistency check of the input satellite measurements. Recurring but subtle clock failures on some of the early satellites provided the motivation: measurements from sub-marginal satellites would corrupt the receiver's output data, producing an out of tolerance accuracy, or an unacceptably noisy velocity. As a consequence the receiver absorbed a simple least squares residual check: if one measurement residual was grossly inconsistent with the others, the receiver would ignore the corresponding measurement. This, however, was the extent of the scheme. Reliability and availability, as the RAIM context has come to define them, were alien concerns; alien also was the notion of attempting to define performance criteria for satellite error detection.

With the advent of precision flight through the national airspace, and precision landing, the focus of GPS navigation integrity has shifted from the black box to the system -- to its impact on the performance of the aircraft, and the success of the mission. System engineers in approaching an implementation should consider integrity monitoring techniques, including RAIM, as components of a system, not as autonomous functions: they should evaluate each -- and the contours of its implementation -- only in the context of the rest of the integrity system. An acceptable false alarm rate for RAIM detection will depend on how the receiver responds to the detection of a failure: annunciation only (with the concomitant failure of all output data) and at the onset of each failure; or a more sophisticated strategy of measurement exclusion and source isolation while maintaining acceptable navigation performance -- with annunciation only after consecutive failures. How the navigation system uses the integrity information, how it filters the detector results, how it annunciates faults, and how this affects subsequent receiver and aircraft operations are questions whose answers will determine the integrity system's implementation.

To satisfy these new requirements (per RTCA-DO-208 via TSO-C129), the enhanced receiver, relying on a ten-channel, all-in-view architecture, uses a minimum of six satellite measurements processed by a modified least squares residual comparison to detect and isolate satellite failures. Algorithmically, this is being inserted into the standard receiver's existing mechanism (in some ways expanding it, in some ways replacing it), and uses the existing annunciation capability. The standard architecture (i.e., five-channel) constrains its operation -- in particular this is true with respect to anti-jamming, minimum signal tracking, and sustainable acceleration and jerk. The paper will describe tradeoffs with respect to navigation performance that are necessary to meet the TSO's requirements in the standard MAGR. The enhanced architecture obviates these compromises: the paper will make a comparison of RAIM performance between the two architectures.

THIS PAGE LEFT BLANK INTENTIONALLY

Integrity Monitoring in the Miniaturized Airborne GPS Receiver

R. W. Hoech
R. G. Bartholomew

Collins Avionics and Communications Division
Rockwell International
350 Collins Road, NE
Cedar Rapids, Iowa 52498

15 March 1995

Approved for Public Release; distribution is unlimited.

THIS PAGE LEFT BLANK INTENTIONALLY

INTEGRITY MONITORING IN THE MINIATURIZED AIRBORNE GPS RECEIVER
R.W. HOECH, R.G. BARTHOLOMEW
COLLINS AVIONICS AND COMMUNICATION DIVISION, ROCKWELL INTERNATIONAL

INTRODUCTION

This paper will present the integrity monitoring capability of the five and ten channel enhanced Miniaturized Airborne GPS Receiver (MAGR), currently being developed by the Collins Avionics and Communications Division, Rockwell International. Early on for the DoD's receivers (ca 1980), the concept of integrity monitoring applied exclusively to the real-time verification of the receiver's hardware and software, and the operating environment in the immediate vicinity. The accuracy of its navigation data was doubtful if, for example, some memory chip failed, or if the GDOP exceeded some value, or if the age of the ionospheric delay measurement increased. As time passed (and experience taught a more subtle appreciation for system errors), test and analysis engineers felt it appropriate to make at least some kind of rudimentary consistency check of the satellite measurements used by the receiver.

Recurring but subtle clock failures on some of the early satellites provided the motivation: measurements from sub-marginal satellites would corrupt the receiver's output data, producing an out of tolerance position accuracy, or an unacceptably noisy velocity. It became difficult to segregate the satellite segment, control segment, and user segment contributions to system error (as revealed in the receiver's output data). As a consequence the receiver absorbed a simple least squares residual check: if one measurement residual was grossly inconsistent with the others, the receiver would ignore it, and log the error in the fault log sent out over the 1553 interface. If it found itself ignoring measurements from the same satellite over a period of several consecutive seconds, it would drop it in favor of some alternate satellite. This, however, was the extent of the scheme.

With the advent of precision guided munitions, and precision landing, the satellite fault detection mechanism has become more rigorous. In the DoD context, improving the integrity of the GPS data to offer a better Precision Landing System may be of limited concern (the case of carrier landings notwithstanding); more compelling presumably is the aid it could provide to the weapon release and weapon targeting capability -- especially where even small, unexpected error could prove lethal -- where unintentional collateral damage is unacceptable. To satisfy new concerns (per RTCA-DO-208 via TSO-C129), the enhanced receivers have absorbed a Receiver Autonomous Integrity Monitoring (RAIM) function that uses a minimum of six satellite measurements processed by a modified least squares residual test to detect and isolate satellite failures. Algorithmically, this is being inserted into the standard receiver's existing fault detection mechanism (in some ways expanding it, in some ways replacing it), using the existing annunciation capability.

This paper will describe the standard MAGR's least squares residual comparison and its other fault detection mechanisms, and will describe the hardware and software architectures that sustain them but that also define their performance limits -- i.e., it will discuss the architecture's impact on the RAIM mechanism, and the RAIM mechanism's impact on the receiver's performance. It will include a discussion of the detection scheme and the isolation scheme, and it will describe the several annunciation capabilities.

SOFTWARE ARCHITECTURE

At a system level, the receiver's capabilities are divided into two groups separated by the boundaries of the receiver's two AAMP2 processors: one group is performed by the Navigation Processor; the other group by

the I/O Processor. The Navigation Processor's software is responsible for all aspects of the performance of the GPS function: selecting satellites, acquiring and tracking them, determining pseudo-range and delta-range, and (therefrom) deriving a position, velocity, and time solution. The I/O processor's software is responsible for communication with the host vehicle interfaces and for performing the relative navigation (i.e. RNAV) functions.

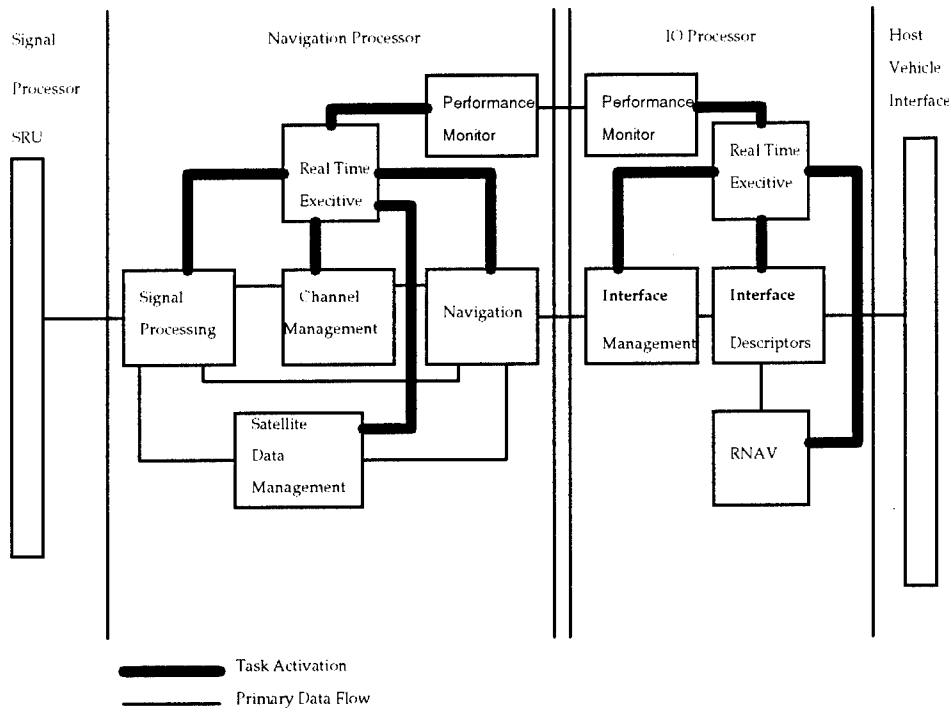


Figure 1. MAGR Software Architecture

Executive: At a secondary level, the receiver's functions are performed by tasks, each of which is initiated and iterated under the control of a multi-tasking executive - independently, to guarantee isolation of operation; so that should it become necessary to modify a function or enhance a capability, the impact is limited to a single task; or in adding a new capability, the impact is confined to a new task operating in isolation. Tasks are prioritized by the executive so that time-critical functions are neither delayed nor interrupted by background tasks. A system of interrupts and timers allows the executive to iterate tasks in either a time driven or an interrupt driven manner (to deal simultaneously with cyclic functions as well as those stimulated by outside events). In this way the executive exerts real-time control over the execution of the GPS functions on the Navigation Processor, while a duplicate executive provides this same control over the several tasks of the I/O Processor. (See Figure 1.)

Navigation Processor Tasks

Satellite Data Management: The first activity in the navigation process is the selection of satellites for acquisition and the collection of data relating to them: this is performed by the Satellite Data

Management task. Four functions are performed: (1) satellite selection, (2) the satellite position and velocity computation, (3) satellite data collection, and (4) the deterministic correction computation.

Each provides data to the Navigation and Channel Management functions based on inputs primarily from the Signal Processing function. The Satellite Selection computation determines the satellite constellation with the lowest DOP. This activity is iterated every two minutes. The Satellite Position/Velocity computation culminates in a list of interpolation coefficients for each visible satellite. This data is updated for each satellite every 30 seconds. The Satellite Data Management task consists of storing the satellite downlink data, monitoring its status, and to reduce data senescence errors, issuing data re-collection requests periodically. Deterministic corrections are predictable and measurable errors inherent in pseudo-range and delta-range measurements: ionospheric delay, tropospheric delay, channel biases, and signal path delays. These corrections are recomputed at regular intervals during the navigation process.

Channel Management: The Channel Management software is the controller of the process by which GPS satellites are acquired and tracked. It also controls the process by which pseudo-range and delta-range measurements are collected and passed on to the navigation function. At the outset of the navigation process it must respond to the environment in which it finds the receiver by determining an acquisition strategy. Subsequently, it must respond to changes in that environment.

On the transition into NAV mode, the goal is to acquire and track the best four Satellite Vehicles (SV's) in the shortest period of time. If the receiver contains neither satellite ephemeris nor almanac data, a Cold Start must be executed, in which the receiver attempts to acquire any available SV and collect the almanac data. The Normal Start is performed when the receiver already contains almanac or ephemeris data. The Hot Start is performed when the code uncertainty (computed from the navigation program's covariance data) is small enough that the P code can be searched directly to reduce acquisition time. This will be the case if the receiver has either almanac or ephemeris data, and precise time. Once all four of the initially selected SV's have been acquired, the initial acquisition phase ends and the normal track phase begins.

Finally, for each of the five channels, Channel Manager performs its acquisition status and measurement processing task. The measurement processing step is performed whenever valid pseudo-range and delta-range have been collected, and the signal strength is still above a minimum threshold. Data is then made available to the Navigation function.

Signal Processing: The signal processing software controls the receiver's signal processing CCA hardware, converting code correlations into pseudo-range and delta-range measurements, and demodulating the 50 Hz satellite downlink data used by the Satellite Management function. Each receiver channel performs all of the basic receiver operations independently, using its own hardware and software interfaces and its own received data.

The Signal Processor hardware interface runs at 100 Hz off a 10 ms interrupt. It collects signal measurements and status data from the preprocessor hardware and issues new commands to the preprocessor when necessary. This is done for each channel in the receiver.

A 50 Hz processing task is the core of the Signal Processing function. Different activities are performed based upon the 20 ms count within this sequence. These activities include computation of pseudo-range and delta-range values, loss-of-lock determination, and preparation of status data needed by the Channel Manager software once per second. The pseudo-range is computed to be the code position effective at 940 ms into the 1 Hz interval, while the delta-range is formulated as the integral of the carrier VCO commands.

Navigation: The Navigation function determines position, velocity, and time (PVT) using the satellite measurements collected and scaled by the Signal Processing and Channel Management functions. It also will use external data from the host vehicle (e.g., INS, Doppler, AHRS) when it is available. The

resulting solution is the basis for all receiver outputs and is used throughout the receiver in support of other functions such as satellite visibility determination, subsequent acquisition, and sequential tracking.

A 12-state Kalman filter mechanized in ECEF coordinates processes pseudo-range and delta-range measurements to determine and maintain a navigation solution. This filter operates in any of three modes - INS, DRS, or PVA - depending first on the availability of host vehicle data, and then on the quality of that data. The Kalman filter is updated at a 1 Hz rate consistent with the satellite measurement rate, and is used to maintain a PVT solution known as the background navigation solution.

In addition to the background navigation solution, there is another that is maintained as close to real time as possible. It is known as the Foreground Navigation solution - consisting of position, velocity, and time - and is driven by host vehicle aiding data inputs (INS, DRS, or attitude); or by an internal 10 Hz rate when aiding data is not available. The goal of the foreground navigation process is to propagate the background solution using the host vehicle velocity and acceleration data, or using the receiver's estimate of velocity and acceleration.

I/O Processor Tasks

Interface Management: The Interface Management task is the conduit through which host vehicle data is passed to the Navigation task (aiding the determination of position, velocity, and time); and through which the GPS navigation solution is disseminated to the various host vehicle subsystems. It consists of three pieces: source selection, input data processing, and output data control. Some host vehicle platforms may have several sources of aiding data available to the MAGR - an INS, a Doppler system, and an AHRS, for example. At a 1-Hz rate, the source selection function will review statistics accumulated by the Interface Descriptors (see below), and select one as the preferred aiding source (based not only on the assumed stability and accuracy of the device, but also its current status). The input data processing function is performed in response to the arrival of new aiding data from the host vehicle. It performs functions common to the processing of all host vehicle aiding data (e.g., block identification, transfer of data from external RAM), and then activates the Interface Descriptor task responsible for the unique processing. If the data being processed is from the preferred source, the Interface Management's processing function will also activate the Foreground Navigation function on the navigation processor. The output data control function will collect and reformat common output data and make it available to the Interface Descriptors' output functions.

Interface Descriptors: The Interface Descriptors provide the part of the I/O processing function that accommodates each interface's peculiarities, that allows the Navigation processor to remain ignorant of and unaffected by the interface unique processing. The MAGR has five - one for each of the two 1553 interfaces (governed by ICD-GPS-059 and ICD-GPS-104), one for the external interfaces (HAVEQUICK and 1 PPS), one for the RS-422 interface (for Instrumentation data), and one for the ARINC 429 Flight Instruments interface. In general each consists of an interrupt handler (several in the case of the 1553 interfaces) that performs a data thinning function and activates the input data processing function; an input data processing function which performs coordinate conversions, validity and reasonableness checks, and accumulates validity and health data for the Interface Management task; and a time driven process initiated by the Interface Management task that collects and reformats receiver computed data, and makes it available to the external interface hardware.

RNAV: The RNAV task provides the receiver with a relative navigation capability: given the receiver's current position, velocity, and time, a desired track, and a set of waypoint data, the receiver will provide direction, distance, and flight progress data that will allow the host vehicle to navigate efficiently from one point to another. It is made up of a collection of functions, each computing a single datum (bearing, range, cross-track deviation, and so on); and a 20 Hz function that controls the rate at which these functions are performed. It contains also a set of utilities that provide for management of the

waypoint data base, including not only waypoint definition data, but flight plan and flight profile data as well.

FAULT DETECTION, ISOLATION, AND ANNUNCIATION

If the purpose of integrity monitoring is to alert the pilot and the other aircraft subsystems that the GPS receiver's output data is valid, then it can be thought of as another of the receiver's several existing on-line performance monitor checks. In the case of the MAGR (and the 3A and EGI), an incipient integrity monitoring already exists as a part of the receiver's Performance Monitor software. RAIM as it generally is understood (and as it is implemented here), is an embellishment of the existing capability. In the context of the baseline receiver's existing fault detection, isolation, and annunciation mechanism (the Performance Monitor function of Figure 1), the standard receiver's consistency check of the satellites is less well developed than other of the performance tests: no attempt at fault isolation is made (even though faults are annunciated), whereas the test for a stuck bit would isolate the fault to a component. Nonetheless, it does very much fit within the receiver's other fault detection schemes; the enhancement -- the RAIM algorithm -- does as well.

Performance Monitor fault detection is divided into two parts: active and passive. The active testing is a non-intrusive check of critical hardware. In a background mode -- so that processor throughput capacity is unaffected -- over as many seconds as are needed, bit sensitivity tests are run on RAM, checksum tests are performed on ROM, processor diagnostics are performed (op codes, arithmetic and logic operations), interprocessor communications, tracking subsystem tests (correlator, antenna electronics), and so on. Typically, a failure from one of these tests will cause the immediate generation of a Receiver Fail message to all external interfaces. The receiver will continue operation, generating position, velocity, and time data; but all its validity indicators will be set to fail, its estimated errors will be set to maximum values, and the Figure of Merit will be set to its worst level (9).

The passive testing consists of a background reviewing of data logged in real-time by the operational software. As input data is received it is evaluated for reasonableness: if a datum exceeds some maximum or minimum limit, if its deviation from average values or filtered values exceeds some limit, if the input rate exceeds some maximum or falls below some minimum, if parity or checksum tests fail, if warp-around tests fail, and so on, the operational software will log errors -- in real-time fault logs -- that are subsequently reviewed by the Performance Monitor software. Periodically -- for most errors, once a second -- the Performance Monitor software will review these fault logs, and should non-zero values appear, it will generate failures, warnings, or informational messages that are then sent out over the receiver's external interfaces (to display systems or other platform subsystems). The baseline MAGR's testing of the satellite measurements uses a least squares residual check to detect anomalies. When a bad measurement is detected, it is discarded. If enough measurements are discarded over a short enough period of time, the satellite is dropped in favor of the alternate whose inclusion yields the best remaining GDOP. The receiver will subsequently attempt using the discarded satellite, providing its 50 Hz health data permits. RAIM is an enhancement of this test, one with a more detailed and rigorously defined set of failure criteria.

The annunciation messages take the form of Position, Velocity, and Time validity flags, a Figure of Merit value, and estimated errors. As a result of this existing reporting mechanism, the incorporation of RAIM need not necessarily require the addition of message traffic, nor the modification of existing integrations: the existing message sets defined by ICD-GPS-059, ICD-GPS-104, and ICD-GPS-073 are more than adequate to the task of providing a qualitative evaluation of the GPS data within the existing interface definitions. A Predictive RAIM Availability function could require platform change; but if the only question asked of the avionics platform by the aircraft is, Can the GPS data continue to sustain the mission; the mechanisms already in use by the platform to identify other anomalies (loss of INS data,

failed memory chip, inadequate GDOP, stale ionospheric delay measurements, and so on) can announce this anomaly as well.

RAIM ARCHITECTURE

Architecturally, RAIM can be divided into four separate activities: measurement delivery, residual computation, integrity determination, and fault annunciation. The Navigation software's residual computation is affected very little by the RAIM inclusion: the same process remains, only now determining up to four additional residuals. The integrity determination -- fault detection and isolation -- is a new functional capability, implemented with new software; but given the nature of a real-time multitasking executive, it can be included in the existing architecture without disrupting the rest of the software (memory and processor throughput permitting) -- another task is added to the cyclic task list, running in a background mode (i.e., its execution is allowed to be spread over as long a period of time as needed so that it interferes with no higher priority task). And, as earlier noted, the Performance Monitor's annunciation task is unchanged -- it has an additional entry in an existing fault log.

The measurement delivery function, however, can be profoundly impacted by the RAIM inclusion. In the ten channel receiver, the Channel Management software suffers the same minimal impact as the Navigation software. With five additional channels, the process remains exactly the same: where it previously managed four channels and their measurements, here using the same mechanism it manages eight. Referring to Figure 1, the Channel Management software continuously tracks eight satellites, the Signal Processing software collects data which it then passes back to the Channel Management function, which in turn creates eight measurements and passes all eight to the Navigation software. This computes residuals which it in turn passes to the RAIM software. This all happens at a 1 Hz rate for all eight satellites. The ten channel MAGR remains, even when the RAIM function is active, a continuous tracking receiver. Not so, the five channel MAGR.

The five channel MAGR must retrieve up to eight measurements using only four channels (the fifth channel -- equally to avoid degrading position accuracy by using stale measurements for the ionospheric delay estimation, as well as to avoid a similar corruption from using modeled delay estimates -- must continue the alternate frequency acquisition task); the continuous tracking receiver must revert in part to a sequencing receiver. The extent of the reversion -- and the extent to which the receiver's performance degrades to that of a sequencing receiver -- is determined by the Channel Management software's measurement delivery strategy -- the satellite acquisition and reacquisition strategy. Note that given the architecture, between the five and the ten channel receivers neither the residual computation nor the integrity determination functions are affected. Since all measurements are time tagged, in the ten channel receiver, the navigation function in effect uses a zero propagation interval for all measurements, whereas in the five channel receiver, prior measurements are propagated to the current interval. How many measurements are propagated and over how long an interval determines the corruption of the standard receiver's performance. Minimizing this corruption becomes the goal of the Channel Management strategy.

A straightforward mechanism is to momentarily acquire and track each of the four additional satellites on the fifth channel, while with the other four channels one at a time acquiring momentarily each of the primary satellites on the opposite frequency (for the ionospheric delay measurement). This way only one of the primary channels' measurements is propagated at a time, and it will only become stale to the extent needed to acquire the opposite frequency and determine a measurement from it: a worst case interval of two seconds. With three current measurements, an input inertial velocity, and a calibrated altimeter input (a not unlikely configuration for a combat aircraft) little performance is lost over this interval except under heavy jamming, in which case the net effect is to lose 3 to 4 dB of jamming resistance under maximum dynamics (1200 m/s, 90 m/s², 100 m/s³). Under constant dynamics (<1 m/s², 1 m/s³) even

under heavy jamming, analysis indicates a negligible fall off in performance (test data confirming this conclusion is scheduled to be available by July 95). Without the inertial and altimeter inputs, the impact of this sequential RAIM is more pronounced, but still is dwarfed by the far more profound impact (an order of magnitude) of having no input inertial velocity to maintain prepositioning data once carrier lock is lost and all four channels are in effect tracking sequentially.

RAIM DESCRIPTION

RAIM capability offers two benefits to the military GPS user: additional integrity for the GPS based targeting solutions; and FAA-compliant GPS integrity within FAA controlled airspace. Much of the RAIM literature to date has, quite properly, addressed the topic of RAIM in the simplest context: an all-in-view receiver which supplies simultaneously valid measurement residuals from all visible satellites. This, however, is an ideal condition, not a necessary one. Studies indicate that a carefully chosen subset of visible satellites offers virtually the same level of RAIM availability as an all-in-view implementation; and the measurement residuals in a RAIM snapshot do not have to be based upon measurements obtained at the same time of validity. Older measurement residuals can be recycled to provide the necessary measurement redundancy to provide timely verification of the integrity of more recent measurements. In short, RAIM is supportable with only modest use of receiver resources to obtain redundant measurement data. RAIM is supportable by a 5-channel receiver without compromising the existing performance of that receiver.

RAIM Detector Algorithm.

A RAIM algorithm quantifies the self-consistency of a set of redundant measurement data and relates this quantity to the expected horizontal error in the least-squares navigation solution derived from that measurement set. The literature describes three RAIM methods: the parity method [5], the least squares residual (LSR) method [6], and the range comparison method [7]. These have been demonstrated to be equivalent for RAIM detection [4]. The parity method seemingly has emerged as the algorithm of choice. This is due partly, perhaps, because of a perception that the parity method uniquely offers a means for identifying the faulted satellite. In actuality, the LSR method offers this same capability at significantly lower throughput cost. The only feature that the LSR method lacks is direct observability of the individual elements of the parity vector. However, this information is not needed for RAIM -- neither for detection nor for isolation.

Some of the equivalencies of the parity and LSR methods are illustrated in Table 1, which uses nomenclature standard to the literature. The one non-standard term is *BSCL*, which is defined as the diagonal matrix comprising the inverse square roots of the main diagonal elements of *I-GA*. The choice between the parity and LSR methods is strictly an implementation decision. The LSR method was selected for use in the MAGR to minimize throughput.

Intuitively, one might think of the RAIM algorithm as an integrity filter which screens all measurement residuals prior to use by the Navigation function (Figure 1). This is both impractical and unnecessary. The RAIM algorithm is specifically intended to detect one type of long term GPS ranging error. This can be accomplished by "spot checking" a measurement source, generally by looking at a specific residual after it has been incorporated by the Navigation function. The RAIM detector detects an anomalous ramp error on a satellite before its systematic use by Navigation function can drive the navigation solution position error beyond the specified RAIM protection limit.

The RAIM detector is one element of an ensemble of monitors which protect the GPS navigation solution from various types of measurement residual errors. To protect against large, short term errors, the GPS receiver complements the RAIM redundancy monitor with other integrity checks on measurement residuals. After the nav solution has converged, the navigation function itself rejects measurement residuals whose magnitude exceeds a priori 10-sigma pseudorange uncertainty. This is the mechanism of the baseline receiver. The navigation function also monitors the difference between successive residuals from the same measurement source, rejecting any residual which differs from its predecessor by more than 400 meters. This latter residual criterion is consistent with a monitor specified in the RTCA Sole Means GPS MOPS draft.

Table 1 Comparison of Parity and Least Squares Residuals Methods

Topic	Parity Method	LSR Method
Detection $P^T P = I - GA$	$\underline{p} = P \underline{y}, \quad \underline{e} = P^T \underline{p}$	$\underline{e} = (I - GA) \underline{y}$
Chi-square distributed test statistic	$\underline{p}^T \underline{p}$	$\underline{e}^T \underline{e}$
Parity space unit vectors	$P_N = P B_{SCL}$	
Vector of parity vector projections onto satellite characteristic lines.	$P_N^T \underline{p}$	$B_{SCL} \cdot \underline{e}$

Receiver Resource Management Strategies For The 5-Channel Receiver.

The 5 tracking channels of the baseline MAGR receiver are organized to support a 4 satellite navigation solution. To support a RAIM fault detection and measurement exclusion/isolation capability, the combined task list for all five receiver channels must be expanded to include the periodic track of at least two additional satellites.

RAIM detection performance is maximized when all available GPS measurements are used in the RAIM snapshot. In devising an appropriate resource management strategy in a five channel receiver, one has the choice of two philosophical approaches: allocate them evenly among satellites in a redundant measurement space; or retain the existing commitment to the best-GDOP four satellite navigation solution and use the spare (fifth) channel to secure the necessary RAIM measurements. Either approach necessitates a sequential tracking strategy, of one sort or another (the issue becomes one of how the ionospheric delay is measured), which could compromise receiver performance to an unacceptable degree.

The implementation strategy chosen (see RAIM Architecture, above) reduces this impact to a negligible level. Two consequences are apparent. The incremental exposure to loss-of-lock on a navigation satellite is limited to one satellite at a time, and only under benign tracking conditions -- i.e., RAIM is effectively unavailable during significant signal masking: even if heavy jamming applies, the weapons release assumption, typically, is a straight (even if not always level) flight path. Furthermore, this exposure involves the relatively low risk associated with switching frequencies on the same satellite when the L1-L2 phase difference is calibrated. Each navigation satellite is exposed to this risk once per two minute interval. The other impact -- a consequence of the frequency switching -- is the benign effect of losing two delta range measurements from each navigation satellite per two minute interval. The net impact is

thereby limited to what one would expect to see shortly after reacquiring a navigation satellite (subsequent to masking of one kind or another).

RAIM Measurement Space.

RAIM detection performance is maximized when all available GPS measurements are used in the RAIM snapshot. However, virtually the same level of RAIM availability is achievable using a carefully selected subset of the visible satellites. An analysis of various satellite selection algorithms was performed [11]. Each algorithm selects additional satellites, designated "RAIM satellites", to be used with the best GDOP set of four navigation satellites. The analysis considered two cases -- 2 RAIM satellites and 4 RAIM satellites -- and considered the following candidate optimization criteria: minimum GDOP, minimum PDOP, minimum HDOP, and minimum SLOPEMAX. As the sole criterion for selecting an entire measurement set, SLOPEMAX minimization leads to bad GDOP.

As the criterion for adding 2 satellites to the best GDOP set of four satellites, however, SLOPEMAX minimization was found to provide the best RAIM availability. For adding 4 satellites to the best GDOP set of four satellites, all four candidate criteria delivered roughly the same availability (within 1%), both for detection and for isolation. GDOP minimization was selected as the RAIM satellite selection criterion for MAGR.

Measurement Space Used For The Navigation Solution.

The RAIM capable 5-channel GPS receiver computes its navigation solution upon a primary set of four navigation satellites. Nominally, this set yields the best GDOP. Periodic incorporation of RAIM satellite measurements overdetermines the navigation solution. The resulting periodic difference in measurement mix from one navigation solution update to another could cause a corresponding hunting cycle in the navigation solution reminiscent of single- or two-channel receivers. Here, however, the Channel Management function continues to provide measurements from the four navigation satellites with only slightly less frequency than in the baseline MAGR. The impact on navigation solution accuracy is negligible and within MAGR performance requirements.

The decision to stay with the best-GDOP four satellite navigation entails two downside issues which are considered manageable. One is that the four satellite navigation solution varies from the RAIM snapshot navigation solution somewhat more than would an all-in-view navigation solution. This issue is addressed in a subsequent section of this paper. The other issue is that an all-in-view navigation solution statistically offers only a modest improvement in navigation solution GDOP. A statistical analysis performed upon the RTCA DO-208 sample space indicated that the all-in-view navigation solution GDOP is 83% as great as that of the best-GDOP four satellite navigation solution. This would have only a negligible impact on performance.

Use Of Measurement Residuals With Different Values For Statistical RMS Error.

References [2] and [7] describe a technique for accommodating baro altitude measurement in a RAIM snapshot. The MAGR's RAIM algorithm expands on this technique by normalizing all measurement residuals to unity variance prior to their incorporation into a RAIM snapshot. The normalized G matrix used in the RAIM computations is derived by pre-multiplying the unweighted measurement line-of-sight matrix, H, by diagonal matrix W, where the elements of W are the inverse of the RMS errors of the measurements. This is a software convenience. There exists an entity, which we call measurement set RMS error, which is given by

$$\sigma \equiv \sqrt{m / \text{trace}(R^{-1})}$$

This variable is not needed for any of the computations required for RAIM availability assessment or for RAIM fault detection and exclusion/isolation. Its only use is for the optional computation of SLOPEMAX or weighted DOP's. Once matrix G is computed, neither measurement set RMS error nor any of the individual measurement variance factor into any RAIM computations, including the computation of RAIM availability. The RAIM test statistic is Chi-square distributed, and, if one assumes that the correlation time constant of the dominant term of pseudorange error is approximately 120 seconds, irrespective of SA level, then a single set of constant false alarm rate (CFAR) RAIM detection thresholds addresses all mixes of RAIM measurements.

Use Of Measurement Residuals Referenced To Different Times Of Validity.

As a result of the 5-channel architecture of the receiver, the RAIM algorithm cannot possibly have access to more than 5 pseudorange measurements with the same time of validity. The preferred receiver resource management strategy described above provides measurement residuals from up to 8 satellites valid at different times within an interval of 32 seconds, worst case. As updates to the navigation solution occur at 1 Hz, these residuals are necessarily referenced to different navigation solutions. The 5-channel RAIM algorithm maintains a database containing the most recent pseudorange measurement residual for each satellite tracked within the past 32 seconds. Each satellite record comprises the following information: measurement time of validity, measurement residual, measurement LOS, and computed measurement RMS error. At 1 Hz (effectively), each residual in the database is adjusted by an increment equal to its LOS vector dotted with the current 1 Hz update to the navigation solution. Thus all residuals in the database are dynamically rereferenced to the current navigation solution. The RAIM detector uses all measurements in this database. The RMS error value used for a measurement residual in the RAIM snapshot is the database value degraded by the age of the measurement.

Accommodation Of The Difference Between GPS Navigation Solution And RAIM Snapshot Nav Solution.

The deviation between the navigation solution and the least squares RAIM solution can be directly monitored in real time. This deviation is safely accommodated by adding its magnitude to the horizontal integrity limit computed for the RAIM snapshot when assessing RAIM availability.

Sole Means GPS

The enhanced MAGR uses a form of the Partial Identification RAIM algorithm, described in reference [10]. The output of the RAIM detector is essentially a list of measurement sources recommended for use by the Navigation function. If more than one measurement source is rejected by RAIM, and one or more

of these rejected measurement sources is used for navigation, the Navigation function immediately ceases to use residuals from this (these) rejected source(s). An excluded RAIM satellite is retained in the RAIM constellation until a consistent pattern of repeated rejection is observed. The RAIM satellite is then dropped by the receiver's channel management function (see figure 1, above) in favor of an alternate satellite. If a navigation satellite is rejected, this satellite is immediately relegated to RAIM satellite status on its channel, and an alternate navigation satellite is tracked. The original rejected navigation satellite remains in the RAIM constellation until it establishes a pattern of repeated rejection and is dropped. Collection of new ephemeris resets the RAIM track history associated with a satellite.

REFERENCES.

- [1] RTCA DO-208, "Minimum Operational Performance Standards (MOPS) for Airborne Supplemental Navigation Equipment Using Global Positioning System", RTCA, 12 July 1991.
- [2] FAA TSO C129.
- [3] R. Grover Brown (Iowa State University), Gerald Y. Chin and John H. Kraemer (US DOT, Volpe Nat'l Transportation Center), "Update on GPS Integrity Requirements of the RTCA MOPS".
- [4] R. Grover Brown (Iowa State University), "A Baseline RAIM Scheme and a Note on the Equivalence of Three RAIM Methods", ION National Technical Meeting, 27-29 January 1992, 28, January 1992.
- [5] Mark Sturza (Litton Systems), "Navigation System Integrity Monitoring Using Redundant Measurements", Navigation: Journal of the ION, Vol. 35, No. 4, Winter 88-89, October 1993.
- [6] Brad Parkinson and Penina Axelrad (Stanford University), "A Basis for the Development of Operational Algorithms for Simplified GPS Integrity Checking", Proceedings of the ION Satellite Division Technical Meeting, Colorado Springs, 1987.
- [7] Young C. Lee (MITRE Corp.), "New Concept for Independent GPS Integrity Monitoring", Navigation: The Journal of the ION, Vol. 36, No. 2, Summer 1988, May 1988.
- [8] Young C. Lee (MITRE Corp.), "Analysis of RAIM Function Availability of GPS Augmented with Barometric Altimeter and Clock Coasting", June 1993.
- [9] Karen L. Van Dyke (U.S. DOT, Volpe NTSC), "RAIM Availability for GPS Supplemental Navigation", Proceedings of 48th Annual Meeting of ION, June 29 - July 1, 1992, Washington DC.
- [10] R. Grover Brown (Iowa State University), John Kraemer (U.S. DOT), Giau Nim (Volpe NTSC), "A Partial Identification RAIM Algorithm for GPS Sole Means Navigation", Proceedings of ION GPS-94, September, 1994.
- [11] GPS Joint Program Office, "Final Report: Enhanced Receiver Study Task CZU-93-0008-F-004", 05 December 1993

THIS PAGE LEFT BLANK INTENTIONALLY

C/A-Only Mode Operation of the DoD Standard MAGR

Abstract

Roger Kirpes and Brent Disselkoen
Rockwell CACD

Most Miniature Airborne GPS Receivers (MAGR) are purchased and operated as authorized receivers that can track Y code (encrypted P code) satellites. However, the increasing number of MAGRs operating as unauthorized receivers, which are restricted to tracking C/A code when the satellites are transmitting Y code, will benefit from ongoing improvements to C/A-only mode operation. C/A-only mode has recently become more important as the GPS satellites started transmitting Y code instead of P code. Until this time MAGR performance in C/A-only mode has not been stressed, except as it was needed for transition to authorized operation.

Normal MAGR initial acquisition of a satellite signal involves correlating a local copy of the C/A (Coarse Acquisition) code with the C/A code transmitted by the satellite. After the two codes are aligned with respect to each other, the 50Hz navigation message is demodulated and the handover word (HOW) is obtained. The HOW provides current P(Y) code phase information for the satellite. Since P and Y code are mutually exclusive, unauthorized receivers cannot use the HOW to acquire P code if information in the HOW indicates the satellite is currently transmitting Y code. This forces unauthorized receivers to continue tracking C/A code on this satellite (C/A-only mode).

Without the benefit of the high quality P(Y) code for accurate positioning, the receiver operating in C/A-only mode must compensate the degraded measurement quality with enhanced software techniques. Several areas for improvement are addressed in this paper: reliable signal acquisitions at high signal power; Kalman filter optimizations which reflect increased pseudorange measurement noise; smoothing pseudorange measurements with continuous carrier-phase data; enhanced satellite selection and management algorithms; and alternate ionosphere delay compensation. Of prime importance is ensuring smooth transitions in and out of C/A-only mode due to changes in either the receiver's authorization or the satellite's transmitted code. Allowance for tracking a mixed constellation of C/A code and P code satellites must also be made.

Incorporation of the previously mentioned enhancements significantly improves the MAGR's tracking reliability and performance in C/A-only mode, which in turn facilitates smooth transitions between C/A-only mode and P(Y) code operation. In addition, some enhancements are applicable to the P(Y) code environment, therefore constituting general MAGR performance improvements.

THIS PAGE LEFT BLANK INTENTIONALLY

Enhancements to C/A-Only Mode Operation of the DoD Standard MAGR

Roger Kirpes
Brent Disselkoen
Barry Breffle

Collins Avionics and Communications Division
Rockwell International
350 Collins Road, NE
Cedar Rapids, Iowa 52498

Approved for Public Release; distribution is unlimited.

THIS PAGE LEFT BLANK INTENTIONALLY

Enhancements to C/A-Only Mode Operation of the DoD Standard MAGR

Roger Kirpes, Brent Disselkoen and Barry Breffle
Collins Avionics & Communications Division, Rockwell International,
Cedar Rapids, Iowa 52498

Biography

Roger Kirpes is a Software Design Engineer in the Standard Airborne GPS Products Department, Collins Avionics & Communications Division, Rockwell International. He received his B.S. in Math and Physics in 1988, and his M.S. in Applied Math in 1993, from Iowa State University. Since joining Rockwell in August 1993, he has been involved in the design and test of channel management and navigation software for the Space Shuttle and other advanced MAGR and embedded GPS products.

Brent Disselkoen is a Software Design Engineer in the Standard Airborne GPS Products Department, Collins Avionics & Communications Division, Rockwell International. He received his B.S. in Electrical Engineering and Computer Science from Dordt College, Sioux Center IA in 1987, and his M.S. in Electrical Engineering from Arizona State University in 1991. Since joining Rockwell in September of 1993, he has been involved in digital signal processing design and analysis for the handheld and airborne GPS products.

Barry Breffle is a Software Design Engineer in the Standard Airborne GPS Products Department, Collins Avionics & Communications Division, Rockwell International. He received his B.S. in Electrical Engineering from The University of Iowa in 1994. Since joining Rockwell in January of 1993, he has been involved in the design and test of Receiver Manager software for MAGR and various MAGR derivative products.

Abstract

Any DoD Standard Miniature Airborne GPS Receiver (MAGR), whether used authorized or unauthorized, will benefit from ongoing enhancements to C/A (coarse/acquisition)-only mode operation. These enhancements complement its Anti-Spoofing capabilities, and include reliable satellite signal acquisitions, optimal channel management, and enhanced solution accuracy under C/A code track conditions. C/A-only mode operation readily and smoothly transitions to authorized operation if MAGR becomes authorized. Ongoing enhancements include differential GPS and continuous carrier smoothing.

1. Introduction

Most MAGRs are purchased with a Precise Positioning Service – Security Module (PPS-SM) and are operated as authorized receivers that can track Y code satellites. Y code is transmitted in place of P (precision) code whenever the satellite Anti-Spoofing (AS) mode of operation is activated. However, the increasing number of MAGRs operating as unauthorized receivers, which are restricted to tracking C/A code when the satellites are transmitting Y code, will benefit from ongoing enhancements to C/A-only mode operation. Until recently MAGR performance in C/A-only mode has not been stressed, except as this weakened state was needed while awaiting the transition to authorized operation.

Normal MAGR initial acquisition of a satellite signal involves correlating a local copy of the C/A code with the C/A code transmitted by the satellite. After the two codes are aligned with respect to each other, the 50 Hz navigation message is demodulated and the hand over word (HOW) is obtained. The HOW provides current P(Y) code phase information for the satellite. Since a satellite transmits either P or Y code at a given time, unauthorized MAGRs cannot acquire P code if information in the HOW indicates the satellite is currently transmitting Y code. This forces unauthorized MAGRs to continue tracking C/A code on this satellite (C/A-only mode).

Without access to the P(Y) code, MAGR operating in C/A-only mode has virtually all the handicaps of a C/A-L1 receiver. It is denied the precision tracking capability, the reduced noise, and the greater resistance to interference offered by the P(Y) code. It is unable to remove the effects of Selected Availability from its measurements. MAGR operating in C/A-only mode compensates for the degraded measurement and tracking quality with enhanced software techniques. These C/A-only enhancements fall into several categories:

- Satellite signal acquisition
- Optimal channel management
- Enhanced solution accuracy
- Assured timely upgrade to non C/A-only operation

These improvements complement MAGR's Anti-Spoofing capabilities. Yet optimal C/A-only mode operation must be constrained by and deferred to MAGR's authorized operation needs, even at the expense of optimal C/A-only mode acquisition, track, and accuracy performance. Hence, of prime importance is ensuring smooth transitions out of and in to C/A-only mode. These transitions may arise due to changes in either the MAGR's authorization status or a satellite's transmitted code.

The C/A-only mode MAGR has an advantage over a C/A-L1 receiver in being able to track P code on L1 or L2 if it is being transmitted by a satellite, and its Anti-Spoofing mode allows. Thus allowance for tracking a mixed constellation of C/A code and P code satellites must also be made. This illustrates the fact that C/A-only mode operation is a *per satellite* attribute, even though the requisite of being unauthorized is a MAGR aggregate attribute.

Incorporation of the previously mentioned enhancements significantly improves MAGR's tracking reliability and performance in C/A-only mode, which in turn facilitates smooth transitions between C/A-only mode and Y code operation. In addition, some enhancements are also applicable to the P(Y) code environment, therefore constituting general MAGR performance improvements.

2. Satellite Signal Acquisition

Acquisition of a C/A code satellite signal is an essential part of MAGR operation. MAGR makes a variety of assumptions and decisions based on its knowledge of C/A code characteristics and past tracking history as well as its current perception of the signal environment (e.g. hostile, friendly) and C/A code properties (e.g. signal strength, multipath).

2.1 C/A Code Characteristics

The C/A codes are actually Gold codes (Gold, 1967) formed as the product of two 1023 bit PN codes, G1(t) and G2(t). These codes have a period of 1023 bits and an autocorrelation function characteristic similar to that shown in Figure 1. Assuming the received C/A code is composed of two discrete levels (-1,1), the autocorrelation can assume 4 possible values: 1023, -65, 63, and -1. With respect to the primary peak at 1023, the signal strengths of the other correlations are 23.94, 24.21, and 60.2 dB lower respectively. These spurious (side) correlations are inherent in all C/A code sequences.

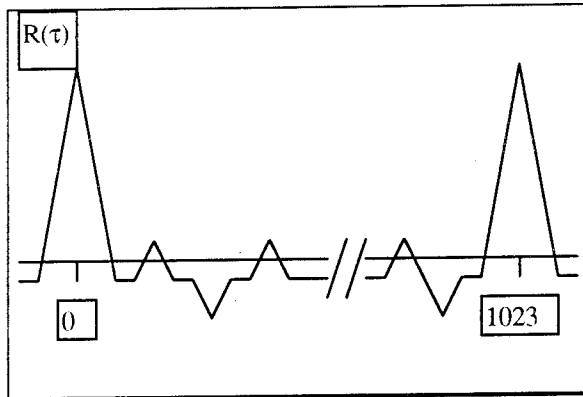


Figure 1: C/A Code Autocorrelation

MAGR is designed to operate over a very wide range of carrier to noise ratio (C/N_0). Hence a very strong true correlation exhibits spurious correlations which may be falsely interpreted by the acquisition logic as weak signal correlations. In these cases the false correlations can initiate an inappropriate transition from the acquisition to the carrier and code tracking algorithms.

2.2 C/A Code Environment

The operation of MAGR in the current C/A code environment is a function of the C/A code signal strength as well as the presence of multipath and spoofers (intentional simulators of GPS signals). During a C/A code acquisition, the presence (or absence) of correlations can imply different things depending on whether the signal environment is hostile or friendly.

In a friendly environment, a weak correlation found during initial acquisition is either the real signal, a side correlation (which implies that the real signal is much stronger), or an out-of-chip multipath signal. Section 2.3, Acquisition Techniques, discusses some design considerations for reliable discrimination between side correlations and true weak signal correlations. The (assumed) absence of spoofers simplifies the decision logic considerably since every correlation found has some relationship to the true correlation.

A hostile environment presents significant challenges to the C/A code search strategy. Here a weak correlation found in initial acquisition is either the real signal, a side correlation from a real signal, an out-of-chip multipath signal, a spoofer, or a side correlation from a spoofer. The number of possible combinations significantly increases the complexity of the decision logic and can mislead the C/A code acquisition process.

2.3 Acquisition Techniques

MAGR uses a series of thresholds to acquire a C/A code signal over a wide range of C/N_0 . During the C/A code search, MAGR correlates a (sliding) local copy of the C/A code with the C/A code transmitted by the satellite. At every C/A code position, a correlation power is computed and compared to the appropriate threshold (which is normalized for the current noise level and establishes a particular probability that this is the true correlation). Different thresholds are used for weak signal mode and strong signal mode, where the mode is dictated by the current perceived environment. Current MAGR logic assumes a weak signal environment in initial acquisition (or when C/N_0 is unknown), making it imperative that strong signals can be identified in weak signal mode. Identification of strong signals is made particularly difficult by the presence of spurious (side) correlations of the C/A code sequences.

MAGR's threshold logic makes a key assumption about the C/A code strong signal characteristics. Specifically, it assumes that if the primary peak is very strong, at least one spurious correlation peak will pass the weak signal mode threshold test within the first 90 C/A chips that are tested. Since there are a

minimum of 10 spurious correlations in 90 C/A chips (for all valid PRN numbers), the probability of missing one of these spurious correlations during the first 90 chip search becomes negligible only for C/A signal strengths above 51 dB-Hz C/N_0 , as shown in Figure 2.

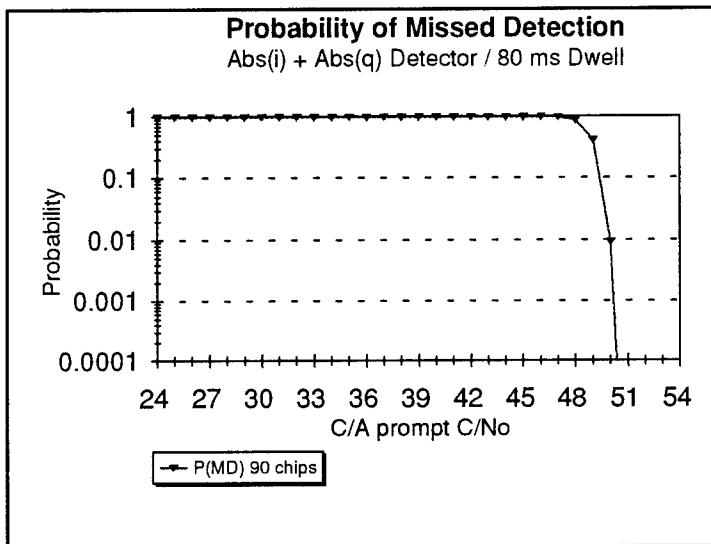


Figure 2: Probability of Missed Detection

The Probability of Missed Detection is only important if there is a high probability of detecting a spurious correlation (after the first 90 chips) before the true correlation would be detected. The maximum number of spurious correlations in 511 C/A chips (over all valid PRN numbers) is 160. Under the assumption that the true correlation can be found by searching half the C/A code (511 chips), one can determine the Probability of False Alarm in 511-90 (=421) C/A chips. This probability becomes significant for C/A signal strengths above 46 dB-Hz C/N_0 , as shown in Figure 3. Therefore, between approximately 47-51 dB-Hz C/N_0 there is a high probability that a spurious correlation could confuse the acquisition logic.

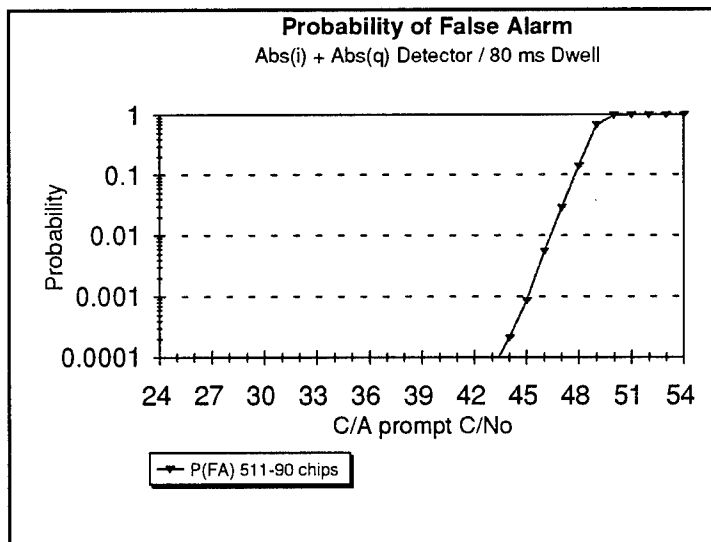


Figure 3: Probability of False Alarm

An additional check has been implemented to help distinguish between spurious correlations and a true weak signal. Upon detecting a possible spurious correlation, a strong signal mode search is initiated to determine if a strong signal is present. If the strong signal mode search yields a candidate correlation, and the correlation power satisfies the criteria for strong signals, then the acquisition logic will pass the strong signal correlation to the carrier and code tracking algorithms; otherwise the previous weak signal correlation will be used. This technique significantly reduces the probability of confusing the acquisition logic with a spurious correlation.

2.4 C/A Code Verification

The probability of continually tracking the wrong C/A correlation is somewhat higher for an unauthorized MAGR than for an authorized MAGR. If MAGR is authorized, the extraneous correlations are only detrimental in that they delay the transition to Y code. If MAGR attempted Y code track on every possible correlation, eventually the real signal should be found and Y code track established. Unfortunately since there are between 200 and 320 side correlations per PRN, this can take a significant amount of time. Once Y code track is established on any satellite, the current downlink data can be collected and used to support the acquisition of subsequent satellites.

An unauthorized MAGR does not have the advantage of being able to verify the real satellite signal by means of tracking Y code. Instead it is forced to remain in C/A-only mode and try to determine which C/A code correlation is most likely the real signal. Prior implementations prevented false track of side correlations by re-commanding a maximal search for the same satellite to locate the strongest correlation. In section 2.3: Acquisition Techniques, a new method was presented which improves MAGR's ability to distinguish between spurious correlations and real weak signals. Regardless of the technique, a hostile environment can cause significant degradation.

If the constellation is comprised of both P and Y code satellites (i.e., a mixed constellation), and the spoofers (if present) are only transmitting C/A code, an unauthorized MAGR can use P code track to verify the real signal. In this situation the downlink and measurement data from the P code satellite can be used to perform consistency checks with the other C/A code satellites, thus providing some degree of protection against C/A code spoofers.

Recent classified enhancements to MAGR under ECP-003 involve improved techniques for distinguishing between real and non-real satellite signals. Many of these changes are only applicable for an authorized MAGR in Y-only mode, during which it will not track a P code signal. Under these circumstances, a variety of additional checks are performed to verify that the C/A code correlation will result in a successful transition to Y code. If the hand over to Y code fails, MAGR employs other new recovery strategies in an attempt to eventually acquire Y code.

Fortunately, some of these new enhancements are also beneficial to an unauthorized MAGR. In particular, the additional verification checks on the C/A code correlation provide some immunity to falsely tracking a non-real satellite signal. However, since it lacks the ability to verify the C/A code correlation by a hand over to Y code, C/A-only mode operation is always susceptible to tracking false satellite signals.

3. Channel Management

As discussed in Section 2, Satellite Signal Acquisition, expedient acquisition of a satellite signal is an essential part of MAGR operation. State 5 track on four satellites is necessary to achieve a fully determined PVT solution. In order to achieve this as rapidly as possible and to maintain this state, MAGR uses its peripheral channel to perform various support tasks (Kacirek and Bartholomew, 1992), which include: aid initial acquisition of satellites, acquire satellites for dual frequency ionospheric delay measurements, and perform acquisition of alternate satellites. For MAGR operating in C/A-only mode, adjustments in the strategies used to fulfill these tasks yield increased efficiency.

3.1 C/A-Only Mode Status

The C/A-only status of each satellite being tracked is monitored each second and saved as part of that satellite's track history. This status reflects how the authorization mode of MAGR as a whole interacts with the Anti-Spoofing status of the satellite being tracked by each individual channel. It is maintained as long as the satellite is visible so that it may be used to influence the type of acquisitions attempted to acquire that satellite. See Table 1 for an explanation on how the individual satellite's C/A-only status is set.

MAGR Authorized	Code Tracked	New HOW collected	Satellite Anti-Spoofing Status	Set C/A-Only Status
Yes	—	—	—	False
—	P	—	—	False
No	C/A	No	False	No Change
No	C/A	No	True	True
No	C/A	Yes	False	False
No	C/A	Yes	True	True

Table 1: Setting the Satellite C/A-Only Status

3.2 Aided Initial Acquisition

Thirty-five seconds after normal start initial acquisition attempts have begun, acquisitions of unacquired primary and alternate satellites are attempted using the fifth channel. This allows a single frequency window to have been searched. If the peripheral channel acquires a satellite while any other channel is still searching, the alternate satellite will be used in place of the unacquired primary satellite.

MAGR's initial acquisition strategy reserves the fifth hardware channel for channel bias measurements to be performed at the start of normal track. This precludes a logical channel switch, so an acquisition command for this satellite must be re-issued on the other hardware channel. As the satellite has been acquired, its range uncertainties are quite small (although current ephemeris for this satellite is probably not resident in the MAGR), and a hot start type reacquisition can be performed. Since the C/A-only status of this satellite has been determined, MAGR operating in C/A-only mode issues a direct C/A L1 acquisition of the alternate satellite. This reduces the acquisition time relative to a C/A to P(Y) code hand over by 6 to 30 seconds.

3.3 Ionospheric Delay Acquisitions

As an L1-L2, P(Y) code capable receiver, MAGR normally compensates for the ionospheric group delay by performing dual frequency pseudorange measurements. Since C/A code is not transmitted on L2, a MAGR operating in C/A-only mode is unable to perform such measurements for satellites transmitting Y

code. An unauthorized MAGR realizes the futility of attempts to acquire L2 P code for such measurements on these satellites. By inhibiting such acquisition attempts, the peripheral channel of a C/A-only mode MAGR can be used to fulfill other requests.

Three distinct types of ionospheric delay acquisitions are performed by MAGR: initial acquisition, high priority acquisitions at the start of normal track, and regular maintenance acquisitions scheduled at 30 second intervals. Inhibiting the initial acquisition type can reduce the time to transition to normal track by up to 6 seconds.

Channel bias measurements are not performed in C/A-only mode, as the C/A code noise variance is much larger than the expected biases in MAGR digital hardware. This moves the alternate satellite acquisitions up in priority. Inhibiting high priority ionospheric delay acquisitions allows a C/A-only mode MAGR to start to acquire and collect ephemeris on alternate satellites sooner as well. Combined, these time savings allow the data collection acquisitions on alternate satellites to begin one whole data frame earlier.

Although of low priority, inhibiting the high rate regular ionospheric delay acquisitions also allows expansion tasks to more frequently visit alternate visible satellites and monitor the constellation for C/A-only mode status changes.

Inhibiting attempts to acquire satellites on L2 does not eliminate a C/A-only mode MAGR's need to compensate for the ionosphere delay on L1. Nor can the C/A-only mode inhibition be allowed to delay the resumption of ionospheric acquisitions if MAGR becomes authorized or the Anti-Spoofing status of the satellite changes. C/A-only mode enhanced MAGR's response to the first need is discussed in section 4.2, Ionospheric Delay Compensation, and its response to the second need is discussed in section 5, C/A-Only Mode Transitions.

3.4 Reacquisitions

Normal MAGR reacquisition strategy calls for use of different code and frequency combinations to reacquire the lost satellite (Kacirek and Bartholomew, 1992). The strategy sequence chosen depends on the code type and frequency stored in track history for the lost satellite. If Y code is enabled on the lost satellite, attempts by an unauthorized MAGR to recover on L1 or L2 P code are futile. MAGR will decrease its expected reacquisition time in most circumstances by not allowing P code reacquisition attempts. This is reflected in both the State 5 and State 3 reacquisition strategies, which will employ only C/A L1 acquisition attempts if MAGR is operating in C/A-only mode.

The reacquisition strategy applicable to an unauthorized MAGR having lost lock on a P code or a Y code satellite is shown in Table 2. The C/A-only status of a P code satellite is false, and the reacquisition strategy functions the same as for an authorized MAGR. Reacquisition of State 5 P code is most probable, so after attempting STEP 0 through STEP 2, STEP 1 is attempted until 20 seconds have elapsed since the loss of lock. If further reacquisition attempts are needed, the strategy resumes with STEP 4.

However if the satellite track history indicates Y code, and MAGR is unauthorized, then the authorization status must have changed. This would cause a loss of signal lock. An authorized MAGR is allowed to toggle code types between P and Y code in its reacquisition attempts, but this is not the case for an unauthorized MAGR. Even though the code in track history is Y code, only unsuccessful P code reacquisition attempts will be made until at least STEP 5. Hence under these circumstances MAGR reacquisition strategy starts with STEP 5, the most likely acquisition to succeed.

STEP	CODE	FREQUENCY	TRACKING TYPE
0	P	Track History	State 3 track
1	P	Track History	State 5
2	P	Opposite Track History	State 5
3	P	Opposite Track History	State 5
4	P	Track History	State 5 slowest search rate
5	C/A to P*	L1	State 5
6	C/A**	L1	State 5

* If jamming is detected, this pass will be skipped.

** If the C/A acquisition is successful but failed the hand over to P code in STEP 5, then a C/A on L1 acquisition will be commanded.

Table 2: Unauthorized State 5 P Code Reacquisition

A different sequence of code and frequency combinations is used for alternate satellite acquisitions by the peripheral channel (Kacirek and Bartholomew, 1992). Once again the strategy builds upon a combination of code and frequency combinations from the alternate satellite's track history. The first acquisitions attempted on C/A-only satellites are C/A L1 acquisitions, the most likely attempts to be successful. Table 3 details this sequence of alternate acquisition attempts as applicable to a C/A-only satellite.

STEP	CODE	FREQUENCY	TRACKING TYPE
1	C/A	L1	State 5
2	C/A	L1	State 5
3	C/A	L1	State 5
4	C/A	L1	State 5
5	C/A to P*	L1	State 5
6	C/A	L1	State 3***
7	C/A	L1	State 3***
8	P**	L1	State 3***
9	P**	L2	State 3***
10	C/A to P	L1	State 5
11	C/A	L1	State 5

* If Jamming detected, then use track history code and frequency

** If track history code is C/A then use P code or Y code if authorized

*** State 3 if INS aided, otherwise acquire state 5 tracking with maximum acquisition sample dwell time

Table 3: Alternate Satellite Acquisition Strategy In C/A-Only Mode

4. Enhanced Accuracy

Selective Availability (SA) dominates the measurement error sources. However, several techniques can be used to reduce some of the C/A-only mode particular errors.

4.1 Measurement Noise

Because of the 10-times larger C/A code chip size, C/A code pseudo-range measurements have a 10^2 -times larger associated measurement noise covariance than do P(Y) code pseudo-range measurements. This translates into a 3^2 -times larger contribution to the navigation solution error for that satellite. In order to decrease the filter gain applied to C/A code measurements, MAGR's Kalman filter measurement noise matrix includes C/A code or P(Y) code appropriate values. Decreasing the gain given to the noisier C/A code measurements decreases the navigation solution error. If MAGR is INS aided, it will also pull the solution closer to the INS solution.

Clearly this does not eliminate the unknown error in the navigation solution due to SA, and does not allow reduction of the covariance augmentation needed to account for biases unaccounted for by the Kalman filter. The extent to which the reduced navigation solution error is mitigated by SA, GDOP, and host vehicle dynamics is still being determined.

4.2 Ionospheric Delay Compensation

Inhibiting ionospheric delay acquisitions frees the peripheral channel for other tasks. The C/A-only mode MAGR must compensate for the ionospheric delay on satellites transmitting Y code by using an alternate method. Left uncompensated, this delay leaves an error of 1 m to more than 100 m in the measured pseudo-ranges (Klobuchar, 1991). By using the Klobuchar single frequency downlink correction model if recent measurements are not available, MAGR compensates for this error.

When dual frequency measurements are available to calibrate the down-link model, a refinement can be made. The short term accuracy of the ionospheric filter correction can be improved by propagating the measurements with the corresponding delay rate of change provided by the model. Although this benefits an authorized MAGR, it will also benefit for a short time a C/A-only mode MAGR which had been previously navigating before transitioning to C/A-only mode.

4.3 Mixed Constellation

MAGR selects satellites for recommended track based upon the best GDOP, weighted with the broadcast URA variance, along with consideration of the satellite health and track history. The unauthorized URA variance reflects a one sigma estimate of the user range errors in the navigation data for the transmitting satellite. It does not include any errors introduced in the receiver or the transmission medium. Other things equal, a satellite transmitting P code contributes less error to the navigation solution, as discussed in section 4.1, Measurement Noise. Yet strict weighting by the URA variance does not favor these satellites when they are available. An appropriate algorithm to favor P code satellites more heavily than C/A code satellites improves the ability of MAGR to choose those four satellites which minimize the navigation solution error. This algorithm multiplies the URA variance by a factor to account for how the augmented covariance matrix reflects the use of C/A code versus P(Y) code measurements.

5. C/A-Only Mode Transitions

Usually MAGR C/A-only mode status will apply for the full duration of a mission. However, at times MAGR may transition from or to C/A-only mode while navigating. For example, it may become

authorized while in NAV mode because a valid crypto key was loaded. Or the Anti-Spoofing status of a satellite may change. Likewise MAGR may be forced to transition into C/A-only mode if its current key expires. It is imperative that any modifications made to enhance C/A-only mode performance must also ensure reliable performance and smooth transitions to and from C/A-only mode.

By default MAGR satellite C/A-only status is false. In addition to updating the C/A-only status for each satellite, MAGR monitors it for changes. The conditions which cause a C/A-only mode transition are shown in Table 4. A transition during initial acquisition to C/A-only mode is benign, as MAGR is simply prevented from handing over to P(Y) code or performing ionospheric delay measurements.

MAGR will transition:	To C/A-Only Mode		From C/A-Only Mode	
	if both of these occur:	<ul style="list-style-type: none"> • Anti-Spoofing enabled • unauthorized 	if either of these occur:	<ul style="list-style-type: none"> • Anti-Spoofing disabled • authorized

Table 4: C/A-Only Mode Transitions

If Anti-Spoofing is ever disabled, or MAGR becomes authorized, the satellite C/A-only status will be cleared. Any satellites being tracked on C/A code as the result of an uncompleted C/A to P hand over acquisition will immediately hand over to P or Y code. Ionospheric delay acquisitions are scheduled at a temporarily high priority for all satellites leaving C/A-only mode, to follow right after channel bias measurements.

Satellites being tracking as the result of a C/A L1 acquisition will not hand over immediately to P(Y) code when their C/A-only status is cleared. This is only temporary as the high priority ionospheric delay acquisition will be used upon completion to upgrade the primary constellation to P(Y) code track. The C/A-only status of alternate satellites is updated periodically when they are visited under a data base expansion or other acquisition. Since an ionospheric delay acquisition is always attempted immediately after an alternate becomes a primary satellite, this C/A to P(Y) hand over acquisition can always be used to update to a more preferred code and frequency combination.

However, recovery from a loss of lock caused by a transition to C/A-only mode because the satellite Anti-Spoofing status changed will be delayed at least until a C/A acquisition is chosen in the reacquisition strategy.

6. Future Enhancements

Several other techniques have been developed which would enhance operation in C/A-only mode. These include differential GPS (DGPS) and continuous carrier smoothing.

6.1 Differential GPS

The commercial user equipment community has used differential GPS for many years to overcome the handicap of being limited to C/A code tracking and vulnerable to the ravages of SA. Likewise, DGPS is beneficial for an unauthorized MAGR operating in C/A-only mode, with the same resultant solution improvement. MAGR will process RTCM format correction messages input via either the 1553 or the RS-422 interface. RTCA format processing is ready for implementation. Although a C/A-only mode MAGR will receive greater benefit from DGPS, it will continue to operate differentially if it becomes authorized or otherwise exits C/A-only mode.

6.2 Continuous Carrier Smoothing

A significant amount of dynamic uncertainty is built into the Kalman filter to cover the dynamic situations MAGR must operate in. As a result the filter has a relatively short filtering time constant. It is capable of reducing the high-frequency pseudo-range noise standard deviation by up to 50%, but is capable of very little filtering on the low-frequency noise from such sources as multipath interference.

Delta-range measurements are derived from low-noise accumulations of the continuous carrier phase. The conventional form of the Kalman filter uses delta-ranges as velocity estimates, and apportions some of the associated uncertainty to the corresponding position estimate. This does not fully utilize the information contained in the continuous carrier phase data.

However a complementary measurement prefilter uses the delta-ranges to smooth the low-frequency noise in the pseudo-range measurements. This alleviates some of the inherent in-chip multipath errors. Provided cycle slips are effectively compensated, carrier smoothing offers great performance improvements, particularly for MAGR operating in C/A-only mode.

References

- Gold, R. "Optimal Binary Sequences for Spread Spectrum Multiplexing," IEEE Transactions on Information Theory, Oct.1967, pp. 619-621
- Kacirek, J. and Bartholomew, R. "Signal Acquisition and Tracking In the DoD Standard Miniature Airborne GPS Receiver," ION 48th Annual Meeting Proceedings, Aug. 1992
- Klobuchar, J. "Ionospheric Effects on GPS," GPS World, April 1991

THIS PAGE LEFT BLANK INTENTIONALLY

**Evaluating the Effects of Different Satellite Selection
Strategies for
Nap Of the Earth (NOE) and Ground-Based
Global Positioning System (GPS) Users**

**Ms. Van Tran
Mr. Paul M. Olson**

US Army CECOM, RD&E Center
Command/Control and Systems Integration Directorate (C2SID)
ATTN: AMSEL-RD-C2-TS, Building 2525
Fort Monmouth, NJ 07703-5603

**Mr. Jim Adametz
Mr. Joe McGowan**



Intermetrics Inc.
1720 State Highway 34
Wall Township, NJ 07719

Approved for Public Release; distribution is unlimited

THIS PAGE LEFT BLANK INTENTIONALLY

1. Abstract

The most common strategy for GPS satellite selection is to optimize the geometric relationship between the receiving antenna and the satellites. This is accomplished by periodically calculating the Geometric Dilution of Precision (GDOP) for each combination of four satellites, and selecting that set which provides the minimum GDOP. Contingency reactions to the unexpected loss or unavailability of a desired satellite signal are also provided. These include the ability to navigate using three satellites by incorporating aiding inputs from another source, typically a barometric altimeter, as well as providing an alternative satellite selection in the event that an outage is sustained.

For GPS host platforms that operate at altitudes well above the local terrain these methods are fine, and generally provide the best available GPS navigation. They were not designed, however, with the peculiar problems of an airborne user flying a Nap Of the Earth (NOE) profile, or a ground based user.

A simulation tool has been developed by C2SID which allows the effects of terrain masking to be evaluated for the current satellite selection strategies in the DOD receiver designs. The object oriented software design of the simulator provides a flexible environment in which to exercise variations on the current selection methods, or to even allow completely new methods (including All-In-View) to be implemented and tested. The simulator allows the evaluation of either GPS only or GPS/INS modes of operation. An enhancement to include GPS/Doppler mode has been started.

Baseline performance simulation runs have been conducted. The results have been evaluated to assess the performance implications of the current satellite selection strategies for the NOE and other low altitude GPS users. The evaluations reveal two particular aspects of behavior of the current methods where revision to reflect the special problems of low altitude users will bring about navigation performance improvement, these are:

1. The current 3 satellite navigation practices.
2. The contingency selection strategy.

Due to the nature of NOE flight profiles and ground based user movements around terrain features, these two aspects of behavior will be frequently encountered.

This paper will summarize:

- The "standard" practices used in GPS satellite selection,
- The Satellite Selection simulation tool developed by C2SID,
- The results of NOE and ground-based simulations,
- The lessons learned from the testing effort.

2. Current GPS Satellite Selection Algorithms

2.1 Purpose of a Satellite Selection Algorithm

A fully determined GPS solution can be formulated using measurements obtained from signals from 4 orbiting satellites. Under the current constellation, between 7 and 12 satellites will be visible to users anywhere on or near the earth. For receivers that incorporate fewer than 12 measurement channels, satellite selection algorithms are used in an attempt to select the subset which provides the best overall navigation performance.

While the features of the local terrain provide a good source of protective concealment for airborne user flying a Nap Of the Earth (NOE) profile or a ground based user, they may also obstruct the signal from a desired satellite. A typical GDOP based algorithm may select a satellite that is masked by the local terrain or man-made obstacle, and the receiver will make a fruitless attempt to lock onto the blocked satellite signal. In addition, a satellite in track can be lost due to its motion or that of the user placing a terrain obstacle in the line of sight. These situations, illustrated in Figure 1, induce short-lived performance anomalies in the navigation outputs of a GPS based navigation system. It will be a common occurrence for a ground-based user, and for ARMY helicopters operating under Nap Of The Earth (NOE) flight profiles.

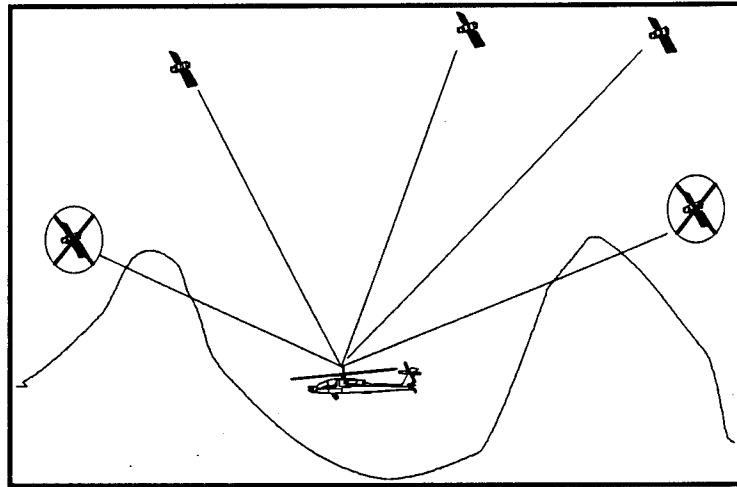


Figure 1 - Satellite Line of Sight Blockage by Terrain

If the navigation system had access to elevation data about local terrain features, it could make more informed decisions about satellite selection in an attempt to mitigate the transient error. With a database of sufficiently dense data points and adequate spatial scope, testing for a clear line of sight to a satellite as part of the selection process can be implemented.

The purpose of this study is to assess current satellite selection algorithms in the context of NOE GPS operation toward the identification of alternative strategies that offer improved performance. In particular, the performance benefit that may be obtained by incorporating knowledge of the local terrain into the satellite selection process will be assessed. One source of such information is the Digital Terrain Elevation Database (DTED) maintained by the Defense Mapping Agency¹. The DTED was used for terrain profiling in the simulations reported herein. Other elevation data sources and formats could be accommodated as well.

2.2 Criteria Incorporated into Existing Algorithms

It was a goal of the project to incorporate the satellite selection strategies of as many existing designs as possible. Most manufacturers of commercial receiver designs were understandably reluctant to divulge the particulars of their design. While some manufacturers provided general descriptions of their selection strategies, none possessed the necessary certainty and detail to warrant the commitment of development resources. Specifications for the GPS receiver designs sponsored by the DOD were available, and provide rich detail about selection strategies employed in those designs.

A study of the Computer Program Development Specifications (the so called "B5s") for the RCVR-OH, RCVR-UH, and the MAGR revealed that the satellite selection strategy has remained virtually constant between the GPS Phase III and MAGR NDI designs, differing primarily in the scheduling of satellite reselection events.

Satellite selection processing must be performed during three specific regimes of receiver operation:

1. During initial acquisition following a transition into NAV operating mode,
2. Periodically during NAV mode to ensure that improving configurations are utilized, and

¹ DMA does not warrant the DTED for flight navigation and safety use, however it does meet the requirements needed in our simulations.

3. Contingency reactions to unexpected loss of lock on an individual satellite.

The initial acquisition phase is not relevant to this study, and is not addressed. The selection strategies employed during the latter two operating regimes, however, greatly effect navigation performance for the NOE flyer, and are addressed in depth.

Satellite selection involves two basic processes. First the visibility of each of the satellites in the constellation must be determined, and then the set of four or more that satisfy some optimization criteria are identified.

2.2.1 Satellite Visibility Determination

The fundamental criteria of satellite visibility is whether or not it is above the user antenna horizon. In addition, it is a common practice to ignore satellites that are at or near the horizon for the following reasons:

1. To avoid signal paths through the most perturbed region of the atmosphere and that produce the greatest susceptibility to multipath problems;
2. To avoid signals with the greatest susceptibility to ground-based jammers;
3. Because the LOS to the satellite impinges on a region of the antenna reception pattern that is typically attenuated by design.

Thus, a widely accepted definition of visibility is that the satellite has a positive elevation angle with respect to the user horizon, and that it is greater than some minimum mask angle (typically 5° during normal tracking and 10° for initial acquisition).

This is the visibility criteria embodied in the Collins DOD receivers. It generates the visible satellites list by propagating the current position estimate halfway to the next scheduled selection, and then applying the visibility test to each satellite for which it has valid almanac. Prior to actually making a constellation change, the DOD receiver attempts to track it on the ancillary measurement channel. If successfully acquired, data collection is performed by the ancillary channel, and the switch is carried out. If the satellite cannot be acquired on the ancillary channel the navigation constellation switch does not occur.

The DTED will be used in the alternative selection strategies to strengthen the visibility criteria to include consideration of the local terrain as well.

2.2.2 Reselection Intervals

In order to avoid the constantly trying to determine which subset of satellites should be used, most receivers will periodically perform this mathematically intense calculation. Once the constellation has been selected, it will be used until the next selection interval occurs. The Collins DOD receivers perform satellite selection at scheduled intervals of 2 minutes in the Phase III designs and in the MAGR.

2.2.3 Contingency Selections

A selection strategy is also needed to handle the contingency of a desired satellite being unavailable or unexpectedly lost. In the Collins DOD receivers, if a signal loss is sustained for 30 seconds, the receiver software declares the satellite unavailable, and commands track on the satellite with the highest elevation angle that is not already in the navigation set. This seems a reasonable strategy for most airborne GPS users. Signal blockage is generally caused by aircraft structures and is generally transient in nature, occurring during a maneuver. The highest satellite in the sky offers the highest likelihood of signal acquisition because:

1. The signal will be among the strongest available, having suffered the least atmospherically induced attenuation;
2. It will have the least susceptibility to ground-based jammers;
3. It is the least likely to be masked by a terrain feature.

Notice that the contingency selection does not consider GDOP and, in fact, will generally result in extremely poor solution geometry. An attempt to restore nominal system geometric relationships would then occur at the next scheduled reselection time.

For a low altitude user, signal blockage on a low elevation satellite can be expected to occur frequently and be sustained for up to several minutes. In particular, a helicopter flying an NOE profile is generally attempting to utilize the local terrain to conceal himself. This important self-protection practice unfortunately aggravates the signal blockage problem. The contingency selection described above may occur frequently for the low altitude GPS user, inducing considerable transients in the navigation performance

3. Algorithm Performance Evaluation Tool: GPS Satellite Selection Covariance Simulator

In order to establish a performance baseline for the evaluation, a series of simulations were run to obtain the performance of the current algorithms under unimpeded and terrain-blocked signal conditions. The alternative algorithms were then exercised under the same simulation profiles, and the effect on performance was gauged against the baseline. For each route plan, 3 standard graphical outputs are provided:

1. A "Sky View" plot which projects the satellite positions onto the user's locally level tangent plane for the duration of the simulation run. The plot contains a superimposed horizon circle. Satellite tracks outside the circle represent satellites that have not risen above the horizon, while those inside represent those that have.
2. A plot of the simulated vehicle ground track, superimposed on a background whose shading (colors on the screen, grayshades on the report plots) represents DTED elevation variations.
3. A plot of the simulated vehicle altitude profile. Plotted on the same axis for reference is the DTED indicated ground elevation directly under the vehicle.

For each simulation run of a route plan a standard set of 4 graphical outputs was produced. These include:

1. Plots of each DOP component vs. time. Included are GDOP, PDOP, TDOP, HDOP, VDOP.
2. A plot showing the track history for each satellite in the almanac or ephemeris database. Using line style and thickness variations, this plot shows four states of track history, not visible (dotted), visible but not used (thin), visible and used (medium), and chosen by GDOP but blocked by terrain (thick).
3. A plot of the time history of the horizontal position 1-sigma error. This is obtained by taking the square root of the sum of the 1,1 and 2,2 diagonal elements of the covariance matrix (R for GPS Only as defined in section 3.1.6.1, and P for GPS/INS as defined in section 3.1.6.2).
4. A plot of the time history of the vertical position 1-sigma error. This is obtained by taking the square root of the 3,3 diagonal element in the covariance matrix.

The simulation tool also allows the operator to define plots of many other system parameters as needed. Examples of each of these plots for the Holloman NOE simulations can be found at the end of the paper in Figure 10-15.

3.1 Simulator Software Architecture

Figure 2 depicts a simplified block diagram of the simulation tool software architecture. The main "engine" of the tool is represented by the *Process Manager*¹ and it's 6 processes labeled *DTED*, *Trajectory Generator*, *Satellite Database*, *Select Satellites*, *GPS Measurement*, and *Navigation Performance*. These provide the fundamental

functional capabilities of simulating vehicle motion, selecting satellites, and forming the GPS measurement inputs to the Performance Analysis modules.

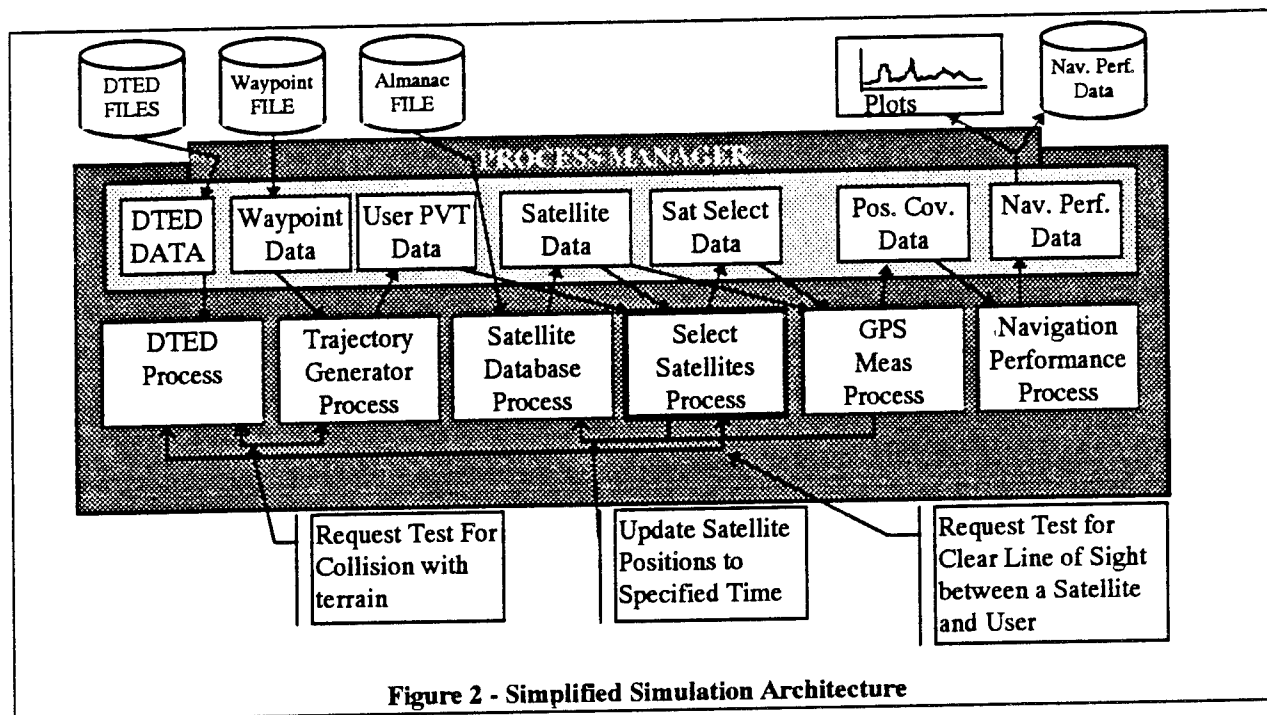


Figure 2 - Simplified Simulation Architecture

3.1.1 Trajectory Generator Process

The trajectory generator process is a rather simple design whose primary function is to place the simulated vehicle at a 3 dimensional waypoint at a specified time. The waypoint list is read into the tool from the Route Plan Database, a plain text input file that can be created with virtually any text editor. Each record of the route plan contains a time, expressed in GPS Time of Week, along with a position specified in latitude, longitude, and altitude.

The trajectory generator executes at a 1 Hz rate (simulator time), and provides vehicle position and velocity along with a time tag. It calculates a velocity and heading that will bring the vehicle to the next waypoint at the specified time. The trajectories used in the performance evaluations were screened to ensure that the vehicle speed did not exceed 50 meters/second (~100 NM/Hr). This is roughly one half of the maximum speed sustainable by the UH-60 Blackhawk helicopter.

The trajectory generator output message is available to all of the other processing modules.

3.1.1.1 Trajectory Editor Tool

An auxiliary tool was also developed to allow the route plan to be generated graphically. It displays a specified collection of DTED cells using color coding to represent variations in elevation contour. The user can establish a route plan using a mouse or other pointing device. A special feature designed into this tool is the ability to "hug the terrain". It will upon user command, follow the line perpendicular to the current heading until the mask angle created by the local terrain is maximized, and output that point as the currently selected waypoint.

3.1.2 Satellite Database Process

The Satellite Database Process manages the almanac or ephemeris database, reading it from an input file and maintaining it in memory where it can be quickly accessed as needed for processing. Almanac files are also plain text. Current almanac files are available from a variety of computer bulletin boards. The common Yuma Proving Ground (YPG) format almanac was used as source data for all of the simulation runs. Ephemeris files may be in either the ICD-GPS-150 Message ID 5 format or the CIGTF Data Acquisition System format.

The Satellite Database Process executes on demand from the Select Satellites and GPS Measurement Processes, and will calculate the position and clock corrections for any one or all of the satellites in its database. It embodies the full orbital model defined in ICD-GPS-200.

3.1.3 DTED Process

The Digital Terrain Elevation Database (DTED) provides a global elevation profile mapped into a latitude/longitude grid. The source data for the DTED is drawn from the historical survey record available for a given region. It may include elevation profiles that were generated using traditional surveying techniques, overhead passes of an orbiting satellite, or digitized entry from paper maps. Thus, the absolute accuracy of the DTED information varies from region to region depending on its source data. The DTED Level 1 used in this study is organized into cells, each of which is a $1^{\circ} \times 1^{\circ}$ grid with 3 arc second divisions. At each point in the grid, an altitude is provided with 1 meter resolution. Header information included in each cell provides an indication of the quality (accuracy) of the data it contains.

The DTED Process manages the DTED database, each cell of which is stored in a separate file. Selected cells of the DTED database can be preloaded into memory to improve program execution speed. If the host computer has limited RAM, however, the DTED Process can be configured to keep only those cells in memory that include the current vehicle position, and those that will allow a cell boundary to be crossed at the current vehicle heading. This file management is carried out in the background, in response to requests from other processes for the elevation at a particular latitude and longitude.

As shown in Figure 2, the Select Satellites Process will request *Test-for-clear-line-of-sight* from the DTED Process as it performs its processing relative to satellite visibility testing. The DTED Process responds by performing the necessary swapping between memory and file needed to respond to the request, and then makes the requested data available to the Satellite Manager.

3.1.4 Select Satellites Process

The Select Satellites Process represents a C++ class definition that provides functions to generate the list of visible satellites and to select the set of four (or more) that satisfies some optimization criteria. It executes at fixed intervals which can be specified by the user at run time. For the evaluations reported herein, this interval was set to 120 seconds to emulate the MAGR. Each time it runs, it will command the Satellite Manager to calculate the positions of all of the satellites in its database.

For the emulation of the Collins DOD designs, the virtual function *GenerateVisibleSVList* applies the visible testing described earlier to each satellite, the satellite must have a positive elevation angle with respect to the local horizon, and it must be above a user specified minimum mask angle. The resulting list is provided to the *SelectSVs* virtual function, where the DOP for all possible combinations of four satellites is calculated. The set which provides the minimum DOP is selected for the navigation constellation. The simulation user can select which particular DOP to minimize at run time. For the simulation runs in which the current algorithms were evaluated, GDOP minimization was selected.

The two virtual functions described above were replaced in derived classes in order to exercise and assess alternative satellite selection strategies.

At a 1 Hz rate, each satellite in the current navigation constellation is tested to determine if it has become occluded by a terrain obstacle. If the satellite is blocked, the *LossOfLockReaction* virtual function is called. This function carries out several tasks:

1. Resets the measurement validity flag for the satellite;
2. If this is the first time the satellite is determined to be blocked, starts a 30 second timer,
or
If the satellite was blocked on the last 1 Hz cycle, check to see if the 30 second timer has elapsed.
3. If the 30 second timer has elapsed, performs the contingency selection.

As described above, for the Collins DOD design emulation the contingency selection will be to select the highest elevation satellite that is not currently in the navigation constellation. It will be established during the performance evaluations below that this aspect of the current satellite selection strategy is responsible for the greatest performance degradation to the NOE GPS user, and as such, warrants investigation of alternatives.

3.1.5 GPS Measurement Formation Process

GPS Measurement Formation Process also executes at a 1 Hz rate, which is the nominal measurement cycle in the Collins DOD receiver design.

The performance analysis software modules (described below) are reused from previous work, and require measurement inputs in the navigation frame. In the GPS/INS Kalman Filter this was provided by generating a least-squares PVT solution using the raw GPS pseudorange and delta range measurements. The measurement noise matrix, R , was calculated by transforming the diagonal line of sight measurement noise matrix, R_{diag} , into the navigation frame. The measurement bias matrix, B , was calculated by transforming the diagonal line of sight measurement bias matrix, B_{diag} , into the navigation frame. For a covariance analysis, the PVT solution is not generated in the simulator. Only the R and B matrixes need be provided, which can be calculated using a G matrix; where G = a matrix such that each row represents the direction cosines between the line of measurement and the solution space axes for one of the measurements (typically this matrix is used to calculate GDOP).

$$R = G^{-1} R_{diag} (G^{-1})^T \quad B = G^{-1} B_{diag} (G^{-1})^T$$

R_{diag} and B_{diag} are diagonal matrixes of variance terms, reflecting the fact that each measurement is independent. After transformation into the navigation frame, however, both contain non-zero off diagonal terms that reflect the spatially correlated nature of GPS measurements.

Each element on the R_{diag} diagonal is set to the GPS specified tracking accuracy of 2.25 meter² for pseudorange, and 0.0004 meter² for delta range². Each element on the B_{diag} diagonal is set to an empirically determined variance value of 16 meters² based on the data collected from the Intelligence Electronics Warfare/Common Sensor (IEWCS) testing at Holloman AFB³.

3.1.6 Navigation Performance Analyzer Process

In selecting the performance analysis techniques to be employed, the primary considerations were to provide a consistent basis for comparison between the baseline runs and the alternative selection strategies. The simulation techniques are required to faithfully represent the navigation performance under nominal conditions, as well as the performance degradation that occur when a satellite signal is lost, causing the GPS solution to be underdetermined,

and those associated with the sub-optimal geometric conditions imposed by the current contingency selection strategy.

In all of the performance evaluation runs aiding input from a barometric altimeter is simulated. If a satellite is blocked, the construction of G and R_{diag} is adjusted to simulate baro altitude aiding. The altimeter is modeled as a measurement source in the vertical direction, having zero mean error and a variance due to its quantization noise. The row of G corresponding to the lost satellite is replaced with $\{0, 0, 1, 0\}$, and the diagonal element of R_{diag} is replaced with the baro quantization noise variance. The AAU-32 baro altimeter provides 100 feet resolution. The probability density function of a quantization noise source is a uniformly distributed random variable with zero mean and range \pm quantization size / 2. The variance used in the simulation reflects the AAU-32 variance of 833 ft^2 (77.4 m^2), or 28.9 ft. (8.8 m) 1-sigma.

3.1.6.1 GPS Only Analysis

Recall from the discussion of GPS measurement formation that R , the measurement noise variance matrix, reflects both the effects of the geometric relationships between the user and the satellites as well as the effect of a 3 satellite condition by introducing an altitude aiding input. Thus it contains all of the features desired to allow the baseline and alternative selection strategies to be comparatively assessed. The time history of the square roots of the diagonal elements of R provide the numerical basis for such comparison.

$$EH = \sqrt{R_{1,1} + R_{2,2} + B_{1,1} + B_{2,2}}$$

$$EV = \sqrt{R_{3,3} + B_{3,3}}$$

Where:

EH is the 1 - sigma horizontal position error,

EV is the 1 - sigma vertical position error

3.1.6.2 GPS/INS Analysis

In a prior effort, a GPS/INS Kalman Filter was developed as a post test processing tool. The filter was designed using a covariance simulation in which a full truth model and the resulting design model existed. The filter is an 11 error state mechanization with 9 INS error states corresponding to the well known Pinson⁴ model along with two states to estimate errors in the receiver clock bias and frequency. The filter design was validated by direct comparison to the Collins INS mode filter outputs. Each filter produced virtually identical performance statistics in 17 test runs. The post processing filter is described in the reference "EH-60 Navigation Upgrade Study", and forms the basis for the GPS/INS evaluations performed in this study.

The filter software was modified slightly for this application so that it would execute only its covariance propagation and update calculations, using the R matrix generated in the GPS Measurement Formation module as its measurement noise matrix. The square roots of the diagonal elements of the covariance matrix provide a numerical basis for performance comparisons. The plotted results show the time history of the covariances after propagation and before the measurement update to provide the most conservative performance prediction. If we denote the filter covariance matrix just prior to measurement incorporation as P^- , then:

Where:

P^- = Covariance Matrix at T^-

T^- = Time just prior to measurement update

B = GPS Range Bias Error Variance

EH is the 1-sigma horizontal position error;

EV is the 1-sigma vertical position error

$$EH = \sqrt{P_{1,1}^- + P_{2,2}^- + B_{1,1} + B_{2,2}}$$

$$EV = \sqrt{P_{3,3}^- + B_{3,3}}$$

3.2 Route Plans

Vehicle Route Plans were created for 4 regions of the continental U. S. for which DTED data was readily available. These were:

1. A route along the Hudson River in New York, using the Palisades on the West as a source of terrain blockage.
2. A route in the area of Carlisle, PA, where the peaks and valleys of the Blue Mountains provide blockage.
3. A route in Holloman AFB, around the area of Holloman AFB. The Sacramento Mountains provide a source of blockage to the East, and Sierra Blanca to the Northeast.
4. A scenario in the Grand Canyon, where blockage can be induced in virtually any direction.

For each plan, the path selected was chosen to maximize the masking effect produced by the local terrain for a simulated vehicle flying at a constant altitude 100 feet above the terrain.

4. Evaluation of Existing Algorithms

Table 1 summarizes the Collins DOD algorithm which will be used as the baseline existing algorithm for comparative purposes.

Table 1 - Collins DOD Satellite Selection Algorithm Summary

FUNCTION	IMPLEMENTATION
Constellation Selection Criteria	Propagate User Position 60 seconds into the future and then select the constellation of 4 satellites with the lowest GDOP.
Satellite Visibility Criteria	5° above User Horizon
Reselection Interval	120 Seconds.
Contingency Selection Strategy	Pick the Satellite with the highest elevation that is not in the current navigation constellation
Delay between Satellite Loss of Lock and Contingency Selection Execution	30 Seconds.
3 Satellite Navigation Strategy	Replace the lost satellite measurement with an altitude measurement (usually a Baro-Altimeter reading).

4.1 Evaluation of Baseline Results

To establish the baseline performance, a first simulation run was conducted for each Route Plan without terrain blockage. The performance exhibited in these runs establishes the best GPS-based performance achievable relative to satellite selection and tracking. A second simulation run was then conducted with DTED-based "loss of lock" detection. From these runs, the performance degradation mechanisms will be identified and examined, and alternative strategies developed.

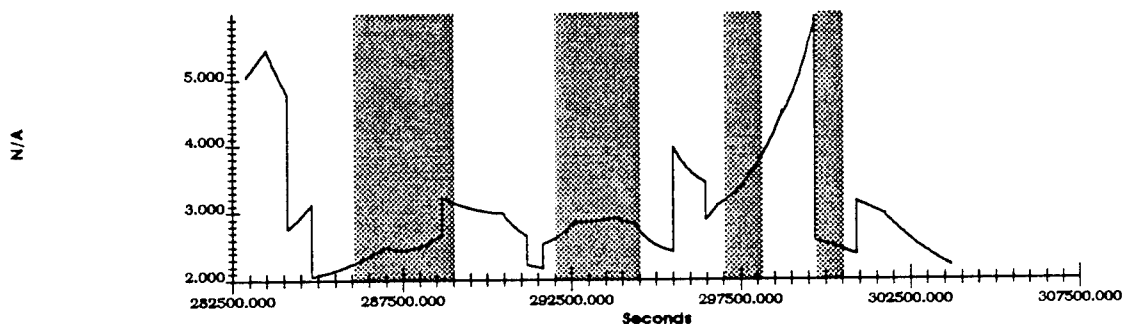
Plots from the results of the Holloman AFB Route Plan baseline runs are used to illustrate the discussion which follows.

A single valued performance parameter was defined from the horizontal and vertical error and from GDOP to provide a basis for comparative performance judgments as alternative selection strategies are exercised.

4.1.1 Baseline DOP Results

By comparing the DOP time histories for the blocked and unblocked runs, a subjective feel for the performance effects of terrain masking is obtained. For example, the DOP plots for the Holloman Route Plan unblocked baseline runs are shown in Figure 3. Typical GPS DOP behavior can be seen, being generally in the range of 2 to 4 during the 6 hour run. The features in the plots are produced as new satellites are chosen under nominal satellite selection conditions, and the slower trends are manifestations of the time varying measurement system geometry.

GDOP vs. Time



VDOP vs. Time

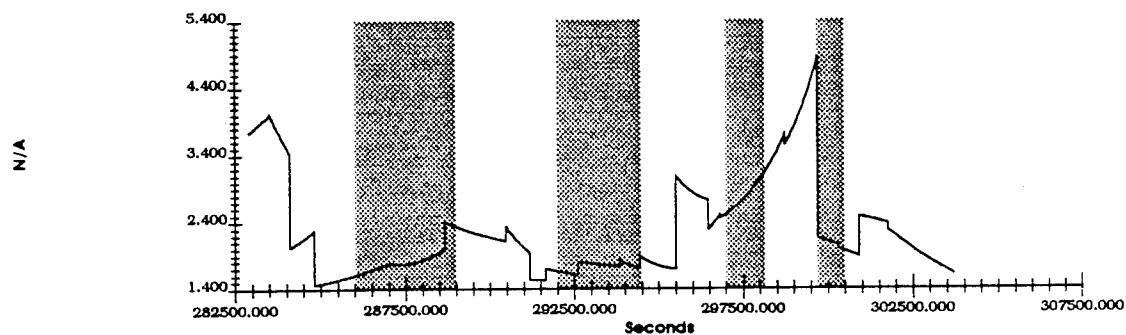
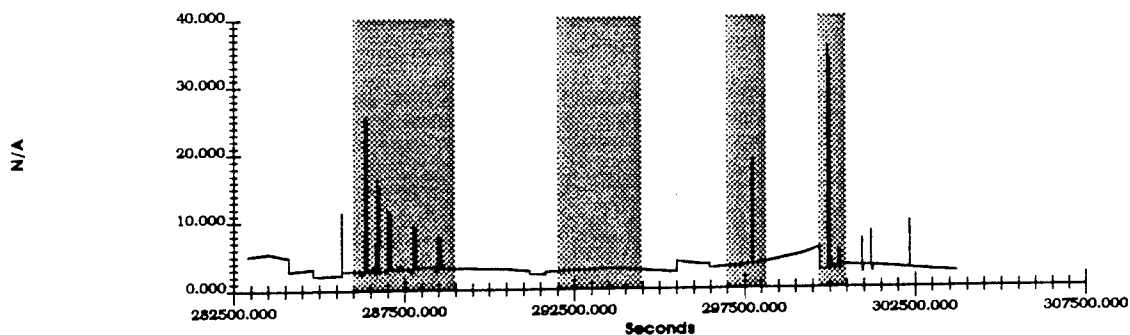


Figure 3 - Holloman Route Unblocked GDOP and VDOP²

Figure 4 was also produced from the Holloman Route Plan, but with DTED-based loss of lock detection enabled. In this figure, the "naturally" occurring features and trends are still apparent, but now the effects of terrain blockage can be seen in the "transient" features. Some of them sustain for of periods up to a couple of minutes, until the blocked satellite becomes unblocked, or the Reselection Interval elapses.

²Gray shading indicates intervals in which the performance metrics were evaluated.

GDOP vs. Time



VDOP vs. Time

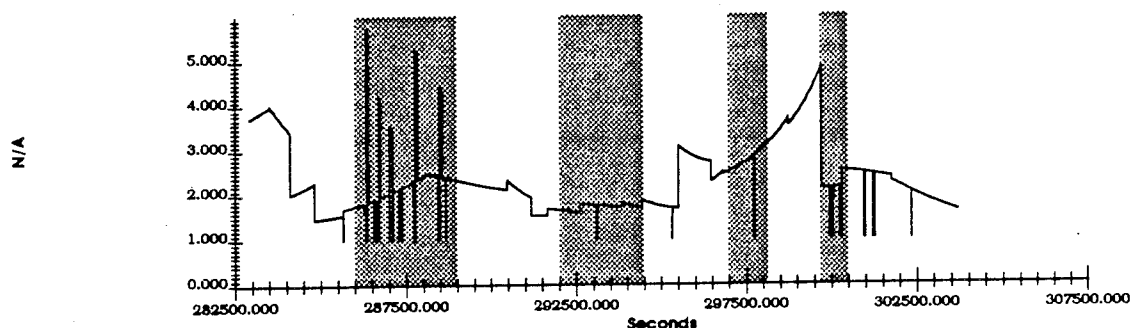


Figure 4 - Holloman Route Blocked GDOP and VDOP

There are three recurring effects that produce the transient DOP behavior, initial signal loss on a single satellite, contingency reselection following a sustained 30 second loss and loss of two or more satellites.

1. During the first 30 seconds following a signal loss, altitude aiding is automatically invoked, replacing the lost satellite with a baro altitude measurement. These events can be readily seen in the VDOP plots, where VDOP goes to 1.0, reflecting a purely vertical channel measurement. The other DOPs can become significantly degraded. For example, during the interval 297000 - 298000 seconds, an occurrence of baro aiding can be seen. During this event, HDOP and TDOP can be seen to exhibit large increases, from an HDOP of about 3 in to nearly 20.
2. If the loss of lock is sustained for more than 30 seconds, the contingency selection described above is invoked. Again, the occurrence can be most readily identified on the VDOP plot, where a VDOP of 1.0 for 30 seconds is followed by a rapid and generally large increase caused by the contingency selection strategy as seen in the interval 286000 to 289000 seconds.
3. When terrain masking blocks two or more satellites, no GPS measurement processing is done, and the DOPs are intentionally set to 0.0 to provide identifiable features on the plot³.

For comparative purposes an Effective DOP, DOP_{eff} , is defined to be the RMS value of its time history over a specific interval. DOP_{eff} is calculated as:

³ NOTE: None of these occur on the plots shown.

$$DOP_{eff} = \sqrt{\frac{1}{t_2 - t_1} \cdot \int_{t_1}^{t_2} DOP(\tau)^2 d\tau}$$

If the Effective DOP for the unblocked baseline run for each route plan is designated DOP'_{eff} , then a relative performance metric for the other runs is:

$$Metric_{DOP} = DOP_{eff} / DOP'_{eff}$$

A metric value of 1.0 indicates that the interval under evaluation is exhibiting the best achievable GPS-based performance, with increasing values indicating performance degradation on a relative basis.

4.1.2 Baseline Covariance Results

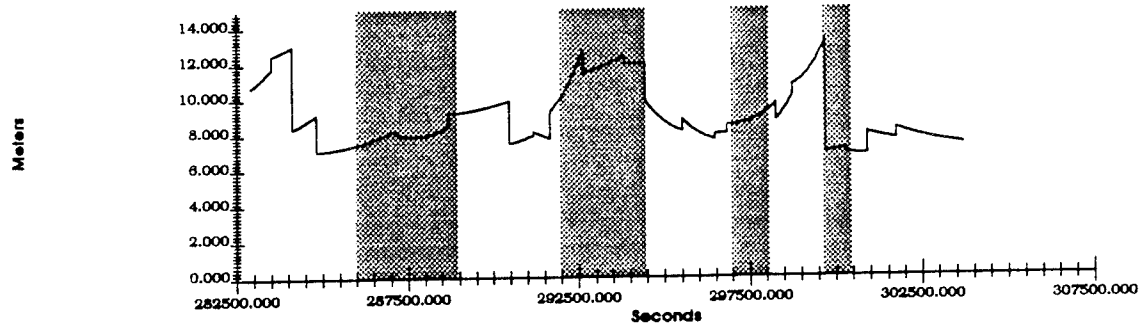
Figure 5 shows the unblocked horizontal and vertical 1-sigma errors for the Holloman Route Plan GPS Only runs, and Figure 6 shows the blocked results. The GPS/INS simulation runs produced the expected result that the hybrid solution is more robust than GPS only. A reduction in the high frequency fluctuation of the navigation errors under nominal conditions was apparent (this is, of course, a well known benefit of GPS/INS integration and is not a revelation resulting from this study). The performance under 3 satellite navigation conditions was greatly improved. In essence, the filter deweights the baro supplied altitude by virtue of its relatively large measurement variance compared to the filter state variance. Under the contingency selection conditions some small benefit is obtained from the integration, however unnecessarily large errors still result.

The performance degradation induced by the terrain masking is readily apparent in the GPS only results, which are used as the basis for the discussion which follows in the remainder of the paper. Some of the alternative algorithms investigated greatly improve the GPS only performance as will be demonstrated later in the paper. It is sufficient to state that with these improvements, integrated system performance will be that much better.

For the unblocked Holloman baseline run, the 1-sigma deviation from the mean position error exhibits typical performance, being generally in the range of 6.0 to 15.0 meters in the horizontal plane, and 8.0 to 20.0 meters in the vertical, as shown in Figure 5.

When the effects of terrain masking are enabled in the simulator, however, Figure 6 shows some remarkable deviations from the nominal performance exhibited in Figure 5. During the periods when baro aiding is used and the contingency selection is carried out, in particular, the 1-sigma errors are greatly increased, 30 to 100 meters in the best cases, and to over 200 meters in one instance. In the vertical channel, the effect of baro aiding is readily apparent, driving the 1-sigma error virtually instantly to reflect the baro uncertainty.

Horizontal Error vs. Time



Vertical Error vs. Time

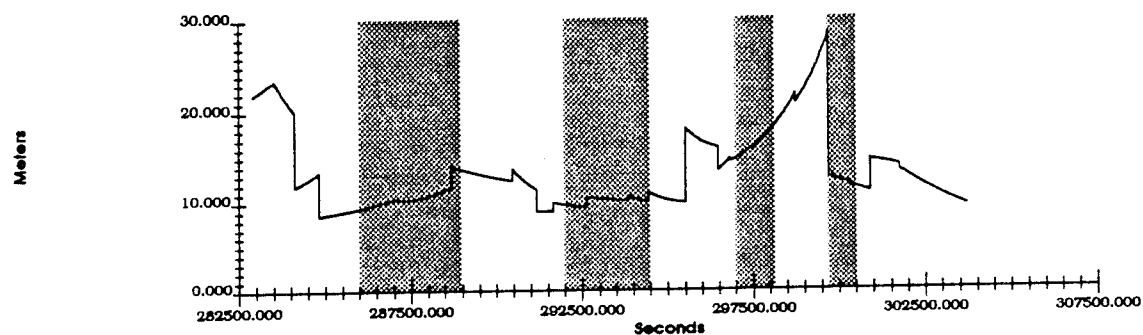
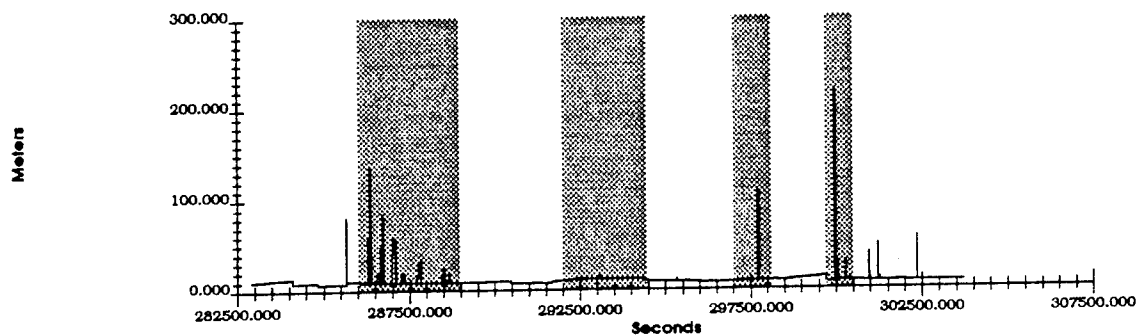


Figure 5 - Holloman Route Unblocked GPS Only 1-Sigma Errors

Horizontal Error vs. Time



Vertical Error vs. Time

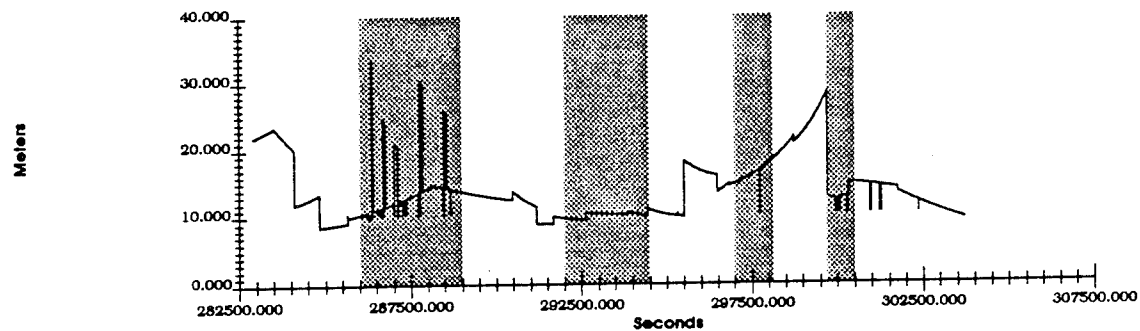


Figure 6 - Holloman Route Blocked GPS Only 1-Sigma Errors

As in the case of DOP, an Effective 1-sigma error is defined as the RMS value of its time history over a specified interval:

$$EH_{eff} = \sqrt{\frac{1}{t_2 - t_1} \cdot \int_{t_1}^{t_2} EH(\tau)^2 d\tau} \quad EV_{eff} = \sqrt{\frac{1}{t_2 - t_1} \cdot \int_{t_1}^{t_2} EV(\tau)^2 d\tau}$$

And for comparative purposes,

$$Metric_{EH} = EH_{eff} / EH'_{eff} \quad \text{and} \quad Metric_{EV} = EV_{eff} / EV'_{eff}$$

4.1.3 Summary of Baseline Results

The baseline effective performance measures are summarized in Table 2 through Table 4 below. In the first, the effective values for GDOP, EH, and EV are given for several intervals of interest during the baseline unblocked run. The second table shows the same values for the terrain blocked run, and the third shows the relative performance metric for each of this run. Next to each table is a bar graph presenting the same information, with each bar representing a metric for one of the intervals.

Intervals were selected to include those periods where the current selection algorithms provides significantly degraded performance. In order to demonstrate the efficacy of the relative performance metric, one interval for each run was selected that did not include significant terrain blockage events. For these latter intervals then, the expected result is for the performance to be similar in each of the baseline runs and for the relative performance metric to be 1.0.

Table 2 - Holloman Route Plan Unblocked Baseline Run Effective Values

Interval	EHeff	VEff	GDOPeff
GPS Only			
286000 - 289000	8.130	10.872	2.544
292000 - 294500	11.711	10.139	2.830
297000 - 298200	8.898	16.455	3.468
299800 - 300500	7.001	12.067	2.510

Table 3 - Holloman Route Plan Blocked Baseline Run Effective Values

Interval	EHeff	VEff	GDOPeff
GPS Only			
286000 - 289000	24.224	14.570	5.114
292000 - 294500	11.742	10.140	2.829
297000 - 298200	17.059	16.356	4.296
299800 - 300500	48.715	12.866	8.195

Table 4 - Holloman Route Plan Baseline Relative Performance Metric

Interval	EH	EV	GDOP
GPS Only			
286000 - 289000	2.980	1.340	2.010
292000 - 294500	1.003	1.000	1.000
297000 - 298200	1.917	0.994	1.239
299800 - 300500	6.959	1.066	3.265

In Table 2, EH_{eff} , EV_{eff} , and DOP_{eff} for the unblocked Holloman GPS only runs can be seen to exhibit expected performance levels under unblocked conditions.

For the terrain blocked runs shown in Table 3, however, considerable performance degradation are shown. During the first interval, from $t = 286000$ to 289000 seconds, two of the three kinds of blockage events described above in section 3.2.1 are encountered. There are 5 separate occurrences of the contingency selection, and 7 periods of 3 satellite visibility that last under 30 seconds. Comparing the effective values in Table 2 and Table 3, indicate significant performance degradation due to satellite blockage. EH_{eff} goes from 8.1 meters to 24.2 meters and EV_{eff} from 10.8 to 14.6 meters. These increases are reflected in Table 4, where the relative performance metric described above is shown. For EH, the metric is about 3 indicating that the effective 1-sigma error over this interval is trebled. For EV, the metric is 1.3. When the alternative satellite selection algorithms are evaluated, it is these metrics which will indicate their effectiveness. Algorithms that result in smaller metrics can be considered to have improved the lot of the NOE flyer.

The second interval, from $t = 292000$ to 294500 does not exhibit much terrain masking, and is included to provide an interval where the metric is expected to indicate no performance degradation. Referring to Table 4 for this interval, it can be seen that the metric is essentially 1.

During the third interval, from $t = 297000$ to 298200 , there are several occurrences of a single satellite being masked for under 30 seconds. For the GPS Only case, the EH metric is 1.9 while for EV it is 1.1.

During the final interval considered for the Holloman runs, from $t = 299800$ to 300500 , a combination of contingency selection and under-30 second outages contributes to the dramatically high values for the metrics in the GPS only case.

Given the level of performance degradation exhibited in the Holloman runs, this route plan will be of great interest in the assessment of alternative selection strategies.

5. Alternative Algorithms Designed to Improve GPS Navigation Performance

In the following sections, we will provide alternatives to the baseline Collins DOD Satellite Selection algorithm. The focus of these revised algorithms will be threefold:

1. Reduce or mitigate the performance degradation induced by the number of Contingency Selections,
2. Reduce or mitigate the performance degradation induced by the effect of a Contingency Selection,
3. Reduce or mitigate the performance degradation induced by the effect of 3 Satellite Navigation Solutions

For each algorithm, we will present a summary of the algorithm, and it's resulting charts indicating the effectiveness of the changes.

5.1 Evaluation of Alternative Algorithms

5.1.1 All in View

Many commercially available GPS receivers incorporate enough hardware channels to track all satellites in view. With all in view tracking, the GPS navigation solution is generally overdetermined, and the performance degradation due to the loss of a single satellite can be considerably mitigated. It seems intuitively apparent that an all in view tracking strategy would provide the optimum navigation performance for an NOE or other low altitude GPS user. While this strategy cannot be implemented in the current DOD receiver designs due to hardware limitations, it will be evaluated in order to establish the potential for NOE performance improvement.

Generally, the loss of a satellite due to terrain blockage removes a significant source of information in the horizontal plane. As expected the results shown in Table 6 and Table 7 indicate that the All in View Algorithm always outperforms the Collins DOD algorithm due to it's elimination of Contingency Selections, and making 3 satellite navigation a remote possibility.

Table 5 - All In View Algorithm Summary

FUNCTION	IMPLEMENTATION
Constellation Selection Criteria	Use all currently visible satellites in the GPS solution.
Satellite Visibility Criteria	5° above the User Horizon + any addition mask indicated by the DTED.
Reselection Interval	Not Applicable.
Contingency Selection Strategy	None Required.
Delay between Satellite Loss of Lock and Contingency Selection Execution	None Required.
3 Satellite Navigation Strategy	Replace the lost satellite measurement with an altitude measurement (usually a Baro-Altimeter reading).

Table 6 - All in View Algorithm Run Effective Values

Interval	EHeff	EVeff	GDOPeff
GPS Only			
286000 - 289000	6.970	10.607	2.485
292000 - 294500	7.254	8.190	2.075
297000 - 298200	6.128	12.987	2.733
299800 - 300500	6.493	10.536	2.354

Table 7 - All in View Algorithm Relative Performance Metric

Interval	EH	EV	GDOP
GPS Only			
286000 - 289000	0.857	0.976	0.977
292000 - 294500	0.619	0.808	0.733
297000 - 298200	0.689	0.789	0.788
299800 - 300500	0.927	0.873	0.938

5.1.2 DTED Based Prediction of Satellite Outages Over the Reselection Interval

The goal of this algorithm change (summarized in Table 8) is to reduce the number of Contingency Selections. This was done by using the DTED Process Line of Sight (LOS) calculations to determine if there will be any satellites which will be masked by the terrain for more than 30 seconds during the next Reselection Interval, and eliminating from the final GDOP selection those satellites which would potentially cause a Contingency Selection. In essence, trading off a little steady state performance to minimize transient performance anomalies.

The results of this modification to the baseline algorithm are shown in Table 9 and Table 10.

Table 8 - DTED Scan Satellite Selection Algorithm Summary

FUNCTION	IMPLEMENTATION
Constellation Selection Criteria	Propagate User Position through the Reselection Interval at 5 second intervals and test the visibility of each satellite eliminating those which would cause a contingency selection to occur. Then select the constellation of 4 satellites with the lowest GDOP.
Satellite Visibility Criteria	5° above the User Horizon + any additional mask indicated by the DTED.
Reselection Interval	120 Seconds.
Contingency Selection Strategy	Pick the Satellite with the largest elevation who has been previously tracked
Delay between Satellite Loss of Lock and Contingency Selection Execution	30 Seconds.
3 Satellite Navigation Strategy	Replace the lost satellite measurement with an altitude measurement (usually a Baro-Altimeter reading).

Table 9 - DTED Scan Algorithm Run Effective Values

Interval	EHeff	EVeff	GDOPeff
GPS Only			
286000 - 289000	15.887	13.745	3.893
292000 - 294500	11.726	10.594	2.901
297000 - 298200	8.713	16.594	3.496
299800 - 300500	14.111	12.791	3.414


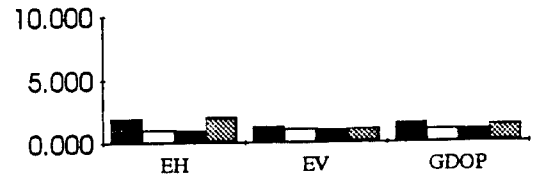


Table 10 - DTED Scan Algorithm Relative Performance Metric

Interval	EH	EV	GDOP
GPS Only			
286000 - 289000	1.954	1.264	1.530
292000 - 294500	1.001	1.045	1.025
297000 - 298200	0.979	1.008	1.008
299800 - 300500	2.016	1.060	1.360



5.1.3 Revised Contingency Selection

The goal of this algorithm change (summarized in Table 11) is to reduce the effect of a Contingency Selection. This was simply done by modifying the Contingency Selection Strategy to select the lowest satellite instead of the highest.

The results of this modification to the baseline algorithm are shown in Table 12 and Table 13. Note that this performed slightly better than the DTED Scan algorithm for the first interval (where many Contingency Selections occur), but much worse than it in the last interval where a significant portion of the position error is induced by satellite blockages lasting less than 30 seconds (thus not inducing the Contingency Selection to occur).

Table 11 - Revised Contingency Satellite Selection Algorithm Summary

FUNCTION	IMPLEMENTATION
Constellation Selection Criteria	Propagate User Position 60 seconds into the future and then select the constellation of 4 satellites with the lowest GDOP.
Satellite Visibility Criteria	5° above User Horizon
Reselection Interval	120 Seconds.
Contingency Selection Strategy	Pick the Satellite with the <u>lowest</u> elevation who has been previously tracked
Delay between Satellite Loss of Lock and Contingency Selection Execution	30 Seconds.
3 Satellite Navigation Strategy	Replace the lost satellite measurement with an altitude measurement (usually a Baro-Altimeter reading).

Table 12 - Revised Contingency Selection Algorithm Run Effective Values

Interval	EHeff	EVeff	GDOPeff
GPS Only			
286000 - 289000	14.116	12.801	3.343
292000 - 294500	11.742	10.140	2.829
297000 - 298200	17.059	16.356	4.296
299800 - 300500	48.715	12.866	8.195

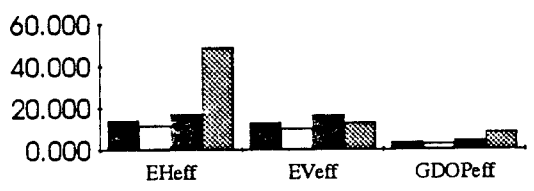
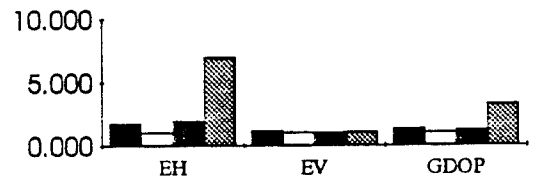


Table 13 - Revised Contingency Selection Algorithm Relative Performance Metric

Interval	EH	EV	GDOP
GPS Only			
286000 - 289000	1.736	1.177	1.314
292000 - 294500	1.003	1.000	1.000
297000 - 298200	1.917	0.994	1.239
299800 - 300500	6.959	1.066	3.265



5.1.4 Revised Aiding Selection for Underdetermined Solutions

The goal of this algorithm change (summarized in Table 14) is to improve navigation accuracy during 3 Satellite Navigating or during underdetermined conditions. This was done by modifying the Aiding strategy of the GPS Measurement Process to test two aiding strategies, and picking the one providing the best 3 Dimensional solution (based on the GPS Position Covariance Matrix). The first aiding strategy is the same one currently employed in the Collins DOD algorithm: Use some form of altitude measurement to substitute for the fourth satellite measurement, thereby providing a fully determined solution. The second aiding strategy is to use the knowledge of our estimate of the receiver clock phase with respect to GPS time from our last fully determined solution, and eliminating the need to calculate clock phase when only 3 satellites are available.

The results of this modification to the baseline algorithm are shown Table 15 and Table 16. Note that this algorithm performed slightly worse than the DTED Scan algorithm for the first interval (where many Contingency Selections occur), but slightly better than it in the last interval where a significant portion of the position error is induced by satellite blockages lasting less than 30 seconds (which is when 3 satellite aiding is used).

Table 14 - Revised Aiding Satellite Selection Algorithm Summary

FUNCTION	IMPLEMENTATION
Constellation Selection Criteria	Propagate User Position 60 seconds into the future and then select the constellation of 4 satellites with the lowest GDOP.
Satellite Visibility Criteria	5° above User Horizon
Reselection Interval	120 Seconds.
Contingency Selection Strategy	Pick the Satellite with the largest elevation who has been previously tracked.
Delay between Satellite Loss of Lock and Contingency Selection Execution	30 Seconds.
3 Satellite Navigation Strategy	Determine which source of aiding will produce the least amount of 3-D Position Error and select that one: <ul style="list-style-type: none"> Altitude Aiding (Baroaltimeter) GPS Clock Phase Propagation

Table 15 - Revised Aiding Satellite Selection Algorithm Run Effective Values

Interval	EHeff	EVeff	GDOPeff
GPS Only			
286000 - 289000	22.602	14.527	4.984
292000 - 294500	11.748	10.159	2.834
297000 - 298200	9.304	16.419	3.485
299800 - 300500	10.841	13.179	3.008

Interval	EHeff	EVeff	GDOPeff
286000 - 289000	22.602	14.527	4.984
292000 - 294500	11.748	10.159	2.834
297000 - 298200	9.304	16.419	3.485
299800 - 300500	10.841	13.179	3.008

Table 16 - Revised Contingency Selection Algorithm Relative Performance Metric

Interval	EH	EV	GDOP
GPS Only			
286000 - 289000	2.780	1.336	1.959
292000 - 294500	1.003	1.002	1.001
297000 - 298200	1.046	0.998	1.005
299800 - 300500	1.549	1.092	1.198

5.1.5 Hybrid Selection

Given the results above, where the Revised Contingency Selection algorithm reduces the errors induced by the contingency selections, and Revised Aiding Selection reduces the errors induced by 3 satellite navigating; it seemed reasonable to expect that combining the effects of each of these algorithms will produce a system that would rival the benefits of knowing when terrain features will induce errors.

The goal of this hybrid algorithm (summarized in Table 17) is to reduce the effect of both Contingency Selections and 3 Satellite Navigating.

The results of this modification to the baseline algorithm are shown in Table 18 and Table 19. As expected, the benefits of both algorithms combined to produce a solution nearly as good as the DTED Scan (refer to Table 10) without the added burden of maintaining the DTED Database, and the intensive scan ahead for satellites which might become blocked.

Table 17 - Hybrid Satellite Selection Algorithm Summary

FUNCTION	IMPLEMENTATION
Constellation Selection Criteria	Propagate User Position 60 seconds into the future and then select the constellation of 4 satellites with the lowest GDOP.
Satellite Visibility Criteria	5° above User Horizon
Reselection Interval	120 Seconds.
Contingency Selection Strategy	Pick the Satellite with the <u>lowest</u> elevation who has been previously tracked.
Delay between Satellite Loss of Lock and Contingency Selection Execution	30 Seconds.
3 Satellite Navigation Strategy	Determine which source of aiding will produce the least amount of 3-D Position Error and select that one: <ul style="list-style-type: none"> Altitude Aiding (Baroaltimeter) GPS Clock Phase Propagation

Table 18 - Hybrid Algorithm Run Effective Values

Interval	EH _{eff}	EV _{eff}	GDOP _{eff}
GPS Only			
286000 - 289000	11.104	12.752	3.141
292000 - 294500	11.748	10.159	2.834
297000 - 298200	9.304	16.419	3.485
299800 - 300500	10.841	13.179	3.008

Table 19 - Hybrid Algorithm Relative Performance Metric

Interval	EH	EV	GDOP
GPS Only			
286000 - 289000	1.366	1.173	1.235
292000 - 294500	1.003	1.002	1.001
297000 - 298200	1.046	0.998	1.005
299800 - 300500	1.549	1.092	1.198

5.2 Summary of the Performance of the Alternative Algorithms

Given that many ARMY GPS receivers use a satellite selection algorithm similar to the Collins DOD algorithm which we used as our baseline, NOE and ground based users operating in terrain which is conducive to satellite blockages would obtain better overall navigation performance by modifying the Contingency Selection strategy, and the 3 Satellite Navigation strategy of these receivers. Figure 7 shows the graphic comparison of the individual metric values calculated above for each algorithm in the Holloman simulations of an NOE flight path. There are 3 conclusions which can be derived from the results of our testing:

1. Where possible, the All In View receiver will be the best choice for low level and NOE users, who do not have the benefits associated with aided (INS, DOPPLER, Ect..) inputs for helping to navigate through terrain features where satellite blockages occur frequently.
2. There are significant benefits associated with knowing when a particular satellite may be blocked in the future. This is clearly shown in the results for the DTED Scan algorithm, where many (if not all) of the contingency selections were eliminated. The drawback to this algorithm are its data storage requirements, and its mathematically intense calculations needed to determine satellite visibility over the next reselection interval.
3. With only a modification to the receiver software, many of the GPS receivers currently used by the ARMY which incorporate a satellite selection algorithm similar to the baseline one tested, could be enhanced to provide better navigation to low level and NOE users. In fact the results show that the Hybrid algorithm is capable of delivering performance which most of the time was better than the DTED Scan algorithm.

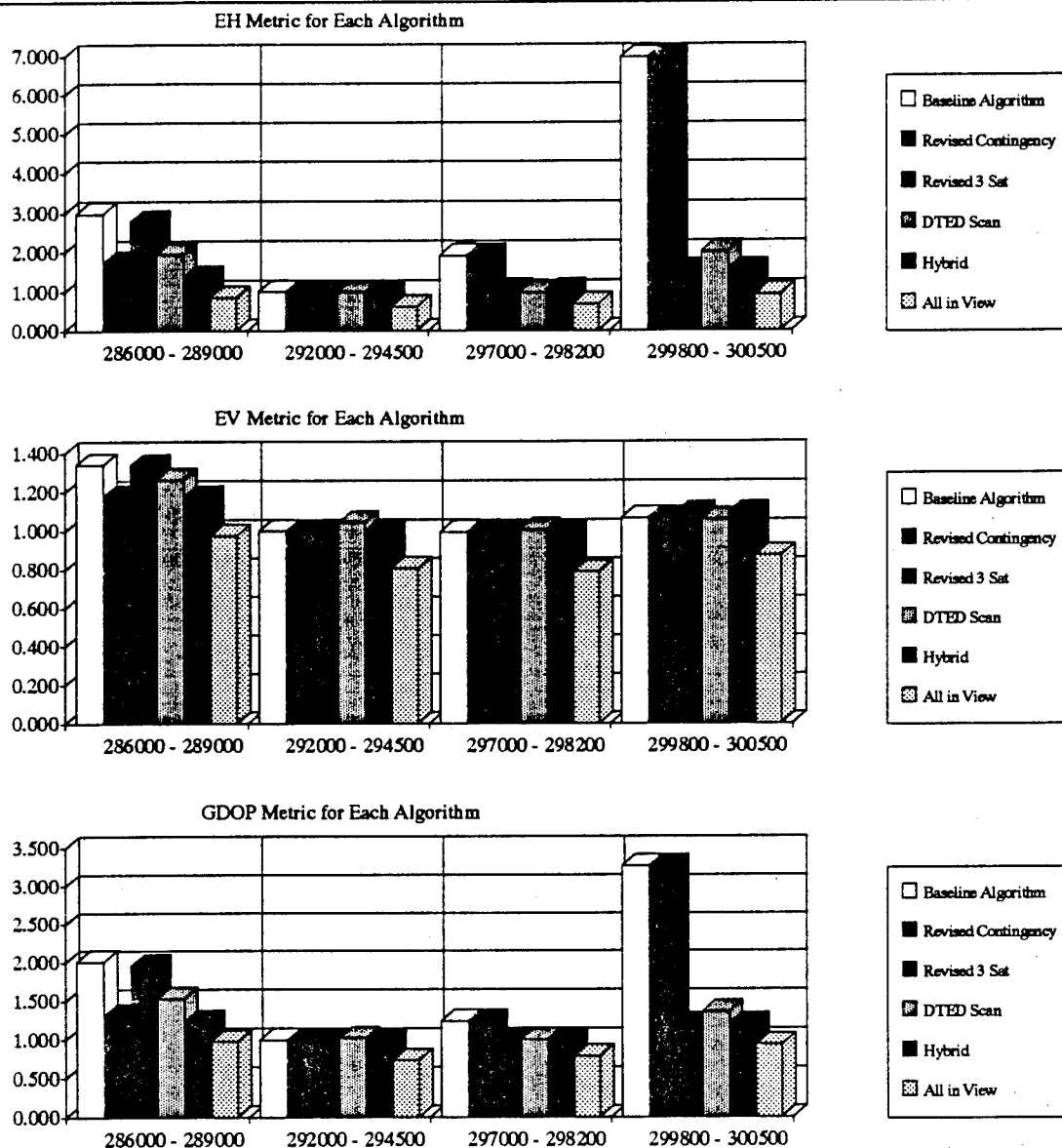


Figure 7 - Metric Values For Each Algorithm

6. Evaluation of Performance for a Ground Based User

One of the goals of our testing was to determine the effectiveness of the new algorithms for ground based users as well as the ARMY NOE flyer. To perform this testing, we simply had the Trajectory Generator lower the users altitude from 100 feet above the terrain, to 10 feet above the terrain.

Figure 8 shows the GPS Only 1-sigma errors for the ground based run of the Holloman AFB path using the Collins DOD satellite selection algorithm. As expected, we see many more satellite blockages and contingency selections.

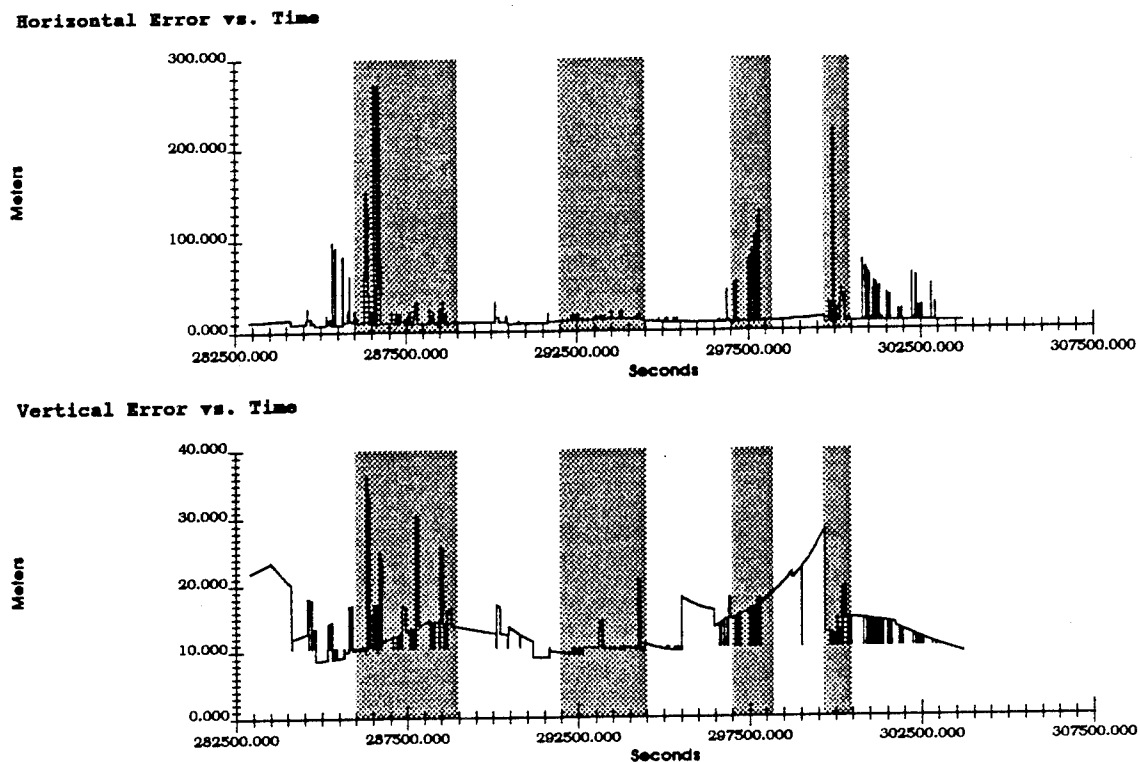
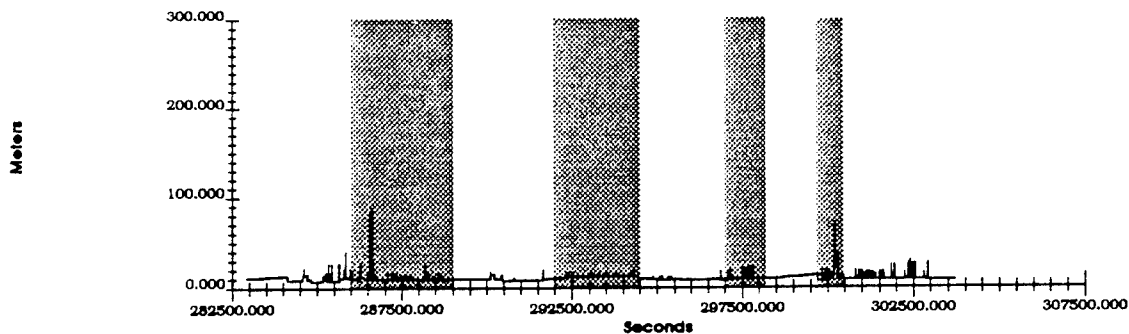


Figure 8 - Baseline Algorithm Ground Based User GPS Only 1-Sigma Errors

Figure 9 shows the same run using the Revised Contingency Selection algorithm, with Time Phase Propagation instead of altitude aiding since a common ground based user would not likely have access to an altitude aiding source. As we saw previously for the NOE user, the ground based users navigation solution can benefit greatly with a change to satellite selection strategy.

Horizontal Error vs. Time



Vertical Error vs. Time

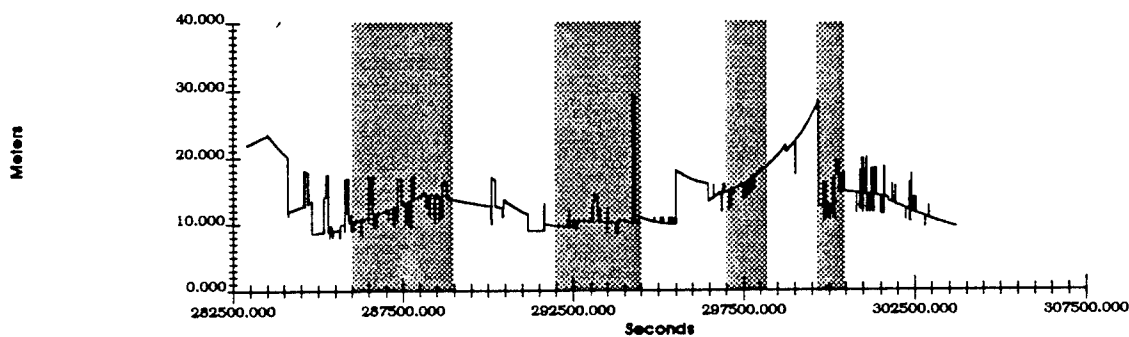


Figure 9 - Revised Contingency and Time Propagate Algo. Ground Based User GPS Only 1-Sigma Errors

7. Future Considerations

The results of this study indicate that the current satellite selection algorithms are in fact inefficient for Nap Of the Earth user or ground based user as was hypothesized. The new algorithms tested here show promise and will be flight tested for validation. Following successful validation, C2SID will pursue the exchange of this technology to interested vendors. It should be noted that these not only include GPS vendors, since many of the newest receivers allow for external control over the selection of satellites.

With the additions of a jamming model, and the utilization of DTED Level 2, the simulation tool used in this study becomes much more capable than originally envisioned. The DOD needs to more fully appreciate the impact of terrain masking and threat jamming as highlighted by the recent DOD Science Board Task Force on GPS vulnerabilities. These impact directly on the systems that depend on accurate and timely navigation data e.g. path guidance, situation awareness and targeting. In addition, the GPS Joint Program Office (JPO) has indicated the need to characterize the performance of varied levels of GPS integration techniques with respect to mission oriented scenarios. This simulation tool has tremendous potential to address these issues, providing key input to architecture configuration decisions.

8. Summary and Conclusions

Most ARMY GPS receivers have less than 12 receiver channels to provide measurements to the full set of observable GPS satellites. This requires that these receivers implement a strategy to select a constellation (of at least 4) which will provide the best navigation solution available for that receiver. The Collins DOD GPS receiver algorithm that we tested performs well for users well above the terrain features which could cause satellite signal blockages. For ARMY aircraft flying NOE profiles, or low altitude users, the terrain features will cause frequent satellite blockages. The purpose of this study was to determine how a receiver's satellite selection algorithm would

react to these blockages and determine the magnitude of the navigation errors which would result from the blockages.

C2SID developed a Satellite Selection Algorithm Simulator to evaluate the existing satellite selection algorithm used in many ARMY GPS receivers. An evaluation of the simulator outputs revealed two aspects of behavior for the receiver which affected the overall navigation errors:

1. The reaction of the algorithm to a Contingency Selection.
2. The method of navigating using less than 4 satellites (underdetermined solution).

Several alternative algorithms were developed and incorporated into the simulator software to be evaluated against the baseline Collins DOD algorithms:

- All in View
- DTED Based Prediction of Satellite Outages Over the Reselection Interval
- Revised Contingency Selection
- Revised Aiding Selection for Underdetermined Solutions
- Hybrid Selection consisting of Revised Contingency and Revised Aiding

Evaluation of the alternative algorithm results revealed that:

1. Where possible, the All In View receiver will be the best choice for low level and NOE users, who do not have the benefits associated with aided (INS, DOPPLER, Ect..) inputs for helping to navigate through terrain features where satellite blockages occur frequently.
2. There are significant benefits associated with knowing when a particular satellite may be blocked in the future. This is clearly shown in the results for the DTED Scan algorithm, where many (if not all) of the contingency selections were eliminated. The drawback to this algorithm are its data storage requirements, and its mathematically intense calculations needed to determine satellite visibility over the next reselection interval.
3. With only a modification to the receiver software, many of the GPS receivers currently used by the ARMY which incorporate a satellite selection algorithm similar to the baseline one tested, could be enhanced to provide better navigation to low level and NOE users. In fact the results show that the Hybrid algorithm is capable of delivering performance which most of the time was better than the DTED Scan algorithm.

Further testing of the alternative methods for improving the navigation performance of low altitude GPS users will include:

- Lab testing of the algorithms using the C2SID GPS Satellite Signal Generator
- Flight testing of the algorithms in specially modified GPS Receivers.

THIS PAGE LEFT BLANK INTENTIONALLY

PLOT TYPE: HOLLOMAN AFB-SIMULATED A/C TRAJECTORY
 PLOT DATE: 6/1/1994

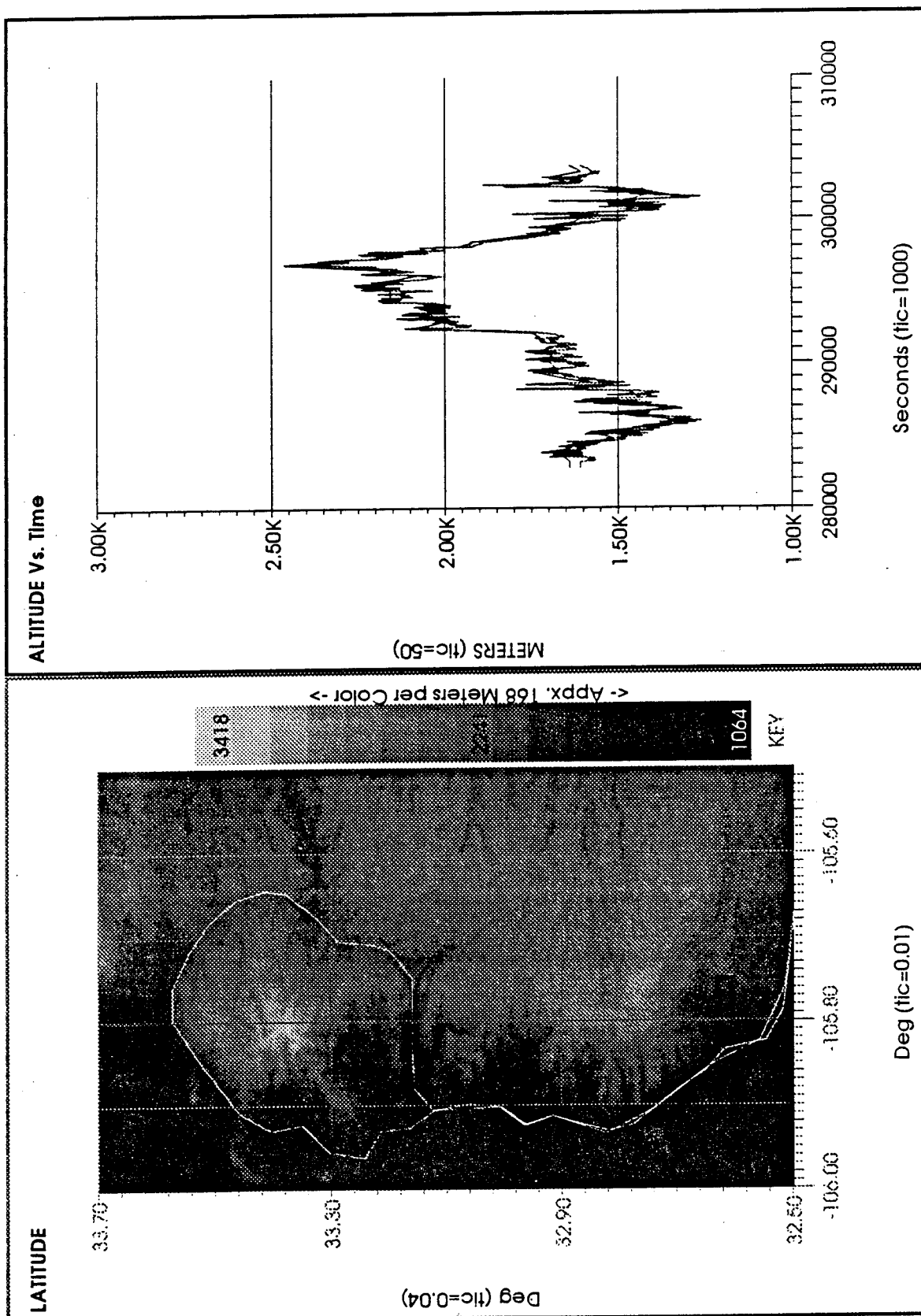


Figure 10 - Sample Holloman AFB Route Plan Map/Altitude Plot

PLOT TYPE: HOLLOMAN AFB SATELLITE TRACK PLOT

PLOT DATE: 6/1/1994

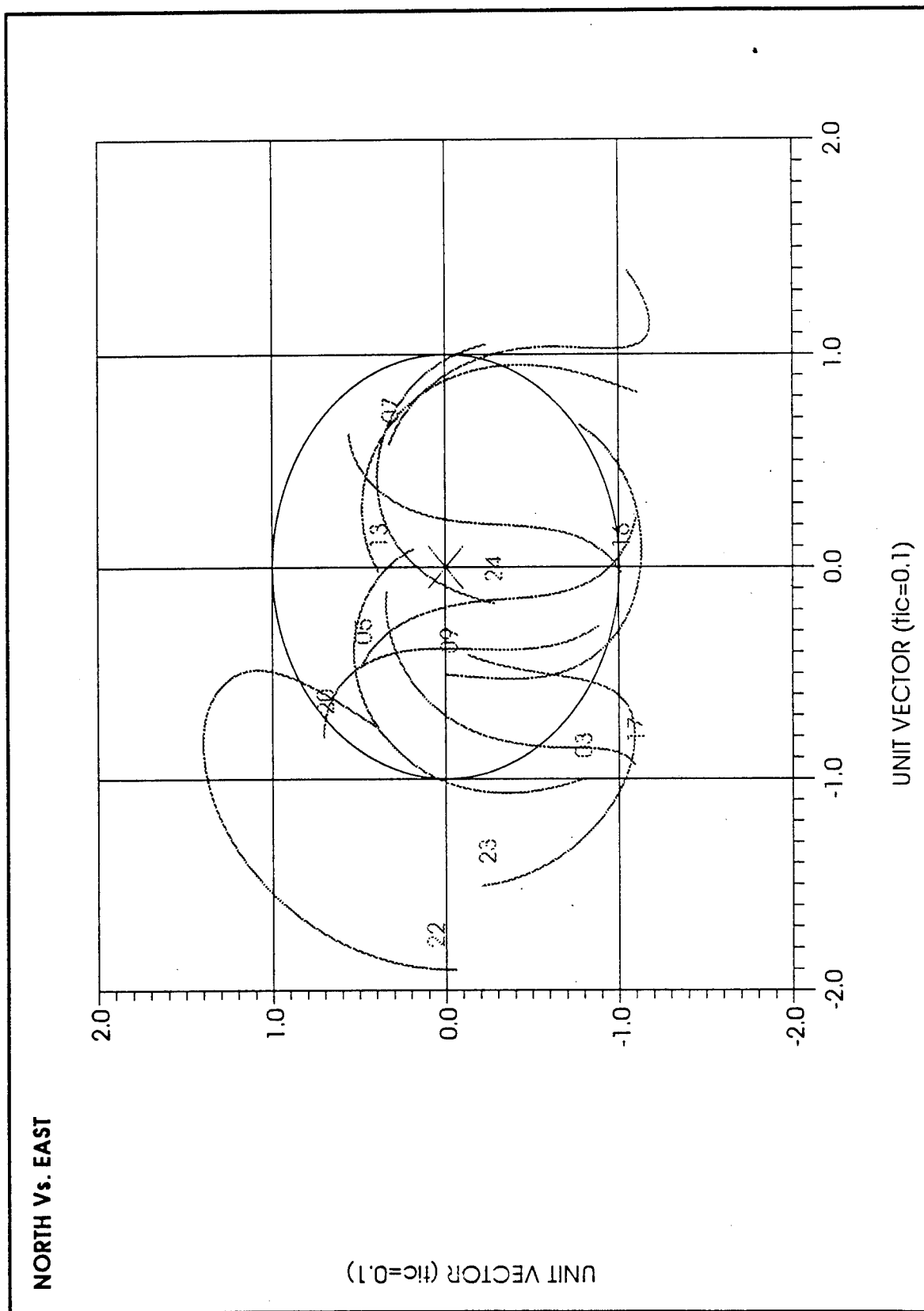


Figure 11 - Relative Satellite Position Plot Sample from Holloman AFB Route Plan

PLOT TYPE: HOLLOMAN AFB-GPS ONLY-COVARIANCE ANALYSIS-WITH DTED-COLLINS DoD
 PLOT DATE: 4/4/1994

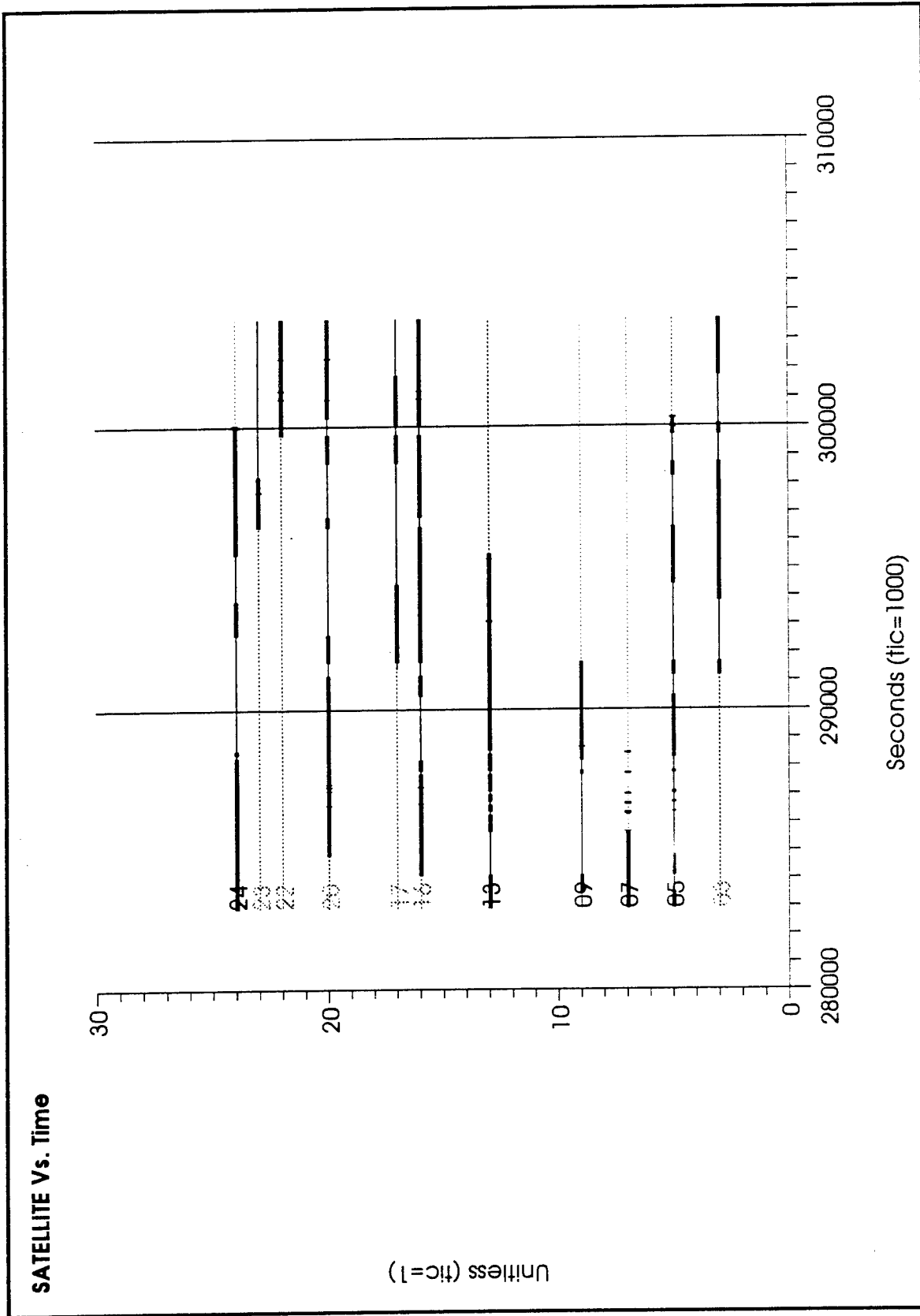


Figure 12 - Satellite Usage Plot Sample from Holloman AFB Route Plan

PLOT TYPE: HOLLOMAN AFB-DOP PLOTS-WITH DTED-COLLINS DoD

PLOT DATE: 4/4/1994

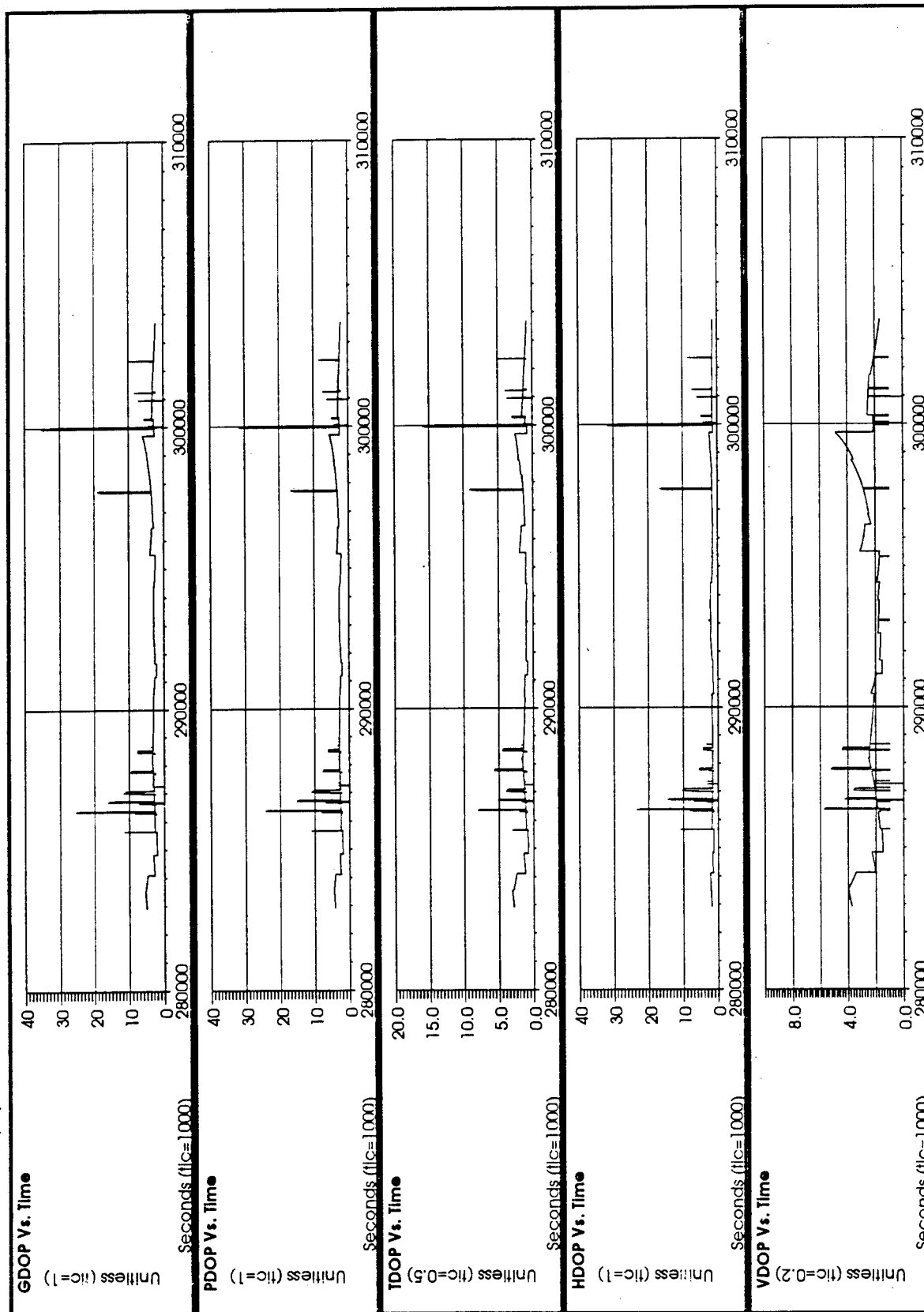


Figure 13 - DOP Plot Sample from Holloman AFB Route Plan

PLOT TYPE: HOLLOMAN AFB-GPS ONLY-COVARIANCE ANALYSIS-WITH DTED-COLLINS DoD
PLOT DATE: 4/4/1994

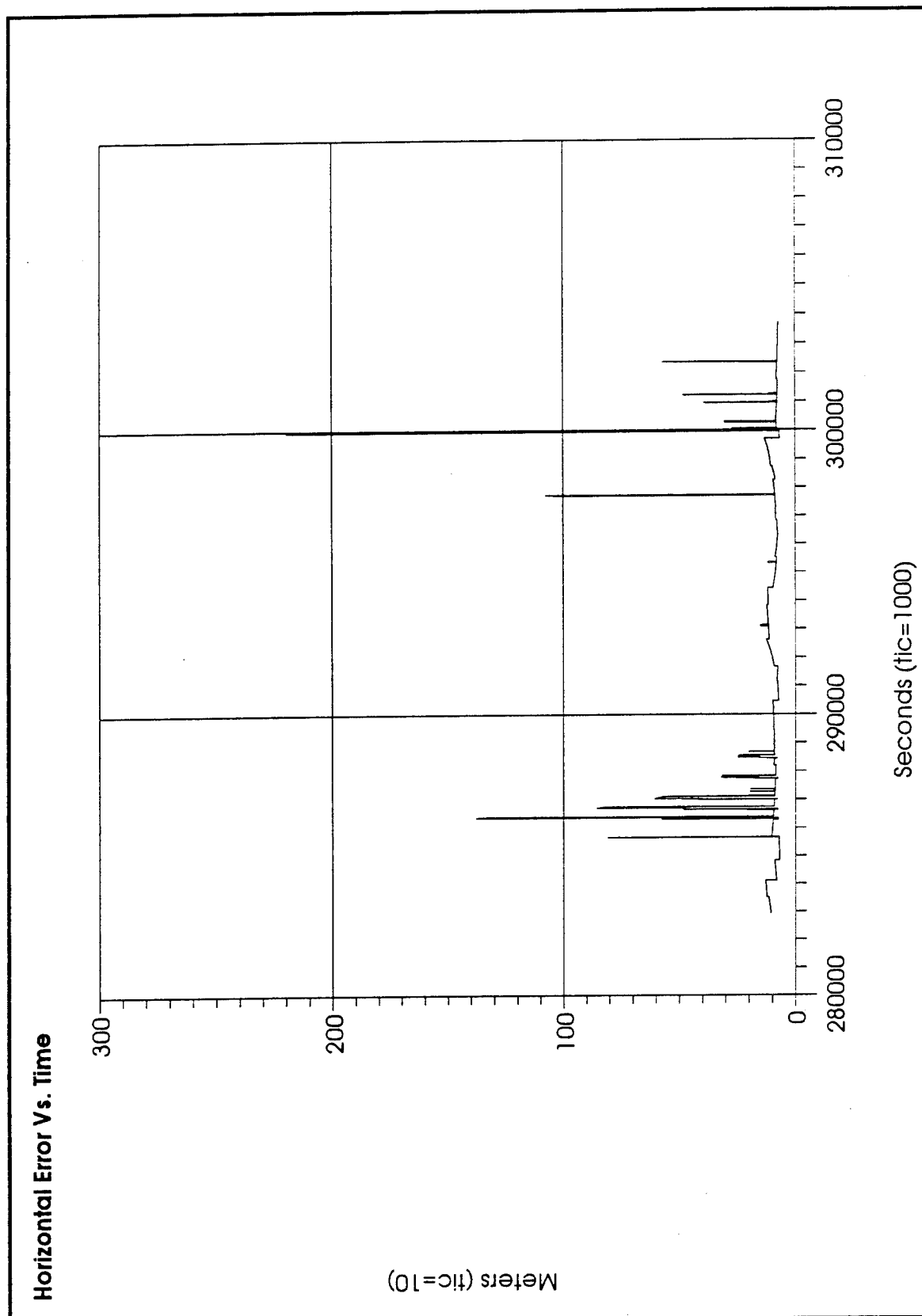


Figure 14 - Horizontal 1-Sigma Error Plot Sample from Holloman AFB Route Plan

PLOT TYPE: HOLLOMAN AFB-GPS ONLY-COVARIANCE ANALYSIS-WITH DTED-COLLINS DoD
PLOT DATE: 4/4/1994

Vertical Error Vs. Time

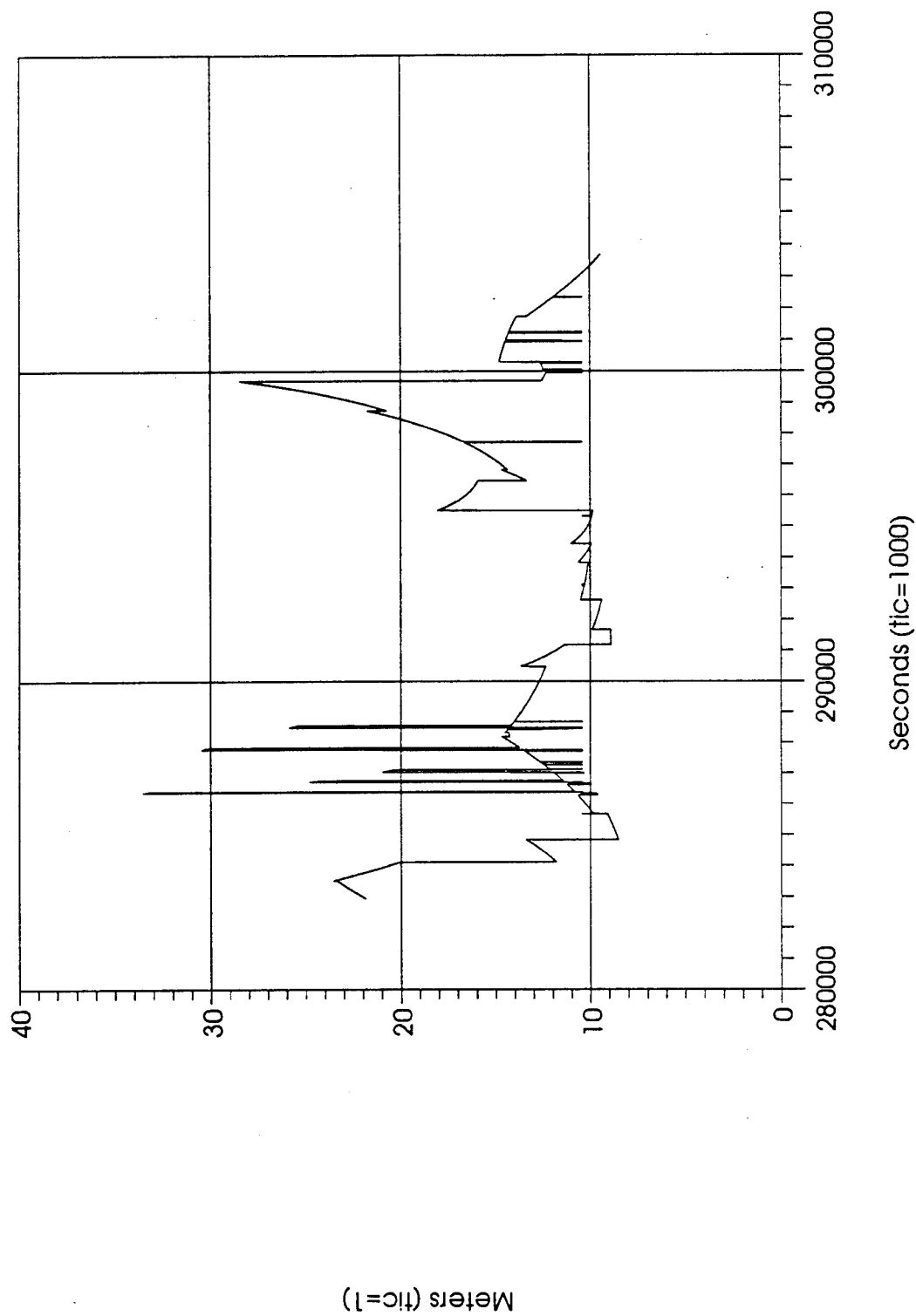


Figure 15 - Vertical 1-Sigma Error Plot Sample from Holloman AFB Route Plan

About the Authors

Ms. Van Tran is an electronics engineer at the Command, Control Systems Integration Directorate (C2SID) Fort Monmouth, US ARMY. Ms. Tran holds a B.S. degree in Electrical Engineering from California State University at Fullerton (1986).

Mr. Paul Olson is the group leader of the Navigation Technology Group of the Command, Control and Systems Integration Directorate (C2SID) and has been working in the area of Army electronics and platform integration since 1982. He has a BS in Electrical and Computer Engineering from Clarkson University, Potsdam New York (1982) and an MS in Electrical Engineering from Fairleigh Dickinson University, Rutherford New Jersey (1987).

Mr. Jim Adametz is a software engineer with Intermetrics Inc., Wall Township, NJ. He holds a B.S. degree in Computer Science from Rutgers University (1982).

Mr. Joe McGowan is a senior electronics engineer specializing in advanced navigation technologies with Intermetrics Inc., Wall Township, NJ. He has been working ARMY GPS applications since 1984 with a focus on high accuracy and special use missions. He holds a B.S. degree in Electronics Engineering from New Jersey Institute of Technology (1980).

Authors would like to acknowledge the contribution of Josh McGowan, who spent so many hours running these simulations and organizing the resulting data for us.

REFERENCES

- ¹ Olson, Paul and Berry, Mark R., The Precision Navigation System, US Army CECOM, RD&E Center Command/Control and Systems Integration Directorate (C2SID) ATTN: AMSEL-RD-C2-TS, Building 2525 Fort Monmouth, NJ 07703-5603
- ² CI-MAGR-300
- ³ C2SID, IEWCS Navigation System Upgrade Performance Test Final Report, US Army CECOM, RD&E Center Command/Control and Systems Integration Directorate (C2SID) ATTN: AMSEL-RD-C2-TS, Building 2525 Fort Monmouth, NJ 07703-5603
- ⁴ Maybeck, Peter S. Stochastic Models, Estimation and Control Volume 1, Academic Press, Inc., 1979

THIS PAGE LEFT BLANK INTENTIONALLY

SESSION IV-A
INERTIAL INSTRUMENTS

CHAIRMAN

COLONEL RICHARD CLARK (USAF Ret)

DESTIN FL

THIS PAGE LEFT BLANK INTENTIONALLY

Thermal Analysis of the HRG to Determine its Gap Sensitivity/Compensation

Lalit Kumar

Delco Systems Operations
6767 Hollister Avenue
Goleta, CA 93117-3000

Approved for Public Release; distribution is unlimited.

Abstract

The hemispherical resonator gyroscope (HRG) is a solid-state inertial rotation sensor. Ideally, in the absence of rotational input about the axis of symmetry, the resonator has two degenerate (identical frequency) modes of vibration. This degeneracy is lifted due to the coupling effect (from Coriolis forces) of the input rotation and frequency of one of the modes is increased by a small amount (proportional to the input rate). At the same time, frequency of the second mode is decreased by a similar amount. The net effect of these opposing changes is a beat phenomena or equivalently precession of the vibration pattern when viewed from the body fixed coordinates.

In order to mechanize this as a practical inertial rotation sensing device, one needs to have a forcing and a pickoff mechanism to sustain the vibration pattern and determine its position relative to body fixed axes, respectively. One of the most convenient methods is to employ capacitive pickoffs and electrostatic forcers. Since these interact with the resonator through an electric field across a small gap, it is important to know the gap behavior under external thermal and mechanical environments. A detailed finite element analysis of the HRG structure is performed to assess thermal gradients and their time constant. Finally, various schemes to monitor the gap in real time are discussed.

THIS PAGE LEFT BLANK INTENTIONALLY

Introduction

HRG's operation is based upon the mode coupling effect of the Coriolis forces which are generated by the interaction between the input rate and the velocity of the shell. The two normal modes of a hemispherical shell can be defined by the following deflection components along the radial, co-latitude (θ) and azimuthal (ϕ) directions [1]:

$$\begin{aligned} w_1 &= A_1 \cos(2\phi) \left[1 + \frac{1}{2} \cos\theta \right] \tan^2 \left[\frac{\theta}{2} \right] \\ u_{\theta 1} &= -\frac{1}{2} A_1 \cos(2\phi) \sin\theta \tan^2 \left[\frac{\theta}{2} \right] \quad \text{---- (1)} \\ u_{\phi 1} &= -\frac{1}{2} A_1 \sin(2\phi) \tan^2 \left[\frac{\theta}{2} \right] \end{aligned}$$

$$\begin{aligned} w_2 &= A_2 \sin(2\phi) \left[1 + \frac{1}{2} \cos\theta \right] \tan^2 \left[\frac{\theta}{2} \right] \\ u_{\theta 2} &= -\frac{1}{2} A_2 \sin(2\phi) \sin\theta \tan^2 \left[\frac{\theta}{2} \right] \quad \text{---- (2)} \\ u_{\phi 2} &= \frac{1}{2} A_2 \cos(2\phi) \tan^2 \left[\frac{\theta}{2} \right] \end{aligned}$$

Equations (1) & (2) show that the resonator lip deforms in an ellipse with antinodes along arbitrarily chosen axes #1 & #2 which are azimuthally separated by 45° (Fig. 1).

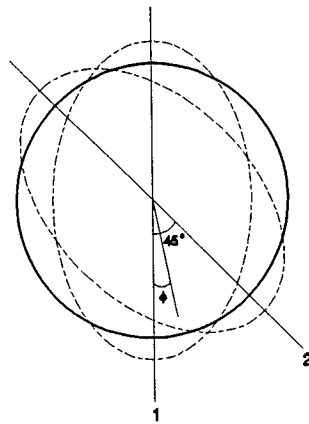


Figure 1

In the absence of rotational input about the axis of revolution (input axis), these two modes are independent of each other, i.e., if the shell is oscillating in its fundamental mode along the principal axis #1, there will be no radial deflection along axis #2. However, in the presence of rotational input Ω rad/sec, these normal modes get coupled due to Coriolis forces generated by the input rate and now there will be some radial deflection along axis #2. For time dependent amplitudes A_1, A_2 along axes #1 & #2, system dynamics can be represented as follows [2,3]:

$$\ddot{A}_1 + 2\xi_1\omega_1\dot{A}_1 + \omega_1^2 A_1 = 2k\Omega\dot{A}_2 \quad \text{----} \quad (3)$$

$$\ddot{A}_2 + 2\xi_2\omega_2\dot{A}_2 + \omega_2^2 A_2 = -2k\Omega\dot{A}_1 \quad \text{----} \quad (4)$$

ω_1, ω_2 = natural frequencies

ξ_1, ξ_2 = fraction of critical damping

At this point, depending on the application requirements, one has a choice between mechanizing Eq. (3) & (4) either as a rate integrating or a rate gyro. In the integrating gyro, resonator's vibration is sustained by parametric forces which have no directional bias. Under these conditions the vibration pattern is free to move. It can be shown that when an input rate is applied, angular velocity of the pattern in an inertial frame of reference is always less than that of the resonator [4]. In other words, vibration pattern precesses with respect to body fixed axes at an angular velocity of $(k\Omega)/2$. Where k is a constant which depends upon the shape of the axisymmetric body. For a hemisphere, its value is approximately .6.

As mentioned earlier, Eq. (3) and (4) can also be mechanized as a rate gyro. In this mode, the vibration pattern is maintained at a fixed location. This can be accomplished, as an example, by maintaining a constant amplitude along axis #1 and a null along axis #2 at 45° . The force required to keep the deflection at null along axis #2, is then a measure of the input rate. In both types of mechanizations, capacitive pickoffs and forcers are employed. Since these function by establishing an electric field across a gap formed between the resonator surface and the metallized pads on the gyro housing, their output depends upon the gap size. However, this sensitivity is not significant in the rate integrating gyro since the pattern location is determined by taking a ratio of two signals. On the other hand in the rate gyro, the force required to maintain a null deflection along axis #2 is directly affected by changes in the gap size. This paper therefore deals with the gap sensitivity and compensation thereof in the rate mode only.

Analysis

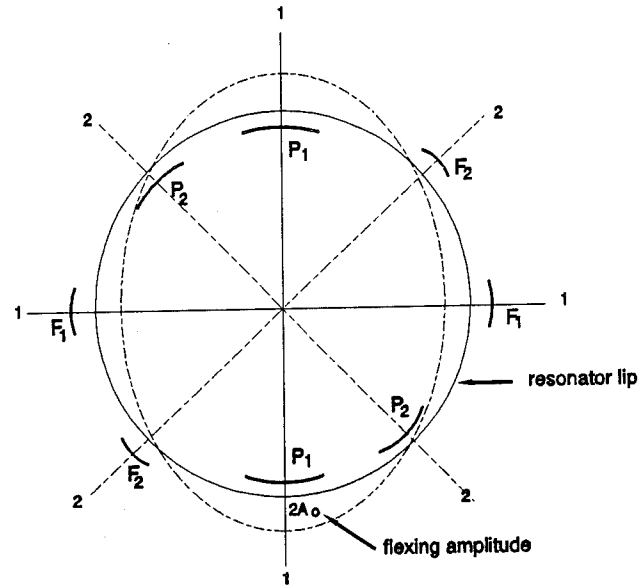


Figure 2

In the presence of external forces, Eq. (3) & (4) can be rewritten as:

$$\ddot{A}_1 + 2\xi_1\omega_1\dot{A}_1 + \omega_1^2 A_1 = F_1 + 2k\Omega\dot{A}_2 \quad \text{----} \quad (5)$$

$$\ddot{A}_2 + 2\xi_2\omega_2\dot{A}_2 + \omega_2^2 A_2 = F_2 - 2k\Omega\dot{A}_1 \quad \text{----} \quad (6)$$

In the rate gyro mode, amplitude along 1-1 axes is maintained at a constant value A_1 by an amplitude control loop. This is accomplished by adjusting forces at F_1 to maintain a fixed voltage output at pickoff P_1 . At the same time a second control loop continuously adjusts forcer F_2 to keep a null output at pickoff P_2 along axes 2-2. Under these conditions:

$$A_1(t) = 2A_o \sin(\omega_1 t)$$

$$\ddot{A}_2(t) = \dot{A}_2(t) = A_2(t) = 0$$

and from equation (6);

$$F_2 - 2k\Omega\dot{A}_1 = 0$$

$$\therefore F_2 = 2k\Omega\dot{A}_1 = 4kA_o\omega_1\Omega\cos(\omega_1 t) \quad \text{----} \quad (7)$$

Amplitude $2A_o$ cannot be measured explicitly since the pickoff output is proportional to the ratio of the flexing amplitude to the gap. Therefore the best that can be achieved in terms of keeping

a constant flexing amplitude is to control the output of pickoff P_1 to a fixed voltage, say V_{ref} . For displacements which are small compared to the gap, pickoff output is given by:

$$V_P = \frac{2A_o}{d_o} V_R = V_{ref}$$

$$\text{or } 2A_o = \frac{V_{ref}}{V_R} d_o \quad \text{---- (8)}$$

where V_P = output voltage at P_1

V_{ref} = a fixed reference voltage

V_R = bias voltage on the resonator

d_o = resonator/pickoff gap

For a given voltage applied at the forcer pad F_2 , the electrostatic force is inversely proportional to the square of the gap:

$$F_2 = \beta \frac{1}{d_o^2} \quad \text{---- (9)}$$

Substituting Eq. (8) & (9) into (7), we get:

$$\beta \frac{1}{d_o^2} = 2k d_o \frac{V_{ref}}{V_R} \omega_1 \Omega \quad \text{---- (10)}$$

Eq. (10) indicates that the scale factor (SF) is only as stable as the gap d_o . Particular care is taken in constructing the device from low coefficient of thermal expansion (CTE) materials. For example, if the CTE is .5 ppm/°C, SF variability at uniform temperatures will be no more than 1.5 ppm/°C. However, this sensitivity increases dramatically for thermal gradients across the gap. This higher sensitivity is due to the amplification factor R_{nom}/d_{nom} (nominal radius over gap).

Assessment of SF Sensitivity to Thermal Gradients

To determine the overall SF thermal stability, a transient thermal analysis was performed using COSMOS/M finite element (FE) code. An axisymmetric FE model of a typical gyro configuration was created as shown in (Fig. 3). The following load conditions were analyzed:

- (1) A temperature step of 10 °C was applied on boundary #1 at time = 0 sec. Temperature versus time output for various parts is shown in (Fig. 4). The analysis shows that the forcer temperature reaches the final value of 10 °C in a relatively short time of ≈ 100 sec. The resonator temperature lags considerably, reaching 4 °C after 1200 sec.
- (2) At boundary #1, temperature was ramped from 0 to 30 °C @ 1 °C/min. Temperature versus time plot is shown in (Fig. 5).
- (3) From load case (1), temperature distribution was input in the structural model to compute displacements at various locations.

Displacement at the forcer = 7.67E-5 mm

Displacement at the pickoff = 3.99E-5 mm

Displacement at the resonator = 4.58E-8 mm

Forcer/resonator gap change = 730 ppm

Pickoff/resonator gap change = 380 ppm

This analysis shows that there is considerable gap sensitivity to thermal gradients and the time constants are of the order of 60 minutes for these to subside.

THIS PAGE LEFT BLANK INTENTIONALLY

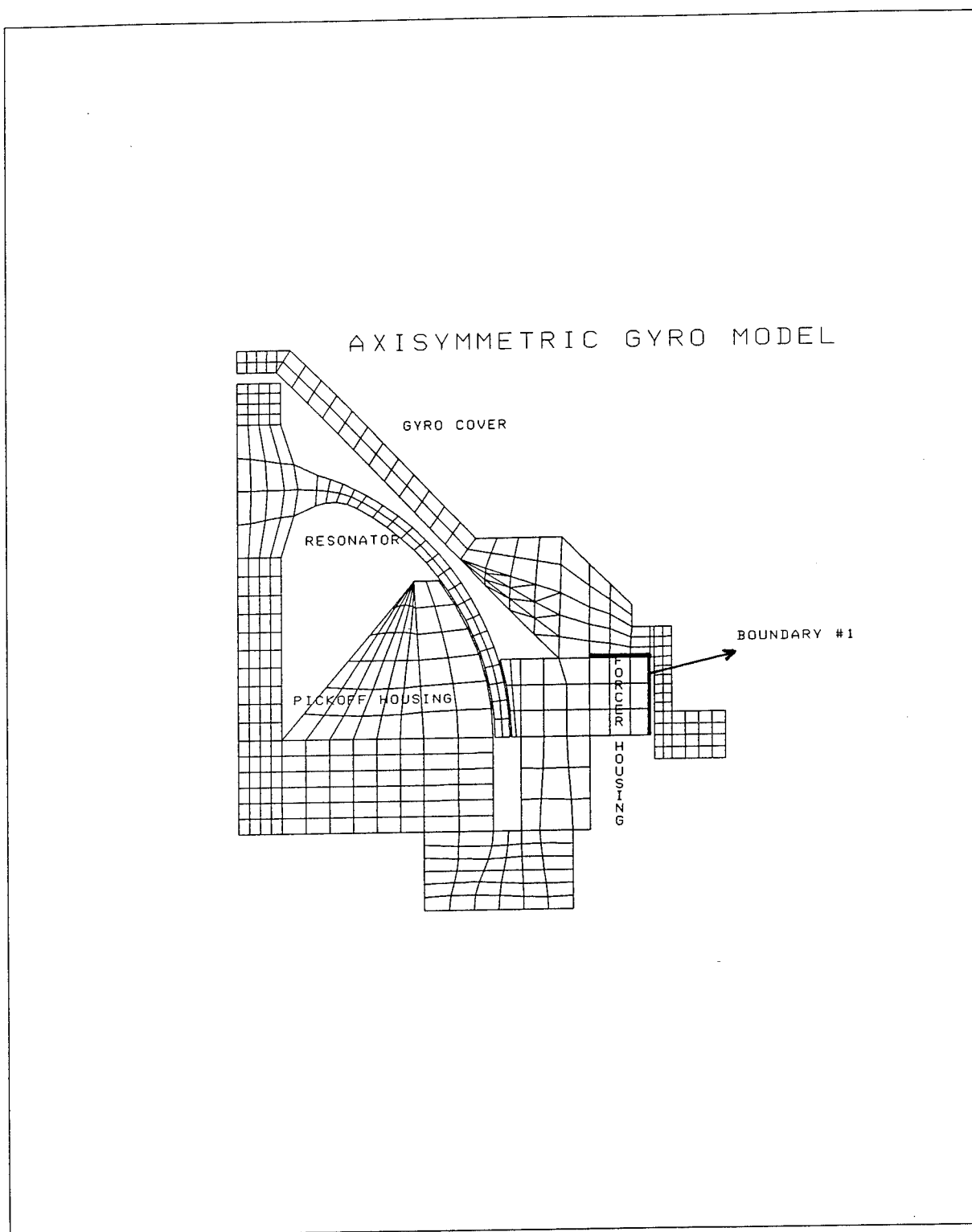


Figure 3

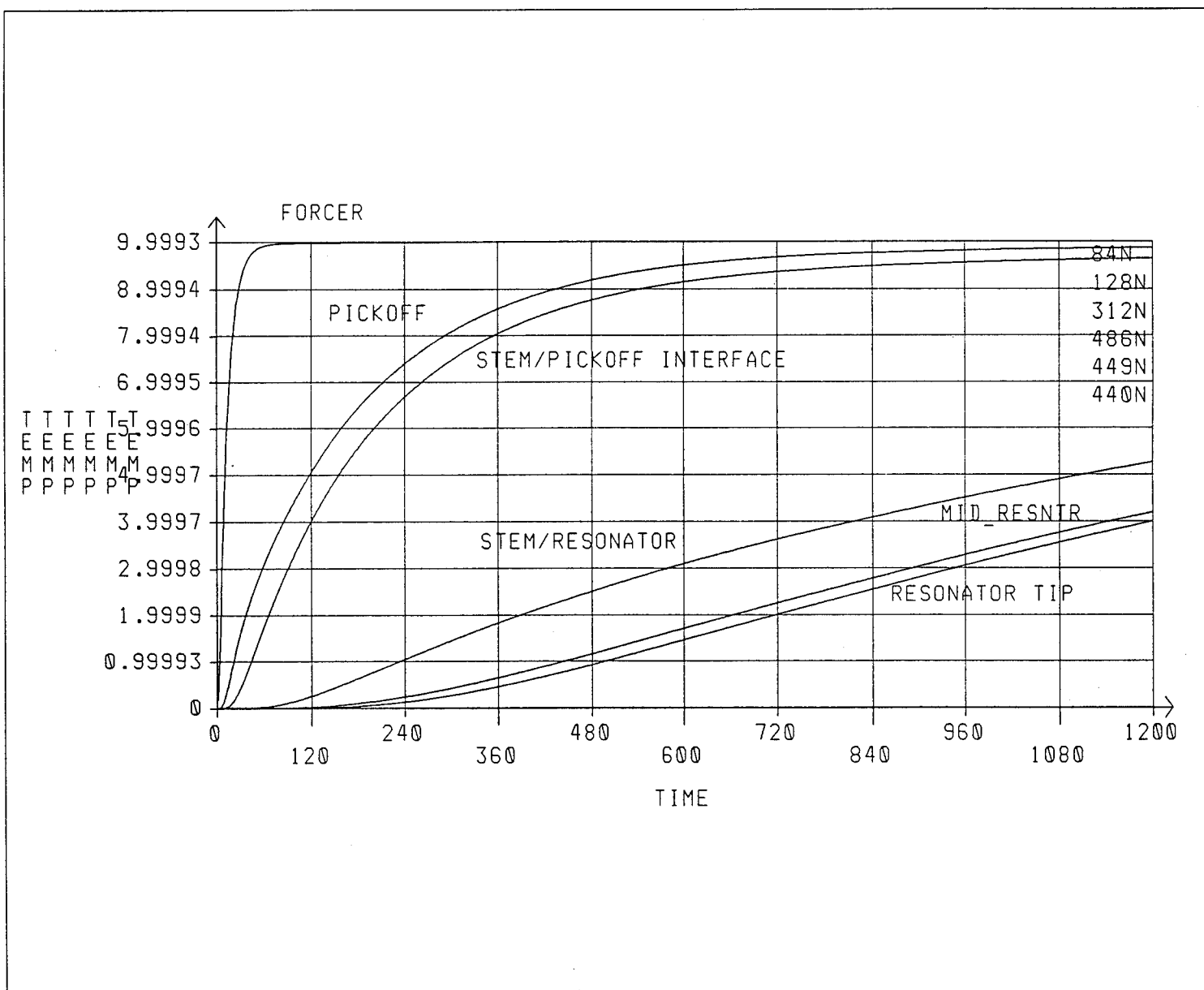


Figure 4

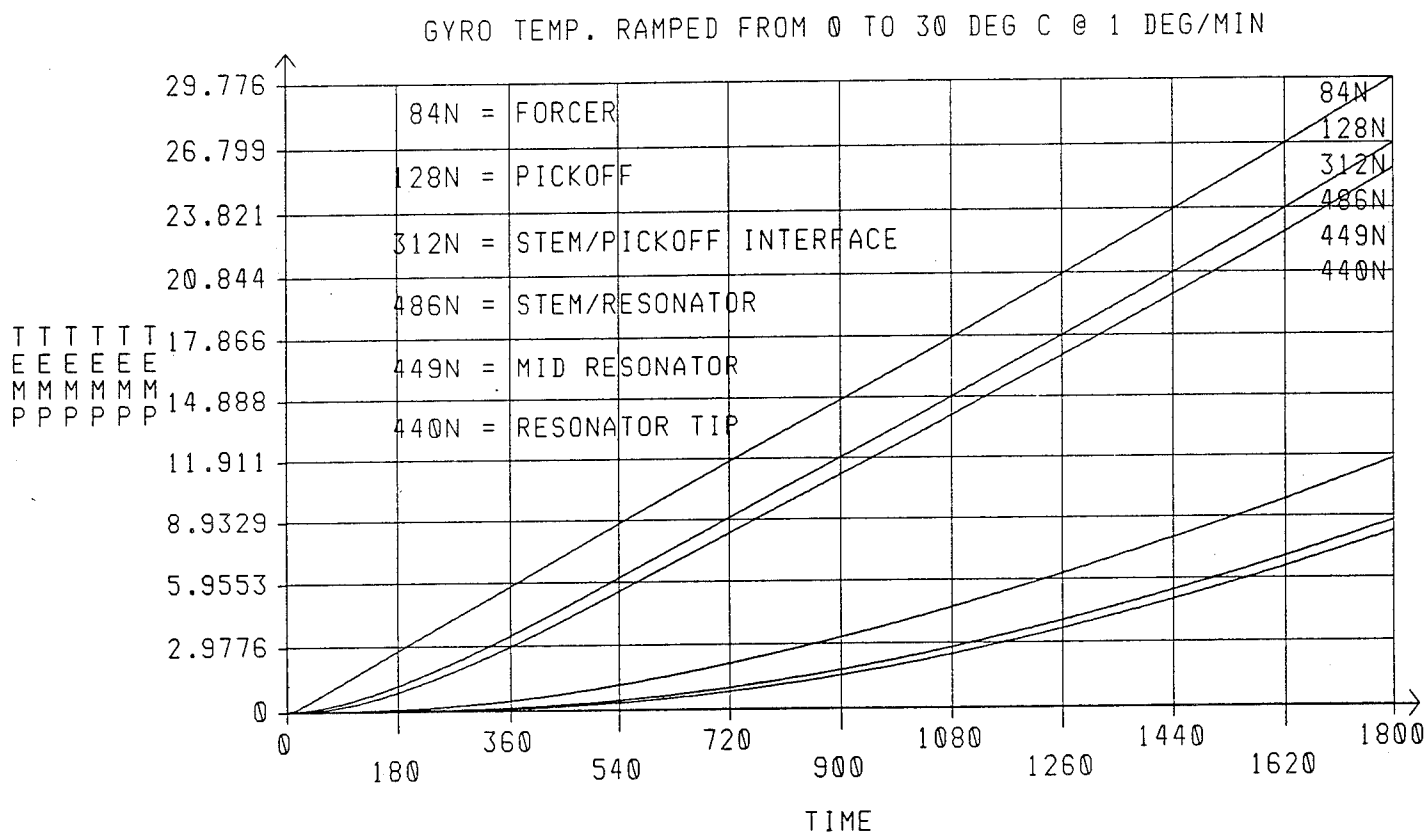


Figure 5

THIS PAGE LEFT BLANK INTENTIONALLY

Compensation

Clearly it is desirable to eliminate the gap sensitivity at the source by making sure that it doesn't change. Since the gaps we are concerned with are between the resonator and pickoff/forcer surfaces, they can vary with changes in dimensions of either surface. Therefore one approach is to construct the pickoff/forcer housing from a material with a negligible CTE. Due to the requirement of high Q for the resonator, it is constructed from fused quartz which has a low but not negligible CTE. Gap change now occurs only due to thermal expansion of the resonator and can be compensated in terms of the resonator frequency which is a very sensitive measure of its temperature.

A second approach is to continuously monitor temperatures of the pickoff and forcer surfaces by appropriately located temperature sensors. These temperature readings along with the resonator frequency allow gap changes to be tracked. This approach is limited by the difficulty of being able to embed temperature sensors close enough to the pickoff/forcer surfaces.

A third and novel approach is based upon sensing signals which can be used to determine the gap explicitly.

Conclusion

In the rate gyro mode, SF stability depends on the gap size. There are several approaches which are effective in compensating for the changes in gap.

References

- [1] Seide, Paul, "*Small Elastic Deformations of Thin Shells*", Noordhoff International Publishing, Leyden, 1975, pages 346-347.
- [2] Lynch, D. "*The Generic Vibratory Gyro*", Delco Systems Operations, 11 December 1990.
- [3] Emslie, A.G. and Simon, I., "*Design of Sonic Gyro*", Arthur D. Little, Inc., Cambridge, MA, July 1967.
- [4] Bryan, G.H., "*On the beats in the vibrations of a revolving cylinder or bell*", Proceedings of the Cambridge Philosophical Society, vol. VII, 1890.

THIS PAGE LEFT BLANK INTENTIONALLY

G2000 MINIATURE GYROSCOPE

Roger F. Burlingame
Litton Guidance and Control Systems Division
Woodland Hills, CA

THIS PAGE LEFT BLANK INTENTIONALLY

G2000 MINIATURE GYROSCOPE

Roger F. Burlingame
Litton Guidance and Control Systems Division
Woodland Hills, CA

Abstract

Dry Tuned Gyro (DTG) technology offers performance and size advantages not offered by emerging optical rate sensor technology. DTG technology has become well established and offers the lowest technical risks and lowest costs when compared to optical technology. The G2000 Miniature Gyroscope advances the art of low cost, high performance, DTG technology in a miniature size package not available until now. The G2000 is a two-axis angular rate sensor capable of high shock and vibration environments. It operates over the MIL-SPEC temperature range (-54 to +100 deg-C) without the need for external temperature control. An available servo electronics board, designed specifically for the G2000, provides DC-DC operation in a small physical envelope.

The design is described and performance data is presented which illustrate the unique capabilities offered by this low cost, miniature size dry tuned gyroscope.

Introduction

Litton Guidance and Control Systems Division began developing dynamically tuned gyro (DTG) technology back in 1974, and the G2000 gyroscope is the latest addition to the Litton family of DTG instruments. The G2000 bridges the gap between rate gyroscopes and medium performance DTGs in a miniature size gyro envelope not previously available. The primary gyro requirements for tactical missile applications, as well as many others, are: low cost, high reliability, and small size. The G2000 meets all these requirements and more. Owing to its highly ruggedized design, the G2000 can be used in applications which previously required shock and vibration isolators to protect the gyro.

From the start of the G2000 design, it was understood that developing a DTG having good performance and utilizing low-cost manufacturing methods can be conflicting requirements which may prove to be the greatest challenge. A review was made as to what tasks made gyro production expensive. Of these, it was found that repeated assembly measurements, inspections, testing, and adjustments made gyros labor intensive and requiring high operator skill levels. It was determined that for the G2000 to be low cost, manufacturing yields must be high with little or no rework. At the same time, labor tasks associated with assembly and calibration testing must be reduced or eliminated. To accomplish these, the traditional methods of gyro build needed to be revised and new criteria for fabricated parts and assembly processes must be established. The fabricated parts design should take advantage of automated Computerized Numerical Control (CNC) machining equipment wherever possible, thereby reducing dimensional variability, as well as hands-on labor. In addition, drawing notes should be relaxed in those areas of the machined part which are non-critical yet add significant costs to the part. Statistical Process Control (SPC) should also be used by vendors to insure lot-to-lot consistency on part dimensions. Assembly processes must also provide high yields with minimal labor. To meet this, the assembly fixtures should control all critical dimensions, rather than control these dimensions by repetitive measurements and adjustments performed by the assembly operator.

The G2000 gyro production incorporates many quality control processes which include a parts quarantine program, and vendor partnerships. To further reduce build cycle times, Demand Flow Technology (DFT) is now being implemented in the factory.

The result is the G2000 miniature gyroscope. The G2000 incorporates many innovative design and manufacturing features making it highly producible in large quantities and with very low costs. The G2000 has proven itself reliable and to exceed the specified performance requirements of many commercial and military applications, both domestic and international.

Features

- Small Size DTG (0.76 diameter, 0.97 long)
- Low Cost, High Volume Production DTG
- High Shock and Vibration Capability
- Mil-Spec Temperature Range Operation
- Temperature Modelable to less than 10 deg/hr
- MTBF of 30,000 Hours
- Low Noise
- High Bias Stability
- High Transient and Continuous Rate Capability
- Rapid Activation Time
- Attached Preamplifier Electronics
- 150 Hz Bandwidth Gyro Servo Electronics Card Available

The G2000 is a miniature two-axis dry-tuned rotor gyroscope capable of operating reliably over high shock and vibration environments. In most applications, temperature compensation of gyro parameters is not necessary owing to the G2000's low temperature sensitivities over the operating temperature extremes from -54 deg-C to 100 deg-C. It is capable of continuous and transient torquing rates of 200 and 400 deg/sec, respectively, and it exhibits the high drift stability and low noise characteristics typical of DTG instruments.

The unique combination of small size, ruggedness, high drift stability, and low cost make it highly suitable for a broad range of gimbaled and strapdown applications including: seeker antenna, tactical missile guidance, torpedo navigation, UAV, commercial autopilot for both marine and aircraft, and oil drilling navigation.

Overall instrument size is 0.76 inch diameter and 0.75 inch long. Length is increased to 0.97 inch with the attached external electronics board. The gyro weight with external electronics board is 25 grams. Figure 1 shows the gyro outline, mounting, and axis definitions.

The G2000 incorporates the well established DTG suspension principle. A schematic diagram of a two-axis gimbal system is shown in Figure 2. The suspension is a single piece design incorporating features which overcome the weaknesses of a traditional DTG suspension.

The Torquer design uses a single axially energized rotor magnet. The Torquer coils mount flat in the housing resulting in a very solid structural support capable of sustaining high shock loading and also providing high thermal dissipation during high continuous torquing rates. This torquer configuration provides reliable performance in a simple low cost design.

The Pickoff coils are designed to attach rigidly to the housing and results in a low cost assembly offering high reliability during severe shock and vibration environments.

An external electronics board attaches to the base of the gyro and contains the preamplifier for the pickoffs. Placement of the preamplifier adjacent to the gyro eliminates pickup noise when long harness lengths are necessary between the gyro and servo electronics.

Though external heaters are not required for broad range temperature operation, the G2000 bias is highly modelable and can be reduced to less than 10 deg/hr over the full Mil-Spec temperature range.

The gyro Mean time Between Failures (MTBF) is in excess of 30,000 hours based upon life test data, reliability models, and no reported field failures.

The performance characteristics of the G2000 gyroscope are summarized in Table 1.

Table 1

G2000 Gyroscope Characteristics

General Features

Size	0.76 inch dia., 0.97 inch long 19.3 mm dia., 24.6 mm long
Weight	25 grams
Nutation Frequency	500 Hz
Rotor Freedom	+/-0.5 degree
Motor	
Type	Synchronous Hysteresis
Phases	2
Resistance	55 ohms per phase
Spin Speed	16,000 rpm
Excitation Frequency	800 Hz
Excitation Waveform	Square or Sine
Start Voltage	28 Vrms
Run Voltage	10 Vrms
Start Power	< 15 watts
Run Power	< 1 watts
Start Time	< 1.4 seconds
Operating Temperature	-54 to +100 deg-C

Pickoff

Type	Variable Reluctance
Excitation Frequency	30-60 kHz sine
Excitation Current	14 mA
Scale Factor	7.0 Vrms/deg

Torquer

Type	Permanent Magnet
Resistance	15 ohms per axis
Scale Factor	1404 deg/hr/mA
Nonlinearity	0.07 percent
Temperature Sensitivity	40 ppm/deg-C
Maximum Continuous Rate	200 deg/sec
Maximum Transient Rate	400 deg/sec
Axis Nonorthogonality	< 1 deg

G-Dependent Drift

Direct Axis	< 25 deg/hr/g
Quadrature Axis	< 15 deg/hr/g
Temperature Sensitivity	0.1 deg/hr/g/deg-C
Anisoelastic Coefficient	0.1 deg/hr/g ²

G-Independent Drift

Fixed	< 300 deg/hr
Random	0.1 deg/hr, 1 sigma

Environmental

Vibration	
Sine	20 Grms (20-2000 Hz)
Random	30 Grms (20-2000 Hz)
Shock	600g, 30msec, halfsine
Temperature Range	-54 to +100 deg-C
Maximum Steady State Load	1000 g
Magnetic Sensitivity	0.5 deg/hr/gauss
Altitude	50 km

Table 2

G2000 Gyro Servo Electronics Card

Dimensions

Size	3.0 x 4.0 x 1.0 inch 76 x 102 x 25 mm
------	--

Input Power

Output Characteristics

Bandwidth	150 Hz
Scale Factor (scaleable)	50 mVdc/(deg/sec)
Output (@200 deg/sec)	10 Vdc (scaleable)
Linearity	0.1 percent
Stability	0.25 percent

Environmental

Vibration	
Sine	20 Grms (20-2000 Hz)
Random	30 Grms (20-2000 Hz)
Shock	600g, 30msec, halfsine
Temperature Range	-54 to +100 deg-C

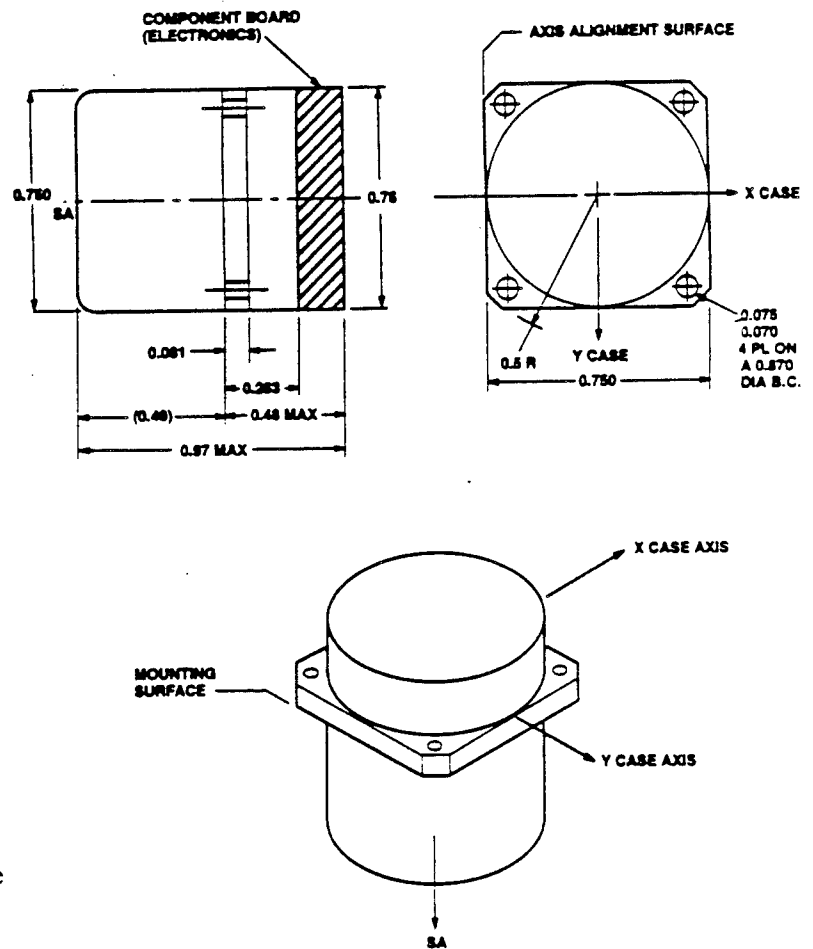
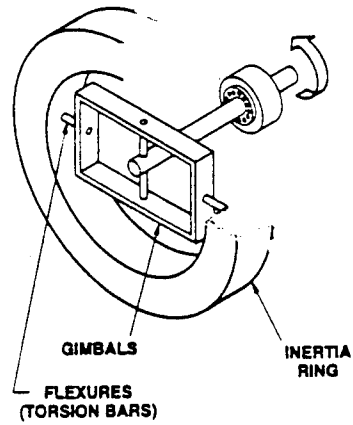


Figure 1. G2000 Gyro Outline and Mounting



$$\begin{aligned} \text{FLEXURE TORQUE} &= K\theta \\ \text{GIMBAL TORQUE} &= (A + B - C) N^2\theta \\ \text{TUNING CONDITION } K &= (A + B - C) N^2 \end{aligned}$$

Figure 2. Principle of Operation of a DTG

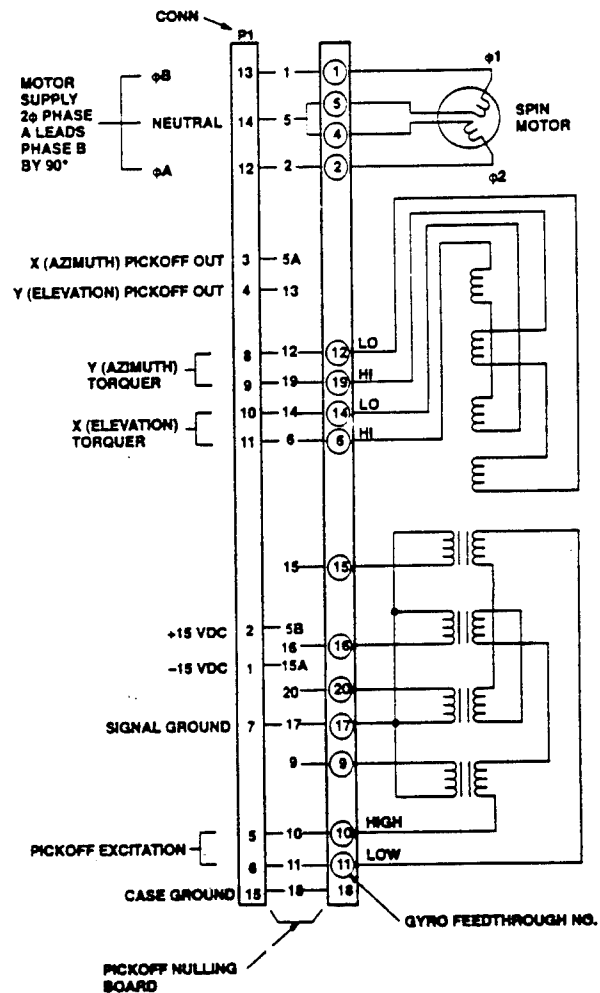


Figure 3. G2000 Electrical Interface Schematic

Technical Description

General Description of a Dry Tuned Rotor Gyro

The two degree of freedom gyro is composed of four major subassemblies: the case, pickoff coils, torquer coils, and the rotor together with the suspension assembly. The case supports the ball bearings which in turn carry the shaft. Attached to one end of the shaft is the rotor assembly and the other end carries the motor hysteresis ring. The torquers and pickoff coils are mounted to the gyro case.

The suspension assembly provides translational support for the rotor against linear accelerations while the torsional coupling between rotor and case about any axis perpendicular to the spin axis is zero. The suspension assembly is analogous to a universal joint which consists of an inertia element (the gimbal) and a torsional element (the flexures). When such a suspension system and rotor are run at a speed corresponding to the tuned frequency, the dynamically induced spring rate of the gimbal is equal to the physical spring rate of the flexures, and the resultant spring rate coupling the rotor to the shaft is zero. This condition is attained by adjusting the inertias of the gimbal such that the tuned frequency is made equal to the frequency of the synchronous motor speed.

The torquers and pickoffs control the attitude of the rotor relative to the case. When an input is applied to the case, the case fixed pickoffs sense this change in rotor attitude relative to the case and cause the caging loop to provide a current to the torquer coils which reduce this change to zero. In an ideal strapdown gyro, the torquer maintains the spin axis of the rotor aligned with the shaft spin axis.

Rotor Suspension

The gyro rotor suspension is a single piece design which lends itself to advanced methods of fabrication. The design permits several suspensions to be made simultaneously with one machine tool set-up. Efforts are currently in progress to perform automatic rotor balancing using a computerized laser balance station.

Two Axis Torquer

The torquer applies the appropriate rebalance torques upon the rotor precessing it to maintain the closed loop null position. Unlike traditional DTG permanent magnet voice coil torquers, which typically use several magnets, the G2000 torquer design uses only one axially energized magnet. This magnet attaches to the rotor in such a way as to provide a radial flux field. This field interacts with axially oriented wire wound coils mounted to the gyro housing. The mounting configuration of the coils provides a very broad, solid, structural support making them capable of withstanding high shock and vibration environments. It also provides a broad conduction area for high thermal dissipation of the coil to the housing during conditions of high continuous torquing rates. The coil winding and mounting tooling tightly control the torquer axis alignments to the housing without the need for additional mechanical or electrical axis adjustment. Axis nonorthogonality is typically below one degree. Another advantage to the magnet and coil mounting configuration allows the torquer scale factor to be adjustable for each application by changing the magnet to coil airgap.

Two Axis Rotor Pickoffs

The rotor pickoffs provide the error signal which indicates the rotor angle from the closed loop null position. The G2000 pickoffs are similar to standard transformer type pickoffs utilizing primary and secondary windings. However, their unique design allows the cores to be mounted rigidly to the housing. The result is a very solid structural support of the pickoff making it capable of undergoing severe shock and vibration while maintaining a stable pickoff null output signal.

Spin Motor

The spin motor is a two phase, six pole, synchronous hysteresis motor operated at 800 Hz excitation. The motor is designed to be self-locating into the housing, eliminating the need for installation alignment tooling. The motor operates in a dual mode start/run configuration. Starting is initiated at 28 Vrms briefly, dropping down to 10 Vrms for continuous operation. This method of overexcitation creates a high starting torque for rapid spin-up time and high power efficiency at operating speed.

Internal Wiring

All internal interconnect wiring is made using a single layer flexprint circuit. This flexprint eliminates the potential for miswiring, and it provides a high yield, high reliability, method for complex internal wiring.

Preamplifier Electronics Board

The pickoff preamplifier board attaches to the base of the gyro. This board provides approximately a gain of 28 to the pickoff output signal. In addition, pickoff electrical trim and compensation components are mounted on the board. The gyro interface cable exits from the board and terminates to a 15 pin MDM style interface connector. The gyro interface connector pin-outs are given in Figure 3.

Gyro Caging Servo Electronics Card

A wide bandwidth servo electronics card has been designed specifically for the G2000 gyro. This servo card provides all the voltages and waveforms necessary to operate the gyro as a closed loop angular rate sensor. The electronics provides gyro rate information through a scaleable DC output voltage which can be tailored to each application. The servo card operates with a nominal input voltage of 28 VDC. The control bandwidth of the gyro in combination with the servo card is 150 Hz. The combination of gyro and servo electronics allows DC-DC operation in a small package size adaptable to any application. A performance summary of the gyro servo electronics card is given in Table 2.

G2000 Gyro Performance Data

Typical performance data of the G2000 gyro when used in conjunction with the wide bandwidth servo electronics are presented in the following figures. Figure 4 is a plot of the gyro fixed bias output over a 15 minute time interval with five second averaging every 30 seconds and operating at 20 deg-C. Figure 5 is a plot of the servo electronics output voltage for gyro input rates from -200 deg/sec to +200 deg/sec. Figure 6 shows a plot of the gyro and servo wideband frequency response.

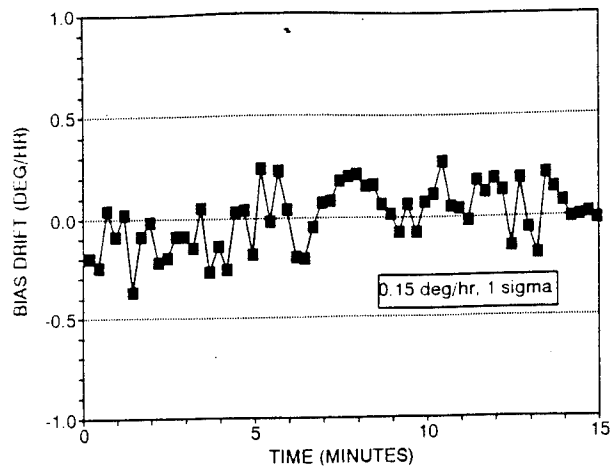


Figure 4. Bias Drift vs. Time

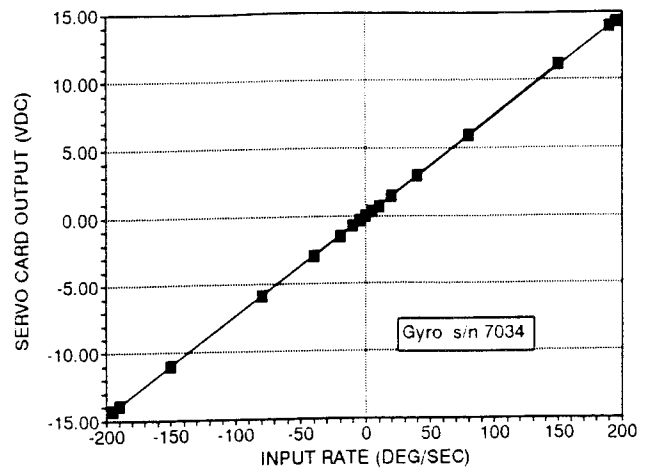


Figure 5. Servo Output Voltage vs. Input Rate

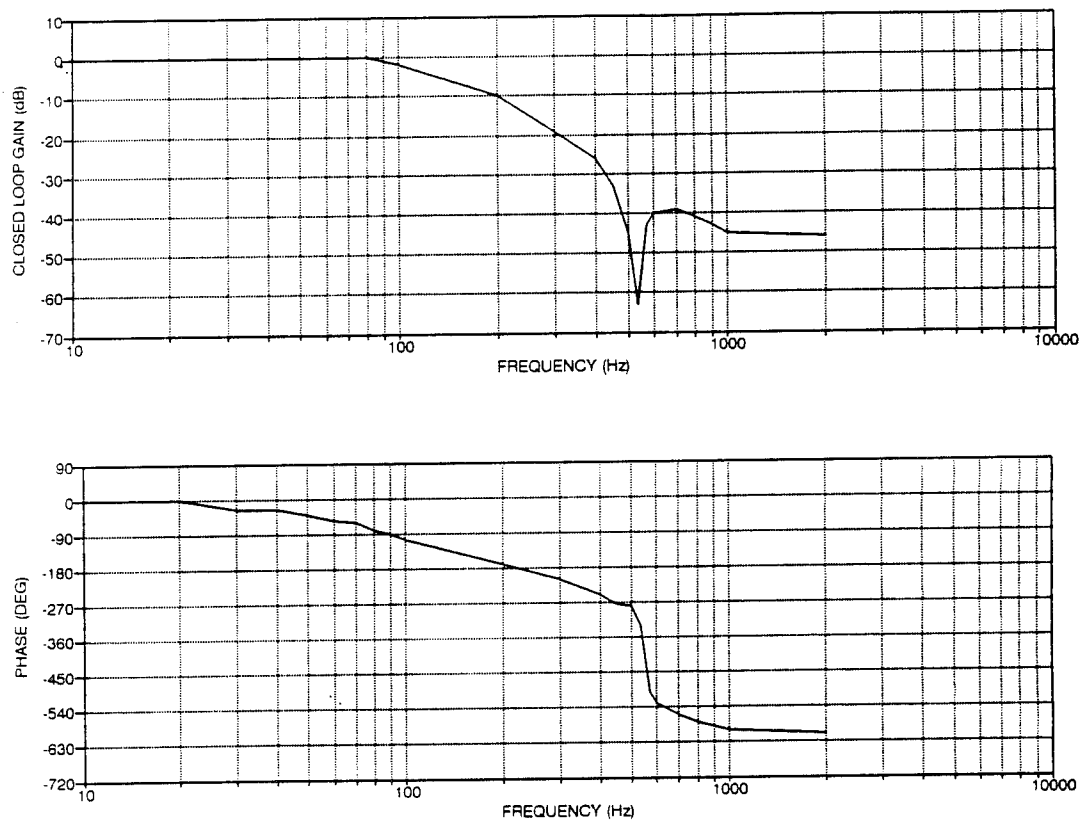


Figure 6. Gyro/Servo Closed Loop Gain and Phase vs. Frequency

THIS PAGE LEFT BLANK INTENTIONALLY

SESSION VI-A

T&E METHODOLOGY II

CHAIRMAN

COLONEL LEONARD SUGERMAN (USAF Ret)

*NEW MEXICO STATE UNIVERSITY
LAS CRUCES NM*

THIS PAGE LEFT BLANK INTENTIONALLY

ONLY PRESENTATIONS WERE GIVEN DURING THIS SESSION

THIS PAGE LEFT BLANK INTENTIONALLY

SESSION VII-A

ADVANCED SYSTEMS II

CHAIRMAN

DR. PAUL RUFFIN

*U. S. ARMY MISSILE COMMAND
REDSTONE ARSENAL AL*

THIS PAGE LEFT BLANK INTENTIONALLY

Fly-by-Light Advanced Systems Hardware (FLASH) Program

By

Carlos A. Bedoya

McDonnell Douglas Corporation

P.O. Box 516, St. Louis, MO 63166-0516

Abstract

Fiber optics are immune to electromagnetic emissions and have the potential to eliminate this concern especially in flight critical applications if they can be developed to the same level of technology as current systems using wire to carry the signals. As aircraft become more and more dependent on digital signals to control all systems, the Electromagnetic Environment (EME) will become more and more a concern for the safe long term operation. The International Severe HIRF electromagnetic environment (EME) is less than 2000 Volts per meter below 400 MHz and reaches a maximum of 6,850 Volts per meter in the 4-6 GHz range. The normal assumption is that a metal or composite aircraft skin with appropriate seals provides 20 dB attenuation of the external environment. This reduces peak levels at the avionics boxes to less than 200 Volts per meter below 400 MHz and a maximum of 685 Volts per meter in the 4-6 GHz range. MIL-STD-461D imposes an additional box level requirement of 200 Volts per meter from 10 KHz to 40 GHz. This requirement equals or surpasses the attenuated HIRF environment over significant portions of the spectrum and implies that the aircraft must be designed to achieve and maintain this value throughout its service life. Although wires can be shielded and designed to achieve these requirements, it is a more expensive process, adds the weight of shielding and requires maintenance of the shielding integrity at all times.

The very light weight and high bandwidth of fiber optics also offer the potential of eliminating the number of connections and weight savings in aircraft. For example on a one to one replacement of wire by fiber, it is estimated that fiber would weigh about 1/20 the weight of wire. Current wire buses used for duplex communications in aircraft applications have a bandwidth of about 1 MHz while equivalent buses using fiber optics have a bandwidth of 20 MHz. For other applications such as video and avionics interfaces, fiber buses in the hundreds of MHz are available. Application of fiber optic buses would then result in the reduction of wires and connections because of reduction in the number of buses needed for information transfer due to the fact that a large number of different signals can be sent across one fiber by multiplexing each signal. The Advanced Research Projects Agency (ARPA) Technology Reinvestment Project (TRP) Fly-by-Light Advanced Systems Hardware (FLASH) program addresses the development of Fly-by-Light Technology in order to apply the benefits of fiber optics to military and commercial aircraft.

1 Direct Benefits to Aircraft - The U.S. Aerospace Industry must develop technology, tools and processes to provide technically superior higher performance products at greatly reduced cost and span time relative to history for the benefit of the Department of Defense (DoD) and the global competitiveness of U.S. industry. Development of carefully chosen technologies and associated tools/processes is the key to establishing this required capability.

There is a need to develop the technologies for integrating the FCS with the other aircraft systems for the completely integrated cost effective Vehicle Management Systems (VMS) of the future. One concept that will benefit from FBL technology is the VMS because fiber optics will provide the inherent EME immunity required in the control of aircraft subsystems as well as the bandwidth needed for this control and diagnostics. Digital controls have threats from many sources of electromagnetic energy which include things such as the outside/inside environment as well as directed threats. In order to implement all the integrated functions that will be required to increase aircraft performance and reduce cost, FBL is the technology that allows the real-time integration necessary. All these functions require high data integrity because they are flight critical as well as high data rates because of real-time control function implementation. Five key direct technical benefits of the integration of fiber optics and photonics at the aircraft level are

shown in figure 1-1. These are substantial benefits which are needed in order to maintain competitiveness in the current military and commercial aircraft business. The detailed benefits are as follows.

Military and Commercial Aircraft Needs

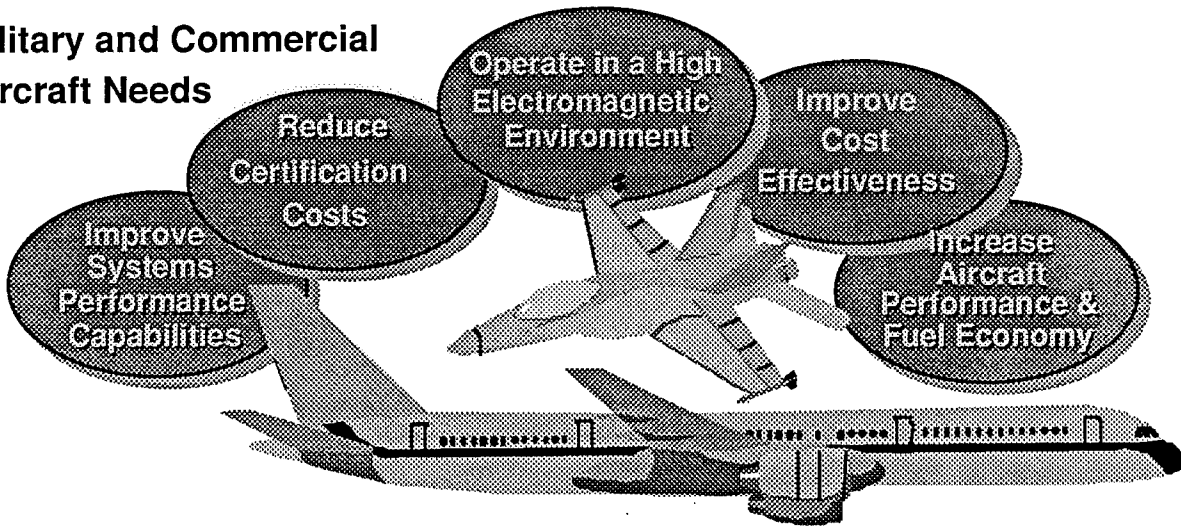


Figure 1-1 Future Aircraft Dual-Use Technology Needs Met by Fiber Optics

(1) Operate in High Electromagnetic Environment (EME): The electromagnetic environment that aircraft must safely operate within is becoming more intense due to the worldwide proliferation of high energy emitting sources, digital electronics and more electric aircraft actuators and control systems. The solution lies in the basic immunity of fiber optics to EME sources. Fiber optics for aircraft applications are needed to provide the necessary technological maturity for cost effective EME protection over the life of the aircraft and its systems.

(2) Improve Cost Effectiveness: Improved cost effectiveness is critical for the U.S. aerospace industry to compete in a global commercial and military aircraft market. Part of the solution can be found through the incorporation of fiber optics technology, as well as new processes to compress development costs and time. Fiber optics will enable the incorporation of power-by-wire (PBW) technology in which U.S. Air Force studies have shown 10% reliability, 14% vulnerability and 12% maintainability improvements, a 20% operational support transport aircraft load reduction and a 15% manpower requirements reduction. Studies indicate that a process using fiber optics and neural networks can significantly reduce the maintenance cost of control systems by identifying control system failures in real-time. Fiber optics are needed to improve the cost effectiveness of future aircraft developments.

(3) Increase Aircraft Performance and Fuel Economy: The commercial and military markets need increased aircraft performance and fuel efficiency to compete. On commercial and military aircraft, weight savings and performance improvements are closely related. One solution is to use lightweight fiber optics in the flight and engine control systems of a commercial wide body aircraft. Over 1000 lb. can be saved by replacing a fly-by-wire control system with its FBL counterpart, and an additional 1400 LB savings could be realized by replacing mechanical control systems. These weight savings could result in a direct increase in passengers or payload and aircraft range or reduction in fuel consumption.

(4) Increased System Performance Capabilities: The demand for increased system performance capabilities has saturated the limits of wire systems and multiplex buses. Fiber optics provides the high bandwidth necessary to permit future aircraft to address these high data rate and volume needs. In addition, neural networks, coupled to fiber optics systems, offer the opportunity to effectively design optimal control systems that maintain higher aerodynamic and engine performance in real-time.

(5) Reduce Certification Cost: The cost and complexity of certifying avionics and control systems in commercial aircraft has increased significantly. The FAA certification cost for EME at the aircraft level on the MD-11 was approximately \$12 million. The solution is to certify all systems at the box level by the use of fiber optic interfaces. Fiber optic interfaces and the cable plant will enable industry to certify aircraft at the box level only and avoid costly aircraft level tests.. In addition, the use of high bandwidth fiber optic buses enables the application of Modern Control Theory to determine control system parameters more rapidly and significantly reduce the time span to develop aircraft control laws and therefore reduce certification costs.

The bottom line is that the ever increasing performance and cost reduction demands (Figure 1-1) placed on new and derivative military and commercial aircraft lead to more complex, highly integrated avionics and control systems. Fiber optics provide a reliable and lightweight solution to the needs identified. FBL technology is needed to develop these key areas in order that the industrial base and suppliers in the U.S. can have this technology ready for flight critical applications which require much more stringent manufacturing controls and processes. Except for some military aircraft, and the current development of the Boeing 777, the U.S. lags behind the Europeans in application of even current technology fly-by-wire (FBW) systems. The Airbus has had a FBW system from the beginning as well as other advanced technologies and the records show that they now own around 40% of the commercial passenger aircraft market of which 90% belonged to the U. S. a decade ago.

As an example of potential benefits in converting a military aircraft from current conventional mechanical to digital/optical control, Figure 1-2 shows the results of an Army/Boeing study for the application to a light weight helicopter of the Advanced Digital Optical Control Actuation (ADOCS) concept.

Parameter

FBL vs. Dual Mech

Flight Safety Reliability	3 Times Better
Mean Time Between Aborts	8 Times Better
Multiple Hit Kill Probability (5Hits)	3 Times Better
Mean Time to Repair	2 Times Better
Mean Time Between Failures	8 Times Better
Control System Weight	27% Reduction
Installation Volume	6 Times Better
Life-Cycle Costs (1450a/c/20yr)	27% Less
Combat Damage Repair	Significant Improvement

Advanced Digital Optical Control Actuation US Army/Boeing

Figure 1- 2 Benefits of Fly-By-Light Technology Study

2. Current FBL Programs Background - The first U.S. digital Fly-by-Wire (FBW) on a production fighter was the F/A-18 in 1978, then the F-16D in 1980's and on a production military transport the C-17 in 1992, which has given industry in this country a large data base of experience in this technology. Therefore, FBL is the next technological step beyond FBW. Fly-By-Light is not a new technology. It has been around since the 1970's in bits and pieces as far as aircraft applications have been concerned as shown in Figure 2-1. It has evolved to the point that it is ready to be applied to flight critical systems. One part that is missing as far as aerospace applications are concerned, is qualified parts, processes and suppliers. There is a need to develop all necessary pieces and to do this by providing realistic system requirements and using as much technology as is available from the telecommunications industry and the use of commercial standards and practices.

<u>Application</u>	<u>Date</u>
Optical FC Data Link, Boeing YC-14	1976
HOFCAS USN/Rockwell	1980
DIGITAC, USAF/Honeywell	1982
AV8-B Data Link, USMC/MDC	1983 Prod a/c
ADOCS US Army/Boeing Vertol	1985
OPMIS NASA/MDC	1985-1992
FOCSI NASA/MDC	1985-1994
FACT NASA/MDC	1993-1995
FBL NASA/Boeing	1993
FLASH ARPA/MDC Team	1994-1996

Figure 2-1 Fly-By-Light Historical Perspective From the 1970's to the Current State

MDC has been developing and testing aircraft fiber optic systems since the mid 1970's. In addition to internal research and development (IRAD), MDA has performed several contracted research and development (CRAD) programs for NASA and the U.S. Navy. Figure 2-2 shows the current FBL configuration installed in the NASA Dryden/MDA Systems Research Aircraft (SRA) which first flew in 1994 and continues to fly today to obtain initial open-loop test information on all the flight control sensors developed for NASA Lewis under the Fiber Optic Control System Integration (FOCSI) program. Figure 2-3 shows the General Electric FOCSI engine control program conducted in parallel and test flown on the same aircraft. These two programs only monitor the performance of the fiber optics in an open-loop configuration and perform no direct control functions. The purpose of both FOCSI programs was to develop sensors and suppliers that could produce flight critical fiber optic components and identify which of the fiber optic sensor technologies were viable for flight control and engine control

applications. Development, laboratory testing and flight testing revealed that in general analog sensors were not desirable for flight control applications and that digital type sensors performed much better and were more reliable as well as weaknesses in the mechanical designs of some suppliers that were not traditional aircraft system suppliers.

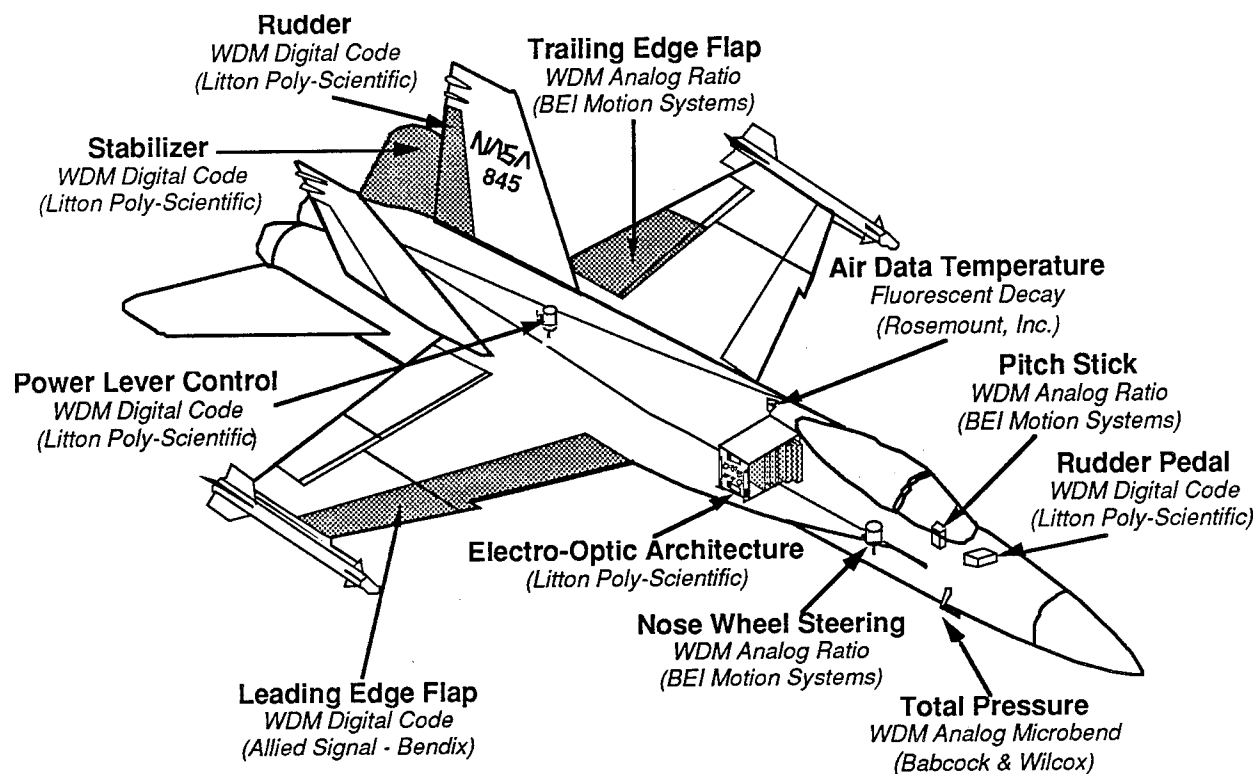


Figure 2-2 The NASA/MDC Fiber Optic Aircraft Controls Research Aircraft

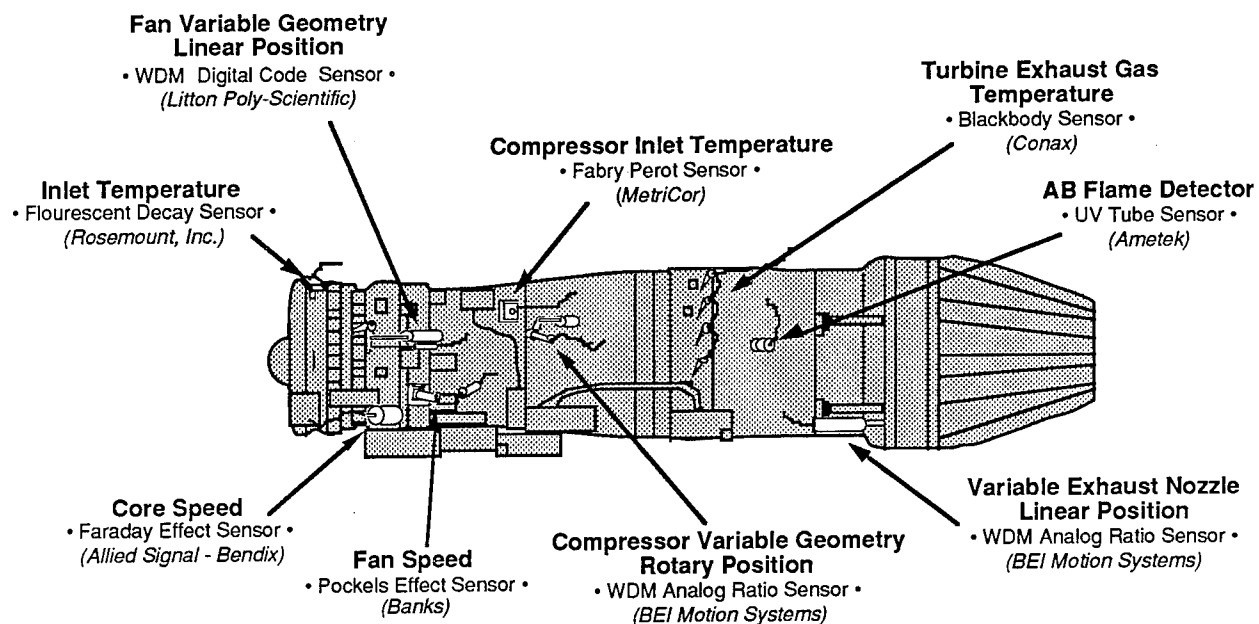


Figure 2-3 The NASA/GE Fiber Optic Engine Controls Research Engine

Why is FBL not a reality yet? In general, the flight control community is extremely conservative and for this reason a methodically planned development is necessary in order to demonstrate a new technology's applicability to flight critical functions. The next step then has to be the demonstration of fiber optics controlling a flight control surface in a realistic flight environment. First the demonstration should be on a surface that is not flight critical, meaning that if there is a failure, the aircraft can still be safely controlled and safely landed. The next step is to then apply the technology to a flight critical surface to demonstrate that it is as safe and reliable as current technology. On the NASA/Dryden F/A-18 SRA aircraft, one rudder and one stabilator respectively meet this criteria, with the added flight test feature of the pilot being able to switch back to the production mechanical control system and safely return to a FBL control configuration if the failure is cleared up.

The NASA subsonic transport office has funded a follow-on program to the FOCSI program using flight worthy optical position sensors developed that fit in the same volume as the F-18 rudder and stabilator production Linear Variable Displacement Transformers (LVDTs) and are dual and quadruplex redundant, respectively. The Fly-by-Light Aircraft Closed-loop Test (FACT) program is under way to perform a closed-loop flight test of one rudder and one stabilator actuator on the same NASA/MDC F-18 SRA as the FOCSI program using fiber optic feed forward, position sensor and feedback with flights scheduled for the end of 1995 at the NASA/Dryden flight test center at Edwards Air Force Base, California. These sensors will close the actuator control loop optically and will be demonstrated in flight. The results of this program will be incorporated into the full FBL system currently being developed under the FLASH program funded by industry and ARPA under the TRP and are considered critical to the future viability of FBL.

Although progress has been slow due to funding limitations and the conservative nature of application of new technology to flight control systems, the FLASH program has provided a \$24 million dollar influx of funding, 50% provided by industry and 50% by ARPA to speed the development of FBL. The FLASH program will bring the state of the art of FBL to the point of being ready for application to current and future aircraft.

3. The FLASH Program Overview- The FLASH program supports the ARPA Technology Development Activity, Defense Dual-Use Critical Technology Partnerships initiative. The FLASH program complements NASA and DoD FBL and power-by-wire (PBW) development efforts by addressing technical gaps that are critical to making FBL/PBW viable military and commercial technologies. The U.S. aerospace industry must "leap frog" its foreign competition with new technology at lower cost to remain competitive and provide affordable weapon systems to the DoD. To accomplish this, the FLASH program is developing key elements of FBL/PBW such as :

- (1) A cost effective and reliable fiber optic cable plant that meets aircraft requirements and enables the implementation of FBL/PBW to reduce costs,
- (2) A low cost flight control system using FBL/PBW sensors and control links, including a new and innovative process for control system design,
- (3) FBL/PBW actuators that provide significant improvements in reliability and maintainability.

The FLASH team includes technology users such as airframe manufacturer McDonnell Douglas, engine manufacturer Pratt Whitney, and various industry suppliers including flight control, avionics, actuator, connector, cable, harness, photonic back planes, and sensor manufacturers, as well as university support. The reason for this approach is to develop the supplier base needed by the aircraft industry to incorporate FBL into its products.

The FLASH program has taken a total system design approach as illustrated in Figure 3-1 in order to develop all the technologies required to implement fly-by-light. FLASH will address the system cable plant including interfaces to sensors, controls and the engine, the flight control computer requirements and its interfaces to sensors, actuators and cross channel data links. Control actuator requirements will also be considered and will include all current technology and advanced actuator technology such as power-by-wire.

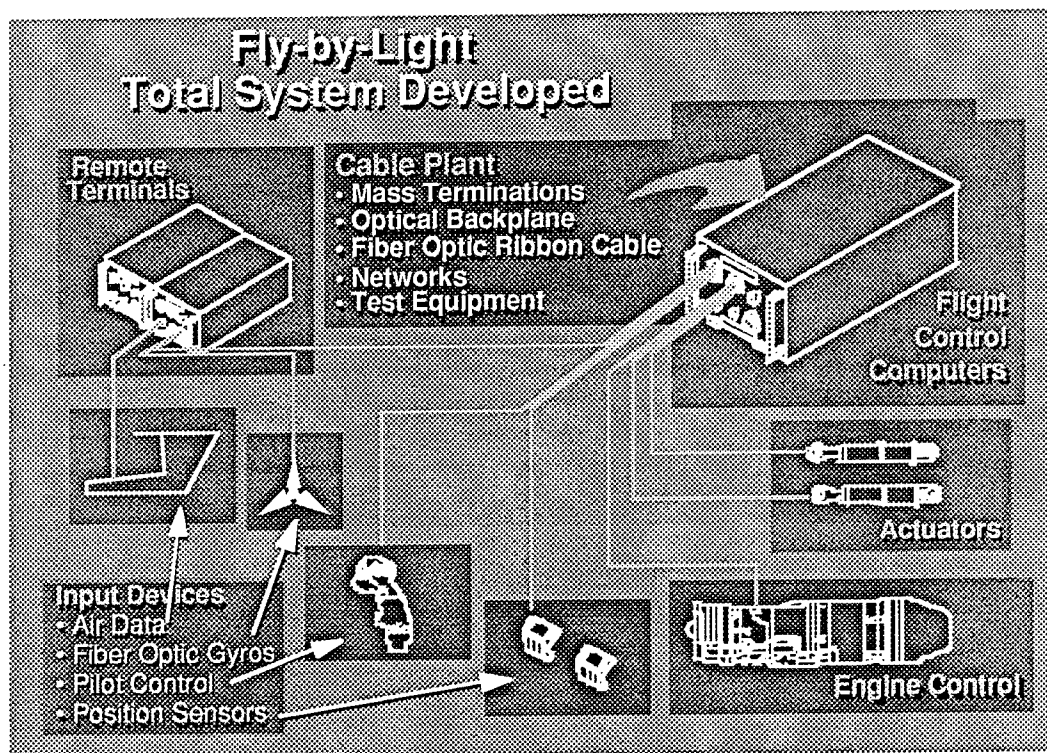


Figure 3-1 FLASH Approach is to Develop the Total FBL System

Technical Approach - The FLASH program organizes the FBL/PBW development efforts into tasks that supply the technical needs not addressed by other programs. These tasks and the technology needs of Figure 1-1 addressed are shown in Table 3-1.

Table 3-1 The FLASH Program Addresses the Needs of Future Aircraft

Technology Needs vs. Tasks Proposed	(1) Operate in High Electromagnetic Environment	(2) Improve Cost Effectiveness	(3) Increase Aircraft Performance and Fuel Efficiency	(4) Improve Systems Performance Requirements	(5) Reduce System Certification Costs
Task 1 - Cable Plant	X	X	X	X	X
Task 2 - Flight Control	X	X	X	X	X
Task 3 - Actuators	X	X			

Task 1: Cable Plant Approach - The FLASH program is developing and demonstrating a cost effective and reliable fiber optic cable plant and backplane that meets future aircraft requirements. There are few (if any) connector, splice, cable, harness, backplane and system test suppliers qualified and certified. The program is developing teammates' capabilities to perform this work as part of the program. This will, in turn, provide viable industry sources of critical FBL/PBW technologies by allowing them to build and test qualified cable plant, backplane and optical connectors.

Task 2: Flight Control Approach - The FLASH program is developing and demonstrating FBL control building blocks including computers, fiber optic sensors and interfaces, fiber optic actuator loops, and fiber optic input commands and integrating them into demonstration systems. FLASH is using neural networks to identify system parameters that can be used to optimize the control laws using modern control theory methods. The program will perform laboratory system demonstrations and will support the planning of a future NASA flight test of selected systems. The approach is to develop versions that can easily be packaged into flight worthy systems. The result will be manufacturers that are qualified suppliers to the global market.

Task 3: Actuators Approach - The FLASH program is developing and demonstrating four different types of actuators which exploit fiber optic sensor and control technologies. These actuators will provide significant improvements in reliability and maintainability over current systems. They consist of: two different 50 hp electric actuators, a thin wing 8000 psi hydraulic pressure actuator and a "smart" actuator. These actuators will be models only requiring proper packaging to be flight worthy and usable for planned future flight test. The result will be several actuator suppliers capable of providing actuators qualified for FBL applications.

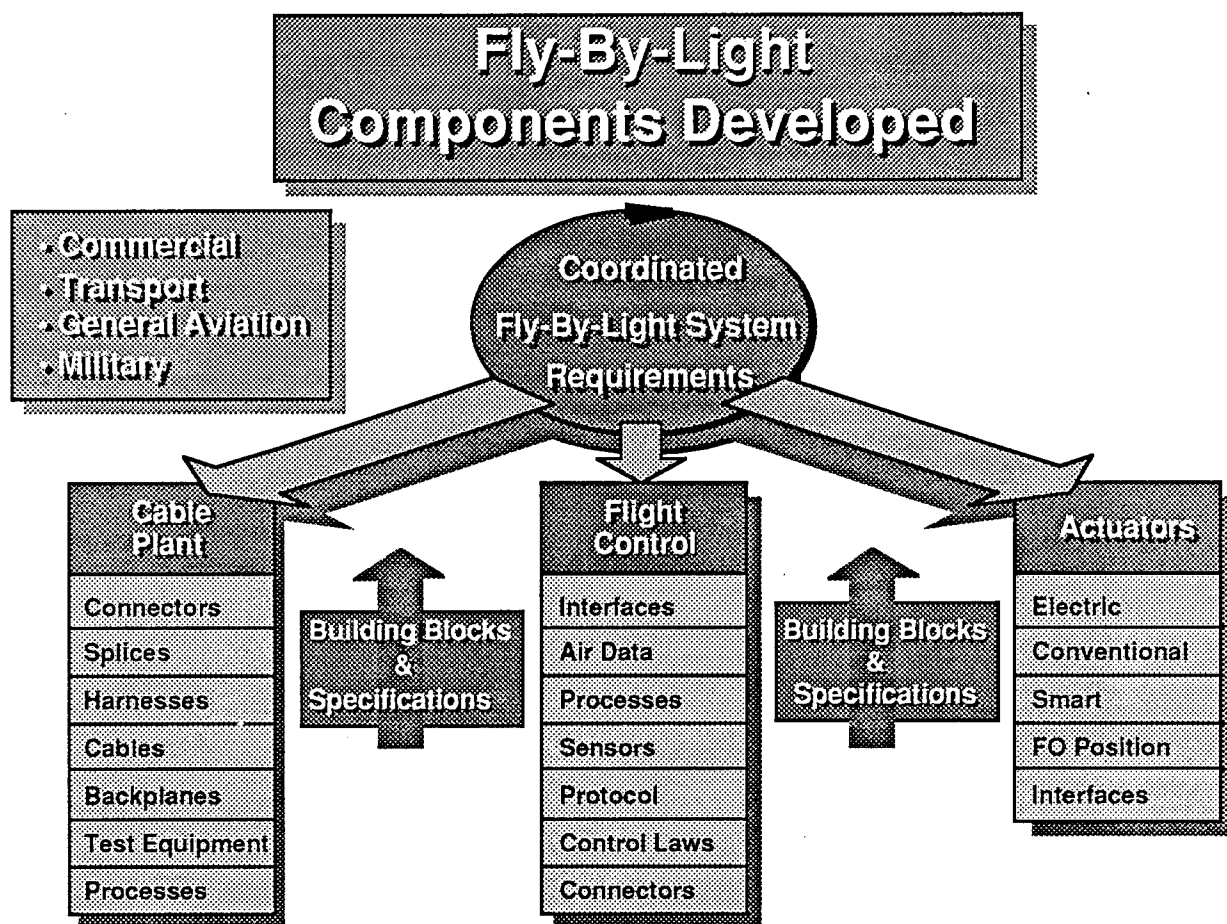


Figure 3-2 The FLASH Technical Approach Develops Requirements and Building Blocks

The overall program approach as shown in Figure 3-2 is to have MDA components, the industry advisory board and technical advisors define top level requirements for military fighters, helicopters and transport aircraft, as well as commercial transport aircraft, and helicopters. As shown in Figure 3-2, requirements are then flowed-up by the teammates in order that they may

develop their individual FBL technologies that meet the sub category needs not being filled by other programs of the overall FBL requirements. This process has resulted in a set of capabilities and specifications which satisfy user needs and providers capabilities. The next step is now developing the building blocks that will be needed by industry to implement FBL. As illustrated in Figure 3-3, the program has been developing the individual pieces with teammates that can provide the needed technology. FLASH is working with traditional flight control, actuator and sensor teammates, as well as fiber optic and photonic component suppliers in order that they establish user/provider relationships to develop FBL building blocks, this is reflected in the composition of the current ARPA-TRP team. Various architectures and buses have been evaluated but have avoided a fixed point design because each user will want to establish the architecture, topology and bus protocol that best meets his application. By providing the necessary building blocks, the user can then select those that meet his current requirement and the suppliers can provide him with the qualified building blocks that they manufacture.

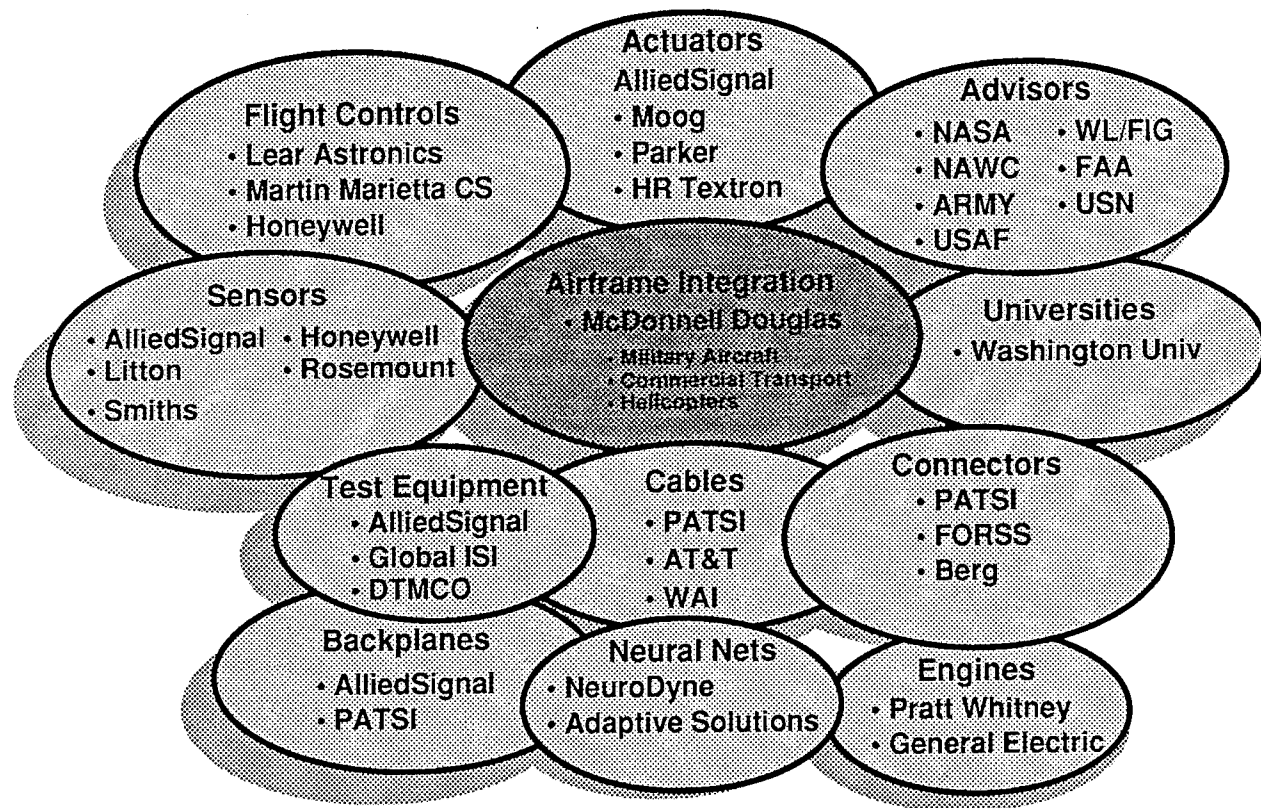
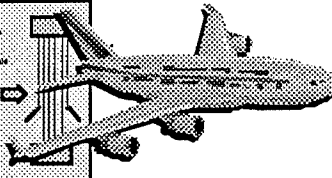
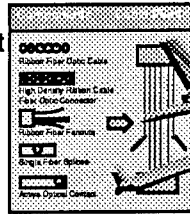


Figure 3-3 The FLASH Team Develops Major and Small FBL Suppliers

4. FLASH Program Products - Figure 4-1 shows the FLASH products that will result from the activities in Task 1. They are subdivided by the three Task 1 sub tasks. Task 1A will have a commercial cable plant for application to commercial aircraft, including ribbon fiber optic cable, connectors, splices and processes. Task 1B will develop a military cable plant including a tester, harnesses, connectors, backplanes, methods and processes for application to fighter aircraft. Task 1C will apply the Task 2B cable plant to military helicopters. During the final milestone of the program, demonstrations will show that these products meet the FLASH derived requirements and are ready for aircraft applications.

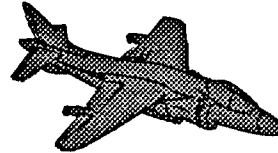
- **Task 1A - Commercial Cable Plant**

- Ribbon Fiber Optic Cable
- High Density Ribbon Cable
- Fiber Optic Connector
- Ribbon Fiber Fanouts
- Single Fiber Splices
- Active Optical Contact



- **Task 1B - Military Fixed Wing Cable Plant**

- Aircraft Cable Plant Tester
- Flight Control Optical Cable Harness
- High Density Optical Connector
- High Density Optical Module Connector
- Optical Backplanes
- High Density Optical Backplane Connector
- Methods and Processes



- **Task 1C - Military Rotary Wing Cable Plant**

- Optical Cable Plant Interface
 - » Flight Control Computers
 - » Cockpit Information Manager

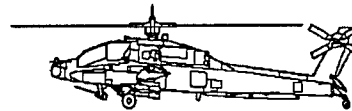
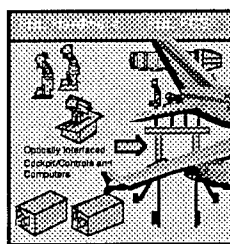


Figure 4-1 Task 1 FLASH Products

Figure 4-2 shows the products that will be developed in Task 2. They are also subdivided into three sub tasks as part of Task 2. Task 2A will develop and demonstrate an optical aileron trim mechanism that will replace the current mechanical cable and pulley system used in commercial aircraft. New FBL Primary Flight Control Computers with optical interfaces to actuators, flight deck and an Active Optical Sidestick Controller all for application to commercial aircraft. Task 2B will result in military FBL flight computers with optical cross channel data links, optical interfaces, fiber optic inertial sensors, air data sensors with optical interfaces and the capability of having centralized or distributed flight control architectures. Task 2C will develop a flight control computer with an optical interface, a neural network board with flight control diagnostic capabilities as well as flight control parameter identification capability.

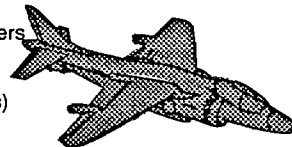


Task 2A

- Fly-By-Light Optical Aileron Trim (FLOAT) System
- New Flight Control Computers for Transport Aircraft
 - Optical Interfaces to Flight Deck
 - Optical Interfaces to Smart Actuator
- Active Sidestick Controller for Transport Aircraft

Task 2B

- Fly-by-Light Versatile Flight Control Computers
 - Optical CCDL
 - Optical Data Interfaces
- FOG IMU With Optical Interfaces (2 Designs)
- Air Data Package With Optical Interfaces
- Centralized and Distributed Architectures



Task 2C

- Flight Worthy Modules for ACTIVE Flight Control Computer (12 Modules + 1 Test)
 - High Capacity 32-Bit Processors
- Neural Network Processor Module (1)
 - Neural Network Chip
 - Digital Signal Processor
 - Optical Interfaces
- Fault Diagnostic Software
- Software for Future Damage Adaptive and Low Cost Control Development

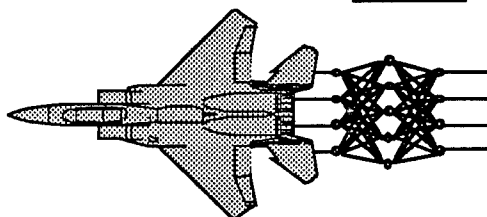


Figure 4-2 Task 2 FLASH Products

Figure 4-3 shows the products that will result from the activities in Task 3. The task will develop two electrohydrostatic actuators in the 50 hp class using optical interfaces and optical position

sensors for applications to fighter aircraft such as the F-15 or a large commercial aircraft stabilator. In addition the task will develop a 8000 LB hydraulic pressure thin wing actuator using an optically driven servo valve and optical position feedback. This task is also developing a so called "smart actuator" which operates as an independent remote unit via a low cost optical bus and closes the control loop of the actuator with self contained electronics.

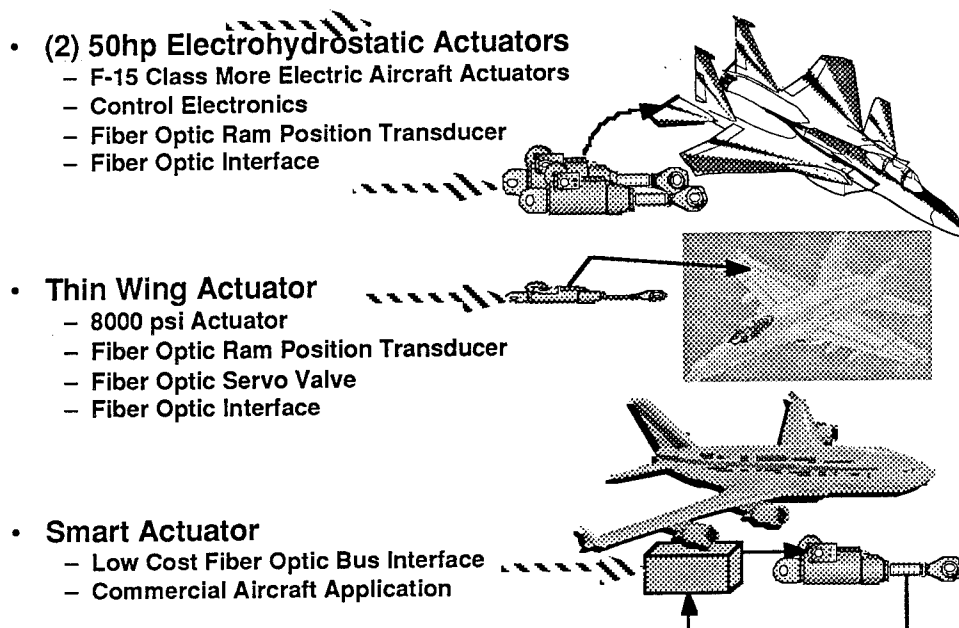


Figure 4-3 FLASH Task 3 Products

5. Remaining Hurdles to Clear in FBL- In order to develop FBL into the system of choice for all types of aircraft flight control, there is a need to prove the technology by flight test of complete systems in each of the target applications. For example a successful fighter, military transport, civilian passenger, military and civilian helicopters demonstrations must be performed. Cost effective optical interfaces must be developed with reliable suppliers for flight-critical and non flight-critical FBL applications. One of the critical needs encountered in the FLASH program was the availability of the 1773A bus hybrids and protocol chips needed as the flight-critical control bus. A standard set of specifications for each application must be developed and agreed upon for civilian aircraft, Federal Aviation Administration (FAA) certification procedures must be developed and approved. Approved processes and maintenance procedures with manuals need developing, as well as training courses for support and maintenance personnel. Finally, the cost/benefit ratio of FBL vs. current technology must be such that it is cost effective to use FBL. This is not only true of the commercial but also true of the military market now as affordability is as important there as in the commercial market place. The user must feel as comfortable with fiber optics and photonics in aircraft control systems as he does with wire and the telecommunications industry does with optical technology.

A viable supplier base is also necessary even though the FLASH program and other FBL programs are beginning to establish some, a larger base is still in need of development. As FBL begins to establish itself, the market place will create this base on a demand basis. As the technology spills over into other industries such as the automobile industry, the base will accelerate due to demand and financial rewards. Once the large scale applications evolve, optical technology will be considered as common as home computers, cellular telephones and cable television, and the cost of components to aerospace applications will be reduced.

6. Other Potential Areas of Technology Applications- As shown in Figure 6-1 all the FLASH team's products are for the global market. AlliedSignal, Moog, Parker and HR Textron provide

actuators to the aircraft market, as well as the tractor and heavy equipment industry. PATSI, FORSS, AlliedSignal, and Berg provide products to the commercial computer and telecommunications industry, as well as the commercial aircraft market. Honeywell, Lear Astronics, Martin Marietta Control Systems, Litton, Rosemount Aerospace and Smiths Industries provide flight control avionics and sensor products to both the commercial and military markets. The FBL products will create high value, advanced technology U.S. jobs by allowing all members of the FLASH team to develop high technology fiber optic products that have dual use applications transcending beyond the aerospace industry into the automobile, telecommunications and computer industry. An example of this dual-use technology is the application of the FBL architecture using distributed components to the automobile industry. In this application the automobile would use fiber optic links to connect the engine compartment with the dashboard, the doors and the rear portion of the automobile using a single fiber bus to multiplex all signals and controls required. By leveraging technology in the extremely high volume auto and telecommunications industry, which use millions of components, the cost of FBL can be significantly reduced and impact military products affordability. One benefit of the FLASH business plan is that it allows the small businesses on the team to interact and work with financially stronger user industries with funding and technical support that they would normally not be able to afford. In the changing global market, U.S. industry needs the benefits of new high technology to compete against industries that are commonly subsidized by their governments or are based on low technology and wages.

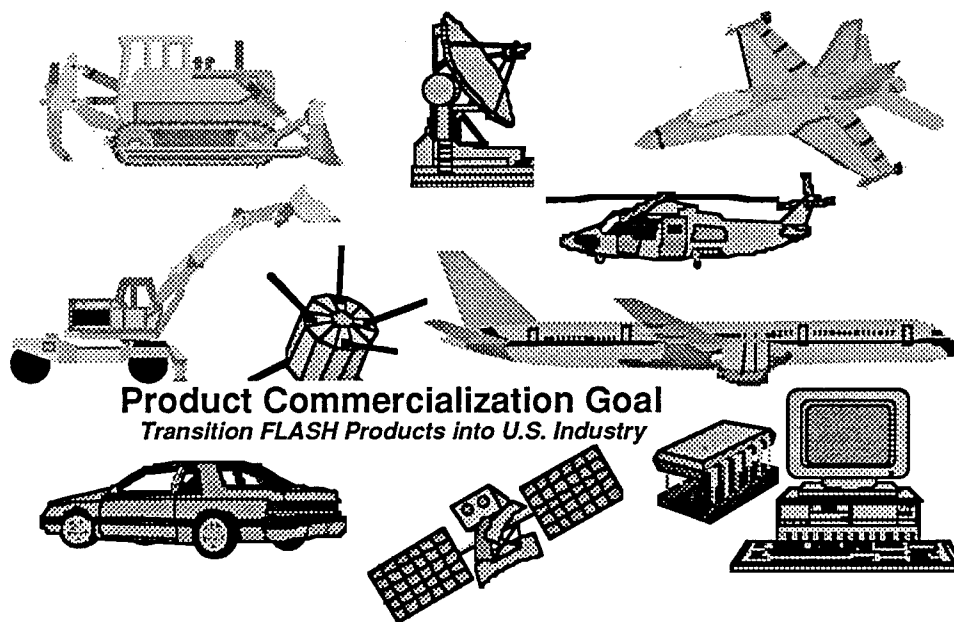
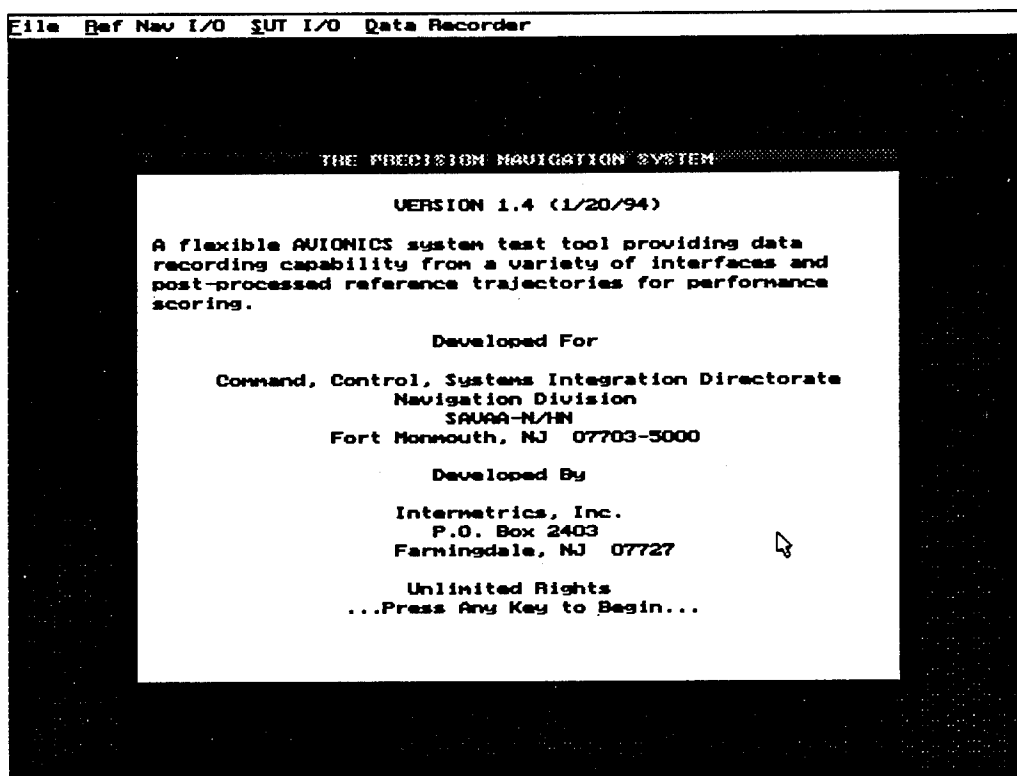


Figure 6-1 Team Members Will Supply Other Markets With FLASH Products

7. Current Status of the FLASH Program- The FLASH program received go-ahead from ARPA on June 15, 1994, as a 24 month technology development program. It has completed its third milestone, the preliminary design of the FBL system, and is currently developing the final design in order to complete its critical design after which fabrication of components and system integration will follow. One of the pacing items of the program has been the availability of components for the 1773A fiber optic bus as it is still in development. This bus was selected as the VMS main interface bus as it has the required flight critical applications characteristics: controlled command/response, a 20 MHz bandwidth, data integrity monitoring, necessary reliability and low cost, as well as very complete documentation developed by the Society of Automotive Engineers (SAE). Delivery of components is expected to be received in sufficient time for subsystem and system integration. The program is developing several FBL products that will be demonstrated by the end of the last milestone.

THIS PAGE LEFT BLANK INTENTIONALLY

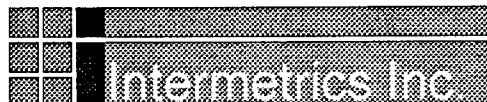
The Precision Navigation System



Paul M. Olson, C²SID

Mark R. Berry, Intermetrics Inc.

US Army CECOM, RD&E Center
Command/Control and Systems Integration Directorate (C²SID)
ATTN: AMSEL-RD-C2-TS, Building 2525
Fort Monmouth, NJ 07703-5603



Intermetrics Inc.
1720 State Highway 34
Wall Township, NJ 07719

Approved for Public Release; distribution is unlimited

THIS PAGE LEFT BLANK INTENTIONALLY

The Precision Navigation System

Paul Olson
CECOM Command, Control and Systems Integration Directorate (C²SID)
System Technology Division
Fort Monmouth, NJ

Mark Berry
Precision Navigation System Project Manager
Intermetrics, Inc.
P.O. Box 2403
Farmingdale, NJ 07727

Abstract

The Precision Navigation System (PNS) was developed to provide a re-useable, flexible, and easily reconfigurable avionics Research, Development, Test and Evaluation (RDT&E) tool. Its purpose is to efficiently facilitate the instrumentation requirements for a System Under Test (SUT) and provide the means to evaluate and analyze the capabilities of the SUT. This paper will describe the components that comprise the PNS and give examples of how this valuable avionics tool has already been utilized as well as some future plans for the system.

PNS is a useful tool by itself these components combine in an integrated system to perform the recurring tasks involved with RDT&E efforts.

The PNS is an IBM-Compatible Personal Computer (PC) based package of tools that allows for the quick-reaction instrumentation of a wide variety of avionics RDT&E efforts. The PNS possesses the Data Acquisition, Data Reduction, and Data Analysis tools in a generic platform that precludes the need to re-invent the instrumentation, the data recording, the data reduction, and data analysis tools for each new effort. Additional features of the PNS are the capability to perform as a MIL-STD-1553 Multiplex Data Bus Controller and the PNS possesses the capability to generate the Truth Reference Data for Navigation testing.

PNS Description

Nearly all RDT&E tasks have a similar set of requirements:

1. Collect Data
2. Reduce the Collected Data
3. Analyze, Display, and Report the Data

Figure 1 illustrates the relationship of the various components of the Precision Navigation System. While each individual component of the

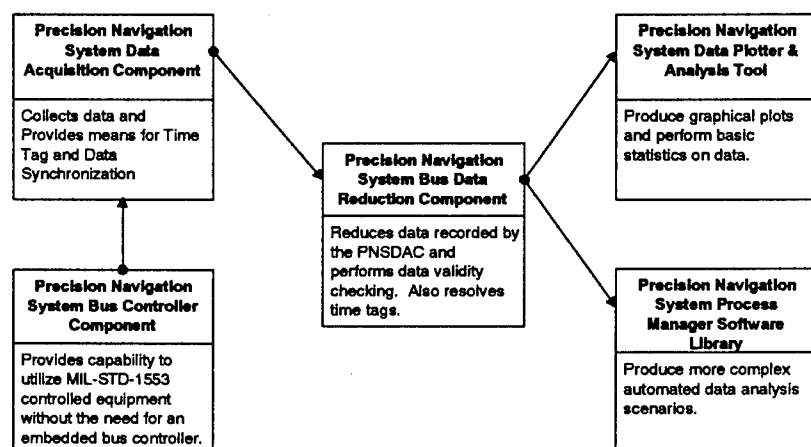


Figure 1 - Relationship of the PNS Family Components

a flexible data collection tool capable of recording data from multiple sources and a variety of data interface protocols. Figure 2 illustrates the Man Machine Interface (MMI) utilized by the PNSDAC to facilitate the set up for a data recording session. The PNSDAC will accommodate simultaneous data recording from any combination of the following interfaces:

- MIL-STD-1553 bus
- multiple channels of ARINC 429
- up to two channels of RS-422
- discrete lines
- architecture of the PNSDAC is designed to easily support the addition of new interfaces.

Data Acquisition Component

The PNS Data Acquisition Component (PNSDAC) is

Figure 2 - The PNSDAC Utilizes a Familiar Graphical User Interface

interfaces.

The PNSDAC is responsible for the recording of data from both the SUT equipment as well as the Truth Reference Navigation Data. Figure 3 illustrates a basic PNSDAC instrumentation configuration.

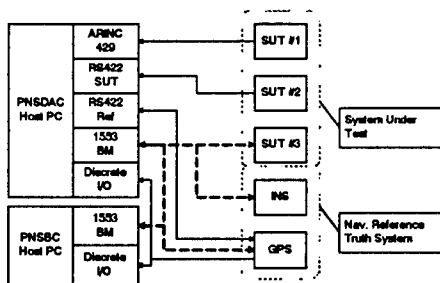


Figure 3 - PNSDAC Typical Application

The PNSDAC Host Computer

The PNSDAC Host computer is an IBM compatible PC with standard ISA bus. The system was designed to be hosted by an Intel based 286 or higher microprocessor and runs under DOS. The use of common computer hardware and commercially available software development products have increased the flexibility of the system and enhanced availability of replacement parts. Costs benefits are also realized by avoidance of exotic or unique components in the PNS.

The intended operation of the PNSDAC is to connect into data lines as an 'eavesdropper' or 'listen-only' device. In this way the instrumentation and data recording functions are transparent to the operation of the SUT equipment and likewise the data acquisition function does not impede the operation of the PNS Bus Controller (PNSBC) in situations where the reference equipment is in place. The control variables (e.g.; baud rate settings, etc.) for some of the interfaces that are available to the user while running the PNSDAC are illustrated in Figure 2.

PNSDAC PC-AT Interface Boards

The interfaces that are available for use by the PNSDAC may be added to a test set up or excluded at the user's discretion. The test set up can vary and no particular interface is required to be present for the PNSDAC software to run. The system will operate with a full complement of interface cards or

any subset of the full complement. This is an important feature because it permits flexibility in the selection of the host computer for the PNSDAC.

For example, when space limitations on the test aircraft call for a very compact data acquisition system the PNSDAC can be hosted in a small 'Lunch-Box' style PC and only the interfaces required for that particular test are present. When conditions are different and the test objectives call for a large number of interfaces and a wide variety of interface types the system can be hosted in a rack-mount industrialized computer chassis. The only requirement placed upon the host PC by the PNSDAC software is that it be truly IBM PC compatible¹ and provide room in the chassis of the Host computer for the insertion of the desired interface cards into the PC-ISA bus. A brief description of the currently supported interface cards is presented in the following sections.

MIL-STD-1553 Interface

The PNSDAC utilizes a PC-AT compatible MIL-STD-1553B Bus interface card for the capture of 1553 data. The interface card used for collection of 1553 data possesses an on-board processor and on-board dual-ported random access memory (RAM). This design permits for the buffering of data on the card to alleviate the work load on the PC-AT host computer CPU. The system can be set to record all bus Remote Terminals (RT) or any subset of RT's. The system will monitor both the A and B sides of the bus or the operator can set the system to record only the data on one side of the bus. Additionally, the PNSDAC incorporates the ability to embed time tag information that will enable the PNS Data Reduction Component to resolve the time tag and-synchronize the time for each and every 1553 message that contains a 1553 bus time tag.

ARINC429 Interface

The PNSDAC possesses an interface card for the collection of up to two channels (provisions exist to expand this to up to 8 channels) of ARINC429 compatible data. The interface card used for this data acquisition is similar to that used for 1553 data collection in that it also utilizes an on-board

¹ Non-standard vendor-proprietary BIOS configurations can cause difficulties with the PNSDAC interface boards that map into the PC-AT memory.

processor and on-board RAM to buffer incoming data. In addition, the ARINC429 board also possesses its own on-board timer circuitry. The card is programmed to time-tag the time of reception of each and every valid 32-bit ARINC429 data word that is transmitted by the system that is being monitored. This time-tag value is recorded along with the data bits in the ARINC429 data word in a manner to permit subsequent time-synchronization of the ARINC data with data collected through other interfaces in the PNSDAC. This capability has proven invaluable when analyzing ARINC data that does not contain time embedded in the data stream itself.

The ARINC429 interface used in the PNS provides the user with the option to select the desired baud rate (usually either 12.5Kbs or 100Kbs) or the user may opt to manually set the baud rate to other non-standard values ranging from 1.25Kbs up to 200Kbs. The parity is also selectable.

The ARINC429 interface also possesses two transmit channels that are currently not used by the PNSDAC but could be utilized for applications that require the PNSDAC instrumentation to actively communicate (rather than the usual 'listen-only' mode) with the SUT or the Reference Navigation suite.

RS232/422/485 Interface

The PNSDAC utilizes a serial coprocessor PC interface board to collect data over RS232/422/485 serial data buses. The system has the capacity for two such interfaces working simultaneously (provisions are in place to expand this number). The serial coprocessor board provides an on-board microprocessor with its own on-board RAM. This RAM is accessed by the host PC through a 'sliding-window' technique. The serial coprocessor board interface provides the user with the options of setting the baud rate (up to 76.8Kbs), the parity, stop bits, and data bits. The board provides separate receive (used in data collection) and transmit channels that have their respective serial communications parameters set independent of each other. This is important for use with common ICD-GPS-150 Instrumentation Port configurations that have different transmit (76.8Kbs) and receive (19.2Kbs) baud rates.

In addition to its data recording capabilities, the coprocessor board used by the PNSDAC has been programmed to provide some special

communications capabilities for use with common GPS Instrumentation Ports. The user is provided the capability to view the contents of the Time Mark Data Block (message ID 3) from the Instrumentation Port in real time. This is useful to verify that the SUT or the Reference Navigation GPS receiver is operating as expected prior to beginning a test. There is a method to view the current list of messages that the Instrumentation Port is transmitting and there is a utility to Connect and Disconnect Instrumentation Port messages. This feature has proven to be extremely useful when working with the Rockwell Collins line of GPS receivers.

Discrete I/O and Timing Interface

The Discrete I/O board in the PNSDAC performs two primary tasks, generation of the local time for the data recorder and input/output of discrete data. The Discrete I/O board possesses an on-board crystal oscillator and timer chip that performs as the local time source. This on-board clock has a resolution of 1 microsecond, a roll-over period of over 3200 days, and once initialized runs completely independent of the host PC. This interface board also provides the ability to synchronize the local time source (the crystal-based clock) with GPS time through the use of an interrupt request.

Time synchronization with GPS is useful to control the drift of the crystal base clock and is accomplished in the following manner.

1. At the beginning of a data recording session the PNS waits for the receipt of up to 7 pulses from the 1PPS port of the connected GPS Receiver's Instrumentation Port.
2. As each pulse is received from the GPS IP 1PPS source the PNS local time is latched on the Discrete I/O board. This time latch function is performed in response to the 1PPS triggering an interrupt in the PNS CPU via the PC ISA IRQ7 (or any other available IRQ line) hardware interrupt request line.
3. Meanwhile, the Time Mark Data Block (message ID 3) corresponding to the 1PPS pulse is collected from the GPS IP serial port via the PNSDAC serial coprocessor interface card. The time latency between the receipt of the 1PPS pulse and the latch of the clock on the Discrete I/O card is insignificant relative to the 1

microsecond resolution of the clock on the Discrete I/O board.

4. For each of the (up to) 7 pulses and corresponding Time Mark Data Blocks there is also a PNS local time to synchronize with. This establishes the initial offset between local time and PNS (GPS-based) time.
5. During the recording session the drift of the local PNS crystal oscillator is accounted for by the repeated once per second synchronization of the 1PPS signal. As each 1PPS pulse is received it results in an interrupt in the PNS host CPU that latches the local PNS time and injects this time into the recorded data stream. The result is a one-second 'time-hack' appearing throughout the recorded data stream.

If desired the timing functions performed by the Discrete I/O board can be disabled and substituted by an IRIG compatible time code reader interface board. This is useful in cases where the PNSDAC is employed on test ranges that normally work with IRIG time code. Most common IRIG time formats are supported.

Recording Media

The PNSDAC can store the incoming data to a variety of storage media devices. Any device that is accessible as a DOS addressable media may be used. In addition to this the PNSDAC has the added features of being able to collect data to a digital 9-Track Tape recorder as well as an 8mm Cartridge Tape System. The 8mm tape option is especially useful for configurations that generate a large amount of test data and high data throughput rates. The 8mm Cartridge Tape system utilized by the PNSDAC interfaces to the PC-AT ISA bus via a SCSI interface board inserted into the ISA bus. The standard 8mm tape format provides data throughput potential exceeding 200Kb/sec (practical use has demonstrated over 80 Kb/sec data rates) and has capacity of up to 2.2 Gbytes on a single removable cartridge tape. The tape device has proven to be very reliable in rough operating conditions¹ and like all components of the PNSDAC is a commercial off-the-shelf item.

¹ This 8mm tape device was used on the sled test facility at Holloman Air Force base and subjected to temperature, humidity, vibration and shock conditions of a wheeled sled test vehicle. During a month-long test effort there were no operational failures of the device.

In less demanding configurations the recorded data may be stored to a floppy diskette or a hard disk drive. One particularly useful configuration is mounting a hard disk drive in a removable slide-bay. With this configuration the test data is easily removed from the instrumentation set up at the conclusion of the data collection effort. This particular method also facilitates the requirements of handling any secure data that may be recorded during a mission. Here again the ability of utilizing common COTS equipment ensures equipment availability and minimizes cost associated with the instrumentation set up.

MIL-STD-1553 Bus Controller Component

Avionics equipment that is MIL-STD-1553B controlled presents a challenge when performing RDT&E type experiments. Equipment that is controlled via a multiplex bus require a bus controller to make the bus operate. Traditionally the development of a bus controller for instrumentation purposes has been difficult and many times involves expensive and unique equipment (i.e.; embedded 1553 bus controllers). The PNS Bus Controller (PNSBC) was added to the PNS family of RDT&E tools to provide this capability.

The PNSBC is a COTS based 1553 bus controller that will operate stand-alone or in conjunction with the PNSDAC. The PNSBC provides a control capability for common navigation avionics components and is designed to accommodate new bus-controlled avionics equipment with a minimal amount of effort. The system is designed to support the addition of new avionics equipment to test avionics bus through the use of a text-based 'ICD-definition' file. This file contains the necessary information to allow the PNSBC hardware to communicate to the new RT(s) on the bus. The PNSBC is commonly used to support the reference navigation suite on board the host vehicle but may also be utilized for controlling the SUT if a bus controller does not currently exist on the host vehicle.

The PNSBC shares the same hardware as the PNSDAC and utilizes the same graphical user interface as the other tools in the PNS family.

Data Reduction Component

Following the collection of test data the engineer is faced with the problem of reducing the data into the desired components of interest and organizing the data in a manner that facilitates the subsequent data analysis. The PNS Data Reduction Component (PNSDRC) performs this task. Figure 4 illustrates the basic function of the PNSDRC.

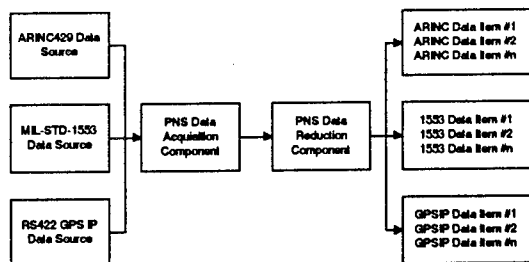


Figure 4 - PNS Data Reduction Process

The data that is recorded by the PNSDAC is contained within a single data file that is actually a composite of all the raw data from the various interfaces as well as data that is created by the PNSDAC during the recording process. Data created by the PNSDAC includes time-tags, time-synchronization messages, checksums, status messages, etc. It is the job of the PNS Data Reduction Component to separate the various components in the aggregate data file and organize them into output data files that can be used by the PNS Data Analysis Tools or by other software data analysis methods.

PNSDRC Validity Checking

In addition to the data parsing and organization tasks, the PNSDRC also performs on-the-fly data integrity checking (verifies embedded checksums) and will monitor the validity bits (when available) in certain types of data and automatically discard data that has bad-validity data bits set. The PNSDRC also maintains statistics on the frequency of each individual data message and performs on-the-fly checking to alert the user if there are anomalies (e.g.; time going backwards, apparent gaps in the data stream, etc.) encountered with respect to the time-tagging of data.

PNSDRC Time Synchronization

Time synchronization of data collected from independent data sources, especially in cases where the incoming data stream does not contain time as one of the data parameters, has always been a difficult problem to solve. The PNSDRC utilizes data that is created by the PNSDAC during the recording process to time-tag all data collected by the system to a common time reference. This time reference is usually GPS-time which provides for time synchronization over a wide area. If GPS time is not available or not desired the common time source may be IRIG based, or simply based upon the PNSDAC local time source. In any case it is the PNSDRC that resolves the time synchronization between all data sources and affixes a time tag to each output data item.

PNSDRC Flexibility

The PNSDRC does not require that the INPUT raw data files be recorded from the PNSDAC. Additionally, it is capable of creating OUTPUT files in a variety of formats that are not dependent on the PNS Data Analysis tools. This software component will currently handle a variety of input data formats including the common "Buffer Box" format (in addition the PNSDAC data file format). The software will also create the popular "Buffer Box" format data files for output data. This flexibility removes any interdependence between the individual components of the PNS Family. Each component may be used with outside data recorders as well as outside data analysis tools (e.g.; a spreadsheet could be used to analyze data output that has been parsed, time-tagged, and validated by the PNSDRC). This feature of the PNS has permitted the cooperative teaming with other organizations (who do not use the PNS) in the collection and the analysis of test data.

Data Analysis Component

After data reduction the final step is the interpretation and analysis of the data that was recorded. The PNS provides a set of tools that enables the analyst to view the data in many different ways and combinations. The following sections will describe the PNS Family of tools available to the analyst for creating and viewing graphical and statistical results. The PNS Navigation Reference capabilities will also be discussed.

PNS Navigation Capabilities

The generation of Truth Navigation Reference data is extremely useful when conducting navigation avionics RDT&E efforts. In the past this sort of testing required that the host aircraft (or vehicle) visit an instrumented navigation range that would generate the navigation reference data from radar, laser, or other techniques. This method restricts the operation of the navigation range to a single location forcing the participants to come to the range as opposed to the range going to the participant. Having a native capability to create the truth reference alleviates this condition. It provides reference navigation data against which the SUT can be evaluated. The range of operation for this navigation reference is not constrained to ground based facilities.

The system performs as an in-house RDT&E tool and is flexible in that the user may configure it to provide the desired level of navigation reference accuracy. In its simplest form the PNS will permit the comparison of the SUT navigation system performance to the Reference navigation system performance. For example, it is possible to observe the relative performance obtainable from a new GPS receiver with respect to another GPS receiver that serves as the control variable. This is a useful capability when considering things such as second source procurements.

PNS Navigation Accuracy

The ultimate accuracy of the Navigation Reference Data generated by the PNS depends upon the configuration of the PNS for the particular task. A high level of accuracy is attained by the use of Differential GPS. In this configuration the PNS will provide navigation reference data with the following accuracy:

Current Data Supports Accuracy Claims of:

POSITION: 8 meters / axis, rms

VELOCITY: .01 meters / sec, rms

These accuracy numbers were obtained during testing at Holloman Air Force Base Sled Test Facility. The accuracy of the PNS was determined by comparison of the PNS Truth Reference to the CIGTF calculated Truth Reference. During the time of this test the GPS receivers were operated in the Authorized Mode (Precise Positioning Service) and

under modest dynamics. Further analysis has indicated that the PNS inertially aided differential GPS navigation accuracy approaches 2 meters per axis (rms) position accuracy and .01 meters per second velocity accuracy.

The Reference Navigation suite on the host vehicle is typically comprised of a GPS receiver (Collins RCVR 3A and MAGR has been used in the past, although many types of receivers will fill this role) and an Inertial Navigation Unit (a Litton LN93 is commonly used, but here also there are many other types of INUs that will fill this role as well).

PNS Navigation Solution Post-Processing Software

The Reference Navigation solution that is accessible to the user of the PNS is calculated in a post-processing environment. The method used for this post processing consists of a variety of possible forms. The following sections will discuss the simplest case (the PNS Plotter tool) and a more complex case (the PNS Process Manager) using the Reference Navigation data generated by the PNS.

The PNS Plotter

The PNS Data Analysis Component provides a rich set of tools that can be used to generate data plots, perform common statistical calculations, and perform error analysis functions.

The PNS plotting tools are designed to accommodate data from a variety of sources. Usually the data has been recorded via the PNSDAC but this is not a requirement. The PNS Plotter tools will work with virtually any fixed length record data files. The user simply defines the data record format using a text editor and creates a 'message definition file' that the PNS plotter software uses to interpret the data. This permits the analysis of data that has been gathered by means other than the PNSDAC.

The PNS Plotter is a versatile data plotting tool that provides for on-screen analysis of data and also generates several output formats to facilitate report generation. All the data plots that follow in this paper were generated as Windows MetaFile format graphics files and imported into this document. Other formats include HPGL and PostScript.

The PNS Plotter provides the basic foundation for more complex data analysis tasks which are automated using the PNS Process Manager.

The PNS Process Manager

The PNS Data Analysis Component also provides a robust navigation process that will permit the generation of a navigation solution from a wide variety of navigation sensor inputs. In this manner the analyst can 'mix-and-match' navigation sensors to determine the optimal combination of equipment for a desired result. The navigation process utilizes a Kalman filter that will accept GPS, inertial, and barometric altimeter inputs to generate the navigation truth reference. Provisions are in place for the application of Differential GPS supplemented by inertial aiding the generation of truth reference navigation data.

Typical post process software will accept data from one or more sources, and combine/manipulate the data until it is in a form which suits the needs of the analysis at hand. If one were to generalize this sequence, he would can define a generic process that performs 3 basic functions:

1. It accepts data from some source
2. It does something to that data
3. It generates results based on the data

Using C++ Object Oriented Programming (OOP) techniques this generic definition of a process has been used to develop a diverse set of specific processes which analyze many different forms of data (from the PNSDAC and other sources). Further enhancements have been added to the generic process definition above to allow these processes to interact with an operating system (OS), a user, and other processes through a device referred to as the PNS Process Manager. In it's purest form the Process Manager's job is as follows:

- maintain and control the system clock which governs the execution of each process,
- provide data to all of the processes in the system,
- allow each process to execute it's analysis of current data,
- allow the user to setup/control a process,

- provide a mechanism for the process to output it's results

The system clock used by the Process Manager is controlled by the user, and can be tied to a time tag field in an incoming message, or a free running clock with a fixed delta between increments, or even a pseudo-clock based on the record number from an input file. In general the system clock is tied to a particular time field (usually GPS Time) in one of the incoming messages. Once the system clock has been defined, the Process Manager is forced to implement a Time Align Strategy for each of the incoming messages so that each of the data fields from one message can be compared to data from another message without the process having to worry about the time alignment of the data.

Time Alignment of Data from Different Sources

Assume that for the simplest case it is desired to compare the position data from one sensor in the SUT to the position data from the Reference Navigation sensor (for example the Collins MAGR). The following formula would be applied to generate the *difference* between the position of the two navigation sensors:

$$Pos_{SUT} - Pos_{Ref} = Pos_{Difference}$$

The problem with the above equation is that it fails to account for the fact the position data calculated by the two navigation sensors is computed completely independent of each other. In order for the position difference to have any meaning the position information must be referenced to the same instant in time.

$$Pos_{SUT}(t_1) - Pos_{Ref}(t_1) = Pos_{Difference}(t_1)$$

Where: t_1 = time of validity for the difference

Since the two navigation sensors in this example act independently of one another it is necessary to interpolate between data points for at least one of the two sensors in order to make the above calculation valid. Figure 5 provides a simple illustration of this time-alignment procedure.

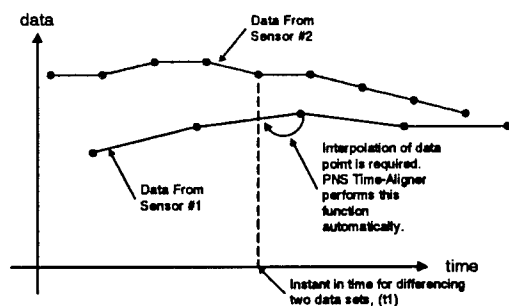


Figure 5 - Time Aligning Data

The example illustrated here is simplified in that it only addresses the case of two values from only two sensors. The Time Align process employed in the PNS Data Analysis Tools will perform the same time-alignment function on data from any number of source data files. This feature makes it extremely useful when there are many data inputs that must be time aligned and processed simultaneously.

Furthermore, it is often necessary to convert units on the data (especially when the sensors being compared are fundamentally different technologies) to a common engineering unit. The PNS Post Processing software provides the units translation and conversion as well as the time correlation functions necessary to enable the calculation shown above. This software is contained in the PNS Data Plotter & Analysis Tool (refer to Figure 1) and is a core component of any special application for more complex processing utilizing the PNS Process Manager Software Library (more on this software library further on).

Reusability Issues

An OOP template has been designed for building new Processes which allows the programmer to quickly build (typically in a few hours) a totally new function for processing data. The design enables the off-loading of special coding for OS interfacing to the Process Manager. In this way, a process can be coded up to run in the DOS Text version of a Process Manager, and simply be re-compiled and re-linked to run in the DOS Graphics or Microsoft Windows™ environment WITH NO CODE CHANGES.

The Process Manager is currently implemented in two operating environments: DOS Text Mode and DOS Graphics Mode. The DOS Graphics Mode will support both Text displaying of data, and Plotting of data (including the ability to generate Windows™

MetaFile, and PostScript outputs). Work is currently underway to implement a Microsoft Windows™ version of the Process Manager.

Approximately 20 specific processes have been developed that can be used by the Process Manager. Examples of these include:

- GPS Measurement Consistency Check
- Laser Tracker data to Aircraft Position Translator
- DTED database manager (including Line Of Sight calculator)
- Simulated Aircraft Trajectory Generator
- GPS Satellite Database Manager (provide satellite positions at specified time)
- GPS Satellite Selection Module
- GPS PVT Solution
- GPS Least Squares PVT Solution
- GPS and GPS/INS Covariance Simulator
- GPS/Doppler-AHRS 14 State Kalman Filter Covariance Simulator
- Differential GPS PVT Solution
- Least Squares DGPS Correction
- Landing Guidance Performance Generator
- Generic Error History Generator
- and many others...

These processes can be linked together to provide information to one another as required through the Process Manager. C²SID has utilized many of these processes in performance of various RDT&E projects.

PNS Process Manager Application Examples

An example of a simple application of the PNS Process Manager follows. For a more comprehensive example and explanation of the PNS process manager refer to the paper entitled "Evaluating the Effects of Different Satellite Selection Strategies for Nap Of the Earth (NOE) and Ground-Based Global Positioning System (GPS) Users", by Ms. Van Tran and Mr. Jim Adametz in this symposium's papers.

The Process Manager Put to Work on a Simple Process

In the simplest case when comparing data from two similar navigation sensors that generate the same

output parameters the mechanization illustrated in Figure 6 of a differencing process is effective.

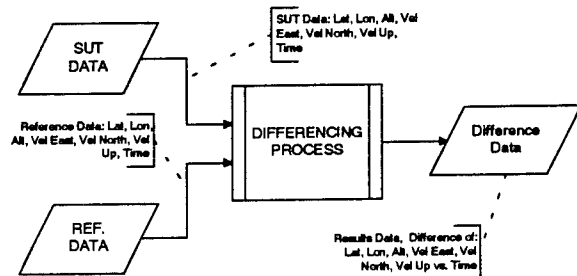


Figure 6 - Simple Process Mechanization

An example of the PNS Process Manager utilized in a modestly more complex task involves data from the AN/ASN-128 Doppler Navigation System. This navigation sensor does not produce the same navigation parameters (in the same engineering units) that are produced by a typical GPS receiver. There have been occasions when it was desirable to compare the position and velocities output by the Doppler Navigation System (the SUT) to those output by the Reference Navigation GPS receiver. In order to accomplish this the Process Manager is used to translate the data produced by the Doppler system into a coordinate system common with the GPS based system. Thus the Doppler parameters;

- Latitude
- Longitude
- Velocity along Heading
- Velocity across Heading
- Velocity Vertical
- Heading Sine
- Heading Cosine
- Time

are combined and translated match the GPS coordinates of;

- Latitude
- Longitude
- Altitude
- Velocity East
- Velocity North
- Velocity Up
- Time

The mechanization necessary to create the Difference of these two sensor outputs involves a

process that is slightly more complex than that of the previous example. Figure 7 illustrates the mechanization of the Doppler/GPS Differencing Process.

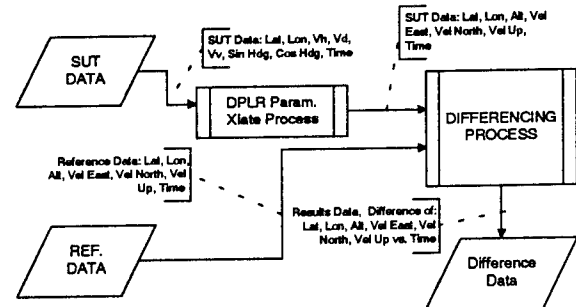


Figure 7 - Slightly More Complex Process Mechanization

Consider that the Time Align process is performed for at least every data point available from the sensor that produces the lowest frequency solution (in this case the GPS at 1Hz) and the fact that there are so many variables being time-aligned, translated into the common coordinate system, then differenced from one another and the utility of this feature of the PNS Software Family begins to become apparent. The Process Manager permits for the assembly of very complex processes with many intermediate steps and many sources of input data (as well as creating many types of output data).

PNS Applications, Past, Present and Future

The PNS has been successfully employed on several large scale RDT&E efforts as well as many small scale short duration tasks as well. Some typical examples of the applications of the PNS are:

- Summer 1992 - NRaD GPS Fiber Optic Link Assessment. PNS served as Lab-based Data Acquisition and Data Reduction tool.
- Fall 1992 - Provide complete end-to-end instrumentation for the Systems Under Test during the EH-60 Navigation System Upgrade Prototype. Tests were performed at the CIGTF Sled Test Facility, HAFB
- Fall 1992 through late Spring 1993 - Data acquisition and reduction for GPS Instrumentation Port Data on board US Army UH-1 aircraft out of Lakehurst Naval Air Station, Lakehurst NJ. Served customer's need in aiding the calibration and initial checkout of a new ground based radar.
- Winter 1992 - Support Army Research Lab/ Survivability, Lethality, Assessment Directorate (ARL/SLAD) in a GPS Jamming test. PNS served as the data acquisition tool.
- Late Summer 1993 - In a small "Lunch-box" style computer the PNS was used to aid in debugging a Honeywell Air Survivability Equipment Aircraft integration. The PNS's unique time-tagging capability proved to be a valuable Systems Integration Laboratory test tool.
- PNS is currently (April '94 through the time of this writing) in service as the Data Acquisition and Analysis tool for the ASN-128B Embedded GPS Doppler Navigation System on board a US Army UH-60A BLACKHAWK helicopter.
- PNS was configured to control the MIL-STD-1553 components and collect GPS IP data in a test conducted by Yuma Proving Grounds on the Embedded GPS Inertial (EGI) in the Kiowa Warrior aircraft.

The following sections will describe past, present and potential future applications of the PNS to RDT&E related tasks.

PNS Past - IEWCS EH-60 Navigation Upgrade Prototype

During the late 1980's the development of the IEWCS included the upgrade of the electronic mission suite on board the EH-60A Advanced QUICKFIX aircraft, imposing velocity accuracy's which were previously considered unprecedented. C²SID conducted computer-based simulations to demonstrate the ability of a GPS/INS system to meet these requirements, resulting in a configuration that included a Miniature Airborne GPS Receiver (MAGR) and a SNU-84 compatible INU. In 1992, the PEO IEW funded C²SID to prototype a navigation system to substantiate the simulation results with this configuration. Employing the PNS, a prototype system was designed based on a configuration in which raw sensor data was collected and system performance was evaluated in post processing. Figure 8 illustrates the configuration that was utilized by the PNS to collect that necessary data to meet the test objectives.

The Intelligence and Electronic Warfare/Common Sensor Navigation Upgrade Project was tested in its prototype configuration in October of 1992 at Holloman Air Force Base, New Mexico. The objective of the test was:

- Evaluate the performance of the GPS MAGR with SNU-84-1 INU aiding.
- Utilize both brands of SNU-84-1 INUs currently being procured by the Government as the source of MAGR aiding.
- Evaluate the capability of two commercially available INUs to support the required accuracy in an integrated system architecture.
- Evaluate the performance of two commercially available Embedded GPS Inertial candidates.

The test was conducted at the HAFB Central Inertial Guidance Test Facility (CIGTF) Test Track. The PNS provided bus control, data acquisition and data reduction of all units under test. Navigation truth reference data was provided by the CIGTF track.

Extensive post processing was conducted and the ability of a properly integrated GPS MAGR/SNU-84 INU to meet the performance requirements of the IEWCS EH-60 mission was established. This milestone positively affected the IEWCS development effort and identified an integration technique for the PEO IEW that avoided a unique point design approach for the navigation suite on the EH-60 aircraft.

The PNS applied itself perfectly to this application, demonstrating its exceptional ability to be configured to a large complement of equipment and recording an enormous volume of data chiefly over the MIL-STD-1553 data bus and GPS Instrumentation Port. The EGI candidates were brought in to the test set up shortly before the start of the test (a few weeks prior to beginning of test) without difficulty. The PNS's data reduction capability handled the data in a rapid and consistent manner providing a data analysis which was meaningful and timely to the customer [reference 1, 2].

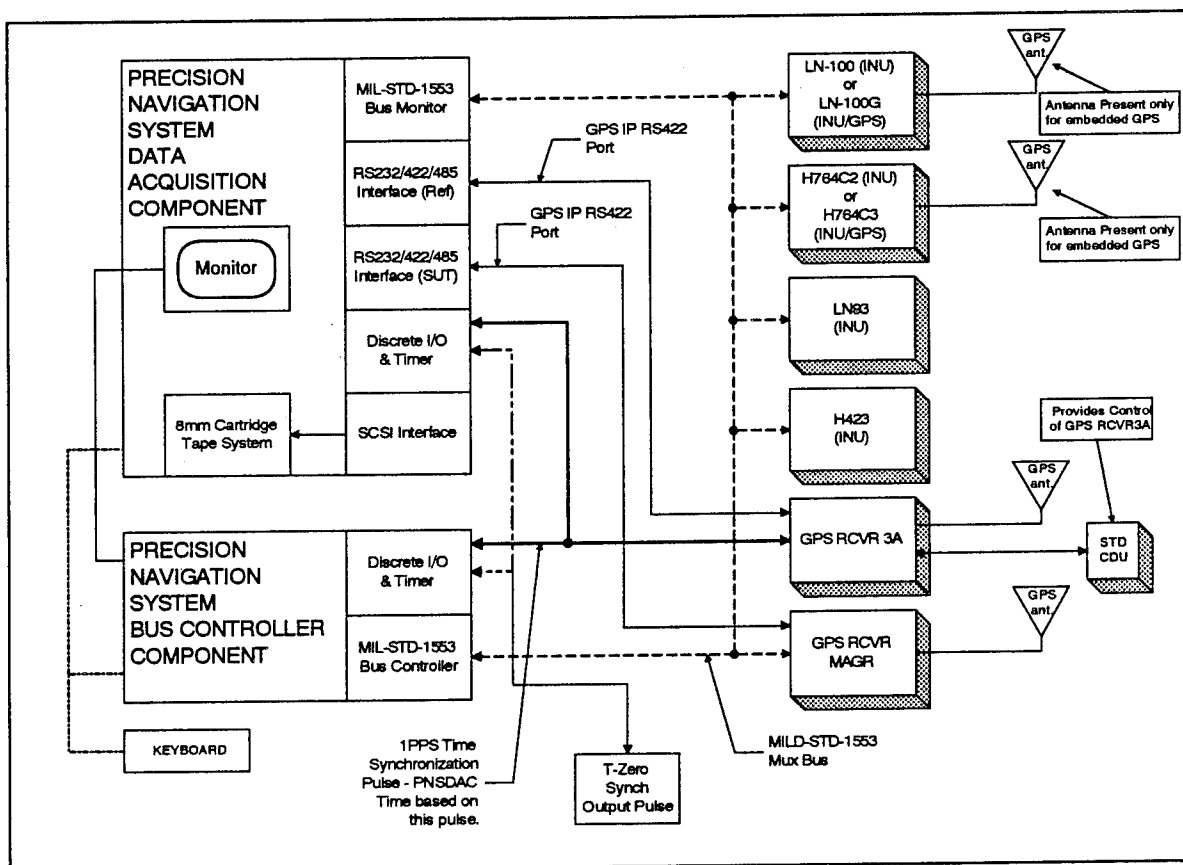


Figure 8 - IEWCS EH-60 Test Set Up

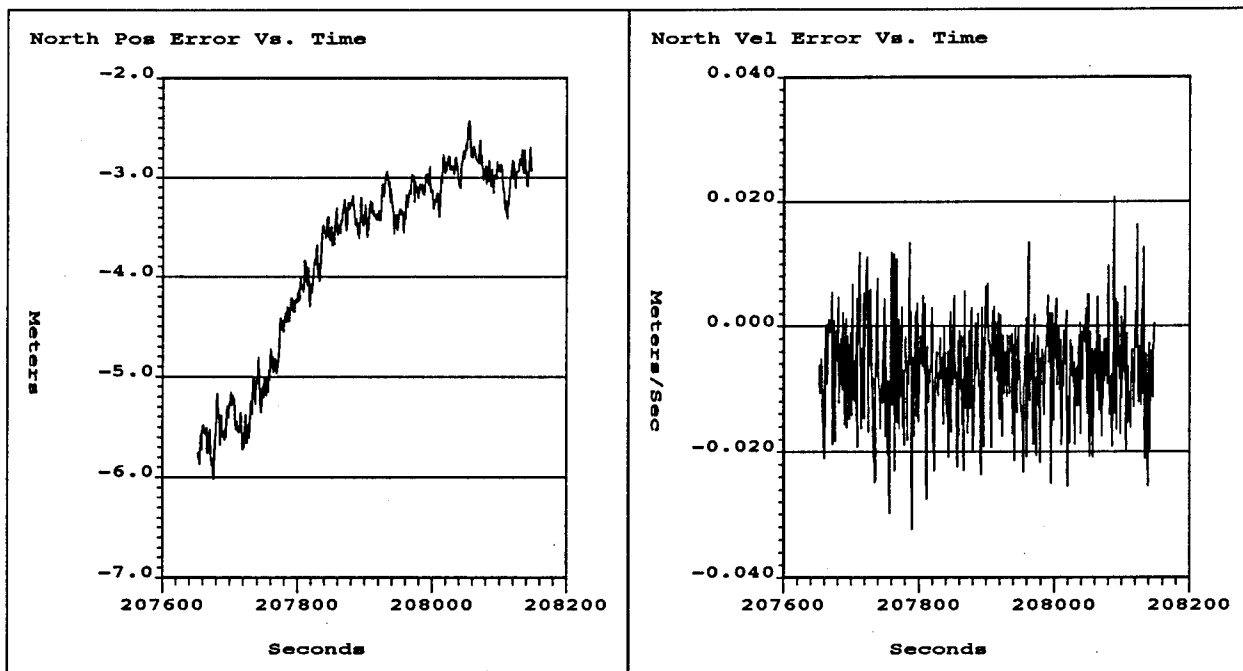


Figure 9 - Sample PNS Data Plot, North Position and Velocity Errors

A sample data plot from the IEWCs EH-60 analysis effort is shown in Figure 9. This plot indicates the North Position and Velocity Errors for the MAGR.

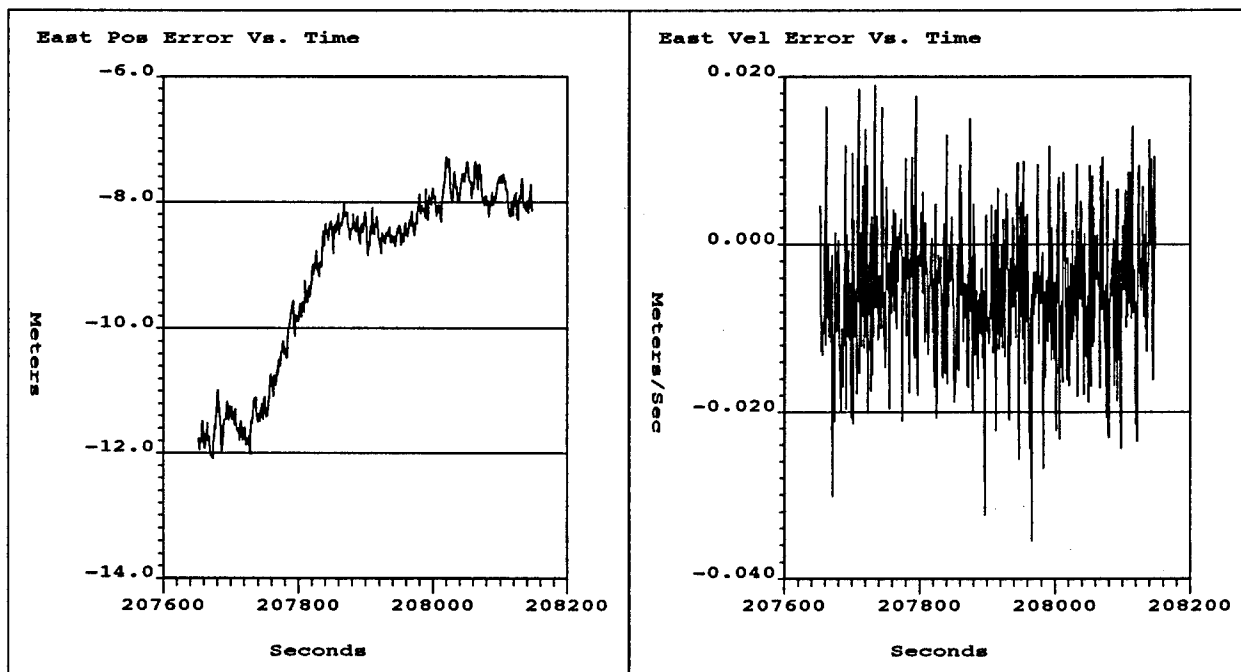


Figure 10 - Sample PNS Data Plot, East Position and Velocity errors

A sample data plot from the IEWCs EH-60 analysis effort is shown in Figure 10. This plot indicates the East Position and Velocity Errors for the MAGR.

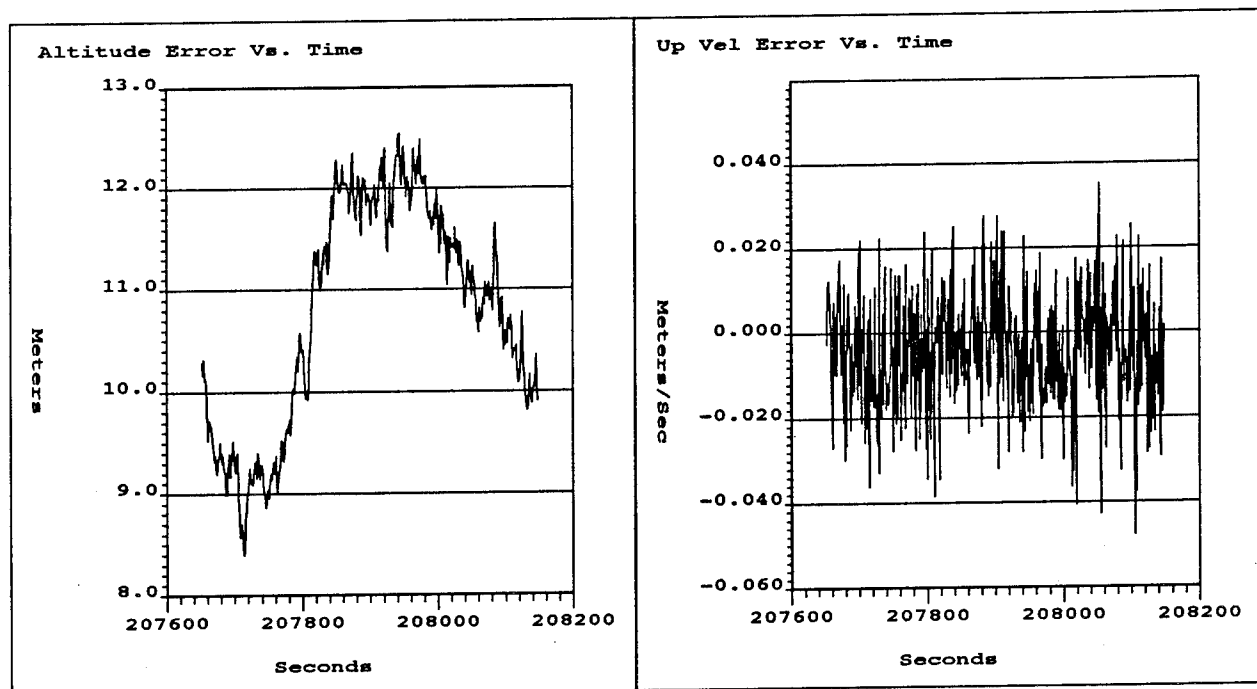


Figure 11 - Sample PNS Plot, Altitude and Up Velocity Error Plot

A sample data plot from the IEWCS EH-60 analysis effort is shown in Figure 11. This plot indicates the Altitude and Up Velocity Errors for the MAGR.

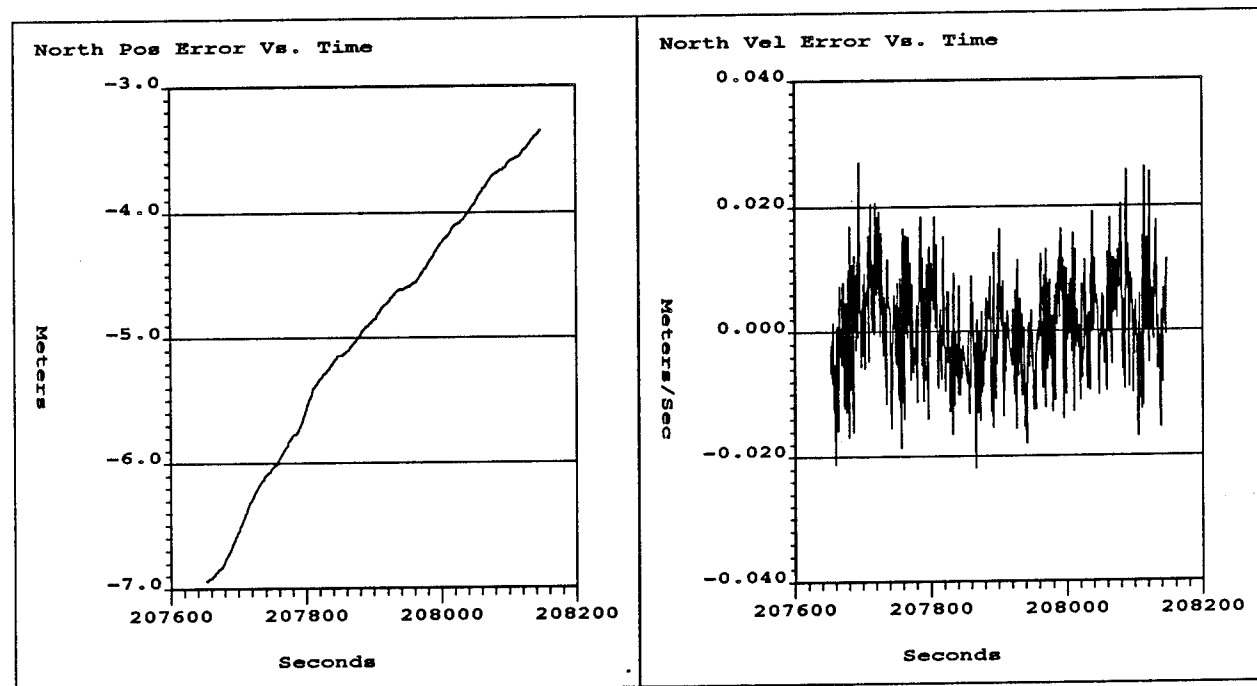


Figure 12 - Sample PNS Data Plot, North Position and Velocity Errors

A sample data plot from the IEWCS EH-60 analysis effort is shown in Figure 12. This plot indicates the North Position and Velocity Errors for the PNS Navigation Solution process.

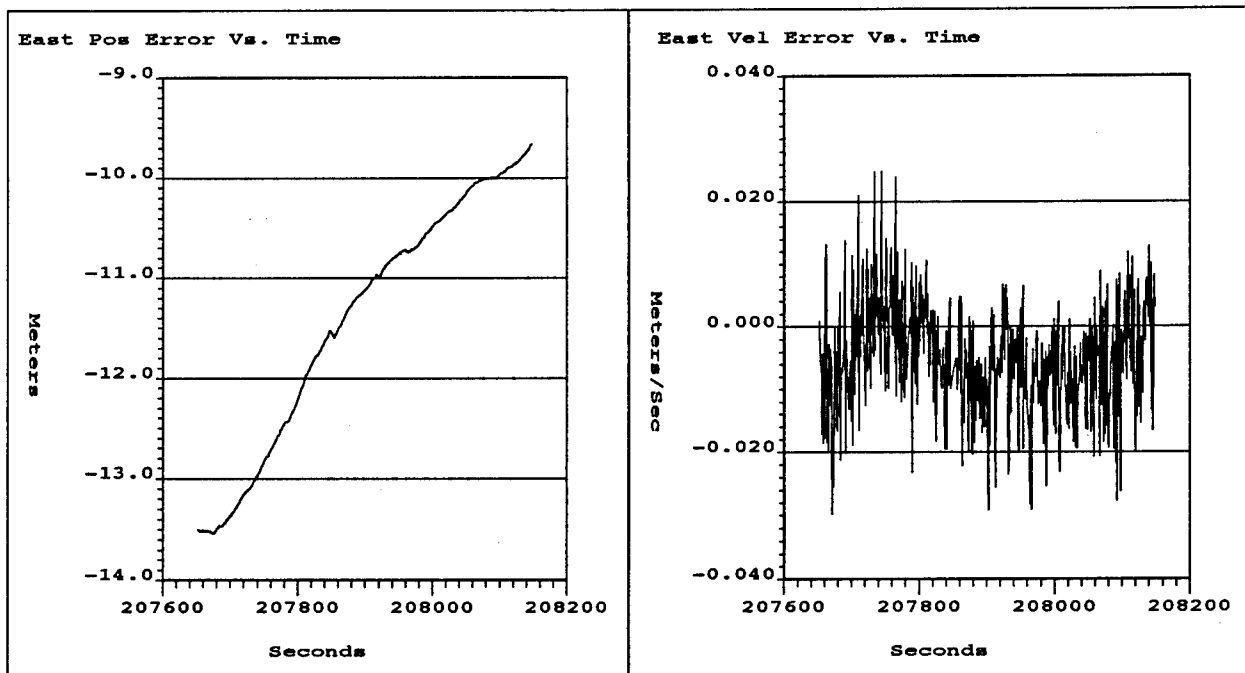


Figure 13 - Sample PNS Plot, East Position and Velocity Errors

A sample data plot from the IEWCs EH-60 analysis effort is shown in Figure 13. This plot indicates the East Position and Velocity Errors for the PNS Navigation Solution process.

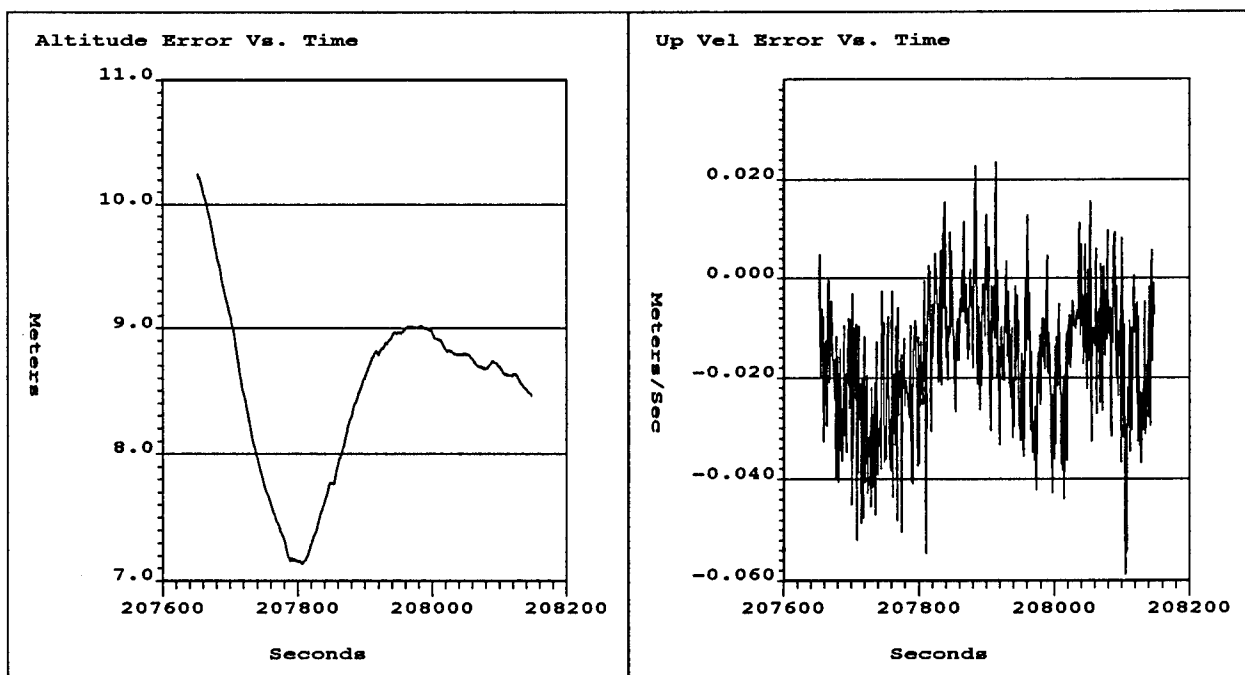


Figure 14 - PNS Sample Plot, Altitude and Up Velocity Error

A sample data plot from the IEWCs EH-60 analysis effort is shown in Figure 14. This plot indicates the Altitude and Up Velocity Errors for the PNS Navigation Solution process.

PNS Present - AN/ASN-128B Embedded GPS/Doppler Navigation System Development

Following a study entitled the GPS Integration Alternative Study (GIAS) conducted by Draper Labs, the PEO Aviation elected to proceed with a feasibility proving program to embed a GPS receiver card within the Signal Data Converter of the AN/ASN-128 Doppler Radar with the intention of fielding the system on UH-60A/L Blackhawks. The PNS was again called upon for this rather difficult RDT&E type effort. The PNS is currently employed to provide system data recording, data reduction, and data analysis tasks.

A Collins MAGR and a Litton LN93 INU on board the UH-60A test bed aircraft are being utilized to generate the truth reference data. Figure 15 illustrates the configuration of the PNS for this effort. Differential GPS truth reference data was generated by the 46th Test Squadron (with support from Intermetrics) at Holloman Air Force Base.

This DGPS solution utilized a GPS ground station provided by the 46th Test Squadron combined with GPS flight data recorded from the Collins MAGR on board the Test Bed UH-60A aircraft. The testing began in April of 1994 and has continued through several phases and is currently on-going.

The testing has included navigation system performance and Electronic Countermeasures (ECM) evaluations. A production contract is set to be awarded this Fiscal Year and will include a number of hardware and software changes to the current configuration demanding further testing.

The strengths and flexibility of the PNS displayed during this test effort demonstrated the PNS ability to record data from a number of different interfaces (ARINC429, MIL-STD-1553, GPS IP, RS-232 and discretes), interface and exchanged data with an external agency, and provide a widely varied set of data plots for analysis [reference 3].

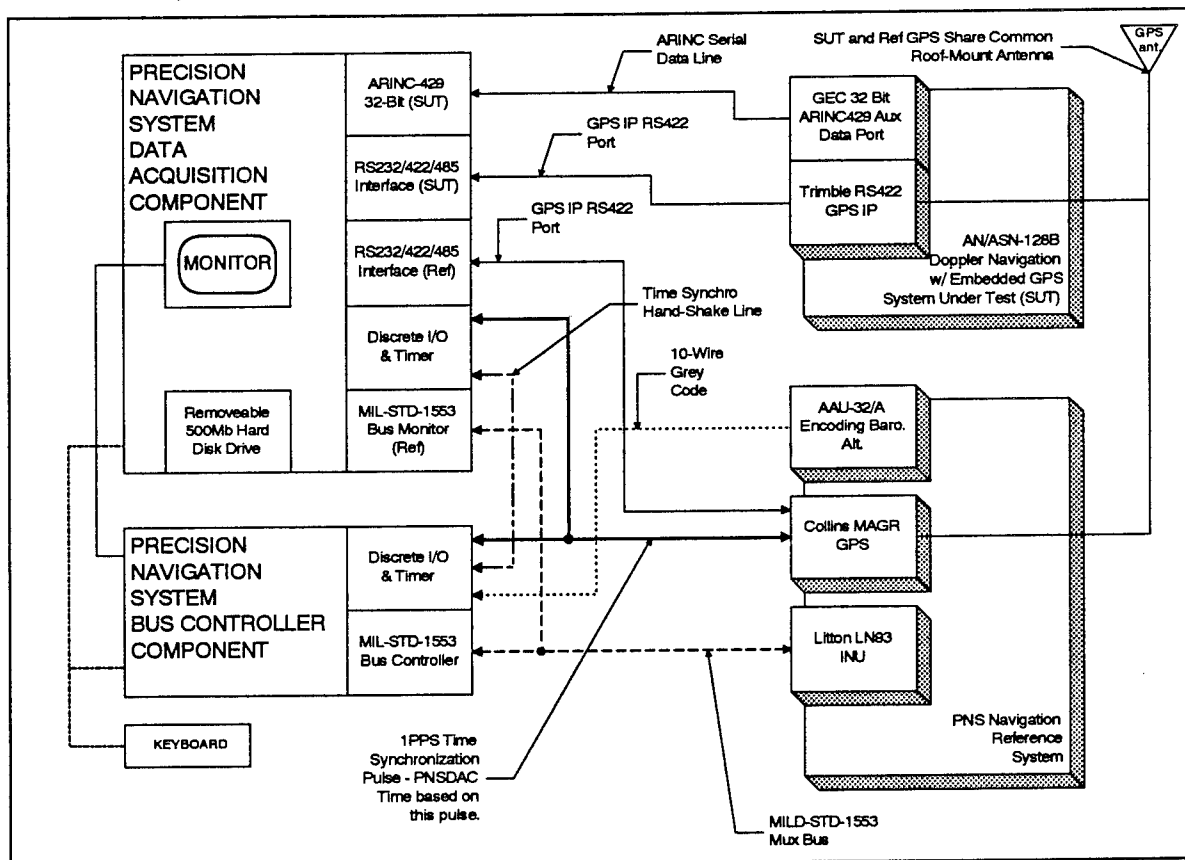


Figure 15 - AN/ASN-128B PNS Configuration

The data package prepared subsequent to each flight of the ASN-128B contained approximate 50 standard data plots produced by the PNS Post Processing Application (a specific variant of the PNS Process Manager) and the more generic data plotting tool, PNS Data Analysis Plotter.

The following data plots illustrate the typical outputs of the Plotter as well as the more specific navigation error plots produced by the Process Manager Tool.

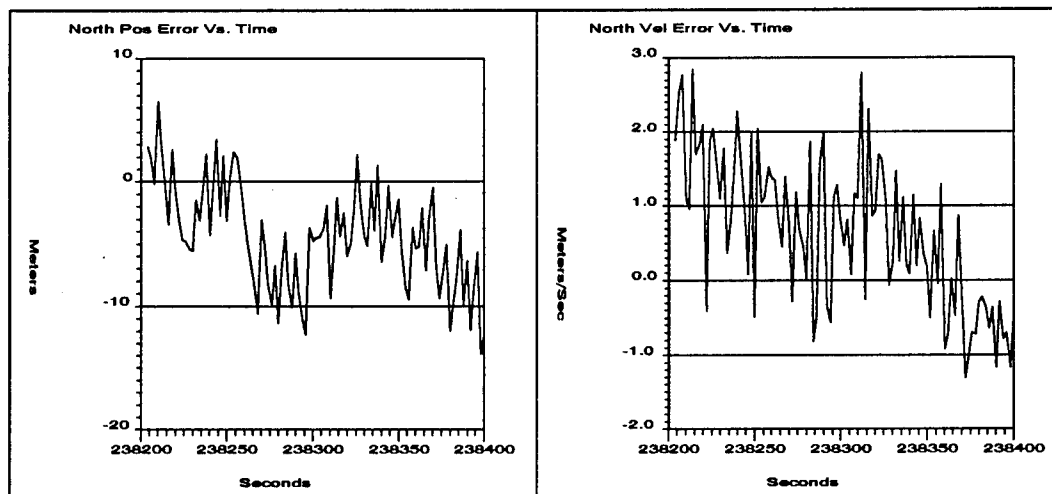


Figure 16 - North Position and North Velocity Error Plot

Figure 16 illustrates the North Position and the North Velocity Error plots. These plots were generated using the 46th Test Squadron Differential Time Space Position Information (TSPI) data product (the navigation truth reference data for this test) differenced with the SUT data from the ASN-128B.

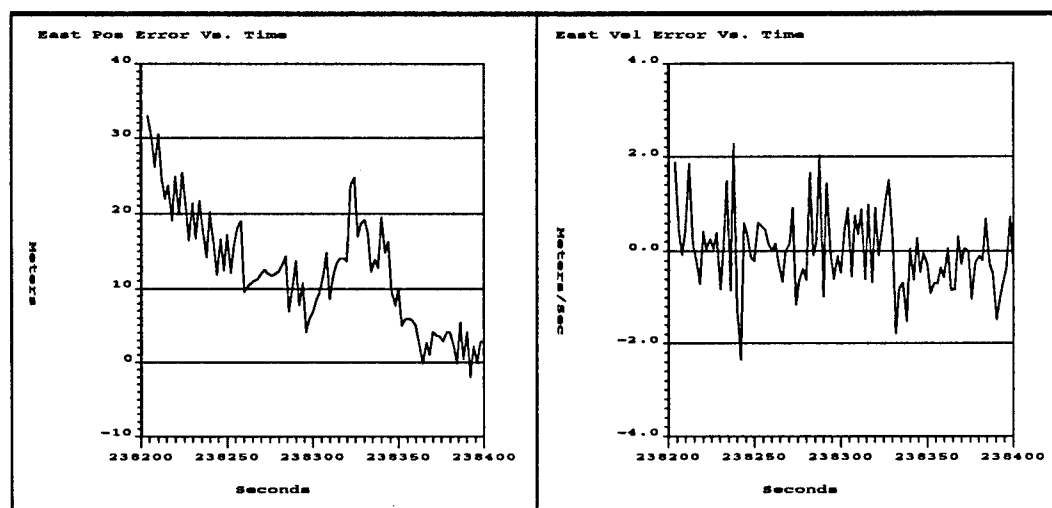


Figure 17 - East Position and Velocity Error Plot

Figure 17 illustrates the East Position and the East Velocity Error plots. These plots were generated using the 46th Test Squadron Differential Time Space Position Information (TSPI) data product (the navigation truth reference data for this test) differenced with the SUT data from the ASN-128B.

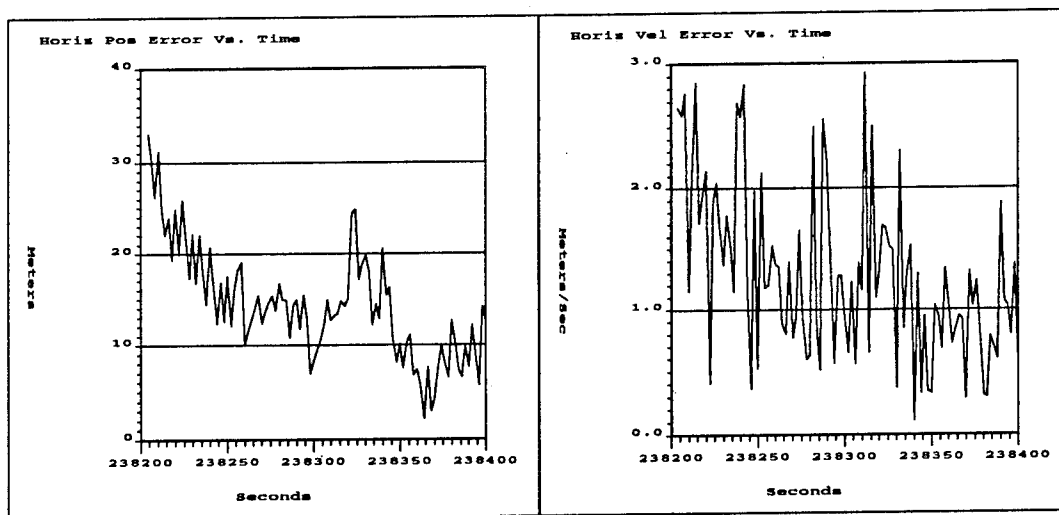


Figure 18 - Horizontal Position and Velocity Error Plot

Figure 18 illustrates the composite Horizontal Position and Velocity Error plots. These plots were generated using the 46th Test Squadron Differential Time Space Position Information (TSPI) data product (the navigation truth reference data for this test) differenced with the SUT data from the ASN-128B.

PNS Future - Comparative Demonstration of GPS Integration Architectures

With the introduction of the Selective Availability/Anti-Spoof Module (SAASM) and GPS Receiver Application Module (GRAM) the GPS Joint Program Office has expressed interest in gathering data that compares varying levels of sophistication in the integration of GPS and sensor data. C²SID has proposed the use of the PNS as a test bed to collect data from a number of GPS receivers and on-board sensors. PNS Post Processing capabilities will be used to demonstrate the benefits and drawbacks associated with various proposed approaches to the GRAM development effort.

The proposed test is based on the same fashion in which the IEWCs test effort was conducted. A large data base of sensor data would be collected allowing for the evaluation of varying Kalman filter techniques and the usage of different levels of processed information. Comparison of results will

be conducted with truth reference data made available from a DGPS system, laser track range, or some other means. This system could be made available to ground or airborne platforms providing valuable data to support integration decisions. An issue of prime importance to Army platforms is the performance of navigation systems following the loss of GPS due to masking or jamming. The PNS is suitably designed to accomplish this demonstration.

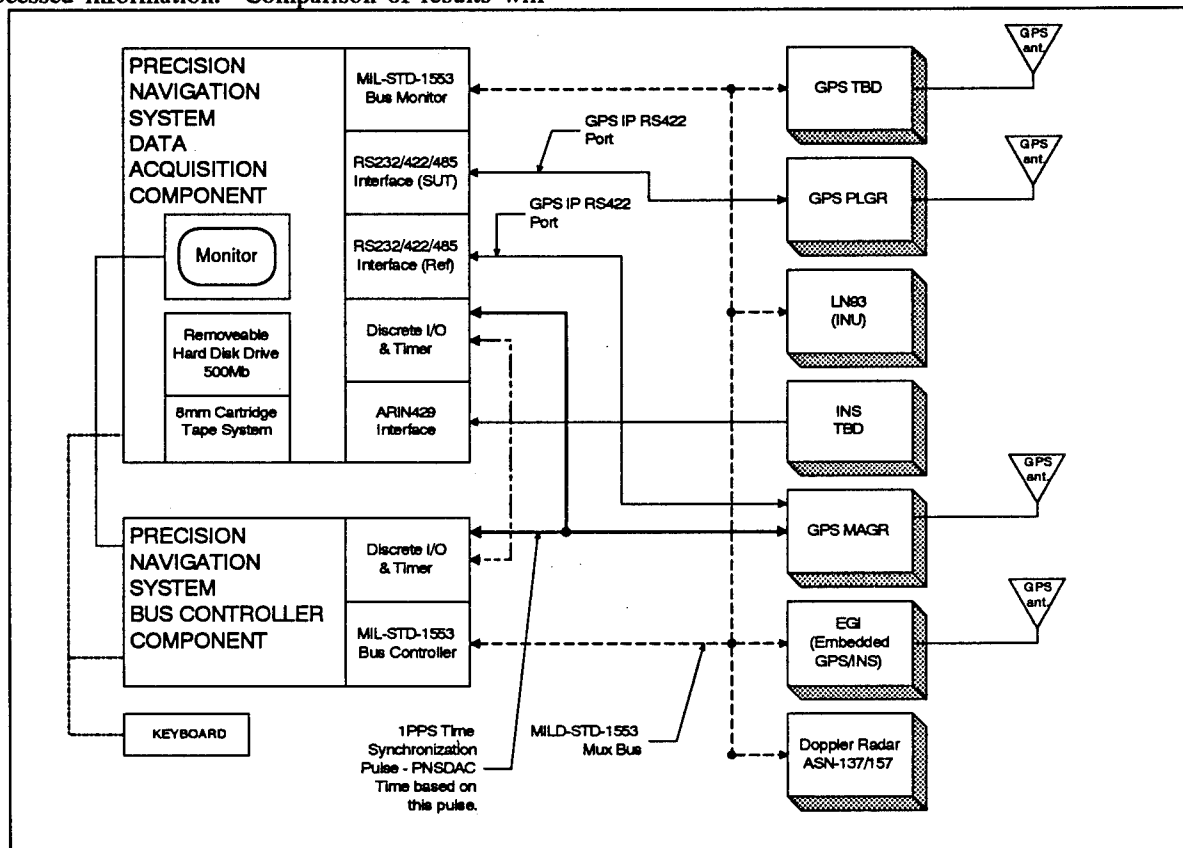


Figure 19 - Proposed Test Set Up for Comparative Demonstration of GPS Integration Architectures

About the Authors

Paul Olson is the group leader of the Navigation Technology Group of the Command, Control and Systems Integration Directorate (C²SID) and has been working in the area of Army electronics and platform integration since 1982. He has a BS in Electrical and Computer Engineering from Clarkson University, Potsdam New York (1982) and an MS in

Electrical Engineering from Fairleigh Dickinson University, Rutherford New Jersey (1987).

Mark Berry is a Senior Engineer at Intermetrics Incorporated and has been involved in the US ARMY Aviation community since 1986. Mr. Berry holds the B.S. degree in Electrical Engineering from Lehigh University in Bethlehem Pennsylvania (1986).

References

1. *"IEWCS Navigation System Upgrade Performance Test Final Report"*, dated July 28, 1993, Prepared for CECOM C²SID, Navigation Technology Division, Fort Monmouth, NJ, Prepared by Intermetrics, Inc., 1720 State Highway 34, Wall, NJ 07719
2. *"Test of an Integrated GPS/INS System for Precision Velocity"*, Brian Mitchell, IEWCS Navigation System Upgrade, CECOM Command/Control and System Integration Directorate, Ft. Monmouth, NJ; and Joseph McGowan, Project Manager, Intermetrics, Inc. Oceanport, NJ; Published in Sixteenth Biennial Guidance Test Symposium, AFDTC-TR-93-06, Vol. 1, Prepared by Central Inertial Guidance Test Facility Guidance Test Division.
3. *"Performance of AN/ASN-128B, an Integrated GPS and Doppler Navigation System"*, Buell, Oleniek, Joint Services Data Exchange, Oct. 1994.

Acknowledgments

The authors acknowledge the following individuals for their contributions to the development of the Precision Navigation System as well as their contributions to the writing of this paper:

Mr. John Weinfeldt, C²SID, Fort Monmouth NJ
Mr. Joe McGowan, Intermetrics Inc.
Mr. Jim Adametz, Intermetrics Inc.

THIS PAGE LEFT BLANK INTENTIONALLY

SESSION IV-B

DIFFERENTIAL GPS

CHAIRMAN

MAJOR KARL KASER

*GPS JPO
LA AFB CA*

THIS PAGE LEFT BLANK INTENTIONALLY

WIDE AREA DIFFERENTIAL GPS NAVIGATION SYSTEM ANALYSIS AND TESTING

D. DeDoes, P. Sinha, D. Wirkkala
Intermetrics Inc.

L. Lupash
LL Consulting

ABSTRACT

There is ever increasing interest in the use of differential GPS, and in particular wide area differential GPS (WDGPS), for enroute/terminal navigation and for precision landing approaches. Both military and civil aircraft will exploit the capabilities offered by WDGPS. For example, the military has considered a communications satellite augmented GPS (CAG) concept and has recently completed a series of GPS precision approach tests, and the FAA is performing flight trials with their wide area test bed and have initiated development of the wide area augmentation system (WAAS). All WDGPS approaches have common technical issues including wide area monitoring of the signal-in-space (SIS), computing differential corrections for all participating satellites and broadcasting integrity messages, under short reaction time limits.

This paper provides an overview of important WDGPS performance parameters, discusses impacts on military GPS receivers and outlines test and evaluations (T&E) issues. Navigation system performance within a service volume encompassing the CONUS, Hawaii, Alaska, and Puerto Rico is evaluated through the use of simulation. Such performance drivers as the location and number of GPS ground monitoring stations, ionospheric disturbances, type of satellite ephemeris and clock error estimation algorithms employed (including Kalman filter, recursive weighted least squares and weighted least-square snapshot algorithms), satellite configurations (including GPS constellation with geostationary satellite (GEO)/Comsat augmentation) and user equipment characteristics on navigation performance within the service volume are explored. Results show performance sensitivity to these parameters.

The DoD family of receivers currently does not have the capability to receive and use the higher navigation message data rates needed to support WDGPS requirements, including differential corrections and integrity warnings. The design issues relative to modifying military receivers are discussed.

Receiver testing approaches must reflect the new WDGPS requirements. In particular, both field and laboratory test configurations will experience changes. The paper identifies impacts to current test methods and overviews required changes to test environments/equipment.

INTRODUCTION

During the past several years there has been much activity to evolve GPS into a navigation system that is capable of supporting instrument flight operation in the National Airspace System (NAS). Milestones achieved toward this objective include use of GPS for

oceanic enroute, supplemental for non-precision approach (as specified in TSO C-129), the FAA WDGPS test bed, the FAA sponsored CAT II/III flight test programs and release of the Wide Area Augmentation System (WAAS) request for proposal (RFP). In addition, the NAVSTAR GPS Joint Program Office (JPO) has conducted studies to determine the feasibility of CAG. This concept is similar to WAAS except military communication satellites would be used instead of commercial GEOs to broadcast the differential correction and integrity messages.

The WAAS concept provides sole means enroute, terminal and precision approach, down to CAT-I conditions. Figure 1 shows the WAAS concept including the Wide-Area Reference Stations (WRSs), the Wide-Area Master Stations (WMSs), the Ground Earth Stations (GESs) and the GEOs. The WRSs provide the WMSs with pseudoranges to the GPS and GEO satellites; satellite position, clock and IONO corrections are estimated in the WMSs and then sent, along with integrity messages, to the GESs for uplink to the GEOs. The User receives differential corrections, ranging signals and integrity messages from each GEO in view. The WAAS specification identifies a service volume (SVOL) and provides system performance requirements; these are shown in Figure 2 and Table 1 respectively [1]. The SVOL extends from the surface up to 50,000 ft. Demonstrating that WAAS meets the availability requirement is particularly demanding because this parameter is defined as, "the probability that the navigation and fault detection functions are operational and that the GPS/WAAS SIS accuracy, integrity, and continuity of function requirements are met."

Analysis to validate WDGPS performance has been performed by many authors during the past two years. Table 2 outlines the contributions of selected researchers and test programs, as they appear in the Reference section. In general, these papers address: (1) algorithms for computing satellite position, clock and IONO corrections, (2) simulations to evaluate user navigation availability and accuracy and (3) results of flight trials using both the FAA Test Bed and Stanford University's network of reference stations. References [2] and [7] represent the type of approach needed to verify the WAAS navigation and availability performance requirements. However, none have performed a comprehensive analysis of all WAAS SVOL requirements as they are stated in the specification. For example, "availability" as defined in [1] has not been treated in its entirety. In general, the SVOL models to date include the impact of GPS and GEO satellite failure probabilities, number of GEOs and their locations, number and location of WRSs, IONO characteristics and use covariance analysis to estimate navigation performance at a number of User locations throughout the SVOL. Results to date seem to indicate that WAAS navigation performance (using various definitions for availability) can be met over the SVOL. However, the outcome of these simulations has shown sensitivity to: (1) number and location of both the GEOs and WRSs, and (2) unmodeled IONO changes. For example, Reference [2] shows that precision approach requirements (vertical accuracy) in the center of CONUS may not be met due to single GEO coverage and to sensitivity of the solution to Grid IONO Vertical Error (GIVE). While much progress has been made to demonstrate WAAS performance there are factors not yet considered in the SVOL models. For example, availability involves a combination of: (1) vertical and horizontal navigation accuracy, (2) continuity of service, and (3) integrity which itself is a function of hazardous misleading information (HMI) potential, time-to-alarm and alarm limit performance. In some cases these parameters depend upon the WAAS ground and space system designs, which must be considered in a comprehensive analysis.

TABLE 1 SUMMARY OF WAAS PERFORMANCE REQUIREMENTS

PARAMETER	INITIAL WAAS		FINAL WAAS	
	ENROUTE	PRECISION	ENROUTE	PRECISION
AVAIL	0.999 OVER 50% OF CONT. 48 STATES	0.95 OVER 50% OF CONT. 48 STATES	0.99999 OVER SERVICE VOLUME AS SPECIFIED	0.999 OVER SERVICE VOLUME AS SPECIFIED
UDRE	N/A	2.0 METERS WITHIN 50% OF CONT. 48 STATES	N/A	1.5 METERS OVER FULL SERVICE VOLUME
GIVE	N/A	2.0 METERS WITHIN 50% OF CONT. 48 STATES	N/A	1.5 METERS OVER FULL SERVICE VOLUME
NAV. ACCURACY	NAV. 100/ 500M HORZ. AT 95% AND 99.999% POINTS	7.6M FOR NAV AT 95%	SAME: NAV INCLUDES THE AVIONICS AND SIS CONTRIBUTIONS.	
INTEGRITY				
HMI	10 ⁻⁷ /HR	4x10 ⁻⁸ /150 SECONDS	10 ⁻⁷ /HR	4x10 ⁻⁸ /150 SECONDS
TIME TO ALARM	8 SECONDS	6.2 SECONDS	8 SECONDS	5.2 SECONDS
ALARM LIMIT	1.0 When PR. exceeds the limit, or 2.0 When UDRE or GIVE exceeds the limit, or 3.0 When active UDRE or GIVE becomes invalid (exceeds the 99.9% point on the distribution)			
CONTINUITY OF FUNCT.		1-5.5x10 ⁻⁵ /150 SEC		1-5.5x10 ⁻⁵ /150 SEC
NAVIGATION	1-10 ⁻⁸ /HR	N/A	1-10 ⁻⁸ /HR	
FAULT DET.	1-10 ⁻⁵ /HR EXCL. 5 MIN OUTAGES	N/A	1-10 ⁻⁵ /HR EXCL. 5 MIN OUTAGES	
LATENCY OF FAST CORR.	5.2 SECONDS	5.2 SECONDS	5.2 SECONDS	5.2 SECONDS

TABLE 2 CONTRIBUTIONS OF SELECTED TECHNICAL PAPERS

REFERENCE	TOPICS ADDRESSED
1	Specifies WAAS requirements
2	Extends the work in [7] to more closely model availability and accuracy across the SVOL.
3	Shows the effects of spatial decorrelation on the WAAS IONO grid
4	Summarizes cross country and approach navigation accuracy results from the FAA WAAS Test Bed flight trials
5	One in a series of papers describing WADGPS algorithms. Shows navigation accuracy results using data from real reference stations
6	Reports on the FAA WAAS Test Bed navigation performance results during flight trials
7	Evaluates availability and navigation performance with various combinations of GPS and GEO satellites under specified satellite failure conditions
8	Reports on algorithms and precision approach results from a Stanford supplied network (3 reference stations in the Western U.S.) using a private aircraft
9	Analyzes IONO data from several monitoring sites. Proposes an IONO estimation algorithm.
10	Describes a simulation of WADGPS algorithms

This paper contributes to the understanding of WAAS by focusing on several issues that are important to system performance and in developing WAAS algorithms. In addition, it provides some insight into the benefit for potential military users.

WAAS PERFORMANCE DRIVERS

This section addresses several of the parameters that drive WAAS performance; namely, number and location of WRSs; algorithms for computing satellite position, clock and IONO corrections; SIS anomaly detection; and performance sensitivity to IONO changes. Each of these is further discussed in the sequel.

PERFORMANCE SENSITIVITY TO REFERENCE STATION GEOMETRY

The WAAS specification identifies the location of 24 WRSs for the initial WAAS, with a requirement to expand up to 50 in the final WAAS. Performance throughout the SVOL depends upon the number, location, reference receiver capability and reliability of these stations. In particular, performance is sensitive to the availability of WRSs around the perimeter of the SVOL. One approach taken by SVOL models [2, 7] is to compute the covariance of the satellite position and clock errors and relate this to User navigation performance. To perform trade studies on WRS geometry with such approaches can result in long duration simulation runs. The objective of the method described herein is to provide a "first cut" at locating the WRSs while at the same time reducing simulation run time. The best candidates can then be refined using covariance analysis, or other more elaborate methods.

The process is straightforward and involves: (1) determining when at least four WRSs can track a given satellite above a specified mask angle (required for satellite error estimation), and (2) at each User location, within a grid covering the SVOL, determine when at least four satellites with good geometry and having up-to-date WAAS corrections can be observed. Figures 3 and 4 show results for the 24 WRS locations defined in the WAAS specification. The criteria in this case was that WAAS corrections were available for at least four GPS satellites and two GEOs. The lack of WRS coverage in the Pacific and Alaska regions is evident in Figure 4. Figures 5 and 6 show the impact of adding additional WRSs in the Caribbean, Newfoundland, Hawaii and Alaska. As illustrated in Figure 6 the objective is to position WRSs so that the "surface" is flat with few or no failure cases.

This process could be enhanced by refining the rule for when sufficiently accurate corrections are available for a given satellite. The error estimation performed by the WMS is a function of the WRS pseudorange measurement error, the geometry of the WRSs in relation to the satellite and the error estimation algorithms. Since geometry is a major consideration, particularly when a satellite first enters and then exits the WAAS tracking network, a parameter similar to the well known GDOP could be used to further refine the site selection process. Instead of using the line-of-sight (LOS) between the User and multiple satellites, the parameter Reverse GDOP (RDOP) can be formed from the LOSs between a single satellite and multiple WRSs. Figure 7 shows an example of RDOP for the 24 satellite GPS constellation. The + indicate RDOP for each GPS satellite, computed at 30 minute intervals, over a 24 hour period, with the satellite's position indicated by the latitude and longitude of its position vector. The surface is a best fit to these points as computed by Matlab. Note the RDOP increase around the perimeter of the tracking network. Due to time limits this approach was not explored completely but it appears to have merit.

SATELLITE POSITION AND CLOCK ERROR ESTIMATION

Background

The WMSs receive pseudorange measurements from the WRSs and use them to compute satellite position and clock corrections. Various algorithms have been proposed in the literature to accomplish this function [5] [10]. The Weighted Least Square (WLS) (snapshot) filter appears to be the common choice. However, there are other candidates including the recursive WLS filter

and the discrete Kalman filter. One advantage of the Kalman filter is its ability to smooth the estimates and to carry across gaps in data.

The following two sections describe a WLS snapshot filter and its use to estimate satellite position and clock errors in a WAAS like environment consisting of 24 GPS satellites, 3 GEOs and up to 32 WRSs.

Estimation Model

The overall estimation model considers as unknowns: (1) 3-D ephemeris error and a clock bias error for each satellite and (2) a clock bias error for each WRS. Therefore, if there are n satellites in view from all reference stations, the total number of unknowns is

$$N_u = 4n + m - 1 \quad (1)$$

where m is total number of reference stations, and clock errors of the reference stations are estimated relative to a fixed reference.

The observation model is based on the measured pseudorange ρ_{ij} from the i -th reference station to the j -th GPS satellite, and is described by

$$\begin{aligned} \rho_{ij} &= D_{ij}^T e_{ij} - b_j + B_i + n_{ij} \\ &= [(R_j + \delta R_j) - S_i]^T e_{ij} - b_j + B_i + n_{ij} \end{aligned} \quad (2)$$

where

- ρ_{ij} - measured pseudorange from i -th reference station to j -th GPS satellite
- D_{ij} - range vector from the i -th reference station to the j -th GPS satellite
- e_{ij} - range unit vector from the i -th reference station to the j -th GPS satellite
- R_j - j -th satellite location calculated from the GPS message
- δR_j - ephemeris error vector of the j -th GPS satellite
- S_i - known i -th reference station position
- b_j - j -th satellite clock error
- B_i - i -th reference station clock error
- n_{ij} - measurement noise for the measured pseudorange ρ_{ij} .

We assume that the measured pseudoranges are adjusted for ionospheric and tropospheric errors.

After combining all equations (2), i.e., for all indices i and j , at a specified time, and executing algebraic manipulations, the observation model is defined by the following equation

$$Z = HX + v \quad (3)$$

where the dimension of the measurement vector Z is given by

$$N_z = \sum_{i=1}^m n_i$$

and n_i is the number of satellites in view from the i -th reference station. Usually the number N_z is greater than the number of unknowns N_u , i.e. there are more measurements than unknowns.

There are several proposed techniques to solving the estimation problem defined by equation (3). The most used approach is the weighted least-squares solution given by

$$X_{est} = (H^T W H)^{-1} H^T W Z \quad (4)$$

where W is the weighting matrix. Note that the system matrix H is sparse, and therefore a significant computational effort can be saved if appropriate sparse matrix techniques are used. Another important remark is the fact that the dimension of the model (3) is time dependent because the total number of available measurements is changing.

Simulation Results

To evaluate estimator performance a simulation including 24 GPS satellites, 3 GEOs, 24 or 32 WRSs and a $5^\circ \times 5^\circ$ grid of User locations within the SVOL was conducted using the WLS algorithm described above. Figure 8 shows an example of RSS satellite position error over a period of time when 23 WRSs were tracking. The modeled WRS receiver pseudorange error was equivalent to that for commercial dual frequency capable receivers. Figure 9 shows the range of RDOP experienced during this tracking period.

SIGNAL-IN-SPACE FAILURE DETECTION

The WAAS specification requires a "DON'T USE" message be transmitted, within the time limits defined in Table 1, in the event that the pseudorange correction exceeds 256 meters, or the UDRE or GIVE exceed their limits. To explore the characteristics of the algorithm described above a ramp clock error, see Figure 10, was simulated. During the test period the number of WRSs tracking the satellite varied between 12 and 14. Figure 11 shows reasonable performance of the WLS algorithm under the ramp error condition. However, in situations where there are only four or five WRSs tracking, with poor RDOP, one may encounter a degradation in the estimator's performance.

IONO CORRECTION PERFORMANCE

The WAAS broadcast message from each GEO contains IONO corrections for a grid of 929 points (IONO Grid Points: IGP) within the GEOs footprint. The grid is further partitioned into bands which contain 5, 10, and 15 degree sub-grids. Due to message transmission limits not all IGPs can be refreshed at the same time. In addition, both the WMSs and the User must interpolate to produce the IGP IONO delays and to calculate the LOS IONO corrections. This provides an opportunity for degraded performance due to: (1) rapid changes in the IONO delay and (2) IONO gradients not adequately accounted for by the interpolation algorithms.

IONO Simulation

To evaluate the magnitude of IONO errors a simulation of the GPS/GEO constellation and IONO grid algorithms was performed. This consisted of 24 GPS satellites, WRSs, and a grid of User locations across the SVOL. Runs were made over 24 hour periods with the models described below.

IONO Truth Model: The Klobuchar model with two additional terms was used to compute the true vertical IONO delay. This model was suggested by Kee, et. al. [10]. The sinusoid term has an amplitude of 5% of cosine peak of Klobuchar and a period of 1/5 of that model. The random term is zero mean and has a standard variation of 5% of the combined Klobuchar and sinusoid terms. Figure 12 shows a typical IONO delay profile from the model. Figure 13 illustrates IONO delays across the SVOL.

WRS Locations: A baseline of 24 stations was used in the simulation and were chosen to be graphically dispersed across the SVOL.

GPS Constellation: Almanac for the 24 satellite constellation was downloaded from the Holloman AFB Bulletin Board.

WRS Measured IONO Delay: These are the LOS delay measurements made from each WRS to each visible satellite. The true IONO from the Klobuchar model, at each pierce point, was multiplied by the obliquity factor to produce the LOS IONO. The WRS receiver noise was assumed to be zero mean with a standard deviation of 0.8 meters.

Estimation of IGP Vertical Delays: Both 5 X 5 and 10 X 10 degree grids were used to cover the SVOL. The "inverse distance weighted with Klobuchar model" was selected as the baseline algorithm for determining vertical delays [9]. A variation of this method was studied in order to reduce the WMS computational load and to decrease errors in the interpolation algorithms. This method sorts the pierce points and uses only the ten closest to the IGP.

The GPS constellation was simulated for a 24 hour period and pierce points computed along with the associated vertical IONO delay. This information was then used to determine the IGP vertical delays.

User IONO Computation: This was based on the Junkins interpolation as defined in the WAAS system specification [1]. User IONO errors for all visible satellites were determined by

differencing the computed delay with "truth" at the pierce point, as computed by the modified Klobuchar model.

Simulation Results:

CASE 1. Sensitivity to Grid Size

Figure 14 shows the results for both 5 X 5 and 10 X 10 degree grids. As indicated, IGP spacing (within this range) appears to have minimal impact on the IONO error, as observed by a User.

CASE 2. Sensitivity to IONO Message Latency

The effect of IONO message latency was simulated using 5 and 10 minute delays between refreshing the IGP's and their use. Figure 15 shows the error growth due to latency. The WAAS specification indicates that the IONO error corrections (message 26) will be broadcast once per 2 - 5 min. Unless the reserved messages are broadcast at high rates, WAAS should be able to refresh all IGP's within several minutes. However, care should be taken to ensure this happens, especially during times of rapid changes in the IONO delays.

CASE 3. Modified IGP IONO Algorithm

Figure 16 shows that selecting the 10 pierce points closest to an IGP has the potential of reducing the Users IONO error. In addition, the WMS processing load is reduced.

CASE 4. Impact of Losing WRSs

Figure 17 illustrates sensitivity of the computed IONO delays at the IGP's to loss of the WRS in Alaska. Because this station is located on the perimeter of the WAAS network the impact on local IONO is an order of magnitude greater than due to the loss of a station near the network's centroid.

WAAS IMPACTS ON MILITARY RECEIVER DESIGN

The primary differences between the signal broadcast by the WAAS GEO satellites and the C/A signal broadcast by the GPS satellites are: (1) the data message content, (2) the C/A coder implementation and (3) the data rate. The latter appears to have the most significant impact on military receiver design, should changes be made to acquire the WAAS signal. The data rate for the WAAS message is 250 bps while that for the GPS is 50 bps. To conserve satellite transmitter power, furthermore, the WAAS data stream is encoded (with a rate 1/2, constraint length 7, Forward Error Correction (FEC) code) before being modulo 2 added to the PRN code. The 250 bps data stream is actually transmitted at 500 symbols per second.

The current generation of DoD receivers will not be able to acquire the WAAS message; both hardware and software modifications will be required to accomplish this. These receivers do not have spare hardware channels; to acquire and track the WAAS signal would require either (i) multiplex utilization of the existing hardware channels with attendant software complexities or (ii) additional hardware channel(s). Additional hardware may be necessary in any case

because the codes assigned to the GEO satellites cannot be implemented using the two-tap selection derived for the GPS C/A codes.

Baseband processing in the current generation of DoD receivers use a Predetection Interval (PDI) of 20 ms (during state 5 tracking), and carrier phase tracking and data demodulation operations are based on detecting the bit transitions that occur at 50 Hz. To extract the WAAS signal in the same manner would require a PDI of 2 ms and monitoring for bit transitions at 500 Hz. In addition a Viterbi decoder would have to be implemented to extract the 250 bps data from the 500 baud symbols. Implementing this higher rate processing within the existing channel management and receiver processing architecture would entail substantial software modification and an extensive re-test and validation effort. The software task is compounded if no additional hardware channels are introduced.

The extensive hardware and software modifications required to make the current generation of DoD receivers compatible with the WAAS signal renders this approach impractical.

An alternative approach would be to install a dedicated multi-channel WAAS receiver card in, for example, a control display unit (CDU), and transfer the WAAS integrity and correction information to the DoD receiver over the 1553 bus. The multi-channel capability would be needed to ensure uninterrupted access to the GEO signals. The drawbacks of this approach are: (1) a separate antenna subsystem may be required, (2) new ICD-GPS-059 messages would have to be defined and implemented and (3) integrating the additional GEO pseudorange measurements with current receiver software (if required) would be difficult. However, these complications are not insurmountable. For example, military flight trials using differential corrections transmitted over the 1553 bus, as described in published technical papers, indicate that this concept is practical and can provide CAT 1 navigation accuracy. In a similar manner, integration of a WAAS receiver card would give full access to the WAAS correction and integrity data.

MILITARY TRAINING AND TEST ACTIVITIES IN THE WAAS ENVIRONMENT

The WAAS will provide WDGPS corrections and integrity messages, with very high availability, to all Users in the SVOL. This could have benefits to certain military activities as described below. However, when assessing any benefits one must recall that WAAS messages are unsecured (at currently defined) and, therefore, would never be used for military operations in hostile environments.

INSTRUMENT FLIGHT IN THE NAS: This application is self evident. Military User Equipment would receive the WAAS messages for navigation during enroute, terminal and precision approach phases of flight in the NAS.

EQUIPMENT FIELD TESTING: Currently, local area differential GPS (DGPS) is used to provide time-space position indication (TSPI) in support of aircraft, ship and land vehicle test programs. Data from WAAS could be used in a similar fashion to provide TSPI over the entire SVOL. There are several ways to achieve such a capability. With modifications, current military receivers should be capable of receiving the WAAS messages. This implies the availability of continuous real time position accuracies in the 3 - 8 meter range across the entire SVOL. Another

method would be to acquire a copy of the data stored by the WMSs. The WAAS specification requires that WRS data be recorded for possible future use, this includes the satellite code and carrier phase measurements made by all WRSs. This data could be selectively used in a post test mode to produce accurate TSPI at locations in the area covered by the WRSs. It should be noted that tests could be conducted outside of the SVOL boundary with adequate measurement coverage. This is due to the strict requirements placed on WAAS performance, e.g., WRS measurements may be available for TSPI but all WAAS requirements may not be met at a test site outside the SVOL.

GPS integrity monitoring by the WAAS could be another benefit to military test programs. For example, during GPS UE tests there are at times questions as to the cause of a "glitch": it could be the receiver or the SIS. The WAAS satellite correction and integrity messages could be used to guide analysts in resolving the problem. In a similar fashion new GPS satellites could be monitored for operation during their initial on-orbit check out phase. And WAAS data could be useful in assisting military test organizations to perform operational testing and evaluation (OT&E).

TRAINING: There are land and sea training situations where enhanced position accuracy would be beneficial. For example, the military currently uses local area DGPS to position personnel and equipment during land exercises. Here, a local GPS reference station is often used in conjunction with low cost mobile receivers. Purchased in quantity, WAAS capable receivers should be available at competitive prices and the entire system would not be subject to the LOS restrictions of a local DGPS system. In addition, the cost and logistics associated with the reference system and transmitters would be eliminated. Another example would be amphibious or at sea training where a low cost C/A receiver, with accuracy comparable to current military GPS, could be used effectively.

GPS LABORATORY TEST ENVIRONMENTS: In the event current military UE (e.g., Receiver 3A and/or MAGR) is modified, or new equipment purchased, to receive the WAAS signals, then the changes must be reflected in GPS signal simulators. Government laboratories use simulators to test bid samples, isolate problems, validate equipment modifications and explore new operational uses for GPS. The following changes will be needed to accommodate WAAS and to test new applications:

- Increase the number of hardware channels to accommodate a minimum of 3 GEO satellites.
- Incorporate the new WAAS L1 gold codes and data messages.
- Add software for simulating: IONO delays throughout the SVOL, GPS/WAAS time offset, flight profiles representing precision approaches and satellite failure modes.
- Modify data collection and post test analysis software to accommodate the new messages and associated data analysis requirements.

SUMMARY

The WAAS specification places stringent requirements on all components: the system design, the ground hardware and software and the space hardware and software. Substantial progress has been made to evaluate design concepts and algorithms, and to demonstrate navigation performance through flight trials. Algorithm analysis and simulations of the SVOL must be extended to fully address the WAAS availability, integrity and continuity of function requirements. This may require the introduction of candidate designs for the WAAS ground and space segments. Because of the potential for reducing equipment costs and due to the availability of accurate navigation over wide areas, the military may find new uses for the WAAS signals-in-space.

REFERENCES

1. Wide Area Augmentation System (WAAS) Specification, U.S. Department of Transportation, FAA-E-2892, May 9, 1994.
2. Sams, M., Van Dierendonck, A.J., Hua, Q., "Satellite Navigation Accuracy and Availability Modeling as an Air Traffic Management Tool", Proceedings of the ION 1995 National Technical Meeting, Anaheim, CA, January 18-20 1995.
3. Pullen, S., Enge, P., Parkinson, B., "Simulation Based Evaluation of WAAS Performance: Risk and Integrity Factors", Proceedings of the ION GPS-94, Salt Lake City, UT, September 20-23 1994.
4. Haas, F. M., Analysis of Recent WAAS Flight Tests", Proceedings of the ION 50th Annual Meeting, Colorado Springs, CO, June 6-8, 1994.
5. Kee, C., Parkinson, B., "Wide Area Differential GPS as a Future Navigation System in the U.S.", Proceedings of the IEEE PLANS '94, Las Vegas, NV, April 11-15 1994.
6. Wulschleger, V., et.al., "FAAs Wide Area Augmentation System (WAAS) Initial Results of Cross Country Flight Tests", Proceedings of the ION-GPS-94, Salt Lake City, UT, September 20-23 1994.
7. Phlong, W., Elrod, B., "Availability Characteristics of GPS and Augmented Alternatives", Navigation, Vol 40, No. 4, Winter 1993-1994.
8. Walter, T., et. al., "Flight Trials of the Wide Area Augmentation System (WAAS)", Proceedings of the ION-GPS-94, Salt Lake City, UT, September 20-23 1994.
9. El-Arini, M. et. al., "The FAA Wide Area Differential GPS (WDGPS) Static Ionospheric Experiment", Proceedings of the ION National Technical Meeting, San Francisco, CA, January 20-22, 1993.
10. Kee, C., Parkinson, B., Alexrad, P., "Wide Area Differential GPS", Navigation, Vol. 38, No. 2, Summer 1991.

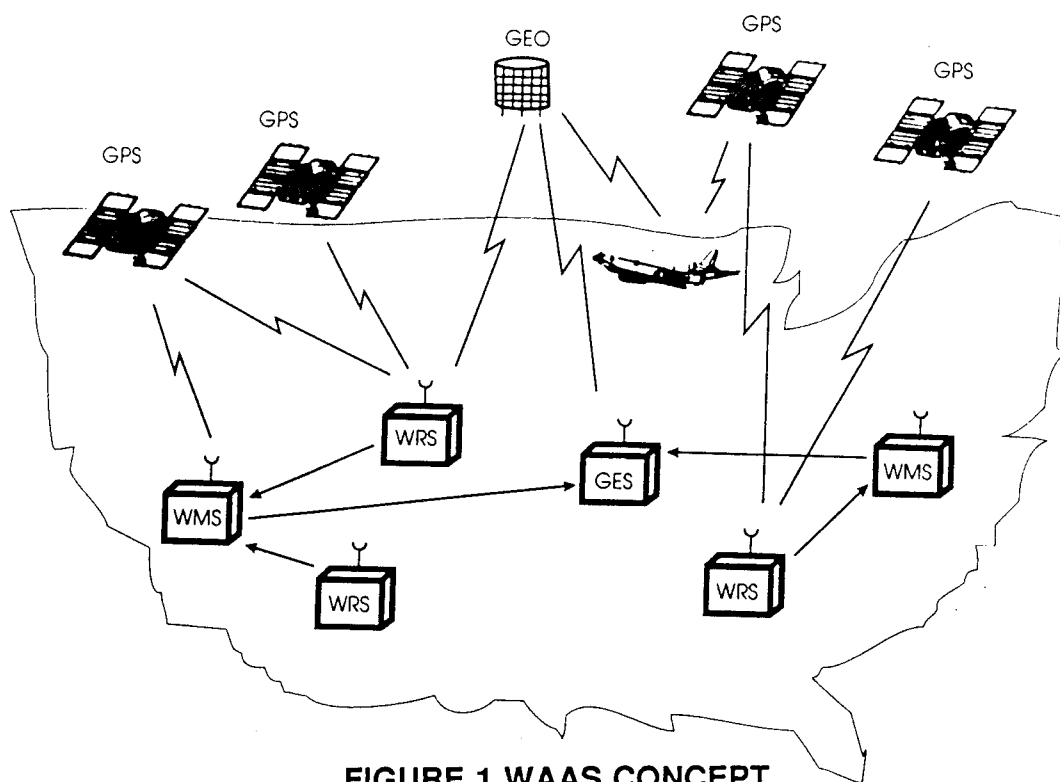


FIGURE 1 WAAS CONCEPT

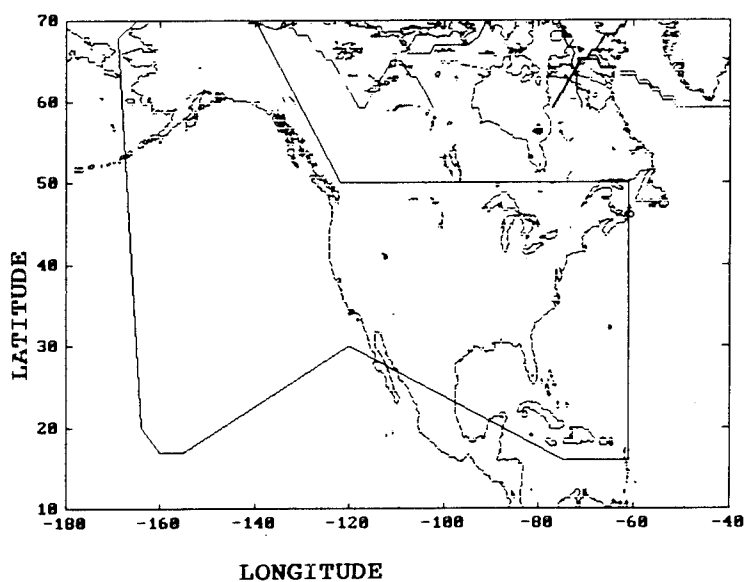


FIGURE 2 WAAS SERVICE VOLUME

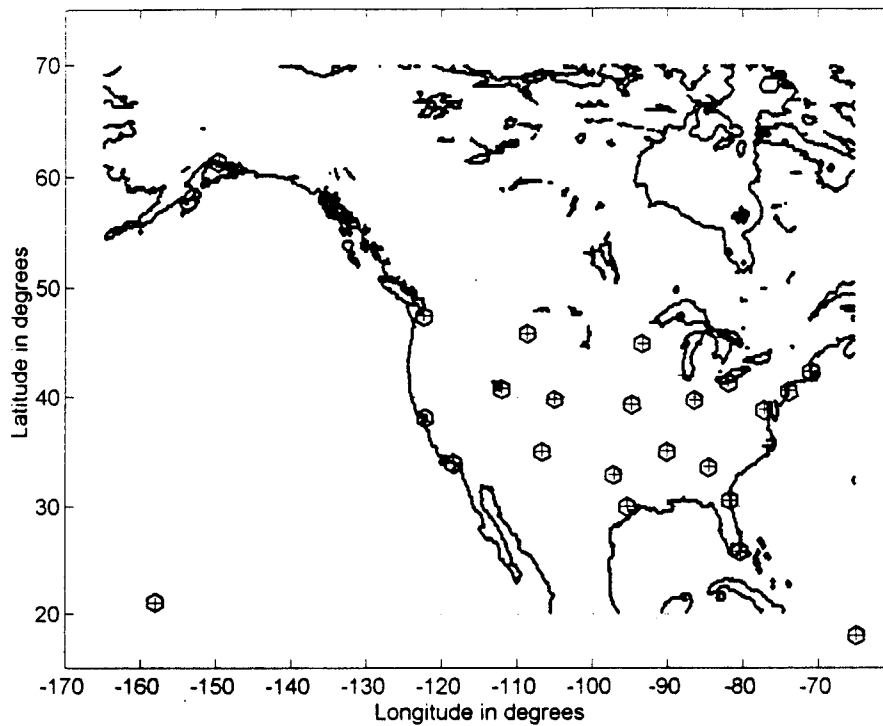


FIGURE 3 NETWORK OF 24 WRSs

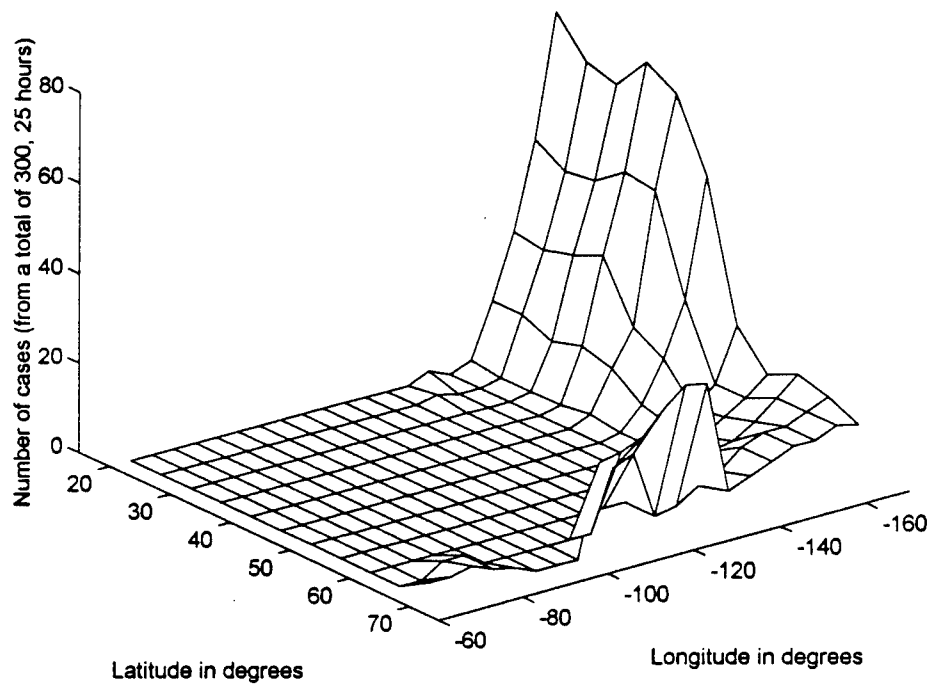


FIGURE 4 FAILURE CASES WITH 24 WRSs

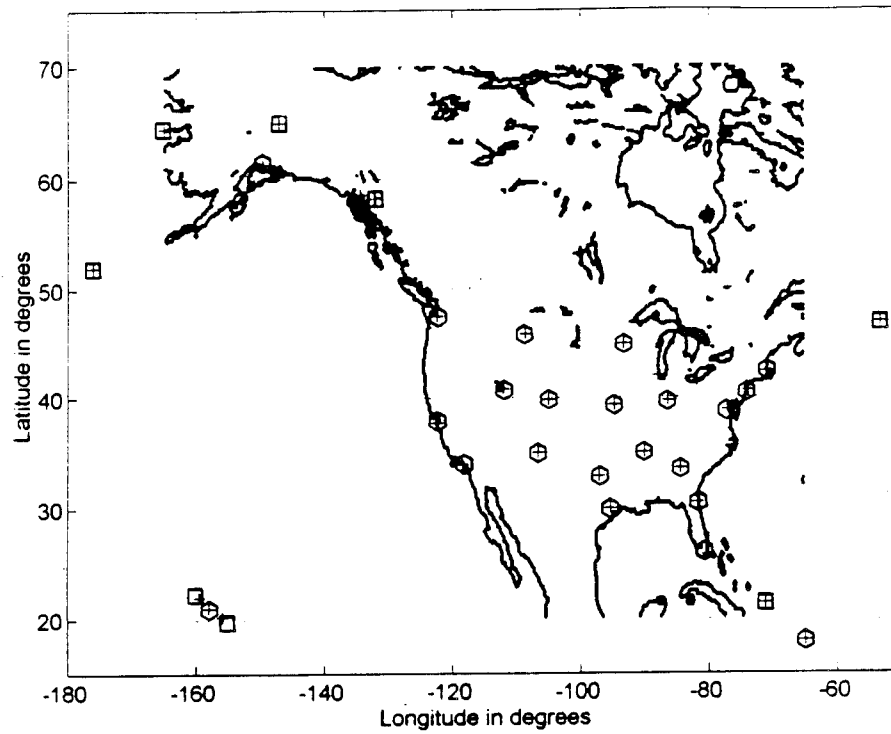


FIGURE 5 NETWORK OF 32 WRSs

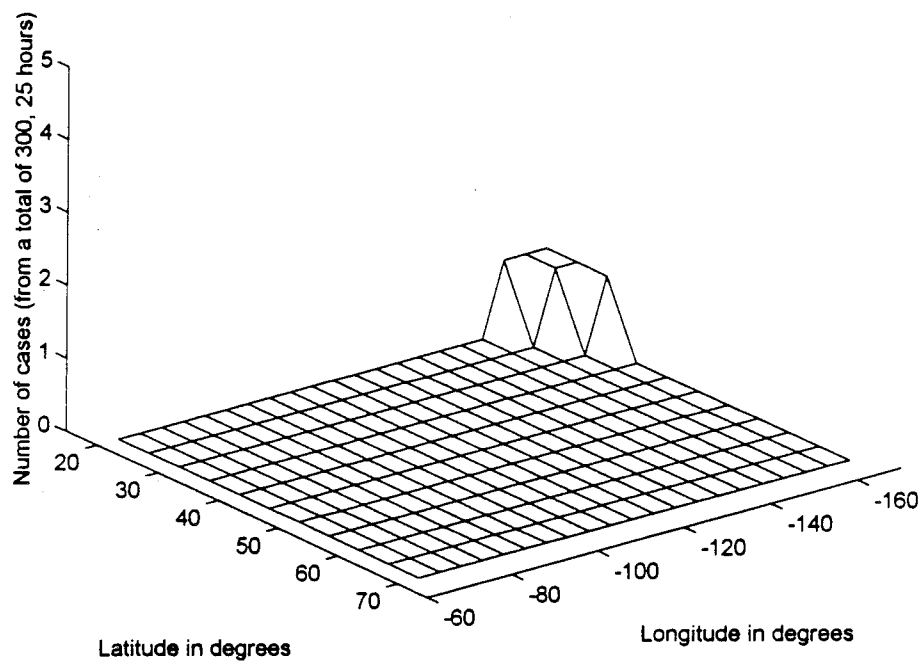


FIGURE 6 FAILURE CASES WITH 32 WRSs

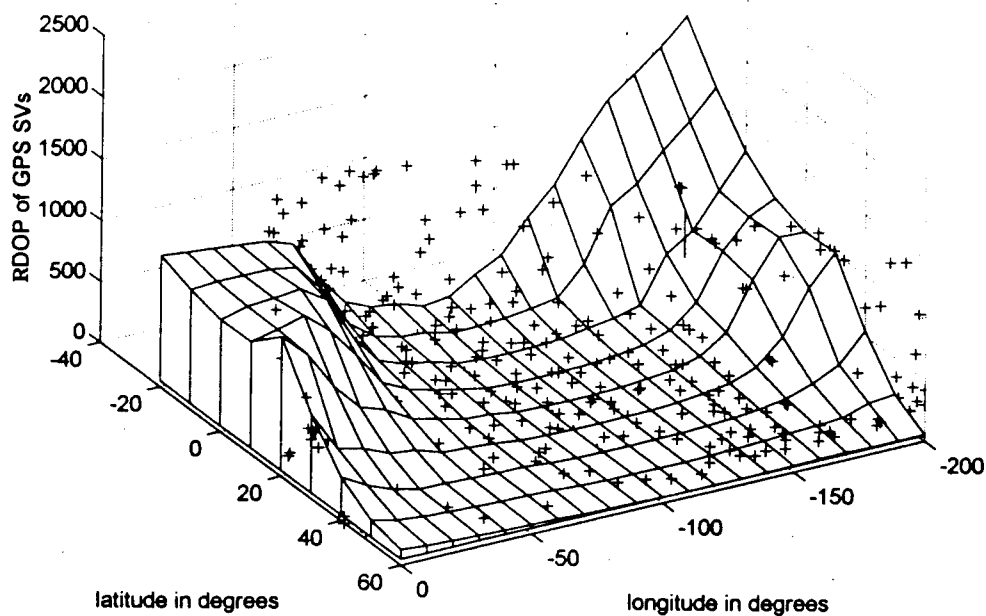


FIGURE 7 EXAMPLE OF RDOP

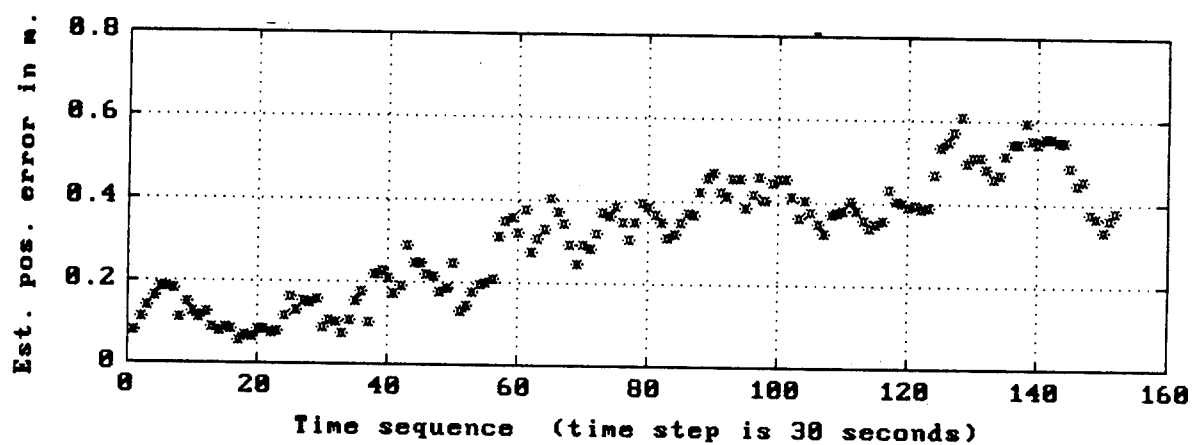


FIGURE 8 POSITION ERROR RESIDUALS FOR SV #21

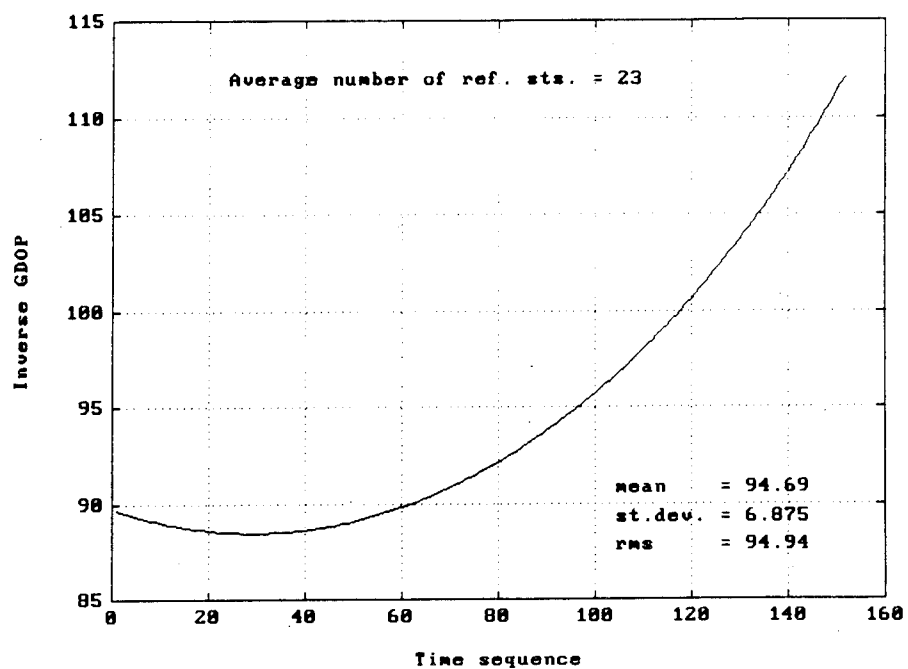


FIGURE 9 RDOP FOR SV #21

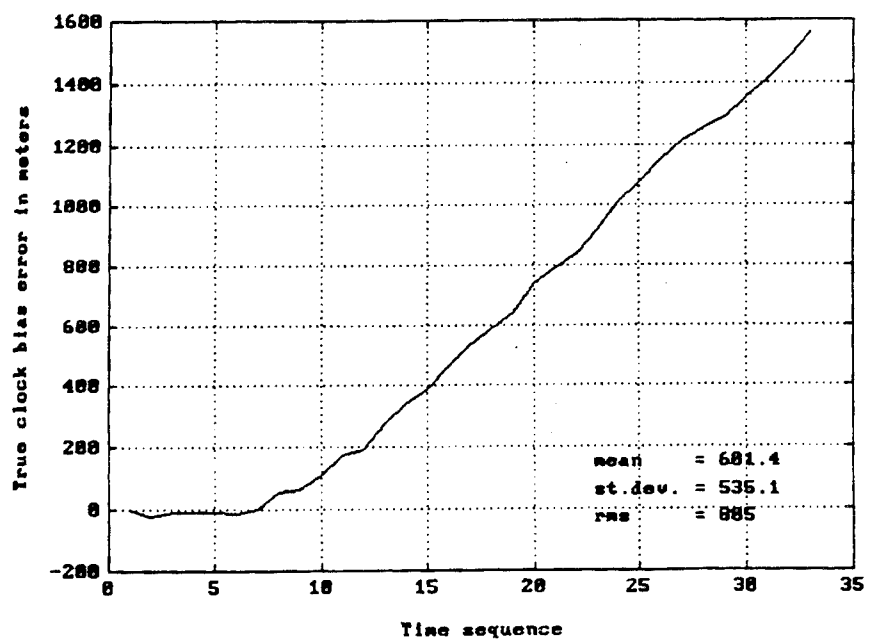


FIGURE 10 SATELLITE CLOCK ERROR

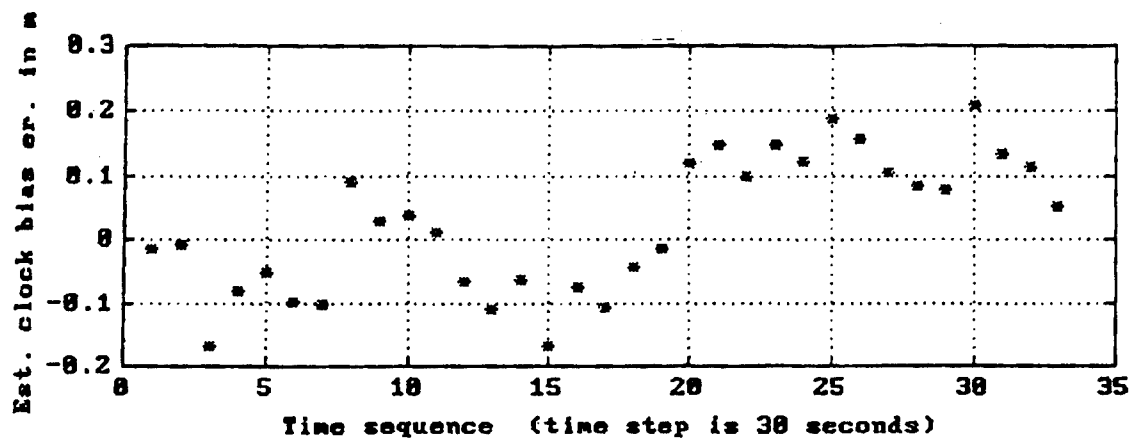


FIGURE 11 CLOCK ERROR RESIDUAL

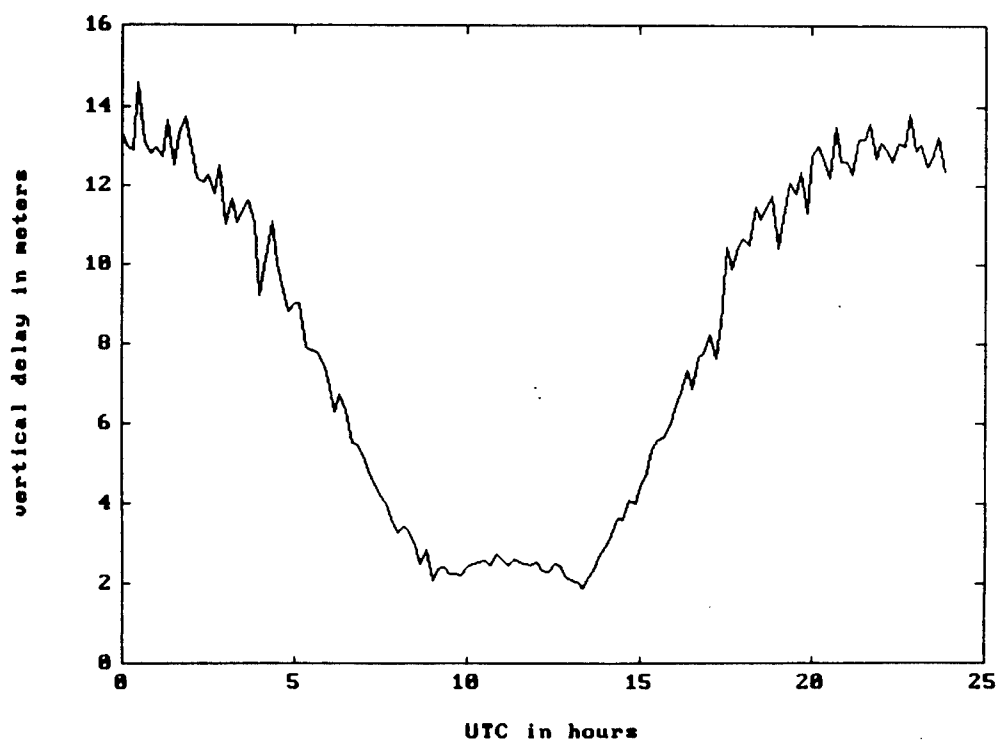


FIGURE 12 IONO TRUTH MODEL

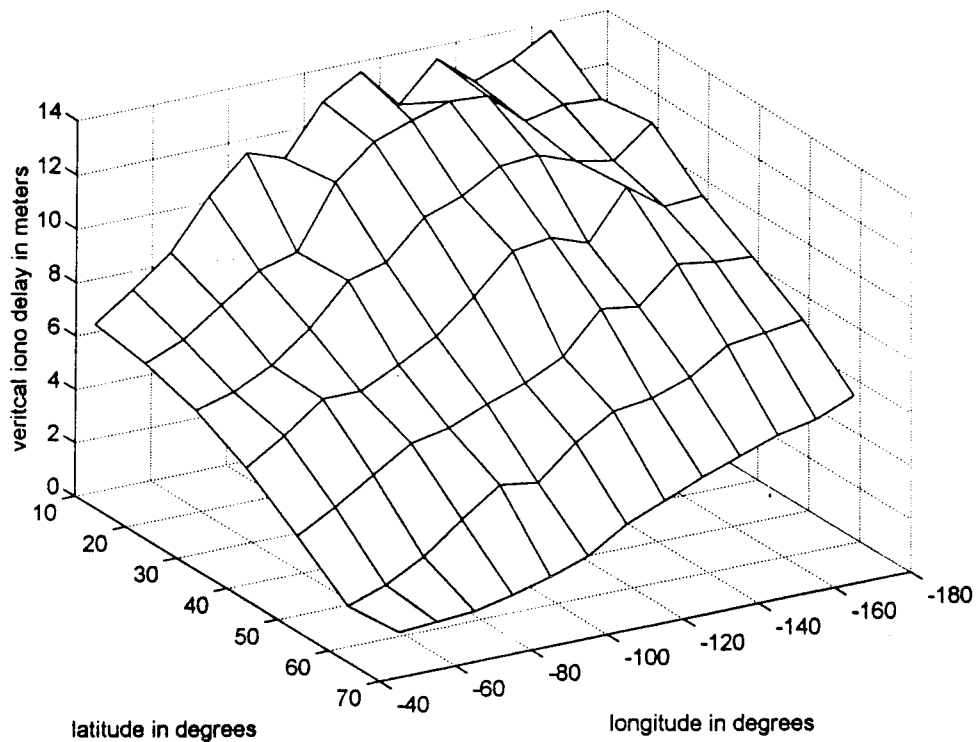


FIGURE 13 VERTICAL IONO DELAY ACROSS THE SV

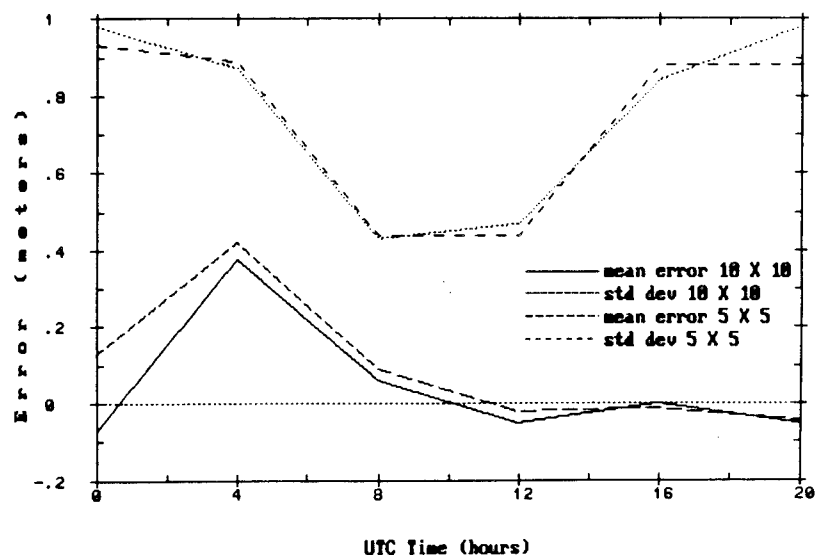


FIGURE 14 SENSITIVITY TO GRID SIZE

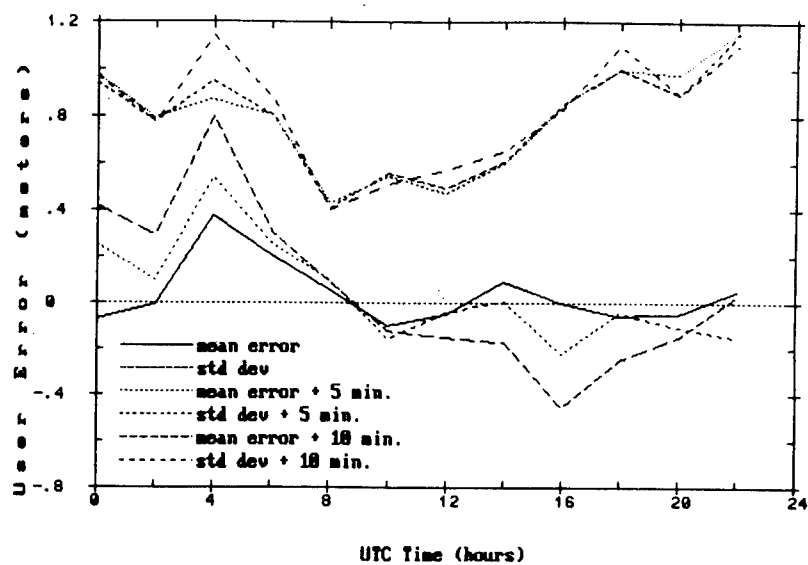


FIGURE 15 SENSITIVITY TO IONO LATENCY

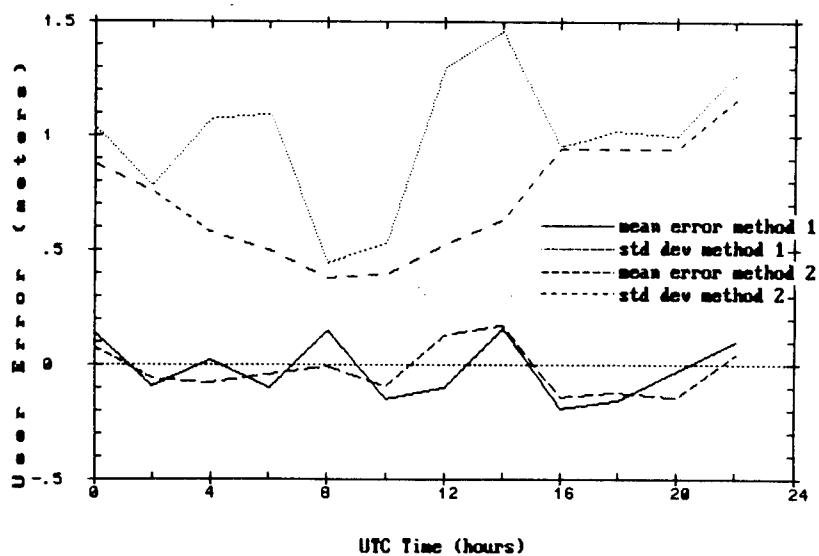


FIGURE 16 SENSITIVITY TO INTERPOLATION ALGORITHM

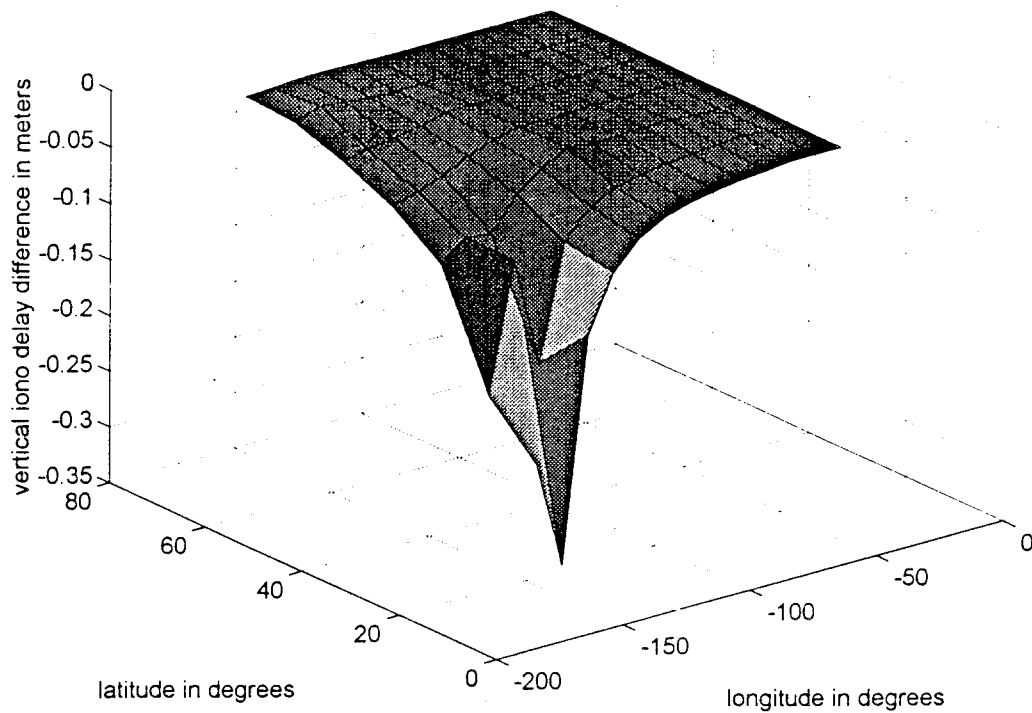


FIGURE 17 SENSITIVITY TO LOSS OF THE HAWAII WRS

THIS PAGE LEFT BLANK INTENTIONALLY

Results of Differential GPS Support for a Coast-to-Coast Flight Test

Capt Daniel Uribe
746th Test Squadron, Holloman AFB, NM

Mr. Dan S. Crouch
746th Test Squadron, Holloman AFB, NM

Mr. Darwin Abby
Intermetrics, Inc., Holloman AFB, NM

Abstract- The 746th Test Squadron (746 TS) established a Test Support Network (TSN) throughout the Continental United States (CONUS) to support flight testing of GPS Integrated Systems. The TSN consists of several Differential GPS (DGPS) ground stations located throughout the CONUS, a data link for data transfer, and a data processing facility at Holloman AFB, NM. GPS data from flight test vehicles and ground stations is transmitted to Holloman AFB and processed to generate a DGPS reference trajectory. The GPS integrated system navigation solution and any navigation or weapon system test item data is processed and evaluated by 746 TS. This paper presents results from a B-2 test mission which was flown from Edwards AFB, CA to Andrews AFB, MD and back in October 1994. During the mission of over 10 hours, data was collected on the aircraft and at the ground stations located along the route. The DGPS reference trajectory data is evaluated and results presented to demonstrate the TSN capability.

BACKGROUND

With the Congressional mandate to integrate GPS user equipment into all DOD avionics systems by the year 2000, a substantial number of DOD platforms have entered the flight test phase of the avionics suite GPS upgrade lifecycle. The increasing number of aircraft requiring effective and cost efficient test reference data and analytical support has yielded an increasing number of flight test support requirements for the 746 TS. In response to the increasing number of platforms requiring test support, the 746 TS developed the TSN which consists of a series of five unique DGPS ground reference stations that can provide continuous Time-Space-Position-Information (TSPI) throughout the greater CONUS.

As the mission capabilities of GPS become more and more valuable and understood by platform integrator's, unique state-of-the-art platform mission requirements must be tested and evaluated to determine system effectiveness. Due to airspace limitations on traditional test ranges, many platform tests requiring TSPI are confined to fly "within" a fixed area, thus limiting extended mission tests. As specialized mission requirements mature, so must the test capabilities. An example of the unique diversity in testing has been the USAF's B-2 bomber.

On 25 October 1994, a B-2 aircraft flew on a record breaking 10.6 hour round-trip avionics and human factors test mission from Edwards AFB, CA to Andrews AFB, MD and back. The first round-trip, coast-to-coast mission flown by the B-2 covered more than 6,000 nautical miles non-stop, taking off at 8 a.m. and landing just after sunset. The mission also included a fly-by for

the former Air Force Chief of Staff's retirement ceremony at Andrews AFB, MD. Aerial refueling tanker support was provided by a KC-10 from Seymour-Johnson AFB, NC and a KC-135R tanker staged out of Edwards AFB, CA.

The B-2 Consolidated Test Force (CTF) uses the 746 TS DGPS reference station at Edwards AFB to support flight testing in the western United States. The possibility of using the 746th TSN which includes several reference stations throughout the US was considered for supporting this flight. This would enable the CTF to collect reference data to support the entire coast-to-coast test mission. Figure 1 shows the flight trajectory and the TSN stations used for this historic mission. The 500 mile circle around each reference station site represents the DGPS coverage for that area. DGPS accuracy of 3-5 meters 3drms in a 500-750 mile radius around a reference station has previously been verified.

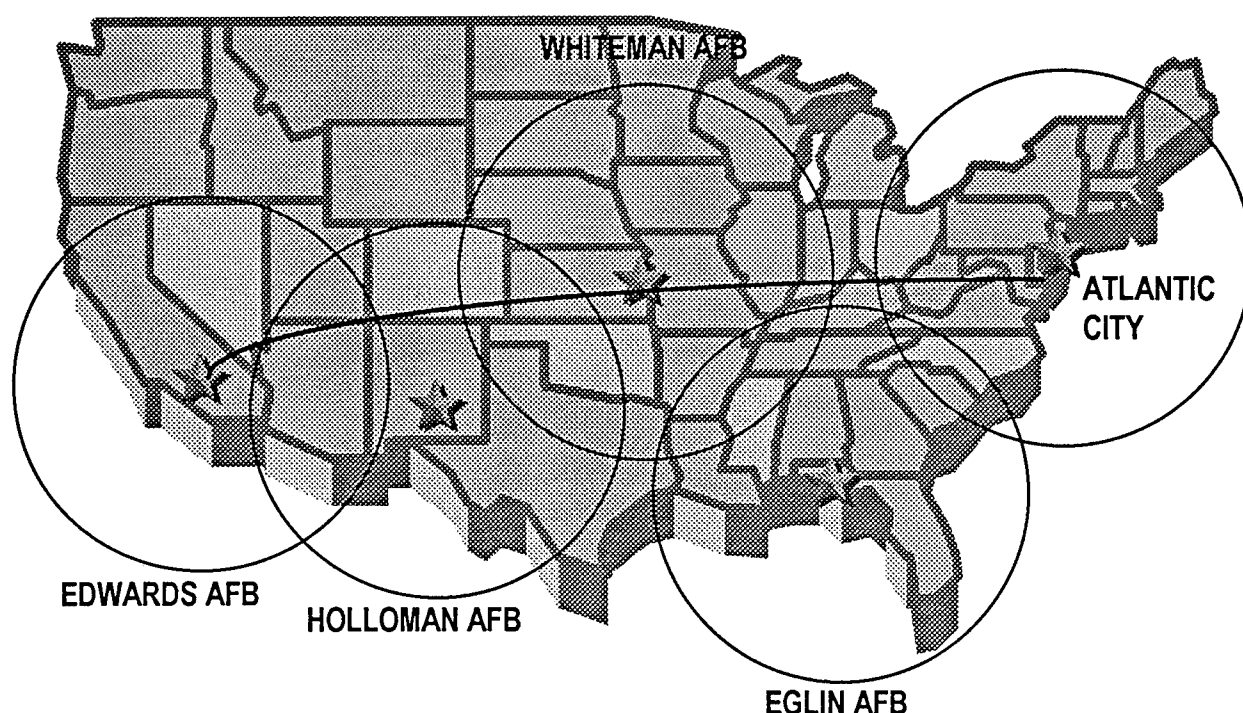


Figure 1. B-2 Flight Test Support Network Stations

Testing over large geographic areas was conducted by flying from test range to test range and obtaining tracking instrumentation support only over the physical range area. Coverage outside the range area was limited to data from flight control radars or some limited DME system to at least monitor the path of the vehicle. The TSN provides a solution for a wide area test support project.

This paper expands on the unique capability of the TSN and provides test results for the B-2 bomber coast-to-coast mission.

TSN CONCEPT ^[1]

The objective of the TSN is to provide a cost effective, centralized, GPS test support capability for integration. TSN support is available at any stage of the integration development and at virtually any location within the continental US. Since the major expenses in any flight test program are range support, system analysis, and the costs associated with moving program test resources (hardware and personnel) to a test range, TSN DGPS capabilities provide a new perspective to the art of system testing.

The TSN consists of a series of Differential GPS ground stations called Satellite Reference Stations (SRS) strategically deployed at military installations throughout the United States. Figure 2 shows the current locations for the network stations. The 500 nautical mile radius circles around each station represents the area of coverage for aircraft operations. During a test mission, the SRS collects all-in-view GPS data and a data acquisition system onboard the test aircraft records raw GPS measurements as well as the GPS integrated navigation solution. Once the mission is complete, an on-site team transmits the data via an electronic link or courier services to the 746 TS data processing facility. The processing team processes the raw GPS measurements with the SRS data to generate a reference trajectory or Time Space Position Information (TSPI). The test team uses this product plus other recorded GPS, INS and system data to evaluate the GPS integration.

The DGPS capability has been used for several years on a local basis to support such programs as the B-2 avionics test program, the T-39 Non-Precision and Precision Approach test programs, the B-52G, F-16C, A-10A, C-130 SCNS, AV-8B, F/RF-111C, F-111A/E, and F-111F GPS integration test programs. Mobile SRS's can be deployed to customer requested locations to support programs in areas not currently covered by an existing TSN station.

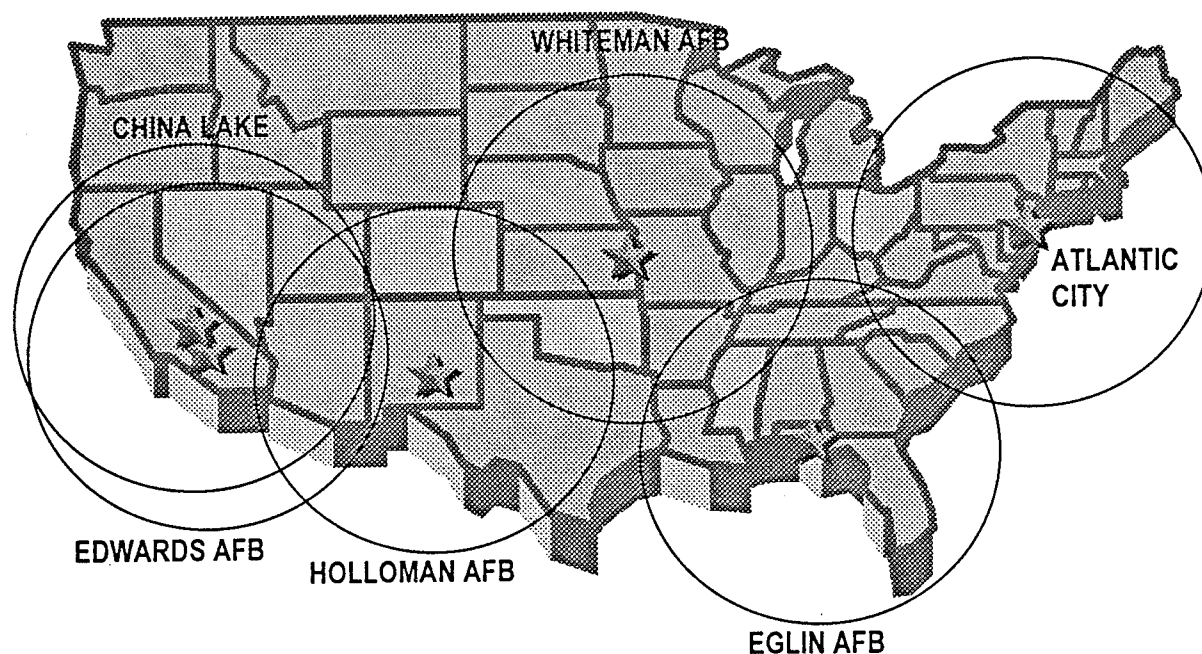


Figure 2. TSN SRS Locations

TSN COMPONENTS ^[1]

Satellite Reference Station (SRS)

The SRS is a self-contained GPS ground reference station which is designed to support two primary functions. It monitors the GPS Space and Control Segment by tracking all-in-view GPS satellites and detects performance anomalies which affect GPS navigation. This quality control or integrity monitoring function is required to isolate space and control segment errors from user equipment errors. Secondly, the SRS tracks all satellites in view and computes pseudo-range and delta-range corrections in real time to produce DGPS TSPI in support of test programs. All data is recorded and processed post-mission.

Aircraft Instrumentation

The TSN is built around the use of the DOD Collins 3A or Miniaturized Airborne GPS Receiver (MAGR) in the aircraft. Raw pseudo-range and delta-range measurements from the front end of the receiver along with other GPS and sensor data such as an INS are recorded on board the test aircraft for post-processing. The primary data interface is the RS-422 Instrumentation Port, however, MIL-STD-1553B data can also be made available for on-board recording.

Data recording is provided by one of two techniques. If room is available, a PC Buffer Box can be interfaced to the IP and digital data recorded directly on a PC compatible disk medium. If space is limited, the RS-422 data can be recorded on one channel of an existing analog recorder which is normally on board to support flight tests. The analog tape is then replayed through a PCBB on the ground after the mission and recorded on PC compatible disk medium. If the aircraft is not integrated with a Collins 3A, MAGR, or does not have a compatible ICD-GPS-150 interface, a small instrumentation pallet can be installed for GPS receiver data collection.

Software

All SRS tracking software and post-processing software supports any GPS receiver using Interface Control Documents such as ICD-GPS-150 and ICD-GPS-059. The test team can use the data products produced by the SRS to evaluate the integrated GPS navigation solution as well as the GPS and INS sensor data. Data products include a wide variety of listings and error plots for any of the recorded parameters. The SRS pseudorange and delta range measurements are processed to generate a "ground truth" which is used as a baseline to compare with the test item and isolate potential anomalies.

Integration Analysis and Reporting

Evaluation of the integration is performed using data from four sources when available. These are SRS ground truth, GPS receiver, INS, and integrated solution. The reference station data helps to isolate any GPS problems or errors. The INS data can be plotted and evaluated to show any INS anomalies. Using all the available data, 746 TS analysts analyze the data from each mission to evaluate the performance of the system, identify problems, evaluate results against

objectives and report the results in a mission summary. They also prepare a report to accompany the data pack for each mission. At the conclusion of the test program, the 746 TS summarizes all the results and prepares a final report for submittal to the integrating agency.

FLIGHT TEST DESCRIPTION

The B-2 aircraft instrumentation used to support the generation of TSPI includes a Collins 3A receiver, Cesium beam frequency standard, and a PC Buffer Box. The high precision external frequency source replaces the internal oscillator and is used by the receiver to support 3 satellite clock aided generation of TSPI. This technique is used when four satellites are not available such as in turns or times of satellite blockage. Flight test data from the receiver Instrumentation Port is collected on a PC Buffer Box hard disk. The data is downloaded after the mission to a Bernoulli disk for transport to the data processing facility.

GPS tracking data was collected at each reference station throughout the entire mission. This would not be necessary in an operational test scenario, but for this mission we wished to do some evaluation of the capability over long distances. All data was shipped to 746 TS for processing.

DATA PROCESSING

This cross-country mission presented a target of opportunity to evaluate the continuity and accuracy of the DGPS TSPI for a 6,000 nautical mile trajectory which utilized data from four TSN reference stations. Due to the sensitivity of the B-2 system, we were unable to include data from the item under test, however, the project personnel indicated the avionics test met the objectives of the mission.

This left us with three types of GPS data to use in our evaluation. First, the Collins 3A GPS navigation solution is always available at one hertz and represents, in this case, a reference of 6-8 meters accuracy.

The second source of data is the TSPI generated from each of the reference stations. As stated earlier, TSPI within 500-750 miles of an SRS meets 3-5 meter 3 drms accuracy. For this mission, TSPI was generated using data from each station for the entire mission so we could perform comparisons. All stations in this case are over 500 miles apart so our comparisons have to extend beyond the normal range.

The third source of data is the "ground truth". Pseudo-range and delta-range measurements from the SRS are run through a navigation filter using the measurements from the same satellite constellation that was used by the aircraft receiver. This static navigation solution is differenced with the SRS antenna surveyed coordinates to derive a navigation error. The major component of this error is due to the space and control segment. The space and control segment errors are then removed from the total GPS navigation error which leaves the user segment error. The user error is then compared with the DGPS TSPI. This process is normally used to isolate space and

control segment problems as a part of the quality control function, but in this case, it provided another source to evaluate the accuracy of the DGPS TSPI.

RESULTS

The data in Table 1 shows the differences between the Collins 3A navigation solution and DGPS TSPI for segments of the mission. The segments are broken down into the areas within each SRS area of coverage. Where there was overlap, the break point was taken to minimize the distance from each station or half way between the two stations. For example, between EAFB and HAFB where there is large overlap, the segments were divided at the midpoint between the two stations. For WAFB and ATL, which are 1,062 miles apart, the segments break very close to the edge of the circle around each point which is the 500 mile point.

Figure 3, see attachment, is a plot of the GPS navigation error for the entire mission using DGPS TSPI as the truth reference. The results shown in Table 1 and Figure 3 are consistent throughout the mission and are typical of GPS navigation accuracy. During the period from approximately 1900 to 2000, the aircraft was orbiting in the Andrews AFB area and participating in the fly-by. The GPS errors during this period are typical of an un-aided GPS receiver during banking maneuvers. The large step functions occurring during the period from 2130 to 2250 are typical of satellite constellation switches when one or more satellites have large errors. A closer review of the

Table 1, GPS - TSPI

REFERENCE STATION	TIME (Z)	RMS ERROR (m)		
		HOR	VERT	TOTAL
EDWARDS AFB (EAFB)	1500-1550	6.5	1.5	6.7
HOLLOMAN AFB (HAFB)	1550-1630	2.1	2.2	3.0
WHITEMAN AFB (WAFB)	1630-1750	4.4	2.7	5.2
ATLANTIC CITY (ATL)	1800-2115	5.0	2.5	5.7
WHITEMAN AFB	2125-0005	5.1	5.0	7.2
HOLLOMAN AFB	2250-0045	1.9	2.5	3.2
EDWARDS AFB	0045-0130	3.5	6.5	7.4

satellites being tracked during that period showed that SV 15, although within specification, was off a few meters from the other satellites in view. Also, during that same period, SV 14 was just rising and low in elevation which could explain the step when the receiver picked it up at 2230. In general, GPS errors were within 6-9 meters RMS throughout the mission.

The second data processing technique involves using ground truth to try to eliminate the space and control segment errors noted above and used to evaluate DGPS TSPI results. A ground truth, as described earlier, was generated for the entire mission and is shown in Figure 4 (Attachment). As seen, there is significant correlation with the GPS TSPI error plot in Figure 3. The next step involves subtracting the space and control segment errors or ground truth from the GPS navigation solution and differencing that with the DGPS TSPI which results in the plot shown in Figure 5 (Attachment). The error includes both the user segment errors and the TSPI errors for the entire mission. The RMS errors, on the order of 2.5 meters, represent an upper limit accuracy for the extended DGPS TSPI mission.

The third data evaluation process included differencing TSPI generated from one reference station with the TSPI generated from a second station. For example, TSPI differences between the EAFB and HAFB segments is the difference between the individual TSPI generated between the two sites. The results are shown in Table 2. Since we have no absolute truth reference this procedure provides, as a minimum, an internal consistency check. The distances between stations are all over 500 miles and in the WAFB/ATL case, the distance is over 1,000 miles which stretches the limits of the process as developed. Special techniques and mission planning have been developed to extend the range in support of the B-2 when they use only the EAFB SRS.

Table 2, TSPI - TSPI

STATIONS	TIME (Z)	RMS ERROR (m)			DISTANCE (miles)
		HOR	VERT	TOTAL	
EAFB-HAFB	1500-1610	5.2	4.2	6.8	690
EAFB-HAFB	0005-0045	0.8	6.9	6.9	
HAFB-WAFB	1610-1715	1.4	2.2	2.6	770
HAFB-WAFB	2255-0005	1.8	0.8	2.0	
WAFB-ATL	1715-1855	2.3	1.2	2.6	1062
WAFB-ATL	2020-2245	1.6	3.1	3.6	

Results comparing the HAFB/WAFB and WAFB/ATL segments show differences of 2-4 meters RMS error which is very good considering the large distances. On the other hand, there is a distinct difference in the results for the differences including EAFB data. Results comparing the EAFB/HAFB segment show differences of 7 meters RMS error. The data still meets the 3-5 meters 3drms accuracy quoted for 500 mile ranges since this data includes the errors from both stations, however, the data does point to a possible problem with the EAFB station. The EAFB antenna was recently moved and an increase in multipath error has been noted. Also, the survey of the new antenna location has not been verified. These two problems could possibly account for the larger errors shown.

SUMMARY

The record breaking October 25, 1994 coast-to-coast B-2 mission was an excellent target of opportunity to evaluate the TSN Concept. Four TSN stations were located in almost perfect position to support the mission. Although there are no other truth references available to support this evaluation, maximum use was made of on-board and ground station data to support the analysis. The continuity of the data was excellent with minimum loss of TSPI for the entire 6,000 nautical mile flight. The GPS navigation error derived by using the DGPS TSPI was typical of a Collins 3A receiver. By using a ground truth technique and comparing TSPI derived from different reference stations, the RMS error for the TSPI was on the order of 2-4 meters. Due to suspected multipath and survey errors with the Edwards AFB data, the TSPI errors from that station were on the order of 7 meters RMS. We were unable to present the test item data due to project sensitivity, however, we were advised that the data looked very good. The B-2 CTF uses the 746th DGPS TSPI on a regular basis and is able to speak from experience. The TSN capability introduces a effective and cost efficient means for testing GPS integrated systems over a large geographic area. While the challenge to integrate GPS into every military system by the year 2000 remains great, the increasing flight test TSPI data requirements can be met through proper planning and utilization of the Test Support Network.

REFERENCES

- [1] Uribe, D. and Abby D., Flight Test Methodology for Global Positioning System (GPS) Integrated Systems, IEEE PLANS-94, Las Vegas NV, April 1994

ATTACHMENT

Figure 3. Collins 3A Navigation - DGPS TSPI

Figure 4. GPS Ground Truth

Figure 5. Collins 3A Navigation - Ground Truth - DGPS TSPI

Mean	-0.36	2.72	2.42	5.31	Horiz	Total	Mean	1.15	1.51	Y	Z	Horiz	Total	Mean	1.61	-1.98	Y	Z	Horiz	Total
RMS	4.56	3.08	3.21	5.50	Horiz	Total	RMS	4.33	4.81	Y	Z	Horiz	Total	RMS	1.98	2.38	Y	Z	Horiz	Total
Std Dev	4.54	1.44	2.11	1.43	Horiz	Total	Std Dev	4.18	4.57	Y	Z	Horiz	Total	Std Dev	1.15	1.32	Y	Z	Horiz	Total

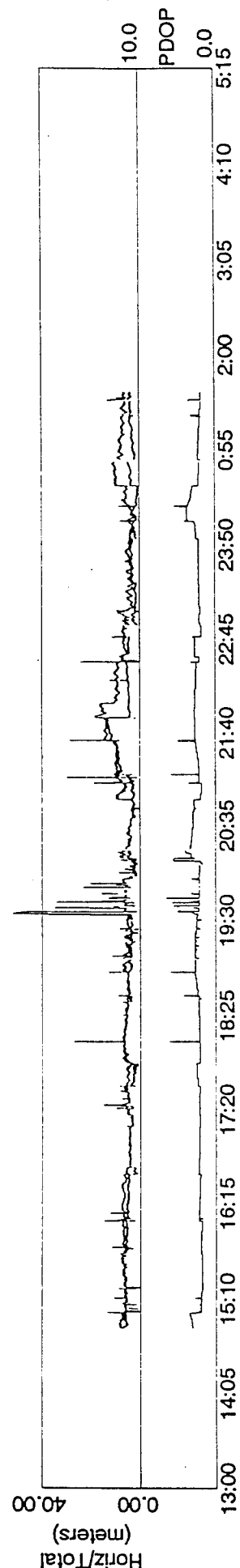
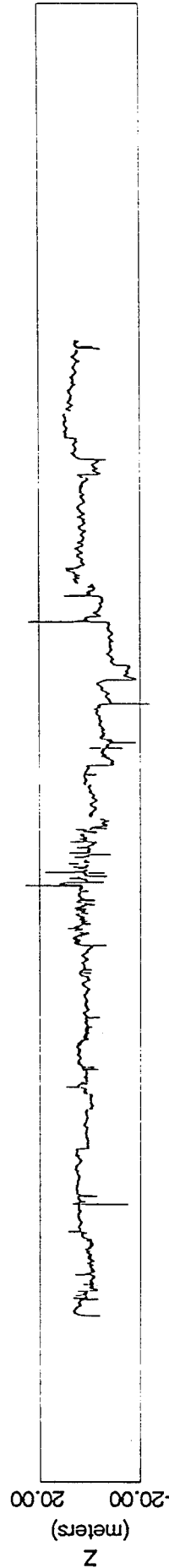
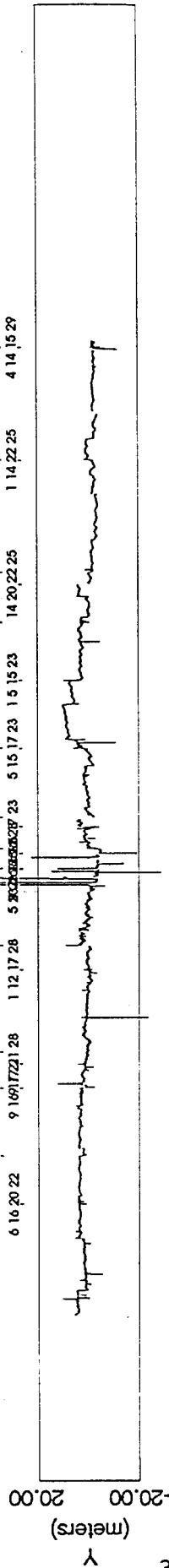
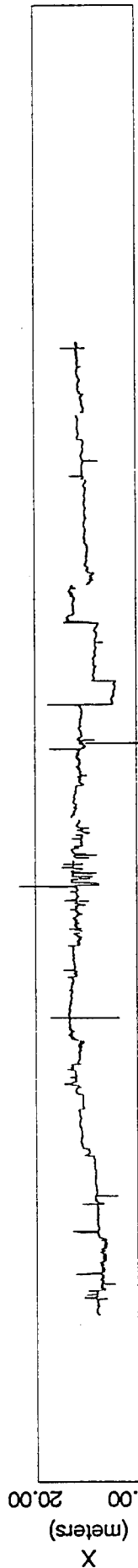


Figure 3. Collins 3A Navigation - DGPS TSPI

	X	Y	Z	Horiz	Total	Mean	X	Y	Z	Horiz	Total	Mean	X	Y	Z	Horiz	Total
Mean	0.89	0.43	-0.72	1.54	2.04		-0.01	0.15	-0.16	1.23	2.05		0.67	-0.02	-0.80	1.11	1.82
RMS	1.61	1.13	1.65	1.96	2.57		1.34	1.05	2.14	1.70	2.73		1.01	0.92	1.79	1.37	2.25
Std Dev	1.33	1.04	1.49	1.22	1.56		1.34	1.04	2.13	1.17	1.80		0.77	0.92	1.59	0.79	1.32

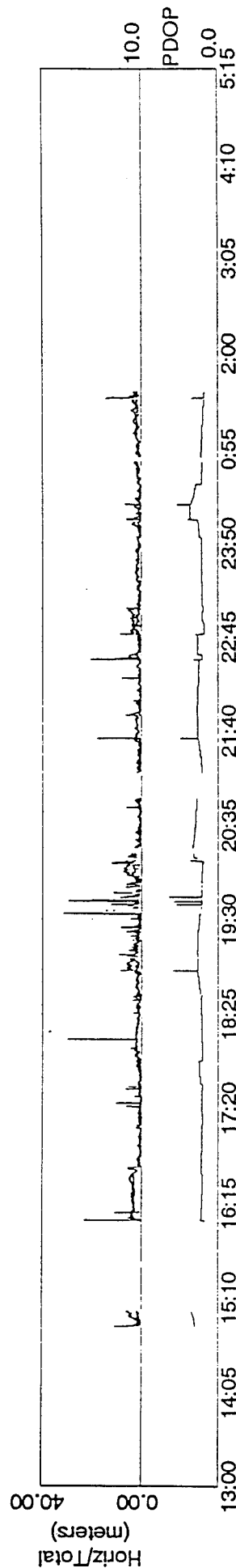
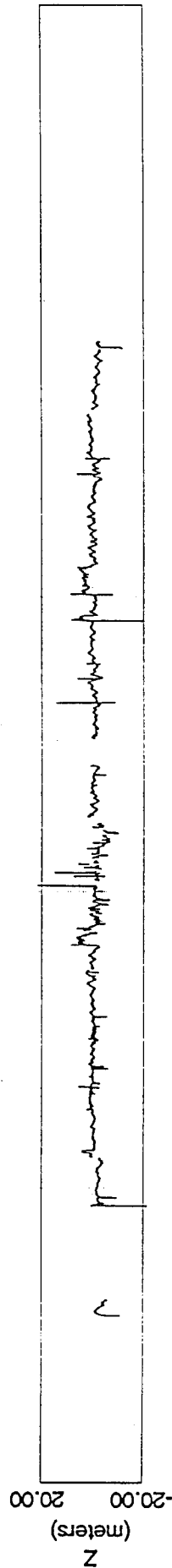
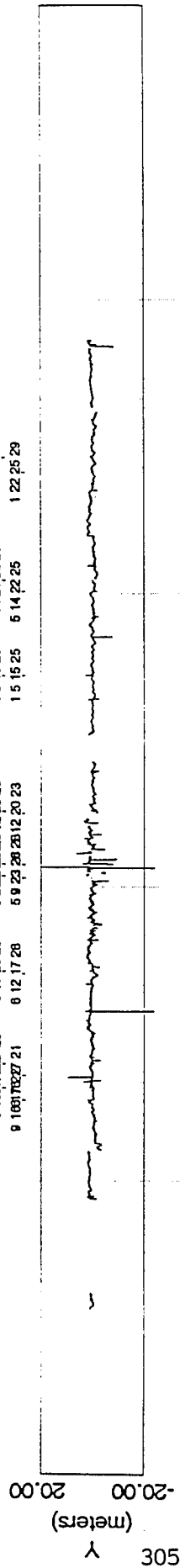
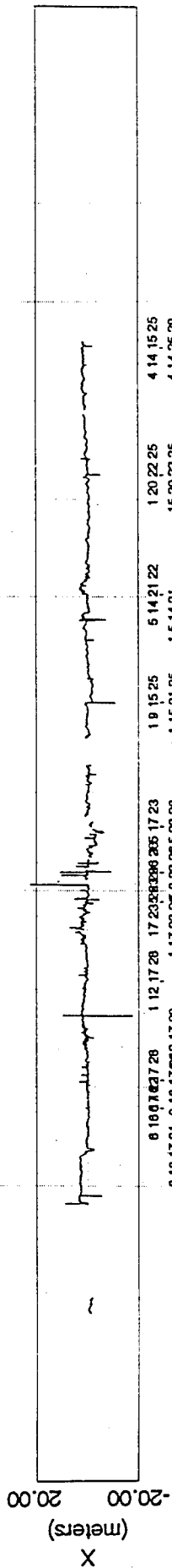


Figure 5. Collins 3A Navigation - Ground Truth - DGPS TSPI

THIS PAGE LEFT BLANK INTENTIONALLY

SESSION V-B
GPS SIMULATORS

CHAIRMAN

A. T. MONROE

*NCCOSC
SAN DIEGO CA*

THIS PAGE LEFT BLANK INTENTIONALLY

REAL TIME GPS SIMULATOR INTEGRATED WITH THE HIGH FIDELITY MANNED FLIGHT SIMULATOR

By

Chris Bartone, ACETEF CNI Laboratory, Athens OH
Gary Green, Pacer Systems, Lexington Park MD
Frederick Ventrone, Jr., Patuxent River, MD

BIOGRAPHY

Christopher Bartone received a Bachelor of Science in Electrical Engineering from the Pennsylvania State University and a Master of Science in Electrical Engineering from the Naval Postgraduate Science. Mr. Bartone has been involved in RDT&E of advanced communication, navigation, and identification systems on Naval aircraft for the past eleven years. He is currently the program manager for the ACETEF CNI laboratory.

Frederick A. Ventrone, Jr. received a Bachelor of Science in Electrical Engineering from The Pennsylvania State University and a Bachelor of Arts degree in Physics from Slippery Rock University. He has worked on the integration of the GPS Test system and other Communication, Navigation, and Identification Laboratory assets with the ACETEF at NAWC-AD Patuxent River, MD.

Gary Green received Bachelor and Master of Science degrees in Electrical Engineering from the University of Missouri-Rolla. He has performed design and analysis of communication and navigation avionics on military aircraft including the National Aerospace Plane, AX, and F-15 programs. He is currently supporting the integration of the GPS Test (GPST) environment into ACETEF at NAWC-AD Patuxent River, Maryland.

ABSTRACT

A real time GPS satellite simulator has been integrated with the Air Combat Environment Test and Evaluation Facility (ACETEF) at the Naval Air Warfare Center - Aircraft Division (NAWC-AD) Patuxent River, Maryland. The ACETEF facility includes a Manned Flight Simulator (MFS) with a 6 Degree-of-freedom (6-DOF) motion bay, high fidelity aircraft and ship motion models that are integrated with the real time GPS simulator. Navigation sensor models that currently run with the stand alone GPS simulator are currently being added

to the real time capability. ACETEF laboratories are integrated via shared memory using a real time network that distributes environment information pertaining to threats, communications, and platform parameters. This man-in-the-loop GPS simulation will be used to evaluate crew and avionics interfaces and will provide air combat effectiveness testing with GPS user equipment in the loop and integrated with platform avionics. It will also be used for Research, Development, and Test (RDT&E) of carrier landing systems where GPS is used as a landing aid. Installed avionics in an aircraft located in an aircraft size anechoic chamber can be interfaced to a cockpit in the MFS dome. At the same time, the real time GPS satellite simulator simultaneously stimulates installed GPS hardware in the aircraft.

Initial demonstration of the real time GPS simulation was performed in March of 1994. The MFS dome at ACETEF was used to generate flight profile data for the demonstration. A 6-DOF F/A-18 strike fighter simulation model was used as the simulated aircraft. Vehicle motion dynamics were passed from the MFS to the GPS simulator over a VME based SCRAMNet real time network. Simulations began with the aircraft sitting idle on the runway until a Rockwell 3A receiver locked onto simulated satellites and began navigating. The aircraft then took off and performed various high g maneuvers with the receiver tracking through each one. Real time video of the pilot's view was provided so vehicle maneuvers and receiver performance could be monitored simultaneously. Platform position truth data and GPS receiver data were recorded for post test analysis.

INTRODUCTION

ACETEF located at NAWC-AD Patuxent River, Maryland provides a fully integrated simulation environment to test battle scenarios involving military aircraft. Each player can have a full suite of simulated sensor and communication avionics. In many cases, actual avionics can be stimulated with simulated RF signals so scenario performance is

evaluated with hardware in the loop. In addition, man/machine interfaces are available, such as in the MFS, so scenarios also include man in the loop effects. All of these simulations are capable of operating in real time.

To meet the need for a real time navigation system simulation, a GPS satellite simulator, the GPS Test (GPST) environment produced by Computing Application Software Technology (CAST), has been modified to operate in real time as an asset in ACETEF. The GPST stand alone configuration provides a full suite of navigation sensor models that are integrated with a GPS satellite signal simulator. With this equipment, a GPS receiver can be exercised with simulated GPS RF signals and navigation sensor models.

The ability of the GPST to drive a receiver with satellite signals derived from real time vehicle state data was demonstrated for the Joint Test Agency Working Group (JTAWG) meeting in March of 1994. In this demonstration, an F/A-18 flight simulator generated vehicle state data while being operated in a 40 foot dome with compuscene visuals and a man in the loop. The GPST received vehicle state data from a real time data network and generated corresponding GPS satellite signals for a GPS receiver under test.

The GPS receiver produced navigation data for the pilot so that a closed loop navigation system was produced.

ACETEF DESCRIPTION

The Systems Engineering Test Directorate (SETD) at NAWC-AD is developing ACETEF which provides a facility for testing, through simulation and stimulation, aircraft avionics systems in a realistic air warfare environment. ACETEF consists of various RF shielded laboratories, an anechoic chamber, a multiple aircraft shielded hanger, and a manned flight simulator, all of which are integrated through electronic interfaces to achieve the needed RDT&E capabilities. Figure 1 shows a block diagram of ACETEF and Figure 2 depict an F/A-18 in the anechoic chamber. The Communications, Navigation and Identification Laboratory (CNIL) is responsible for testing communications, navigation and identification (CNI) and electronic warfare (EW) systems as installed in naval aircraft. An important requirement of the CNIL is to support the testing of GPS receivers that are being integrated into naval aircraft and naval aircraft subsystems (e.g., embedded applications).

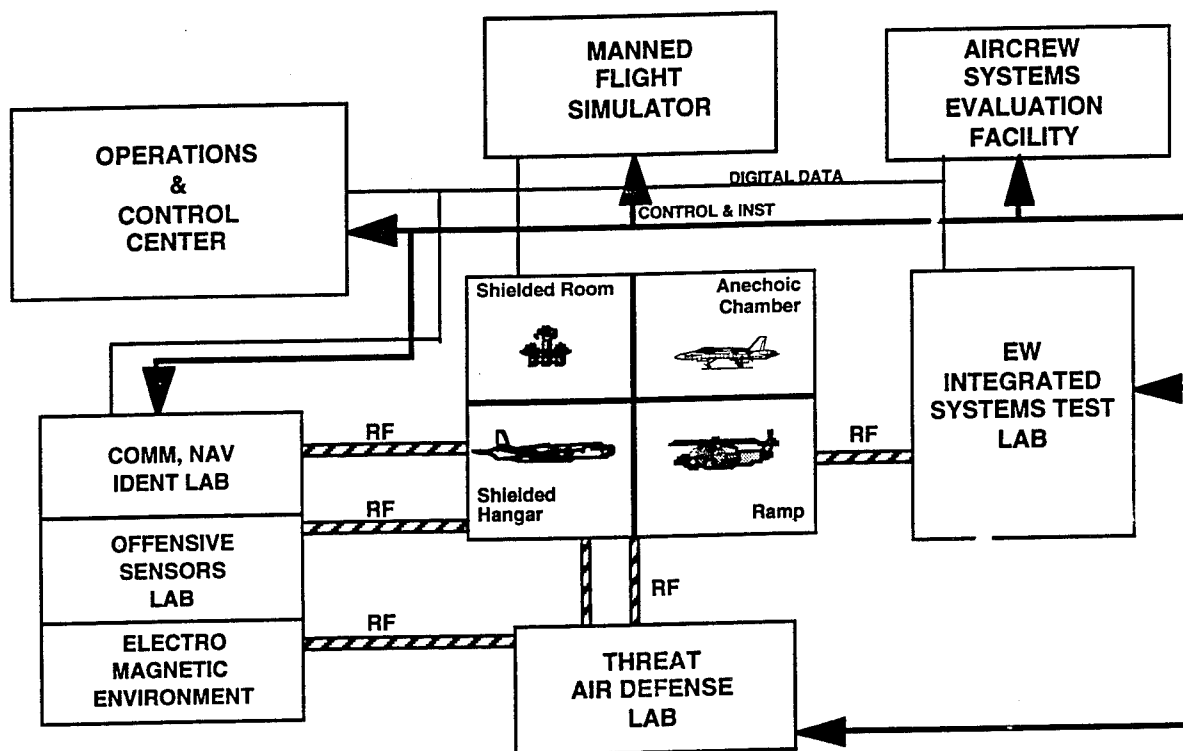


Figure 1. ACETEF Functional Block Diagram

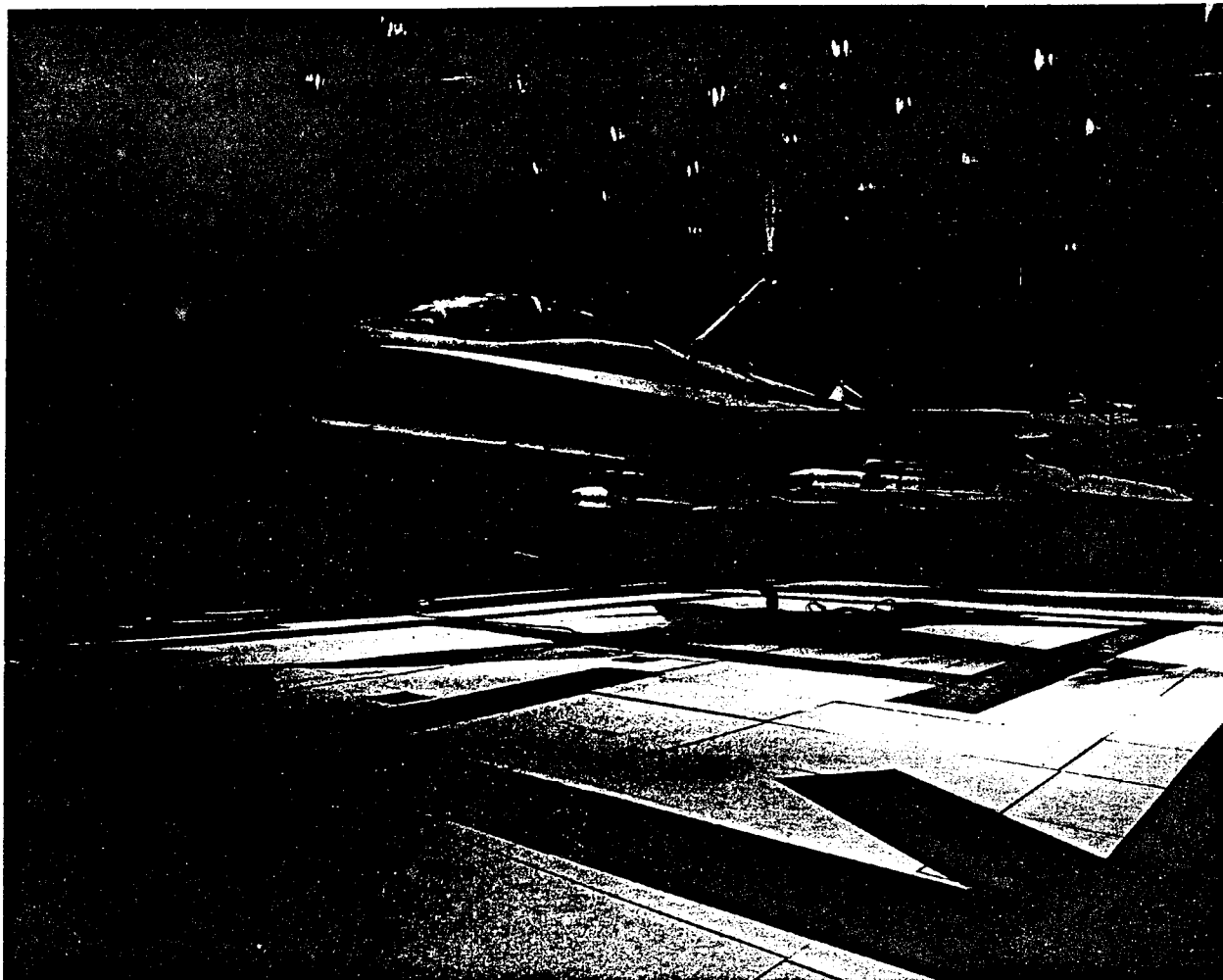


Figure 2. F/A-18 in ACETEF Anechoic Chamber

The CNIL charter within ACETEF is to provide higher fidelity communication, navigation, and identification simulation/stimulation capabilities to meet overall objectives of ACETEF. Friendly, foreign, and threat CNI signal generation and reception are included in the list of CNIL capabilities. These systems include GPS receivers, IFF/ATC, and communications equipment including JTIDS, SATCOM, Link 11, OTCIXS/DAMA, Link 4 etc. The CNIL also provides EW system assets used for recognition and exploitation of threat CNI signals.

GPS AND AUX. NAVIGATION SIMULATION CAPABILITY

Capabilities of the GPS and navigation simulation at NAWC-AD are driven by customer requirements. The customer base at NAWC-AD primarily consists of the military, however, commercial receiver testing has been done. So, providing test capabilities for GPS based navigation on military aircraft is the primary concern for the CNI Laboratory. Current

capabilities allow testing a GPS receiver with aiding from navigation sensors over a variety of interfaces. A rigorous set of test data extraction, reduction, and analysis tools are available for real time and post test analysis.

The GPS based navigation simulation at NAWC-AD is based on the GPST environment that is produced by CAST and is shown in Figure 3 with capabilities available at NAWC-AD. This configuration uses two Stanford Telecom 7200 GPS satellite signal generators to create GPS RF signals. The GPST computer computes pseudoranges and pseudorange rates that are sent to the signal generators to control the simulated GPS satellite signals. The simulated GPS signals include L1 and L2, C/A code, P code, and Y code for the effects of Selective Availability and Antispoofing (SA/AS). These signal characteristics can be used on up to 10 simulated SVs.

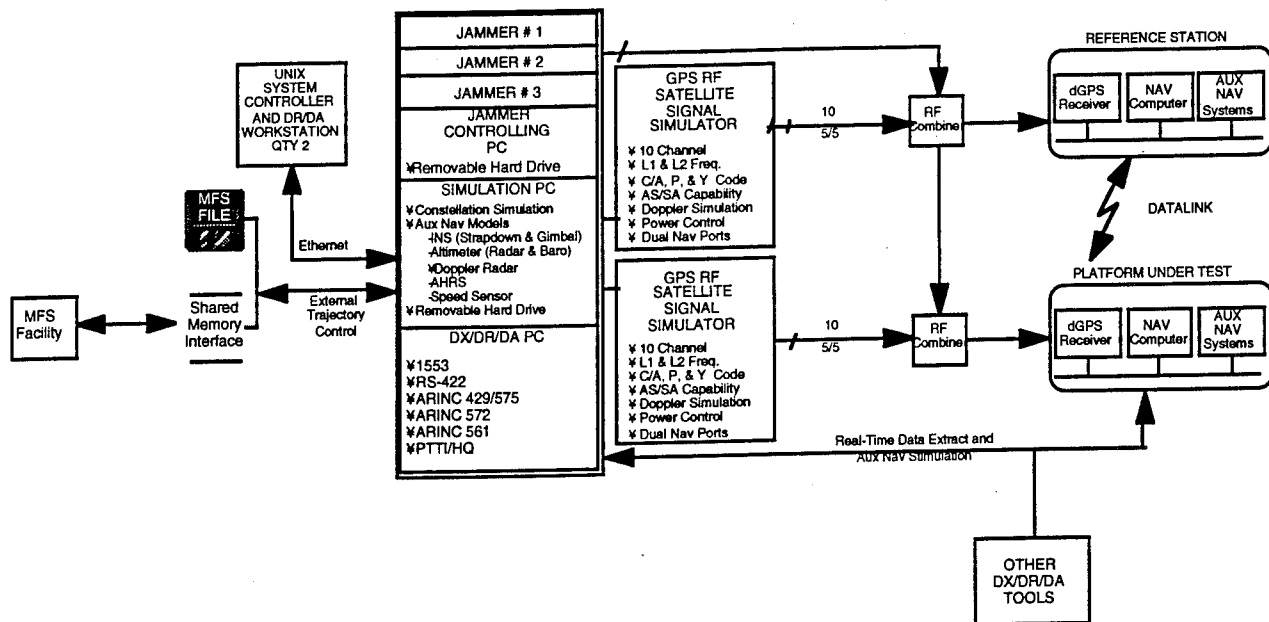


Figure 3. GPST Configuration in the CNIL

The GPST also provides aiding from a variety of navigation sensor models. Information from the navigation sensor models can be interfaced with a GPS receiver over several interfaces. The sensor models and interfaces used in a simulation depend on the receiver under test and the type of test being performed. A list of supported navigation sensor models is shown below:

- Inertial Navigation Systems (INS) (gimbaled and strap down)
- Attitude and Heading Reference Systems (AHRS)
- Speed Sensors
- Barometric Altimeter
- Radar Altimeter
- Doppler Radar

Receiver interfaces that are supported in the GPST at NAWC-AD are shown in Table 1.

Real time data extraction and post test analysis are supported with data reduction utilities that are user definable. A few of the PC based utilities include error plots, receiver operation parameters (such as figure of merit and receiver state), and extraction of simulation parameters (i.e. truth data). Data extracted during a simulation can be made available on a Sun workstation based spreadsheet. On this platform, the user has access to predefined routines and can define routines to suit unique requirements. The spreadsheet format provides a means to select data of interest and perform analysis on it.

Customer requirements for test capabilities are driving the GPS simulator to be able to test aircraft landing systems. As a result of these requirements,

current funding for GPS simulator enhancements are directed to increase the simulator's capability to test GPS as a landing aid. Current efforts for simulator enhancements include adding ten additional simulator channels so that 10 SVs are available to each receiver as a dGPS pair. This capability will be available in a scripted mode and in real time. Navigation sensor aiding is being modified to operate in real time also.

INTERFACE NAME	FUNCTION
ARINC-561	INS Aiding (ICD-GPS-108)
ARINC-429	Digital Flight Inst. (ICD-GPS-073)
ARINC-575	INS Aiding (ICD-GPS-070)
ARINC-572	Baro Altimeter
RS-422	Instrumentation Port (ICD-GPS-204/215)
PTTI/Have Quick	Timing Information (ICD-GPS-060)
Mil-Std-1553	Data Bus Interface (ICD-GPS-059/104)
SCRAMNet	Real Time Data Net.

Table 1. GPST Interfaces.

Modifications that will allow phase kinematic testing are being made. With these capabilities in place, testing of GPS based landing systems will include Category I through Category III requirements and

the flight profile data are triggered on every update of the data by the semaphores, upon which, they read the new data and process it accordingly. One of the processes using this data is the Compuscene IVA visual displays. The visual displays are used to feed data back to the pilot as he/she flies a mission. Another process using this data is the avionics/navigation computer, which converts the data into the correct format required by the mission computer. This data is then used by the mission computer (e.g. AYK-14) to drive the multi-function displays in the cockpit. The final process using the data is the link to the SCRAMNet shared memory interface. This computer is a VAX VMS 3300, which, upon being triggered by the semaphore, reads the data from the multi-port memory at 60 Hz (16.67 ms) and writes the data into the shared memory at 20 Hz (50 ms). This rate corresponds with the rate of the GPST.

The data is transparently, requiring no overhead software, reflected around the network. The rate of the data moving around the network is on the order of micro seconds and is negligible with respect to the overall throughput of the system.

Terrain data within the MFS is in flat earth coordinates. The GPST converts the flat earth coordinate to round earth coordinates as a part of the calculations to drive the GPS simulation. Flat earth data is expected to be replaced by WGS-84 terrain data in the near future.

The GPST architecture is based on 486/50 MHz PC running the real time LYNX operating system. It uses a Bit3 interface between the PC 16 bit ISA bus and the VME based SCRAMNet shared memory board. The data is read from the shared memory at a 20 Hz (50 ms) rate. The MFS and the GPST are running asynchronously so a frame count is attached to each frame of new flight profile data. This does not prevent missed data but allows us to extrapolate our position for one 50 ms piece of time. The timing is such that only one frame of data is can be missed. Minimum and maximum delays expected for the real time GPS simulation is shown in Table 2.

Delay Mechanism		Min Delay (ms)	Max Delay (ms)
From	To		
MFS	GPST	20	70
GPST	RF Out	50	50
Total		70	120

Table 2. Minimum and Maximum Simulation Delays

ACETEF DEVELOPMENT PLAN

The ability to test GPS based navigation systems is evolving with the advancing of GPS technology, and applications. The ACETEF development plan is committed to GPS enhancements to keep GPS testing current with receiver technology.

The basic GPS Test environment was installed at NAWC-AD in April of 1993. It ran only in scripted mode with up to 10 SVs simulated during a run. The navigation sensors and interfaces mentioned previously were available when the system was installed. A dual navigation capability, which supports differential GPS, was added to the basic system during the year as an upgrade. A jammer computer with arbitrary waveform generator cards was also added as an upgrade in September of 1993.

In October of 1993, an effort to modify the GPST to run in real time with the MFS began. The initial capability was demonstrated in-house by NAWC-AD in March of 1994 and was demonstrated again to the GPS Joint Program Office in May of 1994. For the demonstration, simulated GPS RF was sent from the CNI Laboratory to the 40 foot MFS dome through RF cables. A PLGR GPS receiver was connected to the RF cables in the MFS dome and a PC was connected to the PLGR to act as a display device. An F/A-18 flight simulation and cockpit was used in the MFS dome. In this configuration, a test engineer was able to view the cockpit while at the same time watch the GPS receiver's tracking performance.

Tasks related to real time GPS Test are continuing at NAWC-AD. The features were omitted to satisfy the technology demonstration described above in a reasonable time frame, and are now being added. They include ephemeris uploads, power level changes, constellation updates, and the capability to record the instrumentation port data. Except for the navigation sensor models and interfaces, the real time GPS Test environment will operate at the same level that the standalone scripted mode currently operates. This real time configuration will be completed by December of 1994.

The capability to perform differential GPS testing with 10 simulated SVs allocated to each of two receivers is also being added in 1994. Ten additional GPS signal generator channels will be added to the current 10 channels. This feature is called 10/10 dGPS and will be made to operate in scripted mode and in real time. 10/10 dGPS will be used to evaluate GPS based aircraft landing systems that use differential techniques to reduce errors. This effort will continue into 1995.

Navigation sensor models will be added to the real time GPST so that the real time system will have about 90% of the basic GPST configuration. INS models will be made to run in real time and will be provided to a GPS receiver over a MIL-STD-1553 data bus. This effort is expected to be completed by the end of 1994. Other navigation sensors and interfaces will be added during 1995.

[1] R. R. Smullen, Jr, & R. E. Nowak, "Virtual Reality: An Air Combat T&E Perspective", Proceedings of the ITEA, London, England May 1994.

CONCLUSIONS

The basic GPST with the enhancements described herein make ACETEF test capabilities unique for GPS testing. ACETEF allows hardware in the loop stimulation with high fidelity aircraft, flight control, carrier landing, and full aircraft and ship 6 degree of freedom motion models. Ship, ground, and aircraft sensor models (INS, RADAR, baro altimeter, ACLS, ILS, etc.) can be exercised in conjunction with GPS. Displays and control laws can be evaluated with a pilot and GPS hardware in the loop for landing system evaluations. Automatic control for Category III landings can be evaluated. Future plans include adding the capability to have an aircraft in the loop. In this scenario, an aircraft in the anechoic chamber will be stimulated with RF, and it will drive cockpit displays in the MFS.

The Air Combat Environment Test and Evaluation Facility (ACETEF) located at NAWC-AD Pax River provides a laboratory environment for testing air combat scenarios. The GPS Test (GPST) environment is integrated with ACETEF. It adds a navigation system simulation that closely models expected navigation errors observed during a mission. The addition of differential GPS simulation and a real time interface with MFS allows the evaluation of GPS based landing systems. These simulations include both GPS hardware in the loop and a pilot in the loop. Future plans include having ACETEF connected to aircraft in an anechoic chamber so that there can be aircraft in the loop.

ACKNOWLEDGMENTS

We would like to give special thanks to Major Joe Sanford of the GPS JPO for the sponsorship and technical guidance he has provided. Also, Captain Rocky Gmeiner of PMA 213 deserves special thanks for sponsorship and technical guidance applied to landing systems. We also include Glen Colby of Strike Warfare at NAWC-AD in our list of people who made this effort possible. This effort could not have been successful without the support of these individuals.

REFERENCES

THIS PAGE LEFT BLANK INTENTIONALLY

Receiver Time Delay Calibration Using a GPS Signal Simulator

J. Brad
P. Landis
E. Powers
J. White

U.S. Naval Research Laboratory
Washington, D.C. 20375

Abstract.

Time delay calibration of GPS receivers is usually done with live satellites and a local reference clock whose time offset from the U.S. Naval Observatory is precisely known. This method is typically within ten nanoseconds of truth but can be time consuming and usually includes unwanted perturbations such as multipath and UTC-GPS time offset uncertainties. A procedure will be described using GPS signal simulator. This method has the advantage of removing all external perturbations from the calibration process. The key to the method is the calibration of the internal delay of the simulator code transitions of the output signal with respect to the simulator one pulse per second. The simulator calibration method and the receiver calibration process will be presented along with data showing the precision of the measurements.

Background. In addition to providing precise user navigation information, the Global Positioning System (GPS) is capable of providing precise time. Precise Positioning Service (PPS) receivers are typically specified to provide time accurate to one hundred nanoseconds [1]. In order to manufacture a receiver to this accuracy or to recalibrate it later, there must be a procedure to measure the time delays in the receiver with respect to the signals it is receiving.

An Allan Osborne Associates (AOA) receiver model TTR-4P, serial number 155, was provided to NRL for precise delay calibration using the NRL Northern Telecom (NT) simulator. The purpose was to evaluate the simulator calibration procedure and to compare it to live satellite calibrations made by the National Institute of Standards and Technology (NIST) and the U.S. Naval Observatory (USNO) on this same receiver. There are advantages and disadvantages to each method. The appeal of the simulator approach lies in the capability to precisely control the test environment and to identically repeat a test scenario to isolate causes of anomalous results.

Live Satellite Calibration. The time output delay in high performance GPS timing receivers are generally calibrated by using live satellites and comparing the results to a known receiver. The procedure is simply to program the receiver to be calibrated to track the same set of GPS satellites as a reference receiver will track and upon completion of the tracking period to compare the data, measure the average time difference between the receivers and apply the difference to the test receiver as a calibration adjustment. This method has the strong advantage of being a direct measurement of how the receiver will perform with respect to another receiver. By using live satellites, it also verifies that the receiver will actually perform correctly in a real world environment. There are also several disadvantages to the comparison method. These

disadvantages include uncertain calibration of the reference receiver, radio frequency (RF) interference, and multipath effects.

One of the biggest problems is that the calibration is only as good as the reference receiver's calibration. Ideally, calibration should be an absolute process so that when any two receivers calibrated by the same process, regardless of who did the calibration or what reference was used, the results would be the same. In a live satellite environment, there is no absolute reference other than a time standard which is independently compared to the U.S. Naval Observatory time (UTC-USNO) by a means other than GPS. Such resources are generally only available to sites physically close to the Observatory or to laboratories with two-way time transfer capability to USNO.

Another limitation is the RF environment in which the receiver is calibrated. There will be multipath, in-band interference, and out-of-band interference. Unless both receivers are of identical design and share a common antenna, it is possible that there will be measurable differences between the receiver outputs. Use of a common antenna is not always possible due to beating of the local oscillators (LO's) in the receivers. The AOA receiver is particularly difficult in this area since it uses LO's at the GPS L1 and L2 frequencies. These have been shown to cause interference to other receivers whose antennas are close to the AOA antenna. AOA testing at NRL also revealed a susceptibility to 928 through 932 MHz signals from paging transmitters which beat together in the downconverter to produce significant interference at baseband. In some cases, the interference was so strong that the receiver would not operate.

Figure 1 shows the time-recovery performance of a Standard Telecom 5401C receiver tracking live satellites at NRL. The receiver has both Selective Availability (SA) and Anti-Spoofing (AS) or Y-Code capability. The reference clock at NRL is a hydrogen maser whose frequency is stable with respect to the Naval Observatory to within better than 1×10^{-14} over a period of several days, giving a time uncertainty of around a nanosecond per day. The receiver was in the Automatic Track mode which selects one satellite for a 15 minute track and then switches to another satellite. The process is repeated indefinitely, and the receiver will eventually track all visible satellites over a period of time. The residual time errors for this receiver are typically 50 nanoseconds peak-to-peak for the 15 minute averages and the noise on a one day average of the time offsets is less than 15 nanoseconds, one sigma.

Simulator Calibration. The NT simulator, model STR2760, is a six channel unit capable of simulating the GPS satellites' signals in a variety of user motion scenarios. Using a GPS signal simulator as a calibration tool has several significant advantages. The biggest is that the method can be used as an absolute measurement of the receiver's internal delays, dependent only on the calibration of the simulator itself. It also has the benefit of being done in a controlled RF environment where there are no interfering signals and no multipath. Disadvantages include unknown receiver performance in a real RF environment, separate calibration of the GPS antenna, and external interface compatibility issues such as slow rise times on timing pulses supplied to the receiver by other equipment in the end user's configuration.

The key to a high-accuracy receiver calibration is the calibration of the simulator itself. The factor that must be accurately known is the relationship of the one pulse-per-second (1 PPS) reference signal from the simulator and the code phase of the generated GPS signal. Experience with the Northern Telecom model 2760 simulator has shown that from a cold start, without the internal calibration recommended by the manufacturer, there can be 10's of nanoseconds of total delay variation and comparable code phase differences between the L1 and L2 signals. Using the NT internal calibration procedure before the start of each simulation run reduces the total delay variations to a few nanoseconds and the L1 to L2 variations to about one nanosecond. Table 1 shows the results of calibration runs for simulator serial number 147. These results show that NT simulator has very repeatable delays when the internal calibration is used. The absolute and relative delays in the simulator can be quickly measured using a high-speed digitizing oscilloscope as shown in figure 2.

Date	L1 Delay in nanoseconds		L2 Delay in nanoseconds	
2/23/95	99.7		100.9	
2/28/95	98.6		100.2	
3/1/95	98.7		100.9	
3/2/95	98.9		101.6	
3/3/95	98.8		100.26	
3/6/95	101.2		103.2	
Statistics	Average	Std Dev	Average	Std Dev
All Runs	99.3	.9	101.1	1.0

Table 1. Simulator Calibration Data, C/A codes.

The principle that makes this calibration possible is that the amplitude of the carrier envelope is affected by the GPS code structure. Figure 3 is an oscilloscope plot of the amplitude of the GPS L1 carrier near the time of the reference one pulse per second. The effect of C/A code modulation (with the navigation data turned off) is that amplitude of the carrier at the actual time of the reference pulse goes nearly to zero. These dips have an repetition rate of about 3 microseconds. The dip immediately following the 1 PPS signal is the correct response. This method can also be done using the P code but the dips are much closer and there is ambiguity as to which is the correct one to measure.

The process is to trigger the oscilloscope with the simulator reference 1 PPS signal and determine the delay to the carrier response. The difference between the two is the simulator calibration error. Some simulators, such as the STel 7200, have the ability to adjust the reference

pulse output phase to reduce this error to zero. Where it cannot be adjusted, the difference is carried as a calibration adjustment that is removed from the final receiver calibration value.

Once the simulator has been calibrated, the receiver is connected as shown in figure 4. The use of cables with identical delays in the RF and reference lines simplifies calibration by matching delays in the test and reference signal paths. The NRL procedure is to run a fixed-position scenario with nominal ionosphere and troposphere. These factors are included because the modeled ionosphere and tropospheric corrections in many receivers cannot be turned off. A standard GPS constellation is used with no errors in satellite positions or satellite clocks. This method produces receiver output like that in figure 5. This is an STel 5401C like the one used to track live satellites in figure 1. Note that the peak-to-peak excursions are reduced by about 75% and that the average will not vary more than a few nanoseconds.

The final step in completing the calibration is to determine the average time difference for the simulator run, apply corrections for simulator bias, test cables, delay of the antenna and any RF cables used to connect it not previously included in the calibration run.

Stanford Telecom uses their own version of the simulator calibration method to calibrate their 5401C receivers prior to delivery [2]. The receiver has a built-in calibration mode that is compatible with a calibration function of the STel 7200 GPS signal simulator. When used together, the STel method provides calibration in a few minutes. NRL has not done an independent analysis of the STel results.

AOA Calibration Allan Osborne receiver serial number 155 was calibrated at NRL during the period March 1, 1995 through March 15, 1995. This is a much longer period than normally required for a simulator calibration in order to identify any systematic effects in the calibration method or in the receiver. Ten calibration runs were made.

The calibration scenarios used a two-hour and eight-hour static situation with nominal ionosphere and troposphere. The lengths were chosen to provide adequate time to average out short term noise in the measurements. The Northern Telecom Simulator had six L1/L2 channels. No SA/AS effects were generated. AOA SN 155 did not have SA/AS capability at the time of this calibration. Prior to the start of calibration, the receiver memory was cleared and the simulator static position coordinates were entered. The receiver then downloaded the simulator almanac. This step is essential in order for the receiver to know which satellites are available to be tracked. Prior to each individual run, the receiver time was reset to a time several minutes prior to the simulator time and the coordinates were reloaded. The receiver keeps an internal clock and will not track satellites whose broadcast time is significantly earlier than its own time. We also found that sometimes the AOA would renavigate its position for no obvious reason. The coordinates were checked during each run after the initial satellite acquisition.

The AOA printer port output data were captured with a PC using PROCOMM. Data were output at 10 second intervals. No commands were sent to the receiver via the RS-232 port

during the runs. The output data stream includes time offset data for each channel, allowing up to eight satellites to be tracked simultaneously. Since the simulator was only capable of generating six simultaneous channels not all receiver channels could be active at once, but all were exercised since the receiver uses the upper channels to search for rising satellites then continues tracking on those channels.

To arrive at a number describing the difference between the received GPS signal time and the input 1 PPS signal from the simulator, the time offset data from all active channels were averaged. Prior to accepting the average, the data from all channels were plotted to determine whether or not there were any excursions in the data. Figure 6 shows a plot of a calibration run made on 2/28/95. The results of the calibration runs are shown in Table 2.

Date	Mean (nsec)	Standard Deviation (nsec)
2/23/95	-225.0	4.2
2/24/95	-226.4	3.7
2/24/95	-217.5	2.5
2/25/95	-222.7	2.3
2/27/95	-221.4	3.2
2/27/95	-220.0	2.9
2/28/95	-230.5	2.7
3/1/95	-231.8	2.9
3/2/95	-220.7	3.4
3/3/95	-222.2	4.8
Statistics	-223.8	4.4

Table 2. Receiver Calibration Data Summary

Using this data and the simulator correction data described previously, the final calibration is:

System Name	Calibration Value	Standard Deviation
AOA155 measurement	-224 nsec	4.4 nsec

RF Cable delay	12 nsec	0.25 nsec*
Simulator delay	-99 nsec	1 nsec
AOA antenna cable delay	302 nsec	0.25 nsec**
AOA antenna delay	6 nsec	1 nsec**
Calibration	-3 nsec \pm 5 nsec	

* Delay measured independently using network analyzer

** Nominal delay for AOA 200 ft cable and standard antenna (preamp and internal cable measured on analyzer)

The data in Table 2 show a run-to-run variation that is significantly larger than the standard deviations of the individual tests. Some of the changes seemed to correlate with temperature changes in the laboratory. The receiver was placed in a thermal chamber and re-tested at several temperatures to isolate temperature effects. No clear temperature effect was identified. More detailed testing will be needed to document what temperature effects exist and whether or not they are unique to this particular receiver or whether they are generic to the TTR-4P design.

The simulator did not appear to cause timing shifts since its calibration number remained constant over time and various laboratory conditions. However, to increase confidence in it, another experiment was done using an STel 5401C receiver. The scenario length was increased to one day to increase the chance of seeing any irregularity in the simulator signal. The room temperature was changed from 70 to 80 degrees F for several hours and then back to 70 degrees during the run. Within the noise limits of the STel receiver (less than 5 nanoseconds), no changes in the simulator were seen, figure 7.

Data Comparison. The table below shows results from the NIST and USNO live satellite calibrations on AOA receiver Sn 155.

NRL	-3 \pm 5 nsec
NIST	+5 \pm 5 nsec

Conclusion The simulator method for calibrating receivers is a useful method of providing timing calibration of GPS receivers in the laboratory. It allows precise measurement of the receiver delays in a controlled environment. This data must be combined with measured delays for the antenna and antenna cable to produce a final result. It does not necessarily show how the receiver will perform in a real world situation with noise, multipath, and local interface problems. Further investigation into the wide excursions seen in the receiver tested here are necessary to reduce the uncertainty of the calibration. Future work will also include an extensive investigation of temperature effects on simulator calibration and the calibration of other models of receivers.

References.

1. Trimble TASMANT Receiver specification.
2. Private communication, Ben Smith, Stanford Telecom.

STEL Y-CODE GPS RECEIVER

1 PPS TIME DATA LIVE SV

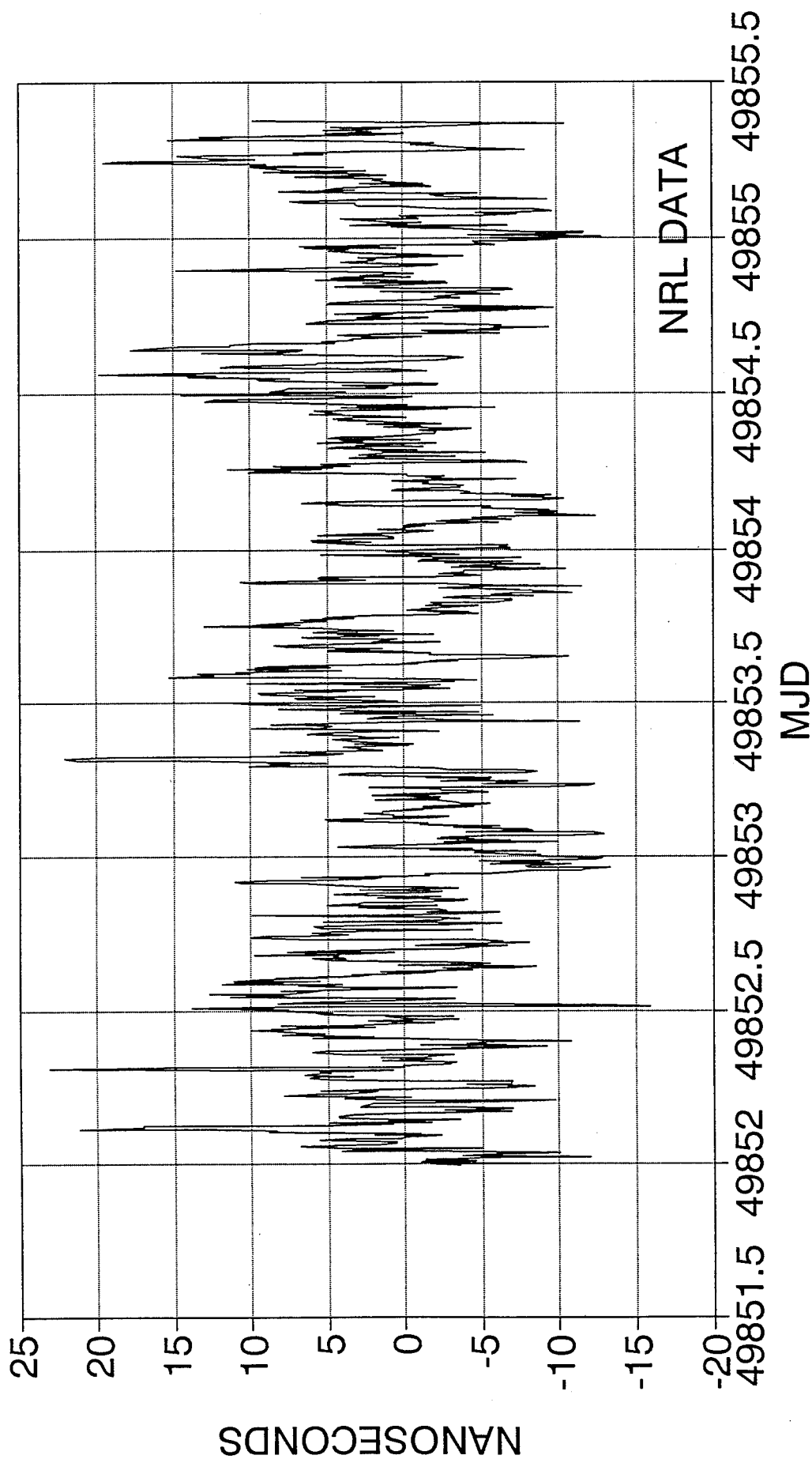


FIGURE 1. Time Recovery Performance

NRL GPS RECEIVER CALIBRATION EXPERIMENT

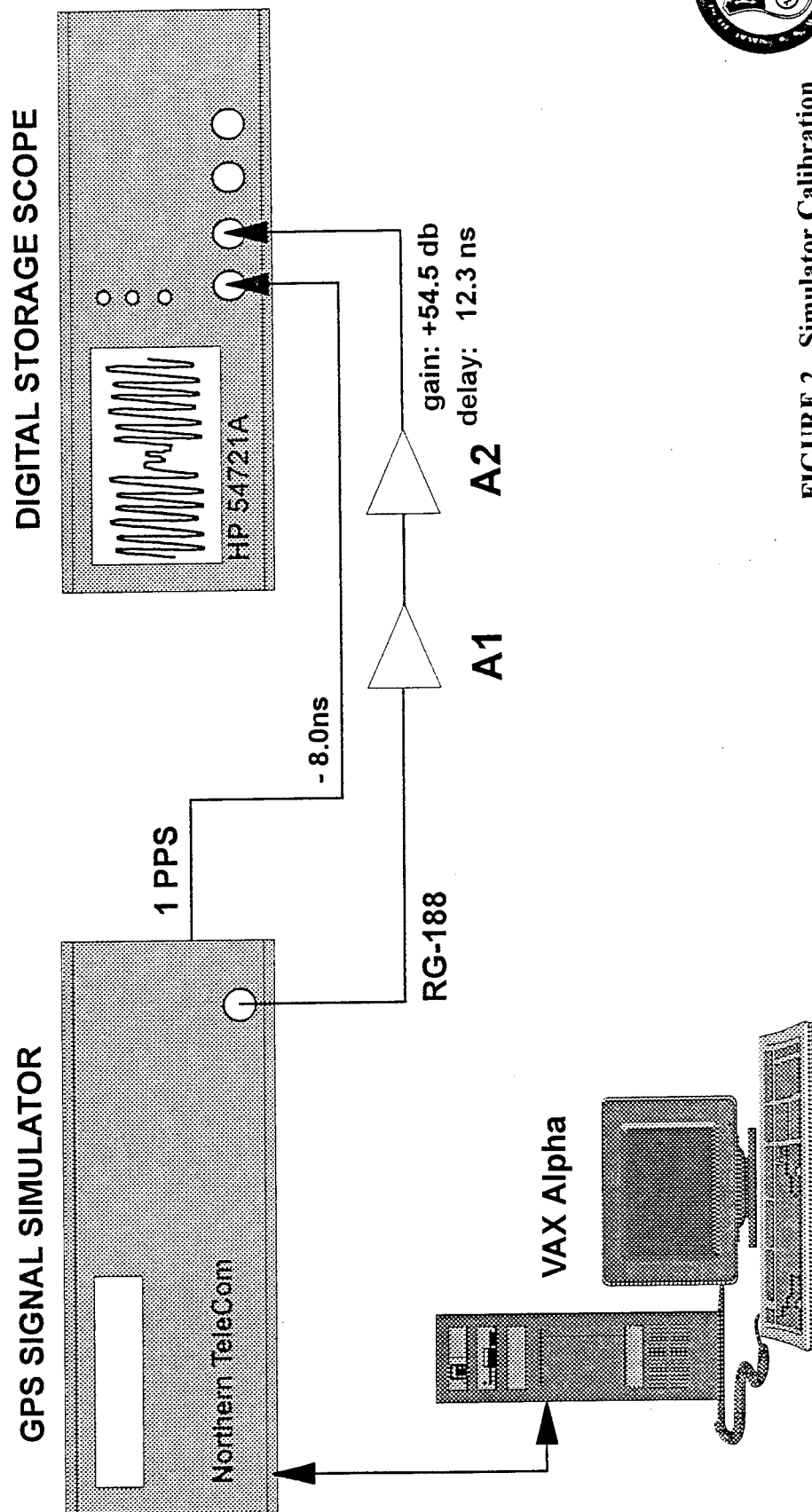


FIGURE 2. Simulator Calibration



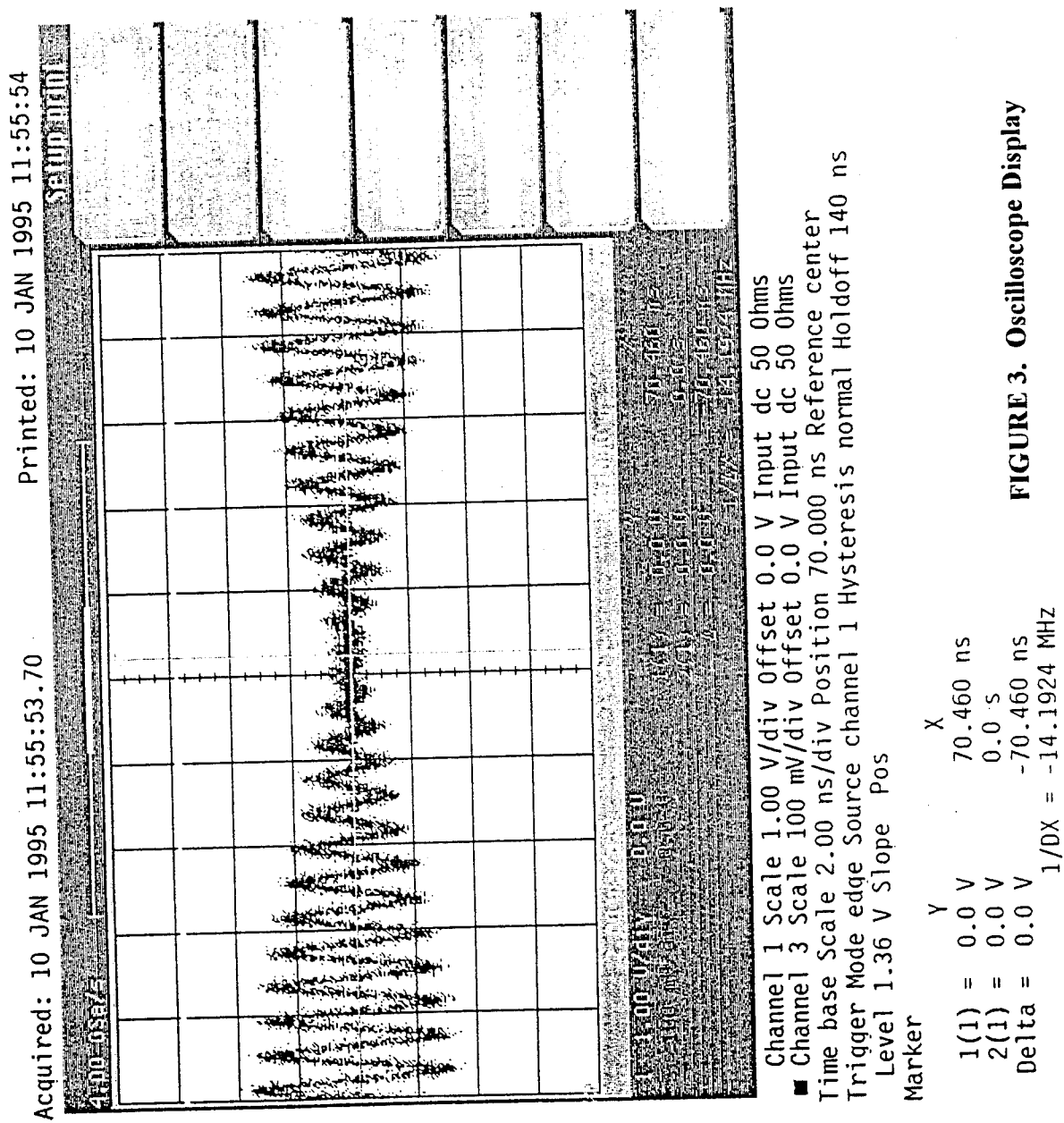


FIGURE 3. Oscilloscope Display

GPS RECEIVER CALIBRATION EXPERIMENT

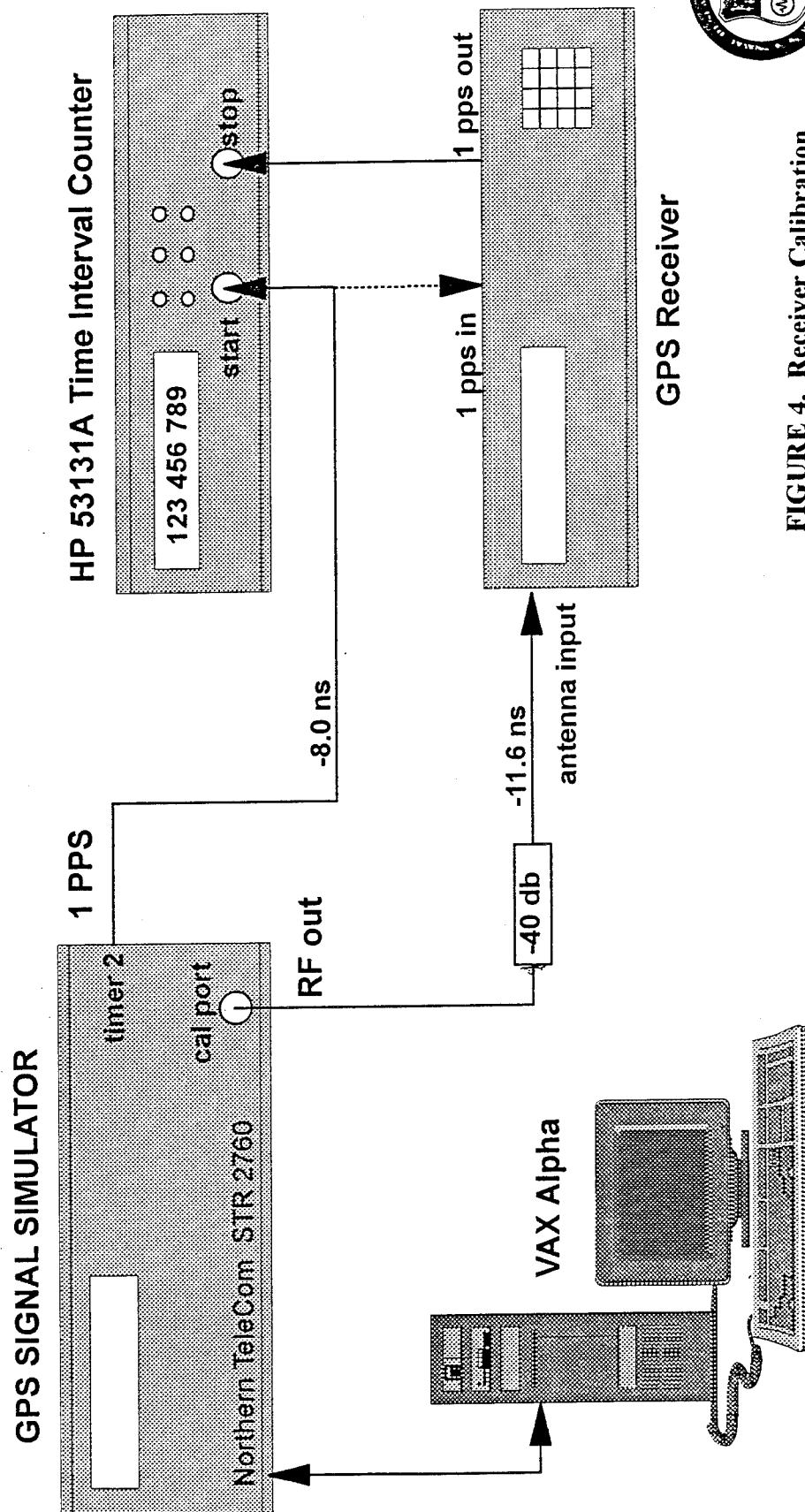


FIGURE 4. Receiver Calibration

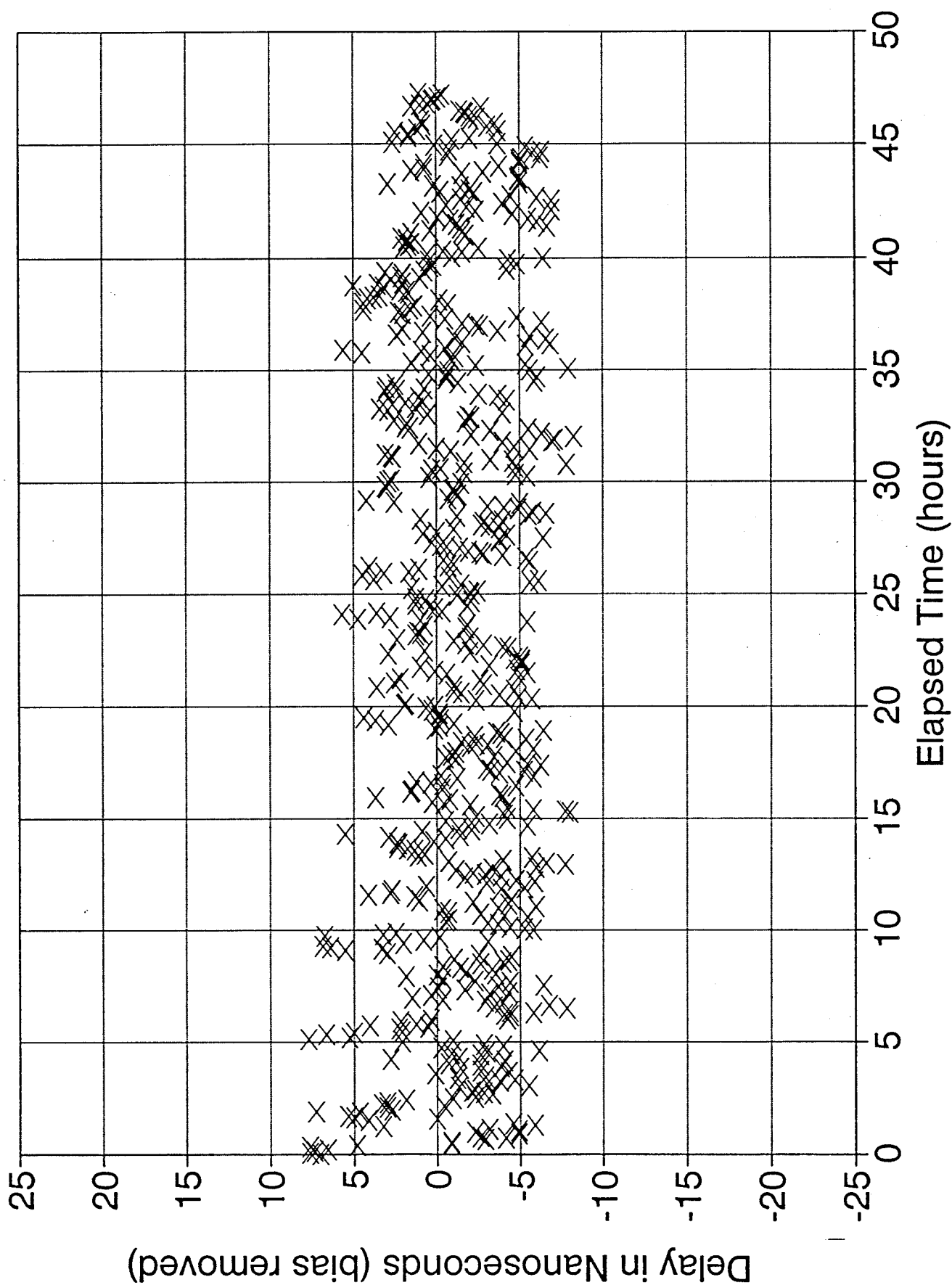
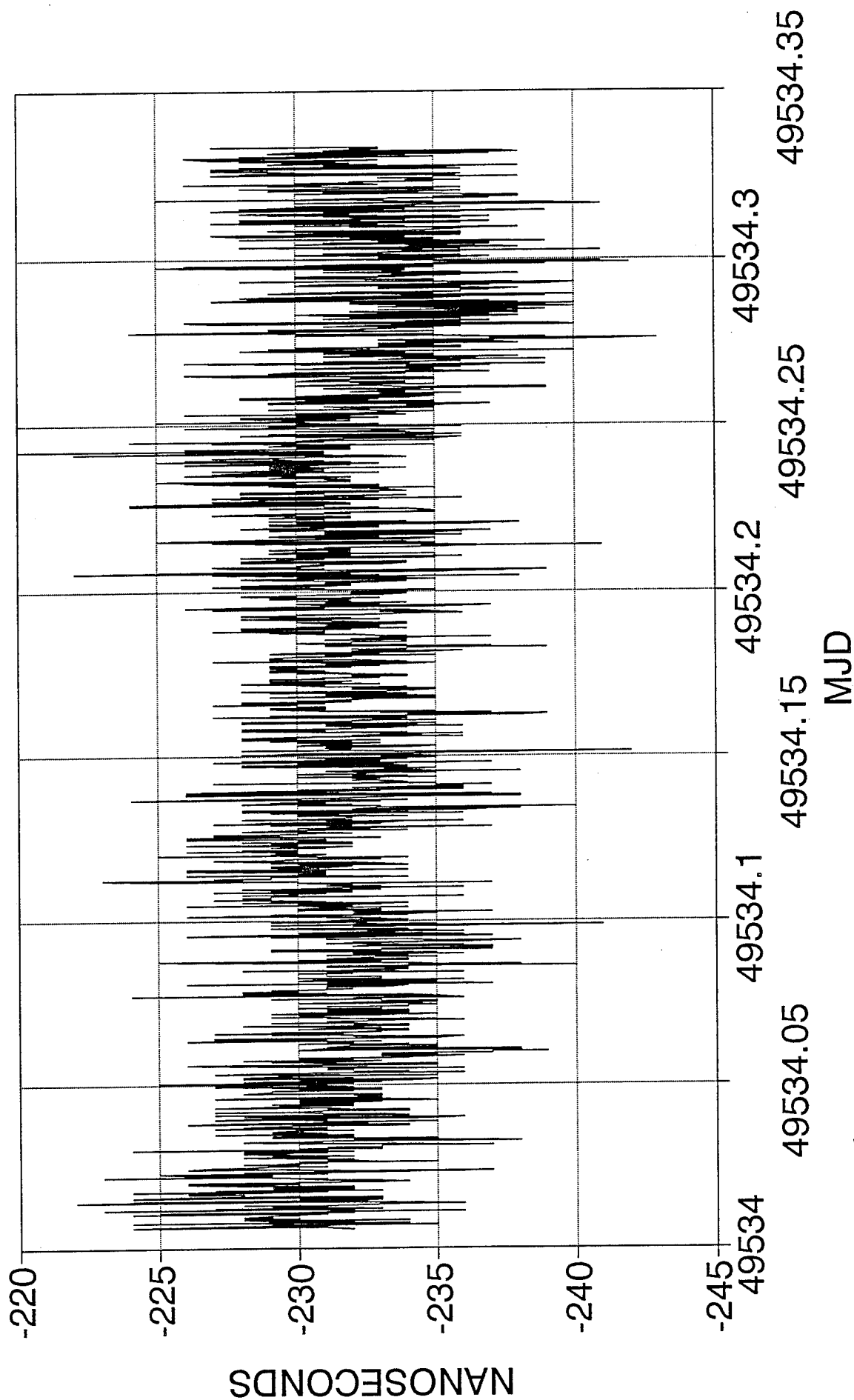


Figure 5. Stel 5401C rcvr on simulator

AOA 155 RUN A

AVG (-231.8) STD (2.9)



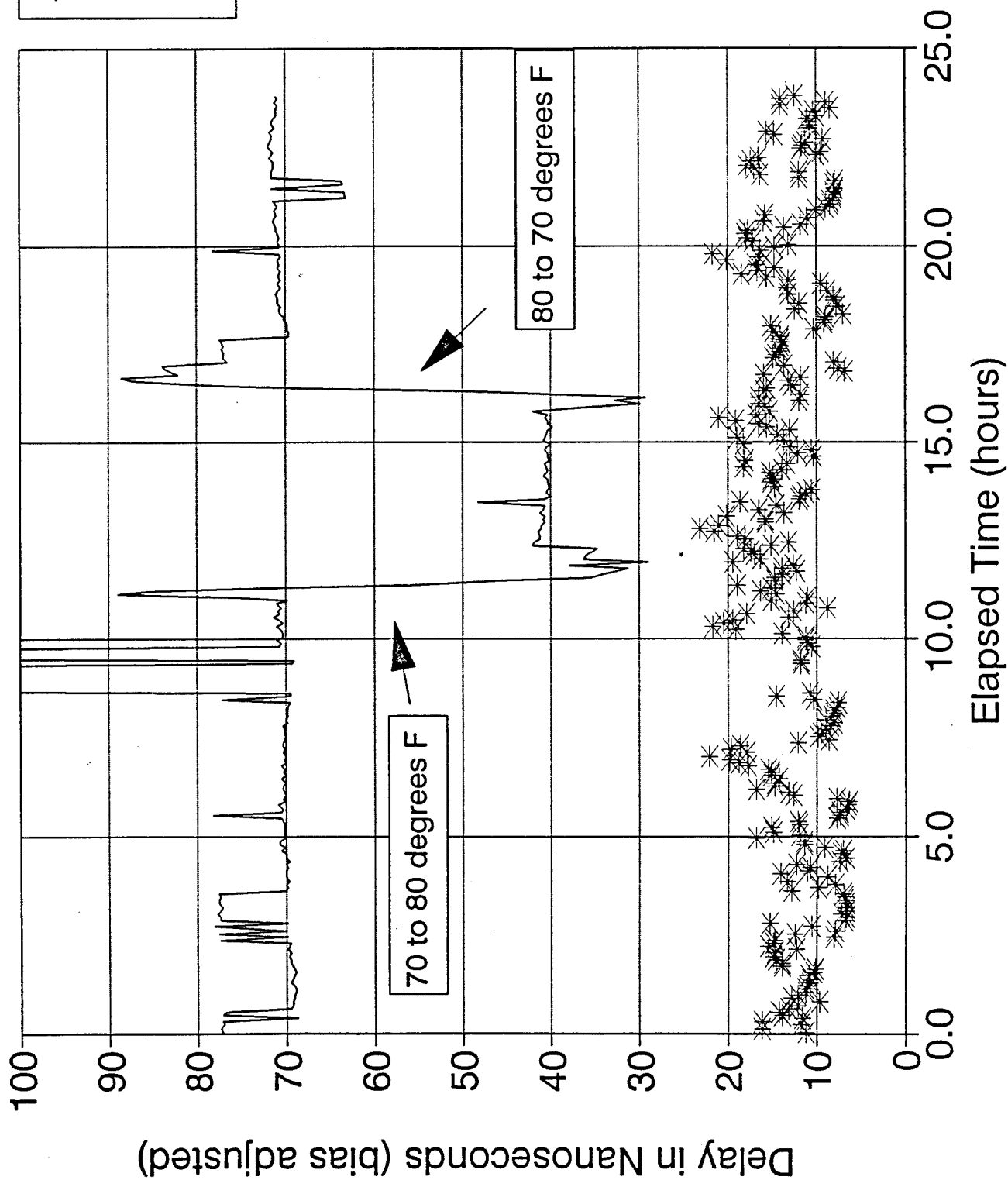


FIGURE 7. Temperature Test

THIS PAGE LEFT BLANK INTENTIONALLY

SESSION VI-B

INTEGRATED GPS II

CHAIRMAN

ROBERT BLIZZARD

*HONEYWELL
CLEARWATER FL*

THIS PAGE LEFT BLANK INTENTIONALLY

Global Positioning System Inertial Navigation Assembly (GINA) Test and Evaluation

Stanley J. Zugay and Richard Hogg
NRaD Warminster
Warminster, PA

Biography:

Stanley J. Zugay is the Test Director for the GINA Program at NRaD Warminster Detachment. He graduated from Villanova University with a BSEE. His experience includes testing of embedded GPS navigation systems and integration of GPS User Equipment into Navy aircraft.

Richard Hogg is the GPS Test Facilities Coordinator at the NRaD Warminster Detachment. In that position he has been involved with the Embedded GPS Inertial Test program and Gem-III Qualification testing.

Abstract:

The advancements of low cost inertial technology combined with the miniaturization of multi-channel Global Positioning System receivers have produced a variety of embedded navigation systems with a range of applications. Embedded systems offer substantial size, weight, performance and power savings as well as improvements in accuracy and GPS receiver performance, without the difficulty of box integration. The U.S. Navy is capitalizing on this technology in order to provide the T-45TS GOSHAWK with GPS capability. The Navy strategy for accomplishing this was through the Non-Developmental Item (NDI) acquisition of the Litton Global Positioning System Inertial Navigation Assembly (GINA). To evaluate the GINA system, a combination of laboratory and field testing was performed. GPS laboratory hardware in the loop

testing with simulated GPS satellites provided error analysis under controlled conditions. Field testing provided a dynamic environment in which the tightly coupled GPS/INS system was evaluated. The focus of this paper is to discuss GINA testing performed at NCCOSC.

1.0 GINA Description

The GPS Inertial Navigation Assembly (GINA) is comprised of a self-contained all attitude world wide, strapdown inertial sensor assembly (ISA) and embedded GPS receiver (EGR). The principle information provided by the GINA consists of acceleration, velocity, position, attitude (pitch, roll and heading), attitude rates and time. Conceptually the GINA consists of three functions: the core sensors, processor function, and the interface function (see figure 1). The core sensors consists of an Embedded GPS receiver (GEM-III) with the necessary hardware and software to implement the GPS requirements, and an Inertial Sensor Assembly (LN-100) with the necessary hardware (gyros, accelerometers, etc.) and software to implement the inertial navigation requirements. The processor function provides the hardware, software and firmware to support a tightly integrated Hybrid navigation function, GPS navigation function and inertial navigation function. The interface function (see figure 2) supports digital and analog communication between the GINA and the host vehicle platform with principle control commands and data exchange provided via MIL-STD-1553 serial digital multiplex bus.

The GINA provides a GPS-only navigation solution and either a integrated GPS/Inertial-only solution or a hybrid navigation solution. The hybrid navigation solution is obtained from a combination of GEM-III and LN-100 sensor data. Both the GPS solution and a hybrid or inertial-only solution are available to the user to determine present position and velocity of the aircraft.

2.0 Test Approach

The government GINA qualification test program consisted of a series of tests conducted in NRAD's GPS Central Engineering Activity (CEA) Laboratory, Strapdown Navigation System Development Laboratory (SNSDL) and Mobile Navigation Test Facility (MNTF). Testing was divided into four primary areas

- Functional Interface
- GPS Performance
- Inertial Performance
- Hybrid Performance

3.0 GPS CEA Laboratory Overview

Figure 3 identifies the test configuration of the GPS Central Engineering Activity (CEA) Facility during GINA testing. Functional interface verification and GPS performance testing was performed in the GPS CEA laboratory. The components which comprise the CEA are described as follows:

Satellites Signal Simulator (SSS): The SSS is a system of processors and transmitters which calculate trajectory data and generate realistic RF signals that reflect the propagation of GPS signals in a live environment. The SSS has ten independent channels which can simulate the output of up to ten SV signals (both L1 and L2 Frequencies). Selective Availability/Anti-Spoofing (SA/AS) can also be simulated on the SSS.

Integrated Satellite Signal Generator (ISSG): The ISSG is a composite of the ISSG VAX and SSS. The ISSG VAX computes platform motion parameters and provides the data to the SSS; the SSS can then produce the correct signal corresponding to platform motion. ISSG data from a test is stored in a data extraction file in the VAX disc memory to be used in post test data processing.

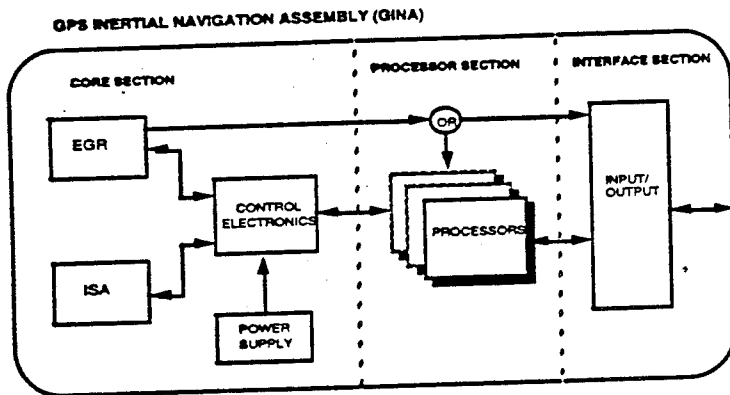


Figure-1 GPS Inertial Navigation Assembly (GINA)

GINA INTERFACES

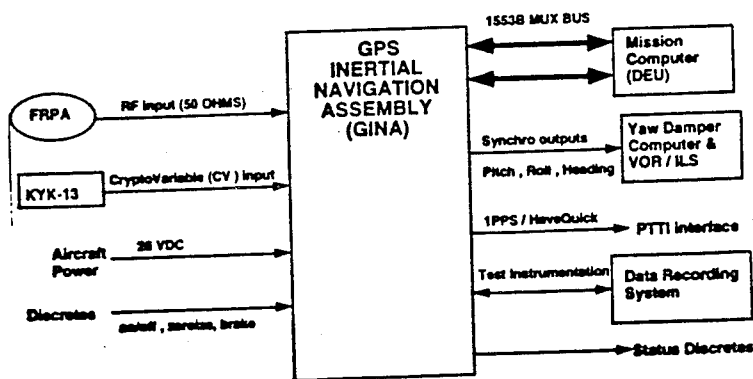


Figure-2 GINA Interfaces

User Equipment test facility (UETF): The UETF provides the capability of real-time simulation of platform navigation subsystem sensor signals and interfaces.

Smart Buffer Box (SBB): The SBB is used to collect data from the GINA instrumentation port (IP) and store it to magnetic tape or disc. In addition the SBB is used to display critical IP data during lab testing.

Bus Controller (BC): The bus controller formats all GINA I/O messages to comply with 1553B protocol. The bus controller displays GINA 1553 data in operator defined page formats tailored for embedded GPS/INS testing. Selected messages are recorded to disc and later transferred to the vax for post test processing via ethernet interface.

Reference GPS Receiver: The GPS MAGR receiver is used for post-test analysis as a reference.

GINA LRIP GPS LABORATORY TEST CONFIGURATION

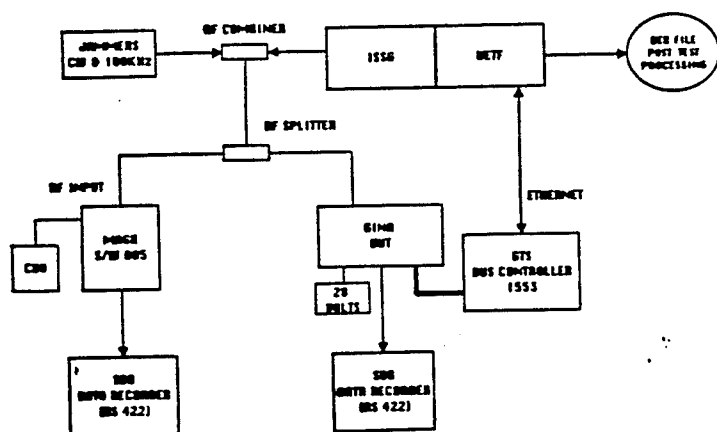


Figure-3 GPS Test Configuration

3.1 Inertial laboratory Overview

The NRAd Strapdown Navigation System Development Laboratory (SNSDL) was used to test the GINA inertial characteristics for specification compliance. The inertial tests were done independently of the GPS function in order to ascertain the "pure" inertial navigation performance. The SNSDL facility contains some equipment in common with the GPS CEA facility; however the SNSDL possesses a variety of instrumentation and equipment unique to its function.

CARCO Three Axis Rate Table: The rate table is capable of simultaneous angular excitation of the GINA in three axes-roll, pitch and yaw. Slip rings contained in all three axes allow for uninterrupted signal transmission to and from the GINA.

Hewlett Packard (HP) 3852a: This device contains an 8-channel power controller with relays and a 16-channel general purpose switch to gate 28 VDC to the GINA and to control the state of GINA input discretes.

GINA LRIP INERTIAL FACILITY TEST CONFIGURATION

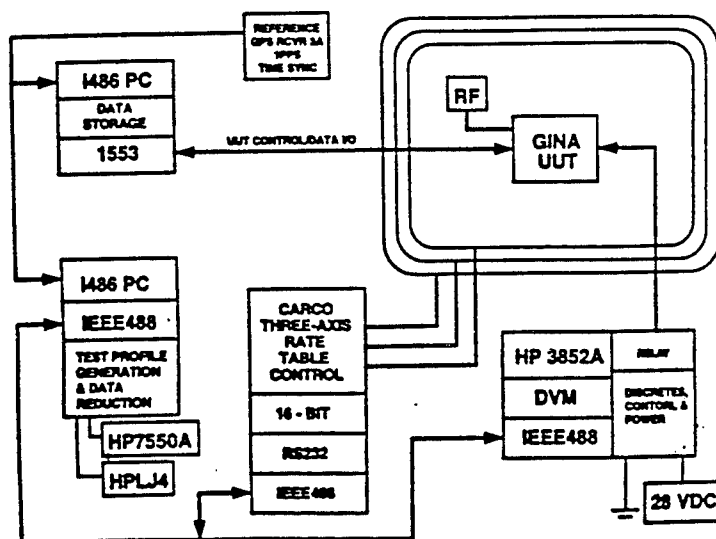


Figure-4 Inertial Test Configuration

3.2 Mobile Test Facility Overview

The Mobile Navigation Test Facility (MNTF) is a completely self-contained mobile laboratory designed for testing navigation and communication equipment. Provided on-board the van are: 15KVA of 115 volt 60 HZ power, 115 volt 400 HZ power and adjustable DC power. Power is distributed to four project work stations, each of which includes a standard 19 inch rack for mounting equipment and adjustable seats for test engineers. Provided as part of the van test facility is a integrated GPS/LTN-72 INS reference system. When used in conjunction with the surveyed and calibrated NRaD airfield test range, the reference system can be used to post-process position and velocity accuracy of less than two meters CEP and two dimensional velocity accuracy of less than 0.05 meters/second. This setup was used during GINA hybrid navigation performance testing.

4.0 Test Results

The result provided in this section were obtained during Government Qualification Test and Evaluation (QT&E) testing performed at the Naval Command, Control and Ocean Surveillance Center, RDT&E Division, Warminster Detachment (NRaD). The GINA inertial navigation performance baseline was established over GINA system processor software versions (GSP-84, GSP-107, GSP-132, GSP-150, GSP-171, GSP-196, GSP-209 and GSP-248) using four GINA QT&E assets. The GEM-III performance results were obtained from GEM-III software release AGL-12.

4.1 GINA Inertial Alignment

The GINA design supports two primary alignment types, either a fixed base alignment or a moving base alignment. The options for a fixed base alignment are a gyrocompass ground align or a stored heading ground align. Entry into a fixed base align mode requires valid latitude/longitude, weight-on-wheels mode discrete set true, parking brake hardware discrete set, and the at sea mode discrete set false. Entry into a moving base alignment will result if GPS navigation data is valid and the weight-on-wheels discrete is false or the shipboard mode discrete is true. The results from GINA gyrocompass alignment and GPS inflight alignment tests will be discussed.

4.1.1 Gyrocompass Alignment Test Results

The gyrocompass alignment is a zero velocity based alignment of the inertial system to the local level and true north. Following entry of present position this alignment can occur based solely on zero velocity updates, or can be augmented by GPS, Doppler and/or baro altitude measurements. If additional measurements are provided, the data is combined in a statistical manner based on the associated Kalman

GINA LAIP
MOBILE TEST FACILITY (MTF) CONFIGURATION

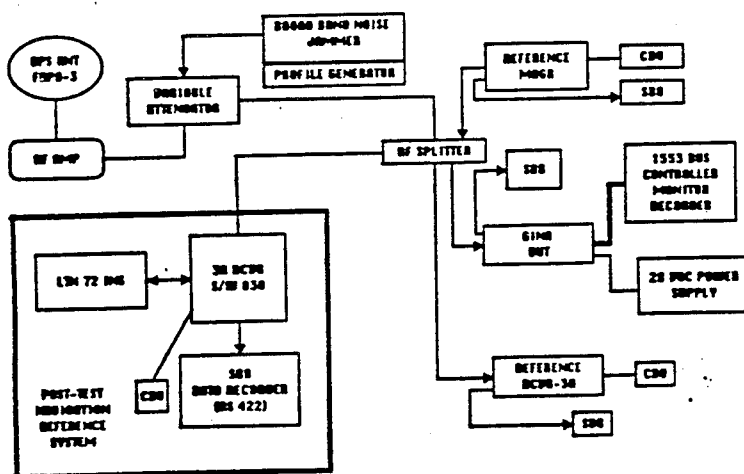


Figure-5 Van Test Configuration

filter noise parameters. The zero velocity update is a strong update relative to all other sources, the effect of additional inputs is a calibration of the filter states associated with these other sources.

In order to evaluate heading alignment, a series of gyrocompass alignments were performed in the SDNL laboratory with the GINA mounted on a single axis Contraves rate table. The mount was boresighted using an optical alignment fixture provided by Litton. The boresight accuracy of the SDNL test fixture is estimated to be better than 5 arc_sec (0.00138 deg.). The SDNL gyrocompass alignment tests were performed with baro altitude aiding only. The results of 124 Gyrocompass alignments over various GINA software versions are provided in table-1. A heading sensitivity problem found in interim GINA software versions was not evident in the latest GSP-248 release.

Table-1
Gyrocompass Alignment Test Results

GSP VERSION	ALIGN TIME (MINS.)	LRIP #2 COMPOSITE HDG ERROR	LRIP #4 COMPOSITE HDG ERROR	LRIP #7 COMPOSITE HDG ERROR	LRIP #8 COMPOSITE HDG ERROR	COMPOSITE SYSTEM HDG ERROR
GSP 084	3	0.0408	0.0825	N/A	N/A	0.0708
	4	0.0441	0.0781	N/A	N/A	0.0687
GSP 132	3	0.0491	0.0958	N/A	N/A	0.0703
	4	0.0464	0.089	N/A	N/A	0.068
GSP 150	3	0.0484	N/A	N/A	N/A	0.0484
	4	0.0424	N/A	N/A	N/A	0.0424
GSP 208	3	N/A	N/A	0.0801	0.0893	0.0848
	4	N/A	N/A	0.0772	0.0722	0.0747
GSP 248	3	N/A	N/A	N/A	0.0275	0.0275
	4	N/A	N/A	N/A	0.0461	0.0461
COMPOSITE SOFTWARE	3	0.0468	0.0889	0.0801	0.0861	0.0879
	4	0.0442	0.0819	0.0772	0.0605	0.0839

4.1.2 Inflight Alignment Test Results

A GPS Inflight alignment is based on position and velocity errors computed from the comparison of the GPS position and velocity with inertial position and velocity. The process results in the alignment of the inertial system to the local level and true north. Entry into the GPS inflight alignment mode requires valid GPS position and velocity data

and the entry of the platform GPS antenna lever arm data. The GINA utilizes GPS derived position and velocity (PVT) data prior to inertial course align complete and individual satellite line of sight (LOS) measurements during fine alignment. The GINA tolerates GPS data dropouts for up to 65 seconds during a inflight alignment. Data dropouts greater than 65 seconds will cause the alignment to restart. Therefore, it is recommended that a reasonable flight profile be maintained prior to completion of inertial course alignment

The inflight alignment capability of the GINA was evaluated during van testing while traveling along a North/South or East/West heading. Other than GPS RF and valid lever arm entry no initialization data was supplied to the GINA. Upon completion of the inflight alignment the GINA was commanded into the standalone mode while the van continued to travel for 1.5 hours in the direction of the alignment. Both keyed and unkeyed inflight alignments were tested.

The test results show that inflight align time and alignment quality are dependent upon the flight path and keyed state of the GINA. Optimal alignments are achieved when the GINA is keyed (PPS accuracy) during moderate platform dynamics. The alignment times and subsequent free inertial performance following both keyed and unkeyed inflight alignments are provided in table-2.

Table-2
Inflight Alignment Test Results

NAVIGATION PERFORMANCE				AFTER AN IN-FLIGHT ALIGNMENT WITH GPS			
KEYED INFLIGHT ALIGNMENT							
LRIP UNIT	REFERENCE	TEST RUN #	GSP VERSION	ALIGNMENT	CEP RATE	KEYED	
NUMBER	HEADING			TIME (SEC)	NM/HR		
1004	E → W	1	171	259	0.776	YES	
1004	S → N	2	171	308	0.299	YES	
		RMS		283.5	0.58803784		
UNKEYED INFLIGHT ALIGNMENT							
LRIP UNIT	REFERENCE	TEST RUN #	GSP VERSION	ALIGNMENT	CEP RATE	KEYED	
NUMBER	HEADING			TIME (SEC)	NM/HR		
1004	W → E	1	171	1143	1.25	NO	

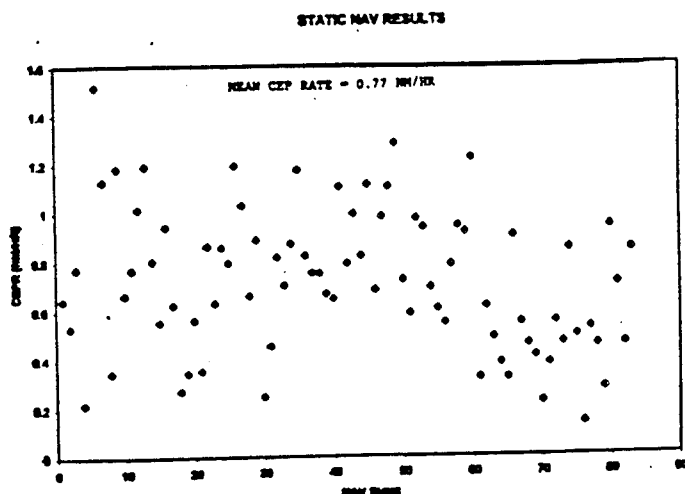
4.2 GINA Standalone Navigation

The GINA outputs a free inertial and GPS-only navigation solution while operating in the standalone mode. The free inertial solution is based solely on inertial sensor data and external barometric altitude aiding. The GPS-only navigation solution is based solely on GEM-III sensor data, with inertial aiding of the GPS tracking loops if the inertial data is available. The failure of either the inertial or GPS sensors does not affect the output of the other navigation solution.

4.2.1 Free Inertial Test Results

The free inertial results presented here are composite results from the standalone navigation performance tests conducted on four GINA QT&E systems. Following a 3 minute gyrocompass alignment at various headings, the GINA was commanded into the standalone mode and allowed to navigate for 90 minutes. The composite navigation performance from 83 trials was 0.77 NM/HR. Table-3 is a plot of the CEPR(NM/HR) of each standalone navigation test.

Table-3
Inertial Navigation Performance Results



4.2.2 GEM-III Test Results

The GINA GEM-III was tested in the NRAd GPS CEA laboratory over specified dynamic range and satellite signal levels. The ability of the GEM-III to provide a standalone PVT solution was successfully tested and verified at maximum dynamics without jamming. Test results are provided in table-4. The GEM-III failed to meet tracking reliability and navigation performance requirements under conditions of state 5 jamming. This shortfall is a documented deficiency with contractor corrective action planned during 4TH quarter FY 96.

Table-4
GPS Navigation Performance Results

GEM III P-Code Navigation Performance Normalized
GEM III AGU-12

Specifications per MIL-GINA XXX		Position Error (M)		Velocity Error (M/S)
Test	Condition	Horizontal	Vertical	3d RMS
GEM III L1/F NAV PERF NO JAMMING	Constant Dynamics	1.262 (pass)	1.035 (pass)	0.036 (pass)
	Maximum Dynamics	1.206 (pass)	0.995 (pass)	0.702 (pass)

4.3 GINA Hybrid Performance

The GINA outputs a hybrid and GPS-only navigation solution while operating in the hybrid mode. The hybrid solution is based on inertial and GPS data (both GPS and inertial "aiding" each other). The hybrid kalman filter solution runs on a 4 second update period. Between GPS updates, the system uses inertial system outputs to propagate the hybrid position, velocity and altitude. In parallel the GEM-III, with tracking loop aiding, continues to track satellites and outputs a GPS based (PVT) solution. Failure of the inertial sensor does not preclude the output of the GPS solution. Upon GPS failure, the hybrid solution will be based on

inertial data only. The hybrid test results in this section were obtained from van testing at NRaD Warminster airfield.

4.3.1 Hybrid Navigation Test Results

The GINA will operate in hybrid mode during cryptographically authorized as well as unauthorized conditions. When operating "unauthorized" the GPS sensor measurements to the blending filter are inhibited by default. The operator must provide an input enabling incorporation of unauthorized GPS measurements into the hybrid solution. During unauthorized hybrid operation GPS C/A code measurements are processed with the GPS figure of merit (FOM) reflecting the accuracy degradation. GINA authorized and unauthorized hybrid navigation results obtained during van testing are summarized in table-5 and table-6 respectively. Position and velocity plots for the hybrid tests are provided on the following page.

Table-5
GINA Authorized Hybrid Performance

MISSION TIME	Position Error Meters (RMS)			Velocity Error Meters/Sec (RMS)		
	LON	LAT	ALT	VE	VN	Vz
15:46 to 16:39	2.51	2.90	4.14	0.049	0.046	N/A

Table-6
GINA Unauthorized Hybrid Performance

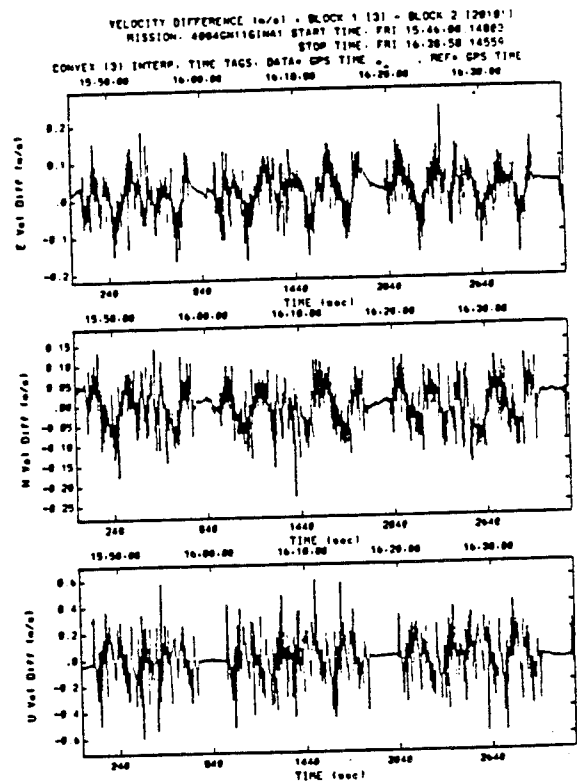
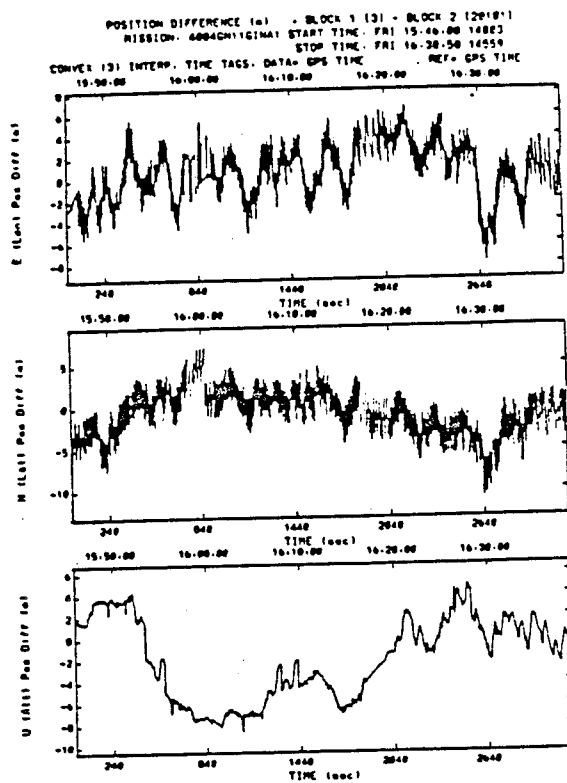
MISSION TIME	Position Error Meters (RMS)			Velocity Error Meters/Sec (RMS)		
	LON	LAT	ALT	VE	VN	Vz
18:40 to 19:44	22.94	23.34	22.12	0.125	0.188	N/A

During hybrid operation after course align is complete the GINA is considered to be operating in a "Fine Align" state. In "Fine Align" the inertial alignment estimate is continuously refined and navigation is performed using all available aiding data such as GPS, baro, etc. The continuous refinement of the inertial alignment in hybrid mode allows for improved free inertial navigation performance following the loss of GPS aiding data. A 3 HR tests was designed where the GINA was operated in standalone mode (after a gyrocompass alignment) during the 1ST HR, hybrid mode during the 2nd HR and hybrid mode with the GPS antenna disconnected during the 3RD hour. Six tests were performed; 3-keyed and 3-unkeyed. A comparison of the "Free Inertial" performance before and after hybrid operation shows marked improvement in inertial performance following "keyed" hybrid operation. The results of the "unkeyed" hybrid test indicate no further refinement of the initial gyrocompass alignment. The individual tests results are summarized in table-7. The graphs in figure-6 and figure-7 provide the GINA inertial CEPR plots resulting from the tests.

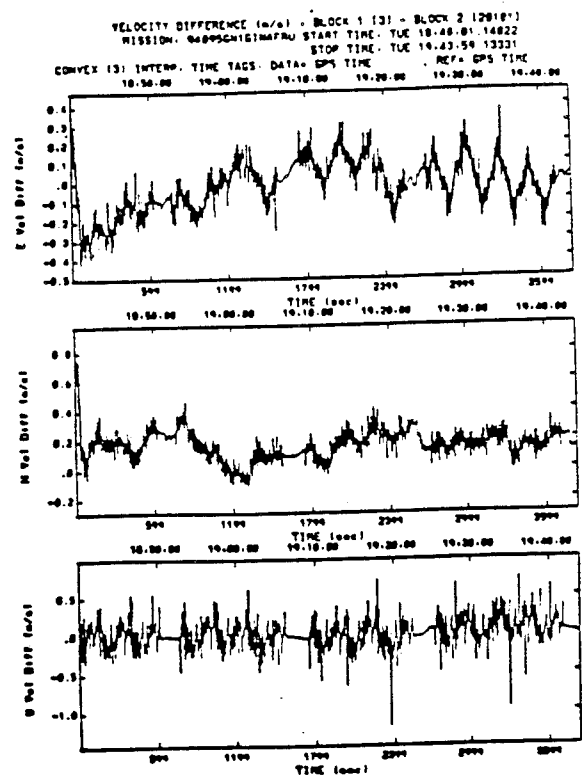
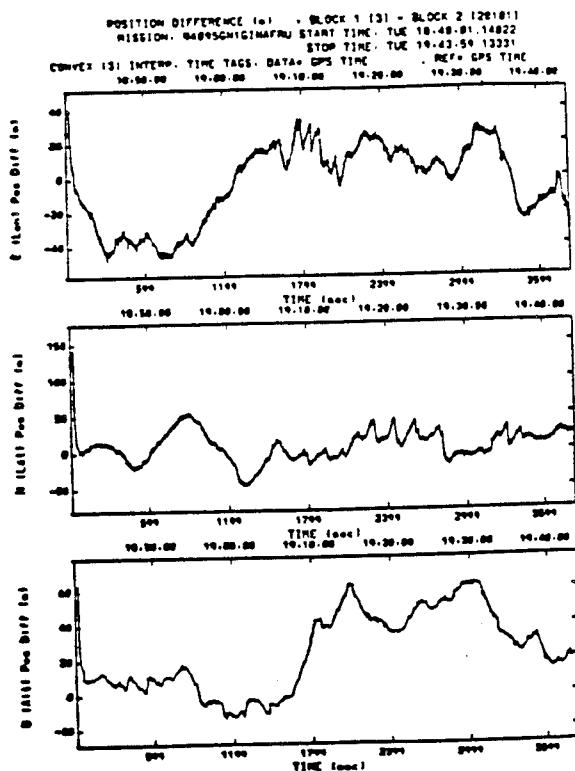
Table-7 GINA CEPR - Composite

STATIC HYBRID NAVIGATION						
TEST RUN #	SCENARIO	ALIGNMENT TIME (MIN)	INAV	HNNAV	HNNAV-GPS REF	
			CEP RATE NM/HR	CEP RATE NM/HR	CEP RATE NM/HR	
601	KEYED	4	0.249921	0.004976	0.192151	
612	KEYED	4	0.706036	0.004786	0.11075	
621	KEYED	4	0.209062	0.005779	0.165164	
632	UNKEYED	4	0.691182	0.026968	0.475502	
641	UNKEYED	4	0.318871	0.028917	0.595842	
671	UNKEYED	4	0.175249	0.037262	0.411918	
KEYED SCENARIO RMS			0.44894478	0.00519818	0.159652452	
UNKEYED SCENARIO RMS			0.45097061	0.03136836	0.500268668	

GINA Hybrid Authorized Navigation Performance



GINA Hybrid Unauthorized Navigation Performance



5.0 Summary

The Government Qualification testing performed at NRaD, certified that the GINA meets critical T-45TS navigation requirements and is recommended for operational testing.

References:

[1] Interim Test Report, Government Laboratory Qualification Test and Evaluation For The GPS Inertial Navigation Assembly (GINA), NRaD Document, January 1995.

[2] David A. Nelthropp, James Campanile and Luci Federici, Integration of Embedded GPS/Inertial Navigation on the T-45TS, Annual meeting of the Institute of Navigation, September 1992

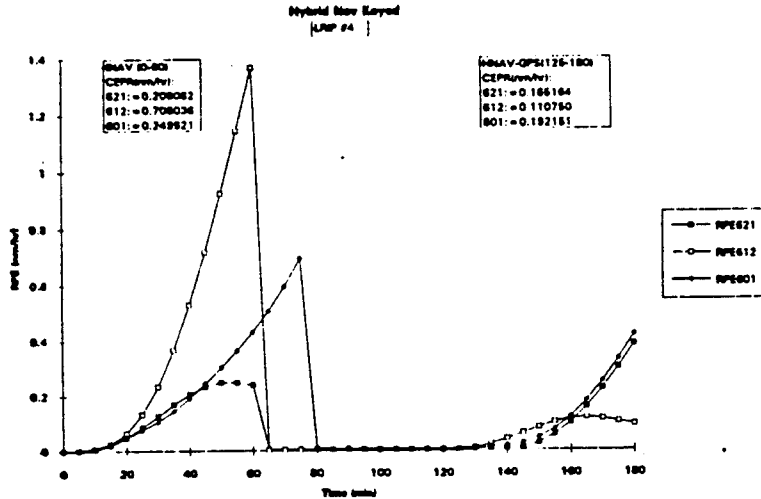


Figure-6 GINA CEPR - Keyed Test

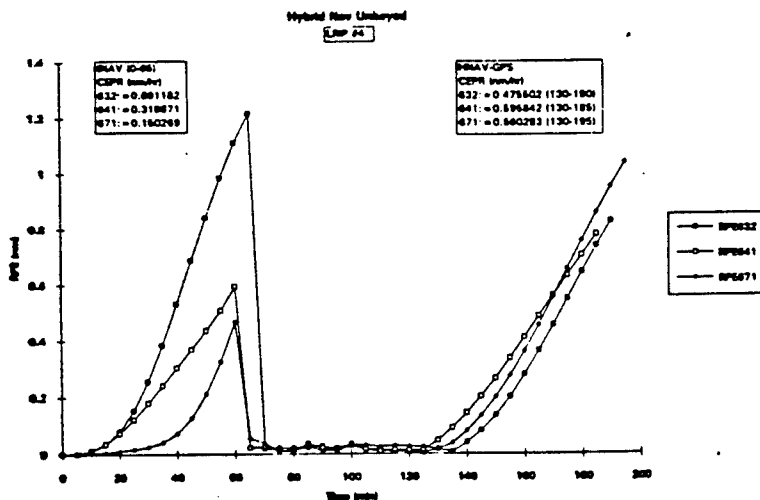


Figure-7 GINA CEPR - Unkeyed Test

THIS PAGE LEFT BLANK INTENTIONALLY

SESSION VII-B

GPS TOPICS II

CHAIRMAN

ROBERT MCADORY

*GEC-MARCONI ELECTRONIC SYSTEMS
DAYTON OH*

THIS PAGE LEFT BLANK INTENTIONALLY

STATISTICAL SIGNIFICANCE
FOR
GLOBAL POSITIONING SYSTEM (GPS)
TESTS AND EVALUATION

by

Robert M. Rogers
Rogers Engineering & Associates
Gainesville, FL 32604

presented at the
Seventeenth Biennial Guidance Test Symposium
Holloman Air Force Base, New Mexico
2-3-4 May 1995

Approved for Public Release; distribution is unlimited.

THIS PAGE LEFT BLANK INTENTIONALLY

Statistical Significance for Global Positioning System (GPS) Tests and Evaluation

Robert M. Rogers
Rogers Engineering & Associates

Abstract

This paper examines a method for establishing the statistical significance of GPS Precise Positioning Service (PPS) test data. The GPS PPS position errors can be ideally characterized by a compound Poisson process with an additive independent random Gaussian process. Using approximating arguments and monte carlo simulation results, the statistical distribution for these errors is shown to be chi-squared with the number of degrees-of-freedom governed by the number of satellite constellation changes.

Introduction

Several GPS PPS receivers, integrated as part of an inertial navigation system, are undergoing tests, i.e. the Miniature Airborne GPS Receiver (MAGR) [Ref. 1] and the Embedded GPS Inertial (EGI) [Ref. 2]. The position data from these tests are compared independent position reference systems. The difference between the navigation system and the reference system forms the basic test data from which to evaluate the navigation system's performance.

Test data analysis has several objectives including system function and performance. After the system's functioning is deemed correct, then attention focuses on the observed performance; however, these are not easily separable. The system performance is typically presented as a mean error and standard deviation, see [Ref. 1], or as error time histories, see [Ref. 2]. The significance of these statistics are not usually addressed.

Errors associated with GPS PPS ranging data include; satellite vehicle ephemeris and clock errors, atmospheric delay error, user equipment and multi-path errors [Ref. 3]. Processing within the user equipment combines the ranging for individual satellites and produces a position navigation solution defined in a local navigation frame. The result of combining individual satellite ranging errors, for a given constellation, is a nominal solution point position error, or mean error, that is shifted from the origin and random scatter about this mean. Accompanying each satellite constellation change, a different group of satellites with their individual errors, is a different mean error.

Shown in Fig. 1 is a typical data scatter plot of GPS position error. This figure shows the shifting of the mean with satellite constellation changes and accompanying scatter about these points.

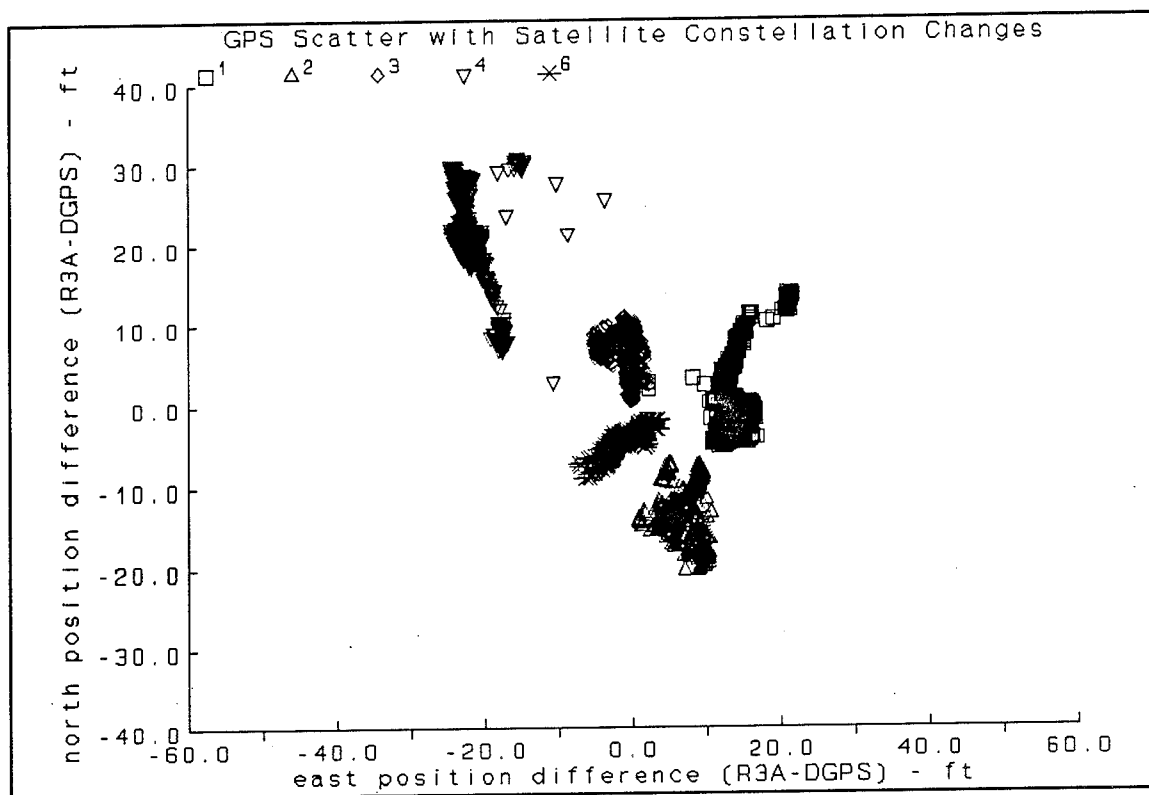


Figure 1: Typical GPS Position Error

The objective of this paper is to develop a methodology to determine the statistical significance of GPS performance from test data like that shown in Fig. 1. This objective is accomplished by considering a single component or axis, and developing the test statistic for this single axis. Extension to two axes follows with the assumption of stochastic independence between axes.

Single axis position error scatter is illustrated in Fig. 2 with simulated data representing several mean shifts, events, for what would be constellation changes. A histogram for this data, presented in this figure, shows the multi-modal nature of this data corresponding to the distribution of the mean errors. Ideally, there are two stochastic processes, one that governs the shifted mean errors and the other that governs the scatter about that mean.

The shifting mean is a compound Poisson process [Ref. 4]. The event occurs randomly in time and is of random duration, and the amplitude of the event (shifted mean) is governed by a Gaussian process. The scatter about the shifted mean is governed by another independent Gaussian process.

In the actual data in Fig. 1, the distribution scatter about the shifted mean is the governed by the satellite geometry with the elongated axis of an ellipse containing the data points being normal to the alignment direction of the satellites being used.

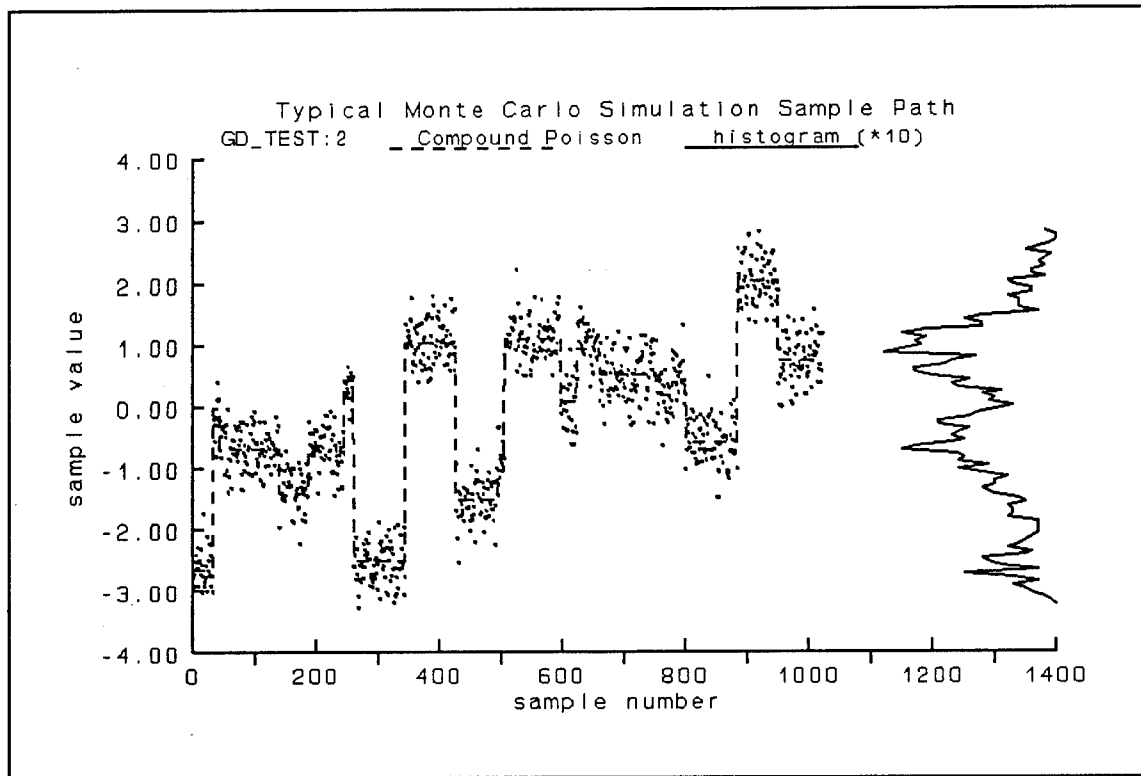


Figure 2: Single Axis Simulated Data

Chi-Squared Statistic

The chi-squared statistic assumes independent, identically distributed, observations of a normally distributed population [Ref. 5]. Clearly, from the figures above, the direct application of this statistic is not consistent with this assumption since subsequent observations are not from an identically distributed population. In the following, the chi-squared statistic for a single shifted mean event is considered.

The variance about a population mean, ξ_x , can be written as the following variation about the j^{th} event sample mean, μ_{x_j} , as

$$\begin{aligned} \sum_{i=1}^{n_j} (x_{i,j} - \xi_x)^2 &= \sum_{i=1}^{n_j} [(x_{i,j} - \mu_{x_j}) + (\mu_{x_j} - \xi_x)]^2 \\ &= \left[\sum_{i=1}^{n_j} (x_{i,j} - \mu_{x_j})^2 + n_j (\mu_{x_j} - \xi_x)^2 \right] \quad (1) \end{aligned}$$

since

$$\sum_{i=1}^{n_j} (x_{i,j} - \mu_{x_j}) \equiv 0 \quad \text{and} \quad (\mu_{x_j} - \xi_x) = \text{constant}$$

Defining a normalized variable

$$u_{i,j} = \frac{x_{i,j} - \xi_x}{\sigma_x} \quad (2)$$

then the chi-squared statistic for the j^{th} event becomes

$$\chi_j^2 = \sum_{i=1}^{n_j} u_{i,j}^2 = \sum_{i=1}^{n_j} (u_{i,j} - \mu_{u_j})^2 + n_j \mu_{u_j}^2 \quad (3)$$

where

$$\mu_{u_j} = \frac{\mu_x - \xi_x}{\sigma_x} \quad (4)$$

and σ_x^2 is the shifted mean variance. In Eq. (3) above, χ^2 has been partitioned into the sum of two terms, with the first being chi-squared distributed with n_j-1 degrees-of-freedom and the second chi-squared distributed with 1 degree-of-freedom [Ref. 5].

Examining the first of the terms in far right part of Eq. (3), if the sample points are closely grouped about the mean, then

$$u_{i,j} \approx \mu_{u_j} \quad (5)$$

and the chi-squared statistic for the j^{th} event is approximated by

$$\chi_j^2 \approx n_j \mu_{u_j}^2 \quad (6)$$

which is chi-squared distributed with 1 degree-of-freedom.

Now consider that the mean shifts occur k times, corresponding to k satellite constellation change events, with each of the resulting chi-squared variables being stochastically independent. From [Ref. 5], the Addition Theorem for a chi-squared distribution is stated as:

"If $\chi_1^2, \chi_1^2, \dots, \chi_k^2$ are stochastically independent and have χ^2 -distributions with f_1, f_2, \dots, f_k degrees of freedom, respectively, then the sum

$$\chi^2 = \chi_1^2 + \chi_2^2 + \dots + \chi_k^2$$

also has a χ^2 -distribution with $f=f_1+f_2+\dots+f_k$ degrees of freedom."

Therefore, with the approximation defined by Eq. (5) above, the chi-squared variable for the ensemble of samples becomes

$$\begin{aligned}
 \chi^2 &= \chi_1^2 + \chi_2^2 + \dots + \chi_k^2 \\
 &\approx n_1 \mu_{u_1}^2 + n_2 \mu_{u_2}^2 + \dots + n_k \mu_{u_k}^2 \\
 &= \frac{1}{\sigma_x^2} \sum_{j=1}^k n_j \mu_{x_j}^2
 \end{aligned} \tag{7}$$

with k degrees of freedom. The population mean, ξ_x , is zero.

This demonstrates that the number of degrees-of-freedom for the entire ensemble of data points is the number of satellite constellation changes and not the total number of observations.

Numerical Experiments

Monte Carlo simulations are used to establish, by numerical experiments, values of the chi-squared statistic. Fig. 2 shows a single sample path generated by the simulation. For the results presented in this section, one-thousand such sample paths were generated to establish the value of the chi-squared statistic as a function of the magnitude of the scatter about the shifted means.

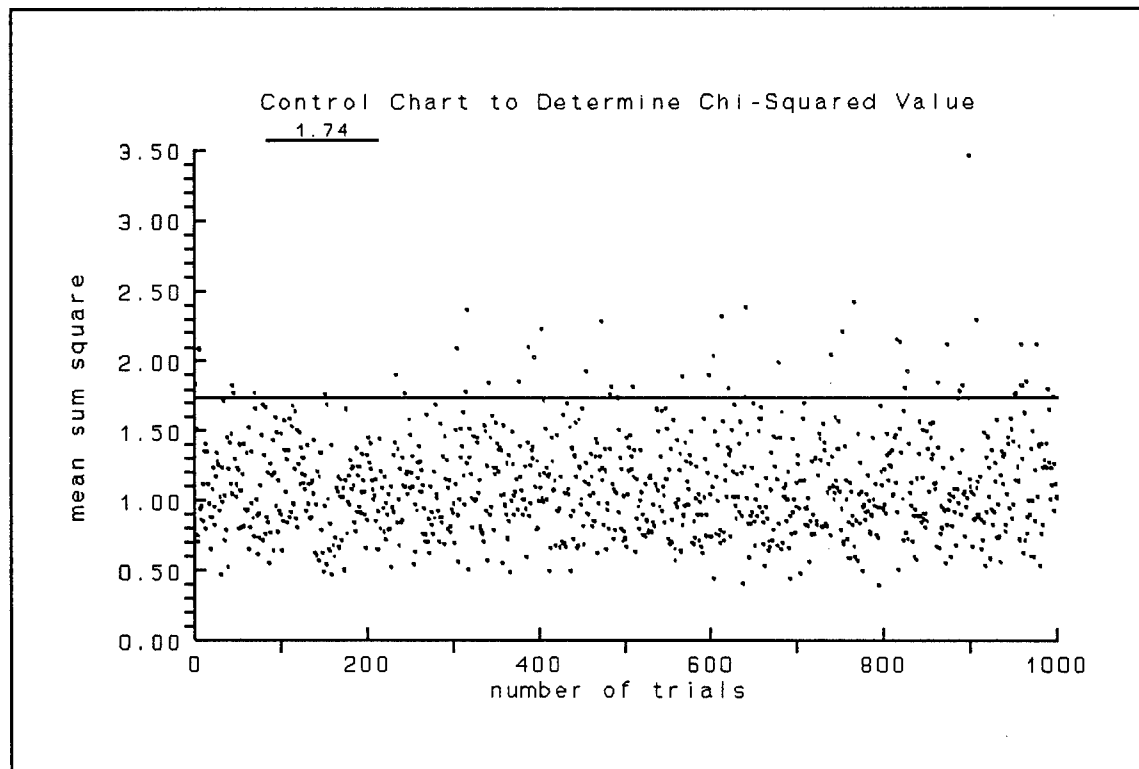


Figure 3: Example Control Chart

A control chart [Ref. 5] is used to determine the probability that an actual chi-squared value exceeds a specified percentage of occurrences. An example of this control chart is shown in Fig. 3. Repeated application of the Monte Carlo simulation yields the results summarized in Table 1. In this table, different values for the scattering about the shifted mean are parameterized as a function of the ratio σ_s/σ .

To establish a cross check for the values generated using this technique, the Monte Carlo simulation was used to generate the chi-squared values with no additional scatter about the shifted mean $\sigma_s/\sigma=0$. The resulting values should be the same as the chi-squared values obtained from statistical tables - $\chi_{\alpha,k}^2/k$ -Tables. Consistently, the Monte Carlo simulation values are slightly higher than the table values, and represents the simulations' imprecision and represents the amount by which the corresponding values in each row of the table should be adjusted. The results in Table 1 conform to the following model.

$$\chi^2/n = \chi_{\alpha,k}^2/k + (\sigma_s/\sigma)^2 \quad (8)$$

Additional Monte Carlo simulations show that the same model holds when the scatter about the shifted mean is governed not by the same σ_s for each shift, but by a random value for each event. In this case, the random value of σ_s was selected from a uniform distribution whose mean value is the same as σ_s used for the table above. This result suggests that the assumption of axis independence is not restrictive in its application to a bi-variate problem for which the number of degrees-of-freedom is $2k$.

Tests of Significance

The tests of significance commonly used include the chi-squared test, and are based on the following unilateral and bilateral fractile definitions [Ref. 5]:

$$\text{Prob} [\chi^2 < \chi_{\alpha,k}^2] = 1 - \alpha, \quad (9)$$

and

$$\text{Prob} [\chi_{\alpha_1,k}^2 < \chi^2 < \chi_{\alpha_2,k}^2] = \alpha_1 - \alpha_2 \quad (10)$$

The second of these fractiles will be used to demonstrate the application of the results obtained in this paper.

The data presented in Fig. 2 is used for this illustration. For the ratio $\sigma_s/\sigma = 1/3$ ($\sigma = 1$), the result is $\chi^2/n = 1.798$. The problem is to determine the confidence interval, defined by Eq. (10), for this result. Two values of α will be used to illustrate the application this test.

Table 1
Numerical Experiment (Monte Carlo Simulation) Results
Prob [$\chi^2 > \chi_{\alpha,k}^2$] = $\alpha = n_\alpha/n$
($n=1000$)

$\alpha=5\%$ ($n_\alpha=50$) χ^2/n					
$k \backslash \sigma_s/\sigma$	0	$1/5$	$1/3$	$1/2$	$\chi_{\alpha,k}^2/k$ -Tables
20	1.64	1.68	1.74	1.88	1.57
50	1.38	1.43	1.49	1.64	1.35
100	1.29	1.33	1.40	1.54	1.24

$\alpha=10\%$ ($n_\alpha=100$) χ^2/n					
$k \backslash \sigma_s/\sigma$	0	$1/5$	$1/3$	$1/2$	$\chi_{\alpha,k}^2/k$ -Tables
20	1.43	1.48	1.56	1.70	1.42
50	1.29	1.33	1.40	1.54	1.26
100	1.20	1.25	1.31	1.45	1.18

$\alpha=50\%$ ($n_\alpha=500$) χ^2/n					
$k \backslash \sigma_s/\sigma$	0	$1/5$	$1/3$	$1/2$	$\chi_{\alpha,k}^2/k$ -Tables
20	0.94	0.98	1.05	1.19	0.96
50	0.97	1.01	1.08	1.22	0.99
100	0.99	1.03	1.10	1.24	0.99

$\alpha=90\%$ ($n_\alpha=900$) χ^2/n					
$k \backslash \sigma_s/\sigma$	0	$1/5$	$1/3$	$1/2$	$\chi_{\alpha,k}^2/k$ -Tables
20	0.58	0.63	0.70	0.84	0.62
50	0.72	0.77	0.83	0.97	0.75
100	0.79	0.83	0.90	1.04	0.82

$\alpha=95\%$ ($n_\alpha=950$) χ^2/n					
$k \backslash \sigma_s/\sigma$	0	$1/5$	$1/3$	$1/2$	$\chi_{\alpha,k}^2/k$ -Tables
20	0.52	0.56	0.63	0.77	0.54
50	0.66	0.70	0.78	0.91	0.70
100	0.75	0.78	0.85	0.99	0.78

For the first, a 90% interval, the Table values [Ref. 6] of the chi-squared variables $\chi_{0.05,20}^2/k$ and $\chi_{0.95,20}^2/k$ are 0.543 and 1.571. Adding $(\sigma_s/\sigma)^2$ to each of these, the test becomes;

$$? \quad 0.654 < \chi^2/n < 1.682$$

$\chi^2/n = 1.798$ falls outside the interval; therefore, the test fails at a 90% confidence level. For the second, a 95% interval, the Table values of the chi-squared variables $\chi_{0.025,20}^2/k$ and $\chi_{0.975,20}^2/k$ are 0.480 and 1.708. Again, adding $(\sigma_s/\sigma)^2$, the test is;

$$? \quad 0.591 < \chi^2/n < 1.819$$

$\chi^2/n = 1.798$ falls inside this interval; therefore, the test is passed at a 95% confidence level.

Close examination of Fig. 3, for the first mean sum square sample result, reveals that this sample did exceed the threshold value of 1.74, corresponding to a unilateral test for an $\alpha=0.05$, which agrees results obtained in this illustration.

Conclusion

The chi-squared statistic, modified by the number of satellite constellation changes as the number of degrees-of-freedom and by the scatter variation about the shifted mean, can be used to assess the statistical significance of GPS PPS test data.

References

1. Peterson, M., Stiles, B.T. and Boykin, L., "CIGTF Verification Testing of the SNU 84-1E", Sixteenth Guidance Test Symposium, AFDTC-TR-93-06, Vol. I, October 1993, pp 703-717.
2. Elchynski, J.J. and Syse, D., "Test and Evaluation Status of the Honeywell H-764G Embedded GPS/INS at CIGTF", Sixteenth Guidance Test Symposium, AFDTC-TR-93-06, Vol. I, October 1993, pp 733-751.
3. Milliken, R.J. and Zoller, C.J., "Principal of Operation of NAVSTAR and System Characteristics", Navigation, Vol. 25, No. 2, Summer 1978, pp 95-106.
4. Snyder, D.L., Random Point Processes, John Wiley and Sons, Inc., New York, 1975.
5. Hald, A., Statistical Theory with Engineering Applications, John Wiley and Sons, Inc., New York, 1952.
6. Abramowitz, M. and Stegun, I.A., Ed., Handbook of Mathematical Functions, Dover, New York, 1972.

THIS PAGE LEFT BLANK INTENTIONALLY

**Investigation into the
Reliability of the
DoD Miniaturized Airborne
Global Positioning System
Receiver (MAGR)**

Prepared By:
Geoffrey J. Barnes
Bruce A. McCullough

Advanced Stand-Alone
GPS Projects IPPD

March 2, 1995

Mail Station 153-160
Collins Avionics and Communications Division
Rockwell Defense Electronics
400 Collins Road, NE
Cedar Rapids, Iowa 52498
TEL: 319 395 8609 / 2682
FAX: 319 395 1642

Approved for Public Release; distribution is unlimited.

THIS PAGE LEFT BLANK INTENTIONALLY

Investigation into the Reliability of the DoD Miniaturized Airborne Global Positioning System Receiver (MAGR)

Geoffrey J. Barnes and Bruce A. McCullough; Collins Avionics & Communications Division,
Rockwell International. Cedar Rapids Iowa 52498.

BIOGRAPHY

Geoffrey Barnes graduated from the Royal Australian Air Force (RAAF) Academy in 1978. He was an air navigator in the RAAF until 1987 with tours including C-130, P-3C and F/A-18. In 1987 he joined Rockwell International and worked at Cedar Rapids on GPS Integration and Development with the U.S. DoD Phase 3 GPS Receivers. In 1992 he left Rockwell to work for the Australian Department of Defence GPS Joint Program Office. In 1994 he joined Collins Avionics & Communications Division as a Senior Design Engineer. His current duties include supporting MAGR Integrations for both domestic and international users.

Bruce McCullough graduated from the University of Missouri-Columbia in 1988. He served as a control systems engineer with McDonnell Aircraft Company and as an avionics systems engineer with ARINC Research Corporation before joining Collins Avionics & Communications Division as a GPS applications engineer. His current duties include support of MAGR Integration activities for both domestic and international users.

ABSTRACT

Production units of the U.S. Department of Defense (DoD) Standard five channel Miniature Airborne GPS Receiver (MAGR) are now being delivered by Collins Avionics & Communications Division (CACD), Rockwell International Corporation. MAGR is required to be highly reliable over a range of environmental and dynamic conditions as experienced by high performance military platforms. This paper presents methods and findings of an investigation of reliability based upon data gathered from factory, field, and integration testing of MAGR Integration Models (IM).

This paper also categorizes those failures found to be caused by design deficiency. A discussion of reported failures that could not be replicated by CACD, as well as currently unresolved discrepancies is also presented.

SECTION 1

INTRODUCTION

1.1 *MAGR Program Background*

The DoD Standard Miniaturized Airborne GPS Receiver (MAGR) is designed and built by the Collins Avionics & Communications Division (CACD) of Rockwell Defense Electronics as a smaller version of the DoD Standard Airborne GPS Receiver (RCVR 3A). The effort to design and build MAGR was a two step process. Step one of this process was an internally funded (IR&D) project that culminated in the development of the RCVR 3M as the bid sample for the MAGR Non-Development Item (NDI) procurement. Subsequently, the U.S. DoD funded Rockwell for the development and production of MAGR, which implemented a number of additional and improved functional capabilities over the RCVR 3A. Among these improvements is a requirement that MAGR shall provide a Mean Time Between Failure (MTBF) of 2000 hours (versus 1350 hours for the RCVR 3A), where failure is defined as "*a deficiency of the receiver in meeting performance requirements ...due to hardware or software, including false indications of failure*"¹.

Phase 1 of the MAGR contract resulted in the delivery of 92 units known as Integration Models (IM) - delivered as 27 Intermediate Frequency (IF - requiring an antenna electronics) and 65 RF (Radio Frequency) versions. These were delivered to the GPS Joint Program Office (JPO) for a variety of test and validation activities. Phase 2 of the MAGR contract was awarded April, 1994 and resulted in delivery of the first of the Production Model MAGRs beginning in July, 1994. This paper focuses largely upon reliability of the IM MAGRs as little reliability data is available at this time for Production Models. (Reliability data for Production Models is presented where available.)

1.2 *MAGR Reliability Estimation*

The ability of the MAGR design to meet reliability requirements was verified by Combined Environmental, Reliability Testing (CERT). The objective of CERT was to test MAGR in a "combined environment of temperature, vibration, humidity, and input power variations to simulate the field environment of a high performance fighter aircraft"². A total of 11,911.73 valid test "ON" hours resulted in two relevant failures. A point estimate of MTBF was thereby derived as:

$$MTBF = \frac{11,911.73}{2} = 5,955.86$$

Appendix 1 to this paper contains the CERT profiles used for this verification.

¹ CI-MAGR-300, Page 50.

² Combined Environmental, Reliability Test Report for MAGR, Page 5.

1.3 Purpose of Investigation

The purpose of this paper is to document verification of CERT results by analyzing failures and deficiencies that have occurred during Phase 1 of the MAGR program. Because this investigation focuses on data captured during Phase 1, it is expected that a greater number of failures will be the result of design deficiencies. The incidence of these type of failures is expected to diminish as the design matures. Similarly, as operational time increases on fielded receivers during Phase 2 and subsequent productions, it can be expected that the incidence of failure due to component breakdown will increase. Nevertheless, this report provides an early assessment and verification of MAGR's actual reliability as defined by the MAGR specification.

SECTION 2

METHOD OF INVESTIGATION

2.1 Scope of Investigation

This investigation includes all data captured to date for both production and integration models. However, because of the relatively low amount of operational hours that have been accumulated by Production Models, the data captured for this investigation comes primarily from IM MAGRs. There are no fundamental differences between IM and Production Model MAGRs.

2.2 Source of Reliability Data

Reported deficiency data for this investigation have been captured primarily from Service Worksheets. The Service Worksheet is initiated upon receipt of Contractor Returned Goods (CRG) by the factory and is used to document the customer complaint as well as all service action. The Service Worksheet therefore serves as a reliable source of information on failures *that resulted in the unit being returned to the factory*.

Other sources of data used for this investigation are the files maintained at Cedar Rapids by the GPS Integration Group including memos and records of telephone conversations relating to suspected MAGR deficiencies. In some cases these deficiencies were not verifiable or were caused by application specific circumstances such as operator error or host system design deficiencies.

2.3 Categorization of Reliability Data

After an initial review of the Service Worksheets, it was decided to categorize deficiencies as follows:

- **Hardware Design (Type 1 Deficiency):** Any incident which is the result of deficiencies within the hardware or firmware design of MAGR, and which is corrected through upgrade of the deficient element.

- **Software Design (Type 2 Deficiency):** Any incident which is the result of deficiencies within the design of the software of MAGR, and which is corrected through release of an updated version of MAGR software.
- **Component (Type 3 Deficiency):** Any incident which is the result of the breakdown or failure of an electronic, electrical or mechanical component of MAGR. These failures are correctable by replacement with a functionally equivalent component.
- **Equipment Misuse (Type 4 Deficiency):** Any incident which is the result of electrical, physical, or environmental trauma beyond that specified by CI-MAGR-300.
- **False Failures (Type 5 Deficiency):** Any false failure reported by Power On Built In Test (BIT), Performance Monitor, or Commanded BIT which did not result in performance or functional degradation.
- **Non-Replicated Failures (Type 6 Deficiency):** Any incident reported from a field activity which could not be replicated, and resulted in no service action being performed.

2.4 *Determination of Operating Hours*

A Failure Rate is calculated based on component deficiencies using an estimated total operating time for each type of MAGR. The estimated total operating time is extrapolated from Time Totalizing Meter data captured during reprogramming and other receiver servicing activities. The total operating time for 65 Integration Model MAGRs was available for this investigation. The total operating time for those receivers was calculated to be 37,095 hours (8,671 hours for IF receivers and 28,424 hours for RF receivers). Using these hours as the baseline and assuming a consistent useage rate across all 92 receivers provided to the JPO, it is estimated that the total operating time for all the Integration Model MAGRs was 52,404 hours (12,292 hours for IF receivers and 40,112 for RF receivers) as of March 1, 1995.

SECTION 3

RESULTS OF INVESTIGATION

3.1 *Deficiency Categories*

As discussed in Section 2, the Service Worksheets were analyzed to develop the source data for this investigation. In particular, the Customer Complaint, Service Summary, and Service Narrative fields of the worksheets were reviewed to determine the type (or category) of the deficiency. Appendix 2 to this paper contains the relevant fields from all the Service Worksheets reviewed. The results of this categorization are presented in Table 1.

Table 1. Summary of Service Worksheet Data

Deficiency Type	Incidence of Occurrence	Comments
1. Hardware Design Deficiency	IF: 64 RF: 50	Upgrades to -002. 1553 Interface firmware change.
2. Software Design Deficiency	IF: 43 RF: 40	Link 007 upgrade. Link 008 upgrade (includes field reprogramming).
3. Component Deficiency	IF: 3 RF: 6	Power Supply failures. Circuit Card failures. Frequency Standard Failures.
4. Equipment Misuse	IF: 4 RF: 1	Broken connector pins. Damaged chassis.
5. False Failures	IF: 15	False AE-1 Fail Report.
6. Non-Replicated Failures	IF: 3 RF: 2	Key erasure, faulty almanac, long TTFF.

3.2 Failure Rate

As discussed in paragraph 2.4, operating times were available for a number of the units. Table 2 presents this data, as well as the calculated Failure Rate based upon Type 3 deficiencies observed prior to March 1, 1995 (the numbers in square parantheses are for the 65 receivers for which elapsed time readings were known).

Only Type 3 deficiencies were included for two reasons:

- although the definition of reliability includes software failures and false failures, most of the returns for Type 1, 2 and 5 deficiencies were due to either improvements to software or fixes incorporated before the receivers were installed in aircraft.
- the CERT profiles only considered Type 3 failures in the calculations.

The Type 3 deficiencies were unique to each receiver - not necessarily common across all units.

Table 2. Operating Times & Computed Failure Rates

Receiver Type	Extrapolated Operating Time to MAR 95 (hrs)	Number of Type 3 Failures	Computed Failure Rate (per 1000 hrs)
IF	12,292 [8,671]	3	0.244 [0.346]
RF	40,112 [28,424]	6	0.150 [0.211]
Composite	52,404 [37,095]	9	0.172 [0.243]

SECTION 4

DISCUSSION OF RESULTS

4.1 *Discussion of Failure Types*

The deficiencies (actual and perceived) fall into the six categories previously defined. Most of the deficiencies are documented in the Service Worksheets and resulted (in the main) in upgrades to either hardware, firmware and/or software.

4.1.1 *Hardware Design Deficiency (Type 1)*

There were two types of reportable incidents in this category - the upgrade from -001 to -002 configuration and an update in the MIL-STD-1553 interface firmware.

The -002 upgrade (42% of Type 1 deficiencies) applied to IM MAGRs (the baseline Production Model was -002) and addressed a number of hardware deficiencies including:

- a change to the Programmable Logic Device (PLD) controlling Input/Output (I/O) processor bus accesses thus improving processor throughput;
- a change to the IP/ARINC microcontroller firmware;
- a change to the 1553 microcontroller firmware significantly reducing lockout problems seen on a very noisy bus;
- incorporation of a jumper to provide the 1553 MASTER CLEAR signal to the Bit Status Register; and
- a change to the PLD controlling Navigation (NAV) processor bus accesses thus improving processor throughput.

The separate MIL-STD-1553 interface firmware change (58% of Type 1 deficiencies) corrected a problem with collecting receiver almanac via the MIL-STD-1553 interface which occurred when output messages containing the Time Of Validity field (such as G-9) were also being commanded. This firmware update was incorporated into four IM MAGRs, and retrofitted into a 62 Production Models prior to shipping from Cedar Rapids.

4.1.2 *Software Design Deficiency (Type 2)*

This category of deficiency included the Link -007 upgrade and the Link -008 (or ECP-005) upgrade plus some miscellaneous (custom or pre-release) software upgrades to meet particular user requirements.

The Link -007 software upgrade provided the security fix to the Link -006 software. Link -008 software provided the ECP-005 changes - which included fixes for 28 software deficiencies (not including Product Improvement Software Deficiency Resolutions).

4.1.3 Component Deficiency (Type 3)

The Service Worksheets showed three types of failures associated with component deficiency; power supply failures, circuit card failures and frequency standard failure. Six power supply failures were reported; these were caused by a defective capacitor used on the 400 hertz input circuit. CACD has changed vendors for this component as a result of these deficiencies. Two circuit card failures have been reported. One of these was due to an open circuit condition on a battery board, and the other was the result of an open trace on the chassis interconnect of the 400 hertz input. The remaining reported component failure was caused by a failed frequency standard. All Type 3 failures occurred in IM MAGRs.

4.1.4 Misuse (Type 4)

The main failure due to misuse or physical abuse of MAGR was broken or bent connector pins (3 of 4). There was also one incidence of damage to a MAGR chassis during transit to the aircraft integrator. This MAGR was repaired under warranty. Three Type 4 deficiencies involved Production Models; one occurred in an IM MAGR.

4.1.5 False Failures (Type 5)

The only false failure shown on the Service Worksheets was a false AE-1 Failure. This problem involved several IF MAGRs that reported a Commanded BIT failure when connected to an AE-1. This was the result of a procedure used to compensate an op-amp controlling DC current gain on L2. The assembly procedure used a simulated AE-4 load, which resulted in large variation in current gain under the AE-1 load condition. Further, it was determined that the BIT tolerances for the L2 current detector were overly restrictive. As a result, a modified production procedure was put in place to adjust the L2 current gain, and to test IF MAGRs under AE-1 load condition during Automated Test Procedure (ATP). Also, new BIT tolerances for the L2 current detector were incorporated into ECP-005 software. Type 5 deficiencies occurred in 14 Production Models and one IM MAGR.

4.1.6 Unable to Replicate (Type 6)

Type 6 deficiencies reported on the Service Worksheets included one Production Model (1553 RT Problem) and four IM MAGRs (bad almanac). Deficiencies not reported on the Service Worksheets included:

a. Closed Discrepancy Reports

- **Keying Failures:** Miscellaneous reports of problems with keying or zeroizing MAGR. None of these problems were replicated, and most were resolved through explanation of the keying and zeroization process.
- **Poor GDOP Configuration:** Reported occurrence of bad satellite constellation selection after an extended period of jamming. This is thought to be caused by the satellite track history maintained by MAGR and is considered to be proper operation of the software design implementation.
- **Poor EHE/EVE during Nonauthorized Operation:** Reported deficiencies to achieve "optimal" SPS performance based on FOM, EHE and EVE. Based upon analysis, MAGR was shown to be operating correctly.

b. Open Discrepancy Reports

- **ICD-GPS-104 Velocity Output:** Reported inconsistency between velocity outputs by GPS25-***** and GPS26-*****. This problem was never reproduced by CACD.
- **Altitude Discrepancies:** Two host vehicle integrators have reported significant differences between GPS and Barometric altitude during flight while GPS Figure of Merit (FOM) was 1. This discrepancy is under investigation.
- **Velocity Noise:** This problem is associated with unreliable satellite tracking (loss of lock and signal interference). Noticed during freeway van testing. This discrepancy is unresolved.
- **Iono Filter Discrepancy:** This reported problem occurs during operation with an AE-1 and is currently under investigation.

4.2 Comparison of Specified MTBF and Computed Failure Rates

The specified MTBF is 2000 hours. The MTBF is derived as the inverse of failure rate ($MTBF = [Failure\ Rate]^{-1}$) if the failure characteristics are assumed to follow an exponential distribution. However, this assumption is not typical of a developing system; failure rate generally decreases with time (during the development period) as shown in Figure 1.

For the purpose of this investigation, it is assumed that MTBF is the inverse of Failure Rate since only Type 3 deficiencies were included in the calculations (decrease in reliability due to software maturity was not included). From the component failures observed to date, the MTBF of the IF Integration Models is better than 2,890 hours (using the calculated operating times) or approximately 4,090 hours (using the extrapolated operating times). Similarly, the MTBF for the RF Integration Models is at least 4,730 hours (calculated times) or approximately 6,660 hours (extrapolated times). Both receiver types show a MTBF in excess of that specified.

It is expected that this MTBF will decrease slightly (i.e. Failure Rate to increase) as production units are fielded in greater numbers - due mainly to the more extreme operational environment as opposed to the relatively benign test environment in which most Integration Models were used. This decrease should be followed by a greatly improved MTBF during regular operational use (as the program approaches the flat portion of the curve shown in Figure 1). The projected MTBFs (based upon parts analysis) for production receivers are 5,533 hours and 5,691 hours for IF and RF MAGRs respectively.

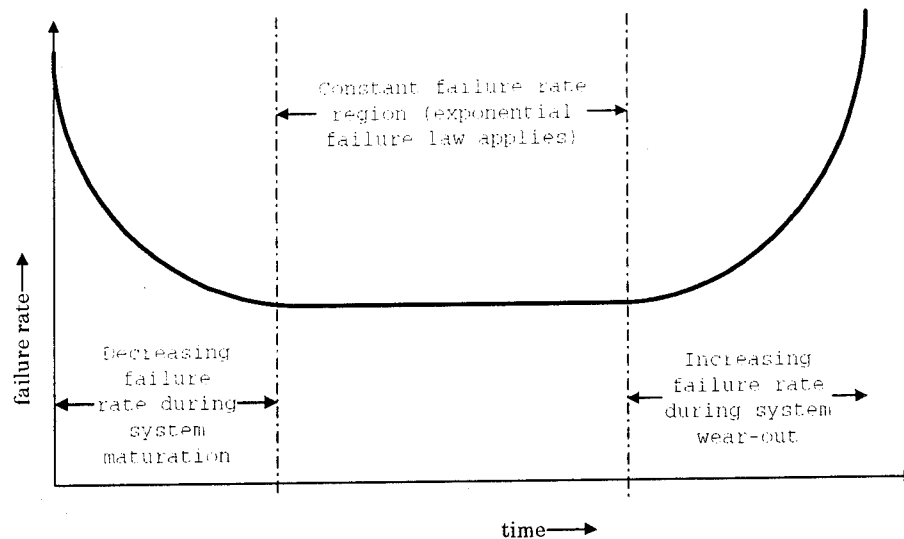


Figure 1. Generic Failure Rate Curve³

SECTION 5

CONCLUSIONS

The purpose of this investigation was to assess MAGR reliability based upon available data captured primarily through the Service Worksheet. This paper also documents those deficiencies that were found to be the result of design deficiency, as well as instances where failures were not replicated by CACD, or have not been resolved.

Receivers returned for service were categorized into six types based upon the deficiency. The majority of returns were for hardware or software upgrade, not directly related to reliability. Deficiencies that resulted in modification to the baseline design of MAGR were not counted as relevant for the calculation of failure rates. Nine returns were the result of component failures (Type 3 Deficiency); these were used to determine failure rate. On this basis, the IF Integration Model MAGR has a failure rate to March 1, 1995 of 0.244 failures per thousand hours of operation. Likewise, the RF Integration Model MAGR has a failure rate of 0.150 failures per thousand hours.

Assuming an exponential failure distribution, the current failure rates are equivalent to MTBFs greatly exceeding the 2000 hour requirement.

³ Adapted From Blanchard and Fabrycky, *Systems Engineering Analysis*, Prentice Hall, New Jersey, Page 355, Figure 13.5.

REFERENCES

Blanchard, B.S., & Fabrycky, W.J., *Systems Engineering Analysis (2nd Ed)*, Prentice Hall, 1990.

CI-MAGR-300, 28 June 1990.

Combined Environmental, Reliability Test Plan for MAGR, CDRL Item 085A2-A002, F04701-91-C-0003, 28 July 1993.

Combined Environmental, Reliability Test Report for MAGR, CDRL Item 087A2-A001, F04701-91-C-0003, 16 December 1993.

Miniature Airborne GPS Receiver Service Worksheets (file maintained at Stand-Alone Airborne Navigation Products IPPD) Collins Avionics & Communications Division, Rockwell Defense Electronics, Cedar Rapids.

Version Description Document for the GPS Receiver MAGR CSCI 613-8379-008, CDRL Item 058A2-004, F04701-91-C-0003, 25 January 1995.

THIS PAGE LEFT BLANK INTENTIONALLY

APPENDIX 1

CERT PROFILES

The following figures (Figure A1-1 through A1-4) show the temperature, power and vibration profiles used for the Combined Environmental, Reliability Tests (CERT) conducted on the Miniature Airborne GPS Receiver.

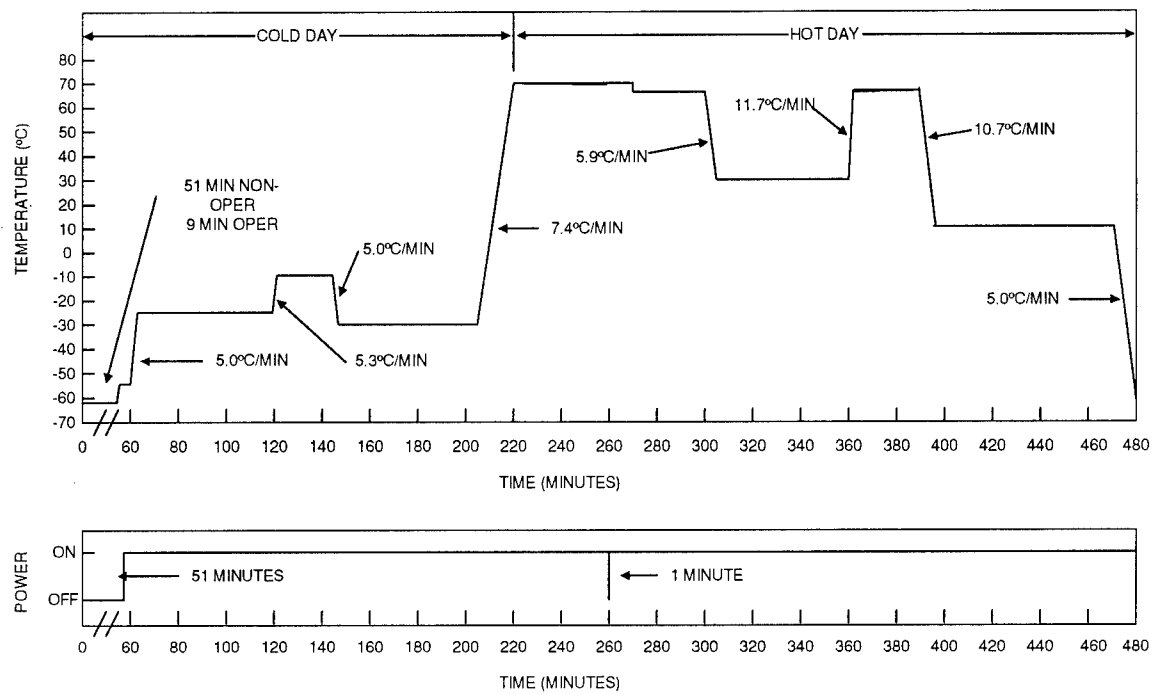


Figure A1-1. CERT Temperature Profile

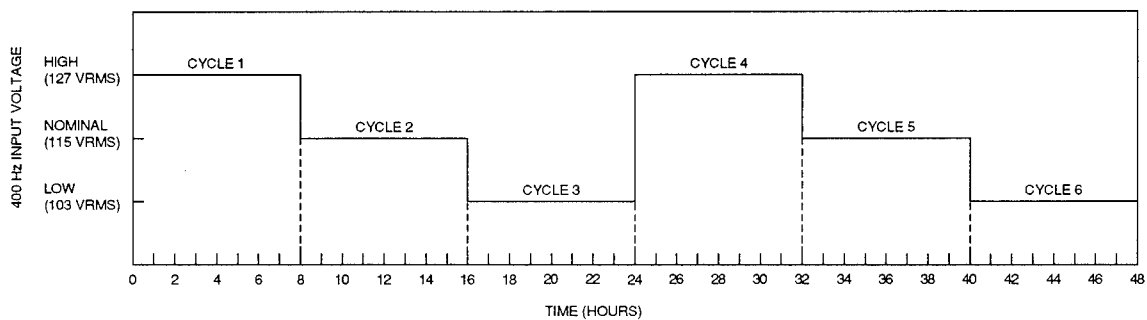


Figure A1-2. Input Voltage Variation Between Cycles

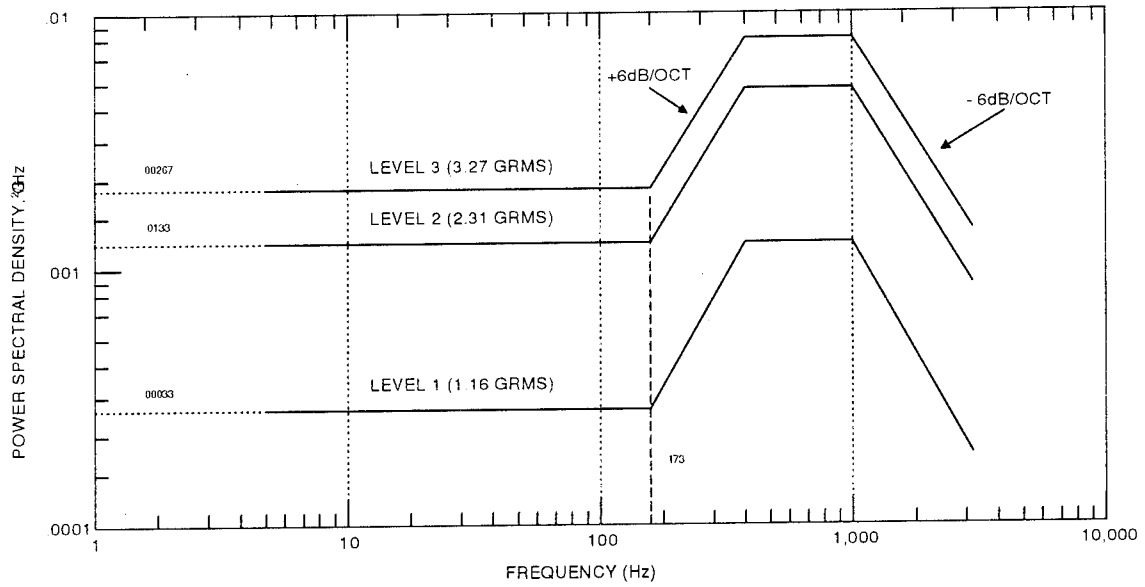


Figure A1-3. Random Vibration Power Spectral Density Curves

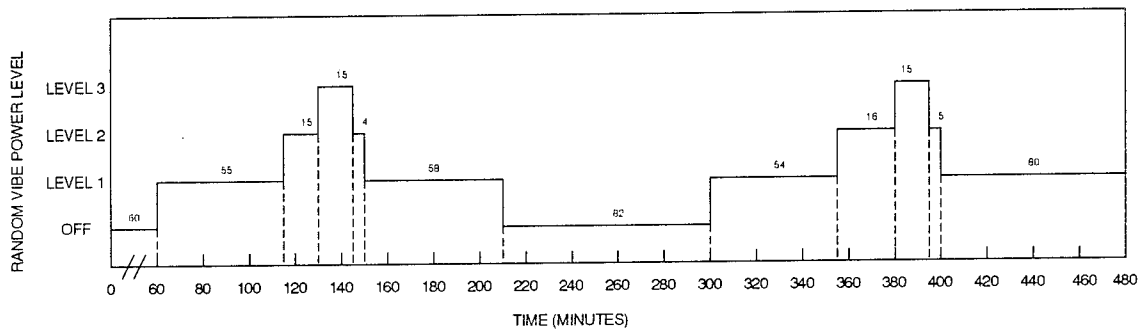


Figure A1-4. Random Vibration Power Level Profile

THIS PAGE LEFT BLANK INTENTIONALLY

APPENDIX 2

SERVICE WORKSHEET SUMMARIES

Table A2-1 contains information extracted from MAGR Service Worksheets maintained by the Coralville factory. The table includes Integration Model and Production MAGRs that have been serviced after initial delivery.

Table A2-1 Service Worksheet Summaries

Receiver Type	Serial Number	Date	Deficiency Category	Comments
IF	101	23-Oct-94	1	002 Upgrade
IF	102	16-Jul-92	2	Software Upgrade
IF	105	28-Oct-93	1	002 Upgrade
IF	105	02-Sep-94	2	Software Upgrade
IF	105	15-Jan-95	1	1553 Firmware
IF	106	14-Jul-94	1	002 Upgrade
IF	106	02-Dec-94	5	FALSE AE-1 Failure
IF	107	07-Jul-93	1	002 Upgrade
IF	109	09-Jun-94	1	002 Upgrade
IF	110	09-Jun-94	1	002 Upgrade
IF	111	27-Jan-94	3	Power Supply Failure
IF	111	08-Apr-94	1	002 Upgrade
IF	112	16-Dec-93	1	002 Upgrade
IF	112	08-Aug-94	2	Software Upgrade
IF	113	03-Nov-93	1	002 Upgrade
IF	114	17-Feb-95	4	Broken connector pins
IF	116	03-Dec-93	1	002 Upgrade
IF	116	25-Oct-93	1	002 Upgrade
IF	117	25-Oct-93	6	TTPF Problem
IF	118	30-Jul-93	1	002 Upgrade
IF	119	25-Oct-93	2	Software Upgrade
IF	119	19-May-94	6	Bad Almanac
IF	120	24-Oct-93	1	002 Upgrade
IF	120	31-Jan-94	2	Software Upgrade
IF	122	15-Aug-94	1	002 Upgrade
IF	123	30-Jul-93	1	002 Upgrade
IF	124	30-Jul-93	1	002 Upgrade
IF	125	30-Jul-93	1	002 Upgrade
IF	126	14-Feb-94	3	Power Supply Failure
IF	127	30-Jul-93	1	002 Upgrade
IF	127	16-Dec-93	2	Software Upgrade
IF	128	30-Jul-93	1	002 Upgrade
IF	128	16-Dec-93	2	Software Upgrade
IF	129	30-Jul-94	1	002 Upgrade
IF	146	02-Sep-94	1	002 Upgrade
IF	146	22-Feb-95	1	1553 Firmware
IF	177	13-Oct-94	1	1553 Firmware
IF	178	13-Oct-94	1	1553 Firmware
IF	179	13-Oct-94	1	1553 Firmware
IF	179	22-Jan-95	5	FALSE AE-1 Failure
IF	180	21-Oct-94	1	1553 Firmware
IF	180	22-Jan-95	5	FALSE AE-1 Failure
IF	181	12-Sep-94	1	1553 Firmware

Table A1-1 (continued)

Receiver Type	Serial Number	Date	Deficiency Category	Comments
IF	182	21-Oct-94	1	1553 Firmware
IF	183	12-Sep-94	1	1553 Firmware
IF	184	21-Oct-94	1	1553 Firmware
IF	185	21-Oct-94	1	1553 Firmware
IF	186	21-Oct-94	1	1553 Firmware
IF	188	12-Sep-94	1	1553 Firmware
IF	189	12-Sep-94	1	1553 Firmware
IF	190	12-Sep-94	1	1553 Firmware
IF	191	12-Sep-94	1	1553 Firmware
IF	192	12-Sep-94	1	1553 Firmware
IF	193	12-Sep-94	1	1553 Firmware
IF	194	12-Sep-94	1	1553 Firmware
IF	194	06-Oct-94	2	Software Upgrade
IF	195	12-Sep-94	1	1553 Firmware
IF	196	12-Sep-94	1	1553 Firmware
IF	197	12-Sep-94	1	1553 Firmware
IF	198	12-Sep-94	1	1553 Firmware
IF	199	12-Sep-94	1	1553 Firmware
IF	200	12-Sep-94	1	1553 Firmware
IF	201	12-Sep-94	1	1553 Firmware
IF	203	12-Sep-94	1	1553 Firmware
IF	205	22-Jan-95	5	FALSE AE-1 Failure
IF	209	22-Jan-95	5	FALSE AE-1 Failure
IF	213	10-Oct-94	5	FALSE AE-1 Failure
IF	220	22-Jan-95	5	FALSE AE-1 Failure
IF	227	18-Oct-94	5	FALSE AE-1 Failure
IF	234	22-Jan-95	5	FALSE AE-1 Failure
IF	235	22-Jan-95	5	FALSE AE-1 Failure
IF	237	22-Jan-95	5	FALSE AE-1 Failure
IF	238	22-Jan-95	5	FALSE AE-1 Failure
IF	239	22-Jan-95	5	FALSE AE-1 Failure
IF	247	22-Jan-95	5	FALSE AE-1 Failure
IF	250	22-Jan-95	5	FALSE AE-1 Failure
IF	342	12-Sep-94	1	1553 Firmware
IF	343	12-Sep-94	1	1553 Firmware
IF	343	16-Dec-94	6	1553 RT Problem
IF	344	12-Sep-94	1	1553 Firmware
IF	345	12-Sep-94	1	1553 Firmware
IF	346	12-Sep-94	1	1553 Firmware
IF	347	21-Oct-94	1	1553 Firmware
IF	348	08-Sep-94	1	1553 Firmware
IF	349	12-Sep-94	1	1553 Firmware
IF	350	12-Sep-94	1	1553 Firmware
IF	351	12-Sep-94	1	1553 Firmware
IF	353	12-Sep-94	1	1553 Firmware
IF	355	12-Sep-94	1	1553 Firmware
IF	356	12-Sep-94	1	1553 Firmware
IF	357	08-Sep-94	1	1553 Firmware
IF	358	08-Sep-94	1	1553 Firmware
IF	359	23-Jan-95	4	Damaged Connector
IF	362	23-Jan-95	4	Damaged Connector
IF	369	12-Sep-94	1	1553 Firmware
IF	401	17-Nov-94	3	Power Supply Failure
IF	408	19-Jan-95	4	Damaged in transit
RF	102	02-Sep-94	1	002 Upgrade

Table A1-1 (continued)

Receiver Type	Serial Number	Date	Deficiency Category	Comments
RF	103	29-Nov-93	1	002 Upgrade
RF	105	20-Sep-93	1	002 Upgrade
RF	108	09-Oct-92	3	Circuit Card Failure
RF	108	01-Nov-93	1	002 Upgrade
RF	113	11-Jan-94	1	002 Upgrade
RF	114	29-Jun-94	2	Software Upgrade
RF	115	29-Nov-93	1	002 Upgrade
RF	115	10-Nov-94	1	1553 Firmware
RF	116	12-Sep-94	1	002 Upgrade
RF	117	07-Jul-93	1	002 Upgrade
RF	119	16-Aug-93	4	Damaged Connector
RF	120	08-Jul-94	3	Power Supply Failure
RF	121	01-Jul-93	2	Software Upgrade
RF	121	23-May-94	1	002 Upgrade
RF	122	15-Jun-94	1	002 Upgrade
RF	124	12-May-94	1	002 Upgrade
RF	125	30-Jul-94	1	002 Upgrade
RF	126	27-Jan-93	3	Circuit Card Failure
RF	126	30-Jul-94	1	002 Upgrade
RF	136	13-May-94	1	002 Upgrade
RF	137	12-Nov-93	1	002 Upgrade
RF	138	29-Jun-94	2	Software Upgrade
RF	139	26-Oct-93	6	Loss of memory/keys
RF	139	01-Sep-94	2	Software Upgrade
RF	140	11-Mar-94	1	002 Upgrade
RF	145	18-Aug-94	1	002 Upgrade
RF	147	14-Jul-93	2	Software Upgrade
RF	147	08-Sep-94	1	002 Upgrade
RF	150	03-Jul-93	1	002 Upgrade
RF	150	14-Oct-94	6	Unknown
RF	151	03-Jul-93	1	002 Upgrade
RF	152	03-Jan-95	3	Power Supply Failure
RF	153	27-Jul-94	1	002 Upgrade
RF	153	15-Jan-95	1	1553 Firmware
RF	153	17-Feb-95	2	Software Upgrade
RF	156	03-Jul-93	1	002 Upgrade
RF	156	29-Jun-94	2	Software Upgrade
RF	157	03-Jul-93	1	002 Upgrade
RF	158	09-Jul-93	1	002 Upgrade
RF	159	09-Jul-93	1	002 Upgrade
RF	160	09-Jul-93	1	002 Upgrade
RF	161	09-Jul-93	1	002 Upgrade
RF	209	05-Nov-93	1	002 Upgrade
RF	214	15-Jul-94	2	Software Upgrade
RF	215	22-Feb-95	1	1553 Firmware
RF	217	23-Dec-94	3	Power Supply Failure
RF	218	10-Feb-95	3	Frequency Standard Failure
RF	220	12-Sep-94	1	1553 Firmware
RF	221	12-Sep-94	1	1553 Firmware
RF	222	12-Sep-94	1	1553 Firmware
RF	223	12-Sep-94	1	1553 Firmware
RF	225	12-Sep-94	1	1553 Firmware
RF	226	12-Sep-94	1	1553 Firmware
RF	227	12-Sep-94	1	1553 Firmware
RF	228	12-Sep-94	1	1553 Firmware

Table A1-1 (continued)

Receiver Type	Serial Number	Date	Deficiency Category	Comments
RF	229	12-Sep-94	1	1553 Firmware
RF	230	12-Sep-94	1	1553 Firmware
RF	231	12-Sep-94	1	1553 Firmware
RF	232	12-Sep-94	1	1553 Firmware
RF	233	12-Sep-94	1	1553 Firmware
RF	234	12-Sep-94	1	1553 Firmware
RF	235	12-Sep-94	1	1553 Firmware
RF	236	12-Sep-94	1	1553 Firmware
RF	237	12-Sep-94	1	1553 Firmware
RF	239	12-Sep-94	1	1553 Firmware
RF	240	12-Sep-94	1	1553 Firmware

THIS PAGE LEFT BLANK INTENTIONALLY

ATTENDANCE LIST

*746TH TEST SQUADRON
CIGTF*

ATTENDANCE LIST
SEVENTEENTH BIENNIAL GUIDANCE TEST SYMPOSIUM
2-4 May 1995

NAME	COMPANY	PHONE #
Adamez, James	Intermetrics, Inc., Victoria Plaza, Bldg. 4, 2nd Floor, 615 Hope Road., Eatontown NJ 07724	(908) 681-5310
Adams, Gary	Honeywell, P. O. Box 2111, Phoenix AZ 85036 M/S 2127A1	(602) 436-6344
Airth, Walter	Magnavox Electronic Systems Co., 2829 Maricopa St., Torrance, CA 90503 MS-B6	(310) 618-1200 Ext 2421
Alianti, David	IIT Research Institute, 185 Admiral Cochrane Drive, Annapolis MD 21401	(410) 573-7285
Anderson, Brian Capt.	AFIWC/SAV, 102 Hall Blvd., Suite 342, San Antonio TX 78243-7020	(210) 977-2706
Anderson, Dave	Honeywell, 11601 Roosevelt Blvd., St. Petersburg FL 33716	(813) 579-6093
Anderson, David	Litton, 2211 N. Temple, Salt Lake City UT 84116	(801) 539-1200
Anderson, Gerald	AGMC/MAE, 813 Irvingwick Dr. W., Newark AFB OH 43057-0005	(614) 522-7402
Araujo, Peter D.	746 TS/TGGML, 1644 Vandergrift Rd., HAFB NM 88330-7850	(505) 679-1629
Armstrong, Woodie	746 TS/TGGML, 1644 Vandergrift Rd., HAFB NM 88330-7850	(505) 679-2237
Aronowitz, Frederick	Rockwell, 3370 Miraloma Ave., Anaheim CA 92803	(714) 762-5397
Ash, Michael	C. S. Draper Lab, M/S 32, 555 Technology Sq., Cambridge MA 02139	(617) 258-2884
Atkins, Paige	DOD Joint Spectrum Center, 120 Washington Basin, Annapolis MD 21402-5064	(410) 293-2681
Bailey, Eric M.	Northrop Grummen, 100 Morse St., Norwood MA	(617) 762-5300
Barker, Cleon	746 TS/TGGPP, 1644 Vandergrift Rd., HAFB NM 88330-7850	(505) 679-1764
Barker, Donald	46 TG/XP, 871 DeZonia Rd., HAFB NM 88330-7715	(505) 475-1356
Barnes, Geoffrey	Rockwell International, MS 153-160, 400 Collins Rd. NE, Cedar Rapids IA 52498	(319) 395-8609
Bartholomev, Redge	Rockwell International, 350 Collins Rd. NE, Cedar Rapids IA 52498	(319) 395-1906
Baumbach, Jason	AFIWC/SAV, 102 Hall Blvd., Suite 342, San Antonio TX 78243-7020	(210) 977-2706
Bedoya, Carlos	McDonnell Douglas, P. O. Box 516, St. Louis MO 63166	(314) 234-1941
Bell, Jack	46 TG/TGR (Ratscat), HAFB NM	(505) 679-3319
Bennett, Sid	Andrew Corporation, 10500 W 153 St., Orland Park IL 60462	(708) 349-3300
Benshoof, Paul H.	SMC/CZTU-ASEC, 2435 Vela Way, Suite 1613, El Segundo CA 90245-5500	(310) 363-3583
Benson, Donald	Dynamics Research Corp., 60 Frontage Rd., Andover MA 01810	(508) 475-9090 Ext 2360
Berry, Mark	Intermetrics, Inc., 615 Hope Rd., Eatontown NJ 07724	(908) 681-1422
Byer, Robert	Naval Air Systems Command, 10505 Indigo Lane, Fairfax VA 22032	(703) 604-3180
Beyers, Ronald, Capt	USAF, Joint STARS, OLAT ESC, 1500 Nasa Blvd., Melbourne FL 32902	DSN 854-5245 x 7905
Blevins, Clay	46 TG/XPX, 871 DeZonia Rd., HAFB NM 88330-7715	(505) 475-1228
Blizzard, Robert	Honeywell, 1027 Grovewood Court, Clearwater FL 34624-4924	(813) 579-6611
Bohenek, Brian	746 TS/TGGDC, 1644 Vandergrift Rd., HAFB NM 88330-7850	(505) 679-1639
Bongiovanni, Stephen	Honeywell, 13350 U.S. Hwy 19 N., Clearwater FL	

ATTENDANCE LIST
SEVENTEENTH BIENNIAL GUIDANCE TEST SYMPOSIUM
2-4 May 1995

NAME	COMPANY	PHONE #
Bouniol, Pierre	LRBA, BP 914 F27207 France	(33) 32-21-43-60
Brad, Jim	Naval Research Lab, 4555 Overlook Ave., SW, Washington DC	(202) 404-7060
Bradford, Robert	746 TS/TGGML, 1644 Vandergrift Rd., HAFB NM 88330-7850	(505) 679-2238
Braunstein, David S.	Stanford Telecommunications, Inc., 1221 Crossman Ave. Sunnyvale CA 94088-3733	
Bredthauer, Dennis	Defense Mapping Agency, P. O. Drawer F, HAFB NM 88330-0406	(505) 457-7056
Brewer, James	746 TS/TGGDA, 1644 Vandergrift Rd., HAFB NM 88330-7850	(505) 679-1730
Brewer, Mark	746 TS/TGGT, 1644 Vandergrift Rd., HAFB NM 88330-7850	(505) 679-1641
Briessmann, Norbert	German Forces Ctr for A/C, 85077 Manching, Flugplatz, Germany	49-8459-802270
Brienza, Domenico	NAWC, 6000 East 21 St., Indianapolis, IN 46219	(317) 352-3887
Buell, Heinz	GEC-Marconi Electronic Systems Corp., 164 Totowa Rd., Wayne NJ 07474 MS 11C76	(201) 633-6130
Burlingame, Roger	Litton A&CS, 2211 W. North Temple, Salt Lake City UT 84116-2993	(901) 539-1200 x 7832
Burt, John A.	Pentagon DTSE&E OUSD(A&T), 3110 Defense Pentagon, Washington DC 20301-3110	(703) 695-7171
Caron, Dennis	746 TS/TGGML, 1644 Vandergrift Rd., HAFB NM 88330-7850	(505) 679-1504
Challendar, Jerry	HP, El Paso TX	
Chewning, Jay	746 TS/TGGTA, 1644 Vandergrift Rd., HAFB NM 88330-7850	(505) 679-1033
Christiansen, R. G.	Rockwell International, 3370 Miraloma Ave., MC-CA30, Anaheim CA 92803-3105	(714) 762-6173
Cicchinelli, Dominick	746 TS/TGGDA, 1644 Vandergrift Rd., HAFB NM 88330-7850	(505) 679-8577
Clark, Richard E. (Ret Col)	1180 Hwy 98E, Destin FL 32541	(904) 837-3765
Coleman, Carolyn F.	46 TW/TSWW, 401 W Choctawhatchee Ave., Eglin AFB FL 32542	DSN 872-9354 x 226
Comallie, Leo	746 TS/TGGML, 1644 Vandergrift Rd., HAFB NM 88330-7850	(505) 679-2073
Comery, Doug	Embassy of Australia, 1601 Massachusetts Ave., Washington DC 20036-2273	(202) 797-3380
Cosentino, Barbara	746 TS/TGGPP, 1644 Vandergrift Rd., HAFB NM 88330-7850	(505) 679-2017
Cranston, Stewart, MGen	AFDTC/CC, 101 W. D. Ave., Eglin AFB FL 32542-5495	(904) 882-5422
Cravets, Art	SAIC, 10770 Wateridge Circle W., San Diego CA 92121	(619) 552-5432
Crouch, Dan	746 TS/TGGPI, 1644 Vandergrift Rd., HAFB NM 88330-7850	(505) 679-1716
Curby, Robert D.	Litton G&C Systems, 5500 Canoga Ave., M.S. 76, Woodland Hills CA 91367	(818) 715-5092
de Brabander, Ed	NAWCAD, 22777 Saufler Rd., MS 1, Patuxent River MD	(301) 826-3181
Decker, Douglas	746 TS/TGGP, 1644 Vandergrift Rd., HAFB NM 88330-7850	(505) 679-1763
DeDoes, Dirk	Intermetics, Inc., 7711 Center Ave., Suite 615, Huntington Beach CA 92647	(714) 891-4631
Denhard, Bill	JSDE, 25 Springvale Rd., Reading MA 01867-3364	(617) 944-1584
Diaz, Jose L.	746 TS/TGGDA, 1644 Vandergrift Rd., HAFB NM 88330-7850	(505) 679-1552

ATTENDANCE LIST
SEVENTEENTH BIENNIAL GUIDANCE TEST SYMPOSIUM
2-4 May 1995

NAME	COMPANY	PHONE #
Dickman, James	846 TS/TGTE, 1521 Test Track Rd., HAFB NM 88330-7847	(505) 679-2650
Disselkoen, Brent	Rockwell International, Cedar Rapids IA	(319) 395-2671
Donaldson, John P.	Rockwell Collins, 350 Collins Rd. NE, Cedar Rapids IA 52498	(319) 395-8047
Doyle, Sean	746 TS/TGGDA, 1644 Vandergrift Rd., HAFB NM 88330-7850	(505) 679-2236
Eitel, Theodore J.	Honeywell Inc., 9013 130th Way North, Seminole FL 34646-2524	(813) 539-3025
Elliott, Patrick	ASC/LYB, 2145 Monahan Way, Bldg. 28, WPAFB OH 45433-7017	(513) 255-4140
Elwell, John	C.S. Draper Lab, 555 Technology Sq., MS 79, Cambridge MA 02139	(617) 258-3832
Estep, Gene	46 TW/TSWGIL, Eglin AFB FL 32542	(904) 882-9940
Fall, Robert	Honeywell, 13350 US Hwy 19 North, Clearwater FL 34624-7290	(813) 539-4490
Faxnag, Fred	Honeywell, 2600 Ridgway Plzy, Minneapolis MN 55413	(612) 951-6211
Feder, Earl	U.S. Army CECOM, AMSEL-RD-C2-TS-N, Fort Monmouth NJ 07703	(908) 544-3907
Feist, Jon	746 TS/TGGDA, 1644 Vandergrift Rd., HAFB NM 88330-7850	(505) 679-2202
Feldmann, Mike	Smith Industries, 4141 Eastern Ave., SE, Grand Rapids MI 49518	(616) 241-8847
Feltquate, Harvey	Draper Laboratory, 555 Technology Sq., Cambridge MA 02139	(617) 258-1760
FitzGerald, Warren J.	C.S. Draper Laboratory, Inc., 555 Technology Sq., Cambridge MA 02139	(617) 258-4577
Flahive, Martin	Kearfott Guidance and Navigation Corp., 14321 Olympic Ct., Dallas TX	(214) 247-1607
Fleenor, Mike	SMC/CZTU, 2435 Vela Way, Suite 1613, LA AFB CA 90245	(310) 363-2917
Flores, Matt	746 TS/TGGTP, 1644 Vandergrift Rd., HAFB NM 88330-7850	(505) 679-1755
Floyd, William	OC-ALC/LKK, 3001 Staff Dr., Oklahoma City, OK 73145-3018	(405) 736-3991
Fly, Brian	Honeywell, 11601 Roosevelt Blvd., St. Petersburg FL 33706	(813) 579-6733
Ford, Michael	Det 2, 645 MATS, P. O. Box 6056, Greenville TX 75403-6056	(903) 457-6255
Furman, Dennis R.	46 TG/TGR, 871 DeZonia Rd., HAFB NM 88330-7715	(505) 457-1367
Garcia, Frank H.	746 TS/TGGTE, 1644 Vandergrift Rd., HAFB NM 88330-7850	(505) 679-1451
Gibbs, George Eddie	WL/MNAG, 101 W Eglin Blvd., Suite 341, Eglin AFB FL 32542-6810	(904) 882-5489 x 3363
Gibson, Richard	CAST, Inc., 5450 Katella Ave., Suite 103, Los Alamitos, CA 90720-2833	(310) 594-8883
Gilbert, Lee	NAWC, 1 Administration Circle (Code 471000D), China Lake CA 93555-6001	(619) 939-3500
Gilmore, Morgan P.	Lockheed Aeronautical Systems Co., 86 South Cobb Drive, Marietta GA 30063	(404) 494-8267
Goodall, David	Lockheed Adv. Dev. Co., 1011 Lockheed Way, Palmdale CA 93599-7217	(805) 572-6012
Grace, Lance C.	46 TG, 871 DeZonia Rd., HAFB NM 88330-7715	(505) 475-1367
Green, Kerry ILt	746 TS/TGGTE, 1644 Vandergrift Rd., HAFB NM 88330-7850	(505) 679-6534
Green, Robert E.	U.S. Army, STEWS-IDD-SA, WSMR NM 88002	(505) 678-2294

ATTENDANCE LIST
SEVENTEENTH BIENNIAL GUIDANCE TEST SYMPOSIUM
2-4 May 1995

NAME	COMPANY	PHONE #
Greenlee, Darrell	Adroit Systems, Inc., 209 Madison St., Alexandria VA 22314	(703) 684-2900
Greenspan, Richard	C. S. Draper Lab, 555 Technology Sq., Cambridge MA 02139	(617) 332-1160
Greskowiak, David F.	NAWC, 1 Administration Circle, China Lake CA 93555	(619) 927-3616
Grey, Filomena	746 TS/TGGMI, 1644 Vandergrift Rd., HAFB NM 88330-7850	(505) 679-2155
Grimaldi, Gerald	Rockwell International, 3370 Miraloma Ave., Anaheim CA 92803-3105	(714) 762-4457
Gruman, Fredrick	746 TS/TGGTE, 1644 Vandergrift Rd., HAFB NM 88330-7850	(505) 679-1665
Hackett, Michael	DASP-2-2, Dept of Defense, Ontario Canada KIA0K2	(613) 993-3380
Hadfield, Michael	746 TS/TGGPM, 1644 Vandergrift Rd., HAFB NM 88330-7850	(505) 679-2234
Handzel, James	Litton G&C, 448 Eucalyptus Dr., Redlands CA 92373	(909) 793-6054
Hansen, Robert	Honeywell Military Avionics, 11601 Roosevelt Blvd., St. Petersburg FL 33716-2202	(813) 579-6640
Harris, George	746 TS/TGGPI, 1644 Vandergrift Rd., HAFB NM 88330-7850	(505) 679-1529
Hauge, Lee	Martin Marietta Defense, 100 Plastics Ave., Pittsfield MA 01201	(413) 494-5312
Hayes, Don	Raytheon Service Co., 2 Wayside Rd., Burlington MA 01801	(617) 238-3131
Hegels, Hermann	SHAPE/NATO, SHAPE Technical Center, The Hague, The Netherlands	31-70-3142370
Hendren, Eric R.	746 TS/TGGPP, 1644 Vandergrift Rd., HAFB NM 88330-7850	(505) 679-4829
Hendrix, Dave	Hewlett Packard, P. O. Box 12903, El Paso TX 79913	
Hicks, Susan	ASC/VFWX, 2300 D St., Bldg. 32, WPAFB OH 45433-7249	DSN 785-3685
Hight, Dalayr	746 TS/TGGDA, 1644 Vandergrift Rd., HAFB NM 88330-7850	(505) 679-2317
Hilty, David	Contraves Inc., 610 Epsilon Drive, Pittsburg PA 15238	(412) 967-7288
Hoech, Robert	Rockwell International, 350 Collins Rd NE, Cedar Rapids IA	(319) 395-2738
Holland, Kenneth	46 TG/CA, 871 DeZonia Rd., HAFB NM 88330-7715	(505) 475-1403
Hogg, Richard	US Navy N&D Center, Warminster PA	
Holsapple, Boyd	WL/AAAI, Bldg. 635, 2185 Avionics Circle, WPAFB OH 45433-7301	(513) 255-5668
Hooser, Michael	846 TS/TGGT, Test Track Rd., HAFB NM 88330-7847	(505) 679-2941
Horn, Randy	Honeywell, 3320 Candelaria, Albuquerque NM 87107	(505) 880-3204
Horner, Parker C.	HQ USAF/TER, 1650 Air Force Pentagon, Washington DC 20330-1650	DSN (227) 1165
Howell, Dana	WL/AAAI-1, 2185 Avionics Circle, WPAFB OH 45433-7301	(513) 255-2766
Hunt, Coy	746 TS/TGGDA, 1644 Vandergrift Rd., HAFB NM 88330-7850	(505) 679-1584
Hymas, Carl E.	TRW, Inc., 1104 Country Hills Drive, Ogden, UT 84403	(801) 776-1410
Ingold, Norman L.	746 TS/CC, 1644 Vandergrift Rd., HAFB NM 88330-7850	(505) 679-2123
Jackson, Lon	Rockwell International, 3370 Miraloma Ave., Anaheim CA 92803	(714) 762-0872

ATTENDANCE LIST
SEVENTEENTH BIENNIAL GUIDANCE TEST SYMPOSIUM
2-4 May 1995

NAME	COMPANY	PHONE #
Jackson, Michael R.	Rockwell International, 1595 Wimbledon, Auburn CA 95603	(916) 885-0137
Kantrowitz, Frank	Aerospace Corporation, P. O. Box 92957-M4/904, Los Angeles CA 90009-2957	(310) 336-0711
Kaser, Karl	GPS/JPO, SMC/CZTU, 2435 Vela Way, Suite 1613, LA AFB CA 90245	(310) 362-1216
Keedy, Glen	FAA, AVN-810, 6500 S. MacArthur, Oklahoma City OK 73125	(405) 954-6438
Keen, Dan	ASC/ENAE, Bldg. 20, 2450 D. St., Ste 2, WPAFB OH 45433-7630	(513) 255-5153
Kelher, Robert S.	746 TS/TGGD, 1644 Vandergrift Rd., HAFB NM 88330-7850	(505) 679-1631
Kelley, Gilbert	Aerotherm Corporation, 2901 Juan Tabo NE, #201, Albuquerque NM 87112	(505) 237-9946
Keltos, Michael	746 TS/TGGTE, 1644 Vandergrift Rd., HAFB NM 88330-7850	(505) 679-1738
Kieffer, Jean-Francois	LRBA, BP 976, R7807 Vernon, France	(33) 38 4333
King, Kerry	746 TS/TGGPI, 1644 Vandergrift Rd., HAFB NM 88330-7850	(505) 679-2499
Kirkpatrick, George	GMK Consulting Service, 202 David Dr., NO, Syracuse NY 13212-1901	(315) 458-0082
Kucej, Michael	46 TG/XP, 871 DeZonia Rd., HAFB NM 88330-7715	(505) 475-1347
Kuhn, Ferdinand, Dr.	SYSTEC, 2107 Dewey Lane, Alamogordo NM 88310	(505) 437-3038
Kumar, Lalit	Delco Systems Operations, 6767 Hollister Ave., Goleta CA 93117-3000	(805) 961-7389
Landers, Jack	P. O. Box 3767, Alamogordo NM 88311-3767	(505) 434-4405
Landers, Mary	746 TS/TGGPP, 1644 Vandergrift Rd., HAFB NM 88330-7850	(505) 679-2500
Lane, Thomas	Det 2, 645 MATS, Greenville TX 75403	(903) 457-5948
Lawrence, Robert	746 TS/TGGDA, 1644 Vandergrift Rd., HAFB NM 88330-7850	(505) 679-1772
Lazar, Steven	Aerospace Corporation, P. O. Box 92957, Los Angeles CA 90009-2957	(310) 336-1938
Lehmann, Axel	LITEF, P. O. Box 774, D-79007, Republic of Germany	
Lloyd, Michael T.	Honeywell Inc., 13350 U.S. Hwy., 19 N., Clearwater FL 34624-7290	(813) 539-5618
Long, Marianne Capt.	746 TS/TGGTA, 911 DeZonia Rd., HAFB NM 88330-7715	(505) 475-1012
Lynman, Jerry	Hewlett Packard, El Paso TX	
Martorana, Richard	C.S. Draper Lab, 555 Technology Sq., Cambridge MA	
Matthews, Fred	746 TS/CC, 1644 Vandergrift Rd., HAFB NM 88330-7850	(505) 679-2786
McCracken, Becky	746 TS/TGGTB, 1644 Vandergrift Rd., HAFB NM 88330-7850	(505) 679-2316
McAdory, Robert	GEC-Marconi Systems, 235 Elm Hill Drive, Dayton OH 45415-2941	(513) 278-9540
McDaniel, Mickey	NAWC AD, 6000 East 21st St., Indianapolis IN	(317) 353-3480
McGowan, Joe	Intermetrics, Inc., Victoria Plaza, Bldg. 2, 2nd Floor, 615 Hope Rd., Eatontown NJ 07724	(908) 681-1205
Mead, Thomas U.	46 TG/CC, 871 DeZonia Rd., HAFB NM 88330-7715	(505) 475-1368
Melendrez, David	746 TS/TGGMI, 1644 Vandergrift Rd., HAFB NM 88330-7850	(505) 679-2762

ATTENDANCE LIST
SEVENTEENTH BIENNIAL GUIDANCE TEST SYMPOSIUM
2-4 May 1995

NAME	COMPANY	PHONE #
Miller, Dennis, Maj.	46 TG/XP, 871 DeZonia Rd., HAFB NM 88330-7715	(505) 475-1344
Miller, Jim	IIT Research Institute, 185 Admiral Cochrane Dr., Annapolis MD 21401	(410) 573-7256
Miller, Matthew	COMOPTEVFOR, 7970 Diven Street, Norfolk VA 23505	(804) 444-5025
Miola, Joe	C.S. Draper Lab, 555 Technology Sq., Cambridge MA 02139	(617) 258-4072
Moen, Verlyn	Rockwell International, 350 Collins Rd., NE, Cedar Rapids IA 52498	(319) 395-8633
Moffitt, Mary C.	746 TS/TGGP, 1644 Vandergrift Rd., HAFB NM 88330-7850	(505) 679-2174
Monier, Jeri	FAA, 6500 S. MacArthur, AMP-100, Oklahoma City OK 73125	(405) 954-5438
Monroe, Athanison	Nise West SD, P. O. Box 85137 Code 322, San Diego CA 92186-5137	(619) 524-2087
Moore, John B.	U.S. Navy, 455 Bob Jones Drive, Virginia Beach VA 23462	(804) 686-7842
Moore, William BGen	AFPEO/ST, Pentagon, Washington DC	DSN 223-7290
Morgan, Marjorie	746 TS/TGGMR, 1644 Vandergrift Rd., HAFB NM 88330-7850	(505) 679-2957
Morris, Alan	USAWSMR-EPG, 3649 Sparton Dr., Sierra Vista, AZ 85635	(520) 833-8134
Morton, Jack	746 TS/TGGML, 1644 Vandergrift Rd., HAFB NM 88330-7850	(505) 679-2602
Mosle, William	746 TS/TGGPI, 1644 Vandergrift Rd., HAFB NM 88330-7850	(505) 679-1532
Myers, Joe, Maj.	746 TS/TGGT, 1644 Vandergrift Rd., HAFB NM 88330-7850	(505) 679-1756
Nadeau, Fredric R.	746 TS/CA, 1644 Vandergrift Rd., HAFB NM 88330-7850	(505) 679-2125
Nash, Tony	746 TS/TGGDC, 1644 Vandergrift Rd., HAFB NM 88330-7850	(505) 679-2317
Nedeau, Joseph	PL/VT-B, 3550 Aberdeen Ave. SE, Kirtland AFB NM 87117	DSN 246-5799 x205
Novy, Michael	746 TS/TGGPI, 1644 Vandergrift Rd., HAFB NM 88330-7850	(505) 679-2154
Nowicki, Richard	Synetics, 23272 Mill Creek Drive, Suite 200, Laguna Hills CA 92653	(714) 458-0663
Olson, Craig	Rockwell International, 350 Collins Road NE M/S 153-250, Cedar Rapids IA	(319) 953-2242
Olson, Paul M.	U.S. Army, CECOM, 304 Timberline Place, Brick NJ 08723	(908) 920-1948
Palmer, Richard	McDonnell Douglas, D318, Bldg. 105, MC 1065425, P. O. Box 516, St. Louis MO 63166-05	(314) 233-6777
Panefieu, Bernard	French MOD LRBA, BP 914 27207 Vernon, France	33 32 21 44 86
Patterson, Ralph	Litton G&C Systems, 5500 Canoga Ave., Woodland Hills CA 91367	(818) 719-7602
Payne, Kevin	746 TS/TGGP, 1644 Vandergrift Rd., HAFB NM 88330-7850	(505) 679-1775
Peck, Robert S.	Rockwell International, 865 E. Sepulveda Blvd., Carson CA 90745-6195	(310) 834-2611
Peters, Rex	Allied Signal Instrument System, 12001 N.E., 36th St., Box 97001, Redmond VA 98073-9701	(206) 885-8029
Phillips, John	GPS/JPO, 5 Orbin Lane, San Pedro CA 90732-4416	(310) 363-2735
Pinson, Ed	Defense Mapping Agency, P. O. Drawer F, WSMR NM 88330-0406	(505) 475-7056
Pluter, Edward J.	Martin Marietta Defense Systems, P. O. Box 62495, Sunnyvale CA 94088-2495	(408) 742-7847

ATTENDANCE LIST
SEVENTEENTH BIENNIAL GUIDANCE TEST SYMPOSIUM
2-4 May 1995

NAME	COMPANY	PHONE #
Porter, Rex	AFPEO/ST, Pentagon, Washington DC	DSN 223-7290
Quigley, Jack	408 Sunnyside Ave., Alamogordo NM 88310	(505) 437-1064
Race, Robert W.	Lockheed Martin Defense Systems, 100 Plastics Ave., Pittsfield MA 01201	(413) 494-3426
Raimondo, Nat	TASC Corporation, 21215 Hawthorne, Suite 1250, Torrance CA 90503	(310) 543-6866
Ramirez, Francisco	746 TS/TGGDA, 1644 Vandergrift Rd., HAFB NM 88330-7850	(505) 679-2855
Redman, William A.	Smith Industries, 4141 Eastern Ave., SE, Grand Rapids MI 49518-8727	(616) 241-7272
Reed, Thomas	MSSA, Inc., 25 Tucker Road, Charlton MA 01507	(508) 248-1952
Reina, Andres	NAWC-AD1, 6000 E. 21St., Indianapolis IN 46219-2189	(317) 322-2931
Riggins, Robert	AFIT/ENG, WPAFB OH 45433	(513) 255-3636 x 4574
Ritter, William	746 TS/TGGP, 1644 Vandergrift Rd., HAFB NM 88330-7850	(505) 679-2174
Robinson, Lesley	HQ USAF/TER, 1650 Air Force Pentagon, Washington DC 20330-1650	DSN 223-6597
Rogers, Charles	Adroit Systems, Inc., 209 Madison St., Alexandria VA 22314	(703) 684-2900
Rogers, Robert M.	Rogers Engineering Assoc., P. O. Box 12232, Gainesville FL 32604	(904) 373-4761
Rosa, John W.	49 OG/CC, 700 Delaware Ave., Suite 114, HAFB NM 88330-8014	(505) 475-7092
Rott, Louisa	PM GPS, SEAE-CM-GPS-RMD, Bldg. 915, Murphy Dr., Fort Monmouth NJ 07703-5000	(908) 532-6134
Ruediger, Friedrich	NATO, B-2010, SHAPE, Belgium	32 65 44 55 38
Ruffin, Paul B.	USAMICOM, ATTN: AMSMI-RD-MG-NC, Redstone Arsenal AL	(205) 876-8331
Sakran, Frank C.	NAWCAD, 22777 Saufley Road, MS 1 (4KJ200A), Patuxent River MD 20670-5304	(301) 826-3181
Sanford, Joseph, Maj.	746 TS/DO, 1644 Vandergrift Rd., HAFB NM 88330-7850	(505) 679-2172
Sapuppo, Mike	Milli Sensor Systems & Actuators, Inc., 93 Border St., West, Newton MA 02165	(617) 965-1346
Schoenfeld, Herbert	JSDE, 7802 NW 77 Ave, Tamarac, FL 33321	(305) 726-2405
Schrader, James P.	Lockheed Aircraft, P. O. Box 33, Ontario CA 91761-0033	(909) 395-2411 x 5431
Scott, Daniel	746 TS/TGGT, 1644 Vandergrift Rd., HAFB NM 88330-7850	(505) 679-1745
Senter, Steven	Northern Telecom Ltd, 475 N. Martingale Rd., Schaumburg IL	(708) 706-8287
Shaw, Bowen W.	NAWC-Weapons Div., 1124 W. Las Cruces Ct., Ridgecrest CA 93555-5900	(619) 939-5988
Siebert, Robert	Honeywell Inc, 13350 U.S. Highway 19 N., Clearwater FL 31624	(813) 539-4097
Siouris, George	ASC/XRES, Bldg. 11A, 1970 Third St., Ste 2, WPAFB OH 45433-7209	DSN 785-2821
Sitomer, James	C.S. Draper Lab, 555 Technology Sq., M.S. 79, Cambridge MA 02139	(619) 258-1752
Sklar, Jay	MIT Lincoln Lab., 244 Wood Street, Lexington MA 02173-9108	(617) 981-7440
Skouson, Mark	586 FLTS/TGOOM, 1117 DeZonia Dr., HAFB NM 88330	(505) 475-5727
Snead, Jack C.	DCS Corporation, 1330 Braddock Place, Alexandria VA 22314	(703) 683-8430 x 289

ATTENDANCE LIST
SEVENTEENTH BIENNIAL GUIDANCE TEST SYMPOSIUM
2-4 May 1995

NAME	COMPANY	PHONE #
Snowball, Allen	SMC/CZTU, 2435 Vela Way, Suite 1613, Los Angeles AFB CA 90245-5500	(310) 363-6481
Spencer, Richard V.	Lockheed Martin, 100 Plastics Ave., Pittsfield MA 01235	(413) 494-3855
Spennik, Adam	746 TS/TGGTE, 1644 Vandergrift Rd., HAFB NM 88330-7850	(505) 679-1725
Spicer, Benny	NAWC AD, 6000 E. 21st, MS-37, Indianapolis IN 46219-2189	(317) 322-2970
Stoneking, Donald	746 TS/TGGML, 1644 Vandergrift Rd., HAFB NM 88330-7850	(505) 679-1651
Stotts, Larry	DOD, ARPA, 3701 North Fairfax Drive, Washington DC	(703) 696-2367
Strandberg, Ron	Draper Lab, Inc., 555 Technology Sq., Cambridge MA 02139	(617) 258-2596
Sturdevant, Reese	746 TS/TGGDA, 1644 Vandergrift Rd., HAFB NM 88330-7850	(505) 679-2053
Stutz, Derryl	746 TS/TGGPM, 1644 Vandergrift, HAFB NM 88330-7850	(505) 679-1676
Surgerman, Leonard	Physical Science Lab, 3025 Fairway Drive, Las Cruces NM 88011	(505) 522-7842
Tafel, Robert W.	NCCOSC RDT&E Det, P. O. Box 5152, Warminster PA 18974-0591	(215) 441-2069
Tan, Henry	Logicon, Inc., 222 W. 6th St., P. O. Box 471, San Pedro CA 90733-0471	(310) 831-0611 x 2617
Taylor, Scott	746 TS/TGGPM, 1644 Vandergrift Rd., HAFB NM 88330-7850	(505) 679-1605
Tehrani, M.M.	Litton G&C, 5500 Canoga Ave., Woodland Hills CA 91367	(818) 715-3753
Thielman, Leroy O.	Honeywell, MN17-2511, 2600 Ridgway Parkway, Minneapolis MN 55413	(612) 951-5642
Thompson, Barbara	746 TS/TGGMR, 1644 Vandergrift Rd., HAFB NM 88330-7850	(505) 679-2666
Tipps, Ben	Litton G&C Systems, 5500 Canoga Ave., MS 28, Woodland Hills CA 91367-6698	(818) 715-2059
Tran, Van	C2SID, Bldg. 2525, Fort Monmouth NJ 08731	(908) 544-3895
Truncalo, Angelo	Rockwell International, 3370 Miraloma Ave., P. O. Box 3105, Anaheim CA 92803-3105	(714) 762-3303
Trunzo, Angelo	746 TS/TGGTB, 1644 Vandergrift Rd., HAFB NM 88330-7850	(505) 679-1744
Tyner, Sam	ASC/LYB, Bldg. 28, 2145 Monahan Way, WPAFB OH 45433-7019	(513) 255-4140
Upadhyay, Triveni	Mayflower Communications Co., Inc., 80 Main Street, Reading MA 01867	(617) 942-2666
Ventrone, Frederick	516300A, MS-3, 48108 Standley Rd., Patuxent River MD 20670-5304	(301) 826-6356
Von Husen, Ray	746 TS/TGGPM, 1644 Vandergrift Rd., HAFB NM 88330-7850	(505) 679-1728
Von Schmittou, Steve	Rockwell International, 3370 Miraloma Ave., Anaheim CA 92803-4921	(714) 762-2093
Walker, Gary	Northrop Grumman, 100 Morse Street, Norwood MA 02062	(617) 762-5300 x2809
Walthers, Phillip A.	Logicon, Inc., 370 South 500 East, Suite 230, Clearfield UT 84015	(801) 773-5274
Welch, Brian	ASC/LYB, 2145 Monahan Way, WPAFB OH 45433-7017	(513) 255-4140
Wells, Rod	Rockwell International, 350 Collins Rd., NE, Cedar Rapids IA	(319) 395-3543
Whalen, Donna	746 TS/IM, 1644 Vandergrift Rd., HAFB NM 88330-7850	(505) 679-1758
Welchel, Toby	746 TS/TGGTE, 1644 Vandergrift Rd., HAFB NM 88330-7850	(505) 679-1661

ATTENDANCE LIST
SEVENTEENTH BIENNIAL GUIDANCE TEST SYMPOSIUM
2-4 May 1995

NAME	COMPANY	PHONE #
White, John	Defense Mapping Agency, P. O. Drawer F, HAFB NM 88330-0406	(505) 475-7056
Whitehead, Dennis	Acutronic USA Inc., 139 Delta Drive, Pittsburgh PA 15238	(412) 963-9400
Whitsel, Ronald	NRaD, P. O. Box 5152, Warminster PA 18974	(215) 441-2777
Wiedemer, Michael	SMC/CZ, 2435 Vela Way, Suite 1613, Los Angeles AFB CA 90245-5500	(310) 363-1526
Wimber, Bud	Litton G&C Systems, 5500 Canoga Ave., Woodland Hills CA 91367	(818) 715-7920
Winterrowd, David	46 TG/TGOR, 225 Polars, WSMR NM 88002	(505) 678-0971
Wong, Christi	746 TS/TGGD, 1644 Vandergrift Rd., HAFB NM 88330-7850	(505) 679-2195
Yerion, Dale	746 TS/TGGPP, 1644 Vandergrift Rd., HAFB NM 88330-7850	(505) 679-2194
Zarzour, Fred	46 TG/CSS, 961 DeZonia Rd., HAFB NM 88330-7717	(505) 475-1004